MycoKeys 103: 1–24 (2024)
DOI: 10.3897/mycokeys.103.116153

Research Article

Molecular phylogeny and morphology reveal two new entomopathogenic species of *Ophiocordyceps* (Ophiocordycipitaceae, Hypocreales) parasitic on termites from China

Qi Fan[1,2,3*], Tao Yang[2,3,4*], Hui Li[2,3], Xue-Mei Wang[2,3,4], He-Fa Liao[2,3,4], Pei-Hong Shen[1], Zhu-Liang Yang[2,3], Wen-Bo Zeng[5], Yuan-Bing Wang[2,3]

1 *College of Life Science and Technology, Guangxi University, Nanning 530004, Guangxi, China*
2 *CAS Key Laboratory for Plant Diversity and Biogeography of East Asia, Kunming Institute of Botany, Chinese Academy of Sciences, Kunming 650201, Yunnan, China*
3 *Yunnan Key Laboratory for Fungal Diversity and Green Development, Kunming Institute of Botany, Chinese Academy of Sciences, Kunming 650201, Yunnan, China*
4 *College of Life Science, Yunnan University, Kunming 650091, Yunnan, China*
5 *Notoginseng Medicine and Pharmacy, Wenshan University, Wenshan 663000, Yunnan, China*
Corresponding authors: Wen-Bo Zeng (zengwenboherb@163.com); Yuan-Bing Wang (wangyuanbing@mail.kib.ac.cn)

Abstract

Two new termite-pathogenic species, *Ophiocordyceps globiperitheciata* and *O. longistipes*, are described from Yunnan Province, China. Six-locus (ITS, nrSSU, nrLSU, *tef-1α*, *rpb1* and *rpb2*) phylogenetic analyses in combination with morphological observations were employed to characterize these two species. Phylogenetically, *O. globiperitheciata* is most closely related to *Hirsutella cryptosclerotium* and *O. communis*, whereas *O. longistipes* shares a sister relationship with *O. fusiformis*. However, *O. globiperitheciata* differs from *H. cryptosclerotium* by parasitizing Blattodea and producing clavate, unbifurcated stromata. *Ophiocordyceps globiperitheciata* is distinguished from *O. communis* by multiple stromata, shorter asci and ascospores. *Ophiocordyceps longistipes* differs from *O. fusiformis* in producing larger stromata, perithecia, asci and ascospores, as well as smaller citriform or oval conidia. Morphological descriptions of the two new species and a dichotomous key to the 19 termite-pathogenic *Ophiocordyceps* species are presented.

Key words: New species, morphology, *Ophiocordyceps*, phylogeny, termites

Academic editor: Marc Stadler
Received: 23 November 2023
Accepted: 11 January 2024
Published: 8 March 2024

Citation: Fan Q, Yang T, Li H, Wang X-M, Liao H-F, Shen P-H, Yang Z-L, Zeng W-B, Wang Y-B (2024) Molecular phylogeny and morphology reveal two new entomopathogenic species of *Ophiocordyceps* (Ophiocordycipitaceae, Hypocreales) parasitic on termites from China. MycoKeys 103: 1–24. https://doi.org/10.3897/mycokeys.103.116153

Introduction

Invertebrate-associated fungi are intriguing and diverse, widely distributed around the world (Araújo et al. 2018; Luangsa-ard et al. 2018; Haelewaters and Kasson 2020; Wilson et al. 2021; Santamaria et al. 2023). There are two typical relationships between fungi and invertebrates. One is mutualism. Mutualism is reciprocally positive interactions between pairs of species (Bronstein 2009). For example, *Termitomyces* Heim (Lyophyllaceae, Agaricomycetes) can decompose plants to provide food for termites; in return, termites shelter *Termitomyces* from external threats (Da Costa et al. 2019). The other is parasitism.

* Contributed equally as the first authors.

Parasitism is the interaction between two species where one party (the parasite) benefits, while the other party (the host) suffers harm (Roper et al. 2019). As exemplified by species of *Cordyceps* Fr. sensu lato (s. l.), fungi parasitize invertebrates and eventually kill them. Invertebrate-pathogenic fungi are considered as the most well-known parasitic fungi (Araújo et al. 2018; Araújo et al. 2021; Wilson et al. 2021). They are ubiquitous inhabitants of forests worldwide, especially in tropical and subtropical regions. Invertebrate-pathogenic fungi are highly virulent and are known to have significant effects on host populations (Evans 1974). *Cordyceps* s. l. represents the most abundant and diverse group among invertebrate-pathogenic fungi (Araújo et al. 2021). Representatives of this group can colonize hosts in more than 10 invertebrate orders (Sanjuan et al. 2015; Araújo and Hughes 2016). They spread primarily through their hosts, evolving extensively in their morphologies and parasitic strategies. (Araújo and Hughes 2016). According to the current status of *Cordyceps* s. l. taxonomy, it belongs to four families: Clavicipitaceae, Cordycipitaceae, Ophiocordycipitaceae and Polycephalomycetaceae (Sung et al. 2007a; Xiao et al. 2023). Among them, the genus *Ophiocordyceps* Petch (Ophiocordycipitaceae) has received significant attention for its unique interactions with hosts and medical values (Zou et al. 2017; Araújo et al. 2018; Luangsa-ard et al. 2018; Khonsanit et al. 2019; Wang et al. 2021a; Zou et al. 2022; Tang et al. 2023a).

Ophiocordyceps is the largest genus in the family Ophiocordycipitaceae (Araújo et al. 2018; Luangsa-ard et al. 2018). The genus was established by Petch based on the type species *O. blattae* Petch (Petch 1931). In recent years, an increasing number of species have been described in *Ophiocordyceps*, with approximately 410 accepted species names to date (http://www.indexfungorum.org/names/Names.asp) (Sung et al. 2007a; Sanjuan et al. 2015; Spatafora et al. 2015; Araújo et al. 2018; Evans et al. 2018; Luangsa-ard et al. 2018; Wijayawardene et al. 2018; Khonsanit et al. 2019; Mongkolsamrit et al. 2023; Tang et al. 2023a, b).

The majority of species in *Ophiocordyceps* exhibit clavate, entirely, or partially darkly pigmented stromata or synnemata, especially those species with a hirsutella-like anamorph, while some species possess brightly colored stromata with hymenostilbe-like anamorph. The stromata are mostly wiry, tough, leathery, and flexible. Perithecia are superficial to pseudo-immersed to fully immersed, and are vertically or obliquely inserted in the stromata. Asci are usually cylindrical with thickened apex and contain eight ascospores. Ascospores are typically cylindrical or clavate, multiseptate, either disarticulating into secondary spores or remaining whole after discharge (Sung et al. 2007a; Quandt et al. 2014; Luangsa-ard et al. 2018). Species in *Ophiocordyceps* mainly attack insects of Coleoptera, Diptera, Hemiptera, Hymenoptera, Lepidoptera, Odonata, and Orthoptera. Generally, they can attack all stages (larva, pupa, nymph, and adult) of the insects, with the majority of targets being larvae of Coleoptera and Lepidoptera living in wood or buried in soil (Sung et al. 2007a; Shrestha et al. 2016). Among species of *Ophiocordyceps*, only 17 species attack termites (Tasanathai et al. 2019; Araújo et al. 2021; Tang et al. 2022; Tasanathai et al. 2022; Xu et al. 2022).

Termites (Termitidae, Blattodea) are typically eusocial soil-dwelling insects, widely distributed around the world, especially in tropical and subtropical regions (Pearce 1997). Most termites are considered pests, causing significant impacts on forest ecosystems, and agricultural and forestry crops, with subterranean termites being particularly destructive (Rust and Su 2012; Scharf 2015).

Some species of termite-pathogenic *Ophiocordyceps* have been regarded as potential biological agents to control termite populations (Rath 2000).

During surveys of invertebrate-pathogenic fungi in Yunnan Province, China, several specimens attacking termites were collected. Morphological and molecular evidence indicates that they belong to two different taxa distinct from previously described species. This study aims to introduce these two new species and discuss their evolutionary placement among related species.

Materials and methods

Collection and isolation

Stromata emerging above fallen leaves were found in subtropical evergreen broad-leaved forests of Ruili City and Jinghong City, Yunnan Province, China. Specimens were documented and photographed in the field using a Canon 90D digital camera, and then each was placed in a sterilized 50 mL plastic centrifugal tube. All samples were stored in a cooler with ice packs until they were taken to the laboratory. Pure cultures were obtained on potato dextrose agar (PDA) with the composition of 200 g/L potato, 20 g/L dextrose, and 20 g/L agar, following the method previously presented (Wang et al. 2020). Subsequently, pure cultures were transferred to PDA slants and stored at the Kunming Institute of Botany Culture Collection (**KUNCC**), Chinese Academy of Sciences. Dried specimens were deposited in the Cryptogamic Herbarium of the Kunming Institute of Botany, Chinese Academy of Sciences (**KUN-HKAS**).

Morphological observations

The newly collected specimens were macroscopically examined with the Canon 750D camera and Olympus SZ60 stereo microscope. The characteristics of stromata (size, texture, shape, and color) were recorded. For the observation of teleomorph, perithecia were removed from the stromata and mounted on a glass slide with either 3% potassium hydroxide (KOH) (w/v) or 0.04% lactophenol cotton blue stain solution (w/v). Subsequently, the sizes and shapes of the perithecia, asci, and ascospores were measured under Olympus BX53 microscope. For each species, at least two specimens are measured, and each characteristic is measured at least 15 times repeatedly. The characteristics of pure cultures (size, texture, and color) were photographed using a Canon 750D camera after six weeks of culturing in an incubator at 25 °C. For the morphological description of anamorph, microscope slide cultures were prepared using the previous described method (Wang et al. 2020). Conidiogenous structures and conidia were measured and photographed using an Olympus BX53 microscope.

DNA extraction, amplification and sequencing

Genomic DNA was extracted from fresh mycelia cultured for three weeks using Ezup Column Fungi Genomic DNA Extraction Kit (Sangon Bio Co., Ltd., Shanghai, China), following the manufacturer's protocol. Polymerase chain reactions (PCRs) were used to amplify genetic markers using the following primer pairs: nrSSU-COF/nrSSU-COR for the nuclear ribosomal small subunits (nrSSU)

(Wang et al. 2015), LR0R/LR5 for the nuclear ribosomal large subunits (nrLSU) (Vilgalys and Hester 1990; Hopple 1994), ITS5/ITS4 for the internal transcribed spacer (ITS) (White et al. 1990), EF1α-EF/EF1α-ER for the translation elongation factor 1α (*tef-1α*) (Bischoff et al. 2006; Sung et al. 2007b), RPB1-5F/RPB1-5R for the largest subunits of RNA polymerase II (*rpb1*) (Bischoff et al. 2006), and RPB2-5F/RPB2-7cR for the second largest subunits of RNA polymerase II (*rpb2*) (Bischoff et al. 2006; Sung et al. 2007b).

Each 25 μL-PCR reaction contained 12.5 μL of 2× Taq PCR Master Mix (Tiangen Biotech Co., Ltd., Beijing, China), 9.5 μL of RNase-Free water (Sangon Bio Co., Ltd., Shanghai, China), 1 μL of each forward and reverse primer (10 μmol/L), 1 μL of DNA template (500 ng/μL). PCR reactions were placed in a LongGene T20 multi-block thermal cycler (Hangzhou LongGene Scientific Instruments Co., Ltd., Hangzhou, China) under the following conditions: For ITS, (1) 3 min at 95 °C, (2) 36 cycles of denaturation at 94 °C for 30 sec, annealing at 55 °C for 50 sec and extension at 72 °C for 1 min, (3) extension at 72 °C for 5 min and 12 °C soak. For nrSSU, (1) 4 min at 95 °C, (2) 22 cycles of denaturation at 94 °C for 1 min, annealing at 51 °C for 1 min and extension at 72 °C for 90 sec, followed by (3) 12 cycles of denaturation at 94 °C for 1 min, annealing at 50 °C for 1 min and extension at 72 °C for 95 sec, (4) extension at 72 °C for 10 min and 12 °C soak. For nrLSU, (1) 4 min at 95 °C, (2) 36 cycles of denaturation at 94 °C for 1 min, annealing at 50 °C for 1 min and extension at 72 °C for 2 min, (3) extension at 72 °C for 10 min and 12 °C soak. For *tef-1α*, (1) 3 min at 95 °C, (2) 36 cycles of denaturation at 94 °C for 30 sec, annealing at 50 °C for 30 sec and extension at 72 °C for 1 min, (3) extension at 72 °C for 10 min and 12 °C soak. For *rpb1*, (1) 4 min at 95 °C, (2) 36 cycles of denaturation at 94 °C for 40 sec, annealing at 50 °C for 40 sec and extension at 72 °C for 90 sec, (3) extension at 72 °C for 10 min and 12 °C soak. For *rpb2*, (1) 3 min at 95 °C, (2) 36 cycles of denaturation at 94 °C for 45 s, annealing at 58 °C for 45 s and extension at 72 °C for 90 s, (3) extension at 72 °C for 10 min and 12 °C soak. Standard DNA markers (Sangon Bio Co., Ltd., Shanghai, China) of known size and weight were used to quantify the PCR products. PCR products were purified using the DiaSpin PCR Product Purification Kit (Sangon Bio Co., Ltd., Shanghai, China), following the manufacturer's instructions. Purified PCR products were sent to Sangon Bio Co., Ltd., (Kunming, China) for Sanger sequencing. The newly generated sequences were checked using MEGA v. 7.0 (Kumar et al. 2016). Consensus sequences were obtained using SeqMan of the Lasergene software package v. 14.1 (DNAstar, Madison, Wisconsin, USA) and deposited in NCBI GenBank (https://www.ncbi.nlm.nih.gov/genbank).

Sequencing alignments and phylogenetic analyses

We generated sequences for six loci from five specimens (Table 1). These were complemented with sequences of 125 related samples downloaded from NCBI GenBank based on BLAST searches and recent publications on Ophiocordycipitaceae (Tang et al. 2022; Xu et al. 2022). *Tolypocladium inflatum* Gams OSC 71235 and *T. ophioglossoides* (J.F. Gmel.) Quandt et al. CBS 100239 were selected as the outgroup. The sequence datasets were aligned using MAFFT v. 7, and alignments were manually corrected in MEGA v. 7.0 (Katoh and Standley 2013; Kumar et al. 2016). Ambiguously aligned sites were manually eliminated and gaps were regarded as missing data. ModelFinder (Kalyaanamoorthy et al.

Table 1. Voucher information and GenBank accession numbers for the sequences included in this study.

Species	Voucher information	GenBank accession no.						Reference
		ITS	nrSSU	nrLSU	*tef-1α*	*rpb1*	*rpb2*	
Hirsutella satumaensis	ARSEF 996	–	KM652082	KM652125	KM652008	KM652047	–	Simmons et al. 2015
H. cf. *haptospora*	ARSEF 2228	KM652166	KM652075	KM652118	KM652001	KM652041	–	Simmons et al. 2015
H. citriformis	ARSEF 1446	KM652154	KM652065	KM652106	KM651990	KM652031	–	Simmons et al. 2015
H. cryptosclerotium	ARSEF 4517	KM652157	KM652066	KM652109	KM651992	KM652032	–	Simmons et al. 2015
H. fusiformis	ARSEF 5474	–	KM652067	KM652110	KM651993	KM652033	–	Simmons et al. 2015
H. gigantea	ARSEF 30	–	–	JX566977	JX566980	KM652034	–	Simmons et al. 2015
H. guyana	ARSEF 878	–	KM652068	KM652111	KM651994	KM652035	–	Simmons et al. 2015
H. haptospora	ARSEF 2226	KM652159	–	–	KM651995	KM652036	–	Simmons et al. 2015
H. illustris	ARSEF 5539	KM652160	KM652069	KM652112	KM651996	KM652037	–	Simmons et al. 2015
H. kirchneri	ARSEF 5551	–	KM652070	KM652113	KM651997	–	–	Simmons et al. 2015
H. lecaniicola	ARSEF 8888	KM652162	KM652071	KM652114	KM651998	KM652038	–	Simmons et al. 2015
H. liboensis	ARSEF 9603	KM652163	KM652072	KM652115	–	–	–	Simmons et al. 2015
H. necatrix	ARSEF 5549	KM652164	KM652073	KM652116	KM651999	KM652039	–	Simmons et al. 2015
H. nodulosa	ARSEF 5473	KM652165	KM652074	KM652117	KM652000	KM652040	–	Simmons et al. 2015
H. radiata	ARSEF 1369	–	KM652076	KM652119	KM652002	KM652042	–	Simmons et al. 2015
H. repens nom. inval.	ARSEF 2348	KM652167	KM652077	KM652120	KM652003	–	–	Simmons et al. 2015
H. rhossiliensis	ARSEF 3747	KM652168	KM652080	KM652123	KM652006	KM652045	–	Simmons et al. 2015
H. strigosa	ARSEF 2197	KM652174	KM652085	KM652129	KM652012	KM652050	–	Simmons et al. 2015
H. subulata	ARSEF 2227	KM652176	KM652086	KM652130	KM652013	KM652051	–	Simmons et al. 2015
H. thompsonii	ARSEF 257	KM652182	–	KM652139	KM652019	KM652056	–	Simmons et al. 2015
	ARSEF 414	KM652184	–	KM652143	KM652021	KM652059	–	Simmons et al. 2015
H. thompsonii var. *vina*	ARSEF 254	–	KM652101	KM652149	KM652028	KM652062	–	Simmons et al. 2015
H. versicolor	ARSEF 1037	–	KM652102	KM652150	KM652029	KM652063	–	Simmons et al. 2015
Ophiocordyceps acicularis	OSC 110988	–	EF468951	EF468804	EF468745	EF468853	–	Sung et al. 2007a
O. agriotidis	ARSEF 5692	JN049819	DQ522540	DQ518754	DQ522322	DQ522368	DQ522418	Spatafora et al. 2007
O. annulata	CEM 303	–	KJ878915	KJ878881	KJ878962	KJ878995	–	Quandt et al. 2014
O. appendiculata	NBRC 106960	JN943326	JN941728	JN941413	AB968577	JN992462	AB968539	Schoch et al. 2012
O. arborescens	NBRC 105891	AB968398	AB968386	AB968414	AB968572	–	AB968534	Ban et al. 2015
O. asiana	MY11878	MW285719	–	MW280213	MW292448	MW296049	–	Khao-ngam et al. 2021
O. asiatica	BCC 30516	MH754722	–	MH753675	MK284263	MK214105	MK214091	Tasanathai et al. 2019
	BCC 86435	MH754723	–	MH753676	–	MK214106	MK214092	Tasanathai et al. 2019
O. barnesii	BCC 28560	–	EU408776	–	–	EU408773	EU418599	Luangsa-ard et al. 2010
O. bidoupensis	YFCC 8793	–	OM304638	–	OK556894	OK556898	OK556900	Zou et al. 2022
O. brunneinigra	BCC 69032	–	–	MF614654	MF614638	MF614668	MF614681	Luangsa-ard et al. 2018
O. brunneiperitheciata	BCC 66167	–	–	MF614659	MF614644	–	MF614684	Luangsa-ard et al. 2018
O. brunneipunctata	OSC 128576	–	DQ522542	DQ518756	DQ522324	DQ522369	DQ522420	Spatafora et al. 2007
O. brunneirubra	BCC 14384	MH754736	–	MH753690	GU797121	MK751465	MK751468	Tasanathai et al. 2019
O. campes	BCC 36938	MT783955	–	MT118175	MT118167	MT118183	MT118188	Tasanathai et al. 2020
O. communis	BCC 1842	MH754726	–	MH753680	MK284266	MK214110	MK214096	Tasanathai et al. 2019
	BCC 1874	MH754725	–	MH753679	MK284267	MK214109	MK214095	Tasanathai et al. 2019
	BCC 2754	MH754727	–	MH753681	MK284268	MK214111	MK214097	Tasanathai et al. 2019
O. cossidarum	MFLU 17-0752	–	MF398186	MF398187	MF928403	MF928404	–	Xiao et al. 2019
O. crinalis	GDGM 17327	–	KF226253	KF226254	KF226256	KF226255	–	Wang et al. 2014
O. dipterigena	OSC 151911	–	KJ878919	KJ878886	KJ878966	KJ879000	–	Quandt et al. 2014
O. elongata	OSC 110989	–	–	EF468808	EF468748	EF468856	–	Sung et al. 2007a

Species	Voucher information	GenBank accession no.						Reference
		ITS	nrSSU	nrLSU	*tef-1α*	*rpb1*	*rpb2*	
O. flavida	BCC 84256	–	–	MT512655	MT533482	MT533476	–	Mongkolsamrit et al. 2021
O. formosana	TNM F13893	–	KJ878908	–	KJ878956	KJ878988	KJ878943	Quandt et al. 2014
O. furcatosubulata	YFCC 902	–	MT774214	MT774221	MT774242	MT774228	MT774235	Wang et al. 2021b
O. fusiformis	BCC 93025	MZ676743	–	MZ675422	MZ707849	MZ707855	MZ707805	Tasanathai et al. 2022
	BCC 93026	MZ676744	–	MZ675423	MZ707850	MZ707856	MZ707806	Tasanathai et al. 2022
O. geometridicola	BCC 35947	–	–	MF614647	MF614631	MF614664	MF614678	Luangsa-ard et al. 2018
O. globiceps	MFLU 18-0661	MH725816	MH725812	MH725830	MH727388	–	–	Xiao et al. 2019
O. globiperitheciata	**HKAS 126130**	**OR015963**	**OR082950**	**OR015968**	**OR030532**	**OR119834**	–	**This study**
	HKAS 126131	**OR015964**	**OR082951**	**OR015969**	**OR030533**	**OR119835**	–	**This study**
O. globosa	BCC 93023	MZ676740		MZ675419	MZ707846	MZ707861	–	Tasanathai et al. 2022
O. halabalaensis	MY5151	GU723763	KM655826	–	GU797110	–	–	Luangsa-ard et al. 2011
O. hydrangea	YFCC 8832	–	OM304636	OM304640	OM831277	OM831280	OM831283	Zou et al. 2022
O. irangiensis	BCC 82795	MH028142	–	–	MH028186	MH028164	MH028174	Khonsanit et al. 2019
O. isopterae	MY12376	MZ676741	–	MZ675420	MZ707847	MZ707859	MZ707803	Tasanathai et al. 2022
	BCC 93042	MZ676742	–	MZ675421	MZ707848		MZ707804	Tasanathai et al. 2022
O. karstii	MFLU 15-3884	–	KU854952	–	KU854945	KU854943	–	Li et al. 2016
O. khokpasiensis	BCC 48071	MH754728	–	MH753682	MK284269	MK214112	–	Tasanathai et al. 2019
	BCC 48072	MH754729	–	MH753683	MK284270	MK214113	–	Tasanathai et al. 2019
	BCC 1764	MH754730	––	MH753684	MK284271	MK214114	MK214098	Tasanathai et al. 2019
	BCC 81464	MK632043	MK632128	MK632103	MK632077	MK632170	MK632159	Tasanathai et al. 2019
O. kimflemingiae	SC09B	–	KX713631	KX713620	KX713698	KX713724	–	Araújo et al. 2018
O. konnoana	EFCC 7315	–	EF468959	–	EF468753	EF468861	EF468916	Sung et al. 2007a
O. longissima	EFCC 6814	–	–	EF468817	EF468757	EF468865	–	Sung et al. 2007a
	NBRC 106965	AB968406	AB968392	AB968420	AB968584	–	AB968546	Ban et al. 2015
O. longistipes	**KUNCC 5224**	**OR015962**	**OR082949**	**OR015967**	**OR030530**	**OR062224**	**OR113082**	**This study**
	HKAS 126186	**OR015960**	**OR082947**	**OR015966**	**OR030531**	**OR062225**		**This study**
	HKAS 126187	**OR015961**	**OR082948**	**OR015965**	**OR030529**	**OR062223**		**This study**
O. longistromata	BCC 44497	MT783956	–	MT118178	MT118170	–	MT118191	Tasanathai et al. 2020
O. macroacicularis	NBRC 100685	AB968400	AB968388	AB968416	AB968574	–	AB968536	Ban et al. 2015
O. megacuculla	BCC 82984	–	–	MH028162	MH028192	–	MH028181	Khonsanit et al. 2019
O. mosingtoensis	BCC 30904	MH754732	–	MH753686	MK284273	MK214115	MK214100	Tasanathai et al. 2019
O. mosingtoensis	BCC 36921	MH754731	–	MH753685	MK284272	MK214116	MK214099	Tasanathai et al. 2019
O. multiperitheciata	BCC 22861	–	–	MF614656	MF614640	MF614670	MF614683	Luangsa-ard et al. 2018
O. myrmecophila	CEM 1710	–	–	KJ878894	KJ878974	KJ879008	–	Quandt et al. 2014
O. nigrella	EFCC 9247	JN049853	EF468963	EF468818	EF468758	EF468866	EF468920	Sung et al. 2007a
O. nutans	OSC 110994	–	DQ522549	DQ518763	DQ522333	DQ522378	–	Spatafora et al. 2007
O. ovatospora	YHH 2206001	OP295105	OP295110	OP295113	OP313801	OP313803	OP313805	Tang et al. 2022
	YFCC 22069184	OP295106	OP295111	OP295114	OP313802	OP313804	–	Tang et al. 2022
O. pauciovoperitheciata	TBRC 8096	–	–	MF614649	MF614636	MF614665	MF614672	Luangsa-ard et al. 2018
O. phuwiangensis	BCC 85351	MT783958	–	–	MT118174	MT118187	MT118195	Tasanathai et al. 2020
	BCC 86208	–	–	MT118180	MT118172	MT118185	MT118193	Tasanathai et al. 2020
O. pruinosa	NHJ 12994	–	EU369106	EU369041	EU369024	EU369063	EU369084	Johnson et al. 2009
O. pseudoacicularis	BCC 53843	–	–	MF614646	MF614630	MF614661	MF614677	Luangsa-ard et al. 2018
O. pseudocommunis	NHJ 12581	–	EF468973	EF468831	EF468775	–	EF468930	Luangsa-ard et al. 2018
	NHJ 12582		EF468975	EF468830	EF468771	–	EF468926	Luangsa-ard et al. 2018
O. pseudocommunis	BCC 16757	MH754733	–	MH753687	MK284274	MK214117	MK214101	Tasanathai et al. 2019

Species	Voucher information	GenBank accession no.						Reference
		ITS	nrSSU	nrLSU	*tef-1α*	*rpb1*	*rpb2*	
O. pseudolloydii	MFLUCC 15-0689	MF351725	–	–	MF372758	MF372761	–	Xiao et al. 2017
O. pseudorhizoidea	BCC 48879	MH754720	–	MH753673	MK284261	MK214104	MK214089	Tasanathai et al. 2019
	BCC 86431	MH754721	–	MH753674	MK284262	MK751469	MK214090	Tasanathai et al. 2019
	NHJ 12522	JN049857	–	EF468825	EF468764	EF468873	EF468923	Tasanathai et al. 2019
	NHJ 12529	–	–	EF468824	EF468765	EF468872	EF468922	Tasanathai et al. 2019
O. puluongensis	YFCC 6442	–	MT141118	MT270528	MT270520	MT270523	MT270526	Xu et al. 2022
	YFCC 6443	–	MT141119	MT270529	MT270521	MT270524	MT270527	Xu et al. 2022
	YHH 16017	–	–	MT270530	MT270522	MT270525	–	Xu et al. 2022
O. pulvinata	TNS-F 30044	AB721302	GU904208	–	GU904209	GU904210	–	Kepler et al. 2011
O. radiciformis	BCC 93036	MZ676746	–	MZ675425	MZ707852	MZ707857	MZ707808	Tasanathai et al. 2022
	BCC 93035	MZ676747	–	MZ675426	MZ707853	MZ707858	MZ707809	Tasanathai et al. 2022
O. ramosissimum	GZUHHN8	KJ028007	KJ028012	–	KJ028014	KJ028017	–	Wen et al. 2014
O. ravenelii	OSC 110995	–	DQ522550	DQ518764	DQ522334	DQ522379	DQ522430	Spatafora et al. 2007
O. rhizoidea	NHJ 12522	JN049857	EF468970	EF468825	EF468764	EF468873	EF468923	Tasanathai et al. 2019
	NHJ 12529	–	EF468969	EF468824	EF468765	EF468872	EF468922	Tasanathai et al. 2019
O. robertsii	KEW 27083	AJ309335	–	EF468826	EF468766	–	–	Sung et al. 2007a
O. rubiginosiperitheciata	NBRC 106966	JN943344	JN941704	JN941437	AB968582	JN992438	AB968544	Kepler et al. 2012
O. salganeicola	Mori01	–	MT741705	MT741719	MT759575	MT759578	MT759580	Araújo et al. 2021
	Mori02	–	MT741704	MT741718	MT759572	MT759579	MT759581	Araújo et al. 2021
O. satoi	J7	–	KX713653	KX713599	KX713683	KX713711	–	Araújo et al. 2018
O. sinensis	ARSEF 6282	KM652173	KM652083	KM652126	KM652009	KM652048	–	Simmons et al. 2015
	EFCC 7287	JN049854	EF468971	EF468827	EF468767	EF468874	EF468924	Kepler et al. 2012
O. sobolifera	NBRC 106967	AB968409	AB968395	AB968422	AB968590	–	–	Ban et al. 2015
O. spataforae	NHJ 12525	–	EF469125	EF469078	EF469063	EF469092	EF469111	Sung et al. 2007a
	OSC 128575	JN049845	EF469126	EF469079	EF469064	EF469093	EF469110	Sung et al. 2007a
O. sphecocephala	NBRC 101752	JN943351	JN941696	JN941445	AB968591	JN992430	AB968552	Schoch et al. 2012
O. spicatus	MFLU 18-0164	MK863254	MK863047	MK863054	MK860192	–	–	Zha et al. 2021
O. stylophora	OSC 111000	JN049828	DQ522552	DQ518766	DQ522337	DQ522382	DQ522433	Spatafora et al. 2007
	OSC 110999	–	EF468982	EF468837	–	EF468882	EF468931	Sung et al. 2007a
O. termiticola	BCC 1920	MH754724	–	MH753678	MK284265	MK214108	MK214094	Tasanathai et al. 2019
	BCC 1770	GU723780	–	MH753677	MK284264	MK214107	MK214093	Tasanathai et al. 2019
	BCC 93002	–	–	MZ675427	MZ707854	MZ707862	MZ707810	Tasanathai et al. 2019
O. thanathonensis	MFLU 16-2909	MF850376	–	MF850377	MF872613	MF872615	–	Xiao et al. 2017
O. tricentri	NBRC 106968	AB968410	AB968393	AB968423	AB968593	–	AB968554	Ban et al. 2015
O. unilateralis	OSC 128574	–	DQ522554	DQ518768	DQ522339	DQ522385	DQ522436	Spatafora et al. 2007
O. unituberculata	YFCC HU1301	–	KY923214	–	KY923216	KY923218	KY923220	Wang et al. 2018
O. xuefengensis	GZUHHN13	KC631804	KC631785	–	KC631790	KC631795	–	Wen et al. 2013
	GZUH2012HN13	KC631801	KC631787	–	KC631792	KC631797	–	Wen et al. 2013
O. trichospora	CBS 109876	–	AF543766	AF543790	AF543779	AY489669	DQ522457	Sung et al. 2007a
Tolypocladium inflatum	OSC 71235	JN049844	EF469124	EF469077	EF469061	EF469090	EF469108	Sung et al. 2007b
T. ophioglossoides	CBS 100239	–	KJ878910	KJ878874	KJ878958	KJ878990	KJ878944	Quandt et al. 2014

Note: Newly-generated sequences are shown in bold.

2017) was used to select the best-fit nucleotide substitution models for Maximum Likelihood (ML) and Bayesian Inference (BI) analyses under the Akaike Information Criterion (AIC). The optimized models for each locus partition are presented in Table 2. Partitioned ML and BI analyses were performed on the

Table 2. Results of the best-ftting model for maximum likelihood (ML) and Bayesian inference (BI) for six loci partitions.

Gene name	ML	BI
ITS	GTR+F+I+G4	GTR+F+I+G4
nrSSU	TNe+I+G4	SYM+I+G4
nrLSU	TIM+F+I+G4	GTR+F+I+G4
tef-1α	TIM2+F+I+G4	GTR+F+I+G4
rpb1	TIM+F+I+G4	GTR+F+I+G4
rpb2	TIM3+F+I+G4	GTR+F+I+G4

concatenated data set. The BI analysis was conducted using the MrBayes v. 3.2 (Ronquist et al. 2012). Four simultaneous Markov chains were run for 2,000,000 generations with a sub-sampling frequency every 100 generations. A burn-in of the first 25% of the total run was discarded. ML analysis was conducted using IQ-TREE v. 2.1.3 (Nguyen et al. 2015) under partitioned models (Chernomor et al. 2016) with 1000 ultrafast bootstrap (Hoang et al. 2018). Trees were visualized with its Maximum-Likelihood bootstrap proportions (ML-BS) and Bayesian posterior probability (BI-PP) in FigTree v. 1.4.4 and edited with Adobe Illustrator CS6.0.

Results

Phylogenetic analyses

The combined dataset of six loci was composed of 5021 bp (585 bp for ITS, 903 bp for nrLSU, 1037 bp for nrSSU, 859 bp for *tef-1α*, 664 bp for *rpb1*, and 973 bp for *rpb2*). Phylogenetic trees inferred from ML and BI analyses exhibited nearly consistent overall topologies and recognized four statistically well-supported clades within *Ophiocordyceps*, namely *Hirsutella* Pat, *O. sphecocephala* (Klotzsch ex Berk.) Sung et al., *O. sobolifera* (Hill ex Watson) Sung et al., and *O. ravenelii* (Berk. & M.A. Curtis) Sung et al. clades (Fig. 1). Among them, the *Hirsutella* clade includes six distinct subclades, namely *H. citriformis* Speare, *H. thompsonii* Fisher, *H. nodulosa* Petch, *H. guyana* Minter & Brady, *H. sinensis* (Berk.) Sung et al., and the *Hirsutella* ant pathogen subclades. As revealed from phylogenetic analyses, all specimens collected in this study were placed in the *H. thompsonii* subclade. Three samples (HKAS 126185, HKAS 126186, and HKAS 126187), newly described as *O. longistipes*, were clustered closely with *O. fusiformis* Tasan et al. However, the phylogenetic evidence indicated that these three samples formed a monophyletic clade in *Ophiocordyceps*, with high statistical support (ML-BS/BI-PP=100/1). The other two samples (HKAS 126130 and HKAS 126131), newly described as *O. globiperitheciata*, clustered together and formed a separate clade, distinguishing from other species in *Ophiocordyceps* with moderate bootstrap support (ML-BS/BI-PP=84/0.99). Therefore, the phylogenetic data supported the recognition of *O. longistipes* and *O. globiperitheciata* as distinct species in *Ophiocordyceps*.

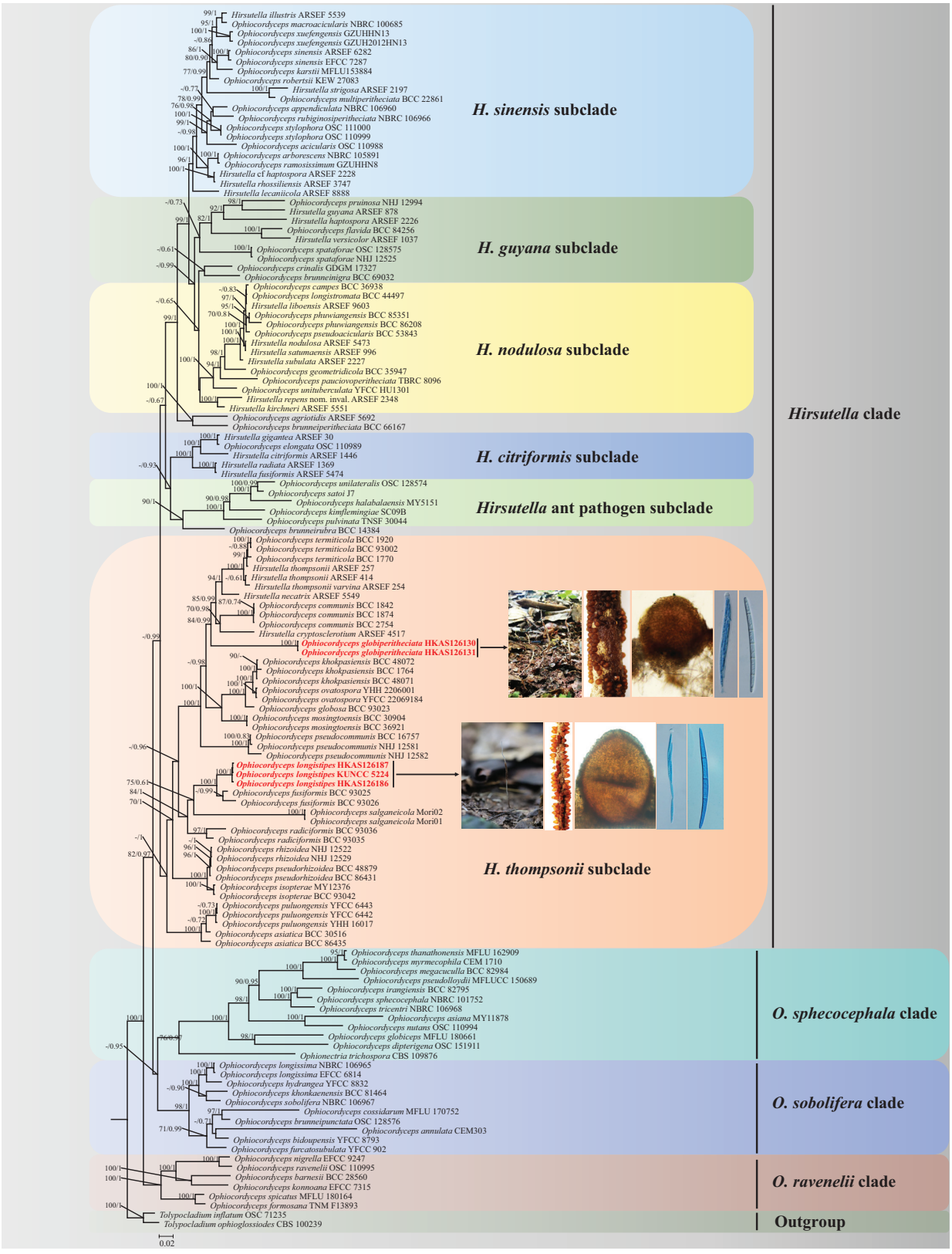

Figure 1. Phylogenetic tree based on the combined dataset of nrSSU, nrLSU, *tef-1α*, *rpb1*, *rpb2*, and ITS showing the relationship of two new species on termites from China with other *Ophiocordyceps* species. Values at the nodes before and after the backslash are BI posterior probabilities (BI-PP greater than 0.60) and ML bootstrap proportions (ML-BP greater than 70%), respectively. New species described in this paper are shown in bold red.

Taxonomy

***Ophiocordyceps longistipes* Y.B. Wang, T. Yang, Q. Fan & Zhu L. Yang, sp. nov.**
Index Fungorum: IF901029
Fig. 2

Etymology. Referring to the long stipe of stromata.

Type. *Holotype*: China, Yunnan Province, Ruili City, 26°1.07'N, 97°51.33'E, alt. 1140 m, on a termite buried in soil, 2 July 2022, Tao Yang (holotype HKAS 126185, ex-type culture KUNCC 5224). Ex-type sequences (ITS: OR015962, nrLSU: OR015967, nrSSU: OR082949, *tef-1α*: OR030530, *rpb1*: OR062224, *rpb2*: OR113082).

Description. Stromata arising from the back of termites buried in soil, solitary, unbranched, cylindrical, flexible, leathery, 17–24 cm long, 0.5–1.0 mm wide, grayish white to yellowish brown. Fertile parts cylindrical, yellowish brown, 3–5.5 cm long, generating toward the upper part of stromata, covered by a spinous surface, with a sterile tip of 11–28 × 0.5–1.0 mm. Perithecia superficial, pale yellow at early stage, brown at maturity, pyramidal to oval, densely distributed in the upper of stromata, arranged in a disordered manner, 390–420 × 295–350 µm. Asci 8-spored, filiform, hyaline, 160–195 × 4.5–6.5 µm, with hemispheric apical cap. Ascospores whole, hyaline, filiform, tapering at both ends, 70–85 × 3.5–4.5 µm, multiseptate, septa 4.5–13.8 µm long.

Anamorph. hirsutella-like. Colonies on PDA growing very slowly, reaching 3–3.5 cm diam after six weeks at 25 °C, felty, irregularly convex, cream, reverse pale brown to dark brown. Hyphae hyaline, branched, septate, smooth-walled, 2–3 µm wide. Conidiogenous cells arising from aerial mycelia, monophialidic or rarely polyphialidic, on hyphae laterally or terminally, hyaline, smooth, flask-shaped, 29–60 µm long, with a swollen base, 4–4.5 µm wide, tapering sharply into a thin neck, 0.5–0.8 µm wide. Conidia borne directly on the tip of phialides, hyaline, one-celled, solitary, smooth-walled, citriform or oval, 7–10 × 4.5–7 µm, with a mucous sheath.

Additional specimens examined. China, Yunnan Province, Ruili City, 26°1.07'N, 97°51.33'E, alt. 1140 m, on a termite buried in soil, 2 July 2022, Tao Yang (HKAS 126186), sequences (ITS: OR015960, nrLSU: OR015966, nrSSU: OR082947, *tef-1α*: OR030531, *rpb1*: OR062225). *Ibid.*, (HKAS 126187), sequences (ITS: OR015961, nrLSU: OR015965, nrSSU: OR082948, *tef-1α*: OR030529, *rpb1*: OR062223).

Habitat and ecology. Parasitic on termites buried in soil of the subtropical evergreen broad-leaved forests, emerging from fallen leaves on the forest floor.

Known distribution. Ruili City, Yunnan Province, China.

Notes. *Ophiocordyceps longistipes* is characterized by solitary stromata, superficial and pyramidal to oval perithecia, filiform asci, and filiform ascospores, hirsutella-like anamorph with monophialidic or rarely polyphialidic, flask-shaped conidiogenous cells, and citriform or oval conidia embedded in a mucous sheath. Phylogenetically, all specimens of *O. longistipes* are clustered in the *H. thompsonii* subclade of *Hirsutella* lineages and form a monophyletic clade, which is placed sister to *O. fusiformis* with maximum support (Fig. 1). However, *O. longistipes* exhibits significant morphological differences from *O. fusiformis* in its both teleomorph and anamorph. For the teleomorph, *O. longistipes* produce longer stromata of 17–24 cm (up to 6 cm

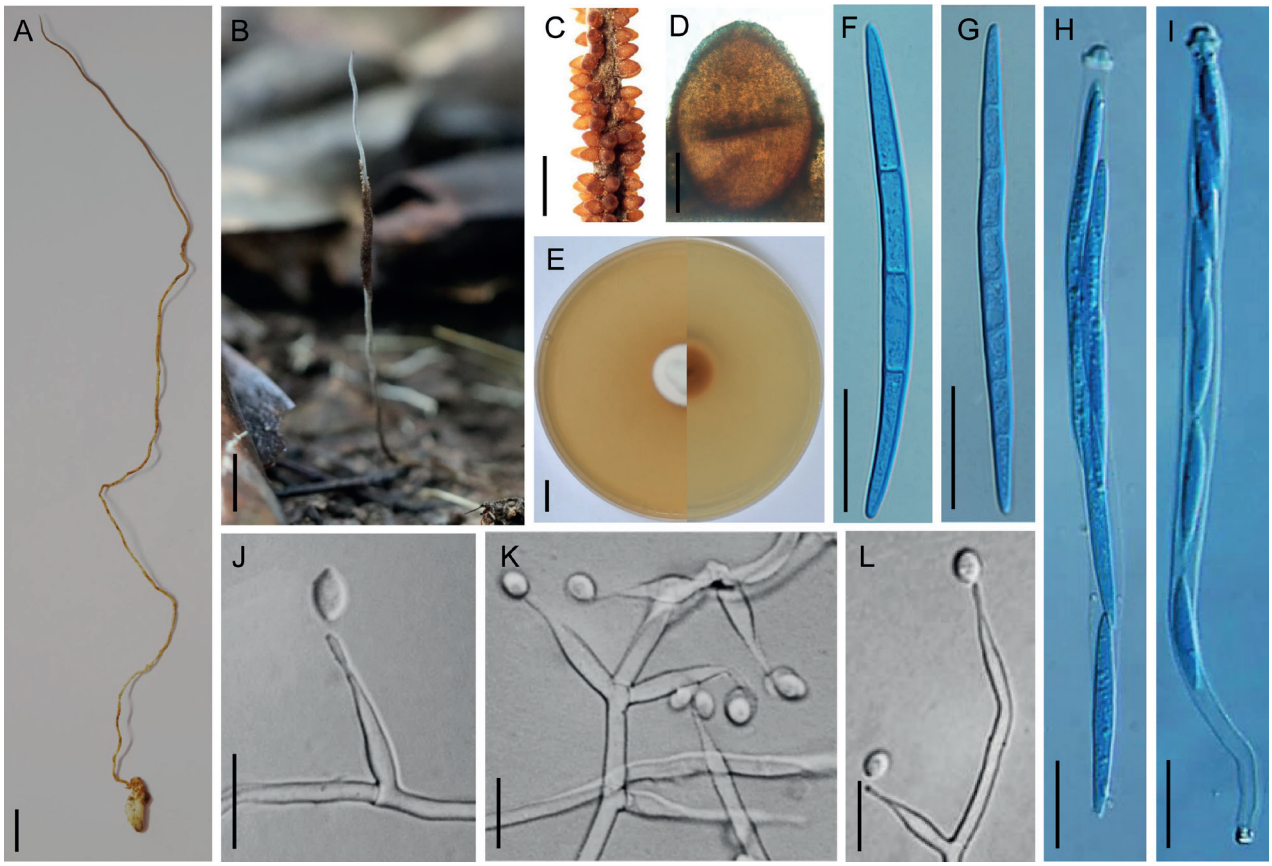

Figure 2. *Ophiocordyceps longistipes* **A, B** stromata of fungus arising from termites **C** fertile part **D** perithecia **E** colony on PDA (obverse and reverse) **F, G** ascospores **H, I** asci **J–L** conidiogenous cells and conidia. Scale bars: 1 cm (**A, B, E**); 2 mm (**C**); 100 μm (**D**); 20 μm (**F–L**).

long for *O. fusiformis*), larger perithecia of 390–420 × 295–350 μm (300–360 × 180–270 μm for *O. fusiformis*). For the anamorph, *O. longistipes* possess both monophialidic and polyphialidic conidiogenous cells, but *O. fusiformis* is only monophialidic. Moreover, *O. longistipes* produces oval conidia, while *O. fusiformis* produces narrower fusiform conidia (Table 3).

Ophiocordyceps globiperitheciata **Y.B. Wang, T. Yang, Q. Fan & Zhu L. Yang, sp. nov.**

Index Fungorum: IF901030

Fig. 3

Etymology. Referring to the shape of perithecia, with "*globi*" meaning globose.

Type. *Holotype*: China, Yunnan Province, Jinghong City, Puwen Town, 22°26.35'N, 101°1.32'E, alt. 970 m, on a termite buried in soil, 28 Sep. 2022, Tao Yang (HKAS 126130). Holotype sequences (ITS: OR015963, nrLSU: OR015968, nrSSU: OR082950, *tef-1α*: OR030532, *rpb1*: OR119834).

Description. Stromata arising from the termite buried in soil, multiple (2–5), clavate, unbranched, flexible, leathery, 8–15 cm long, 1–1.5 mm wide, tapering from base to tip, base brown, tip gray. Fertile parts cylindrical, pale brown, generating toward the upper part of stromata, covered by a spinous surface, with a sterile

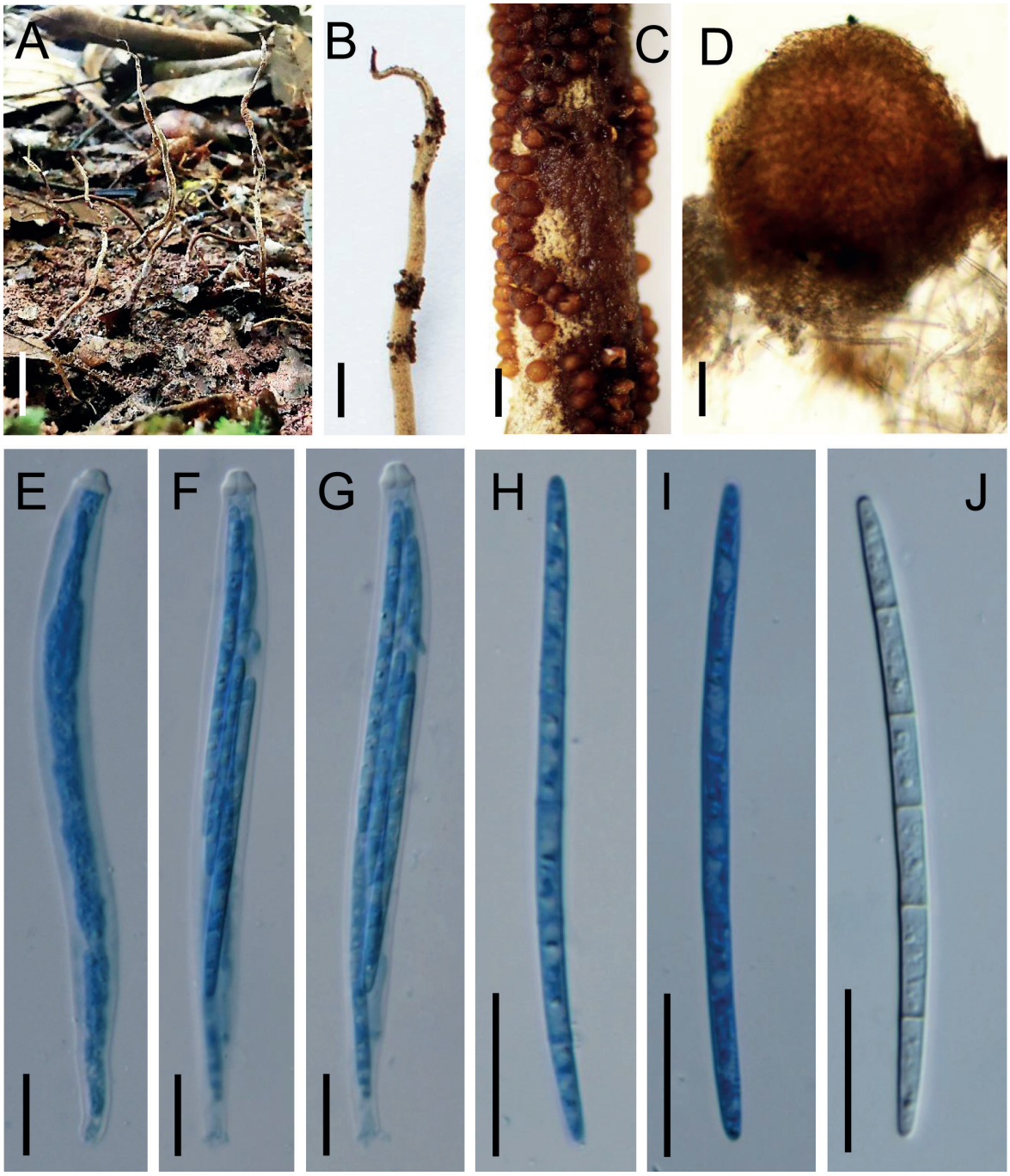

Figure 3. *Ophiocordyceps globiperitheciata* **A** stromata of fungus arising from termites **B** sterile tip and fertile part **C** fertile part **D** perithecia **E–G** asci **H–J** ascospores. Scale bars: 1 cm (**A**); 2 mm (**B**); 500 µm (**C**); 50 µm (**D**); 20 µm (**E–J**).

tip. Perithecia superficial, pale brown to brown, subglobose, aggregating loosely at the upper of stromata, arranged in a disordered manner, 240–295 × 215–280 µm. Asci 8-spored, filiform, hyaline, 135–170 × 8.5–13.5 µm, with a hemispheric apical cap. Ascospores whole, hyaline, tapering at both ends, filiform, 85–110 × 3.5–4.5 µm, multiseptate, septa 11–14.5 µm long. Anamorph not detected.

Additional specimens examined. China, Yunnan Province, Jinghong City, Puwen Town, 22°26.35'N, 101°1.32'E, alt. 970 m, on a termite buried in soil, 28 Sep. 2022, Tao Yang (HKAS 126131). Sequences (ITS: OR015964, nrLSU: OR015969, nrSSU: OR082951, *tef-1α*: OR030533, *rpb1*: OR119835).

Table 3. Morphological comparison between *Ophiocordyceps* species parasitic on termites.

Species	Host	Stromata (cm)	Perithecia (μm)	Asci (μm)	Ascospore (μm)	Conidiogenous cells (μm)	Conidia (μm)	Reference
O. asiatica	Termites	Solitary, simple, filiform, orange brown, up to 15 long	Superficial, globose to subglobose, 240–320 × 180–260	Filiform, 92.5–175 × 5–6.3	Filiform, septate, whole, 80–132.5 × 1–2	Monophialidic or rarely polyphialidic, 15–20 × 2–3	Fusiform, 7–9 × 2–3	(Tasanathai et al. 2019)
O. bispora	Termites	Multiple (20–30), simple or branched, clavate	Immersed, globose, 300–375 × 375	Clavate, 162–163 × 58–61	Elliptical closely appressed, septate, 95–105 × 34–35.4			(Blackwell and Gilbertson 1984; Ochiel et al. 1997)
O. brunneirubra	Termites	Solitary, simple or branched, narrowly clavate, orange brown to red brown, 9.5 long	Immersed, ovoid, 300–400 × 130–200	Cylindrical, 155–225 × 4.5–8	Filiform, septate, whole, 156.5–197.5 × 2–3	Monophialidic, 32–50 × 2–3	Fusiform, 12–17 × 2–4	(Tasanathai et al. 2019)
O. communis	Termites	Solitary, simple, filiform, base whitish-grey, upper part yellow-brown, 5–13 long	Superficial, 285–675 × 195–390	Filiform, 215–250 × 15	Filiform, septate, whole, 100–180 × 5–6	Monophialidic or rarely polyphialidic, 10–14 × 2.7–3.3	Almond-shaped, 7–9 × 2.5–3	(Sung et al. 2007a)
O. fusiformis	Termite	Solitary, simple, cylindrical, brown, up to 6 long	Superficial, ovoid, 300–360 × 180–270	Cylindrical, 141–227 × 7–15	Cylindrical, septate, whole, 36–78 × 5–6.5	Monophialidic, 9–24 × 2–4	Fusiform, 6–18 × 2–4	(Tasanathai et al. 2022)
O. globosa	Termites	Solitary, simple, cylindrical, brown, up to 8 long	Pseudo-immersed, ovoid, 190–245 × 120–190	Filiform, 100–157 × 7–13	Filiform, septate, whole, 58–118 × 2–3	Monophialidic or polyphialidic, 9–15 × 3–5	Globose, 2–4	(Tasanathai et al. 2022)
O. globiperitheciata	**Termites**	**Multiple (2–5), unbifurcated, clavate, base brown, tip gray, 8–15 long**	**Superficial, subglobose, 240–295 × 215–280**	**Filiform, 135–170 × 8.5–13.5**	**Filiform, septate, whole, 85–110 × 3.5–4.5**			**This study**
O. isopterae	Termites	Solitary, simple, cylindrical, brown, up to 10 long	Superficial, ovoid, 270–320 × 140–180	Filiform, 81–137 × 5–9	Filiform, septate, whole, 55–78 × 2–2.5	Monophialidic, 14–28 × 2–4	Fusiform, 6–11 × 1.5–3	(Tasanathai et al. 2022)
O. khokpasiensis	Termites	Solitary, simple, cylindrical, brown, 16 long	Pseudo-immersed, subglobose, 200–250 × 120–200	Filiform, 62.5–125 × 4–5	Filiform, whole, 46–90 × 2–3	Monophialidic or polyphialidic, 15–28 × 3–5	Globose to oval, 4–6 × 2.5–4	(Khonsanit et al. 2019)
O. koningsbergeri	Termites	Solitary, filiform, gray-white, 8–10 long	Immersed, 450 × 90	Cylindrica, 180–200 × 4–5	Filiform, whole, 150 × 1			(Penzig and Saccardo 1904)
O. longistipes	**Termites**	**Solitary, unbifurcated, cylindrical, grayish white to yellowish brown, 17–24 long**	**Superficial, pyramidal to oval, 390–420 × 295–350**	**Filiform, 160–195 × 4.5–6.5**	**Filiform, septate, whole, 70–85 × 3.5–4.5**	**Monophialidic or rarely polyphialidic, on hyphae laterally or terminally, 29–60 long, with a swollen base, 4–4.5 wide, tapering sharply into a thin neck, 0.5–0.8 wide.**	**Citriform or oval, 7–10 × 4.5–7**	**This study**
O. mosingtoensis	Termites	Solitary, simple, cylindrical, brown to grey, 11 long	Pseudo-immersed, ovoid, 400–500 × 200–300	Filiform, 187.5–287.5 × 4.5–7.5	Filiform, septate, whole, 230–315 × 1.5–3	Monophialidic, 10–17 × 2–3	Oval, 3–5 × 2–3	(Tasanathai et al. 2019)
O. octospora	Termites	Multiple, clavate, white to pale tan, 0.2–0.3 long	Immersed, subglobose to ovoid, 180–220 × 200	Clavate, about 250 × 60	Cylindrical, septate, 40–70 × 15–30			(Blackwell and Gilbertson 1981)
O. ovatospora	Termites	Solitary, simple, cylindrical or clavate, light-yellow, up to 13 long	Pseudo-immersed, ovoid to pyriform, 110–140 × 80–110	Filiform, 110–125 × 5–7	Filiform, septate, whole, 110–130 × 1–2	Monophialidic or rarely polyphialidic, 15–35 × 3–6	Oval, 3–5 × 3–4	(Tang et al. 2022)
O. pseudocommunis	Termites	Solitary, simple, cylindrical, brown, 21 long	Superficial, Subglobose, 520–600 × 360–440	Filiform, 160–165 × 14–17	Filiform,septate, whole, 107.5–147.5 × 6–7.5	Arising from hyphae laterally or terminally	Fusiform, septate (2–3), 13–27 × 3–5	(Tasanathai et al. 2019)

Species	Host	Stromata (cm)	Perithecia (μm)	Asci (μm)	Ascospore (μm)	Conidiogenous cells (μm)	Conidia (μm)	Reference
O. pseudorhizoidea	Termites	Solitary, simple, filiform, light brown, up to 21 long	Superficial, ovoid, 280–390 × 160–220	Cylindrical, 120–150 × 5–7	Filiform, whole, 65–82.5 × 2–3	Monophialidic, 9–21 × 2–4	Fusiform, 5–10 × 1–2	(Tasanathai et al. 2019)
O. puluongensis	Termites	Solitary, simple or branched, filiform, pale orange to red brown, 7.1–13.3 long	Superficial, subglobose, 181.8–251.0 × 123.7–205.4	Fliform, 74.3–138.5 × 4.6–6.5	Filiform, septate, whole, 67.0–124.5 × 1.5–2.5	Monophialidic or rarely polyphialidic, 7.9–21.2 × 1.7–5.0	Fusiform or citriform, 2.8–6.1 × 1.9–3.4	(Xu et al. 2022)
O. radiciformis	Termites	Solitary, simple, cylindrical, brown, up to 11 long	Superficial, ovoid, 330–460 × 200–320	Cylindrical, 140–296 × 6–10	Filiform septate, whole, 154–215 × 2–3	6–15 × 2–5	Fusiform, 5–7 × 2–3	(Tasanathai et al. 2022)
O. termiticola	Termites	Solitary, simple, filiform, yellow brown, up to 14 long	Pseudo-immersed, globose to subglobose, 200–280 × 150–250	Filiform 62.5–110 × 4–6	Filiform, whole, 85 × 2	Monophialidic to polyphialidic, 7–11 × 2.5–4	Globose, 2.5–3.5	(Tasanathai et al. 2019)

Habitat and ecology. Parasitic on termites buried in soil of tropical evergreen broad-leaved forests, emerging from fallen leaves on the forest floor.

Known distribution. Puwen Town, Jinghong City, Yunnan Province, China.

Notes. *Ophiocordyceps globiperitheciata* is characterized by multiple and unbranched stromata, superficial and subglobose perithecia, and filiform asci and ascospores. Phylogenetically, *O. globiperitheciata* forms a separate clade from other *Ophiocordyceps* species in the *H. thompsonii* subclade with moderate bootstrap support (Fig. 1). It is closed to *H. cryptosclerotium* Fern. et al. and *O. communis* Hywel-Jones & Samson. However, it differs from *H. cryptosclerotium* in parasitizing Blattodea (*H. cryptosclerotium* parasitic on Hemiptera), producing multiple clavate stromata (*H. cryptosclerotium* stroma absence). *Ophiocordyceps globiperitheciata* is distinguished from *O. communis* by multiple and thicker stromata, shorter asci of 135–170 μm (215–250 μm for *O. communis*) and ascospores of 85–110 μm (100–180 μm for *O. communis*) (Table 3).

Key to species of *Ophiocordyceps* parasitic on termites

1 Stromata multiple **2**
– Stromata solitary **4**
2 Perithecia superficial ..... ***O. globiperitheciata***
– Perithecia immersed **3**
3 Perithecia subglobose to ovoid ..... ***O. octospora***
– Perithecia globose ..... ***O. bispora***
4 Perithecia nonsuperficial **5**
– Perithecia superficial **11**
5 Perithecia immersed **6**
– Perithecia pseudo-immersed **7**
6 Stromata orange brown to red brown ..... ***O. brunneirubra***
– Stromata gray-white ..... ***O. koningsbergeri***
7 Only monophialidic ..... ***O. mosingtoensis***
– Possessing polyphialidic **8**
8 Large asci (100–160 μm long) ..... ***O. globosa***
– Small asci (60–130 μm long) **9**
9 Large ascospores (> 100 μm long) ..... ***O. ovatospora***
– Small ascospores (< 100 μm long) **10**

10 Conidia globose ..... ***O. termiticola***
– Conidia globose to oval ..... ***O. khokpasiensis***
11 Stromata sometimes branched ..... ***O. puluongensis***
– Stromata unbranched **12**
12 Long stromata (≥ 15 cm long) **13**
– Short stromata (< 15 cm long) **16**
13 Conidia have septa ..... ***O. pseudocommunis***
– Conidia have no septa **14**
14 Short stromata (< 16 cm long) ..... ***O. asiatica***
– Long stromata (> 16 cm long) **15**
15 Long conidiogenous cells (> 25 µm long) ..... ***O. longistipes***
– Short conidiogenous cells (< 25 µm long) ..... ***O. pseudorhizoidea***
16 Conidia almond-shaped ..... ***O. communis***
– Conidia fusiform **17**
17 Short asci (< 140 µm long) ..... ***O. isopterae***
– Long asci (≥ 140 µm long) **18**
18 Long stromata (> 6 cm long) ..... ***O. radiciformis***
– Short stromata (≤6 cm long) ..... ***O. fusiformis***

Discussion

Thus far, only 17 species of *Ophiocordyceps* parasitic on termites were described, mainly clustered in the *H. thompsonii* subclade (Tasanathai et al. 2019; Tasanathai et al. 2022). These species are: *O. asiatica* Tasanathai et al., *O. bispora* (Stifler) G.H. Sung et al., *O. brunneirubra* Tasanathai et al., *O. communis* Hywel-Jones & Samson, *O. fusiformis* Tasanathai et al., *O. globosa* Tasanathai et al., *O. isopterae* Tasanathai et al., *O. khokpasiensis* Tasanathai et al., *O. koningsbergeri* (Penz. & Sacc.) G.H. Sung et al., *O. mosingtoensis* Tasanathai et al., *O. octospora* (M. Blackw. & Gilb.) G.H. Sung et al., *O. ovatospora* H. Yu et al., *O. pseudocommunis* Tasanathai et al., *O. pseudorhizoidea* Tasanathai et al., *O. puluongensis* H. Yu et al., *O. radiciformis* Tasanathai et al., and *O. termiticola* Tasanathai et al. Most the termite-pathogenic *Ophiocordyceps* species are found in tropical and subtropical regions, which may be related to the higher diversity of both *Ophiocordyceps* fungi and their termite hosts in these climatic zones (Sung et al. 2007a; Tasanathai et al. 2019; Cerezer et al. 2020; Araújo et al. 2021; Wilson et al. 2021; Tang et al. 2022; Tasanathai et al. 2022; Xu et al. 2022).

Phylogenetically, almost all *Ophiocordyceps* species parasitic on termites are placed in the *H. thompsonii* subclade, except for *O. brunneirubra*. Termite-pathogenic species exhibit significant morphological variation overall. Among these species, the length of stromata ranges from extremely short to very long, the existence pattern of perithecia from superficial to pseudo-immersed to immersed, and the size of perithecia ranges from about 100 to 600 µm (Tasanathai et al. 2019; Araújo et al. 2021; Tasanathai et al. 2022; Xu et al. 2022). However, some of these species exhibit minimal interspecific morphological variation, making it challenging to distinguish them only through morphological studies. Therefore, the use of molecular systematics is necessary to accurately identify these species. For example, *O. asiatica* and *O. puluongensis*, as well as *O. khokpasiensis* and *O. termiticola*, share similar morphological char-

acteristics. *Ophiocordyceps asiatica* and *O. puluongensis* produce subglobose superficial perithecia, similar asci, ascospores, conidiogenous cells, and conidia (Tasanathai et al. 2019; Xu et al. 2022). *Ophiocordyceps khokpasiensis* and *O. termiticola* possess similar colored and shaped stromata, pseudo-immersed perithecia, and similar asci, ascospores, and conidiogenous cells (Tasanathai et al. 2019). Although these species are morphologically indistinguishable, phylogenetic analyses support them as separate taxa.

It's worth noting that the hosts of these termite-pathogenic *Ophiocordyceps* species are usually buried underground, typically 5 to 15 cm below the ground, which may be relevant to the subterranean living habits of the host termites (Martelossi et al. 2023). However, this can pose a challenge for species identification, as hosts are often lost due to separation from fragile stromata during excavation (Tasanathai et al. 2022).

Termites are notorious pests known for damaging wood, cultivated plants, buildings, pastures, forests, and even non-cellulosic materials like cables, causing annual economic losses amounting to tens of billions of dollars. Subterranean termites are responsible for about 80% of the total damage (Rust and Su 2012; Scharf 2015; Oi 2022). Therefore, the control of termites has become the focus of attention in various industries. Previously, many chlorinated hydrocarbon insecticides were used for termite control, but they were banned due to their irreversible environmental impact and negative effects on crop production. Consequently, environmentally friendly and sustainable control measures for termites are urgently needed. Entomopathogenic fungi may represent a potent solution (Afzal et al. 2019; Tasanathai et al. 2019; Oi 2022; Moon et al. 2023). These fungi, with strong infectivity, can continuously spread spores in the field to control pests and are considered environmentally non-polluting, so they have significant advantages in pest control (Shimazu et al. 1995; Meyling and Eilenberg 2007). Most members of *H. thompsonii* subclade have been found to obligately parasitize termites, they may have a regulatory effect on natural termite populations. Particularly, *O. bispora*, for which field investigations have revealed a high infection rate against termites, and laboratory experiments have also shown that it can effectively kill termites (Blackwell and Gilbertson 1984; Suh et al. 1998). Although laboratory experiments have not been conducted with *O. longistipes*, field observations have found that termites infected by this fungus often appear in groups. This may indicate that it has strong lethality against termites and possesses the potential to become a biological control agent for termites.

Acknowledgements

The authors gratefully acknowledge Mr. Maolin Yan, Mr. Shouhua Cun, Mr. Haijun Yin, and Ms. Zhaolin Yang of the Tongbiguan Provincial Nature Reserve in Yunnan for their invaluable assistance and support during the sample collection process.

Additional information

Conflict of interest

The authors have declared that no competing interests exist.

Ethical statement

No ethical statement was reported.

Funding

This work was financially supported by the Science and Technology Planning Project of Yunnan Province (202207AB110016, 202001BA070001-078), the High Level Talent Introduction Plan, Kunming Institute of Botany, CAS (E16N61), and the Innovation Project of Guangxi Graduate Education (YCBZ2022028).

Author contributions

All authors contributed to the study conception and design. Material preparation, data collection and analysis were performed by Xue-Mei Wang, He-Fa Liao, Qi Fan and Tao Yang. The first draft of the manuscript was written by Qi Fan and Tao Yang. Pei-Hong Shen, Zhu-Liang Yang, Wen-Bo Zeng, and Yuan-Bing Wang reviewed and revised the manuscript. All authors commented on previous versions of the manuscript.

Author ORCIDs

Qi Fan https://orcid.org/0000-0003-3168-0347
Tao Yang https://orcid.org/0009-0000-8579-1574
Hui Li https://orcid.org/0000-0003-4255-8312
Xue-Mei Wang https://orcid.org/0009-0001-0171-4924
He-Fa Liao https://orcid.org/0009-0006-7287-1384
Pei-Hong Shen https://orcid.org/0000-0003-0980-9562
Zhu-Liang Yang https://orcid.org/0000-0001-9745-8453
Wen-Bo Zeng https://orcid.org/0009-0000-0251-5890
Yuan-Bing Wang https://orcid.org/0000-0002-3305-9418

Data availability

All of the data that support the findings of this study are available in the main text.

References

Afzal M, Farman M, Rasib KZ, Qureshi NA (2019) Biocidal action of silver oak (*Grevillea robusta*) leaf extract on the termite *Heterotermes indicola* wasmann (Blattodea: Rhinotermitidae). International Biodeterioration & Biodegradation 139: 1–10. https://doi.org/10.1016/j.ibiod.2019.02.001

Araújo JPM, Hughes DP (2016) Diversity of entomopathogenic fungi: Which groups conquered the insect body? Advances in Genetics 94: 1–39. https://doi.org/10.1016/bs.adgen.2016.01.001

Araújo JPM, Evans HC, Kepler R, Hughes DP (2018) Zombie-ant fungi across continents: 15 new species and new combinations within *Ophiocordyceps*. I. Myrmecophilous hirsutelloidÂ species. Studies in Mycology 90(1): 119–160. https://doi.org/10.1016/j.simyco.2017.12.002

Araújo JPM, Moriguchi MG, Uchiyama S, Kinjo N, Matsuura Y (2021) *Ophiocordyceps salganeicola*, a parasite of social cockroaches in Japan and insights into the evolution of other closely-related Blattodea-associated lineages. IMA Fungus 12(1): 1–17. https://doi.org/10.1186/s43008-020-00053-9

Ban S, Sakane T, Nakagiri A (2015) Three new species of *Ophiocordyceps* and overview of anamorph types in the genus and the family Ophiocordyceptaceae. Mycological Progress 14(1): 1–12. https://doi.org/10.1007/s11557-014-1017-8

Bischoff JF, Rehner SA, Humber RA (2006) *Metarhizium frgidum* sp. nov.: A cryptic species of *M. anisopliae* and a member of the *M. flavoviride* complex. Mycologia 98(5): 737–745. https://doi.org/10.1080/15572536.2006.11832645

Blackwell M, Gilbertson RL (1981) *Cordycepioideus octosporus*, a termite suspected pathogen from Jalisco, Mexico. Mycologia 73(2): 358–362. https://doi.org/10.1080/00275514.1981.12021355

Blackwell M, Gilbertson RL (1984) New information on *Cordycepioideus bisporus* and *Cordycepioideus octosporus*. Mycologia 76(4): 763–765. https://doi.org/10.1080/00275514.1984.12023912

Bronstein JL (2009) The evolution of facilitation and mutualism. Journal of Ecology 97(6): 1160–1170. https://doi.org/10.1111/j.1365-2745.2009.01566.x

Cerezer FO, de Azevedo RA, Nascimento MAS, Franklin E, de Morais JW, de Sales Dambros C (2020) Latitudinal gradient of termite diversity indicates higher diversification and narrower thermal niches in the tropics. Global Ecology and Biogeography 29(11): 1967–1977. https://doi.org/10.1111/geb.13167

Chernomor O, Von Haeseler A, Minh BQ (2016) Terrace aware data structure for phylogenomic inference from supermatrices. Systematic Biology 65(6): 997–1008. https://doi.org/10.1093/sysbio/syw037

Da Costa RR, Vreeburg SME, Shik JZ, Aanen DK, Poulsen M (2019) Can interaction specificity in the fungus-farming termite symbiosis be explained by nutritional requirements of the fungal crop? Fungal Ecology 38: 54–61. https://doi.org/10.1016/j.funeco.2018.08.009

Evans HC (1974) Natural control of arthropods, with special reference to ants (Formicidae), by fungi in the tropical high forest of Ghana. Journal of Applied Ecology 11(1): 37–49. https://doi.org/10.2307/2402003

Evans HC, Araújo JPM, Halfeld VR, Hughes DP (2018) Epitypification and re-description of the zombie-ant fungus, *Ophiocordyceps unilateralis* (Ophiocordycipitaceae). Fungal Systematics and Evolution 1(1): 13–22. https://doi.org/10.3114/fuse.2018.01.02

Haelewaters D, Kasson MT (2020) Animal-associated fungi. Mycologia 112(6): 1045–1047. https://doi.org/10.1080/00275514.2020.1841469

Hoang DT, Chernomor O, Von Haeseler A, Minh BQ, Vinh LS (2018) UFBoot2: Improving the ultrafast bootstrap approximation. Molecular Biology and Evolution 35(2): 518–522. https://doi.org/10.1093/molbev/msx281

Hopple JS (1994) Phylogenetic investigations in the genus *Coprinus* based on morphological and molecular characters. PhD dissertation, Duke University.

Johnson D, Sung GH, Hywel-Jones NL, Luangsa-ard JJ, Bischoff JF, Kepler RM, Spatafora JW (2009) Systematics and evolution of the genus *Torrubiella* (Hypocreales, Ascomycota). Mycological Research 113(3): 279–289. https://doi.org/10.1016/j.mycres.2008.09.008

Kalyaanamoorthy S, Bui Quang M, Wong TKF, von Haeseler A, Jermiin LS (2017) ModelFinder: Fast model selection for accurate phylogenetic estimates. Nature Methods 14(6): 587–589. https://doi.org/10.1038/nmeth.4285

Katoh K, Standley DM (2013) MAFFT multiple sequence alignment software version 7: Improvements in performance and usability. Molecular Biology and Evolution 30(4): 772–780. https://doi.org/10.1093/molbev/mst010

Kepler RM, Kaitsu Y, Tanaka E, Shimano S, Spatafora JW (2011) *Ophiocordyceps pulvinata* sp. nov., a pathogen of ants with a reduced stroma. Mycoscience 52(1): 39–47. https://doi.org/10.1007/S10267-010-0072-5

Kepler RM, Sung GH, Ban S, Nakagiri A, Chen MJ, Huang B, Li Z, Spatafora JW (2012) New teleomorph combinations in the entomopathogenic genus *Metacordyceps*. Mycologia 104(1): 182–197. https://doi.org/10.3852/11-070

Khao-ngam S, Mongkolsamrit S, Rungjindamai N, Noisripoom W, Pooissarakul W, Duangthisan J, Himaman W, Luangsa-ard JJ (2021) *Ophiocordyceps asiana* and *Ophiocordyceps tessaratomidarum* (Ophiocordycipitaceae, Hypocreales), two new species on stink bugs from Thailand. Mycological Progress 20(3): 341–353. https://doi.org/10.1007/s11557-021-01684-x

Khonsanit A, Luangsa-ard JJ, Thanakitpipattana D, Kobmoo N, Piasai O (2019) Cryptic species within *Ophiocordyceps myrmecophila* complex on formicine ants from Thailand. Mycological Progress 18(1–2): 147–161. https://doi.org/10.1007/s11557-018-1412-7

Kumar S, Stecher G, Tamura K (2016) MEGA7: Molecular evolutionary genetics analysis version 7.0 for bigger datasets. Molecular Biology and Evolution 33(7): 1870–1874. https://doi.org/10.1093/molbev/msw054

Li GJ, Hyde KD, Zhao RL, Hongsanan S, Abdel-Aziz FA, Abdel-Wahab MA, Alvarado P, Alves-Silva G, Ammirati JF, Ariyawansa HA, Baghela A, Bahkali AH, Beug M, Bhat DJ, Bojantchev D, Boonpratuang T, Bulgakov TS, Camporesi E, Boro MC, Ceska O, Chakraborty D, Chen JJ, Chethana KWT, Chomnunti P, Consiglio G, Cui BK, Dai DQ, Dai YC, Daranagama DA, Das K, Dayarathne MC, De Crop E, De Oliveira RJV, Fragoso de Souza CA, de Souza JI, Dentinger BTM, Dissanayake AJ, Doilom M, Drechsler-Santos ER, Ghobad-Nejhad M, Gilmore SP, Goes-Neto A, Gorczak M, Haitjema CH, Hapuarachchi KK, Hashimoto A, He MQ, Henske JK, Hirayama K, Iribarren MJ, Jayasiri SC, Jayawardena RS, Jeon SJ, Jernimo GH, Jesus AL, Jones EBG, Kang JC, Karunarathna SC, Kirk PM, Konta S, Kuhnert E, Langer E, Lee HS, Lee HB, Li WJ, Li XH, Liimatainen K, Lima DX, Lin CG, Liu JK, Liu XZ, Liu ZY, Luangsa-ard JJ, Luecking R, Lumbsch HT, Lumyong S, Leano EM, Marano AV, Matsumura M, McKenzie EHC, Mongkolsamrit S, Mortimer PE, Thi Thuong Thuong N, Niskanen T, Norphanphoun C, O'Malley MA, Parnmen S, Pawlowska J, Perera RH, Phookamsak R, Phukhamsakda C, Pires-Zottarelli CLA, Raspe O, Reck MA, Rocha SCO, de Santiago ALCMA, Senanayake IC, Setti L, Shang QJ, Singh SK, Sir EB, Solomon KV, Song J, Srikitikulchai P, Stadler M, Suetrong S, Takahashi H, Takahashi T, Tanaka K, Tang LP, Thambugala KM, Thanakitpipattana D, Theodorou MK, Thongbai B, Thummarukcharoen T, Tian Q, Tibpromma S, Verbeken A, Vizzini A, Vlasak J, Voigt K, Wanasinghe DN, Wang Y, Weerakoon G, Wen HA, Wen TC, Wijayawardene NN, Wongkanoun S, Wrzosek M, Xiao YP, Xu JC, Yan JY, Yang J, Yang SD, Hu Y, Zhang JF, Zhao J, Zhou LW, Persoh D, Phillips AJL, Maharachchikumbura SSN (2016) Fungal diversity notes 253–366: Taxonomic and phylogenetic contributions to fungal taxa. Fungal Diversity 78(1): 1–237. https://doi.org/10.1007/s13225-016-0366-9

Luangsa-ard JJ, Ridkaew R, Mongkolsamrit S, Tasanathai K, Hywel-Jones NL (2010) *Ophiocordyceps barnesii* and its relationship to other melolonthid pathogens with dark stromata. Fungal Biology 114(9): 739–745. https://doi.org/10.1016/j.funbio.2010.06.007

Luangsa-ard JJ, Ridkaew R, Tasanathai K, Thanakitpipattana D, Hywel-Jones N (2011) *Ophiocordyceps halabalaensis*: A new species of *Ophiocordyceps* pathogenic to *Camponotus gigas* in Hala Bala Wildlife Sanctuary, Southern Thailand. Fungal Biology 115(7): 608–614. https://doi.org/10.1016/j.funbio.2011.03.002

Luangsa-ard JJ, Tasanathai K, Thanakitpipattana D, Khonsanit A, Stadler M (2018) Novel and interesting *Ophiocordyceps* spp. (Ophiocordycipitaceae, Hypocreales) with superficial perithecia from Thailand. Studies in Mycology 89(1): 125–142. https://doi.org/10.1016/j.simyco.2018.02.001

Martelossi J, Forni G, Iannello M, Savojardo C, Martelli PL, Casadio R, Mantovani B, Luchetti A, Rota-Stabelli O (2023) Wood feeding and social living: Draft genome of the subterranean termite *Reticulitermes lucifugus* (Blattodea; Termitoidae). Insect Molecular Biology 32(2): 118–131. https://doi.org/10.1111/imb.12818

Meyling NV, Eilenberg J (2007) Ecology of the entomopathogenic fungi *Beauveria bassiana* and *Metarhizium anisopliae* in temperate agroecosystems: Potential for conservation biological control. Biological Control 43(2): 145–155. https://doi.org/10.1016/j.biocontrol.2007.07.007

Mongkolsamrit S, Noisripoom W, Pumiputikul S, Boonlarppradab C, Samson RA, Stadler M, Becker K, Luangsa-ard JJ (2021) *Ophiocordyceps flavida* sp. nov. (Ophiocordycipitaceae), a new species from Thailand associated with *Pseudogibellula formicarum* (Cordycipitaceae), and their bioactive secondary metabolites. Mycological Progress 20(4): 477–492. https://doi.org/10.1007/s11557-021-01683-y

Mongkolsamrit S, Noisripoom W, Hasin S, Sinchu P, Jangsantear P, Luangsa-ard JJ (2023) Multi-gene phylogeny and morphology of *Ophiocordyceps laotii* sp. nov. and a new record of *O. buquetii* (Ophiocordycipitaceae, Hypocreales) on ants from Thailand. Mycological Progress 22(1): 1–5. https://doi.org/10.1007/s11557-022-01855-4

Moon JH, Ajuna HB, Won SJ, Choub V, Choi SI, Yun JY, Hwang WJ, Park SW, Ahn YS (2023) Entomopathogenic potential of *Bacillus velezensis* CE 100 for the biological control of termite damage in wooden architectural buildings of korean cultural heritage. International Journal of Molecular Sciences 24(9): e8189. https://doi.org/10.3390/ijms24098189

Nguyen LT, Schmidt HA, Von Haeseler A, Minh BQ (2015) IQ-TREE: A fast and effective stochastic algorithm for estimating maximum-likelihood phylogenies. Molecular Biology and Evolution 32(1): 268–274. https://doi.org/10.1093/molbev/msu300

Ochiel GS, Evans HC, Eilenberg J (1997) *Cordycepioideus*, a pathogen of termites in Kenya. The Mycologist 1(11): 7–9. https://doi.org/10.1016/S0269-915X(97)80059-6

Oi F (2022) A review of the evolution of termite control: A continuum of alternatives to termiticides in the United States with emphasis on efficacy testing requirements for product registration. Insects 13(1): 1–50. https://doi.org/10.3390/insects13010050

Pearce MJ (1997) Termites: Biology and Pest Management. CAB International, Wallingford, 172 pp. https://doi.org/10.1079/9780851991306.0000

Penzig O, Saccardo PA (1904) Icones Fungorum Javanicorum. Buchhandlung and Druckerei EJ Brill, Leiden, 55–57. https://doi.org/10.5962/bhl.title.17234

Petch T (1931) Notes on entomogenous fungi. Transactions of the British Mycological Society 16(1): 55–75. https://doi.org/10.1016/S0007-1536(31)80006-3

Quandt CA, Kepler RM, Gams W, Araújo JPM, Ban S, Evans HC, Hughes D, Humber R, Hywel-Jones N, Li Z, Luangsa-ard JJ, Rehner SA, Sanjuan T, Sato H, Shrestha B, Sung GH, Yao YJ, Zare R, Spatafora JW (2014) Phylogenetic-based nomenclatural proposals for Ophiocordycipitaceae (Hypocreales) with new combinations in *Tolypocladium*. IMA Fungus 5(1): 121–134. https://doi.org/10.5598/imafungus.2014.05.01.12

Rath AC (2000) The use of entomopathogenic fungi for control of termites. Biocontrol Science and Technology 10(5): 563–581. https://doi.org/10.1080/095831500750016370

Ronquist F, Teslenko M, Van Der Mark P, Ayres DL, Darling A, Höhna S, Larget B, Liu L, Suchard MA, Huelsenbeck JP (2012) MrBayes 3.2: Efficient Bayesian phylogenetic

inference and model choice across a large model space. Systematic Biology 61(3): 539–542. https://doi.org/10.1093/sysbio/sys029

Roper C, Castro C, Ingel B (2019) *Xylella fastidiosa*: Bacterial parasitism with hallmarks of commensalism. Current Opinion in Plant Biology 50: 140–147. https://doi.org/10.1016/j.pbi.2019.05.005

Rust MK, Su NY (2012) Managing social insects of urban importance. Annual Review of Entomology 57(1): 355–375. https://doi.org/10.1146/annurev-ento-120710-100634

Sanjuan TI, Franco-Molano AE, Kepler RM, Spatafora JW, Tabima J, Vasco-Palacios AM, Restrepo S (2015) Five new species of entomopathogenic fungi from the Amazon and evolution of neotropical *Ophiocordyceps*. Fungal Biology 119(10): 901–916. https://doi.org/10.1016/j.funbio.2015.06.010

Santamaria B, Verbeken A, Haelewaters D (2023) Mycophagy: A Global Review of Interactions between Invertebrates and Fungi. Journal of Fungi 9(2): e163. https://doi.org/10.3390/jof9020163

Scharf ME (2015) Termites as targets and models for biotechnology. Annual Review of Entomology 60(1): 77–102. https://doi.org/10.1146/annurev-ento-010814-020902

Schoch CL, Seifert KA, Huhndorf S, Robert V, Spouge JL, Levesque CA, Chen W, Bolchacova E, Voigt K, Crous PW, Miller AN, Wingfield MJ, Aime MC, An KD, Bai FY, Barreto RW, Begerow D, Bergeron MJ, Blackwell M, Boekhout T, Bogale M, Boonyuen N, Burgaz AR, Buyck B, Cai L, Cai Q, Cardinali G, Chaverri P, Coppins BJ, Crespo A, Cubas P, Cummings C, Damm U, de Beer ZW, de Hoog GS, Del-Prado R, Dentinger B, Dieguez-Uribeondo J, Divakar PK, Douglas B, Duenas M, Duong TA, Eberhardt U, Edwards JE, Elshahed MS, Fliegerova K, Furtado M, Garcia MA, Ge ZW, Griffith GW, Griffiths K, Groenewald JZ, Groenewald M, Grube M, Gryzenhout M, Guo LD, Hagen F, Hambleton S, Hamelin RC, Hansen K, Harrold P, Heller G, Herrera G, Hirayama K, Hirooka Y, Ho HM, Hoffmann K, Hofstetter V, Hognabba F, Hollingsworth PM, Hong SB, Hosaka K, Houbraken J, Hughes K, Huhtinen S, Hyde KD, James T, Johnson EM, Johnson JE, Johnston PR, Jones EB, Kelly LJ, Kirk PM, Knapp DG, Koljalg U, Kovacs GM, Kurtzman CP, Landvik S, Leavitt SD, Liggenstoffer AS, Liimatainen K, Lombard L, Luangsa-ard JJ, Lumbsch HT, Maganti H, Maharachchikumbura SS, Martin MP, May TW, McTaggart AR, Methven AS, Meyer W, Moncalvo JM, Mongkolsamrit S, Nagy LG, Nilsson RH, Niskanen T, Nyilasi I, Okada G, Okane I, Olariaga I, Otte J, Papp T, Park D, Petkovits T, Pino-Bodas R, Quaedvlieg W, Raja HA, Redecker D, Rintoul TL, Ruibal C, Sarmiento-Ramirez JM, Schmitt I, Schussler A, Shearer C, Sotome K, Stefani FOP, Stenroos S, Stielow B, Stockinger H, Suetrong S, Suh SO, Sung GH, Suzuki M, Tanaka K, Tedersoo L, Telleria MT, Tretter E, Untereiner WA, Urbina H, Vagvolgyi C, Vialle A, Vu TD, Walther G, Wang QM, Wang Y, Weir BS, Weiss M, White MM, Xu J, Yahr R, Yang ZL, Yurkov A, Zamora JC, Zhang N, Zhuang WY, Schindel D, Fungal Barcoding C (2012) Nuclear ribosomal internal transcribed spacer (ITS) region as a universal DNA barcode marker for Fungi. Proceedings of the National Academy of Sciences of the United States of America 109(16): 6241–6246. https://doi.org/10.1073/pnas.1117018109

Shimazu M, Tsuchiya D, Sato H, Kushida T (1995) Microbial control of *Monochamus alternatus* Hope (Coleoptera: Cerambycidae) by application of nonwoven fabric strips with *Beauveria bassiana* (Deuteromycotina: Hyphomycetes) on infested tree trunks. Applied Entomology and Zoology 30(1): 207–213. https://doi.org/10.1303/aez.30.207

Shrestha B, Tanaka E, Hyun MW, Han JG, Kim CS, Jo JW, Han SK, Oh J, Sung GH (2016) Coleopteran and lepidopteran hosts of the entomopathogenic genus *Cordyceps* sensu lato. Journal of Mycology 2016: 1–14. https://doi.org/10.1155/2016/7648219

Simmons DR, Kepler RM, Rehner SA, Groden E (2015) Phylogeny of *Hirsutella* species (Ophiocordycipitaceae) from the USA: Remedying the paucity of *Hirsutella* sequence data. IMA Fungus 6(2): 345–356. https://doi.org/10.5598/imafungus.2015.06.02.06

Spatafora JW, Sung GH, Sung JM, Hywel-Jones NL, White Jr JF (2007) Phylogenetic evidence for an animal pathogen origin of ergot and the grass endophytes. Molecular Ecology 16(8): 1701–1711. https://doi.org/10.1111/j.1365-294X.2007.03225.x

Spatafora JW, Quandt CA, Kepler RM, Sung GH, Shrestha B, Hywel-Jones NL, Luangsa-ard JJ (2015) New 1F1N species combinations in Ophiocordycipitaceae (Hypocreales). IMA Fungus 6(2): 357–362. https://doi.org/10.5598/imafungus.2015.06.02.07

Suh SO, Spatafora JW, Ochiel GRS, Evans HC, Blackwell M (1998) Molecular phylogenetic study of a termite pathogen *Cordycepioideus bisporus*. Mycologia 90(4): 611–617. https://doi.org/10.1080/00275514.1998.12026950

Sung GH, Hywel-Jones NL, Sung JM, Luangsa-ard JJ, Shrestha B, Spatafora JW (2007a) Phylogenetic classification of *Cordyceps* and the clavicipitaceous fungi. Studies in Mycology 57: 5–59. https://doi.org/10.3114/sim.2007.57.01

Sung GH, Sung JM, Hywel-Jones NL, Spatafora JW (2007b) A multi-gene phylogeny of Clavicipitaceae (Ascomycota, Fungi): Identification of localized incongruence using a combinational bootstrap approach. Molecular Phylogenetics and Evolution 44(3): 1204–1223. https://doi.org/10.1016/j.ympev.2007.03.011

Tang DX, Zhu JY, Luo LY, Hou DH, Wang ZQ, Yang SD, Yu H (2022) *Ophiocordyceps ovatospora* sp. nov. (Ophiocordycipitaceae, Hypocreales), pathogenic on termites from China. Phytotaxa 574(1): 105–117. https://doi.org/10.11646/phytotaxa.574.1.8

Tang DX, Huang O, Zou WQ, Wang YB, Wang Y, Dong QY, Sun T, Yang G, Yu H (2023a) Six new species of zombie-ant fungi from Yunnan in China. IMA Fungus 14(1): 1–9. https://doi.org/10.1186/s43008-023-00114-9

Tang DX, Xu ZH, Wang Y, Wang YB, Tran NL, Yu H (2023b) Multigene phylogeny and morphology reveal two novel zombie-ant fungi in *Ophiocordyceps* (Ophiocordycipitaceae, Hypocreales). Mycological Progress 22(4): 1–22. https://doi.org/10.1007/s11557-023-01874-9

Tasanathai K, Noisripoom W, Chaitika T, Khonsanit A, Hasin S, Luangsa-ard JJ (2019) Phylogenetic and morphological classification of *Ophiocordyceps* species on termites from Thailand. MycoKeys 56: 101–129. https://doi.org/10.3897/mycokeys.56.37636

Tasanathai K, Thanakitpipattana D, Himaman W, Phommavong K, Dengkhhamounh N, Luangsa-ard JJ (2020) Three new *Ophiocordyceps* species in the *Ophiocordyceps pseudoacicularis* species complex on Lepidoptera larvae in Southeast Asia. Mycological Progress 19(10): 1043–1056. https://doi.org/10.1007/s11557-020-01611-6

Tasanathai K, Khonsanit A, Noisripoom W, Kobmoo N, Luangsa-ard JJ (2022) Hidden species behind *Ophiocordyceps* (Ophiocordycipitaceae, Hypocreales) on termites: Four new species from Thailand. Mycological Progress 21(10): 86–102. https://doi.org/10.1007/s11557-022-01837-6

Vilgalys R, Hester M (1990) Rapid genetic identification and mapping of enzymatically amplified ribosomal DNA from several *Cryptococcus* species. Journal of Bacteriology 172(8): 4238–4246. https://doi.org/10.1128/jb.172.8.4238-4246.1990

Wang L, Li HH, Chen YQ, Zhang WM, Qu LH (2014) *Polycephalomyces lianzhouensis* sp. nov., a new species, co-occurs with *Ophiocordyceps crinalis*. Mycological Progress 13(4): 1089–1096. https://doi.org/10.1007/s11557-014-0996-9

Wang YB, Yu H, Dai YD, Wu CK, Zeng WB, Yuan F, Liang ZQ (2015) *Polycephalomyces agaricus*, a new hyperparasite of *Ophiocordyceps* sp. infecting melolonthid larvae

in southwestern China. Mycological Progress 14(9): 1–70. https://doi.org/10.1007/s11557-015-1090-7

Wang YB, Thi Tra N, Dai YD, Yu H, Zeng WB, Wu CK (2018) Molecular phylogeny and morphology of *Ophiocordyceps unituberculata* sp. nov. (Ophiocordycipitaceae), a pathogen of caterpillars (Noctuidae, Lepidoptera) from Yunnan, China. Mycological Progress 17(6): 745–753. https://doi.org/10.1007/s11557-017-1370-5

Wang YB, Wang Y, Fan Q, Duan DE, Zhang GD, Dai RQ, Dai YD, Zeng WB, Chen ZH, Li DD, Tang DX, Xu ZH, Sun T, Nguyen TT, Tran NL, Dao VM, Zhang CM, Huang LD, Liu YJ, Zhang XM, Yang DR, Sanjuan T, Liu XZ, Yang ZL, Yu H (2020) Multigene phylogeny of the family Cordycipitaceae (Hypocreales): New taxa and the new systematic position of the Chinese cordycipitoid fungus *Paecilomyces hepiali*. Fungal Diversity 103(1): 1–46. https://doi.org/10.1007/s13225-020-00457-3

Wang Y, Dai YD, Yang ZL, Guo R, Wang YB, Yang ZL, Ding L, Yu H (2021a) Morphological and molecular phylogenetic data of the Chinese medicinal fungus *Cordyceps liangshanensis* reveal its new systematic position in the family Ophiocordycipitaceae. Mycobiology 49(4): 297–307. https://doi.org/10.1080/12298093.2021.1923388

Wang Y, Wu HJ, Tran NL, Zhang GD, Souvanhnachit S, Wang YB, Yu H (2021b) *Ophiocordyceps furcatosubulata*, a new entomopathogenic fungus parasitizing beetle larvae (Coleoptera: Elateridae). Phytotaxa 482(3): 268–278. https://doi.org/10.11646/phytotaxa.482.3.5

Wen TC, Zhu RC, Kang JC, Huang MH, Tan DB, Ariyawansha H, Hyde KD, Liu H (2013) *Ophiocordyceps xuefengensis* sp. nov. from larvae of *Phassus nodus* (Hepialidae) in Hunan Province, southern China. Phytotaxa 123(1): 41–50. https://doi.org/10.11646/phytotaxa.123.1.2

Wen TC, Xiao YP, Li WJ, Kang JC, Hyde KD (2014) Systematic analyses of *Ophiocordyceps ramosissimum* sp. nov., a new species from a larvae of Hepialidae in China. Phytotaxa 161(3): 227–234. https://doi.org/10.11646/phytotaxa.161.3.6

White TJ, Bruns T, Lee S, Taylor J (1990) Amplification and Direct Sequencing of Fungal Ribosomal RNA Genes for Phylogenetics. PCR Protocols: A Guide to Methods and Applications. Academic Press, San Diego, 315–322. https://doi.org/10.1016/B978-0-12-372180-8.50042-1

Wijayawardene NN, Hyde KD, Lumbsch HT, Liu JK, Maharachchikumbura SSN, Ekanayaka AH, Tian Q, Phookamsak R (2018) Outline of Ascomycota: 2017. Fungal Diversity 88(1): 167–263. https://doi.org/10.1007/s13225-018-0394-8

Wilson M, Barden P, Ware J (2021) A review of ectoparasitic fungi associated with termites. Annals of the Entomological Society of America 114(4): 373–396. https://doi.org/10.1093/aesa/saab001

Xiao YP, Wen TC, Hongsanan S, Sun JZ, Hyde KD (2017) Introducing *Ophiocordyceps thanathonensis*, a new species of entomogenous fungi on ants, and a reference specimen for *O. pseudolloydii*. Phytotaxa 328(2): 115–126. https://doi.org/10.11646/phytotaxa.328.2.2

Xiao YP, Hongsanan S, Hyde KD, Brooks S, Xie N, Long FY, Wen TC (2019) Two new entomopathogenic species of *Ophiocordyceps* in Thailand. MycoKeys 47: 53–74. https://doi.org/10.3897/mycokeys.47.29898

Xiao YP, Wang YB, Hyde KD, Eleni G, Sun JZ, Yang Y, Meng J, Yu H, Wen TC (2023) Polycephalomycetaceae, a new family of clavicipitoid fungi segregates from Ophiocordycipitaceae. Fungal Diversity 120(1): 1–76. https://doi.org/10.1007/s13225-023-00517-4

Xu ZH, Tran NL, Wang Y, Zhang GD, Dao VM, Nguyen TT, Wang YB, Yu H (2022) Phylogeny and morphology of *Ophiocordyceps puluongensis* sp. nov. (Ophiocordycipitaceae, Hypocreales), a new fungal pathogen on termites from Vietnam. Journal of Invertebrate Pathology 192: e107771. https://doi.org/10.1016/j.jip.2022.107771

Zha LS, Kryukov VY, Ding JH, Jeewon R, Chomnunti P (2021) Novel taxa and species diversity of *Cordyceps* sensu lato (Hypocreales, Ascomycota) developing on wireworms (Elateroidea and Tenebrionoidea, Coleoptera). MycoKeys 78: 79–117. https://doi.org/10.3897/mycokeys.78.61836

Zou J, Wu L, He ZM, Zhang P, Chen ZH (2017) Determination of the main nucleosides and nucleobases in natural and cultured *Ophiocordyceps xuefengensis*. Molecules 22(9): e1530. https://doi.org/10.3390/molecules22091530

Zou WQ, Tang DX, Xu ZH, Huang O, Wang YB, Tran NL, Yu H (2022) Multigene phylogeny and morphology reveal *Ophiocordyceps hydrangea* sp. nov. and *Ophiocordyceps bidoupensis* sp. nov. (Ophiocordycipitaceae). MycoKeys 92: 109–130. https://doi.org/10.3897/mycokeys.92.86160

MycoKeys

MycoKeys 103: 25–35 (2024)
DOI: 10.3897/mycokeys.103.115462

Data Paper

The Dolichens database: the lichen biota of the Dolomites

Luana Francesconi[1], Matteo Conti[2], Gabriele Gheza[1], Stefano Martellos[2], Pier Luigi Nimis[2], Chiara Vallese[3], Juri Nascimbene[1]

1 *BIOME Lab, Alma Mater Studiorum - University of Bologna, Bologna, Italy*
2 *Department Of Life Sciences, University of Trieste, Trieste, Italy*
3 *Department Of Earth, Environmental and Life Sciences, University of Genova, Genova, Italy*
Corresponding author: Luana Francesconi (luana.francesconi3@unibo.it)

Abstract

The Dolichens project provides the first dynamic inventory of the lichens of the Dolomites (Eastern Alps, Italy). Occurrence records were retrieved from published and grey literature, reviewed herbaria, unpublished records collected by the authors, and new sampling campaigns, covering a period from 1820 to 2022. Currently, the dataset contains 56,251 records, referring to 1,719 infrageneric taxa, reported from 1820 to 2022, from hilly to nival belts, and corresponding to about half of the species known for the whole Alpine chain. Amongst them, 98% are georeferenced, although most of them were georeferenced a posteriori. The dataset is available through the Global Biodiversity Information Facility (GBIF; https://www.gbif.org/es/dataset/cea3ee2c-1ff1-4f8e-bb37-a99600cb4134) and through the Dolichens website (https://italic.units.it/dolichens/). We expect that this open floristic inventory will contribute to tracking the lichen diversity of the Dolomites over the past 200 years, and providing the basis for future taxonomic, biogeographical, and ecological studies.

Key words: Georeferencing, herbarium specimens, historical records, lichen diversity, occurrence, open inventory

Academic editor: Pradeep Divakar
Received: 9 November 2023
Accepted: 4 January 2024
Published: 11 March 2024

Citation: Francesconi L, Conti M, Gheza G, Martellos S, Nimis PL, Vallese C, Nascimbene J (2024) The Dolichens database: the lichen biota of the Dolomites. MycoKeys 103: 25–35. https://doi.org/10.3897/mycokeys.103.115462

Introduction

The Dolomites, in the Southeastern Italian Alps, were declared a UNESCO World Heritage Site in June 2009, because of the uniqueness of their geology and landscapes. Such a variety of spectacular forms are related to their complex geological origin, as well as to the processes that have modeled the landscape (Messner and Tappeiner 2010). The Dolomites, along with the surrounding areas, constitute a complex mosaic of habitats, which underpin their high biodiversity (Pignatti and Pignatti 2016; Rota et al. 2022).

The Dolomites are one of the lichenologically best-known areas in Italy. Here, lichen diversity is strictly related to the variety of climatic conditions and substrates (Nimis 1993). Trentino-Alto Adige, in particular, is the lichenologically richest administrative region of Italy, with 1,684 infrageneric taxa reported to date, while 1,234 and 1,364 infrageneric taxa are known for the neighboring Veneto and Lombardia regions (Nimis and Martellos 2024).

These comparatively high figures are due to the long tradition of lichenological research in the area, which has been explored since the 19th century. The majority of historical contributions are attributed to Ferdinand Arnold (1828–1901), who surveyed South Tyrol in the last years of the 1800s and published the results in his Lichenologische Ausfluge in Tirol (1868–1897). Another relevant contribution was provided by Ernst Kernstock (1852–1900) in his Lichenologische Beitrage (1890–1896). The lichen records collected in the area until 1901 were summarized by Dalla Torre and Sarnthein (1902) in one of the oldest "checklists". In the first half of the 20th century, these territories were mainly explored by Pio Bolzon (1867–1940) and Maria Cengia Sambo (1888–1939), who published several contributions on local lichen flora (Nimis 1993).

Despite the lichenological relevance of the Dolomites, no modern synthesis of their lichen diversity was ever attempted. There are important resources on the lichens of the Alps (Nimis et al. 2018), and on the lichen biotas of Italian Alpine regions (Martellos et al. 2023), but neither of these resources recognizes the Dolomites as an independent operational geographic unit. In addition, to our knowledge, no geo-referenced occurrence records of lichens are available online for the Dolomites.

Inventories based on new field explorations (Vondrák et al. 2016; Spribille et al. 2020), review of herbarium specimens, and literature records (Isocrono et al. 2007; Himelbrant et al. 2018) provide fundamental information on ecology and distribution of species. Furthermore, they foster taxonomic discoveries, including the description of new species and higher groups (Spribille et al. 2020; Leavitt et al. 2021; Nascimbene et al. 2022). Finally, if occurrence records are geo-referenced, it is possible to perform spatial analyses, such as biogeographical studies or distribution modeling (Bloom et al. 2018; Guttová et al. 2019; Marsico et al. 2020), which are pivotal for revealing biodiversity patterns, predicting potential shifts in a global change scenario and contributing to effective conservation guidelines (Ellis et al. 2007; Eaton et al. 2018; Nelsen and Lumbsch 2020).

The Dolichens project was launched in 2022. It aims at building a dynamic geo-referenced inventory of the lichen biota of the Dolomites by aggregating occurrence records from published and gray literature (such as university research theses), unpublished data, and herbaria from the 19th century onwards. The project aims at aggregating occurrence records from recent surveys as well. The result is a database accessible online (https://italic.units.it/dolichens/), which is continuously updated.

Sampling methods

Description: The Dolichens system hosts georeferenced occurrence records of lichens in the Dolomites, from the 19th century onwards. The geographical delimitation of the Dolomites region was, however, not simple, since several contrasting definitions exist (Bentivoglio and De Simoni 1980; Bosellini 1989; Marazzi 2005; Messner and Tappeiner 2010). In this study, a core area was selected (Fig. 1), which is wider than the most common geographical definition for the Dolomites provided by the Partition of the Alps and the SOIUSA (Marazzi 2005). It spans an area of 11,735 km^2, encompassing the territories surrounding the 9 UNESCO systems (Messner and Tappeiner 2010), thereby incorporating the Friulian and Brenta Dolomites, extending southward to the Venetian and Carnic

Prealps, in order for us to be able to include the area of the "Little Dolomites" (Bosellini 1989) as well. In addition, a buffer area was delimited (Fig. 1), which extends northward and eastward to the national borders, enclosing the Stelvio National Park and the Adamello Brenta Natural Park on the west, and reaching the border of the Po-Valley near Verona, covering a surface of 29,299 km^2. Data aggregation was focused on the core area, while data from the buffer area were aggregated when they were included in the same resource reporting data from the core area. Thus, the Dolichens project provides a preliminary baseline for the development of a future lichen inventory of the Eastern Italian Alps.

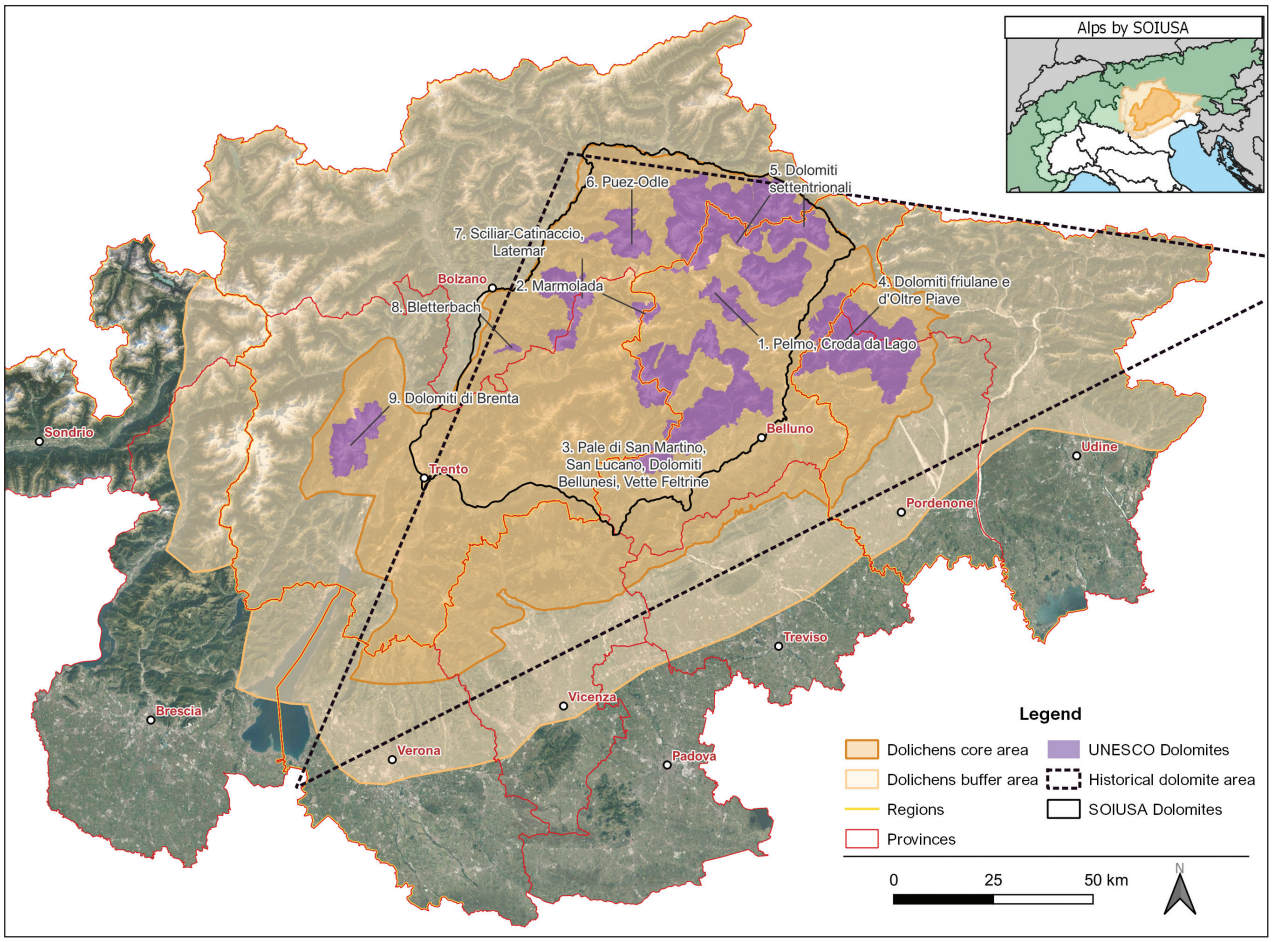

Figure 1. Study area of the project. The core area (dark orange) is wider than the SOIUSA definition (black line, Marazzi 2005). It includes all the 9 UNESCO systems (purple) and it extends southward to the Prealps including the Little Dolomites as well, retracing the historical definition (dotted black line, Bosellini 1989).

Sampling description: For this study occurrence records were collected from different sources. First of all, to compile a baseline inventory of the lichens of the Dolomites, we gathered records from literature starting from the 19th century (such as checklists, vegetation surveys, and taxonomic revisions). Among them, the most exhaustive historical source is the catalogue of Dalla Torre and Sarnthein (1902), from which 10,299 records referring to 885 taxa were retrieved. Furthermore, unpublished records collected by the authors, as well as from gray literature, were gathered. Herbarium specimen data were retrieved from historical herbaria, some of which were reviewed by the authors of this contribution, such as those of Alberto Parolini (1788–1867), Francesco Ambrosi (1821–1897), or

Giacomo Bresadola (1847–1929). Finally, sampling campaigns were carried out and are still ongoing, mainly in the Paneveggio Pale di San Martino Natural Park, the Adamello Brenta Natural Park, and the Dolomiti Bellunesi National Park. They are focused on protected areas and allow the investigation of both historical sites and new locations, which have been poorly explored by lichenologists.

Quality control: Specimens were collected and identified/revised by the experienced lichenologists of our group (e.g. Nascimbene, Nimis) and colleagues from other universities. However, the current database is not a critical checklist. The latter will be developed in the future by critically evaluating all the collected records.

Scientific names were automatically aligned to the latest version of the annotated checklist of Italian lichens (Nimis 2016), available on ITALIC 7.0 (Martellos et al. 2023) by means of a customized version of the FlorItaly name-matching tool (Conti et al. 2021). Then, the scientific names were normalized against the GBIF backbone (GBIF Secretariat 2023). The verbatim names have been always retained together with the currently accepted name.

When geographical coordinates of the collection locality were missing, the records were georeferenced a posteriori using Google Maps, Google Earth, and regional GIS maps, following the best practices proposed by Chapman and Wieczorek (2020).

Geographic coverage

Description: The dataset contains occurrence data of lichens reported for 4 administrative regions and 11 provinces of Italy: Friuli Venezia Giulia (Udine 366 and Pordenone 410), Lombardy (Brescia 11 and Sondrio 2), Trentino Alto Adige (Trento 18,052 and Bolzano 20,543), Veneto (Belluno 14,270, Padova 1, Treviso 779, Verona 106 and Vicenza 325). The distribution of records in the study area is shown in Fig. 2.

Coordinates: 10.2782 and 13.7173 Latitude; 45.3834 and 47.0918 Longitude.

Taxonomic coverage

Description: According to the GBIF Taxonomic Backbone, the dataset comprises taxa from 39 orders, 102 families, and 416 genera.

The following families are represented: Acarosporaceae, Adelococcaceae, Arctomiaceae, Arthoniaceae, Arthopyreniaceae, Arthrorhaphidaceae, Ascodichaenaceae, Baeomycetaceae, Biatorellaceae, Byssolomataceae, Caliciaceae, Candelariaceae, Catillariaceae, Chrysotrichaceae, Cladoniaceae, Coccocarpiaceae, Coenogoniaceae Collemataceae, Coniocybaceae, Cystocoleaceae, Dacampiaceae, Didymellaceae, Elixiaceae, Epigloeaceae, Fuscideaceae, Gomphillaceae, Graphidaceae, Gyalectaceae, Haematommataceae, Helocarpaceae, Hygrophoraceae, Hymeneliaceae, Hysteriaceae, Icmadophilaceae, Lecanographaceae, Lecanoraceae, Lecideaceae, Leprocaulaceae, Lichenotheliaceae, Lichinaceae, Lobariaceae, Lopadiaceae, Malmideaceae, Massalongiaceae, Megasporaceae, Melaspileaceae, Microcaliciaceae, Monoblastiaceae, Mycocaliciaceae, Mycoporaceae, Mycosphaerellaceae, Myriangiaceae, Naetrocymbaceae, Nephromataceae, Ochrolechiaceae, Opegraphaceae, Ophioparmaceae, Pannariaceae, Parmeliaceae, Patellariaceae, Peltigeraceae, Peltulaceae, Pertusariaceae, Phlyctidaceae, Physciaceae, Placynthiaceae, Polycoccaceae, Porinaceae, Porpidiaceae,

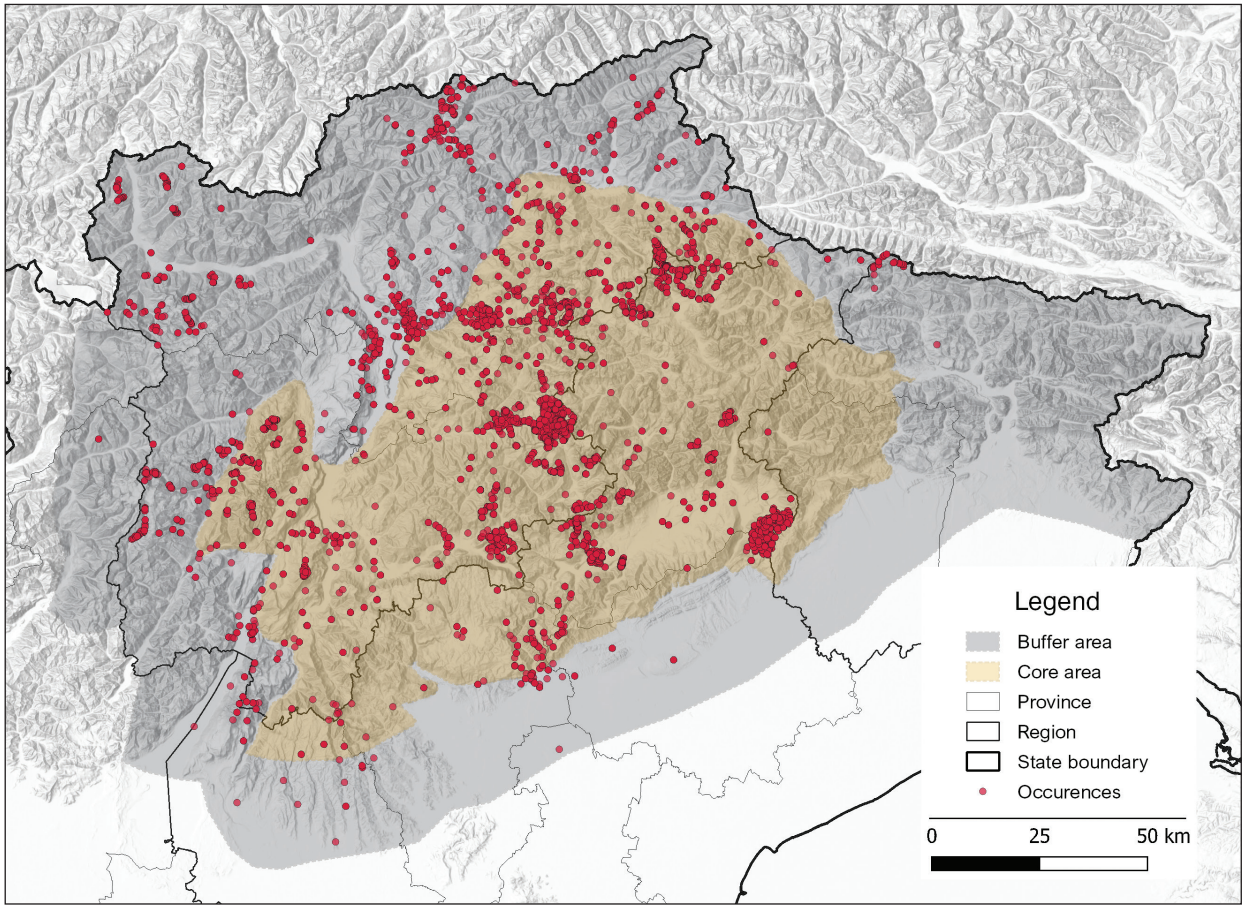

Figure 2. Distribution map of the Dolichens database occurrences and specimens in the study area. Map created using the Free and Open Source QGIS

Psilolechiaceae, Psoraceae, Pycnoraceae, Pyrenulaceae, Ramalinaceae, Ramboldiaceae, Rhizocarpaceae, Roccellaceae, Sagiolechiaceae, Sareaceae, Sarrameanaceae, Schaereriaceae, Sclerococcaceae, Scoliciosporaceae, Sphaerophoraceae, Sphinctrinaceae, Sporastatiaceae, Stereocaulaceae, Stictidaceae, Strangosporaceae, Strigulaceae, Teloschistaceae, Tephromelataceae, Thelenellaceae, Thelocarpaceae, Trapeliaceae, Trypetheliaceae, Umbilicariaceae, Vahliellaceae, Varicellariaceae, Verrucariaceae, Xanthopyreniaceae, and Xylographaceae.

Taxonomic distribution (Fig. 3) and distribution of occurrences (Fig. 4) among each kingdom, phylum, class, order, family, and genus can be graphically visualized as a Krona graph, an interactive multi-layered pie chart that allows the exploration of hierarchical data (the interactive file is provided in Suppl. material 1).

Temporal coverage

Data were reported from 1820 to 2022. Occurrences per year are shown in Fig. 5. The highest number of occurrences in 1902 corresponds to the data retrieved from the most exhaustive historical source, the catalogue of Dalla Torre and Sarnthein (1902), which collects data derived from the publications of previous authors, like Ferdinand Arnold, who explored the Tyrol during the 19th century. Then, the more recent peaks of occurrences from the 1990s correspond to the newfound national interest in lichenology, and the lichenological exploration by the research group of the University of Bologna.

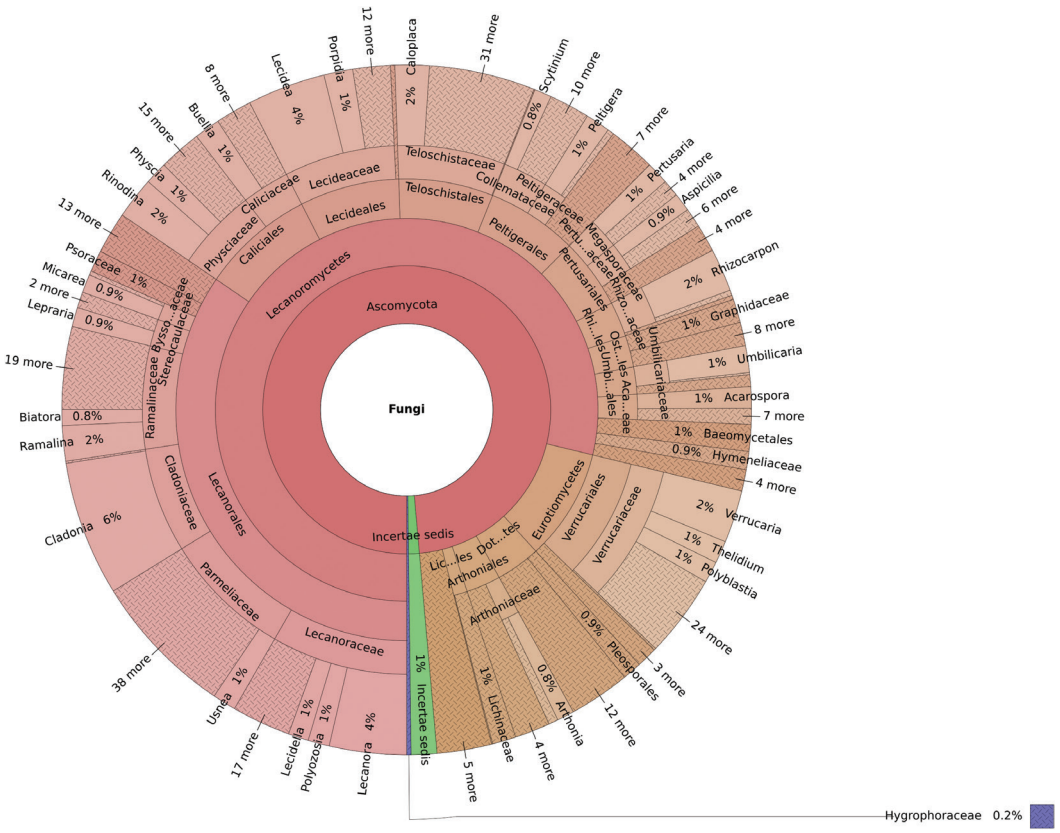

Figure 3. Relative abundance at the genus level referred to the total number of taxa (1994), created using the Krona graph tool (Ondov et al. 2011).

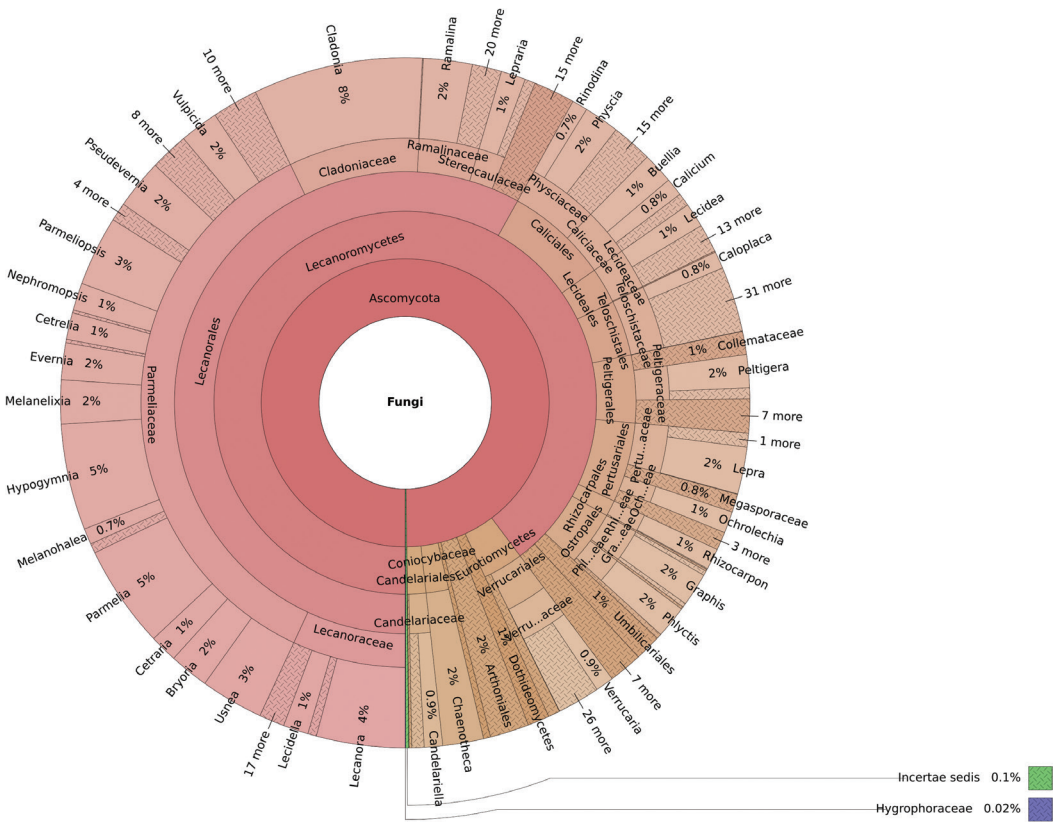

Figure 4. Relative abundance at the genus level referred to the total number of occurrences (56251), created using the Krona graph tool (Ondov et al. 2011).

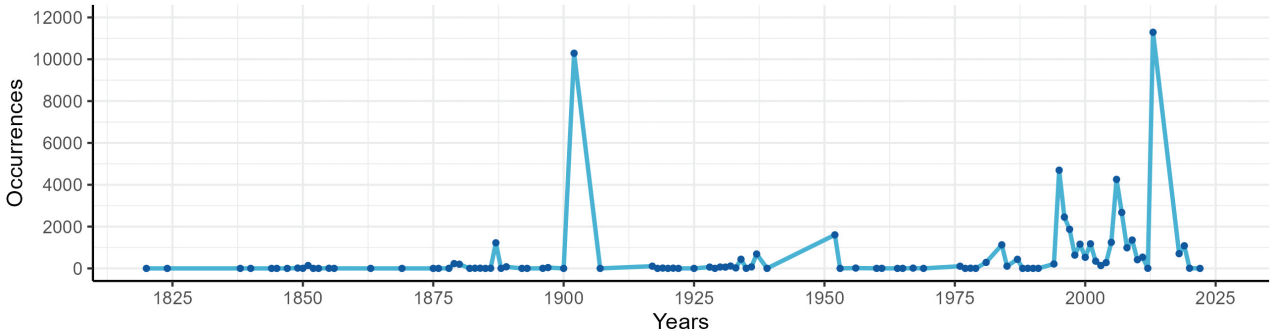

Figure 5. Lichen occurrences of the Dolichens dataset per year.

Usage licence

Data resources

Data package title: Dolichens project: the lichen biota of the Dolomites.

Resource link: https://doi.org/10.15468/64sy7b.

Alternative identifiers: https://cloud.gbif.org/eca/resource?r=dolichens_project.

Number of data sets: 1.

Data set name: Dolichens project: the lichen biota of the Dolomites.

Download URL: https://www.gbif.org/occurrence/download?dataset_key=cea3ee2c-1ff1-4f8e-bb37-a99600cb4134.

Data format: Darwin Core.

Description: Launched in 2022 the Dolichens project aims to assemble an inventory of the lichens reported from the Dolomite area since the 19th century. Data of lichen occurrences have been retrieved and aggregated from herbaria, literature, unpublished data, and new sampling campaigns.

Column label	Column description
occurrenceID	A unique identifier for the occurrence.
basisOfRecord	The source or nature of the record.
verbatimIdentification	The original, unaltered identification of the organism.
scientificName	The scientifically accepted name of the organism.
Kingdom	The taxonomic kingdom to which the organism belongs.
eventDate	The date when the occurrence was observed or recorded.
stateProvince	The administrative region in which the organism was recorded.
County	The name of the next smaller administrative region than state Province in which the organism was recorded.
Locality	The location where the organism was observed.
decimalLatitude	The latitude coordinates of the occurrence in decimal format.
decimalLongitude	The longitude coordinates of the occurrence in decimal format.
geodeticDatum	The reference geodetic datum for the coordinate data.
coordinateUncertaintyInMeters	The level of uncertainty associated with the geographic coordinates, in meter
minimumElevationInMeters	The lowest elevation at which the organism was found.
maximumElevationInMeters	The highest elevation at which the organism was found.

Column label	Column description
Continent	The continent where the occurrence was recorded.
Country	The country where the occurrence was recorded.
countryCode	The code of the country where the occurrence was recorded.
recordedBy	The person responsible for recording the occurrence.
identifiedBy	The person responsible for identifying the organism.
associatedReferences	References or sources of information associated with the occurrence.
License	The terms and conditions under which data can be used and shared
Language	The language in which the data or metadata for the occurrence is written

Acknowledgements

LF gratefully acknowledges MUR and EU-FSE for financial support of the Ph.D. fellowship PON Research and Innovation 2014–2020 (D.M. 1061/2021) XXXVII Cycle in Future Earth, Climate Change and Societal Challenges.

Additional information

Conflict of interest

The authors have declared that no competing interests exist.

Ethical statement

No ethical statement was reported.

Funding

No funding was reported.

Author contributions

Conceptualization: JN. Data curation: MC, PLN, LF, GG, JN, CV. Formal analysis: LF, MC. Funding acquisition: JN. Methodology: SM, JN. Project administration: JN. Supervision: SM, JN. Validation: PLN. Visualization: LF. Writing - original draft: MC, LF. Writing - review and editing: CV, JN, SM, LF, GG, PLN, MC.

Author ORCIDs

Luana Francesconi https://orcid.org/0000-0003-1745-7069
Matteo Conti https://orcid.org/0009-0003-4917-2639
Stefano Martellos https://orcid.org/0000-0001-5201-8948
Pier Luigi Nimis https://orcid.org/0000-0003-3523-0183
Chiara Vallese https://orcid.org/0000-0002-8531-5954
Juri Nascimbene https://orcid.org/0000-0002-9174-654X

Data availability

All of the data that support the findings of this study are available in the main text or Supplementary Information.

References

Arnold F (1869) Lichenologische Ausflüge in Tirol. IV. Der Schlern. Zoologisch-Botanische Gesellschaft, Wien, 606–656.

Arnold F (1871) Lichenologische Ausflüge in Tirol. VI. Der Waldrast. Zoologisch-Botanische Gesellschaft, Wien, 1103–1148.

Arnold F (1874) Lichenologische Ausflüge in Tirol. XIII. Der Brenner. Zoologisch-Botanische Gesellschaft, Wien, 231–284.

Arnold F (1876) Lichenologische Ausflüge in Tirol. XVI. Ampezzo. Zoologisch-Botanische Gesellschaft, Wien, 389–414.

Arnold F (1879) Lichenologische Ausflüge in Tirol. XX. Predazzo. Zoologisch-Botanische Gesellschaft, Wien, 351–394.

Arnold F (1886) Lichenologische Ausflüge in Tirol. XXII. Sulden. Zoologisch-Botanische Gesellschaft, Wien, 61–88.

Arnold F (1887) Lichenologische Ausflüge in Tirol. XXII. Predazzo und Paneveggio. Zoologisch-Botanische Gesellschaft, Wien, 81–150.

Arnold F (1896) Lichenologische Ausflüge in Tirol. XXVI. Pians. XXVII. Galtür. XXVIII. Wolkenstein. XXIX. Plansee. Zoologisch-Botanische Gesellschaft, Wien, 1–43.

Bentivoglio G, De Simoni G (1980) Partizione delle Alpi (in 220 gruppi). Tipografia Alzani, Pinerolo.

Bloom TDS, Flower A, DeChaine EG (2018) Why georeferencing matters: Introducing a practical protocol to prepare species occurrence records for spatial analysis. Ecology and Evolution 8: 765–777. https://doi.org/10.1002/ece3.3516

Bosellini A (1989) La storia geologica delle Dolomiti. Ed. Dolomiti, 148 pp.

Chapman AD, Wieczorek JR (2020) Georeferencing best practices. Version 1.0. GBIF Secretariat. [Report] https://doi.org/10.15468/doc-gg7h-s853

Conti M, Nimis PL, Martellos S (2021) Match Algorithms for Scientific Names in FlorItaly, the Portal to the Flora of Italy. Plants 10: 974. https://doi.org/10.3390/plants10050974

Dalla Torre KW, Sarnthein LG (1902) Die Flechten (Lichenes) von Tirol, Vorarlberg und Liechtenstein. In: K.W. Dalla Torre, Sarnthein LG (Eds) Flora der gefürsteten Grafschaft Tirol, des Landes Vorarlberg und des Fürstenthumes Liechtenstein. Nach eigenen und fremden Beobachtungen, Sammlungen und den Litteraturquellen. Verlag der Wagner'-schen Universitäts-Buchhandlung, Innsbruck, 1–693.

Eaton S, Ellis C, Genney D, Thompson R, Yahr R, Haydon DT (2018) Adding small species to the big picture: Species distribution modelling in an age of landscape scale conservation. Biological Conservation 217: 251–258. https://doi.org/10.1016/j.biocon.2017.11.012

Ellis CJ, Coppins BJ, Dawson TP, Seaward MRD (2007) Response of British lichens to climate change scenarios: Trends and uncertainties in the projected impact for contrasting biogeographic groups. Biological Conservation 140: 217–235. https://doi.org/10.1016/j.biocon.2007.08.016

GBIF Secretariat (2023) GBIF Backbone Taxonomy. https://doi.org/10.15468/39OMEI

Guttová A, Fačkovcová Z, Martellos S, Paoli L, Munzi S, Pittao E, Ongaro S (2019) Ecological specialization of lichen congeners with a strong link to Mediterranean-type climate: a case study of the genus *Solenopsora* in the Apennine Peninsula. The Lichenologist 51: 75–88. https://doi.org/10.1017/S0024282918000543

Himelbrant DE, Stepanchikova IS, Kuznetsova ES, Motiejūnaitė J, Konoreva LA (2018) Konevets Island (Leningrad Region, Russia) – a historical refuge of lichen diversity in Lake Ladoga. Folia Cryptogamica Estonica 55: 51–78. https://doi.org/10.12697/fce.2018.55.07

Isocrono D, Matteucci E, Ferrarese A, Pensi E, Piervittori R (2007) Lichen colonization in the city of Turin (N Italy) based on current and historical data. Environmental Pollution 145: 258–265. https://doi.org/10.1016/j.envpol.2006.03.031

Kernstock E (1890a) Lichenologische Beiträge I. Pinzolo (Südtirol). Zoologisch-Botanische Gesellschaft, Wien 40, 317–339.

Kernstock E (1890b) Lichenologische Beiträge II. Bozen. Zoologisch-Botanische Gesellschaft, Wien 40, 339–350.

Kernstock E (1891) Lichenologische Beiträge III. Jenesien bei Bozen. Zoologisch-Botanische Gesellschaft, Wien 41, 701–738.

Kernstock E (1892a) Lichenologische Beiträge. IV. M. Gazza (Paganella, 2120 m) in Südtirol. Zoologisch-Botanische Gesellschaft, Wien 42, 319–325.

Kernstock E (1892b) Lichenologische Beiträge. V. Judicarien. Zoologisch-Botanische Gesellschaft, Wien 42, 325–349.

Kernstock E (1894) Lichenologische Beiträge. VI. Möltener Alpen. Zoologisch-Botanische Gesellschaft, Wien 44, 191–224. https://doi.org/10.1007/BF01790222

Kernstock E (1896) Lichenologische Beiträge. VII. Ehrenburg im Pusterthale. Zoologisch-Botanische Gesellschaft, Wien 46, 279–310.

Leavitt SD, Hollinger J, Summerhays S, Munger I, Allen J, Smith B (2021) Alpine lichen diversity in an isolated sky island in the Colorado Plateau, USA—Insight from an integrative biodiversity inventory. Ecology and Evolution 11: 11090–11101. https://doi.org/10.1002/ece3.7896

Marazzi S (2005) Atlante orografico delle Alpi: SOIUSA : suddivisione orografica internazionale unificata del sistema alpino. Priuli & Verlucca, 422 pp.

Marsico TD, Krimmel ER, Carter JR, Gillespie EL, Lowe PD, McCauley R, Morris AB, Nelson G, Smith M, Soteropoulos DL, Monfils AK (2020) Small herbaria contribute unique biogeographic records to county, locality, and temporal scales. American Journal of Botany 107: 1577–1587. https://doi.org/10.1002/ajb2.1563

Martellos S, Conti M, Nimis PL (2023) Aggregation of Italian Lichen Data in ITALIC 7.0. Journal of Fungi 9: 556. https://doi.org/10.3390/jof9050556

Messner R, Tappeiner G (2010) Dolomiti. Patrimonio dell'umanità. Mondadori Electa, 268 pp.

Nascimbene J, Gheza G, Bilovitz PO, Francesconi L, Hafellner J, Mayrhofer H, Salvadori M, Vallese C, Nimis PL (2022) A hotspot of lichen diversity and lichenological research in the Alps: the Paneveggio-Pale di San Martino Natural Park (Italy). MycoKeys 94: 37–50. https://doi.org/10.3897/mycokeys.94.95858

Nelsen MP, Lumbsch HT (2020) A data-driven evaluation of lichen climate change indicators in Central Europe. Biodiversity and Conservation 29: 3959–3971. https://doi.org/10.1007/s10531-020-02057-8

Nimis P (2016) The Lichens of Italy. A Second Annotated Catalogue. EUT Edizioni Università di Trieste.

Nimis PL (1993) The lichens of Italy: an annotated catalogue. Museo regionale di scienze naturali, Torino, 897 pp.

Nimis PL, Martellos S (2024) ITALIC - The Information System on Italian Lichens. Version 7.0. [Available from:] https://italic.units.it/

Nimis PL, Hafellner J, Roux C, Clerc P, Mayrhofer H, Martellos S, Bilovitz PO (2018) The lichens of the Alps – an annotated checklist. MycoKeys 31: 1–634. https://doi.org/10.3897/mycokeys.31.23568

Ondov BD, Bergman NH, Phillippy AM (2011) Interactive metagenomic visualization in a Web browser. BMC Bioinformatics 12: 385. https://doi.org/10.1186/1471-2105-12-385

Pignatti E, Pignatti S (2016) Plant Life of the Dolomites: Atlas of Flora. Springer, 495 pp. https://doi.org/10.1007/978-3-662-48032-8

Rota F, Casazza G, Genova G, Midolo G, Prosser F, Bertolli A, Wilhalm T, Nascimbene J, Wellstein C (2022) Topography of the Dolomites modulates range dynamics of narrow endemic plants under climate change. Scientific Reports 12: 1398. https://doi.org/10.1038/s41598-022-05440-3

Spribille T, Fryday AM, Pérez-Ortega S, Svensson M, Tønsberg T, Ekman S, Holien H, Resl P, Schneider K, Stabentheiner E, Thüs H, Vondrák J, Sharman L (2020) Lichens and associated fungi from Glacier Bay National Park, Alaska. The Lichenologist 52: 61–181. https://doi.org/10.1017/S0024282920000079

Vondrák J, Malíček J, Palice Z, Coppins B, Kukwa M, Czarnota P, Sanderson N, Acton A (2016) Methods for obtaining more complete species lists in surveys of lichen biodiversity. Nordic Journal of Botany 34: 619–626. https://doi.org/10.1111/njb.01053

Supplementary material 1

Krona graph taxa and occurrences

Authors: Luana Francesconi, Matteo Conti

Data type: html

Explanation note: Interactive file of the krona graph, showing relative abundance of the total taxa and the total occurrences in in each class, order, family and genus.

Link: https://doi.org/10.3897/mycokeys.103.115462.suppl1

MycoKeys 103: 37–55 (2024)
DOI: 10.3897/mycokeys.103.116605

Research Article

Multiple evidence reveals two new species and new distributions of *Calocybe* species (Lyophyllaceae) from northeastern China

Ao Ma[1*], Jia-Jun Hu[2,3,4*], Yue-Qu Chen[5], Xin Wang[2], Yong-Lan Tuo[2,3], Lei Yue[2], Xue-Fei Li[2,3], Dan Dai[6], Yun-Hui Wei[6], Bo Zhang[2,3], Yu Li[2]

1 *School of Life Science, Northeast Normal University, Changchun 130024, China*
2 *Engineering Research Centre of Edible and Medicinal Fungi, Ministry of Education, Jilin Agricultural University, Changchun 130118, China*
3 *Joint Laboratory of International Cooperation in Modern Agricultural Technology, Ministry of Education, Jilin Agricultural University, Changchun 130118, Jilin Province, China*
4 *College of Life Science, Zhejiang Normal University, Jinhua 321004, Zhejiang Province, China*
5 *Forestry Resources Protection Institute, Jilin Provincial Academy of Forestry Sciences, Changchun 130033, Jilin Province, China*
6 *Institute of Agricultural Applied Microbiology, Jiangxi Academy of Agricultural Sciences, Nanchang 330200, Jiangxi Province, China*

Corresponding authors: Bo Zhang (zhangbofungi@126.com); Yu Li (yuli966@126.com)

Abstract

The *Calocybe* species possess notable economic and medicinal value, demonstrating substantial potential for resource utilization. The taxonomic studies of *Calocybe* are lacking in quality and depth. Based on the specimens collected from northeast China, this study provides a detailed description of two newly discovered species, namely *Calocybe betulicola* and *Calocybe cystidiosa*, as well as two commonly found species, *Calocybe decolorata* and *Calocybe ionides*. Additionally, a previously unrecorded species, *C. decolorata*, has recently been discovered in Jilin Province, China. The two newly discovered species can be accurately distinguished from other species within the genus *Calocybe* based on their distinct morphological characteristics. The primary distinguishing features of *C. betulicola* include its grayish-purple pileus, grayish-brown to dark purple stipe, smaller basidiomata, absence of cellular pileipellis, and its habitat on leaf litter within birch forests. *Calocybe cystidiosa* is distinguished by its growth on the leaf litter of coniferous forests, a flesh-pink pileus, a fibrous stipe with a white tomentose covering at the base, non-cellular pileipellis, larger basidiospores, and the presence of cheilocystidia. The reconstruction of phylogenetic trees using combined ITS, nLSU, and *tef1-α* sequences, employing maximum likelihood and Bayesian inference analyses, showed that *C. betulicola* formed a cluster with *C. decurrens*, while *C. cystidiosa* clustered with *C. vinacea*. However, these two clusters formed separate branches themselves, which also supported the results obtained from our morphological studies. A key to the *Calocybe* species reported from northeast China is provided to facilitate future studies of the genus.

Key words: Colorful basidiomata, economic values, habitat, new taxa

OPEN ACCESS

Academic editor: Zai-Wei Ge
Received: 30 November 2023
Accepted: 22 February 2024
Published: 13 March 2024

Citation: Ma A, Hu J-J, Chen Y-Q, Wang X, Tuo Y-L, Yue L, Li X-F, Dai D, Wei Y-H, Zhang B, Li Y (2024) Multiple evidence reveals two new species and new distributions of *Calocybe* species (Lyophyllaceae) from northeastern China. MycoKeys 103: 37–55. https://doi.org/10.3897/mycokeys.103.116605

* These two authors contributed equally.

Introduction

The genus *Calocybe* Kühner ex Donk is widely distributed in the Northern Hemisphere and has significant economic value. It belongs to the family Lyophyllaceae. However, the genus *Calocybe* is always neglected by researchers. The genus *Calocybe* was officially published in 1962 and is typified by *Calocybe gambosa* (Fr.) Donk (Donk 1962). At first, it was treated as a section of *Lyophyllum* P. Karst. (Kühner and Romagnesi 1953). Then, Singer (1962) elevated it to genus rank based on the obvious colorful pileus, separated it from *Lyophyllum*, and belongs to the family Lyophyllaceae. Moreover, Singer divided *Calocybe* into five sections, namely Sect. *Calocybe* Singer, Sect. *Echinosporae* Singer, Sect. *Heterosporae* Singer, Sect. *Pseudoflammulae* Singer, and Sect. *Carneoviolaceae* Sing, by the combination of three characterizes, viz. the color of pileus, spores, and types of pileipellis (Singer 1962). Later, Singer (1986) assigned Sect. *Heterosporae* to the genus *Lyophyllum*, and, thus, the genus *Calocybe* was divided into four sections (Singer 1986).

By applying molecular methods to research *Calocybe*, it was reconfirmed that *Calocybe* is separate from the genus *Lyophyllum* and belongs to the Lyophyllaceae family (Hofstetter et al. 2002; Moncalvo et al. 2002; Matheny et al. 2006; Garnica et al. 2007). However, the taxonomic systems of *Calocybe* were full of arguments. Hofstetter et al. (2002) and Matheny et al. (2006) revealed that *Calocybe* formed a monophyletic group when the combined ITS, nLSU, or mitSSU fragments were used in phylogenetic analysis. Nevertheless, Bellanger concluded from a multi-gene phylogenetic analysis that *Calocybe* forms a monophyletic clade with *Rugosomyces* Raithelh (Bellanger et al. 2015). Vizzini et al. (2015), Li et al. (2017), and Xu et al. (2021a) also conducted a familiar conclusion with Bellanger. Recent research suggests that the genus *Calocybe* could be divided into five main clades. Based on continuous studies, 62 species of *Calocybe* are listed in the Index Fungorum (www.indexfungorum.org, accessed 20 March 2023).

There have been few studies focusing on the taxonomic and molecular studies of the genus *Calocybe* in China until now. Tai (1979) first reported *Calocybe* species from China, however, under the name *Lyophyllum leucophaeatum* (P. Karst.) P. Karst., later, confirmed to be *Calocybe gangraenosa* (Fr.) V. Hofst., Moncalvo, Redhead & Vilgalys. Seven species were recorded from China (Mao 2000; Bau et al. 2003; Fan and Bau 2006). Furthermore, a preliminary taxonomic study on *Calocybe* was performed in recent years (Zhou 2022). And recently, more than ten new species have been described in northeast China (Li et al. 2017; Xu et al. 2021a, 2021b; Qi et al. 2022; Mu and Bau 2023), and proposed their perspective on the taxonomic systematic on *Calocybe*. As a result, a total of 19 species of *Calocybe* have been reported, including *Calocybe aurantiaca* X.D. Yu & Jia J. Li, *Calocybe badiofloccosa* J.Z. Xu & Yu Li, and *Calocybe carnea* (Bull.) Donk, etc.

This study aims to describe and illustrate two new species, one new record from Jilin Province, and one common species based on both morphological and molecular data. Additionally, a key to the reported *Calocybe* species from northeast China is provided.

Materials and methods

Sampling and morphological studies

The studied specimens were photographed in situ. The size of the basidiomata was measured when fresh. After examination and description of the fresh macroscopic characters, the specimens were dried in an electric drier at 40–45 °C (Hu et al. 2022a, 2022b).

Descriptions of the macroscopic characteristics were based on field notes and photographs, with the colors corresponding to the Flora of British fungi: colour identification chart (Royal Botanic Garden 1969). The dried specimens were rehydrated in 94% ethanol for microscopic examination, and then mounted in 3% potassium hydroxide (KOH), 1% Congo red (0.1 g Congo red dissolved in 10 mL distilled water), and Melzer's reagent (1.5 g potassium iodide, 0.5 g crystalline iodine, and 22 g chloral hydrate dissolved in 20 mL distilled water) (César et al. 2018); they were then examined with a Zeiss Axio lab. A1 microscope at magnifications up to 1000 ×. All measurements were taken from the sections mounted in the 1% Congo red. For each specimen, a minimum of 40 basidiospores, 20 basidia, 20 cheilocystidia, and 20 widths of pileipellis were measured from two different basidiomata. When reporting the variation in the size of the basidiospores, basidia, cheilocystidia, and width of the pileipellis, 5% of the measurements were excluded from each end of the range, and are given in parentheses. The basidiospores measurements are given as length × width (L × W). Q denotes the variation in the ratio of L to W among the studied specimens, Qm denotes the average Q value of all the basidiospores ± standard deviation. The specimens examined have been deposited in the Herbarium of Mycology of Jilin Agricultural University (HMJAU).

DNA extraction, PCR amplification and sequencing

The total DNA was extracted from dried specimens using the NuClean Plant Genomic DNA Kit (Kangwei Century Biotechnology Company Limited, Beijing, China), according to the manufacturer's instructions. Sequences of the internal transcribed spacer region (ITS), nuclear large ribosomal subunits (nLSU), and translation elongation factor (*tef-1α*) were used for phylogenetic analysis. The ITS sequence was amplified using the primer pair ITS4 and ITS5 (Gardes and Burns 1993), and the nLSU sequence was amplified using the primer pair LROR and LR5 (Vilgalys and Hester 1990; Cubeta et al. 1991), and *tef1-α* regions were using *tef1-F* and *tef1-R* (Rehner and Samuels 1994). PCR reactions (25 μL) contained dd H_2O 9.5 μL, 2 × Taq PCR MasterMix 12.5 μL, upstream primer 0.5 μL, downstream primer 0.5 μL, DNA sample 2 μL. Cycle parameters were as follows 2 min at 94 °C; 35 s at 95 °C, 35 s at 48 °C, 1 min at 72 °C for 30 cycles; 10 min at 72 °C; storage at 4 °C (Xu et al. 2021a, 2021b). The PCR products were visualized via UV light after electrophoresis on 1.2% agarose gels stained with ethidium bromide and purified using the Genview High-Efficiency Agarose Gels DNA Purification Kit (Gen-View Scientific Inc., Galveston, TX, USA). The purified PCR products were then sent to Sangon Biotech Limited Company (Shanghai, China) for sequencing using the Sanger method. The new sequences were deposited in GenBank (http://www.ncbi.nlm.nih.gov/genbank; Table 1).

Table 1. Voucher/specimen numbers, country, and GenBank accession numbers of the specimens included in this study. Sequences produced in this study are in bold.

Taxa	Gen Bank accession numbers			Voucher/specimen number	Country	References
	ITS	nLSU	*tef1-α*			
Calocybe aurantiaca	KU528828	KU528833		SYAU-FUNGI-005	China	Li et al. 2017
Calocybe badiofloccosa	NR_173865	MN172334		HMJU:00098	China	Xu et al. 2021a
Calocybe buxea	KP885633	KP885625		EB 20140228	Italy	Xu et al. 2021b
Calocybe betulicola	**OR771918**	**OR771923**	**OR757443**	**HMJAU48265**	**China**	**This study**
Calocybe betulicola	**OR771919**	**OR771924**	**OR757444**	**HMJAU48266**	**China**	**This study**
Calocybe betulicola	**OR771920**	**OR771925**	**OR757445**	**HMJAU48267**	**China**	**This study**
Calocybe carnea	AF357028	AF223178	DQ367425	CBS552.50	Unknown	Xu et al. 2021a
Calocybe carnea	OM905971	OM906008		CC01	Netherlands	Van et al. 2022
Calocybe carnea	OQ321901			MQ22-KEG090-HRL3511	Canada	Unpublished
Calocybe carnea	MZ159709			K(M):250529	United Kingdom	Unpublished
Calocybe chrysenteron	KP885640	KP885629		L05-87	Germany	Xu et al. 2021b
Calocybe coacta	OK649907	OL687156		HMJU269	China	Xu et al. 2021a
Calocybe convexa	NR_156303	NG_058936		SYAU-FUNGI-008	China	Li et al. 2017
Calocybe cyanella	MF686498			HMA16	USA	Unpublished
Calocybe cyanea	OM905975			K(M):56506	Puerto Rico	Unpublished
Calocybe cystidiosa	**OR771915**		**OR757440**	**HMJAU48268**	**China**	**This study**
Calocybe cystidiosa	**OR771916**		**OR757441**	**HMJAU48269(1)**	**China**	**This study**
Calocybe cystidiosa	**OR771917**		**OR757442**	**HMJAU48269(2)**	**China**	**This study**
Calocybe decolorata	NR_156302	NG_058938		SYAU-FUNGI-004	China	Li et al. 2017
Calocybe decolorata	**OR771922**	**OR771927**		**HMJAU48262**	**China**	**This study**
Calocybe decurrens	MT080028	MW444857		HMJU00382	China	Xu et al. 2021a
Calocybe erminea	NR_173864	NG_153875		HMJU00100	China	Xu et al. 2019
Calocybe favrei	AF357034	AF223183		HAe234.97	Unknown	Xu et al. 2021b
Calocybe fulvipes	OK649910	OK649880		HMJU03027	China	Xu et al. 2021b
Calocybe gambosa	AF357027	AF223177		HC78/64	Unknown	Xu et al. 2019
Calocybe gangraenosa	AF357032	AF223202	DQ367427	Hae251.97	Unknown	Xu et al. 2021a
Calocybe graveolens	KP192590			FR2014044	France	Unpublished
Calocybe hebelomoides	MW672342			HUP-10254	Unknown	Li et al. 2017
Calocybe indica	OQ326668	OQ326667		APK2	Unknown	Xu et al. 2021a
Calocybe ionides	AF357029	AF223179	EF421057	HC77/133	Unknown	Xu et al. 2021a
Calocybe ionides		**OR771926**	**OR757446**	**HMJAU48264**	**China**	**This study**
Calocybe lilacea	OM203538	OM341407		SYAU-FUNGI-066	China	Qi et al. 2022
Calocybe longisterigma	OM203543	OM341406		SYAU-FUNGI-069	China	Qi et al. 2022
Calocybe naucoria	KP192543			FR2013213	France	Xu et al. 2019
Calocybe naucoria	KP885642	KP885630		AMB17094	Italy	Xu et al. 2019
Calocybe obscurissima	KP192650			BBF-GC01100203	France	Xu et al. 2021a
Calocybe obscurissima	KP192652			BBF-GC97111127	France	Bellanger et al. 2015
Calocybe obscurissima	MW862295			HBAU15474	China	Unpublished
Calocybe obscurissima	OQ133619			HFRG-LG211104-1	United Kingdom	Unpublished
Calocybe obscurissima	AF357031	AF223181	EF421058	HC79/181	Unknown	Xu et al. 2021b

Taxa	Gen Bank accession numbers			Voucher/specimen number	Country	References
	ITS	nLSU	*tef1-α*			
Calocybe ochracea	AF357033	AF223185		BSI94.cp1	Unknown	Bellanger et al. 2015
Calocybe onychina	KP192651			FR2014102	France	Bellanger et al. 2015
Calocybe onychina	KP192622			FR2014064	France	Bellanger et al. 2015
Calocybe onychina	MW084664	MW084704		CAON-RH19-563	USA	Xu et al. 2021b
Calocybe persicolor	AF357026	AF223176	EF421059	HC80/99	Unknown	Xu et al. 2019
Calocybe pilosella	KJ883237			TR gmb 00697	Italy	Floriani and Vizzini 2016
Calocybe pseudoflammula	MW862362			HBAU15678	Unknown	Unpublished
Calocybe pseudoflammula	KP192649			FR2014100	France	Bellanger et al. 2015
Calocybe vinacea	OK649908	OK649876		HMJU5135	China	Xu et al. 2021b
Lyophyllum atratum	KJ461896	KJ461895		PDD87010	New Zealand	Xu et al. 2021a
Lyophyllum caerulescens	AF357052	AF223209		HC80.140	Unknown	Xu et al. 2019
Lyophyllum decastes	AF357059	AF042583		JM87/16(T1)	Unknown	Xu et al. 2021b
Lyophyllum deliberatum		MK278318		G0631	Austria	Xu et al. 2019
Lyophyllum oldea	OM905959	OM906001	OM974134	BR5020029402116	Unknown	Unpublished
Lyophyllum semitale	AF357049	AF042581		HC85/13	Unknown	Xu et al. 2021b
Asterophora lycoperdoides	OM905969	OM906006		AL01	Netherlands	Unpublished
Asterophora mirabilis	NR_173484			MEL228691	Unknown	Unpublished
Asterophora parasitica	OM905970	OM906007		AP01	Netherlands	Unpublished
Hypsizygus tessulatus	KP192623			FR2014065	France	Bellanger et al. 2015
Hypsizygus ulmarius	EF421105	AF042584		DUKE-JM/HW	Unknown	Unpublished
Tricholomella constricta	DQ825429	AF223188		HC84/75	Unknown	Xu et al. 2021a
Tricholomella constricta	JN790692			EC8205	Italy	Unpublished
Tephrocybe ambusta	AF357058	AF223214		CBS450.87	Unknown	Unpublished
Tephrocybe rancida	OM905966	OM906004		CORT012400	Unknown	Unpublished
Tephrocybe rancida	OM905965	OM906003	OM974135	CORT012399	Unknown	Unpublished
Tephrocybe rancida	OM905967	OM906005	OM974137	TR2017	Unknown	Unpublished
Tricholoma terreum	JN389319	JN389374		F130649	Sweden	Unpublished

Data analysis

Based on the results of BLAST and morphological similarities, the sequences obtained and related to these samples were collected and are listed in Table 1. The dataset of ITS, nLSU, and *tef1-α* resign comprised sequences from this study, with 67 representative sequences showing the highest similarity to *Calocybe* spp. This dataset included all *Calocybe* species with sequences deposited in GenBank to further explore the relationships of the newly sequenced Chinese specimens within the genus. Moreover, representative species within family Lyophyllaceae were also included to explore the relations within it. The sequences of *Tricholoma terreum* (Schaeff.) P. Kumm. were selected as the outgroup taxon.

Of the dataset, each gene region was aligned using Clustal X (Thonpson et al. 1997), MACSE 2.03 (Ranwez et al. 2018), or MAFFT 7.490 (Katoh and Standley 2013), and then manually adjusted in BioEdit 7.0.5.3 (Hall 1999). The datasets first were aligned, and then the ITS, nLSU, and *tef1-α* sequences were

combined with Phylosuite 1.2.2 (Zhang et al. 2020). The best-fit evolutionary model was estimated using Modelfinder (Kalyaanamoorthy et al. 2017). Following the models, Bayesian inference (BI) algorithms were used to perform the phylogenetic analysis. Specifically, BI was calculated with MrBayes 3.2.6 with a general time-reversible DNA substitution model and a gamma distribution for rate variation across the sites (Ronquist and Huelsenbeck 2003). Four Markov chains were run for two runs from random starting trees for two million generations until the split deviation frequency value was < 0.01; the trees were sampled every 100 generations. The first 25% of the sampled trees were discarded as burn-in, while all the remaining trees were used to construct a 50% majority consensus tree and for calculating the Bayesian posterior probabilities (BPPS). RaxmlGUI 2.0.6 (Edler et al. 2021) was used for maximum likelihood (ML) analysis along with 1,000 bootstraps (BS) replicates using the GTRGAMMA algorithm to perform a tree inference and search for the optimal topology. Then the FigTree 1.3.1 was used to visualize the resulting trees.

Results

Phylogenetic analysis

The concatenated matrix contained 106 sequences (40 for nLSU, 58 for ITS, and eight for *tef1-α*) representing 61 samples were used to build a phylogenetic analysis (the concatenated matrix was deposited at treebase under the acc. no. S31166). Modelfinder selected the best-fit model for the combined dataset, and the best fit model for BI is GTR+F+I+G4. The results of the Bayesian analysis (Fig. 1) and the maximum likelihood analysis (Fig. 2) are generally in agreement.

After trimming, the combined ITS, nLSU, and *tef1-α* dataset represented 46 taxa and 3120 characters. The Bayesian analysis was run for two million generations and resulted in an average standard deviation of split frequencies of 0.009440. The same dataset and alignment were analyzed using the ML method. Six clades were revealed within Lyophyllaceae, representing *Calocybe*, *Tricholomella* Zerova ex Kalamees, *Tephrocybe* Donk, *Asterophora* Ditmar, *Lyophyllum*, and *Hypsizygus* Singer (Figs. 1 and 2). Moreover, from our results, the genus *Calocybe* was split into six independent clades, representing five sections and one newly recognized clade. Five sampled specimens formed two independent clades, representing two new species, *C. betulicola* and *C. cystidiosa*.

Taxonomy

***Calocybe betulicola* J.J. Hu, A. Ma, B. Zhang & Y. Li**
Fungal Names: FN 571739
Figs 3, 4D

Etymology. "*betulicola*" refers to this species that grows on the leaf litter of *Betula* forests.

Diagnosis. This species differs from other species by its grayish-purple pileus, grayish-brown to dark purple stipe, non-cellular pileipellis, and grows on the leaves' litter of *Betula* forest.

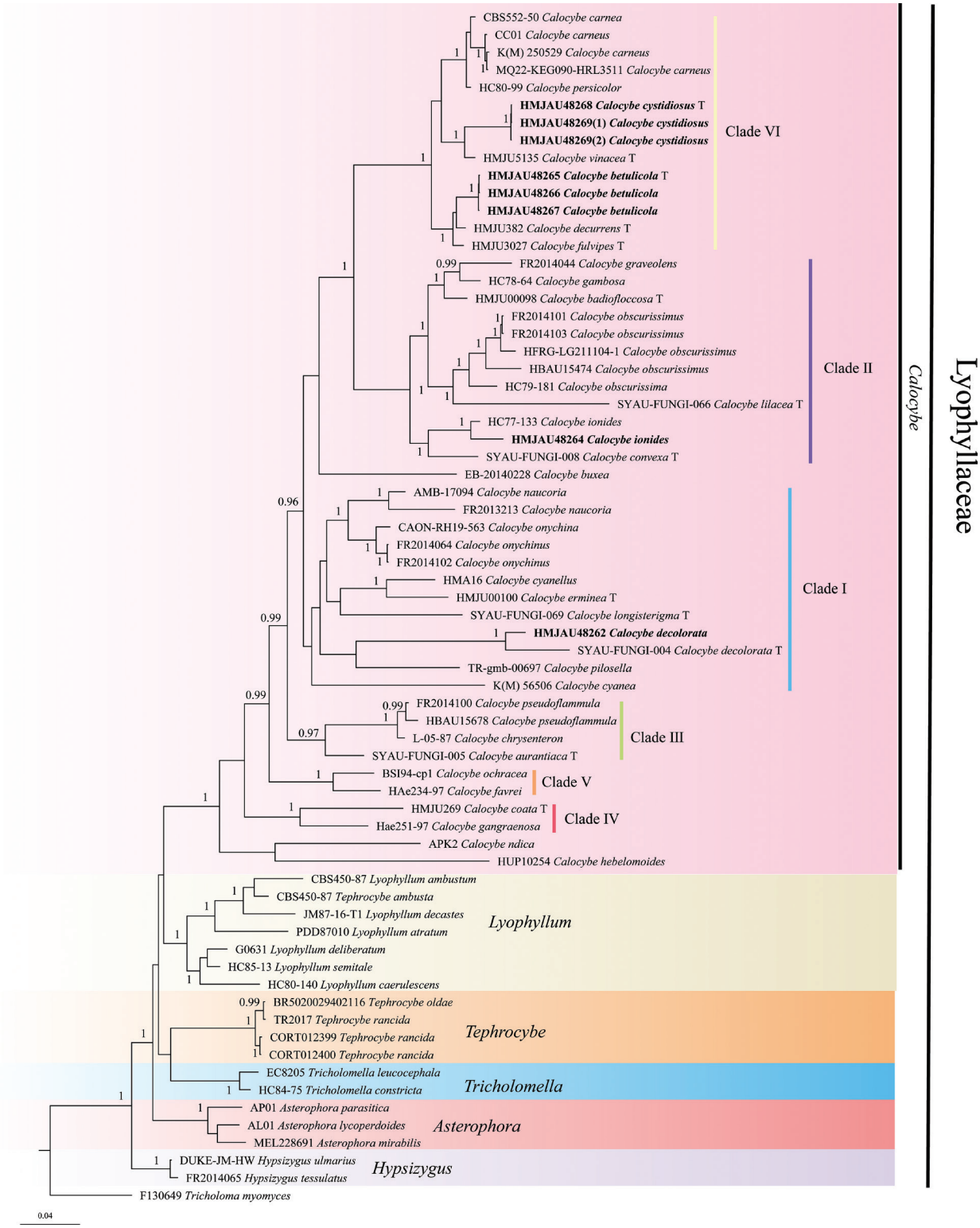

Figure 1. Bayesian analysis phylogenetic tree generated from the ITS, nLSU and *tef1-a* dataset. Bayesian posterior probabilities ≥ 0.95 from BI analysis are shown on the branches. Newly sequenced collections are indicated in bold, and the type specimens are denoted by (T).

Type. China. Jilin Province, Changchun City, Jilin Agricultural University, 20 September 2021, Jia-Jun Hu and Gui-Ping Zhao, HMJAU48265 (Collection No.: Hu J.J. 1089).

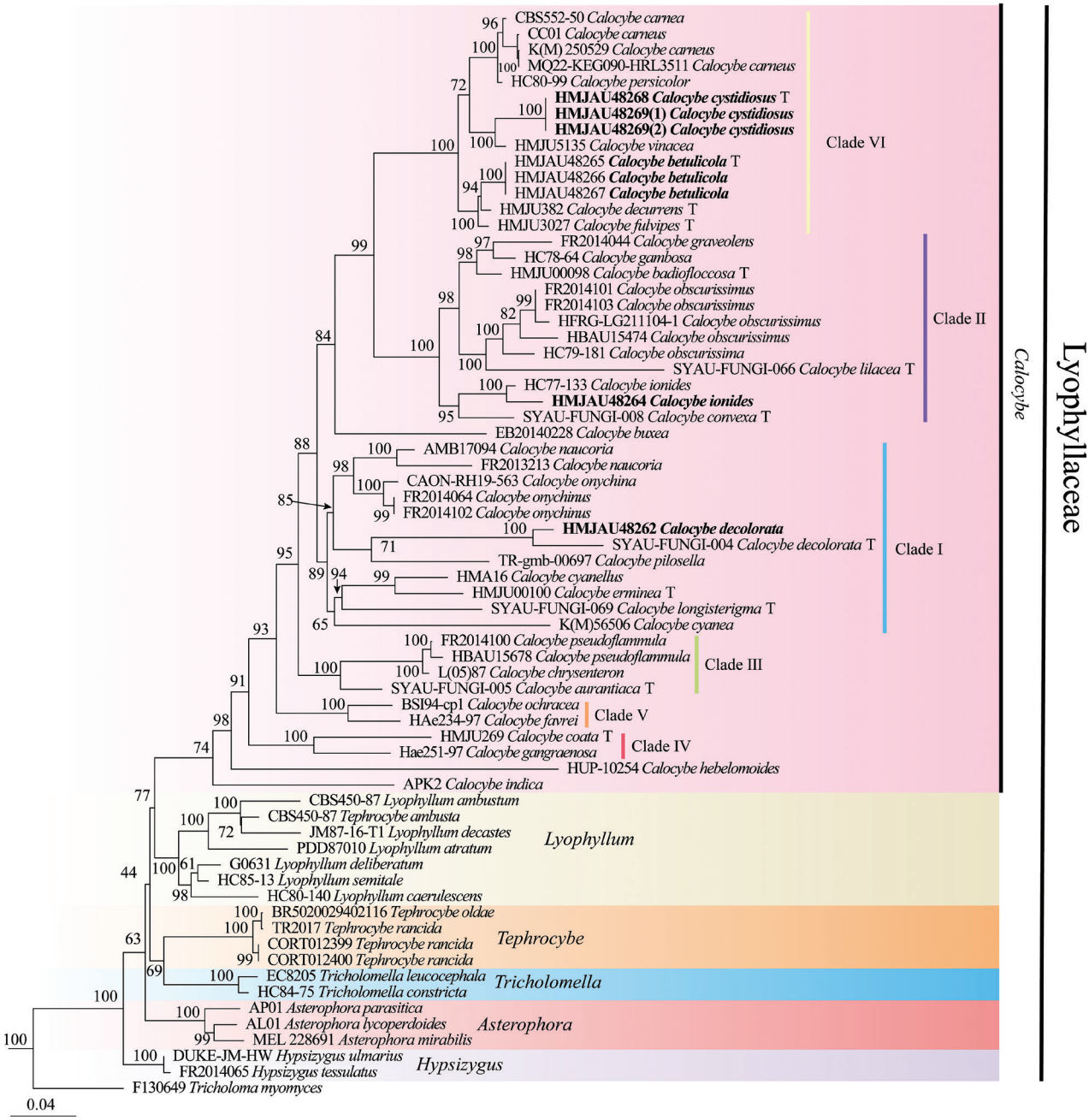

Figure 2. Maximum likelihood phylogenetic tree generated from the ITS, nLSU and *tef1-α* dataset. Bootstrap values ≥ 75% from ML analysis are shown on the branches. Newly sequenced collections are indicated in bold, and the type specimens are denoted by (T).

Description. Basidiomata gregarious, small. Pileus convex with an umbo, 2.0–3.5 cm diameter, smooth, violet (18F6) entirely; margin entire, wavy, involute, or reflex occasionally. Lamellae subdecurrent, beige (4B5) to light yellow (30A4), entire, crowded, with 1–3 lamellulae. Stipe cylindrical or tapering downwards, 1.5–3.0 cm long and 0.5–0.8 cm wide, central, with longitudinal stripe, solid, smooth, grayish-brown (18F6) to dark purple (20F7). Context thin, concolor or paler with pileus, odorless.

Basidiospores (2.0)3.0–6.0 × (2.0)3.0–4.0 µm, Q = (1.25)1.33–2.35(2.50), Qm = 1.90, hyaline, oval, smooth, inamyloid, thin-walled. Basidia 10.0–19.0 × 4.0–6.0 µm, clavate, 2- or 4-spored, hyaline, thin-walled. Hymenophoral tra-

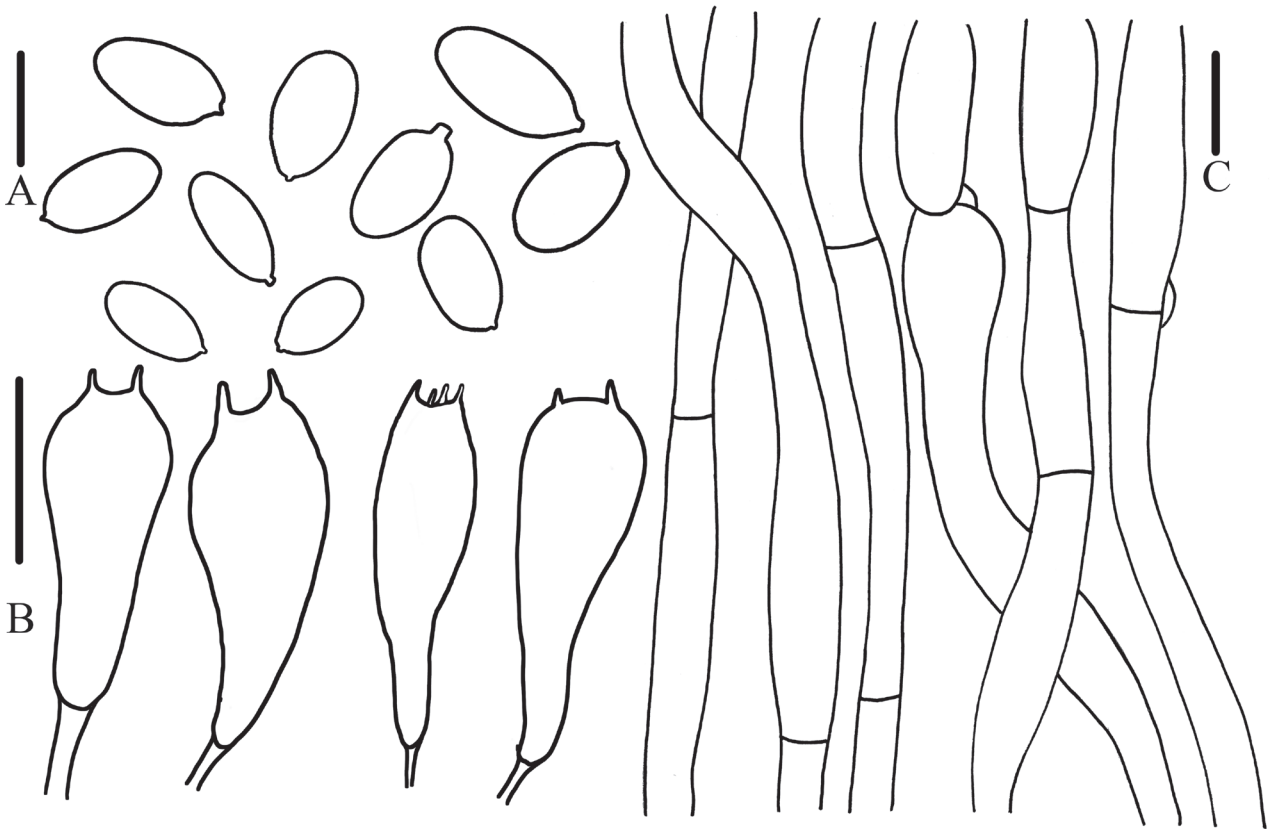

Figure 3. Microcharacteristics of *Calocybe betulicola* **A** basidiospores **B** basidia **C** pileipellis. Scale bars: (**A**) 5 μm; (**B, C**) 10 μm.

ma regular and hyphae arranged parallel, not pigmented, hyaline, thin-walled. Pileipellis hyphae 4.0–7.5 μm wide, smooth, hyaline, thin-walled. Stipitipellis hyphae 3.8–9.0 μm wide, hyaline, thin-walled, not pigmented. Clamp connections present.

Habitat. Growing on the leaf litters in birch forests.

Additional specimens examined. China. Jilin Province, Changchun City, Jilin Agricultural University, 18 September 2022, Jia-Jun Hu and Lei Yue, HMJAU48266; Jilin Province, Changchun City, Jilin Agricultural University, 27 September 2023, Lei Yue, HMJAU48267.

Comments. *Calocybe betulicola* is characterized by its grayish-purple pileus, grayish-brown to dark purple stipe, smaller basidiomata, non-cellular pileipellis, and its growth on the leaf litter in birch forests. According to these characteristics, *C. betulicola* is a member of Sect. *Carneoviolaceae.* Sect. *Carneoviolaceae* mainly includes four other species, viz. *Calocybe decurrens* J.Z. Xu & Yu Li, *Calocybe fulvipes* J.Z. Xu & Yu Li, *Calocybe ionides* (Bull.) Donk, and *Calocybe coacta* J.Z. Xu & Yu Li.

This species is macroscopically similar to *C. ionides* due to the purple basidiomata. However, *C. betulicola* differs from *C. ionides* in terms of its unique habitat, subdecurrent lamellae, and wider basidiospores. *Calocybe decurrens* has an intimate affinity in phylogenetic analysis. However, it differed from *C. betulicola* by the gradual fading from pinkish purple to brownish red to grayish brown stipe, carneous pileus, and larger basidiospores ((5.8) 6.0–8.5 (9.3) × (2.1) 2.7–3.8 (4.3) μm) (Xu et al. 2021b). *Calocybe fulvipes* differs by its tone

brown to dark violet stipe, and the changes it undergoes when injured, bigger Qm, and slightly longer sterigmata (Xu et al. 2021a). *Calocybe coacta* can be distinguished from *C. betulicola* by its cream-gray pileus, the presence of hymenial cystidia, and larger basidiospores (Xu et al. 2021a).

***Calocybe cystidiosa* A. Ma, J.J. Hu, B. Zhang & Y. Li**
Fungal Names: FN 571740
Figs 4C, 5

Etymology. "cystidiosa" refers to the presence of cheilocystidia.

Diagnosis. This species is differentiated from other species by its fresh-pink basidiomata, uncurved margin of the pileus, whitish pink stipe covered with tomentose at the base, lager basidiospores, and the presence of cheilocystidia.

Type. China. Liaoning Province, Fushun City, Xinbin Manchu Autonomous County, Gangshan Provincial Forest Park, Fushun City, August 28, 2018, Ao Ma, HMJAU48268.

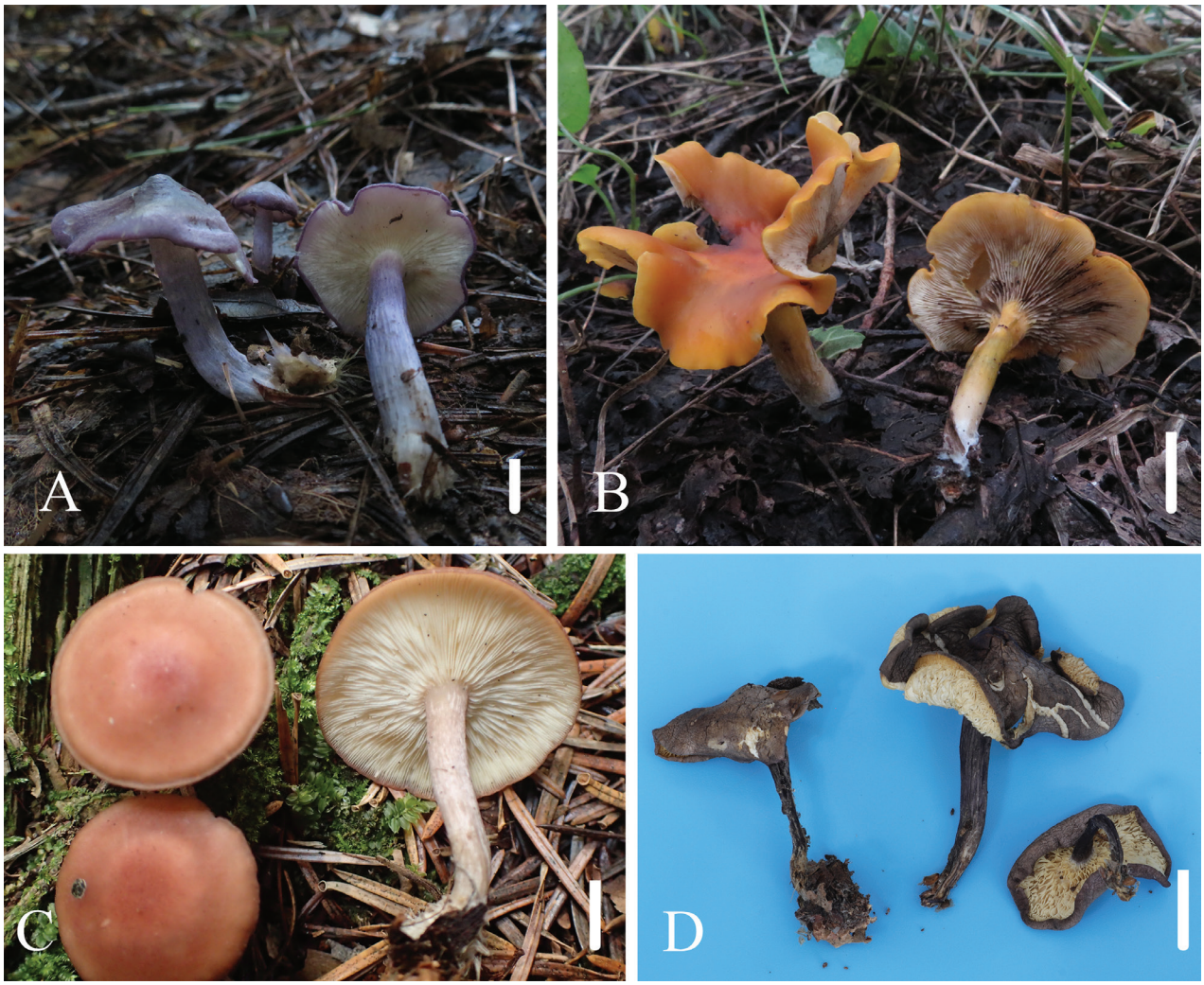

Figure 4. Habitat of *Calocybe* species in this study **A** *Calocybe ionides* **B** *Calocybe decolorata* **C** *Calocybe cystidiosa* **D** *Calocybe betulicola*. Scale bars: 1 cm (**A–E**).

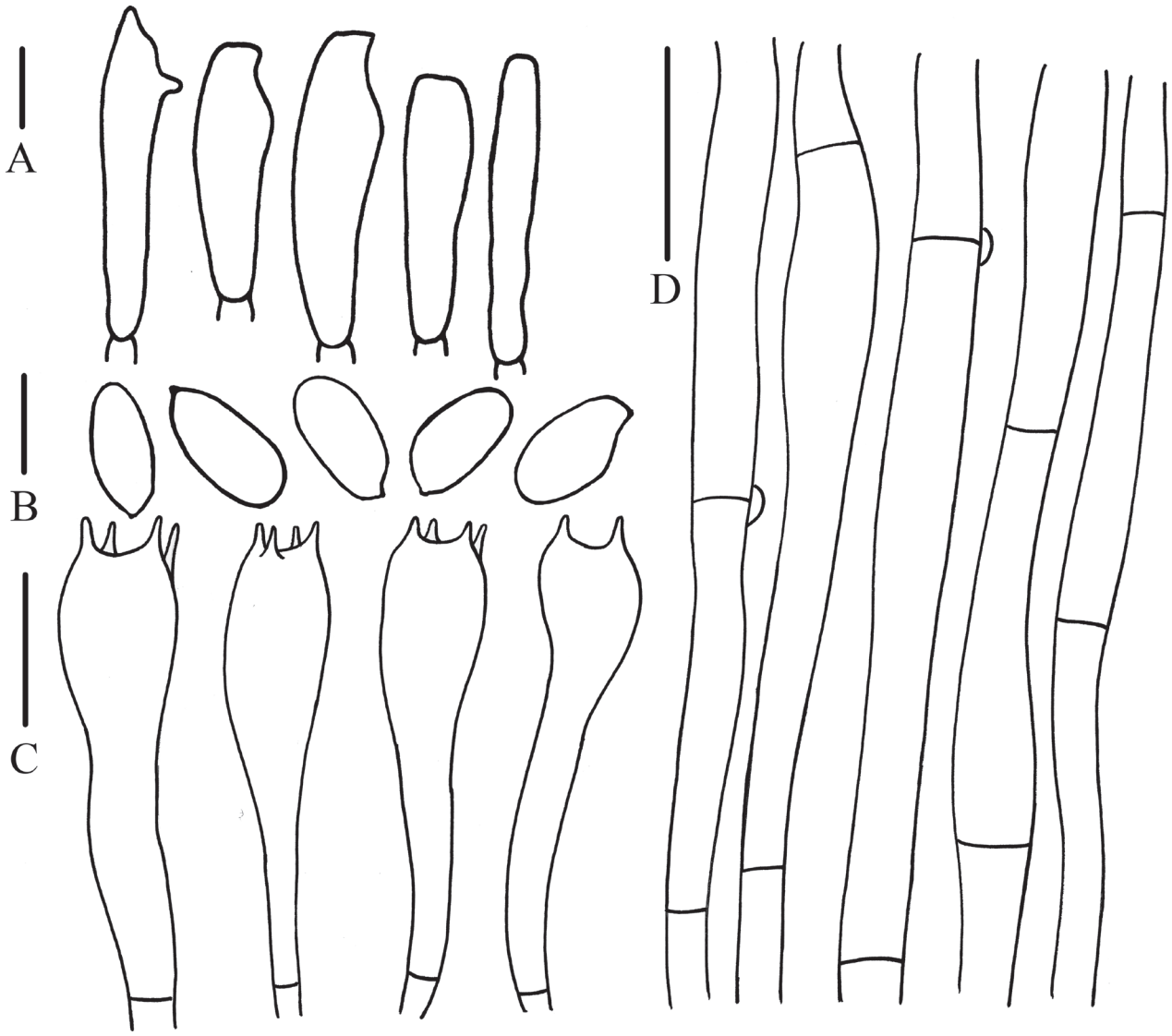

Figure 5. Microcharacteristics of *Calocybe cystidiosa* **A** cheiocystidia **B** basidiospores **C** basidia **D** pileipellis. Scale bars: 5 µm (**A, B**); 10 µm (**C, D**).

Description. Basidiomata solitary to gregarious, small to medium. Pileus 1.8–3.7 cm diameter, convex when young, plane and umbonatus when mature, smooth, dull, flesh-pink (7B4), entire; margin entire, inrolled to incurved. Lamellae white (7A1) to cream (30A2), subdecurrent, adnate, crowded, with a serious lamellulae. Stipe 2.8–4.5 cm long and 0.3–0.6 cm wide, central, paler pink (7B3) to pink (7B44), white (7A1) at apex, solid when younger, then becoming hollow, cylindrical, smooth, fibrous, slightly enlarged towards the base, with white tomentose at base. Context white (7A1), thin, odorless, tastes mild and not distinctive.

Basidiospores (4.0)5.0–6.5(6.9) × (2.0)2.1–2.5 µm, Q = (2.00)2.27–3.00(3.10), Qm = 2.58, hyaline, oval, smooth, inamyloid, thin-walled. Basidia 22.0–28.0 × 5.0–7.0 µm, clavate to cylindrical, 2- or 4-spored, hyaline, thin-walled. Hymenophoral trama regular and hyphae arranged parallel, not pigmented. Cheilocystidia 13.0–20.0 × 3.0–6.0 µm, clavate with an umbo occasionally, or bifurcated, hyaline, thin-walled. Pileipellis hyphae wide 5.0–12.0 µm diameter, smooth, hyaline, thin-walled. Stipitipellis hyphae 3.8–9.0 µm diameter, hyaline, thin-walled. Clamp connections present.

Additional specimens examined. China. Liaoning Province, Fushun City, Xinbin Manchu Autonomous County, Gangshan Provincial Forest Park, Fushun City, 23 June 2018, Ao Ma, HMJAU48269.

Habitat. Grows on the leaf litter in coniferous forests.

Comments. This species is characterized by its growth on the leaf litter in coniferous forests, flesh-pink pileus, fibrous stipe covered with white tomentose at the base, non-cellular pileipellis, larger basidiospores, and the presence of cheilocystidia. These characteristics suggest that *C. cystidiosa* belongs to Sect. *Carneoviolaceae* according to Singer's opinion (Singer 1986).

This species is closely related to *C. carnea* due to its pinkish pileus. However, this species can be distinguished from *C. carnea* by its unique habitat, deep color of basidiomata, light yellow lamellae, and larger basidiospores. In the Sect. *Carneoviolaceae*, *C. vinacea* J.Z. Xu & Yu Li is another species recorded from China with pinkish basidiomata. However, *C. vinacea* differs from this species by the curved margin of pileus, white stipe, smaller basidiospores, and the absence of cystidia (Xu et al. 2021b).

***Calocybe decolorata* X.D. Yu & Jia J. Li**

Figs 4B, 6

Description. Basidiomata scattered or gregarious, small to medium. Pileus 1.3–5.0 cm diameter, convex to applanate, involute then becoming reflex, orange-brown (7C8) at center, paler outwards, smooth, hygrophanous; margin petaloid, wavy, orange (6B8). Lamellae subdecurrent, close, white (6A1) at first, black (6E2) at the base to the three-quarter towards the margin when mature, with 1–5 lamellulae, edge denticulate. Stipe 2.3–4.2 cm long and 0.3–0.9 cm wide, central, cylindrical, or enlarged at apex, light orange-brown (6A6), with green tone at center, covered with white tomentose at base, hollow when mature. Context fleshy, thin, odorless.

Basidiospores (2.0)2.9–5.0 × (1.5)2.0–3.2 μm, Q = (1.15)1.17–1.50(1.60), Qm = 1.34, subglobose, hyaline, inamyloid, smooth, thin-walled. Basidia 11.1–21.5 × 3.7–6.0 μm, clavate, 2-spored, occasionally 4-spored, hyaline, thin-walled. Hymenophoral trama regular and hyphae arranged parallel, not pigmented, 2–3 μm wide. Pileipellis an epicutis composed of dense, radially parallel, hyphae 2.5–11.3 μm in width, smooth, hyaline, terminal cells a bulbous shape. Stipitipellis hyphae smooth, pigmented, 2.5–8.8 μm diameter.

Specimen examined. China. Jilin Province, Changchun City, Jilin Agricultural University, 21 Aug 2019, Jia-Jun Hu and Gui-Ping Zhao, HMJAU48262 (Collection no.: Hu J.J. 591).

Habitat. Grows on the leaves' litter in broad-leaved forests.

Comments. This species was originally described from Liaoning Province, China by Li et al. (2017) and is mainly characterized by a brighter orange or yellow color pileus, light orange-brown stipe, and smaller basidiospores. The species was classified as a species of Sect. *Carneoviolaceae* based on its main morphological characteristics.

However, there are some differences between our specimen and the type specimen. The specimens observed in this study have bulbous-like terminal hyphae in the pileipellis, which were not described in the type species.

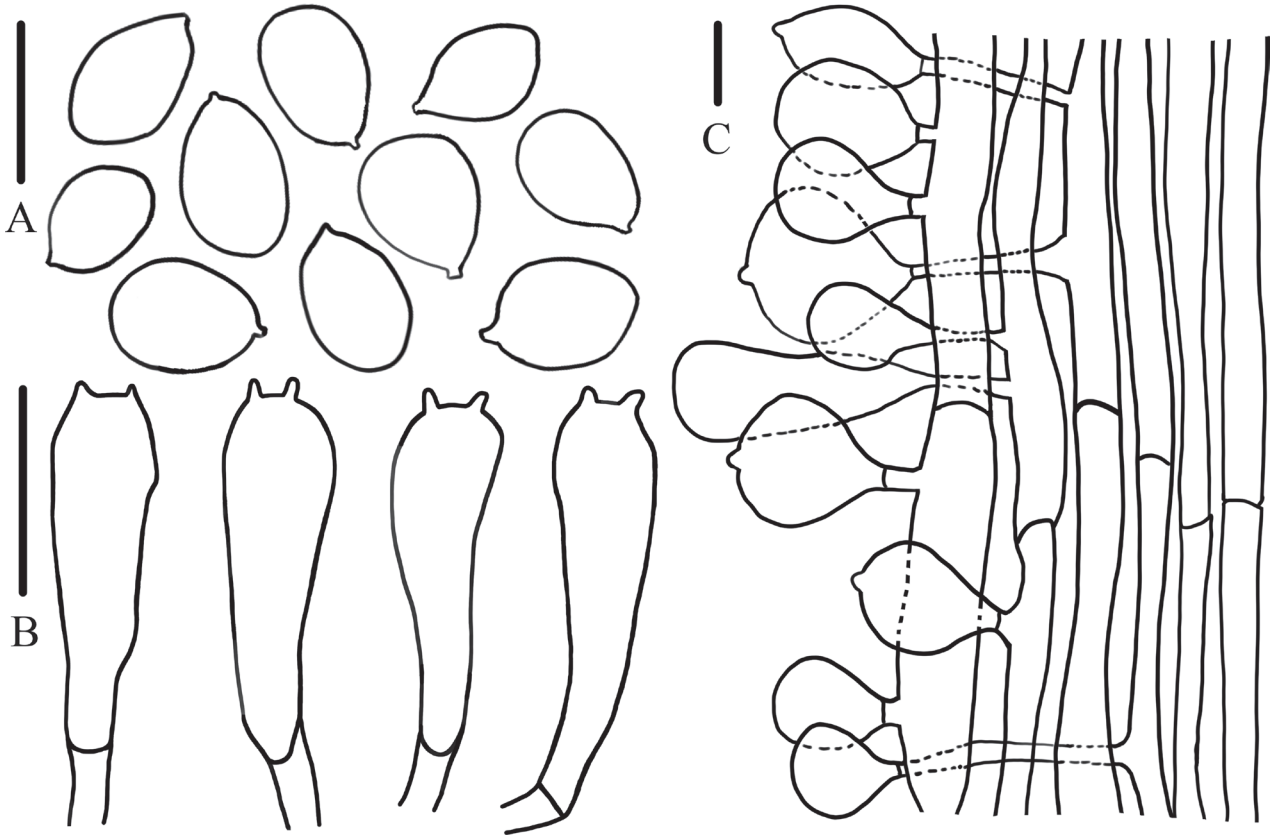

Figure 6. Microcharacteristics of *Calocybe decolorata* **A** basidiospores **B** basidia **C** pileipellis. Scale bars: 5 µm (**A**); 10 µm (**B, C**).

***Calocybe ionides* (Bull.) Donk**
Figs 4A, 7

Description. Basidiomata gregarious, small. Pileus 1.3–2.8 cm diameter, convex to oblate semispherical, with an umbo at center, hygrophanous, smooth, entire, involute, violet (16E8) to purple-black (17E8), occasionally deeper at center. Lamellae white (16A1), crowded, adnate, with 1–3 lamellulae. Stipe 1.5–3.0 cm long and 0.1–1.2 cm wide, center, paler violet (16E8), cylindrical, hollow, smooth, fibrous, covered with white tomentose at base. Context thin, white, fleshy, odorless.

Basidiospores (3.0)4.0–6.0 × (2.0)2.2–3.0 µm, Q = (1.50)1.67–2.40(2.50), Qm = 2.11, oblong, smooth, hyaline, inamyloid. Basidia 12.0–19.0 × 3.0–6.0 µm, clavate, 2- or 4- spored, hyaline, thin-walled. Pileipellis hyphae 3.0–6.0 µm wide, smooth, hyaline. Stipitipellis hyphae smooth, 3.0–7.5 µm wide, annulated, with a litter thick-walled.

Specimen examined. China. Jilin Province, Changchun City, Jingyuetan National Forest Park, 27 Aug 2019, Jia-Jun Hu and Gui-Ping Zhao, HMJAU48264; Liaoning Province, Fushun City, Xinbin Manchu Autonomous County, Gangshan Provincial Forest Park, 13 September 2018, Ao Ma, HMJAU 49165; Heilongjiang Province, Da Hinggan Ling Prefecture, Shuanghe National Nature Reserve, 18 July 2019, Di-Zhe Guo, HMJAU 48270.

Habitat. Grows on the leaf litter in coniferous or broad-leaved forests.

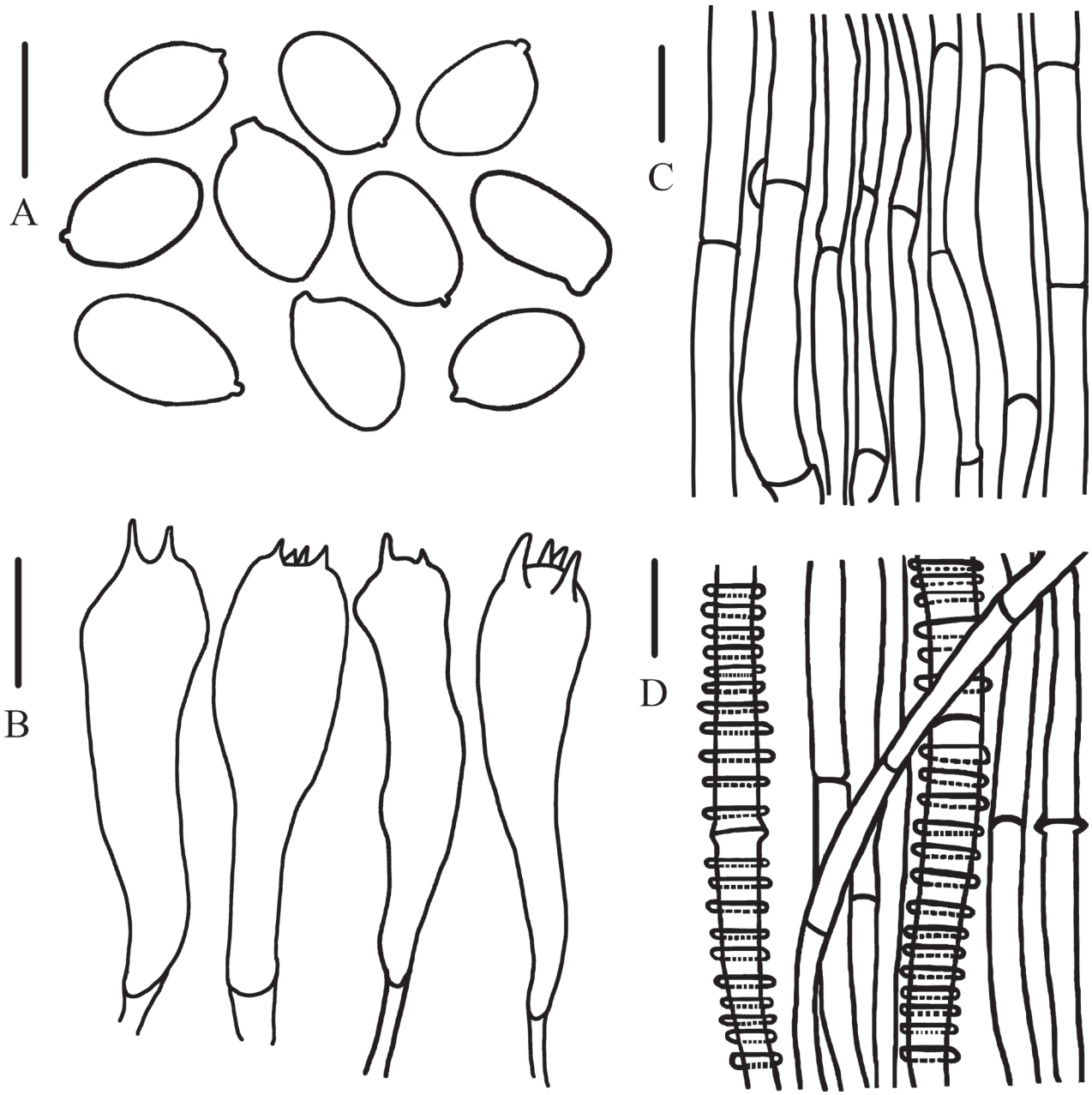

Figure 7. Microcharacteristics of *Calocybe ionides* **A** basidiospores **B** basidia **C** pileipellis **D** stipitipellis. Scale bars: 5 μm (**A**); 10 μm (**B–D**).

Comments. The main characteristics of this species are small basidiomata, a purple-blue color of the pileus, white lamellae, and a stipe that is either of the same color or lighter than the pileus. According to its main morphological characteristics, this species can be assigned to Sect. *Carneoviolaceae*.

Key to the reported species of *Calocybe* from northeast China

1 Pileus with orange to gray-brown tones, usually grows on coniferous forest, or mix **3**

– Pileus without orange-yellow to gray-brown tones, usually grows on broad-leaved forest **2**

2 Pileus with pink to red tones.....**7**
– Pileus without pink to red tones.....**11**
3 Lamellae blue when bruised, cystidia present.....***C. decolorata***
– Lamellae color unchanged when bruised, cystidia usually absent.....**4**
4 Lamellae yellow, covered with dense white fibrils at base .....***C. aurantiaca***
– Lamellae not yellow, not covered with dense white fibrils at base **5**
5 Pileipellis cellular, basidiospores subglobose.....***C. erminea***
– Pileipellis noncellular, basidiospores not subglobose.....**6**
6 Pileus felty, sterigmata shorter than 5 µm..... ***C. coacta***
– Pileus not felty, sterigmata longer than 5 µm..... ***C. longisterigma***
7 Pileus dull-red, color of stipe not similar with pileus .....***C. vinacea***
– Pileus not dull-red, color of stipe similar or paler than pileus **8**
8 Habitat is white birch forest, basidiomata grows on leaf litter of *Betula*..... .....***C. betulicola***
– Habitat not white birch forest, basidiomata does not grow on leaf litter of *Betula* **9**
9 Lamellae grayish-orange when bruised, stipe usually smooth....***C. fulvipes***
– Lamellae unchanged, greyish-orange when bruised, stipe not smooth.....**10**
10 Stipe turn purple when mature, cystidia not present .....***C. decurrens***
– Stipe does not turn purple when mature, cystidia present ..... ***C. cystidiosa***
11 Pileus with purple tones, pileipellis a trichoderm..... ***C. ionides***
– Pileus without purple tones, pileipellis not trichoderm.....**12**
12 Stipe with white pubescence at base, basidiospores biger than 5 µm..... .....***C. badiofloccosa***
– Stipe without white pubescence at base, basidiospores shorter than 5 µm .....***C. convexa***

Discussion

The genus *Calocybe* exhibits a wide distribution in China, but the full extent of its species diversity remains uncertain. This study provides a detailed description of two new species, namely *C. betulicola* and *C. cystidiosa*, as well as one previously unrecorded species, *C. decolorata*, found in Jilin Province. Additionally, a common species, *C. ionides*, was also identified in northeastern China. Moreover, the phylogenetic analysis confirmed all of the species that were previously reported.

The phylogenetic analysis, based on the combined ITS, nLSU, and *tef1-α* dataset, revealed that Lyophyllaceae forms a monophyletic clade. Moreover, the Lyophyllaceae clade was divided into six subclades, representing six independent genera, viz. *Calocybe*, *Lyophyllum*, and *Tricholomella*, etc. In addition, the genus *Calocybe* forms a monophyletic clade with "*Rugosomyces*", consisting of Bellanger et al. (2015), Li et al. (2017), and Xu et al. (2021a). Thus, the demarcation between the genus *Calocybe* and other genera within the Lyophyllaceae family is more distinct.

However, our phylogenetic analysis reveals certain discrepancies when compared to the findings of Li et al. (2017) and Xu et al. (2021a). In the present study, we identified six distinct sectional clades within the genus *Calocybe*, supported by robust evidence. These clades have been designated as clade I to clade VI. Notably, a new sectional clade, referred to as clade VI, has been identified for the first time in this study. This clade (clade VI) is featured by the

presence of a pinkish to reddish pileus and primarily consists of two newly discovered species, namely *C. carnea*, and *C. persicolor*, etc.

In addition, Clade I consists of *Calocybe onychina* (Fr.) Donk, *Calocybe naucoria* (Murrill) Singer, and *Calocybe erminea* J.Z. Xu & Yu Li, etc., distinguished by a pileus that ranges in color from white to yellow. The Clade II comprises primarily of *Calocybe obscurissima* (A. Pearson) M.M. Moser, *Calocybe lilacea* X.D. Yu, Ye Zhou & W.Q. Qin, *Calocybe graveolens* (Pers.) Singer, etc., characterized by pileus color ranging from white, yellow to violet shades. The Clade III consistent with *Calocybe chrysenteron* (Bull.) Singer, *C. aurantiaca*, and *Calocybe pseudoflammula* (J.E. Lange) M. Lange ex Singer, and is characterized by a yellow pileus. The main distinguishing characteristics of Clade IV, which includes *C. gangraenosa* and *C. coacta*, are the white-colored to grayish-yellow pileus. The Clade V is distinguished by the presence of a gilded pileus and includes two species, *Calocybe ochracea* (R. Haller Aar.) Bon and *Calocybe favrei* (R. Haller Aar. & R. Haller Suhr) Bon.

Based on the findings of the present study, we increased the species diversity of the genus *Calocybe* in China. The taxonomic system of this genus remains a subject of debate due to insufficient species sampling and the inadequate genetic variation in the DNA loci. Therefore, additional evidence is needed to contribute to a more comprehensive understanding of the genus. Furthermore, despite the recent identification of new species of *Calocybe* from northeast China, the true extent of its species diversity remains uncertain and calls for a comprehensive systematic analysis.

Acknowledgements

The authors would like to express our great appreciation to Mr. Di-Zhe Guo from Hebei Normal University of Science and Technology for his kind help in specimen collections.

Additional information

Conflict of interest

The authors have declared that no competing interests exist.

Ethical statement

No ethical statement was reported.

Funding

This study is funded by the Research on the Creation of Excellent Edible Mushroom Resources and High Quality & Efficient Ecological Cultivation Technology in Jiangxi Province (20212BBF61002), the Diversity and conservation of characteristic macrofungi resources in different vegetation zones in Changbai Mountain of China (20230202119NC), Youth Doctoral Program of Zhejiang Normal University - Study on species diversity of macrofungi in Baishanzu National Park (2023QB043), Zhejiang Normal University Doctoral Initiation Fund (YS304024921), the Natural Science Foundation of China (Nos. 31970020), Investigation of macrofungal Resources in Tongjiang County, China, Investigation of macrofungal resources in Anhui Province, China (jwg202307), and Construction of edible mushroom resource bank and Fungal Resource Conservation System.

Author contributions

Conceptualization: BZ. Data curation: AM. Investigation: YHW, XFL, LY, AM, YQC, YLT, XW, JJH. Project administration: YL, BZ. Software: JJH, DD. Supervision: YL, BZ. Writing - review and editing: BZ.

Author ORCIDs

Ao Ma https://orcid.org/0000-0001-8635-9767
Jia-Jun Hu https://orcid.org/0000-0002-7562-7612
Yong-Lan Tuo https://orcid.org/0000-0001-6019-1038
Xue-Fei Li https://orcid.org/0009-0005-2556-6494
Dan Dai https://orcid.org/0000-0002-9642-2480
Bo Zhang https://orcid.org/0000-0001-9508-8188
Yu Li https://orcid.org/0000-0003-4719-7210

Data availability

All of the data that support the findings of this study are available in the main text.

References

Bau T, Wang CY, Li Y (2003) Notes on Basidiomycetes of Jilin Province (V). Journal of Fungal Research 1: 13–16. https://doi.org/10.13341/j.jfr.2003.01.010

Bellanger JM, Moreau PA, Corriol G, Bidaud A, Chalange R, Dudova Z, Richard F (2015) Plunging hands into the mushroom jar: A phylogenetic framework for Lyophyllaceae (Agaricales, Basidiomycota). Genetica 143(2): 169–194. https://doi.org/10.1007/s10709-015-9823-8

César E, Bandala VM, Montoya L, Ramos A (2018) A new *Gymnopus* species with rhizomorphs and its record as nesting material by birds (Tyrannideae) in the subtropical cloud forest from eastern Mexico. MycoKeys 21: 21–34. https://doi.org/10.3897/mycokeys.42.28894

Cubeta M, Echandi E, Abernethy T, Vilgalys R (1991) Characterization of anastomosis groups of binucleate *Rhizoctonia* species using restriction analysis of an amplified ribosomal RNA gene. Phytopathology 81(11): 1395–1400. https://doi.org/10.1094/Phyto-81-1395

Donk MA (1962) The generic names proposed for Agaricaceae. J. Cramer, Weinheim, German. Taxon 11(3): 75–104. https://doi.org/10.2307/1216021

Edler D, Klein J, Antonelli A, Silvestro D (2021) RaxmlGUI 2.0: A graphical interface and toolkit for phylogenetic analyses using RAxML. Methods in Ecology and Evolution 12(2): 373–377. https://doi.org/10.1111/2041-210X.13512

Fan YG, Bau T (2006) Notes on basidiomycetes of Jilin province (VII). Journal of Fungal Research 4: 34–37. https://doi.org/10.13341/j.jfr.2006.02.008

Floriani M, Vizzini A (2016) *Calocybe pilosella* sp. nov., a distinctive new lyophylloid agaric collected near Trento (Italy). Studi Trentini di Scienze Naturali 95: 17–24.

Gardes M, Bruns TD (1993) ITS primers with enhanced specificity for basidiomycetes-application to the identification of mycorrhizae and rusts. Molecular Ecology 2(2): 113–118. https://doi.org/10.1111/j.1365-294X.1993.tb00005.x

Garnica S, Weiss M, Walther G, Oberwinkler F (2007) Reconstructing the evolution of agarics from nuclear gene sequences and basidiospore ultrastructure. Mycological Research 111(9): 1019–1029. https://doi.org/10.1016/j.mycres.2007.03.019

Hall TA (1999) BioEdit: a user-friendly biological sequence alignment editor and analysis program for Windows 95/98/NT. Nuclc Acids Symposium Series 41: 95–98. doi:https://doi.org/10.1021/bk-1999-0734.ch008

Hofstetter V, Clémençon H, Vilgalys R, Moncalvo JM (2002) Phylogenetic analyses of the Lyophylleae (Agaricales, Basidiomycota) based on nuclear and mitochondrial rDNA sequences. Mycological Research 106(9): 1043–1059. https://doi.org/10.1017/S095375620200641X

Hu JJ, Song LR, Tuo YL, Zhao GP, Lei Y, Zhang B, Li Y (2022a) Multiple evidences reveal new species and a new record of smelly *Gymnopus* (Agaricales, Omphalotaceae) from China. Frontiers in Microbiology 13: 968617. https://doi.org/10.3389/fmicb.2022.968617

Hu JJ, Zhao GP, Tuo YL, Rao G, Zhang ZH, Qi ZX, Yue L, Liu YJ, Zhang T, Li Y, Zhang B (2022b) Morphological and Molecular Evidence Reveal Eight New Species of *Gymnopus* from Northeast China. Journal of Fungi 8(4): 349. https://doi.org/10.3390/jof8040349

Kalyaanamoorthy S, Minh BQ, Wong TK, Von Haeseler A, Jermiin LS (2017) ModelFinder: Fast model selection for accurate phylogenetic estimates. Nature Methods 14(6): 587–589. https://doi.org/10.1038/nmeth.4285

Katoh K, Standley DM (2013) MAFFT multiple sequence alignment software version 7: Improvements in performance and usability. Molecular Biology and Evolution 30(4): 772–780. https://doi.org/10.1093/molbev/mst010

Kühner R, Romagnesi H (1953) Flore analytique des champignons supérieurs (agarics,bolets,chanterelles). Masson et Cie, Paris, France.

Li JJ, Wu SY, Yu XD, Zhang SB, Cao DX (2017) Three new species of *Calocybe* (Agaricales, Basidiomycota) from northeastern China are supported by morphological and molecular data. Mycologia 109(1): 55–63. https://doi.org/10.1080/00275514.2017.1286570

Mao XL (2000) The macrofungi in China. Henan science and technology press, Zhengzhou, China.

Matheny PB, Curtis JM, Hofstetter VM, Aime MC, Moncalvo JM, Ge ZW, Yang ZL, Slot JC, Ammirati JF, Baroni TJ, Bougher NL, Hughes KW, Lodge DJ, Kerrigan RW, Seidl MT, Aanen DK, DeNitis M, Daniele GM, Desjardin DE, Kropp BR, Norvell LL, Parker A, Vellinga EC, Vilgalys R, Hibbett DS (2006) Major clades of *Agaricales*: A multilocus phylogenetic overview. Mycologia 98(6): 984–997. https://doi.org/10.1080/15572536.2006.11832627

Moncalvo JM, Vilgalys R, Redhead SA, Johnson JE, James TY, Aime MC, Hofstetter V, Verduin SJ, Larsson E, Baroni TJ (2002) One hundred and seventeen clades of euagarics. Molecular Phylogenetics and Evolution 23(3): 57–400. https://doi.org/10.1016/S1055-7903(02)00027-1

Mu L, Bau T (2023) A new species of *Calocybe* (Agaricales, Basidiomycota) from China. Phytotaxa 600(2): 73–78. https://doi.org/10.11646/phytotaxa.600.2.2

Qi Y, Xu A, Zhou Y, Bi K, Qin W, Guo H, Yu X (2022) Morphological and phylogenetic studies of three new species of *Calocybe* (Agaricales, Basidiomycota) from China. Diversity 14(8): 643. https://doi.org/10.3390/d14080643

Ranwez V, Douzery EJ, Cambon C, Chantret N, Delsuc F (2018) MACSE v2: Toolkit for the alignment of coding sequences accounting for frameshifts and stop codons. Molecular Biology and Evolution 35(10): 2582–2584. https://doi.org/10.1093/molbev/msy159

Rehner SA, Samuels GJ (1994) Taxonomy and phylogeny of *Gliocladium* analysed from nuclear large subunit ribosomal DNA sequences. Mycological Research 98(6): 625–634. https://doi.org/10.1016/S0953-7562(09)80409-7

Ronquist F, Huelsenbeck JP (2003) MrBayes 3: Bayesian phylogenetic inference under mixed models. Bioinformatics 19(12): 1572–1574. https://doi.org/10.1093/bioinformatics/btg180

Royal Botanic Garden E (1969) Flora of British fungi: colour identification chart. HM Stationery Office.

Singer R (1962) The Agaricales in modern taxonomy 2ED. J. Cramer, Germany.

Singer R (1986) The Agaricales in modern taxonomy 4ED. Koeltz Botanical Books, Koenigstein, Germany.

Tai FL (1979) Sylloge Fungorum Sinicorum. Science Press, Academic Sinica, Beijing, China, 419–420.

Thompson JD, Gibson TJ, Plewniak F, Jeanmougin F, Higgins DG (1997) The CLUSTAL X windows interface: Flexible strategies for multiple sequence alignment aided by quality analysis tools. Nucleic Acids Research 25(24): 4876–4882. https://doi.org/10.1093/nar/25.24.4876

Van de Peppel LJJ, Aime MC, Læssøe T, Pedersen OS, Coimbra VRM, Kuyper TW, Stubbe D, Aanen DK, Baroni TJ (2022) Four new genera and six new species of lyophylloid agarics (Agaricales, Basidiomycota) from three different continents. Mycological Progress 21(10): 1–14. https://doi.org/10.1007/s11557-022-01836-7

Vilgalys R, Hester M (1990) Rapid genetic identification and mapping of enzymatically amplified ribosomal DNA from several *Cryptococcus* species. Journal of Bacteriology 172(8): 4238–4246. https://doi.org/10.1128/jb.172.8.4238-4246.1990

Vizzini A, Antonin V, Sesli E, Contu M (2015) *Gymnopus trabzonensis* sp. nov. Omphalotaceae and *Tricholoma virgatum* var. *fulvoumbonatum* var. nov. Tricholomataceae, two new white-spored agarics from Turkey. Phytotaxa 226(2): 119–130. https://doi.org/10.11646/phytotaxa.226.2.2

Xu JZ, Yu XD, Zhang CL, Li Y (2019) Two new species of *Calocybe* (Lyophyllaceae) from northeast China. Phytotaxa 425(4): 219–232. https://doi.org/10.11646/phytotaxa.425.4.3

Xu JZ, Yu X, Suwannarach N, Jiang Y, Zhao W, Li Y (2021a) Additions to Lyophyllaceae s.l. from China. Journal of Fungi 7(12): 1101. https://doi.org/10.3390/jof7121101

Xu JZ, Yu XD, Zhang CL, Li Y (2021b) Morphological characteristics and phylogenetic analyses revealed a new *Calocybe* (Lyophyllaceae, Basidiomycota) species from northeast China. Phytotaxa 490(2): 203–210. https://doi.org/10.11646/phytotaxa.490.2.7

Zhang D, Gao F, Jakovlić I, Zou H, Zhang J, Li WX, Wang GT (2020) PhyloSuite: An integrated and scalable desktop platform for streamlined molecular sequence data management and evolutionary phylogenetics studies. Molecular Ecology Resources 20(1): 348–355. https://doi.org/10.1111/1755-0998.13096

Zhou Y (2022) Morphological classification and molecular systematics of *Calocybe*. Master's thesis, Shenyang agricultural university, Shenyang, China.

MycoKeys 103: 57–70 (2024)
DOI: 10.3897/mycokeys.103.119027

Research Article

Molecular and morphological data reveal two new species of *Tropicoporus* (Hymenochaetaceae, Basidiomycota) from Australia and tropical Asia

An-Hong Zhu[1,2*], Zhan-Bo Liu[1*], Yue Li[1], Hong-Gao Liu[3,4], Yuan Yuan[1], Shuang-Hui He[1]

1 *State Key Laboratory of Efficient Production of Forest Resources, School of Ecology and Nature Conservation, Beijing Forestry University, Beijing, 100083, China*
2 *Rubber Research Institute, Chinese Academy of Tropical Agricultural Sciences, Haikou, 571101, China*
3 *Yunnan Key Laboratory of Gastrodia and Fungi Symbiotic Biology, Zhaotong University, Zhaotong, 657000, China*
4 *Yunnan Engineering Research Center of Green Planting and Processing of Gastrodia, Zhaotong University, Zhaotong, 657000, China*
Corresponding authors: Yuan Yuan (yuanyuan1018@bjfu.edu.cn); Shuang-Hui He (heshuanghui@bjfu.edu.cn)

Abstract

Phylogenetic analyses and morphological examination confirmed two new species in the tropical polypore genus *Tropicoporus*, *T. oceanianus* and *T. zuzaneae*, from Australia and tropical Asia, respectively. A phylogenetic analysis based on the two DNA markers including the nuclear ribosomal internal transcribed spacer (ITS) region and the large subunit (nLSU) gene shows that these two new species form two independent lineages nested in the genus *Tropicoporus*. *T. oceanianus* is characterized by perennial and ungulate basidiomata, the occasional presence of hymenial setae, a trimitic hyphal structure in the context and a dimitic hyphal system in the trama, and broadly ellipsoid to subglobose basidiospores measuring 5.2–6 × 4–5 µm. *T. zuzaneae* is characterized by perennial and resupinate basidiomata with distinct receding margin, glancing pores, very thin to almost lacking subiculum, a dimitic hyphal structure, the absence of any setal elements, broadly ellipsoid to subglobose basidiospores measuring 3.8–4.9 × 3–4.2 µm. The differences among the new species and their phylogenetically related and morphologically similar species are discussed.

Key words: *Phellinus*, Phylogenetic analysis, polypore, wood-rotting fungi

Academic editor: R. Henrik Nilsson
Received: 18 January 2024
Accepted: 29 February 2024
Published: 19 March 2024

Citation: Zhu A-H, Liu Z-B, Li Y, Liu H-G, Yuan Y, He S-H (2024) Molecular and morphological data reveal two new species of *Tropicoporus* (Hymenochaetaceae, Basidiomycota) from Australia and tropical Asia. MycoKeys 103: 57–70. https://doi.org/10.3897/mycokeys.103.119027

Introduction

Tropicoporus L.W. Zhou et al. (Hymenochaetaceae, Basidiomycota) is mainly a tropical polypore genus, and it is characterized by annual to perennial, resupinate to distinctly pileate basidiomata with yellow-brown to umber pore surface, a dimitic hyphal system at least in the trama, the presences of hymenial setae, and yellowish, slightly thick-walled, smooth, and usually collapsed basidiospores which become darker in a 5% KOH solution in a few species (Salvador-Montoya et al. 2018, 2020). Most species of the genus grow on angiosperm wood and cause a white rot (Zhou et al. 2016). As of early 2024, 49 species are

* These authors have contributed equally to this work and share first authorship.

accepted in the genus, 40 species exist in tropical region, and 25 species occur in tropical Asia and Australia (Tian et al. 2013; Xavier de Lima et al. 2022; Wu et al. 2022a, b; Gunaseelan et al. 2024; Liu et al. 2024). *Tropicoporus excentrodendri* L.W. Zhou & Y.C. Dai is the type species of the genus.

Tropical Pacific areas are rich for species of Hymenochaetales, and many new taxa have been described from these areas recently (Ji et al. 2017; Bian and Dai 2020; Chen et al. 2020; Du et al. 2020; Guo et al. 2022; Wu et al. 2022a; Zhao et al. 2022; Cui et al. 2023; Dong et al. 2023). However, there are still many unknown taxa in Hymenochaetales from certain regions of tropical Pacific areas.

A study on tropical polypores recovered four specimens from Australia and tropical Asia that morphologically fit the definition of *Tropicoporus*. Phylogenetic analyses assigned these specimens to two independent lineages nested in the *Tropicoporus* clade. Morphological comparison with all the taxa in *Phellinus* s.l. was carried out, and no existing taxa fit them. We thus describe two new species based on our studied samples and molecular data.

Materials and methods

Morphological studies

The studied specimens are deposited in the Fungarium of the Institute of Microbiology, Beijing Forestry University (BJFC), the private herbarium of Josef Vlasák (JV), and the Royal Botanic Gardens Victoria (MEL). Morphological descriptions are based on field notes and voucher specimens. The microscopic analysis follows Dai (2010) and Wu et al. (2022a). Sections were studied at a magnification of up to 1 000× using a Nikon Eclipse 80i microscope and phase contrast illumination. Microscopic features and measurements were made from slide preparations stained with Cotton Blue and Melzer's reagent. Basidiospores were measured from sections cut from the tubes stained with Cotton Blue. To represent the variation in the size of spores, 5% of measurements were excluded from each end of the range and are given in parentheses. In the description: KOH = 5% potassium hydroxide, IKI = Melzer's reagent, IKI– = neither amyloid nor dextrinoid, CB = Cotton Blue, CB(+)= weakly cyanophilous in Cotton Blue, CB– = acyanophilous in Cotton Blue, L = arithmetic average of spore length, W = arithmetic average of spore width, Q = L/W ratios, and n = number of basidiospores/measured from given number of specimens. Color terms follow Anonymous (1969) and Petersen (1996).

DNA extraction, amplification, and sequencing

A CTAB rapid plant genome extraction kit-DN14 (Aidlab Biotechnologies Co., Ltd, Beijing) was used to obtain DNA from dried specimens, and to perform the polymerase chain reaction (PCR) according to the manufacturer's instructions with some modifications (Han et al. 2016; Cui et al. 2019). The nuclear ribosomal internal transcribed spacer (ITS) and large subunit nuclear ribosomal (nLSU) RNA gene were amplified using the primer pairs ITS5/ITS4 and LR0R/LR7 (White et al. 1990; Hopple and Vilgalys 1999) (https://sites.duke.edu/vilgalyslab/rdna_primers_for_fungi/).

The PCR procedure for ITS was as follows: initial denaturation at 95 °C for 3 min, followed by 34 cycles at 94 °C for 40 s, annealing at 54 °C for 45 s and extension 72 °C for 1 min, and a final extension of 72 °C for 10 min. The PCR procedure for nLSU was as follows: initial denaturation at 94 °C for 1 min, followed by 34 cycles of denaturation at 94 °C for 30 s, annealing at 50 °C for 1 min and extension at 72 °C for 1.5 min, and a final extension at 72 °C for 10 min. The PCR products were purified and sequenced at the Beijing Genomics Institute (BGI), China, with the same primers. DNA sequencing was performed at the Beijing Genomics Institute and the newly generated sequences were deposited in GenBank. All sequences analysed in this study are listed in Table 1. Sequences generated from this study were aligned with additional sequences downloaded from GenBank using BioEdit (Hall 1999). The final ITS and nLSU datasets were subsequently aligned using MAFFT v.7 under the G-INS-i strategy with

Table 1. Taxa information and GenBank accession numbers of the sequences used in this study. New species are shown in bold. * Holotype.

Species	Locality	Voucher No.	GenBank accession numbers	
			ITS	nLSU
Inonotus compositus	China	Wang 552	KP030781	KP030768
Inonotus cuticularis	Canada	QFB-888	AF237730	–
Perenninotus shoreicola	China	Dai 13614	KJ575522	KT749416
Perenninotus shoreicola	China	Dai 13615	KJ575523	KT749417
Sanghuangporus alpinus	China	Cui 9658 *	JQ860310	KP030771
Sanghuangporus alpinus	China	Cui 9646	JQ860313	–
Sanghuangporus australianus	Australia	Dai 18847 *	MZ484581	MZ437411
Sanghuangporus lagerstroemiae	Vietnam	Dai 18337 *	MZ484582	MZ437412
Sanghuangporus lonicericola	China	Cui 10994	MF772786	MF772804
Sanghuangporus lonicericola	China	Dai 8376	JQ860308	KP030772
Sanghuangporus pilatii	Czechia	BRNM 771989	KT428764	KT428765
Sanghuangporus sanghuang	China	Wu 0903-1	JN794061	–
Sanghuangporus weigelae	China	Yuan 5526	JN169786	JN169790
Tropicoporus angustisulcatus	Brazil	Dai 17409 *	MZ484584	MZ437417
Tropicoporus angustisulcatus	French Guiana	JV 1808/83	MZ484585	MZ437418
Tropicoporus boehmeriae	China	Dai 20522	MZ484586	MZ437419
Tropicoporus boehmeriae	China	Dai 20617	MZ484587	MZ437420
Tropicoporus boehmeriae	Thailand	LWZ 20140729-10 *	KT223640	–
Tropicoporus cleistanthicola	India	MUBL1089 *	OR272292	OR272337
Tropicoporus cleistanthicola	India	MUBL1090	OR272291	OR272336
Tropicoporus cubensis	Cuba	MUCL 47079 *	JQ860325	KP030776
Tropicoporus cubensis	Cuba	MUCL 47113	JQ860324	KP030777
Tropicoporus dependens	USA	JV 0409/12-J	KC778777	MF772818
Tropicoporus dependens	USA	JV 1207/3.4-J	KC778779	–
Tropicoporus detonsus	USA	IDR 1300012986	KF695121	KF695122
Tropicoporus detonsus	French Guiana	MUCL 45517	MZ484589	EF429237
Tropicoporus drechsleri	Argentina	CTES 570140	MG242439	MG242444
Tropicoporus drechsleri	Argentina	CTES 570144 *	MG242437	MG242442
Tropicoporus excentrodendri	China	Yuan 6227	KP030788	–
Tropicoporus excentrodendri	China	Yuan 6232 *	KP030790	–

Species	Locality	Voucher No.	GenBank accession numbers	
			ITS	nLSU
Tropicoporus flabellatus	Brazil	VRTO873 *	MT908376	MT906643
Tropicoporus flabellatus	Brazil	JB7	MT925653	MT925654
Tropicoporus guanacastensis	Costa Rica	JV 1408/25	KP030793	KP030778
Tropicoporus guanacastensis	Costa Rica	O 19228	KP030794	MF772819
Tropicoporus hainanicus	China	Dai 17705 *	MZ484588	MZ437421
Tropicoporus indicus	India	MUBL1083 *	OR272293	OR272338
Tropicoporus indicus	India	MUBL1084	OR272294	OR272339
Tropicoporus lineatus	Malaysia	Dai 21196 *	MZ484594	MZ437426
Tropicoporus linteus	USA	JV 0904/140	JQ860323	KP030780
Tropicoporus linteus	USA	JV 0904/64	JQ860322	JX467701
Tropicoporus melleoporus	USA	CBS 145357	NR_168219	NG_068906
Tropicoporus melleoporus	USA	TX8	MN108123	MN113949
Tropicoporus minor	China	Dai 18487A	MZ484590	MZ437422
Tropicoporus minor	Malaysia	Dai 18601	MZ484591	MZ437423
Tropicoporus minor	Malaysia	Dai 21139 *	MZ484592	MZ437424
Tropicoporus minor	Malaysia	Dai 21183	MZ484593	MZ437425
Tropicoporus natarajaniae	India	MUBL4020 *	OP003882	–
Tropicoporus nullisetus	Brazil	VRTO195	MN795118	MN812254
Tropicoporus nullisetus	Brazil	VRTO131	MN795117	MN812253
Tropicoporus nullisetus	Brazil	VXLF616 *	MN795129	MN812261
***Tropicoporus oceanianu*s**	**Australia**	**Dai 18859 ***	**PP034280**	–
Tropicoporus oceanianus	**Australia**	**MEL 2382654**	**KP013017**	**KP013017**
Tropicoporus oceanianus	**Australia**	**MEL 2382727**	**KP012908**	**KP012908**
Tropicoporus oceanianus	**Australia**	**MEL 2382781**	**KP012961**	**KP012961**
Tropicoporus pseudoindicus	MUBL1087	India *	OR272295	OR272340
Tropicoporus pseudoindicus	MUBL1088	India	OR272296	OR272341
Tropicoporus pseudolinteus	USA	JV 0312/22.10-J	KC778780	–
Tropicoporus pseudolinteus	Venezuela	JV 0404/35-K *	KC778781	MF772820
Tropicoporus pseudolinteus	Costa Rica	O 906288	KP030795	–
Tropicoporus ravidus	China	Dai 18165 *	MZ484595	MZ437427
Tropicoporus rudis	Rwanda	O 915614	KP030796	–
Tropicoporus rudis	Tanzania	O 915617	KP030797	MH101016
Tropicoporus sideroxylicola	USA	JV 0409/30-J *	KC778782	–
Tropicoporus sp.	Brazil	URM 80348	MZ484596	MZ437428
Tropicoporus stratificans	Brazil	SMDB 14731	KM199688	–
Tropicoporus subramaniae	India	MUBL4021 *	OP003881	–
Tropicoporus substratificans	French Guiana	JV 1908/80 *	MZ484597	MZ437429
Tropicoporus substratificans	Brazil	VRTO884	MN795124	MN812266
Tropicoporus tamilnaduensis	India	MUBL1085 *	OR272297	OR272343
Tropicoporus tamilnaduensis	India	MUBL1086	–	OR272344
Tropicoporus tenuis	China	Dai 19699 *	MZ484598	MZ437430
Tropicoporus tenuis	China	Dai 19724	MZ484599	MZ437431
Tropicoporus zuzaneae	**China**	**Dai 22168**	**PP034281**	**PP034283**
Tropicoporus zuzaneae	**China**	**Dai 22171 ***	**PP034282**	**PP034284**
Tropicoporus zuzaneae	**Indonesia**	**JV 1502/5-Zuz**	**PP383896**	**–**
Tropicoporus zuzaneae	**Thailand**	**TBP00705**	**KT800054**	**–**
Tropicoporus zuzaneae	**Thailand**	**BCC 23706**	**KP059109**	**KP059108**

no cost for opening gaps and equal cost for transformations (command line: mafft –genafpair –maxiterate 1000) (Katoh and Standley 2013) and visualized in BioEdit (Hall 1999).

Phylogenetic analyses

The two genetic markers were concatenated into a single multiple sequence alignment for phylogenetic analysis (TreeBase accession ID 31179; Study Accession URL: http://purl.org/phylo/treebase/phylows/study/TB2:S31179). Sequences of *Phellinus betulinus* (Murrill) Parmasto, obtained from GenBank, were used as the outgroups following Wu et al. (2022a). The phylogenetic analyses followed the approach of Du et al. (2021). Maximum Likelihood (ML) and Bayesian Inference (BI) analyses were performed based on the two datasets. The best-fit evolutionary model was selected by Hierarchical Likelihood Ratio Tests (HLRT) and Akaike Information Criterion (AIC) in MrModeltest 2.2 (Nylander 2004) after scoring 24 models of evolution in PAUP* version 4.0 beta 10 (Swofford 2002).

Sequences were analysed using Maximum Likelihood (ML) with RAxML-HPC through the CIPRES Science Gateway (www.phylo.org; Miller et al. 2009). Branch support for ML analysis was determined by 1000 bootstrap replicates. Bayesian phylogenetic inference was done in MrBayes 3.2.7a (Ronquist et al. 2012). Four Markov chains were run for 2 million generations (2-gene dataset) until the split deviation frequency value was less than 0.01, and trees were sampled every 1000 generations. The first 25% of the sampled trees were discarded as burn-in and the remaining ones were used to reconstruct a majority rule consensus and calculate Bayesian Posterior Probabilities (BPP) of the clades. All trees were viewed in FigTree v. 1.4.3 (http://tree.bio.ed.ac.uk/software/figtree/). Branches that received ML bootstrap support of at least ≥75% and BPP of at least ≥ 0.90 BPP were considered as significantly supported. The significant ML bootstrap values and the BBP are presented on the topology from the ML analysis, respectively.

Results

Molecular phylogeny

The concatenated two-marker dataset included sequences from 77 samples representing 41 taxa. The dataset had an aligned length of 2371 characters, of which 1664 (70%) were constant, 193 (8%) were variable and parsimony-uninformative, and 514 (22%) were parsimony informative. The phylogenetic reconstructions performed with Maximum Likelihood (ML) and Bayesian Inference (BI) analyses produced similar topologies and only minor differences in statistical support. The best model-fit applied in the Bayesian analysis was GTR+I+G. Bayesian analysis resulted in a nearly congruent topology with respect to the ML analysis, and thus only the ML tree is provided (Fig. 1). And the average standard deviation of split frequencies was 0.005467 (BI).

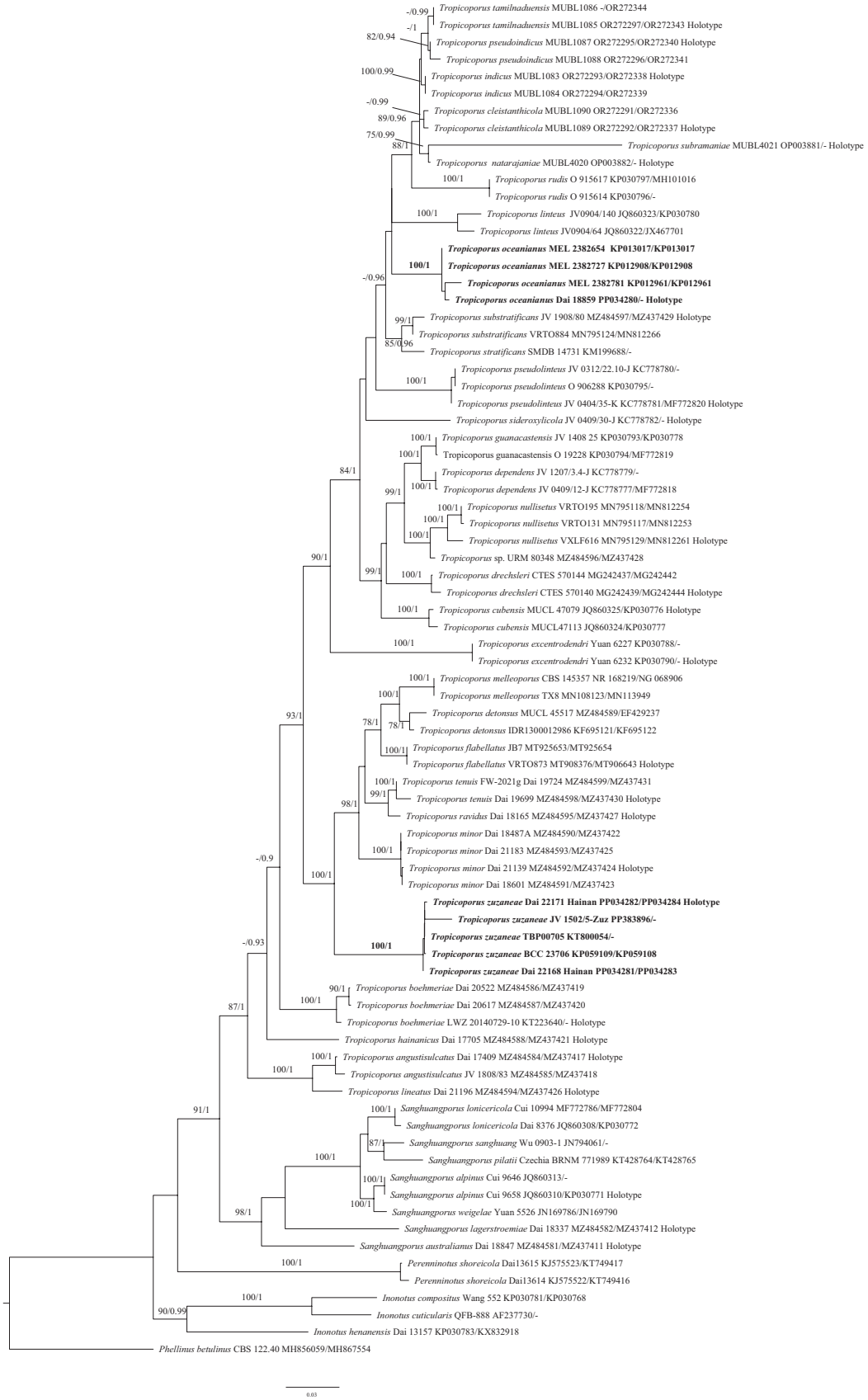

Figure 1. Phylogeny of *Tropicoporus* generated by ML analyses based on combined ITS+nLSU sequences. Branches are labelled with maximum likelihood bootstrap higher than 75% and Bayesian posterior probabilities higher than 0.90. New species are indicated in bold.

Taxonomy

***Tropicoporus oceanianus* A.H. Zhu, Yuan Yuan & S.H. He, sp. nov.**
MycoBank No: 851484
Figs 2, 3

Type. Australia. Queensland, Cains, Whitfield Conservation Park, on living tree of *Eucalyptus*, 18.V.2018, Dai 18859 (holotype, BJFC027327, isotype will be sent to MEL).

Etymology. *Oceanianus* (Lat.): refers to the species being found in Oceania.

Description. *Basidiomata*. Perennial, pileate, solitary, woody hard and without odor or taste when fresh, bone hard when dry; pilei ungulate to triquetrous, projecting up to 2 cm, 3 cm wide, and 2.5 cm thick at base; pileal surface vinaceous gray to black when fresh and dry, concentrically sulcate with narrow zones, velutinate to glabrous, encrusted with age, distinctly cracked; margin more or less acute, snuff brown. Pore surface fawn brown when fresh, becoming umber when dry, glancing; sterile margin fawn brown when fresh and dry, distinctly paler than pores, up to 2 mm wide; pores circular, 6–7 per mm; dissepiments thick, entire. Context homogeneous, fulvous, woody hard, up to 3 mm thick, a black crust present at pileal surface. Tubes concolorous with pore surface, bone hard to brittle, up to 22 mm long, annual layers indistinct.

***Hyphal structure*.** Hyphal system trimitic in context, dimitic in trama; generative hyphae simple septate; all hyphae IKI–, CB–; tissue becoming blackish brown in KOH.

***Context*.** Generative hyphae infrequent, pale yellowish, thin- to thick-walled, rarely branched, frequently septate, 2–3 µm in diam; skeletal hyphae dominant, yellowish to brown, thick-walled with a narrow to medium lumen, dichotomous-

Figure 2. Basidiomata of *Tropicoporus oceanianus* (Dai 18859, holotype).

ly branched like the so-called skeleto-binding hyphae, strongly flexuous, interwoven, skeletal parts 3–5 µm in diam.

***Trama of the tubes*.** Generative hyphae hyaline to pale yellowish, thin- to thick-walled, rarely branched, frequently septate, 2–2.5 µm in diam; skeletal hyphae thick-walled with a medium lumen, rarely branched, aseptate, flexuous, loosely interwoven, 2.5–3 µm in diam; hymenial setae occasionally present, subulate, dark brown, 22–30 × 4.5–6.5 µm; cystidioles present, fusoid, hyaline, thin-walled, 10–18 × 3.5–5 µm; basidia barrel-shaped, with four sterigmata and a simple septum at the base, 9–12 × 4–5 µm; basidioles capitate, slightly smaller than basidia.

***Spores*.** Basidiospores broadly ellipsoid to subglobose, thick-walled, mostly collapsed, IKI–, CB–, (5–)5.2–6(–6.1) × (3.8–)4–5(5.1) µm, L = 5.60 µm, W = 4.61 µm, Q = 1.21 (n = 30/1).

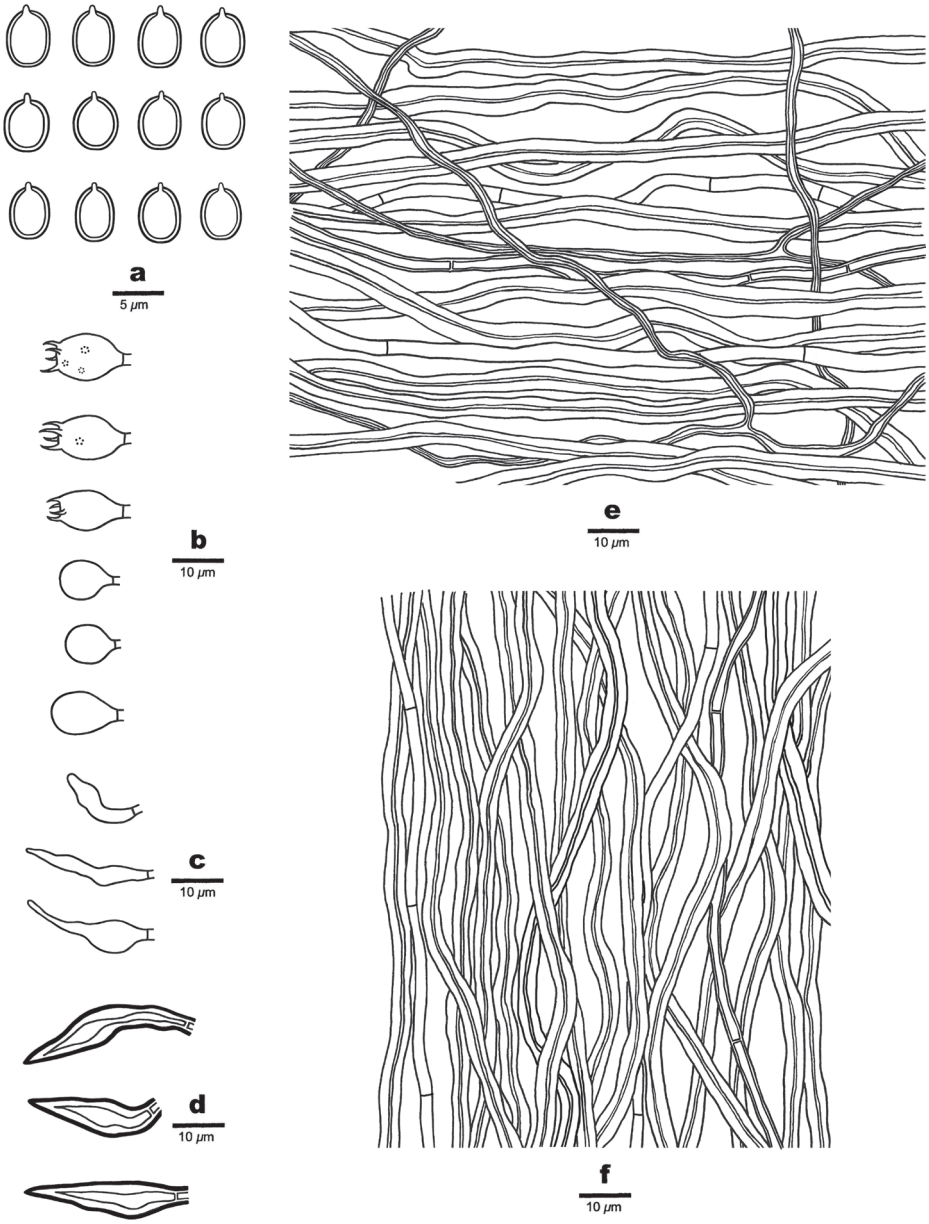

Figure 3. Microscopic structures of *Tropicoporus oceanianus* (drawn from the holotype Dai 18859) **a** basidiospores **b** basidia and basidioles **c** cystidioles **d** hymenial setae **e** hyphae from context **f** hyphae from trama. Scale bars: 5 µm (**a**); 10 µm (**b–f**).

Tropicoporus zuzaneae **A.H. Zhu, Yuan Yuan & S.H. He, sp. nov.**
MycoBank No: 851485
Figs 4, 5

Type. China. Hainan Province, Haikou, Guanlan Lake, on dead tree of *Sonneratia*, 28.XII.2020, Dai 22171 (holotype, BJFC036063).

Etymology. *Zuzaneae* (Lat.): in honour of the collector Zuzana Egertova.

Description. ***Basidiomata*****.** Perennial, resupinate, firmly attached to the substrate, corky and without distinctive odor or taste when fresh, hard corky when dry, up to 40 cm long, 3 cm wide, and 3 mm thick at center. Pore surface pinkish buff when fresh, fawn to snuff brown and cracked when dry, distinctly glancing; sterile margin paler than pores when fresh, pale mouse gray when dry, up to 3 mm wide, distinctly receding; pores angular to circular, 6–8 per mm; dissepiments thin, entire. Subiculum very thin to almost lacking, yellowish brown, corky, less than 0.1 mm thick. Tubes paler than pore surface, brittle, up to 2.9 mm long, annual layers indistinct.

Hyphal structure**.** Hyphal system dimitic; generative hyphae simple septate; all hyphae IKI–, CB–; tissue becoming blackish brown in KOH.

Subiculum**.** Generative hyphae hyaline to pale brownish, thin- to thick-walled, unbranched, frequently septate, 2–3 µm in diam; skeletal hyphae brownish, thick-walled with a wide lumen, unbranched, aseptate, strongly flexuous, interwoven, 2–3.5 µm in diam.

Trama of the tubes**.** Generative hyphae hyaline to pale yellowish, thin- to thick-walled, rarely branched, frequently septate, 1.8–2.8 µm in diam; skeletal hyphae yellowish, thick-walled with a wide lumen, unbranched, aseptate, more or less straight, subparallel along tubes, 2.5–3 µm in diam; hymenial setae absent; cystidioles present, fusoid, hyaline, thin-walled, 15–20 × 3.5–4.5 µm; basidia barrel-shaped, with four sterigmata and a simple septum

Figure 4. Basidiomata of *Tropicoporus zuzaneae* (Dai 22171, holotype).

at the base, 9–11 × 7–8 µm; basidioles dominant in hymenium, capitate, slightly smaller than basidia; rhomboid crystals frequently present in trama and hymenium.

***Spores*.** Basidiospores broadly ellipsoid to subglobose, pale yellowish, slightly thick-walled, mostly collapsed, IKI–, CB(+), 3.8–4.9(–5.1) × (3–)3.1–4.2(–4.4) µm, L = 4.42 µm, W = 3.69 µm, Q = 1.2 (n = 30/1).

Additional specimens (paratypes) examined. China. Hainan Province, Haikou, Guanlan Lake, on dead tree of *Sonneratia*, 28.XII.2020, Dai 22168 (BJFC036060, sterile). Indonesia, Borneo, on *Rhizopora apiculata*, 17.II.2015, Zuzana Egertova, Vlasák JV1502/5-Zuz (JV and BJFC, sterile).

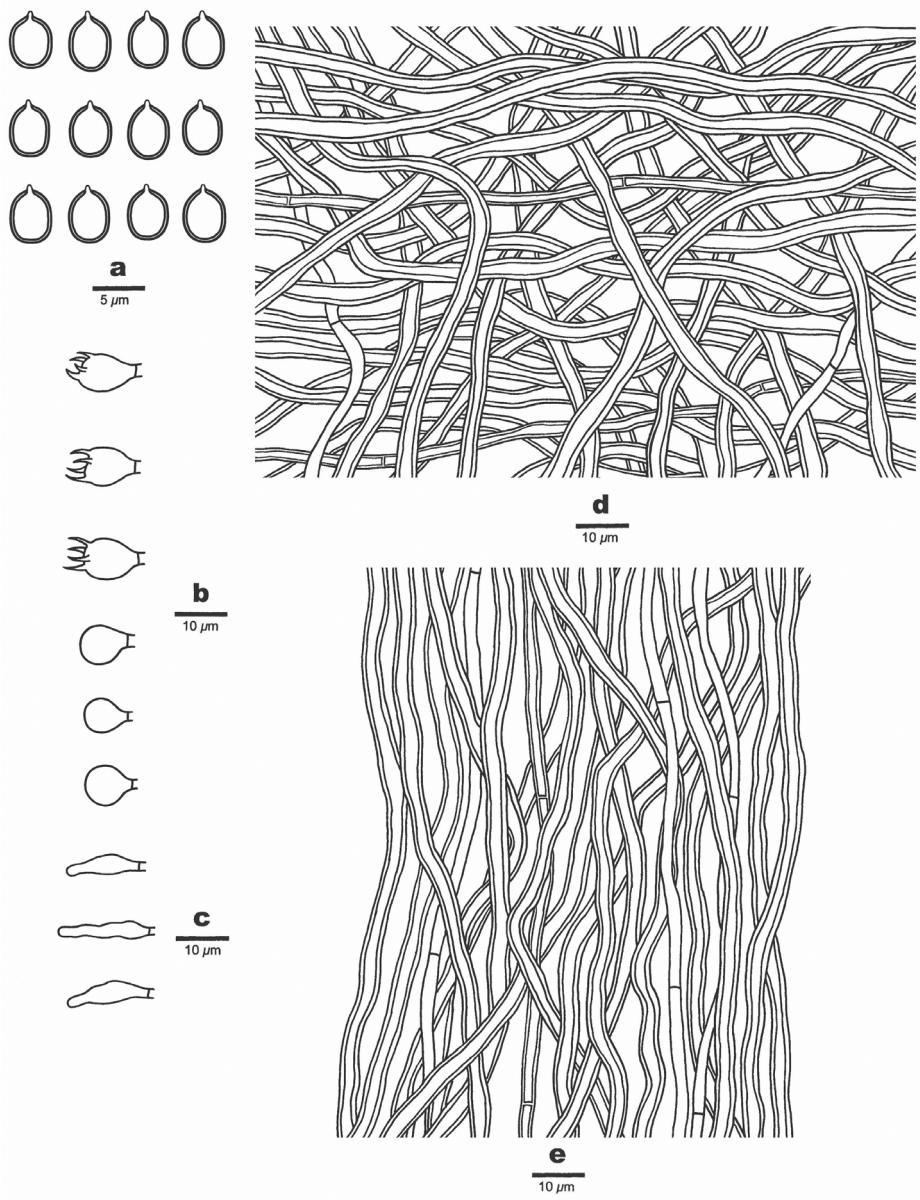

Figure 5. Microscopic structures of *Tropicoporus zuzaneae* (drawn from the holotype Dai 22171) **a** basidiospores **b** basidia and basidioles **c** cystidioles **d** hyphae from subiculum **e** hyphae from trama. Scale bars: 5 µm (**a**); 10 µm (**b–e**).

Discussion

Tropicoporus oceanianus is characterized by perennial and ungulate basidiomata with glancing pores, hymenial setae occasionally present, context with a trimitic and tube trama with a dimitic hyphal system, and broadly ellipsoid to subglobose basidiospores measuring 5.2–6 × 4–5 µm. Although we studied a single specimen (Dai 18859), three samples (MEL 2382654, MEL 2382727 and MEL 238278) from Australia have available sequences in GenBank, and their sequences (KP013017, KP012908 and KP012961) are identical to those of Dai 18859. We thus treat MEL 2382654, MEL 2382727 and MEL 238278 as *Tropicoporus oceanianus* in the present paper.

Phylogenetically, *T. oceanianus* seems to be unrelated to other species in *Tropicoporus* (Fig. 1). Morphologically, *T. oceanianus* is similar to *T. cambodiensis* (L.W. Zhou & W.M. Zhang) Y.C. Dai & F. Wu and *T. inamoenus* (Mont.) Y.C. Dai & F. Wu by sharing pileate and solitary basidiomata with concentrically sulcate and zonate at pileal surface, similar size of pores and basidiospores, but *T. cambodiensis* differs from *T. oceanianus* by a dimitic hyphal structure without skeleto-binding hyphae in context, and it has a distribution in Cambodia (Wu et al. 2022a). *T. inamoenus* is different from *T. oceanianus* by a dimitic hyphal structure without skeleto-binding hyphae in context, longer hymenial setae (28–45 × 10–15 µm vs. 22–30 × 4.5–6.5 µm), and has a distribution in India (Wu et al. 2022a).

Tropicoporus zuzaneae is characterized by perennial and resupinate basidiomata with receding margin, glancing pores as 6–8 per mm, very thin to almost lacking subiculum, a dimitic hyphal structure, the absence of any setal elements, broadly ellipsoid to subglobose basdiospores measuring 3.8–4.9 × 3.1–4.2 µm. We studied two Chinese specimens (Dai 18859, Dai 22168) and one Indonesian sample (JV 1502/5-Zuz), but two other samples (TBP00705 and BCC 23706) from Thailand have available sequences in GenBank, and their ITS sequences (KT800054 and KP059109) are identical to our studied samples. So, we treat TBP00705 and BCC 23706 as *Tropicoporus zuzaneae*.

Phylogenetically, the new species is closely related to *Tropicoporus tenuis* Y.C. Dai & F. Wu, *T. ravidus* Y.C. Dai & F. Wu, *T. minor* Y.C. Dai & F. Wu, *T. detonsus* (Fr.) Y.C. Dai & F. Wu, *T. flabellatus* V.R.T. Oliveira et al. and *T. melleoporus* (Murrill) Salvador-Montoya & Drechsler-Santos with strong support (Fig. 1), but these species are readily distinguished from *T. zuzaneae* by the presence of hymenial setae (Salvador-Montoya et al. 2020; Xavier de Lima et al. 2022; Wu et al. 2022a). Morphologically, *Tropicoporus zuzaneae* resembles *T. anchietanus* (Decock & Ryvarden) Y.C. Dai & F. Wu, *T. carteri* (Berk. ex Cooke) Y.C. Dai & F. Wu, *T. purpureogilvus* (Petch) Y.C. Dai & F. Wu and *T. shaferi* (Murrill) Y.C. Dai & F. Wu by sharing perennial and resupinate basidiomata with pore 6–9 per mm, and broadly ellipsoid to subglobose basidiospores, but the latter four species are different from *T. zuzaneae* by the presence of hymenial setae (Wu et al. 2022a).

Two new members of *Tropicoporus* are described in the present paper. *Tropicoporus oceanianus* is unique in the genus by its trimitic hyphal structure in context, and *T. zuzaneae* is unique in the genus by its absence of any setal elements. We thus modify the definition of *Tropicoporus* to be annual to perennial, resupinate to distinctly pileate basidiomata with yellow-brown to umber pore surface, mostly a dimitic hyphal system at least in trama, a few with trimitic or monomitic hyphal sys-

tem in context, hymenial setae present in most species, and yellowish, slightly thick-walled, smooth, usually collapsed basidiospores which become darker in a 5% KOH solution in a few species, growing on angiosperm wood and causing a white rot.

Acknowledgements

Special thanks are due to Prof. Yu-Cheng Dai (Beijing Forestry University) and Dr. Josef Vlasák (Biology Centre of the Academy of Sciences of the Czech Republic) who allowed us to study their specimens. We thank Qiu-Yue Zhang and Kai-Yue Luo (Beijing Forestry University) for helping in the laboratory examination of the samples. The language was improved by Dr. Genevieve Gates (Hobart, Australia).

Additional information

Conflict of interest

The authors have declared that no competing interests exist.

Ethical statement

No ethical statement was reported.

Funding

The research was supported by the Research Project of Yunnan Key Laboratory of Gastrodia and Fungi Symbiotic Biology (TMKF2023A03), the Yunnan Province expert workstation program (No. 202205AF150014) and the National Natural Science Foundation of China (Project No. 32161143013).

Author contributions

An-Hong Zhu and Zhan-Bo Liu designed the research and contributed to data analysis and interpretation. Hong-Gao Liu, Yue Li, Yuan Yuan and Shuang-Hui He prepared the samples, drawing and drafted the manuscript. Yuan Yuan and Shuang-Hui He discussed the results and edited the manuscript. All authors contributed to the article and approved the submitted version.

Author ORCIDs

Zhan-Bo Liu https://orcid.org/0000-0002-3894-5398
Yue Li https://orcid.org/0000-0003-4091-1506
Yuan Yuan https://orcid.org/0000-0001-6674-9848
Shuang-Hui He https://orcid.org/0000-0003-4702-3034

Data availability

The sequences are deposited in the GenBank database (Table 1).

References

Anonymous (1969) Flora of British fungi. Colour identification chart. Her Majesty's Stationery Office, London.

Bian LS, Dai YC (2020) Molecular phylogeny and morphology reveal two new species of *Coltricia* (Hymenochaetaceae Basidiomycota) from China. Mycological Progress 19(7): 657–666. https://doi.org/10.1007/s11557-020-01583-7

Chen Q, Du P, Vlasák J, Wu F, Dai YC (2020) Global diversity and phylogeny of *Fuscoporia* (Hymenochaetales, Basidiomycota). Mycosphere 11(1): 1477–1513. https://doi.org/10.5943/mycosphere/11/1/10

Cui BK, Li HJ, Ji X, Zhou JL, Song J, Si J, Yang ZL, Dai YC (2019) Species diversity, taxonomy and phylogeny of Polyporaceae (Basidiomycota) in China. Fungal Diversity 97(1): 137–302. https://doi.org/10.1007/s13225-019-00427-4

Cui BK, Pan XH, Pan F, Sun YF, Xing JH, Dai YC (2023) Species diversity and resources of *Ganoderma* in China. Mycosystema 42: 170–178.

Dai YC (2010) Hymenochaetaceae (Basidiomycota) in China. Fungal Diversity 45(1): 131–343. https://doi.org/10.1007/s13225-010-0066-9

Dong JH, Gu JY, Zhao CL (2023) Diversity of wood-decaying fungi in Wenshan Area, Yunnan Province, China. Mycosystema 42: 638–662.

Du R, Wu F, Gate GM, Dai YC, Tian XM (2020) Taxonomy and phylogeny of *Sidera* (Hymenochaetales, Basidiomycota): Four new species and keys to species of the genus. MycoKeys 68: 115–135. https://doi.org/10.3897/mycokeys.68.53561

Du P, Cao TX, Wu YD, Zhou M, Liu ZB (2021) Two new species of Hymenochaetaceae on *Dracaena cambodiana* from tropical China. MycoKeys 80: 1–17. https://doi.org/10.3897/mycokeys.80.63997

Gunaseelan S, Kezo K, Karunarathna SC, Yang E, Zhao C, Elgorban AM, Tibpromma S, Kaliyaperumal M (2024) New species of *Tropicoporus* (Basidiomycota, Hymenochaetales, Hymenochaetaceae) from India, with a key to Afro-Asian *Tropicoporus* species. MycoKeys 102: 29–54. https://doi.org/10.3897/mycokeys.102.117067

Guo T, Yang RH, Tang MX, Hou D, Sun XL, Wang L, Li Y, Bao DP, Zhou XW (2022) Species diversity of macrofungi in the Mount Huangshan, East China. Mycosystema 41: 1398–1415.

Hall TA (1999) BioEdit: A user-friendly biological sequence alignment editor and analysis program for Windows 95/98/NT. Nucleic Acids Symposium Series 41: 95–98.

Han ML, Chen YY, Shen LL, Song J, Vlasak J, Dai YC, Cui BK (2016) Taxonomy and phylogeny of the brown-rot fungi: Fomitopsis and its related genera. Fungal Diversity 80(1): 343–373. https://doi.org/10.1007/s13225-016-0364-y

Hopple Jr JS, Vilgalys R (1999) Phylogenetic relationships in the mushroom genus *Coprinus* and dark-spored allies based on sequence data from the nuclear gene coding for the large ribosomal subunit RNA: Divergent domains, outgroups, and monophyly. Molecular Phylogenetics and Evolution 13(1): 1–19. https://doi.org/10.1006/mpev.1999.0634

Ji XH, He SH, Chen JJ, Si J, Wu F, Zhou LW, Vlasák J, Tian XM, Dai YC (2017) Global diversity and phylogeny of *Onnia* (Hymenochaetaceae) species on gymnosperms. Mycologia 109(1): 27–34. https://doi.org/10.1080/00275514.2016.1274619

Katoh K, Standley DM (2013) MAFFT multiple sequence alignment software version 7: Improvements in performance and usability. Molecular Biology and Evolution 30(4): 772–780. https://doi.org/10.1093/molbev/mst010

Liu SL, Wang XW, Li GJ, et al. (2024) Fungal diversity notes 1717–1817: taxonomic and phylogenetic contributions on genera and species of fungal taxa. Fungal Diversity 124: 1–216. https://doi.org/10.1007/s13225-023-00529-0

Miller MA, Holder MT, Vos R, Midford PE, Liebowitz T, Chan L, Hoover P, Warnow T (2009) The CIPRES Portals. http://www.phylo.org/sub_sections/portal [Archived by WebCite(r) at http://www.webcitation.org/5imQlJeQa]

Nylander JAA (2004) MrModeltest v2. Program distributed by the author. Evolutionary Biology Centre, Uppsala University.

Petersen JH (1996) The Danish Mycological Society's colour-chart. Foreningen til Svampekundskabens Fremme, Greve.

Ronquist F, Teslenko M, Mark P, Ayres DL, Darling A, Höhna S, Larget B, Liu L, Suchard MA, Huelsenbeck JP (2012) MrBayes 3.2: Efficient Bayesian phylogenetic inference and model choice, across a large model space. Systematic Biology 61(3): 539–542. https://doi.org/10.1093/sysbio/sys029

Salvador-Montoya CA, Costa-Rezende DH, Ferreira-Lopes V, Borba-Silva MA, Popoff OF (2018) *Tropicoporus drechsleri* (Hymenochaetales, Basidiomycota), a new species in the "*Inonotus linteus*" complex from northern Argentina. Phytotaxa 338(1): 75–89. https://doi.org/10.11646/phytotaxa.338.1.6

Salvador-Montoya CA, Popoff OF, Góes-Neto A, Drechsler-Santos ER (2020) Global phylogenetic and morphological reassessment of *Fomitiporella* s.l. (Hymenochaetales, Basidiomycota): Taxonomic delimitation of *Fomitiporella* s.s. and segregation of *Rajchenbergia*, gen. nov. Plant Systematics and Evolution 306(2): 1–27. https://doi.org/10.1007/s00606-020-01648-w

Swofford DL (2002) PAUP*: phylogenetic analysis using parsimony (*and other methods), version 4.0b10. Sinauer Associates, Sunderland, Massachusetts.

Tian XM, Yu HY, Zhou LW, Decock C, Vlasák J, Dai YC (2013) Phylogeny and taxonomy of the Inonotus linteus complex. Fungal Diversity 58(1): 159–169. https://doi.org/10.1007/s13225-012-0202-9

White TJ, Bruns T, Lee S, Taylor J (1990) Amplification and direct sequencing of fungal ribosomal RNA genes for phylogenetics. In: Innis MA, Gelfand DH, Sninsky JJ, White JT (Eds) PCR Protocols: A guide to methods and applications. Academic Press, San Diego, 315–322. https://doi.org/10.1016/B978-0-12-372180-8.50042-1

Wu F, Zhou LW, Vlasák J, Dai YC (2022a) Global diversity and systematics of Hymenochaetaceae with poroid hymenophore. Fungal Diversity 113(1): 1–192. https://doi.org/10.1007/s13225-021-00496-4

Wu F, Man XW, Tohtirjap A, Dai YC (2022b) A comparison of polypore funga and species composition in forest ecosystems of China, North America, and Europe. Forest Ecosystems 9: 100051. https://doi.org/10.1016/j.fecs.2022.100051

Xavier de Lima V, Oliveira VRT, Lima-Júnior NC, Oliveira-Filho JRC, Santos C, Lima N, Gibertoni TB (2022) Taxonomy and phylogenetic analysis reveal one new genus and three new species in *Inonotus* s.l. (Hymenochaetaceae) from Brazil. Cryptogamie. Mycologie 43(1): 1–21. https://doi.org/10.5252/cryptogamie-mycologie2022v43a1

Zhao H, Zhou M, Liu XY, Wu F, Dai YC (2022) Phylogeny, divergence time estimation and biogeography of the genus *Onnia* (Basidiomycota, Hymenochaetaceae). Frontiers in Microbiology 13: 907961. https://doi.org/10.3389/fmicb.2022.907961

Zhou LW, Vlasák J, Decock C, Assefa A, Stenlid J, Abate D, Wu SH, Dai YC (2016) Global diversity and taxonomy of the *Inonotus linteus* complex (Hymenochaetales, Basidiomycota): *Sanghuangporus* gen. nov., *Tropicoporus excentrodendri* and *T. guanacastensis* gen. et spp. nov., and 17 new combinations. Fungal Diversity 77(1): 335–347. https://doi.org/10.1007/s13225-015-0335-8

MycoKeys 103: 71–95 (2024)
DOI: 10.3897/mycokeys.103.117580

Research Article

Four new species of Dothideomycetes (Ascomycota) from Pará Rubber (*Hevea brasiliensis*) in Yunnan Province, China

Rui-Fang Xu[1,2,3], Samantha C. Karunarathna[1,4], Chayanard Phukhamsakda[2], Dong-Qin Dai[1], Abdallah M. Elgorban[5], Nakarin Suwannarach[6,7], Jaturong Kumla[6,7], Xiao-Yan Wang[8,9], Saowaluck Tibpromma[1]

1 *Center for Yunnan Plateau Biological Resources Protection and Utilization, College of Biological Resource and Food Engineering, Qujing Normal University, Qujing, Yunnan 655011, China*
2 *Center of Excellence in Fungal Research, Mae Fah Luang University, Chiang Rai, Thailand*
3 *School of Science, Mae Fah Luang University, Chiang Rai, 57100, Thailand*
4 *National Institute of Fundamental Studies (NIFS), Kandy, Sri Lanka*
5 *Department of Botany and Microbiology, College of Science, King Saud University, Riyadh 11451, Saudi Arabia*
6 *Department of Biology, Faculty of Science, Chiang Mai University, Chiang Mai, Thailand*
7 *Center of Excellence in Microbial Diversity and Sustainable Utilization, Chiang Mai University, Chiang Mai, Thailand*
8 *Edible Fungus Research Institute of Hunan Province, Changsha 410013, China*
9 *Luliang cuan Lu yuan Mushroom Co., LTD, Luliang 655607, China*

Corresponding authors: Xiao-Yan Wang (wangxiaoyan1206@sohu.com); Saowaluck Tibpromma (saowaluckfai@gmail.com)

Abstract

The tropical areas in southern and south-western Yunnan are rich in fungal diversity. Additionally, the diversity of seed flora in Yunnan Province is higher than in other regions in China and the abundant endemic species of woody plants provide favourable substrates for fungi. Rubber plantations in Yunnan Province are distributed over a large area, especially in Xishuangbanna. During a survey of rubber-associated fungi in Yunnan Province, China, dead rubber branches with fungal fruiting bodies were collected. Morphological characteristics and multigene phylogenetic analyses (ITS, LSU, SSU, *rpb*2 and *tef*1-α) revealed four distinct new species, described herein as *Melomastia puerensis*, *Nigrograna lincangensis*, *Pseudochaetosphaeronema lincangensis* and *Pseudochaetosphaeronema xishuangbannaensis*. Detailed descriptions, illustrations and phylogenetic trees are provided to show the taxonomic placements of these new species.

Key words: Dothideomycetes, four new species, multigene phylogeny, Pará rubber, saprobic fungi, taxonomy

Academic editor: S. Maharachchikumbura
Received: 19 December 2023
Accepted: 29 January 2024
Published: 22 March 2024

Citation: Xu R-F, Karunarathna SC, Phukhamsakda C, Dai D-Q, Elgorban AM, Suwannarach N, Kumla J, Wang X-Y, Tibpromma S (2024) Four new species of Dothideomycetes (Ascomycota) from Pará Rubber (*Hevea brasiliensis*) in Yunnan Province, China. MycoKeys 103: 71–95. https://doi.org/10.3897/mycokeys.103.117580

Introduction

Hevea brasiliensis (Pará rubber tree) is native to the Amazon River Basin; however, it shows a pantropical species distribution through introductions (Basik et al. 2021). Pará rubber plantations have increased intensely worldwide in the past few decades, with the global consumption of natural rubber increasing by about 3% in 2019 (Bhattacharjee et al. 2021). Yunnan Province is one of the rubber-producing provinces in China and Xishuangbanna Prefecture (located in the south of Yunnan) contributes up to 77% of the rubber production in the

province, representing 37% of the national rubber production (National Bureau of Statistics of China 2011, Statistical Bureau of Yunnan Province 2011).

Besides rubber, Yunnan Province is also rich in fungal diversity (Feng and Yang 2018). Approximately 104,000 fungal species are expected to be discovered in Yunnan; however, around 6,000 fungal species have been reported from the Province, leaving much to be described (Feng and Yang 2018; Bhunjun et al. 2022; Phukhamsakda et al. 2022). Surprisingly, a few fungal species have been described on Pará rubber in China (Senwanna et al. 2021; Xu et al. 2022a, 2022b, 2023; Hyde et al. 2023).

Senwanna et al. (2021) listed 67 orders, 168 families and 513 genera of fungi on Pará rubber and reported eight new taxa, two asexual-sexual linkages, 20 new host records and one reference specimen of saprobic fungi from Thailand. In addition, Senwanna et al. (2021) reported that three species from their collections had previously been reported from Pará rubber in the Amazon Forest (Spaulding 1961) and most of the taxa reported on Pará rubber have been found in Thailand. Moreover, Senwanna et al. (2019) discovered that *Muyocopron dipterocarpi* may have jumped from its original host. *Dipterocarpus tuberculatus*, to the Pará rubber host and adapted to the new host in Thailand.

Dothideomycetes is the largest class of Ascomycota, currently encompassing more than 25 orders, 110 families and over 19,000 species (Wijayawardene et al. 2022). They can be endophytes, epiphytes, saprobes, lichenised or lichenicolous fungi and are found in terrestrial, freshwater and marine habitats worldwide (Hyde et al. 2013). In Pará rubber, Dothideomycetes are predominant amongst ascomycetes (Senwanna et al. 2021).

Fungi associated with rubber in China were poorly studied compared with other countries in the Greater Mekong Subregion (GMS), especially in Thailand. Moreover, saprobic fungal taxa, described in earlier studies, do not have sequence data. Continuing the fungal diversity studies in the GMS (Chaiwan et al. 2021), this study introduces four new taxa of Dothideomycetes associated with Pará rubber trees in Yunnan Province, China. Morphological characteristics and phylogenetic analyses were conducted to find accurate taxonomic placements of these new taxa.

Materials and methods

Collection, morphological examination and isolation

Dead rubber (*Hevea brasiliensis*) branches with fungal fruiting bodies were collected from Yunnan Province, China, during the summers of 2021 and 2022. The samples were stored in sealable plastic bags and taken to the mycology laboratory at Qujing Normal University. Morphological observations and single spore isolations were conducted following the methods described by Senanayake et al. (2020). Morphological characteristics were observed using a stereomicroscope Leica S8AP0 and photographed with an OLYMPUS BX53 compound microscope. Measurements were obtained using Tarosoft (R) Image Frame Work software. Adobe Photoshop CC 2017 software was used for preparing photo-plates. Herbarium specimens of the new species were deposited at the Herbarium of Zhongkai University of Agriculture and Engineering (**ZHKU**), China. The living cultures were deposited at the culture collection of Zhongkai University of Agriculture and Engineering (**ZHKUCC**), China. Facesoffungi (FoF)

numbers and Index Fungorum (IF) numbers were obtained as per Jayasiri et al. (2015) and Index Fungorum (2024).

DNA extraction, PCR amplification and sequencing

Genomic DNA was extracted directly from scraped fresh mycelia grown on one-month-old artificial culture media (PDA), using an E.Z.N.A. Forensic DNA Kit (BIO-TEK), in accordance with the manufacturer's protocol. The different gene regions, primers and protocols used for the amplification are summarised in Table 1. Polymerase chain reaction (PCR) amplifications were conducted using 25 µl PCR mixture containing 8.5 µl ddH2O, 12.5 µl 2 × Master Mix (Bioteke Corporation, Beijing, China), 2 µl DNA template and 1 µl each reverse and forward primer (Tibpromma et al. 2018). Purification and sequencing of PCR products were carried out in Bioteke, P.R. China.

Table 1. Primers, PCR thermal cycles for SSU, ITS, LSU, *rpb*2 and *tef*1-α amplification and reference(s).

Genes	Primers/Loci	PCR condition	References
ITS	ITS4	(94 °C: 30 s, 55 °C: 50 s, 72 °C: 90 s) × 35 cycles	White et al. (1990)
	ITS5		
LSU	LR0R	(94 °C: 30 s, 55 °C: 50 s, 72 °C: 90 s) × 35 cycles	Vilgalys and Hester (1990)
	LR5		
SSU	NS1	(94 °C: 30 s, 55 °C: 50 s, 72 °C: 90 s) × 35 cycles	White et al. (1990)
	NS4		
*tef*1-α	983F	(95 °C: 30 s, 55 °C: 50 s, 72 °C: 90 s) × 35 cycles	Carbone and Kohn (1999)
	2218R		
*rpb*2	fRPB2-5f	(94 °C: 60 s, 58 °C: 60 s, 72 °C: 90 s) × 40 cycles	Liu et al. (1999)
	fRPB2-7cR		

Phylogenetic analyses

Sequences with high similarities (> 90%) were identified by BLASTn searches to determine the closest match to the taxa. Initial alignments of the sequence data were processed using MAFFT v.7 (http://mafft.cbrc.jp/alignment/server) using default settings (Katoh et al. 2019). The sequences were trimmed using TrimAl V 1.2 with 'gappyout' automated trimming option (Capella-Gutiérrez et al. 2009). The alignments were checked visually and improved manually wherever necessary. Multiple genes were concatenated by Sequence Matrix.

Multigene phylogenetic analyses for the concatenated genes were conducted using Maximum Likelihood (ML) and Bayesian Inference (BI) analyses. The CIPRES Science Gateway portal (Miller et al. 2012) was used to run both RAxML and Bayesian analyses. Maximum Likelihood analysis was made with RAxML-HPC2 on XSEDE v.8.2.10 tool (Stamatakis 2014) employing the GTR+GAMMA model with 1000 bootstrap repetitions. Bayesian analysis was performed by MrBayes v.3.0b4 (Huelsenbeck and Ronquist 2001) with the best-fit model of sequence evolution estimated using MrModelTest 2.2 (Nylander 2004). MrBayes analyses were performed with GTR+I+GAMMA for one million generations, sampling every 100th generation and ending the run automatically when the standard deviation of split frequencies dropped below 0.01 with a 25% burn-in. Phylograms were visualised with the FigTree v.1.4.0 programme (Rambaut 2012) and edited in Microsoft PowerPoint 2021. The final alignments and trees were deposited in TreeBASE, under submission ID 31039 (Fig. 1) and ID 31040 (Fig. 3) (http://www.treebase.org/).

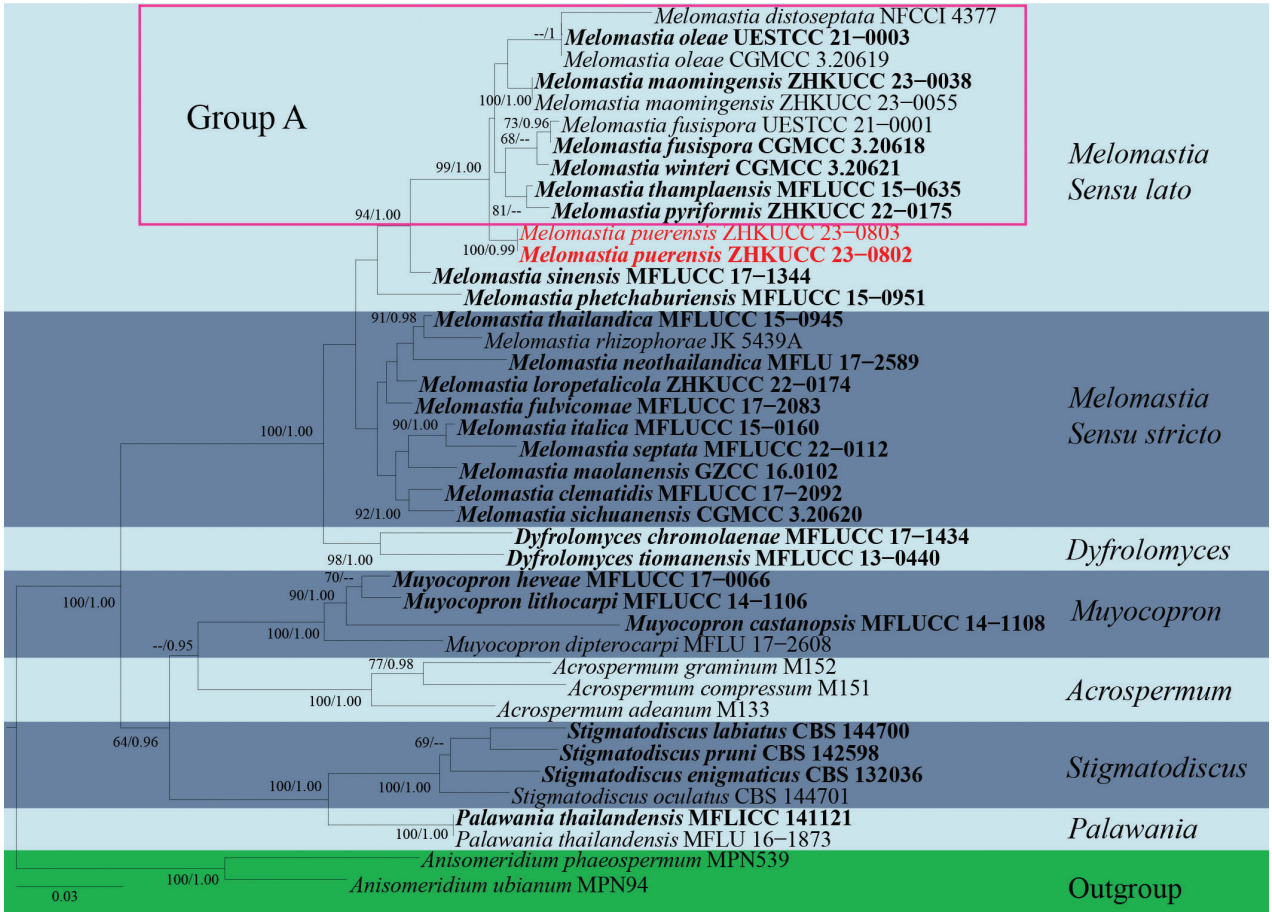

Figure 1. Phylogram generated from Maximum Likelihood analysis, based on combined LSU, SSU and *tef*1-α sequence data of 41 taxa, which comprised 2836 base pairs (LSU = 902 bp, SSU = 1031 bp, *tef*1-α = 903 bp). The best scoring RAxML tree with a final likelihood value of -14798.632437 is presented. The matrix had 1013 distinct alignment patterns, with 24.90% of undetermined characters or gaps. Estimated base frequencies were as follows: A = 0.241740, C = 0.258134, G = 0.292403, T = 0.207722; substitution rates: AC = 0.834723, AG = 2.021967, AT = 1.126143, CG = 1.032150, CT = 7.231944, GT = 1.000000; gamma distribution shape parameter α = 0.320795. Bootstrap support values for ML equal to or greater than 60% and Bayesian Inference analysis values equal to or greater than 0.90 PP are labelled at each node. The tree is rooted with *Anisomeridium phaeospermum* (MPN539) and *A. ubianum* (MPN94). Related sequences were collected following Li et al. (2022), Kularathnage et al. (2023) and Dong et al. (2023). The new isolates are indicated in red and the ex-type strains are in bold. Group A indicates the taxa used to compare the morphology with our new species (*Melomastia puerensis*).

Results

Taxonomy and phylogenetic results

Dothideomycetes O.E. Erikss. & Winka
Dyfrolomycetales Pang, K.D. Hyde & E.B.G. Jones

Pleurotremataceae Watson

Notes. Pleurotremataceae was introduced by Watson (1929) and it comprises three genera viz. *Dyfrolomyces*, *Melomastia* and *Pleurotrema* (Wijayawardene et al. 2022). Species in this family are saprobes on wood in terrestrial and aquatic habitats (Hongsanan et al. 2020). Pleurotremataceae has been classified in several orders. Pleurotremataceae was excluded from Sordariomycetes

and placed in Dothideomycetes, based on morphology and DNA sequences (Maharachchikumbura et al. 2016).

Melomastia Nitschke ex Sacc.

Notes. *Melomastia* was introduced by Saccardo (1875) with *M. mastoidea* as the type species (Kang et al. 1999). *Melomastia* has been recorded with 63 epithets in Index Fungorum (2024). Most *Melomastia* species have been found in terrestrial, freshwater and marine habitats and they have a wide geographical distribution in Africa, China, Germany, Italy, Japan, Poland and the United States of America (Norphanphoun et al. 2017; Dayarathne et al. 2020; Li et al. 2022; Kularathnage et al. 2023). *Melomastia* was discovered to be closely related to *Dyfrolomyces* and their exact relationship is still unknown. Li et al. (2022) reclassified *Dyfrolomyces* as *Melomastia*, based on morphology and phylogeny of four newly-introduced species from Olive in Sichuan Province, China. *Melomastia tiomanensis* and *M. chromolaenae* exhibit spindle-shape, 6–11-septate ascospores with acute ends. Additionally, the phylogenetic analysis conducted by Kularathnage et al. (2023) showed that *M. tiomanensis* and *M. chromolaenae* form a distinct lineage. Thus, *M. tiomanensis* and *M. chromolaenae* were moved into *Dyfrolomyces* and named *Dyfrolomyces tiomanensis* and *Dyfrolomyces chromolaenae*. *Melomastia* is characterised by immersed, ostiolate ascomata, multiple layered, dark brown peridium, filamentous pseudoparaphyses, unitunicate, cylindrical, 8-spored asci and ovoid, hyaline, 1–10-septate, fusiform to oblong ascospores with rounded or acute ends, with or without gelatinous sheath (Norphanphoun et al. 2017; Dayarathne et al. 2020; Li et al. 2022; Kularathnage et al. 2023). However, the asexual morph of *Melomastia* is still unknown (Norphanphoun et al. 2017; Li et al. 2022; Kularathnage et al. 2023).

Melomastia puerensis R.F. Xu & Tibpromma, sp. nov.

Index Fungorum number: IF901419
Facesoffungi number: FoF15195
Fig. 2

Etymology. The name refers to the location "Pu'er, Yunnan, China", where the holotype was collected.

Holotype. ZHKU 23–0106.

Description. ***Saprobic*** on a dead branch of *Hevea brasiliensis*. ***Sexual morph:*** Ascomata 260–720 µm high, 225–850 µm diam. ($\bar{x}$ = 540 × 520 µm, n = 10), visible as black dots on the host surface, solitary or gregarious, immersed to slightly erumpent, subglobose or pyriform, carbonaceous, dark brown to black, ostiolate, papillate. Ostioles 205–220 × 195–258 µm ($\bar{x}$ = 233 × 207 µm, n = 5), central, carbonaceous, dark brown to black. Peridium 40–120 µm wide, two-layered, outer layer, thick, carbonaceous, inner layer composed of several layers, brown to pale brown cells of textura angularis. Hamathecium comprises 2–4.5 µm wide, filiform, unbranched, hyaline, aseptate, guttulate, pseudoparaphyses, longer than asci. Asci 175–205 × 6–10 µm ($\bar{x}$ = 190 × 8, n = 15), 8-spored, hyaline, bitunicate, cylindrical, flexuous, apically obtuse, with an ocular chamber, smooth-walled, short pedicellate. Ascospores 20–30 × 5–8 µm ($\bar{x}$ = 24 × 7, n = 30), uniseriate, hyaline,

Table 2. Morphological comparison of *M. puerensis* and closely-related species viz. *M. distoseptata*, *M. fusispora*, *M. maomingensis*, *M. oleae*, *M. pyriformis*, *M. thamplaensis* and *M. winteri*.

Species	Ascomata	Peridium	Pseudoparaphyses	Asci	Ascospores	References
M. distoseptata	550–630 × 450–600 µm, perithecial, immersed, erumpent neck with pseudoparaphyses, clypeate	40 µm, with two strata, outer thick, and inner brown and hyaline cells of textura angularis to *epidermoidea* cells	1.8–2.1 µm, flamentous, septate, unbranched, dense, longer than asci	126.7–146.2 × 4.7–6.3 µm, apical ends obtuse, short pedicellate	19.7–24.9 × 4.3–5 µm, fusoid, obtuse ends, apical ends slightly bent	Hongsanan et al. (2020)
M. fusispora	432–624 × 527–618 µm, cone-shaped structures on the host surface, immersed to erumpent through host tissue, pyriform	25.5–61.5 µm, two-layered, outer layer of cells of *textura intricata*, inner layer of textura angularis	2–2.6 µm, dense, filiform, unbranched, hyaline, aseptate	200–231 × 7.6–9.2 µm, slightly flexuous, apically round, with well-developed ocular chamber, cylindrical pedicellate	27.5–32 × 6.5–7.5 µm, fusiform, with rounded to acute ends, narrow towards apex, constricted at the central septum, surrounded by an irregular and thin gelatinous sheath	Li et al. (2022)
M. maomingensis	300–550 µm high × 250–500 µm diam., solitary, semi-immersed to immersed, visible on the host surface as black, obvious, raised spots, black, uni-loculate, globose to subglobose	35–100 µm wide, comprising dense, thick, brown to dark brown cells of textura angularis, fusion with host tissue	1.5–3.5 µm wide, comprising numerous, filamentous, hyaline, septate, sometimes branched, longer than asci, attached at the base and between the asci	175–195 × 7–9 µm, cylindrical pedicel, rounded in apex, J-	(23–)24.5–29 × 6–8 µm, fusiform with acute ends, constricted at the septum, with a large guttule in each cell when mature	Du et al. (2024)
M. oleae	410–440 × 493–520 µm, cone-shaped structures on host surface, semi-immersed, globose to compressed globose	54–65 µm, two-layered, outer thick and inner composed of 5–6 layers of textura angularis to textura prismatica	2–2.5 µm, dense, filiform, unbranched, aseptate	209–237 × 7.5–9 µm, slightly flexuous, apically rounded with ocular chamber, cylindrical pedicellate	28–34 × 6–7 µm, fusiform with obtuse ends, slightly constricted at the septa	Li et al. (2022)
M. puerensis	**260–720 × 225–850 µm, black dot on the host surface, immersed to erumpent to superficial, pyriform**	**40–120 µm, two-layered, outer thick, carbonaceous, inner composed of several layers, pale brown to brown cells of *textura angularis***	**2–4.5 µm, filiform, unbranched, guttulate, pseudoparaphyses, longer than asci**	**175–205 × 6–10 µm, flexuous, apical ends obtuse, with ocular chamber, smooth-walled, short pedicellate**	**20–30 × 5–8 µm, fusiform, obtuse or conical ends, narrow towards apex, constricted at the central septum, with guttules in each cell**	**This study**
M. pyriformis	330–640 × 275–420 µm, erumpent to superficial when mature, pyriform, papillate, ostiolate	20–50 µm, thin at the base and become thick towards sides, comprised of brown, thick-walled, cells of *textura intricata* in sides; and thin-walled, pale brown, cells of textura angularis in base	1.8–2.5 µm wide, dense, filiform, unbranched, septate, anastomosing between and above the asci	135–160 × 5.5–7.5 µm, fissitunicate, apically round, with an indistinct ocular chamber, short pedicellate	20–25 × 4.5–7 µm, , fusiform with acute ends, not constricted at the septa, with guttules in each cell	Kularathnage et al. (2023)
M. thamplaensis	550–630 × 450–600 µm, black spots on the host surface, immersed, clypeate, subglobose to obpyriform, some with a broad, flattened base	14–49 µm, composed of three strata, an outer stratum, dense, amorphous, thick-walled cells fusing with host tissue, a middle layer of thick-walled, black cells of textura angularis and an inner layer of thin-walled black cells of textura angularis	1.8–2.1 µm, attached at the base and between the asci, embedded in a gelatinous matrix	126.7–146.2 × 4.7–6.3 µm, long cylindrical, short-pedicellate, apically rounded with an obvious apical ring	19.7–24.9 × 4.3–5 µm, fusiform with acute angular ends, constricted at the septum, smooth-walled, containing several guttules when young	Zhang et al. (2017)
M. winteri	340–365 × 364–410 µm, semi-immersed to immersed, globose	55–62.5 µm, two-layered, outer thick, and inner composed of 3–4 layers of hyaline to lightly brown cells of textura angularis to textura prismatica	1.5–3.5 µm, dense, filiform, unbranched, septate	165–189 × 7–8.5 µm, slightly flexuous, apically round, with a distinct ocular chamber, cylindrical pedicellate	25–30 × 5–6.5 µm, partially overlapping, fusiform with acute ends, deeply constricted at the median septum	Li et al. (2022)

fusiform, obtuse or conical ends, narrow towards the apex, 3-septate, constricted at the central septum, with guttulate in each cell. ***Asexual morph:*** Undetermined.

Culture characteristics. Colonies on PDA that grow at 28 °C, flat, rough surface, entire edges, culture from above, brownish-grey, forming zonate grey, reverse dark brown, brown at the edge, turning reddish-brown.

Material examined. China, Yunnan Province, Pu'er on a dead branch of *Hevea brasiliensis*, 16 September 2021, Rui-Fang Xu, XPER–14 (ZHKU 23–0106, holotype); ex-type ZHKUCC 23–0802, ZHKUCC 23–0803.

GenBank numbers. ZHKUCC 23–0802 = ITS: OR941077, LSU: OR922309, SSU: OR922340, *tef*1-α: OR966284; ZHKUCC 23–0803 = ITS: OR941078, LSU: OR922310, SSU: OR922341, *tef*1-α: OR966285.

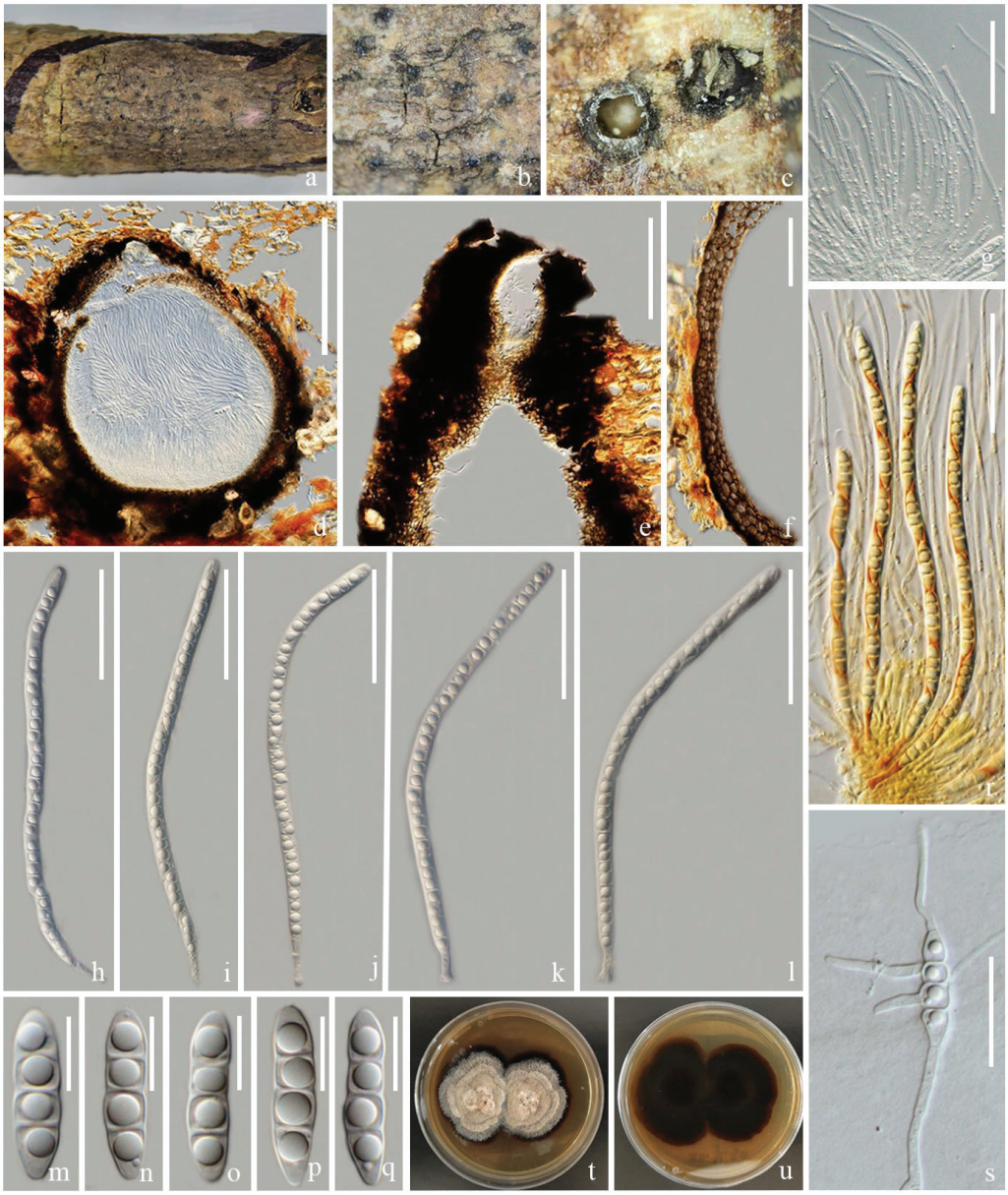

Figure 2. *Melomastia puerensis* (ZHKU 23–0106, **holotype**) **a–c** appearance of ascomata on host surface **d** vertical section of an ascoma **e** vertical section of ostiole **f** section of peridium **g** hamathecium **h–l** asci **m–q** ascospores **r** asci stained in Lugol's iodine **s** germinated ascospore **t, u** colonies on PDA (t-front and u-reverse views). Scale bars: 100 μm **(d–f)**; 50 μm **(g–l)**; 10 μm **(m–q)**; 30 μm **(s)**.

Notes. The phylogenetic analyses showed that *Melomastia puerensis* clustered basal to *M. distoseptata*, *M. fusispora*, *M. maomingensis*, *M. oleae*, *M. pyriformis*, *M. thamplaensis* and *M. winteri* with 99% MP, 1.00 PP support (Fig. 1). We compared the morphology of our collection with closely-related species and the differences are mentioned in Table 2. Our collection has slight differences from other closely-related species by having larger ascomata and wider peridium, but the phylogenetic tree shows that they are different species (Fig. 1, Table 2). Therefore, we introduce *M. puerensis* as a new species, based on morphology and phylogenetic analyses.

Pleosporales Luttrell ex M.E. Barr

Nigrogranaceae Jaklitsch & Voglmayr

Notes. Nigrogranaceae was introduced by Jaklitsch and Voglmayr (2016), with *Nigrograna* as the type genus. The members of Nigrogranaceae can be found on a wide range of hosts in marine and terrestrial habitats (Dayarathne et al. 2020; Boonmee et al. 2021; Lu et al. 2022; Hyde et al. 2023).

***Nigrograna* Gruyter, Verkley & Crous**

Notes. *Nigrograna* was introduced by De Gruyter et al. (2013) with *N. mackinnonii* as the type species. *Nigrograna* has 32 epithets in Index Fungorum (2024). Ahmed et al. (2014) transferred *N. mackinnonii* to *Biatriospora*, based on multigene phylogenetic analysis. Kolařík et al. (2017) introduced four new endophytic species viz. *B. antibiotica*, *B. carollii*, *B. peruviensi*, and *B. yasuniana* in *Biatriospora*, based on morphology and multigene phylogeny and, later, Kolařík (2018) synonymised these four species under *Nigrograna*. The sexual morph of *Nigrograna* is characterised by globose, immersed or less commonly superficial ascomata, bitunicate, fissitunicate 8-spored asci with short stipe and knob-like base, asymmetric, fusoid, 1–3-septate, pale to chocolate brown, smooth or faintly verrucose ascospores (Jaklitsch and Voglmayr 2016). The asexual morph is characterised by globose to subglobose or pyriform pycnidia, solitary terminal phialides conidiophores, ampulliform, lageniform or subcylindrical phialides, oblong, cylindrical or allantoid conidia, sometimes ellipsoid and 1-celled (Jaklitsch and Voglmayr 2016; Lu et al. 2022). In this study, we introduced one new species isolated from rubber tree, based on morphology and phylogeny.

***Nigrograna lincangensis* R.F. Xu & Tibpromma, sp. nov.**
Index Fungorum number: IF901420
Facesoffungi number: FoF15196
Fig. 4

Etymology. The name refers to the location "Lincang, Yunnan, China", where the holotype was collected.

Holotype. ZHKU 23–0104.

Description. ***Saprobic*** on a dead branch of *Hevea brasiliensis*. ***Sexual morph:*** Ascomata 285–360 µm high, 230–307 µm diam. ($\bar{x}$ = 337 × 272 µm, n = 5), immersed, under the clypeus, sometimes inconspicuous on host surface and small bumps can be seen, solitary, dark brown, globose or ellipsoid, with papilla. Ostioles 117–217 × 68–124 µm ($\bar{x}$ = 152 × 99 µm, n = 10), central, brown, papillate. Peridium 16–45 µm wide, comprising several layers with dark-brown to dark cells of textura angularis. Hamathecium comprises 1.5–3 µm wide, unbranched, septate, hyaline, pseudoparaphyses. Asci 45–70 × 9–12 µm ($\bar{x}$ = 57 × 10 µm, n = 10), 8-spored, bitunicate, pedicellate, club shape, cylindrical to clavate, straight or slightly curved, apically rounded, thick-walled. Ascospores 10–15 × 4–6 µm ($\bar{x}$ = 13 × 4.8 µm, n = 30), 1–2-seriate, initially 1-septate, becoming 3-septate at the maturity, fusoid to narrowly ellipsoid, upper part or second cell slightly wider and tapering towards narrow ends, constricted at the septa, hyaline to yellow-brown to brown with age, guttulate, think-walled. ***Asexual morph:*** Undetermined.

Culture characteristics. Spores germinated within 12 hours, colonies grow on PDA at 28 °C, circular, floppy, entire edge, raised, grey to taupe, reverse dark brown.

Material examined. China, Yunnan Province, Lincang, on a dead branch of *Hevea brasiliensis*, 28 July 2022, Rui-Fang Xu, LCR06, (ZHKU 23–0104, holotype); ex-type ZHKUCC 23–0798, ZHKUCC 23–0799.

GenBank numbers. ZHKUCC 23–0798 = ITS: OR853099, LSU: OR922323, SSU: OR941079, *tef*1-α: OR966282, *rpb*2: OR966280; ZHKUCC 23–0799 = ITS: OR853100, LSU: OR922324, SSU: OR941080, *tef1-α*: OR966283, *rpb*2: OR966281.

Notes. In the phylogenetic analyses, *Nigrograna lincangensis* (ZHKUCC 23–0798) forms a closely-related clade to *N. asexualis* (ZHKUCC 22–0214), *N. aquilariae* (ZHKUCC 23–0070) and *N. verniciae* with 100% ML and 1.00 PP support (Fig. 3). However, we could not compare the morphological characteristics of *N. lincangensis* and *N. asexualis*, because *N. lincangensis* was described only from its sexual morph in nature, while *N. asexualis* was described by its asexual morph in nature from coffee in China. A comparison of the ITS region of *N. lincangensis* and *N. asexualis* revealed 16 base pair differences (3.46%) across 462 nucleotides, 40 base pair differences (4.21%) across 949 nucleotides in *tef*1-α gene, 124 base pair differences (12%) across 1033 nucleotides in *rpb*2 gene. *Nigrograna aquilariae* and *N. verniciae* have very similar morphological characteristics, but they can be differentiated by having wider ascomata (285–360 µm vs. 180–270 µm), larger asci (45–70 × 9–12 µm vs. 49–57 × 7–9 µm) and larger ascospores (10–15 × 4–6 µm vs. 10–13 × 3.5–4.5 µm) in *N. lincangensis* (Du et al. 2024); while *N. verniciae* has larger ascomata (340–360 × 350–370 µm vs. 85–360 µm × 230–307 µm) and asci with knob-like to furcate pedicels (Li et al. 2023).

Nigrograna lincangensis has similar ascomata, asci and ascospore characteristics similar to other *Nigrograna* species (Jaklitsch and Voglmayr 2016; Hyde et al. 2017; Tibpromma et al. 2017; Dayarathne et al. 2020; Mapook et al. 2020; Lu et al. 2022). However, *N. lincangensis* differs from *N. cangshanensis* by having larger ascomata (285–360 × 230–307 µm vs. 120–135 × 135–155 µm) (Tibpromma et al. 2017). *Nigrograna chromolaenae* can be distinguished from *N. lincangensis* in having smaller ascomata (160–280 × 115–130 µm vs. 285–360 × 230–307 µm), smaller asci (40–55 × 7–10 µm vs. 45–70 × 9–12 µm), and greyish-brown to dark brown ascospores (Mapook et al. 2020). *Nigrograna coffeae* differs from *N. cangshanensis* by having smaller ascomata (90–140 × 140–200 µm vs. 285–360 × 230–307 µm), 1-septate ascospores (Lu et al. 2022). *Nigrograna novergica* differs

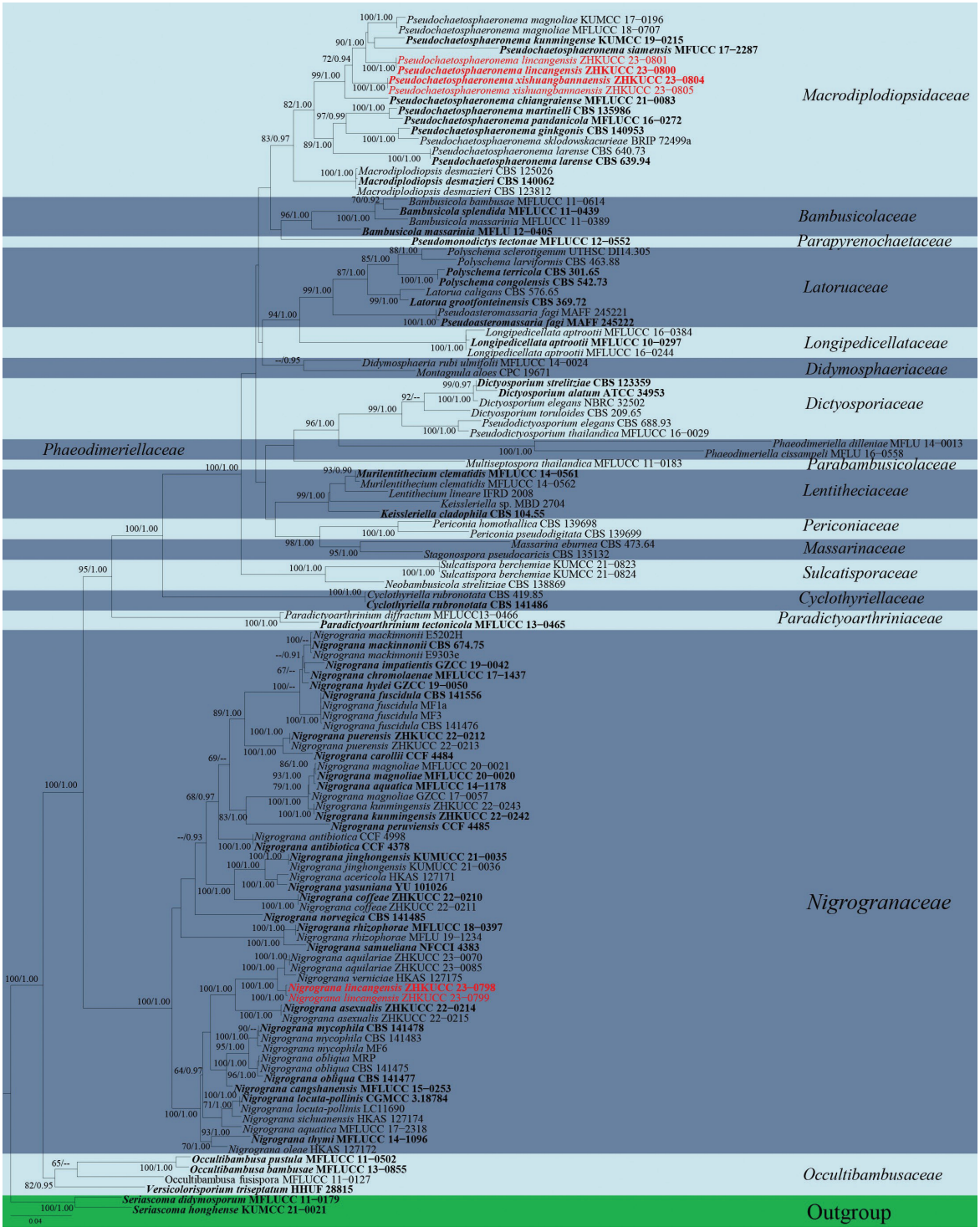

Figure 3. Phylogram generated from Maximum Likelihood analysis based on combined LSU, ITS, SSU, *tef*1-α and *rpb*2 sequence data of 119 taxa, which comprised 4399 base pairs (LSU = 908 bp, ITS = 512 bp, SSU = 1000 bp, *tef*1-α = 925 bp, *rpb*2 = 1054 bp). The best scoring RAxML tree with a final likelihood value of -38918.764563 is presented. The matrix had 2023 distinct alignment patterns, with 39.00% of undetermined characters or gaps. Estimated base frequencies were as follows: A = 0.245191, C = 0.247520, G = 0.268228, T = 0.239061; substitution rates: AC = 1.533778, AG = 3.877174, AT = 1.672983, CG = 1.254032, CT = 8.838860, GT = 1.000000; gamma distribution shape parameter α = 0.208600. Bootstrap support values for ML equal to or greater than 60% and Bayesian Inference analysis values equal to or greater than 0.90 PP are labelled at each node. The tree is rooted with *Seriascoma didymospora* (MFLUCC 11–0179) and *S. didymospora* (MFLUCC 11–0194). Related sequences were obtained from De Silva et al. (2022), Lu et al. (2022) and Li et al. (2023). The new isolates are indicated in red and the ex-type strains are in bold.

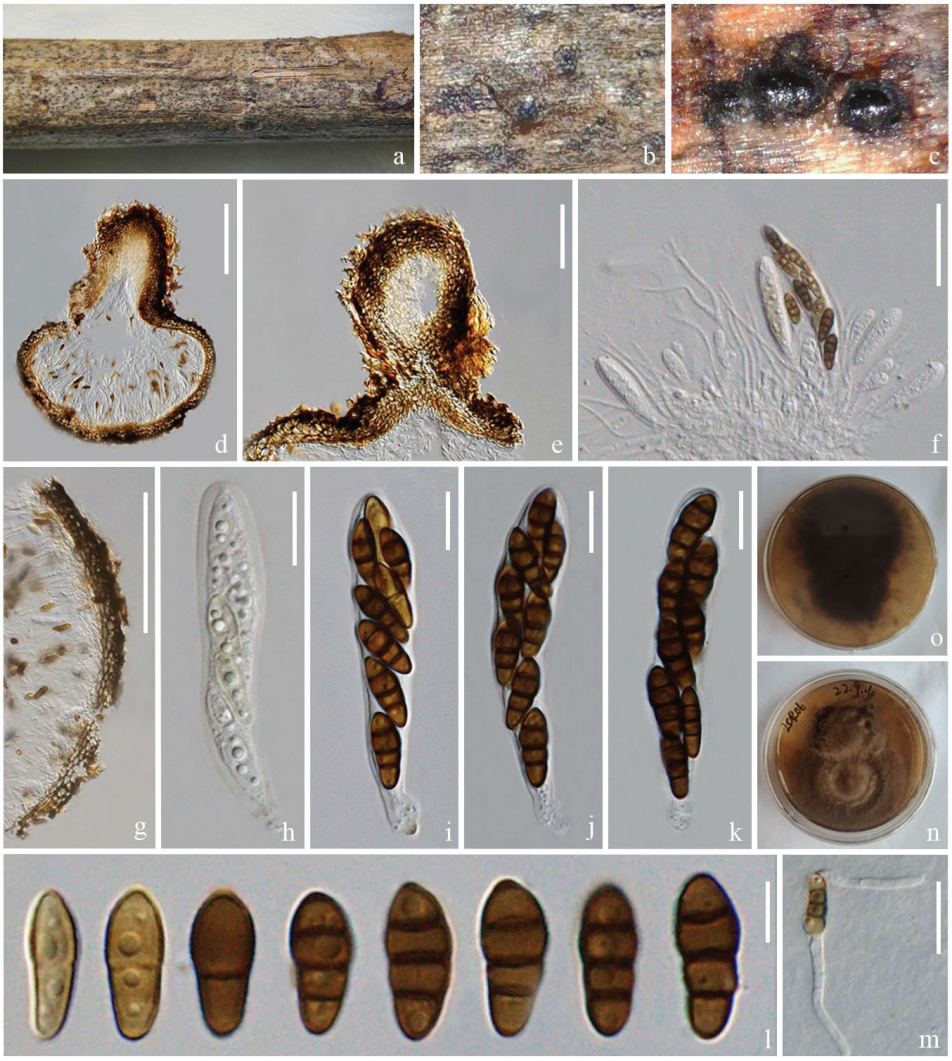

Figure 4. *Nigrograna lincangensis* (ZHKU 23–0104, **holotype**) **a–c** appearance of ascomata on the host surface **d** vertical section of an ascoma **e** vertical section of ostiole **f** hamathecium and asci **g** section of peridium **h–k** asci **l** ascospores **m** a germinated ascospore **n, o** colonies on PDA (n-front and o-reverse views). Scale bars: 100 µm (**d**); 50 µm (**e**); 30 µm (**f**); 200 µm (**g**); 10 µm (**h–k**); 5 µm (**l**); 20 µm (**m**).

from *N. lincangensis* as it occurs on pseudostromata from the host of *Diaporthe* sp. (Jaklitsch and Voglmayr 2016). *Nigrograna mycophila* and *N. obliqua* are distinct from *N. lincangensis* by having dark brown ascospores (Jaklitsch and Voglmayr 2016). *Nigrograna puerensis* differs from *N. lincangensis* by having acute apical and basal cells and the apical cells are wider than the basal cells (Lu et al. 2022). *Nigrograna samueliana* differs from *N. lincangensis* by the absence of ostiole (Dayarathne et al. 2020). *Nigrograna thymi* can be easily distinguished from *N. lincangensis* in having 4–5 septate (Hyde et al. 2017). Therefore, *N. lincangensis* is described here as a new species, based on phylogeny and morphology.

Macrodiplodiopsidaceae Voglmayr, Jaklitsch & Crous

Notes. Macrodiplodiopsidaceae was introduced by Crous et al. (2015) with *Macrodiplodiopsis* as the type genus. There are two genera viz. *Macrodiplodiopsis* and *Pseudochaetosphaeronema* in this family (Wijayawardene et al. 2022).

***Pseudochaetosphaeronema* Punith.**

Notes. *Pseudochaetosphaeronema* was introduced by Punithalingam (1979), with *P. larense* as the type species. The members of this genus have been reported as human pathogens, endophytes and saprobes (Boonmee et al. 2021). Nine epithets are listed in Index Fungorum (2024), i.e. one sexual *P. chiangraiense* and eight asexual species viz. *P. ginkgonis*, *P. kunmingense*, *P. larense*, *P. magnoliae*, *P. martinelli*, *P. pandanicola*, *P. siamense* and *P. sklodowskacurieae*. The asexual morph of *Pseudochaetosphaeronema* is characterised by globose, conidiomata, monophialidic, cylindrical conidiogenous cells and hyaline, subglobose to oval, aseptate conidia (De Silva et al. 2022). The sexual morph is characterised by immersed, uni-loculate ascomata, peridium with the cells of textura angularis, unbranched, septate pseudoparaphyses, 8-spored, bitunicate, fissitunicate, short distinct pedicel asci with rounded end and fusiform, 1-septate, guttulate ascospores with pointed ends (Boonmee et al. 2021).

***Pseudochaetosphaeronema lincangensis* R.F. Xu & Tibpromma, sp. nov.**
Index Fungorum number: IF901421
Facesoffungi number: FoF15197
Fig. 5

Etymology. The name refers to the location "Lincang, Yunnan, China", where the holotype was collected.

Holotype. ZHKU 23–0105.

Description. ***Saprobic*** on a dead branch of *Hevea brasiliensis*. ***Sexual morph:*** Ascomata 140–245 µm high, 255–290 µm diam., ($\bar{x}$ = 190 × 267 µm, n = 5), immersed, visible as dark-brown dots on the host surface, solitary, uni-loculate, ampulliform, without ostiole. Peridium 18–50 µm wide, several layers, comprising dark-brown to pale-brown cells of textura angularis. Hamathecium comprises 2–3 µm wide, numerous, hyaline, unbranched, pseudoparaphyses. Asci 90–145 × 15–30 µm ($\bar{x}$ = 112 × 22 µm, n = 15), 8-spored, bitunicate, cylindrical to clavate, apically rounded, short pedicelate, with a small ocular chamber, thick-walled. Ascospores 25–40 × 8–15 µm ($\bar{x}$ = 30 × 11 µm, n = 35), overlapping, 2-seriate, fusiform, 1-septum in the middle of cell, widest at the centre and tapering towards narrow ends, constricted at the septum, hyaline, guttulate, with ellipsoid mucilaginous sheath, thick and smooth-walled. ***Asexual morph:*** Undetermined.

Culture characteristics. culture on PDA, colonies slow growing on 28 °C, low convex, entire, smooth, edge is off-white from above, dark brown, edge is orange on reverse side.

Material examined. China, Yunnan Province, Lincang on a dead branch of *Hevea brasiliensis*, 28 July 2022, Rui-Fang Xu, LCR07 (ZHKU 23–0105, holotype); ex-type ZHKUCC 23–0800, ZHKUCC 23–0801.

GenBank numbers. ZHKUCC 23–0800 = ITS: OR853095, LSU: OR922336, SSU: OR922342, *tef*1-α: OR966290; ZHKUCC 23–0801 = ITS: OR853096, LSU: OR922337, SSU: OR922343, *tef*1-α: OR966291.

Notes. In the phylogenetic analyses, *Pseudochaetosphaeronema lincangensis* clusters distinctly, sister to *P. kunmingense*, *P. magnoliae* and *P. siamensis* with 90% MP, 1.00 PP support (Fig. 3). The base pair differences in ITS, LSU,

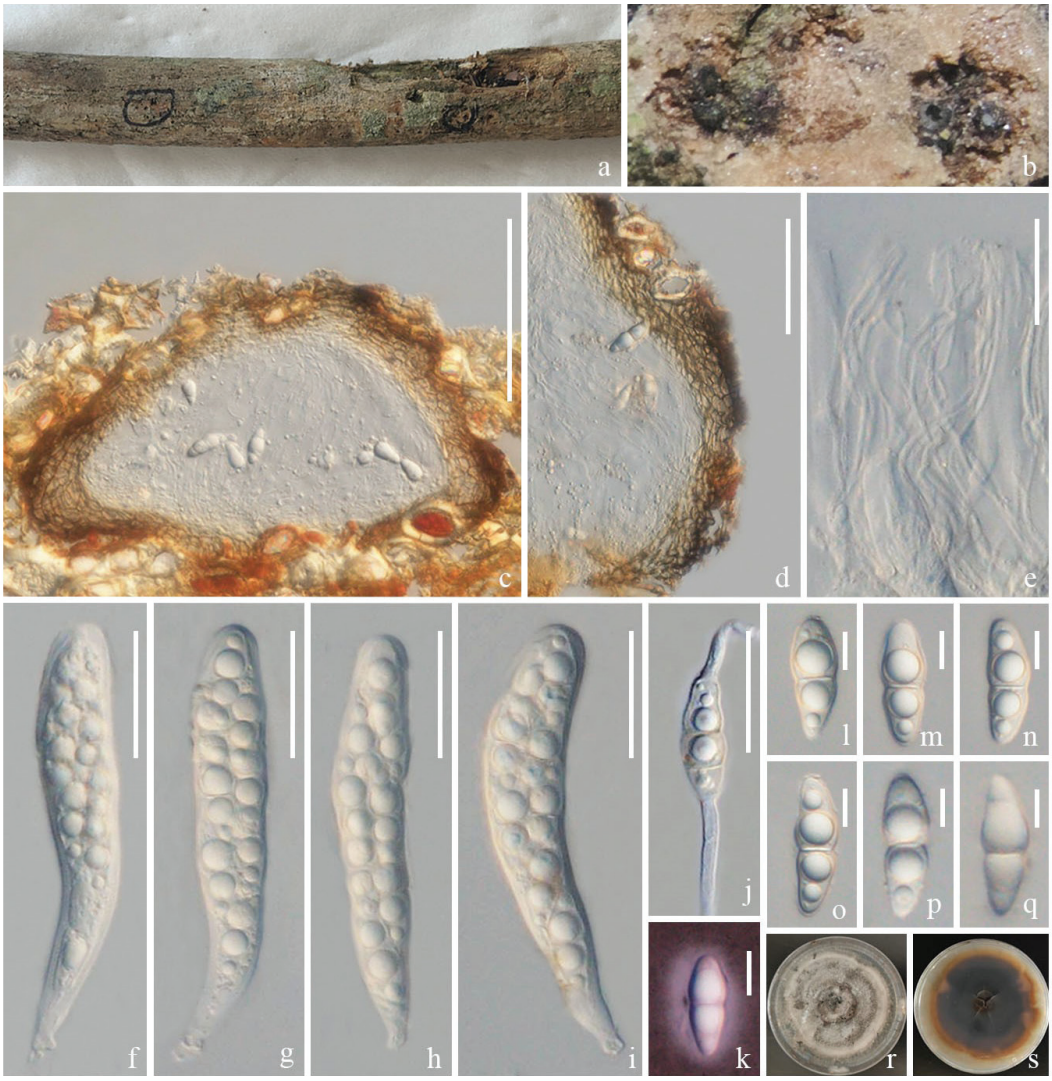

Figure 5. *Pseudochaetosphaeronema lincangensis* (ZHKU 23–0105, **holotype**) **a, b** appearance of ascomata on host substrate **c** vertical section of an ascoma **d** section of peridium **e** pseudoparaphyses **f–i** asci **j** a germinated ascospore **l–q** ascospores **k** ascospore stained with Indian ink **r, s** colonies on PDA (r-front and s-reverse views). Scale bars: 100 µm (**c**); 50 µm (**d**); 30 µm (**e–j**); 200 µm (**g**); 10 µm (**k, l–q**).

SSU and *tef*1-α sequences of our new species are compared with *P. kunmingense*, *P. magnoliae* and *P. siamensis* (Table 3). However, we could not compare the morphological characteristics of the species above, as they were described, based on asexual morphs. Therefore, based on morphology and phylogeny, we introduce *Pseudochaetosphaeronema lincangensis* as a new species.

Pseudochaetosphaeronema xishuangbannaensis **R.F. Xu & Tibpromma, sp. nov.**
Index Fungorum number: IF901422
Facesoffungi number: FoF15198
Fig. 6

Etymology. The name refers to the location "Xishuangbanna, Yunnan, China", where the holotype was collected.

Holotype. ZHKU 23–0107.

Table 3. Nucleotide differences in the ITS, LSU, SSU and *tef*1-α of *P. lincangensis* (ZHKUCC 23–0800) compared with *P. kunmingense*, *P. magnoliae* and *P. siamensis*.

Strains	ITS	LSU	SSU	*tef*1-α
P. kunmingense (KUMCC 19–0215)	30/506 (5.93%)	10/855 (1.16%)	4/1012 (0.39%)	38/893 (4.26%)
P. magnoliae (KUMCC 17–0196)	51/539 (9.46%)	19/854 (2.22%)	8/939 (0.85%)	32/899 (3.56%)
P. siamensis (MFUCC 17–2287)	43/480 (8.96%)	11/848 (1.29%)	1/1005 (0.09%)	98/645 (15.19%)

Description. ***Saprobic*** on a dead branch of *Hevea brasiliensis*. ***Sexual morph:*** Ascomata 270–410 µm high, 370–480 µm diam., ($\bar{x}$ = 350 × 420 µm, n = 5), solitary, scattered, immersed, globose to subglobose, uni-loculate, black. Peridium 40–90 µm wide, thin-walled, composed of several layers of small, brown to pale brown cells of textura intricata. Hamathecium comprises 2–3 µm wide, numerous, dense, filiform, unbranched, hyaline, cellular pseudoparaphyses. Asci 130–180 × 25–35 µm ($\bar{x}$ = 155 × 32 µm, n = 20), 8-spored, bitunicate, obovoid, short distinct pedicel with conical end, apex rounded with a minute ocular chamber. Ascospores 30–50 × 10–20 µm ($\bar{x}$ = 42 × 13 µm, n = 30), hyaline, fusiform, with pointed ends, 3–5-septate, larger upper third cell, constricted at the septa, guttulate, thick-walled, with mucilaginous sheath, the sheath constricted at the middle. ***Asexual morph:*** Undetermined.

Culture characteristics. Colony on PDA, colonies slow growing on 28 °C, umbonate, filiform, smooth, edges brown, from above, brown, dark brown on reverse side.

Material examined. China, Yunnan Province, Xishuangbanna on a dead branch of *Hevea brasiliensis*, 12 September, 2021, Rui-Fang Xu, XSBNR–41 (ZHKU 23–0107, holotype); ex-type ZHKUCC 23–0804, ZHKUCC 23–0805.

GenBank numbers. ZHKUCC 23–0804 = ITS: OR853097, LSU: OR922338, SSU: OR922344, *tef*1-α: OR966286; ZHKUCC 23–0805 = ITS: OR853098, LSU: OR922339, SSU: OR922345, *tef*1-α: OR966287.

Notes. In the phylogenetic analyses, *Pseudochaetosphaeronema xishuangbannaensis* clusters with *P. lincangensis* with 99% ML and 1.00 PP support (Fig. 3). Morphologically, *P. xishuangbannaensis* differs from *P. lincangensis* in having longer asci (130–180 µm vs. 90–145 µm), 3–5-septate ascospores with sheath constricted at the central septum and brown to dark brown colonies, while *P. lincangensis* has ascospores with a normal sheath in a circle, 1-septate ascospores with obtuse ends and colonies off-white from the forward edge, orange in reverse. *Pseudochaetosphaeronema xishuangbannaensis* shares similar morphologies with *P. chiangraiense*, but can be differentiated by having the peridium with the cells of *textura intricate*, larger ascomata (270–410 × 370–480 µm vs. 190–255 × 190–200 µm), longer asci (130–180 µm vs. 50–110 µm), larger (30–50 × 10–20 µm vs. 20–45 × 15–30 µm) and 3–5 septate ascospores with a sheath constricted at the central septum and brown to dark brown colonies. *Pseudochaetosphaeronema chiangraiense* has textura angularis peridium, ascospores surrounded by a normal sheath in a circle, 1-septum, obtuse ends, from above, greenish-grey in the middle and pale brown at the margin, yellowish-brown on the reverse side (Boonmee et al. 2021). In addition, *P. xishuangbannaensis* formed a different lineage with *P. chiangraiense* (Fig. 3). Therefore, *P. xishuangbannaensis* is described as a new species, based on phylogenetic analyses and morphological comparison.

Figure 6. *Pseudochaetosphaeronema xishuangbannaensis* (ZHKU 23–0107, **holotype**) **a–c** appearance of ascomata on host substrate **d** section of an ascoma **e** peridium **f** pesudoparaphyses **g–j** asci **m–t** ascospores **u** ascospore stained with Indian ink **k, l** colonies on PDA (k-front and l-reverse view). Scale bars: 200 μm **(d)**; 100 μm **(e)**; 50 μm **(f–j)**; 10 μm **(m–t)**; 20 μm **(u)**.

Discussion

Global fungal diversity is astounding. Although around 155,000 fungal species have been described, up to 19 million have yet to be described (Hyde 2022; Phukhamsakda et al. 2022). Fungi have been classified into five different phyla: Chytridiomycota, Zygomycota, Glomeromycota, Ascomycota and Basidiomycota (Agui-

lar-Marcelino et al. 2020; Wijayawardene et al. 2022). Fungi play an important role in litter decomposition by breaking down lignin and other refractory components in the litter, thereby affecting the decomposition of terrestrial ecosystems, especially by activities of Basidiomycota and Ascomycota (Osono and Takeda 2002; Bucher et al. 2004; Phukhamsakda et al. 2022). Discovering more saprophytic fungi associated with rubber will enrich our knowledge on saprobic fungi and their functions as litter degraders. Microfungi from warm climates have a more significant decomposition capacity than from cool climates (Osono et al. 2011). Previous studies have reported that Ascomycota, Basidiomycota and Oomycota are abundant on Pará rubber leaf and branch litter (Monkai et al. 2017; Meeboon and Takamatsu 2020; Senwanna et al. 2021). Nizamani et al. (2023) provided a checklist comprising 788 species and 179 taxa identified at the genus level from 57 countries. The taxa listed in the checklist belong to 515 genera, 180 families and 68 orders and more than half of these taxa were isolated from leaf and branch litter.

In Southeast Asia, Pará rubber plantations have been expanding rapidly since the 20th century and, currently, supply over 90% of the world's natural rubber (Fox and Vogler 2005; Mann 2009; Ziegler et al. 2009). More than one million hectares of lands in Cambodia, Laos, Myanmar, South China, Thailand and Vietnam have been converted into Pará rubber plantations (Li and Fox 2012). In 1904, China planted rubber for the first time in Yingjiang, Dehong, in Yunnan Province (Chapman 1991). Pará rubber is widely cultivated in the Hainan, Guangdong, Guangxi, Fujian and Yunnan Provinces in China as an economically important plant (Wang et al. 2015).

Pará rubber is vulnerable to many pests and diseases, but it is still a mystery why only a few fungal species have been found on rubber (Senwanna et al. 2021). Pará rubber tree was introduced to China from Malaysia, presumably by seed and endemic fungi are unlikely to follow; therefore, new fungi colonise Pará rubber through host-shifting or host-jumping (Roy 2001; Senwanna et al. 2019, 2021). Fungi associated with Pará rubber are found in different life modes such as saprobic, endophytic and pathogenic (Gazis and Chaverri 2010; Monkai et al. 2017; Senwanna et al. 2021). On Pará rubber, Dothideomycetes predominate amongst ascomycetes (Senwanna et al. 2021) and four species described in our study also belong to Dothideomycetes.

Fungal pathogens and endophytes were also isolated from the Pará rubber trees. Additionally, studies have been conducted to analyse the richness and diversity of endophytic fungi in different tissues of *Hevea brasiliensis* (Martin et al. 2015; Rojas-Jimenez et al. 2016; Araújo et al. 2020). Pathogens cause potential disease threats to *Hevea brasiliensis*; for example, *Corynespora cassiicola* causes *Corynespora* leaf fall disease (Jayasinghe and Fernando 1998), *Microcyclus ulei* causes South American leaf blight (Júnior et al. 2014), the basidiomycete genera *Phellinus*, *Rigidoporus* and *Ganoderma* cause stem- and root-rots (Mohammed et al. 2014). In addition, the estimated richness of endophytic fungi does not significantly differ amongst the leaves, stems and roots; and the fungal diversity is higher in the stems and roots compared to the leaves (Martin et al. 2015; Araújo et al. 2020). Mahendran et al. (2021) revealed that *Aspergillus terreus* has a good inhibitory potential against *Rigidoporus microporus* and *Corynespora cassiicola* and has potential for biological control. Therefore, it is important to understand the fungi associated with Pará rubber trees to manage and prevent rubber tree diseases.

Only a few reports are available for the saprobic fungi on *Hevea brasiliensis* in China and many taxa lack molecular data (Seephueak et al. 2010, 2011; Senwanna et al. 2021). Therefore, a revised taxonomic approach with multi-gene phylogenetic analyses is necessary to understand the fungal diversity associated with Pará rubber. In this study, we introduce four new saprobic fungi from branches and twigs of rubber trees, based on morphology and molecular phylogenetic analyses. This enriches the fungal diversity in Pará rubber and provides information for host jumping.

Acknowledgements

Rui-Fang Xu thanks Ying Gao for her support in uploading protein genes to GenBank and Jing-Yi Zhang and Ya-Ru Sun for their help in submitting the alignments to TreeBASE. The authors extend their appreciation to the Researchers Supporting Project Number (RSP2024R56), King Saud University, Riyadh, Saudi Arabia.

Additional information

Conflict of interest

The authors have declared that no competing interests exist.

Ethical statement

No ethical statement was reported.

Funding

This study was supported by the National Natural Science Foundation of China (Numbers NSFC 32260004 and 31760013) and High-Level Talent Recruitment Plan of Yunnan Province ("Young Talents" and "High-End Foreign Experts" programmes); the central government guides local projects of Yunnan Provincial Science and Technology Department (No. 202307AC110003); Researchers Supporting Project Number (RSP2024R56), King Saud University, Riyadh, Saudi Arabia. This study was partially supported by Chiang Mai University, Thailand.

Author contributions

Conceptualization: SCK, ST. Data curation: RFX. Formal analysis: SCK. Funding acquisition: DQD, SCK, JK. Investigation: ST, SCK, RFX. Methodology: CP, SCK, ST, RFX. Project administration: SCK. Resources: RFX. Software: ST, RFX, CP. Validation: AME, NS. Visualization: RFX. Writing – original draft: RFX. Writing – review and editing: AME, CP, DQD, NS, JK, XYW, RFX, SCK, ST.

Author ORCIDs

Rui-Fang Xu https://orcid.org/0000-0003-1207-8254
Samantha C. Karunarathna https://orcid.org/0000-0001-7080-0781
Chayanard Phukhamsakda https://orcid.org/0000-0002-1033-937X
Dong-Qin Dai https://orcid.org/0000-0001-8935-8807
Abdallah M. Elgorban https://orcid.org/0000-0003-3664-7853
Nakarin Suwannarach https://orcid.org/0000-0002-2653-1913
Jaturong Kumla https://orcid.org/0000-0002-3673-6541

Xiao-Yan Wang https://orcid.org/0009-0009-6430-3637
Saowaluck Tibpromma https://orcid.org/0000-0002-4706-6547

Data availability

All of the data that support the findings of this study are available in the main text.

References

Aguilar-Marcelino L, Mendoza-de-Gives P, Al-Ani LKT, López-Arellano ME, Gómez-Rodríguez O, Villar-Luna E, Reyes-Guerrero DE (2020) Chapter 26 – Using molecular techniques applied to beneficial microorganisms as biotechnological tools for controlling agricultural plant pathogens and pest. In: Sharma V, Salwan R, Al-Ani LKT (Eds) Molecular Aspects of Plant Beneficial Microbes in Agriculture. Academic Press, 333–349. https://doi.org/10.1016/B978-0-12-818469-1.00027-4

Ahmed SA, Van De Sande WWJ, Stevens DA, Fahal A, Van Diepeningen AD, Menken SBJ, De Hoog GS (2014) Revision of agents of black-grain eumycetoma in the order Pleosporales. Persoonia – Molecular Phylogeny and Evolution of Fungi 33: 141–154. https://doi.org/10.3767/003158514X684744

Araújo KS, Brito VN, Veloso TGR, de Leite TS, Alves JL, da Hora BT Junior, Moreno HLA, Pereira OL, Mizubuti ESG, de Queiroz MV (2020) Diversity and distribution of endophytic fungi in different tissues of *Hevea brasiliensis* native to the Brazilian Amazon forest. Mycological Progress 19(10): 1057–1068. https://doi.org/10.1007/s11557-020-01613-4

Basik AA, Sanglier J-J, Yeo CT, Sudesh K (2021) Microbial degradation of rubber: Actinobacteria. Polymers 13(12): 1989. https://doi.org/10.3390/polym13121989

Bhattacharjee A, Bhowmik M, Paul C, Das Chowdhury B, Debnath B (2021) Rubber tree seed utilization for green energy, revenue generation and sustainable development–A comprehensive review. Industrial Crops and Products 174: 114186. https://doi.org/10.1016/j.indcrop.2021.114186

Bhunjun CS, Niskanen T, Suwannarach N, Wannathes N, Chen Y-J, McKenzie EHC, Maharachchikumbura SSN, Buyck B, Zhao C-L, Fan Y-G, Zhang J-Y, Dissanayake AJ, Marasinghe DS, Jayawardena RS, Kumla J, Padamsee M, Chen Y-Y, Liimatainen K, Ammirati JF, Phukhamsakda C, Liu J-K, Phonrob W, Randrianjohany É, Hongsanan S, Cheewangkoon R, Bundhun D, Khuna S, Yu W-J, Deng L-S, Lu Y-Z, Hyde KD, Lumyong S (2022) The numbers of fungi: Are the most speciose genera truly diverse? Fungal Diversity 114(1): 387–462. https://doi.org/10.1007/s13225-022-00501-4

Boonmee S, Wanasinghe DN, Calabon MS, Huanraluek N, Chandrasiri SKU, Jones GEB, Rossi W, Leonardi M, Singh SK, Rana S, Singh PN, Maurya DK, Lagashetti AC, Choudhary D, Dai Y-C, Zhao C-L, Mu Y-H, Yuan H-S, He S-H, Phookamsak R, Jiang H-B, Martín MP, Dueñas M, Telleria MT, Kałucka IL, Jagodziński AM, Liimatainen K, Pereira DS, Phillips AJL, Suwannarach N, Kumla J, Khuna S, Lumyong S, Potter TB, Shivas RG, Sparks AH, Vaghefi N, Abdel-Wahab MA, Abdel-Aziz FA, Li G-J, Lin W-F, Singh U, Bhatt RP, Lee HB, Nguyen TTT, Kirk PM, Dutta AK, Acharya K, Sarma VV, Niranjan M, Rajeshkumar KC, Ashtekar N, Lad S, Wijayawardene NN, Bhat DJ, Xu R-J, Wijesinghe SN, Shen H-W, Luo Z-L, Zhang J-Y, Sysouphanthong P, Thongklang N, Bao D-F, Aluthmuhandiram JVS, Abdollahzadeh J, Javadi A, Dovana F, Usman M, Khalid AN, Dissanayake AJ, Telagathoti A, Probst M, Peintner U, Garrido-Benavent I, Bóna L, Merényi Z, Boros L, Zoltán B, Stielow JB, Jiang N, Tian C-M, Shams E, Dehghanizadeh F, Pordel A, Javan-Nikkhah M, Denchev TT, Denchev CM, Kemler M, Begerow D, Deng C-Y, Harrower E, Bozorov T, Kholmuradova T, Gafforov Y, Abdurazakov A, Xu J-C, Mortimer PE, Ren G-C, Jeewon R, Maharachchi-

kumbura SSN, Phukhamsakda C, Mapook A, Hyde KD (2021) Fungal diversity notes 1387–1511: Taxonomic and phylogenetic contributions on genera and species of fungal taxa. Fungal Diversity 111(1): 1–335. https://doi.org/10.1007/s13225-021-00489-3

Bucher VVC, Hyde KD, Pointing SB, Reddy CA (2004) Production of wood decay enzymes, mass loss and lignin solubilization in wood by marine ascomycetes and their anamorphs. Fungal Diversity 15: 1–14.

Capella-Gutiérrez S, Silla-Martínez JM, Gabaldón T (2009) trimAl: A tool for automated alignment trimming in large-scale phylogenetic analyses. Bioinformatics (Oxford, England) 25(15): 1972–1973. https://doi.org/10.1093/bioinformatics/btp348

Carbone I, Kohn L (1999) A Method for designing primer sets for speciation studies in filamentous ascomycetes. Mycologia 91(3): 553–556. https://doi.org/10.1080/00275514.1999.12061051

Chaiwan N, Gomdola D, Wang S, Monkai J, Tibpromma S, Doilom M, Wanasinghe DN, Mortimer PE, Lumyong S, Hyde KD (2021) An online database providing updated information of microfungi in the Greater Mekong Subregion. Mycosphere 12(1): 1513–1526. https://doi.org/10.5943/mycosphere/12/1/19

Chapman EC (1991) The Expansion of Rubber in Southern Yunnan, China. The Geographical Journal 157(1): 36–44. https://doi.org/10.2307/635142

Crous PW, Carris LM, Giraldo A, Groenewald JZ, Hawksworth DL, Hemández-Restrepo M, Jaklitsch WM, Lebrun M-H, Schumacher RK, Stielow JB, Van Der Linde EJ, Vilcāne J, Voglmayr H, Wood AR (2015) The Genera of Fungi – fixing the application of the type species of generic names – G 2: *Allantophomopsis*, *Latorua*, *Macrodiplodiopsis*, *Macrohilum*, *Milospium*, *Protostegia*, *Pyricularia*, *Robillarda*, *Rotula*, *Septoriella*, *Torula*, and *Wojnowicia*. IMA Fungus 6(1): 163–198. https://doi.org/10.5598/imafungus.2015.06.01.11

Dayarathne M, Maharachchikumbura S, Hyde K, Devadatha B, Jones G, Chomnunti P, Khongphinitbunjong K (2020) Morpho-molecular characterization of microfungi associated with marine based habitats. Mycosphere: Journal of Fungal Biology 7019(1): 1–188. https://doi.org/10.5943/mycosphere/11/1/1

De Gruyter J, Woudenberg JHC, Aveskamp MM, Verkley GJM, Groenewald JZ, Crous PW (2013) Redisposition of phoma-like anamorphs in Pleosporales. Studies in Mycology 75: 1–36. https://doi.org/10.3114/sim0004

De Silva N, Hyde KD, Lumyong S, Phillips A, Bhat D, Maharachchikumbura S, Thambugala K, Tennakoon D, Suwannarach N, Karunarathna SC (2022) Morphology, phylogeny, host association and geography of fungi associated with plants of Annonaceae, Apocynaceae and Magnoliaceae. Mycosphere: Journal of Fungal Biology 13(1): 955–1076. https://doi.org/10.5943/mycosphere/13/1/12

Dong W, Hyde KD, Jeewon R, Liao CF, Zhao HJ, Kularathnage ND, Li H, Yang YH, Pem D, Shu YX, Gafforov Y, Manawasinghe IS, Doilom M (2023) Mycosphere notes 449–468: Saprobic and endophytic fungi in China, Thailand, and Uzbekistan. Mycosphere: Journal of Fungal Biology 14(1): 2208–2262.

Du TY, Tibpromma S, Hyde KD, Dai D-Q, Mapook A, Zhang G-Q, Stephenson SL, Suwannarach N, Elgorban AM, Rajeshkumar KC, Maharachchikumbura SSN, Li Q, Karunarathna SC (2024) The polyphasic approach reveals twelve novel ascomycota taxa from terrestrial agarwood-producing trees. [Not published]

Feng B, Yang Z (2018) Studies on diversity of higher fungi in Yunnan, southwestern China: A review. Plant Diversity 40(4): 165–171. https://doi.org/10.1016/j.pld.2018.07.001

Fox J, Vogler JB (2005) Land-Use and Land-Cover Change in Montane Mainland Southeast Asia. Environmental Management 36(3): 394–403. https://doi.org/10.1007/s00267-003-0288-7

Gazis R, Chaverri P (2010) Diversity of fungal endophytes in leaves and stems of wild rubber trees (*Hevea brasiliensis*) in Peru. Fungal Ecology 3(3): 240–254. https://doi.org/10.1016/j.funeco.2009.12.001

Hongsanan S, Hyde KD, Phookamsak R, Wanasinghe DN, McKenzie EHC, Sarma VV, Lücking R, Boonmee S, Bhat JD, Liu N-G, Tennakoon DS, Pem D, Karunarathna A, Jiang S-H, Jones GEB, Phillips AJL, Manawasinghe IS, Tibpromma S, Jayasiri SC, Sandamali D, Jayawardena RS, Wijayawardene NN, Ekanayaka AH, Jeewon R, Lu Y-Z, Phukhamsakda C, Dissanayake AJ, Zeng X-Y, Luo Z-L, Tian Q, Thambugala KM, Dai D, Samarakoon MC, Chethana KWT, Ertz D, Doilom M, Liu J-K, Pérez-Ortega S, Suija A, Senwanna C, Wijesinghe SN, Niranjan M, Zhang S-N, Ariyawansa HA, Jiang H-B, Zhang J-F, Norphanphoun C, de Silva NI, Thiyagaraja V, Zhang H, Bezerra JDP, Miranda-González R, Aptroot A, Kashiwadani H, Harishchandra D, Sérusiaux E, Abeywickrama PD, Bao D-F, Devadatha B, Wu H-X, Moon KH, Gueidan C, Schumm F, Bundhun D, Mapook A, Monkai J, Bhunjun CS, Chomnunti P, Suetrong S, Chaiwan N, Dayarathne MC, Yang J, Rathnayaka AR, Xu J-C, Zheng J, Liu G, Feng Y, Xie N (2020) Refined families of Dothideomycetes: Orders and families incertae sedis in Dothideomycetes. Fungal Diversity 105(1): 17–318. https://doi.org/10.1007/s13225-020-00462-6

Huelsenbeck JP, Ronquist F (2001) MRBAYES: Bayesian inference of phylogenetic trees. Bioinformatics (Oxford, England) 17(8): 754–755. https://doi.org/10.1093/bioinformatics/17.8.754

Hyde KD (2022) The numbers of fungi. Fungal Diversity 114(1): 1. https://doi.org/10.1007/s13225-022-00507-y

Hyde KD, Jones EBG, Liu J-K, Ariyawansa H, Boehm E, Boonmee S, Braun U, Chomnunti P, Crous PW, Dai D-Q, Diederich P, Dissanayake A, Doilom M, Doveri F, Hongsanan S, Jayawardena R, Lawrey JD, Li Y-M, Liu Y-X, Lücking R, Monkai J, Muggia L, Nelsen MP, Pang K-L, Phookamsak R, Senanayake IC, Shearer CA, Suetrong S, Tanaka K, Thambugala KM, Wijayawardene NN, Wikee S, Wu H-X, Zhang Y, Aguirre-Hudson B, Alias SA, Aptroot A, Bahkali AH, Bezerra JL, Bhat DJ, Camporesi E, Chukeatirote E, Gueidan C, Hawksworth DL, Hirayama K, De Hoog S, Kang J-C, Knudsen K, Li W-J, Li X-H, Liu Z-Y, Mapook A, McKenzie EHC, Miller AN, Mortimer PE, Phillips AJL, Raja HA, Scheuer C, Schumm F, Taylor JE, Tian Q, Tibpromma S, Wanasinghe DN, Wang Y, Xu J-C, Yacharoen S, Yan J-Y, Zhang M (2013) Families of Dothideomycetes. Fungal Diversity 63(1): 1–313. https://doi.org/10.1007/s13225-013-0263-4

Hyde KD, Norphanphoun C, Abreu VP, Bazzicalupo A, Thilini Chethana KW, Clericuzio M, Dayarathne MC, Dissanayake AJ, Ekanayaka AH, He M-Q, Hongsanan S, Huang S-K, Jayasiri SC, Jayawardena RS, Karunarathna A, Konta S, Kušan I, Lee H, Li J, Lin C-G, Liu N-G, Lu Y-Z, Luo Z-L, Manawasinghe IS, Mapook A, Perera RH, Phookamsak R, Phukhamsakda C, Siedlecki I, Soares AM, Tennakoon DS, Tian Q, Tibpromma S, Wanasinghe DN, Xiao Y-P, Yang J, Zeng X-Y, Abdel-Aziz FA, Li W-J, Senanayake IC, Shang Q-J, Daranagama DA, de Silva NI, Thambugala KM, Abdel-Wahab MA, Bahkali AH, Berbee ML, Boonmee S, Bhat DJ, Bulgakov TS, Buyck B, Camporesi E, Castañeda-Ruiz RF, Chomnunti P, Doilom M, Dovana F, Gibertoni TB, Jadan M, Jeewon R, Jones EBG, Kang J-C, Karunarathna SC, Lim YW, Liu J-K, Liu Z-Y, Plautz Jr HL, Lumyong S, Maharachchikumbura SSN, Matočec N, McKenzie EHC, Mešić A, Miller D, Pawłowska J, Pereira OL, Promputtha I, Romero AI, Ryvarden L, Su H-Y, Suetrong S, Tkalčec Z, Vizzini A, Wen T-C, Wisitrassameewong K, Wrzosek M, Xu J-C, Zhao Q, Zhao R-L, Mortimer PE (2017) Fungal diversity notes 603–708: Taxonomic and phylogenetic notes on genera and species. Fungal Diversity 87(1): 1–235. https://doi.org/10.1007/s13225-017-0391-3

Hyde K, Norphanphoun C, Hongde Y, Zhang J, Du T, Gao Y, Farias A, Gui H, He S, Yuke H, Cuijinyi L, Lu L, Hongli S, Tang X, Tian X-G (2023) Mycosphere notes 387–412 – novel species of fungal taxa from around the world. Mycosphere: Journal of Fungal Biology 14(1): 663–744. https://doi.org/10.5943/mycosphere/14/1/8

Index Fungorum (2024) Index Fungorum. https://www.indexfungorum.org [January 15, 2024]

Jaklitsch WM, Voglmayr H (2016) Hidden diversity in *Thyridaria* and a new circumscription of the Thyridariaceae. Studies in Mycology 85(1): 35–64. https://doi.org/10.1016/j.simyco.2016.09.002

Jayasinghe CK, Fernando THPS (1998) Growth at different temperatures and on fungicide amended media: Two characteristics to distinguish *Colletotrichum* species pathogenic to rubber. Mycopathologia 143(2): 93–95. https://doi.org/10.1023/A:1006958623733

Jayasiri SC, Hyde KD, Ariyawansa HA, Bhat J, Buyck B, Cai L, Dai Y-C, Abd-Elsalam KA, Ertz D, Hidayat I, Jeewon R, Jones EBG, Bahkali AH, Karunarathna SC, Liu J-K, Luangsa-ard JJ, Lumbsch HT, Maharachchikumbura SSN, McKenzie EHC, Moncalvo J-M, Ghobad-Nejhad M, Nilsson H, Pang K-L, Pereira OL, Phillips AJL, Raspé O, Rollins AW, Romero AI, Etayo J, Selçuk F, Stephenson SL, Suetrong S, Taylor JE, Tsui CKM, Vizzini A, Abdel-Wahab MA, Wen T-C, Boonmee S, Dai DQ, Daranagama DA, Dissanayake AJ, Ekanayaka AH, Fryar SC, Hongsanan S, Jayawardena RS, Li W-J, Perera RH, Phookamsak R, de Silva NI, Thambugala KM, Tian Q, Wijayawardene NN, Zhao R-L, Zhao Q, Kang J-C, Promputtha I (2015) The Faces of Fungi database: Fungal names linked with morphology, phylogeny and human impacts. Fungal Diversity 74(1): 3–18. https://doi.org/10.1007/s13225-015-0351-8

Júnior BT da H, Macedo DM de, Barreto RW, Evans HC, Mattos CRR, Maffia LA, Mizubuti ESG (2014) Erasing the Past: a new identity for the damoclean pathogen causing south American Leaf Blight of Rubber. PLOS ONE 9: e104750. https://doi.org/10.1371/journal.pone.0104750

Kang J-C, Hyde K, Kong RYC (1999) Studies on Amphisphaeriales: The genera excluded from the Amphisphaeriaceae, Cainiaceae and Clypeosphaeriaceae. Fungal Diversity 2: 135–151. https://doi.org/10.1007/BF02464294

Katoh K, Rozewicki J, Yamada K (2019) MAFFT online service: Multiple sequence alignment, interactive sequence choice and visualization. Briefings in Bioinformatics 20(4): 1160–1166. https://doi.org/10.1093/bib/bbx108

Kolařík M (2018) New taxonomic combinations in endophytic representatives of the genus *Nigrograna*. Czech Mycology 70(2): 123–126. https://doi.org/10.33585/cmy.70202

Kolařík M, Spakowicz DJ, Gazis R, Shaw J, Kubátová A, Nováková A, Chudíčková M, Forcina GC, Kang KW, Kelnarová I, Skaltsas D, Portero CE, Strobel SA, Narváez-Trujillo A (2017) *Biatriospora* (Ascomycota: Pleosporales) is an ecologically diverse genus including facultative marine fungi and endophytes with biotechnological potential. Plant Systematics and Evolution 303(1): 35–50. https://doi.org/10.1007/s00606-016-1350-24

Kularathnage N, Tennakoon D, Zhu X, Zhou J, Su B, Xie Y, Chen Q, Calabon M, Kirk P, Senanayake I, Doilom M, Xu B, Dong W, Song J (2023) Reinstating *Dyfrolomyces* and introducing *Melomastia pyriformis* sp. nov. (Pleurotremataceae, Dyfrolomycetales) from Guangdong Province, China. Current Research in Environmental & Applied Mycology 13(1): 13. https://doi.org/10.5943/cream/13/1/16

Li Z, Fox JM (2012) Mapping rubber tree growth in mainland Southeast Asia using time-series MODIS 250m NDVI and statistical data. Applied Geography (Sevenoaks, England) 32(2): 420–432. https://doi.org/10.1016/j.apgeog.2011.06.018

Li W-L, Maharachchikumbura SSN, Cheewangkoon R, Liu J-K (2022) Reassessment of *Dyfrolomyces* and four new species of *Melomastia* from Olive (*Olea europaea*) in Sichuan Province, China. Journal of Fungi (Basel, Switzerland) 8(1): 76. https://doi.org/10.3390/jof8010076

Li W-L, Liang R-R, Dissanayake A, Liu J-K (2023) Mycosphere Notes 413–448: Dothideomycetes associated with woody oil plants in China. Mycosphere: Journal of Fungal Biology 14(1): 1436–1529. https://doi.org/10.5943/mycosphere/14/1/16

Liu YJ, Whelen S, Hall BD (1999) Phylogenetic relationships among ascomycetes: Evidence from an RNA polymerse II subunit. Molecular Biology and Evolution 16(12): 1799–1808. https://doi.org/10.1093/oxfordjournals.molbev.a026092

Lu L, Karunarathna SC, Dai D, Jayawardena RS, Suwannarach N, Tibpromma S (2022) Three new species of *Nigrograna* (Dothideomycetes, Pleosporales) associated with Arabica coffee from Yunnan Province, China. MycoKeys 94: 51–71. https://doi.org/10.3897/mycokeys.94.95751

Maharachchikumbura SSN, Hyde KD, Jones EBG, McKenzie EHC, Bhat JD, Dayarathne MC, Huang S-K, Norphanphoun C, Senanayake IC, Perera RH, Shang Q-J, Xiao Y, D'souza MJ, Hongsanan S, Jayawardena RS, Daranagama DA, Konta S, Goonasekara ID, Zhuang W-Y, Jeewon R, Phillips AJL, Abdel-Wahab MA, Al-Sadi AM, Bahkali AH, Boonmee S, Boonyuen N, Cheewangkoon R, Dissanayake AJ, Kang J, Li Q-R, Liu JK, Liu XZ, Liu Z-Y, Luangsa-ard JJ, Pang K-L, Phookamsak R, Promputtha I, Suetrong S, Stadler M, Wen T, Wijayawardene NN (2016) Families of Sordariomycetes. Fungal Diversity 79(1): 1–317. https://doi.org/10.1007/s13225-016-0369-6

Mahendran TR, Thottathil GP, Surendran A, Nagao H, Sudesh K (2021) Biocontrol potential of *Aspergillus terreus*, endophytic fungus against *Rigidoporus microporus* and *Corynespora cassiicola*, pathogens of rubber tree. Archiv für Phytopathologie und Pflanzenschutz 54(15–16): 1014–1032. https://doi.org/10.1080/03235408.2021.1884952

Mann CC (2009) Addicted to Rubber. Science 325(5940): 564–566. https://doi.org/10.1126/science.325_564

Mapook A, Hyde KD, McKenzie EHC, Jones EBG, Bhat DJ, Jeewon R, Stadler M, Samarakoon MC, Malaithong M, Tanunchai B, Buscot F, Wubet T, Purahong W (2020) Taxonomic and phylogenetic contributions to fungi associated with the invasive weed *Chromolaena odorata* (Siam weed). Fungal Diversity 101(1): 1–175. https://doi.org/10.1007/s13225-020-00444-8

Martin R, Gazis R, Skaltsas D, Chaverri P, Hibbett D (2015) Unexpected diversity of basidiomycetous endophytes in sapwood and leaves of *Hevea*. Mycologia 107(2): 284–297. https://doi.org/10.3852/14-206

Meeboon J, Takamatsu S (2020) Hosts of asexual morph of *Erysiphe quercicola* from Thailand. Tropical Plant Pathology 45(2): 122–135. https://doi.org/10.1007/s40858-019-00326-8

Miller MA, Pfeiffer W, Schwartz T (2012) The CIPRES science gateway: enabling high-impact science for phylogenetics researchers with limited resources. Proceedings of the 1st Conference of the Extreme Science and Engineering Discovery Environment: Bridging from the Extreme to the campus and beyond. Association for Computing Machinery, New York, 1–8. https://doi.org/10.1145/2335755.2335836

Mohammed CL, Rimbawanto A, Page DE (2014) Management of basidiomycete root- and stem-rot diseases in oil palm, rubber and tropical hardwood plantation crops. Forest Pathology 44(6): 428–446. https://doi.org/10.1111/efp.12140

Monkai J, Hyde KD, Xu J, Mortimer PE (2017) Diversity and ecology of soil fungal communities in rubber plantations. Fungal Biology Reviews 31(1): 1–11. https://doi.org/10.1016/j.fbr.2016.08.003

National Bureau of Statistics of China (2011) China Statistical Yearbook 2011. http://www.stats.gov.cn/tjsj/ndsj/2011/indexch.htm [Accessed 31 January 2015]

Nizamani MM, Zhang Q, Zhang H, Wang Y (2023) Checklist of the fungi associated with the rubber tree (*Hevea brasiliensis*). Journal of Fungal Biology 13(1): 439–488.

Norphanphoun C, Jeewon R, Mckenzie EHC, Wen T-C, Camporesi E, Hyde KD (2017) Taxonomic position of *Melomastia italica* sp. nov. and phylogenetic reappraisal of Dyfrolomycetales. Cryptogamie. Mycologie 38(4): 507–525. https://doi.org/10.7872/crym/v38.iss4.2017.507

Nylander J (2004) MrModeltest V2. Program Distributed by the Author. Bioinformatics (Oxford, England) 24: 581–583. https://doi.org/10.1093/bioinformatics/btm388

Osono T, Takeda H (2002) Nutrient contents of beech leaf litter decomposed by fungi in Basidiomycota and Ascomycota. Applied Forest Science 11(1): 7–11. https://doi.org/10.20660/applfor.11.1_7

Osono T, Hobara S, Hishinuma T, Azuma J (2011) Selective lignin decomposition and nitrogen mineralization in forest litter colonized by *Clitocybe* sp. European Journal of Soil Biology 47(2): 114–121. https://doi.org/10.1016/j.ejsobi.2010.12.002

Phukhamsakda C, Nilsson RH, Bhunjun CS, de Farias ARG, Sun Y-R, Wijesinghe SN, Raza M, Bao D-F, Lu L, Tibpromma S, Dong W, Tennakoon DS, Tian X-G, Xiong Y-R, Karunarathna SC, Cai L, Luo Z-L, Wang Y, Manawasinghe IS, Camporesi E, Kirk PM, Promputtha I, Kuo C-H, Su H-Y, Doilom M, Li Y, Fu Y-P, Hyde KD (2022) The numbers of fungi: Contributions from traditional taxonomic studies and challenges of metabarcoding. Fungal Diversity 114(1): 327–386. https://doi.org/10.1007/s13225-022-00502-3

Punithalingam E (1979) Sphaeropsidales in culture from humans. Nova Hedwigia 31: 119–158.

Rambaut A (2012) FigTree v1. 4.0. University of Oxford, Oxford, UK.

Rojas-Jimenez K, Hernandez M, Blanco J, Vargas LD, Acosta-Vargas LG, Tamayo G (2016) Richness of cultivable endophytic fungi along an altitudinal gradient in wet forests of Costa Rica. Fungal Ecology 20: 124–131. https://doi.org/10.1016/j.funeco.2015.12.006

Roy BA (2001) Patterns of association between crucifers and their flower-mimic pathogens: Host jumps are more common than coevolution or cospeciation. Evolution. International Journal of Organic Evolution 55(1): 41–53. https://doi.org/10.1111/j.0014-3820.2001.tb01271.x

Saccardo P (1875) Conspectus generum pyrenomycetum italicorum additis speciebus fungorum Venetorum novis vel criticis, systemate carpologico dispositorum. Atti della Società Veneto-Trentina di Scienze Naturali 4: 77–100.

Seephueak P, Petcharat V, Phongpaichit S (2010) Fungi associated with leaf litter of para rubber (*Hevea brasiliensis*). Mycology 1(4): 213–227. https://doi.org/10.1080/21501203.2010.536594

Seephueak P, Phongpaichit S, Hyde K, Petcharat V (2011) Diversity of saprobic fungi on decaying branch litter of the rubber tree (*Hevea brasiliensis*). Mycosphere: Journal of Fungal Biology 2: 307–330.

Senanayake IC, Rathnayaka AR, Marasinghe DS, Calabon MS, Gentekaki E, Lee HB, Hurdeal VG, Pem D, Dissanayake LS, Wijesinghe SN, Bundhun D, Nguyen TT, Goonase-

kara ID, Abeywickrama PD, Bhunjun CS, Jayawardena RS, Wanasinghe DN, Jeewon R, Bhat DJ, Xiang MM (2020) Morphological approaches in studying fungi: Collection, examination, isolation, sporulation and preservation. Mycosphere: Journal of Fungal Biology 11(1): 2678–2754. https://doi.org/10.5943/mycosphere/11/1/20

Senwanna C, Hongsanan S, Phookamsak R, Tibpromma S, Cheewangkoon R, Hyde KD (2019) *Muyocopron heveae* sp. nov. and *M. dipterocarpi* appears to have host-jumped to rubber. Mycological Progress 18(5): 741–752. https://doi.org/10.1007/s11557-019-01484-4

Senwanna C, Mapook A, Samarakoon MC, Karunarathna A, Wang Y, Tang A, Haituk S, Suwannarach N, Hyde K, Cheewangkoon R (2021) Ascomycetes on Para rubber (*Hevea brasiliensis*). Mycosphere: Journal of Fungal Biology 12(1): 1334–1512. https://doi.org/10.5943/mycosphere/12/1/18

Spaulding P (1961) Foreign Diseases of Forest Trees of the World: An Annotated List. U.S. Department of Agriculture, 372 pp.

Stamatakis A (2014) RAxML version 8: A tool for phylogenetic analysis and post-analysis of large phylogenies. Bioinformatics (Oxford, England) 30(9): 1312–1313. https://doi.org/10.1093/bioinformatics/btu033

Statistical Bureau of Yunnan Province (2011) Yunnan Statistical Yearbook 2011. http://tongji.cnki.net/kns55/brief/result.aspx?stab=shuzhi&t=1&f=0&tt=%E6%A9%A1%E8%83%B6&areaname=%E8%A5%BF%E5%8F%8C%E7%89%88%E7%BA%B3%E5%82%A3%E6%97%8F%E8%87%AA%E6%B2%BB%E5%B7%9E [Accessed 21 September 2014]

Tibpromma S, Hyde KD, Jeewon R, Maharachchikumbura SSN, Liu J-K, Bhat DJ, Jones EBG, McKenzie EHC, Camporesi E, Bulgakov TS, Doilom M, de Azevedo Santiago ALCM, Das K, Manimohan P, Gibertoni TB, Lim YW, Ekanayaka AH, Thongbai B, Lee HB, Yang J-B, Kirk PM, Sysouphanthong P, Singh SK, Boonmee S, Dong W, Raj KNA, Latha KPD, Phookamsak R, Phukhamsakda C, Konta S, Jayasiri SC, Norphanphoun C, Tennakoon DS, Li J, Dayarathne MC, Perera RH, Xiao Y, Wanasinghe DN, Senanayake IC, Goonasekara ID, de Silva NI, Mapook A, Jayawardena RS, Dissanayake AJ, Manawasinghe IS, Chethana KWT, Luo Z-L, Hapuarachchi KK, Baghela A, Soares AM, Vizzini A, Meiras-Ottoni A, Mešić A, Dutta AK, de Souza CAF, Richter C, Lin C-G, Chakrabarty D, Daranagama DA, Lima DX, Chakraborty D, Ercole E, Wu F, Simonini G, Vasquez G, da Silva GA, Plautz Jr HL, Ariyawansa HA, Lee H, Kušan I, Song J, Sun J, Karmakar J, Hu K, Semwal KC, Thambugala KM, Voigt K, Acharya K, Rajeshkumar KC, Ryvarden L, Jadan M, Hosen MI, Mikšík M, Samarakoon MC, Wijayawardene NN, Kim NK, Matočec N, Singh PN, Tian Q, Bhatt RP, de Oliveira RJV, Tulloss RE, Aamir S, Kaewchai S, Marathe SD, Khan S, Hongsanan S, Adhikari S, Mehmood T, Bandyopadhyay TK, Svetasheva TY, Nguyen TTT, Antonín V, Li W-J, Wang Y, Indoliya Y, Tkalčec Z, Elgorban AM, Bahkali AH, Tang AMC, Su H-Y, Zhang H, Promputtha I, Luangsa-ard J, Xu J, Yan J, Ji-Chuan K, Stadler M, Mortimer PE, Chomnunti P, Zhao Q, Phillips AJL, Nontachaiyapoom S, Wen T-C, Karunarathna SC (2017) Fungal diversity notes 491–602: Taxonomic and phylogenetic contributions to fungal taxa. Fungal Diversity 83(1): 1–261. https://doi.org/10.1007/s13225-017-0378-0

Tibpromma S, Hyde KD, McKenzie EHC, Bhat DJ, Phillips AJL, Wanasinghe DN, Samarakoon MC, Jayawardena RS, Dissanayake AJ, Tennakoon DS, Doilom M, Phookamsak R, Tang AMC, Xu J, Mortimer PE, Promputtha I, Maharachchikumbura SSN, Khan S, Karunarathna SC (2018) Fungal diversity notes 840–928: Micro-fungi associated with Pandanaceae. Fungal Diversity 93(1): 1–160. https://doi.org/10.1007/s13225-018-0408-6

Vilgalys R, Hester M (1990) Rapid genetic identification and mapping of enzymatically amplified ribosomal DNA from several *Cryptococcus* species. Journal of Bacteriology 172(8): 4238–4246. https://doi.org/10.1128/jb.172.8.4238-4246.1990

Wang Z, Zhang X, Tao L, Bi B, Niu G, Han X, Deng J (2015) The potential development value of rubber seed. Journal of Yunnan Agricultural University 30: 642–647.

Watson W (1929) The Classification of Lichens. The New Phytologist 28(1): 1–36. https://doi.org/10.1111/j.1469-8137.1929.tb06745.x

White TJ, Bruns T, Lee S, Taylor J (1990) Amplification and direct sequencing of fungal ribosomal RNA genes for phylogenetics. In: Innis MA, Gelfand DH, Sninsky JJ, White TJ (Eds) PCR Protocols. Elsevier, 315–322. https://doi.org/10.1016/B978-0-12-372180-8.50042-1

Wijayawardene NN, Hyde KD, Dai D-Q, Sánchez-García M, Goto B, Saxena R, Erdoğdu M, Selçuk F, Rajeshkumar K, Aptroot A, Błaszkowski J, Boonyuen N, Da Silva G, De Souza F, Dong W, Ertz D, Haelewaters D, Jones E, Karunarathna S, Kirk P, Kukwa M, Kumla J, Leontyev D, Lumbsch H, Maharachchikumbura S, Marguno F, Martínez-Rodríguez P, Mešić A, Monteiro J, Oehl F, Pawłowska J, Pem D, Pfliegler W, Phillips A, Pošta A, He M, Li J, Raza M, Sruthi O, Suetrong S, Suwannarach N, Tedersoo L, Thiyagaraja V, Tibpromma S, Tkalčec Z, Tokarev Y, Wanasinghe D, Wijesundara D, Wimalaseana S, Madrid H, Zhang G, Gao Y, Sánchez-Castro I, Tang L, Stadler M, Yurkov A, Thines M (2022) Outline of Fungi and fungus-like taxa – 2021. Mycosphere: Journal of Fungal Biology 13(1): 53–453. https://doi.org/10.5943/mycosphere/13/1/2

Xu R-F, Thiyagaraja V, Dai D-Q, Karunarathna SC, Tibpromma S (2022a) Additions to *Fitzroyomyces* (Stictidaceae, Ascomycota) from Yunnan Province, China. Phytotaxa 548(2): 253–266. https://doi.org/10.11646/phytotaxa.548.2.8

Xu R-F, Hyde K, Karunarathna S, Xu J-C, Mortimer P, Tibpromma S (2022b) Morphology and multi-gene phylogeny reveal a new fungal genus and species from *Hevea brasiliensis* latex in Yunnan, China. Phytotaxa 530(1): 65–76. https://doi.org/10.11646/phytotaxa.530.1.5

Xu R-F, Phukhamsakda C, Dai D-Q, Karunarathna SC, Tibpromma S (2023) *Kirschsteiniothelia xishuangbannaensis* sp. nov. from pará rubber (*Hevea brasiliensis*) in Yunnan, China. Current Research in Environmental & Applied Mycology 13(1): 34–56. https://doi.org/10.5943/cream/13/1/3

Zhang J, Liu J-K, Hyde KD, Chen Y-Y, Liu Y-X, Liu Z-Y (2017) Two new species of *Dyfrolomyces* (Dyfrolomycetaceae, Dothideomycetes) from karst landforms. Phytotaxa 313: 267. https://doi.org/10.11646/phytotaxa.313.3.4

Ziegler AD, Fox JM, Xu J (2009) The Rubber Juggernaut. Science 324(5930): 1024–1025. https://doi.org/10.1126/science.1173833

MycoKeys 103: 97–128 (2024)
DOI: 10.3897/mycokeys.103.118980

Research Article

Species diversity and taxonomy of *Vararia* (Russulales, Basidiomycota) with descriptions of six species from Southwestern China

Yinglian Deng[1,2], Sana Jabeen[3], Changlin Zhao[1,2,4]

1 *The Key Laboratory of Forest Resources Conservation and Utilization in the South-west Mountains of China Ministry of Education, Key Laboratory of National Forestry and Grassland Administration on Biodiversity Conservation in Southwest China, Yunnan Provincial Key Laboratory for Conservation and Utilization of In-forest Re-source, Southwest Forestry University, Kunming 650224, China*
2 *College of Biodiversity Conservation, Southwest Forestry University, Kunming 650224, China*
3 *Department of Botany, Division of Science and Technology, University of Education, Township, Lahore, Punjab, Pakistan*
4 *Yunnan Academy of Biodiversity, Southwest Forestry University, Kunming 650224, China*
Corresponding author: Changlin Zhao (fungi@swfu.edu.cn)

Abstract

Vararia is a species-rich genus in the family Peniophoraceae and has been shown to be polyphyletic. In this study, sequences of ITS and LSU rRNA markers of the studied samples were generated and phylogenetic analyses were performed with the maximum likelihood, maximum parsimony, and Bayesian inference methods. Seventeen lineages including six new species from China, i.e., *V. fissurata*, *V. lincangensis*, *V. punctata*, *V. isabellina*, *V. sinensis*, and *V. yaoshanensis* were recognized, in which *V. fissurata* is characterized by the brittle basidiomata with pruinose and cracking hymenophore having white to olivaceous buff hymenial surface, the clamped generative hyphae, presence of the two types gloeocystidia; *V. lincangensis* is characterized by the simple-septa generative hyphae, and thick-walled skeletal hyphae, and ellipsoid basidiospores; *V. punctata* is delimited by its thin to slightly thick-walled generative hyphae, and thick-walled skeletal hyphae, present thick-walled, clavate to cylindrical gloeocystidia; *V. isabellina* is characterized by having the cream to isabelline to slightly brown hymenial surface, thin to slightly thick-walled generative hyphae, and sub-fusiform to navicular basidiospores; *V. sinensis* is distinguishable by its white to slightly pink hymenial surface, thick-walled skeletal hyphae, and sub-fusiform to navicular basidiospores; *V. yaoshanensis* is characterized by cream to pinkish buff to cinnamon-buff hymenial surface, slightly thick-walled generative hyphae, the presence of two types gloeocystidia, and slightly thick-walled, ellipsoid basidiospores. Phylogram based on the ITS+nLSU rDNA gene regions included nine genera within the family Peniophoraceae as *Amylostereum*, *Asterostroma*, *Baltazaria*, *Dichostereum*, *Michenera*, *Peniophora*, *Scytinostroma* and *Vararia*, in which the six new wood-inhabiting fungi species were grouped into genus *Vararia*. The phylogenetic tree inferred from the combined ITS and LSU tree sequences highlighted that *V. fissurata* was found to be the sister to *V. ellipsospora* with strong supports. Additionally, *V. lincangensis* was clustered with *V. fragilis*. Furthermore, *V. punctata* was retrieved as a sister to *V. ambigua*. Moreover, *V. sinensis* was grouped with five taxa as *V. breviphysa*, *V. pirispora*, *V. fusispora*, *V. abortiphysa* and *V. insolita*. The new species *V. isabellina* formed a monophyletic lineage, in which it was then grouped closely with *V. daweishanensis*, and *V. gracilispora*. In addition, *V. yaoshanensis* was found to be the sister to *V. gallica* with strong supports. The present results increased the knowledge of *Vararia* species diversity and taxonomy of corticioid fungi in China. An identification key to 17 species of *Vararia* in China is provided.

Academic editor: María P. Martín
Received: 17 January 2024
Accepted: 1 March 2024
Published: 22 March 2024

Citation: Deng Y, Jabeen S, Zhao C (2024) Species diversity and taxonomy of *Vararia* (Russulales, Basidiomycota) with descriptions of six species from Southwestern China. MycoKeys 103: 97–128. https://doi.org/10.3897/mycokeys.103.118980

Key words: Biodiversity, China, phylogenetic analyses, taxonomy, wood-inhabiting fungi, Yunnan Province

Introduction

Fungi represent one of the most diverse groups of organisms on the earth, with an indispensable role in the processes and functioning of forest ecosystems (Hyde 2022). The genus *Vararia* P. Karst. belongs to the family Peniophoraceae of the order Russulales (Larsson and Larsson 2003; Miller et al. 2006; Larsson 2007). The Russulales is a well-known order that contains morphologically diverse mushrooms (Miller et al. 2006). Species from this order comprise many representative wood-inhabiting fungal taxa, including hydnoid, corticioid, and polyporoid basidiomes with diverse hymenophoral and cystidial morphology (Yurchenko and Wu 2016; Riebesehl and Langer 2017; Yurchenko et al. 2017; Cui et al. 2019; Riebesehl et al. 2019; Jiang et al. 2021; Wu et al. 2022).

The genus *Vararia* is a corticioid wood-inhabiting fungal genus with a wide distribution, typified by *V. investiens* (Schwein.) P. Karst. It was first described by Karsten as a subgenus of *Xerocarpus* P. Karst. for *Xerocarpus alutarius* (Berk. & M. A. Curtis) P. Karst., which was later found to be a synonym of *Radulum investiens* Schwein. Karsten raised *Xerocarpus* subgen. *Vararia* to the generic rank (Karasinski 2010). The genus is characterized by the resupinate basidiomata, a dimitic hyphal structure with simple-septate or clamped generative hyphae and often dextrinoid dichohyphae in Melzer's reagent, the presence of gloeocystidia, and variously shaped smooth basidiospores with or without an amyloid reaction (Karnste 1898; Boidin and Lanquetin 1975; Boidin 1980; Bernicchia and Gorjón 2010). The species of *Vararia* are found on fallen angiosperm branches, dead woody or herbaceous stems or occasionally on gymnosperm wood (Yurchenko et al. 2017). Based on the MycoBank database (http://www.mycobank.org, accessed on 17 January 2024) and the Index Fungorum (http://www.indexfungorum.org, accessed on 17 January 2024), *Vararia* has registered 99 specific and infraspecific names, and the actual number of the species has reached up to 76, currently known, and they occur mainly in the tropical and subtropical areas of the world (Cunningham 1955; Gilbertson 1965; Boidin 1967; Pouzar 1982; Boidin and Lanquetin 1987; Stalpers 1996; Boidin and Gilles 1999; Larsson and Larsson 2003; Bernicchia and Gorjón 2010; Duhem and Buyck 2012; Sanyal et al. 2012; Nakasone 2015; Liu and He 2016; Dai et al. 2021; Zou et al. 2022; Deng and Zhao 2023).

Classification of the kingdom of fungi has been updated continuously, based on the frequent inclusion of data from DNA sequences in many phylogenetic studies (Yurchenko et al. 2020). These pioneering research studies into the family Peniophoraceae were just the prelude to the molecular systematics period (Zou et al. 2022). The phylogenetic diversity displayed by corticioid fungal species, based on ITS1-5.8S-ITS2-nrLSU nuclear rDNA, revealed that the taxa of Peniophoraceae were nested in the russuloid clade, which holds a considerable share of the phylogenetic framework, and included the genera of *Asterostroma* Massee, *Baltazaria* Leal-Dutra, Dentinger & G.W. Griff., *Dichostereum* Pilát, *Gloiothele* Bres., *Lachnocladium* Lév., *Michenera* Berk. & M.A. Curtis, *Peniophora* Cooke, *Scytinostroma* Donk, *Vesiculomyces* E. Hagstr. and *Vararia* (Larsson and

Larsson 2003; Larsson and Larsson 2004; Larsson 2007; Leal-Dutra et al. 2018; Zou et al. 2022; Li et al. 2023). Morphologically, *Scytinostroma* was similar to *Vararia*, which usually differed in having the typical dichohyphae (Bernicchia and Gorjón 2010). The taxonomic distinction between *Scytinostroma* and *Vararia* has been questioned (Hallenberg 1985; Boidin and Lanquetin 1987; Stalpers 1996; Boidin et al 1998). However, there has been general agreement that the two genera were closely related and that they together made up a natural group. Larsson and Larsson (2003) strongly suggested that neither skeletal hyphae nor their branching patterns have any predictive power in a phylogenetic context.

During investigations on the wood-inhabiting fungi in the Yunnan province of China, the samples representing six additional species belonging to genera *Vararia* were collected. To clarify the placement and relationships of the six species, we carried out a phylogenetic and taxonomic study on *Vararia*, based on the ITS and LSU sequences.

Materials and methods

Morphology

Fresh fruiting bodies of the fungi were collected from Dali, Dehong, Lincang, Puer, Yuxi and Zhaotong of Yunnan Province, P.R. China. Specimens were dried in an electric food dehydrator at 40 °C, then sealed and stored in an envelope bag and deposited in the herbarium of the Southwest Forestry University (SWFC), Kunming, Yunnan Province, P.R. China. Macromorphological descriptions are based on field notes and photos captured in the field and lab. Color terminology follows Petersen (Petersen 1996). Micromorphological data were obtained from the dried specimens when observed under a light microscope following the previous study (Zhao et al. 2023; Guan et al. 2023). The following abbreviations are used: KOH = 5% potassium hydroxide water solution, CB = Cotton Blue, CB– = acyanophilous, IKI = Melzer's Reagent, IKI– = both inamyloid and indextrinoid, L = mean spore length (arithmetic average for all spores), W = mean spore width (arithmetic average for all spores), Q = variation in the L/W ratios between the specimens studied and n = a/b (number of spores (a) measured from given number (b) of specimens).

Molecular phylogeny

The EZNA HP Fungal DNA Kit (Omega Biotechnologies Co., Ltd., Kunming, China) was used to extract DNA with some modifications from the dried specimens. The nuclear ribosomal ITS region was amplified with primers ITS5 and ITS4 (White et al. 1990). The PCR procedure for ITS was as follows: initial denaturation at 95 °C for 3 min, followed by 35 cycles at 94 °C for 40 s, 58 °C for 45 s and 72 °C for 1 min, and a final extension of 72 °C for 10 min. The nuclear LSU region was amplified with primer pair LR0R and LR7 (Vilgalys and Hester 1990; Rehner and Samuels 1994). The PCR procedure for LSU was as follows: initial denaturation at 94 °C for 1 min, followed by 35 cycles at 94 °C for 30 s, 48 °C for 1 min and 72 °C for 1.5 min, and a final extension of 72 °C for 10 min. The PCR procedure for ITS and LSU followed a previous study (Zhao and Wu 2017). All of the newly generated sequences were deposited in NCBI GenBank (https://www.ncbi.nlm.nih.gov/genbank/) (Table 1).

Table 1. List of species, specimens and GenBank accession numbers of sequences used in this study. [* Indicates type materials].

Species name	Specimen No.	GenBank accession No.		Country	References
		ITS	nLSU		
Amylostereum chailletii	NH8031	AF506406	AF506406	Sweden	Larsson and Larsson 2003
A. laevigatum	NH12863	AF506407	AF506407	Sweden	Larsson and Larsson 2003
Asterostroma bambusicola	He4132	KY263865	KY263871	Thailand	Liu et al. 2017
A. cervicolor	He2314	KY263859	KY263869	China	Unpublished
A. cervicolor	He4020	KY263860	KY263868	Thailand	Unpublished
A. muscicola	He4397	MK625630	MK625563	China	Unpublished
Baltazaria galactina	He4999	MK625618	MK625547	China	Unpublished
B. octopodites	FLOR63715	MH260042	MH260060	United Kingdom	Leal-Dutra et al. 2018
Confertobasidium olivaceoalbum	FP90196	AF511648	AF511648	Sweden	Larsson and Larsson 2003
Dichostereum boidinii	He4410	MH538315	MH538331	China	Vu et al. 2019
D. boidinii	He5026	MH538324	MH538330	China	Liu et al. 2019
D. pallescens	CBS:718.81	MH861456	MH873198	USA	Vu et al. 2019
Metulodontia nivea	NH13108	AF506423	AF506423	Sweden	Larsson and Larsson 2003
Michenera artocreas	GHL-2016-Oct	MH204688	MH204691	USA	Liu et al. 2019
M. incrustata	He5368	MH204689	MH204690	China	Liu et al. 2019
Peniophora cinerea	CBS:261.37	MH855905	MH867412	Belgium	Vu et al. 2019
P. cinerea	He3725	MK588769	MK588809	China	Unpublished
P. incarnata	CBS 430.72	MH860518	MH872230	Netherlands	Vu et al. 2019
P. incarnata	NH10271	AF506425	AF506425	Sweden	Larsson and Larsson 2003
P. nuda	LZ15-07	MT859929	—	China	Unpublished
P. quercina	CBS 407.50	MH856687	MH868204	France	Vu et al. 2019
P. quercina	CBS:410.50	MH856690	MH868207	France	Vu et al. 2019
Scytinostroma acystidiatum	He5646	MK625568	MK625494	China	Unpublished
S. alutum	CBS:762.81	MH861482	MH873221	France	Vu et al. 2019
S. beijingensis	He7768	OQ731943	OQ729731	China	Li et al. 2023
S. boidinii	He6911	OQ731934	OQ729724	China	Li et al. 2023
S. duriusculum	He3590	MK625571	MK625499	China	Unpublished
S. hemidichophyticum	CBS:702.84	MH861818	MH873509	Belgium	Vu et al. 2019
S. renisporum	CBS:771.86	MH862051	MH873738	Bali	Vu et al. 2019
S. subrenisporum	He4792	MK625566	MK625493	China	Unpublished
Vararia abortiphysa	CBS:632.81	MH861387	—	Gabon	Vu et al. 2019
V. ambigua	CBS 634.81	MH861388	MH873137	France	Vu et al. 2019
V. amphithallica	CBS:635.81	MH861389	MH873138	Gabon	Vu et al. 2019
V. amphithallica	CBS:687.81	MH861431	—	France	Vu et al. 2019
V.aurantiaca	CBS:641.81	MH861393	—	France	Vu et al. 2019
V. aurantiaca	CBS:642.81	MH861394	—	Gabon	Vu et al. 2019
V. breviphysa	CBS:643.81	MH873144	MH873144	Gabon	Vu et al. 2019
V. breviphysa	CBS:644.81	MH861396	—	Gabon	Vu et al. 2019
V. calami	CBS:646.81	MH861398	—	France	Vu et al. 2019
V. calami	CBS:648.81	MH861399	—	France	Vu et al. 2019
V. callichroa	CBS:744.91	MH874000	MH874000	France	Vu et al. 2019

Species name	Specimen No.	GenBank accession No.		Country	References
		ITS	nLSU		
V. cinnamomea	CBS:641.84	MH861794	—	Madagascar	Vu et al. 2019
V. cinnamomea	CBS:642.84	MH873488	MH873488	Madagascar	Vu et al. 2019
V. cremea	CBS:651.81	MH873147	MH873147	France	Vu et al. 2019
V. daweishanensis	CLZhao 17911	OP380613	—	China	Zou et al. 2022
V. daweishanensis	CLZhao 17936	OP380614	—	China	Zou et al. 2022
V. dussii	CBS:652.81	MH873148	MH873148	France	Vu et al. 2019
V. dussii	CBS:655.81	MH861405	—	France	Vu et al. 2019
V. ellipsospora	HHB-19503	MW740328	—	New Zealand	Zou et al. 2022
V. fissurata	**CLZhao 10118**	**PP083288**	—	**China**	**Present study**
V. fissurata	**CLZhao 10181**	**PP083289**	—	**China**	**Present study**
V. fissurata	**CLZhao 22538**	**PP083290**	—	**China**	**Present study**
V. fissurata	**CLZhao 4614**	**PP083283**	—	**China**	**Present study**
V. fissurata	**CLZhao 5218**	**OQ025218**	**OR539502**	**China**	**Present study**
V. fissurata	**CLZhao 6070**	**PP083284**	—	**China**	**Present study**
V. fissurata	**CLZhao 8171***	**OQ025219**	**OR539503**	**China**	**Present study**
V. fissurata	**CLZhao 9618**	**PP083285**	—	**China**	**Present study**
V. fissurata	**CLZhao 9668**	**PP083286**	—	**China**	**Present study**
V. fissurata	**CLZhao 9697**	**PP083287**	—	**China**	**Present study**
V. fragilis	CLZhao 16475	OP380612	—	China	Zou et al. 2022
V. fragilis	CLZhao 2628	OP380611	—	China	Zou et al. 2022
V. fusispora	PDD:119539	OL709443	—	New Zealand	Zou et al. 2022
V. gallica	CBS 234.91	MH862250	MH873932	Canada	Vu et al. 2019
V. gallica	CBS 656.81	MH861406	MH873152	France	Vu et al. 2019
V. gillesii	CBS:660.81	MH873153	MH873153	Cote d'Ivoire	Vu et al. 2019
V. gomezii	CBS:661.81	MH873154	MH873154	France	Vu et al. 2019
V. gracilispora	CBS:663.81	MH861411	—	Gabon	Vu et al. 2019
V. gracilispora	CBS:664.81	MH861412	—	Gabon	Vu et al. 2019
V. insolita	CBS:668.81	MH861413	—	France	Vu et al. 2019
V. intricata	CBS:673.81	MH861418	—	France	Vu et al. 2019
V. investiens	FP-151122ITS	MH971976	—	USA	Liu et al. 2019
V. investiens	UC2023140	KP814286	—	USA	Rosenthal et al. 2017
V. isabellina	**CLZhao 22852**	**OR048789**	**OR506350**	**China**	**Present study**
V. isabellina	**CLZhao 22887**	**OR048788**	**OR506351**	**China**	**Present study**
V. lincangensis	**CLZhao 22791***	**OR048819**	**OR506348**	**China**	**Present study**
V. lincangensis	**CLZhao 22799**	**OR048818**	**OR506349**	**China**	**Present study**
V. malaysiana	CBS:644.84	MH873490	MH873490	Singapore	Vu et al. 2019
V. minispora	CBS:682.81	MH861426	—	France	Vu et al. 2019
V. ochroleuca	CBS:465.61	MH858109	—	France	Vu et al. 2019
V. ochroleuca	JS24400	AF506485	AF506485	Norway	Larsson and Larsson 2003
V. parmastoi	CBS:879.84	MH861852	MH861852	Uzbekistan	Vu et al. 2019
V. pectinata	CBS:685.81	MH861429	—	Cote d'Ivoire	Vu et al. 2019
V. perplexa	CBS:695.81	MH861438	—	France	Vu et al. 2019
V. pirispora	CBS:720.86	MH862016	—	France	Vu et al. 2019
V. punctata	**CLZhao 22423**	**OR048813**	**OR539685**	**China**	**Present study**

Species name	Specimen No.	GenBank accession No.		Country	References
		ITS	nLSU		
V. punctata	**CLZhao 22439***	**OR048812**	**OR510675**	**China**	**Present study**
V. rhombospora	CBS:743.81	MH861470	—	France	Vu et al. 2019
V. rosulenta	CBS:743.86	MH862028	—	France	Vu et al. 2019
V. rugosispora	CBS:697.81	MH861440	—	Gabon	Vu et al. 2019
V. sigmatospora	CBS:748.91	MH874001	MH874001	Netherlands	Vu et al. 2019
V. sinensis	**CLZhao 25160***	**OR102494**	**OR510678**	**China**	**Present study**
V. sinensis	**CLZhao 25161**	**OR102495**	**OR510679**	**China**	**Present study**
V. sphaericospora	CBS:700.81	MH873185	MH873185	Gabon	Vu et al. 2019
V. sphaericospora	CBS:703.81	MH861446	—	Gabon	Vu et al. 2019
V. sphaericospora	He4847	MK625592	MK625521	China	Unpublished
V. trinidadensis	CBS:650.84	MH873495	MH873495	Madagascar	Vu et al. 2019
V. trinidadensis	CBS:651.84	MH861803	—	Madagascar	Vu et al. 2019
V. tropica	CBS 704.81	MH861447	MH873189	France	Vu et al. 2019
V. vassilievae	UC2022892	KP814203	—	USA	Unpublished
V. verrucosa	CBS:706.81	MH861449	MH861449	France	Vu et al. 2019
V. yaoshanensis	**CLZhao 20528**	**PP091673**	—	**China**	**Present study**
V. yaoshanensis	**CLZhao 20531**	**PP091674**	—	**China**	**Present study**
V. yaoshanensis	**CLZhao 20565**	**PP091675**	**PP091683**	**China**	**Present study**
V. yaoshanensis	**CLZhao 20605**	**PP091676**	—	**China**	**Present study**
V. yaoshanensis	**CLZhao 20608**	**PP091677**	—	**China**	**Present study**
V. yaoshanensis	**CLZhao 20617**	**PP091678**	—	**China**	**Present study**
V. yaoshanensis	**CLZhao 20619**	**PP091679**	—	**China**	**Present study**
V. yaoshanensis	**CLZhao 20624**	**PP091680**	—	**China**	**Present study**
V. yaoshanensis	**CLZhao 20646**	**PP091681**	—	**China**	**Present study**
V. yaoshanensis	**CLZhao 20656**	**PP091682**	—	**China**	**Present study**
V. yaoshanensis	**CLZhao 20669**	**PP091666**	—	**China**	**Present study**
V. yaoshanensis	**CLZhao 20677**	**PP091667**	—	**China**	**Present study**
V. yaoshanensis	**CLZhao 20693***	**PP091665**	**PP091684**	**China**	**Present study**
V. yaoshanensis	**CLZhao 20697**	**PP091668**	—	**China**	**Present study**
V. yaoshanensis	**CLZhao 20709**	**PP091669**	—	**China**	**Present study**
V. yaoshanensis	**CLZhao 20713**	**PP091670**	—	**China**	**Present study**
V. yaoshanensis	**CLZhao 20717**	**PP091671**	—	**China**	**Present study**
V. yaoshanensis	**CLZhao 20724**	**PP091672**	—	**China**	**Present study**

The sequences were aligned in MAFFT version 7 (Katoh et al. 2019) using the G-INS-i strategy. The alignment was adjusted manually using AliView version 1.27 (Larsson 2014). Sequences of *Confertobasidium olivaceoalbum* (Bourdot & Galzin) (AF511648) Jülich and *Metulodontia nivea* (P. Karst.) Parmasto () retrieved from GenBank were used as the outgroups in the ITS+LSU analysis (Fig. 1); Sequences of *Peniophora incarnata* (Pers.) P. Karst. (AF506425) and *Peniophora nuda* (Fr.) Bres. (MT859929) retrieved from GenBank were used as the outgroups in the ITS analysis (Fig. 2) (Leal-Dutra et al. 2018; Zhao et al. 2021).

Maximum parsimony (MP), Maximum Likelihood (ML), and Bayesian Inference (BI) analyses were applied to the combined three datasets following

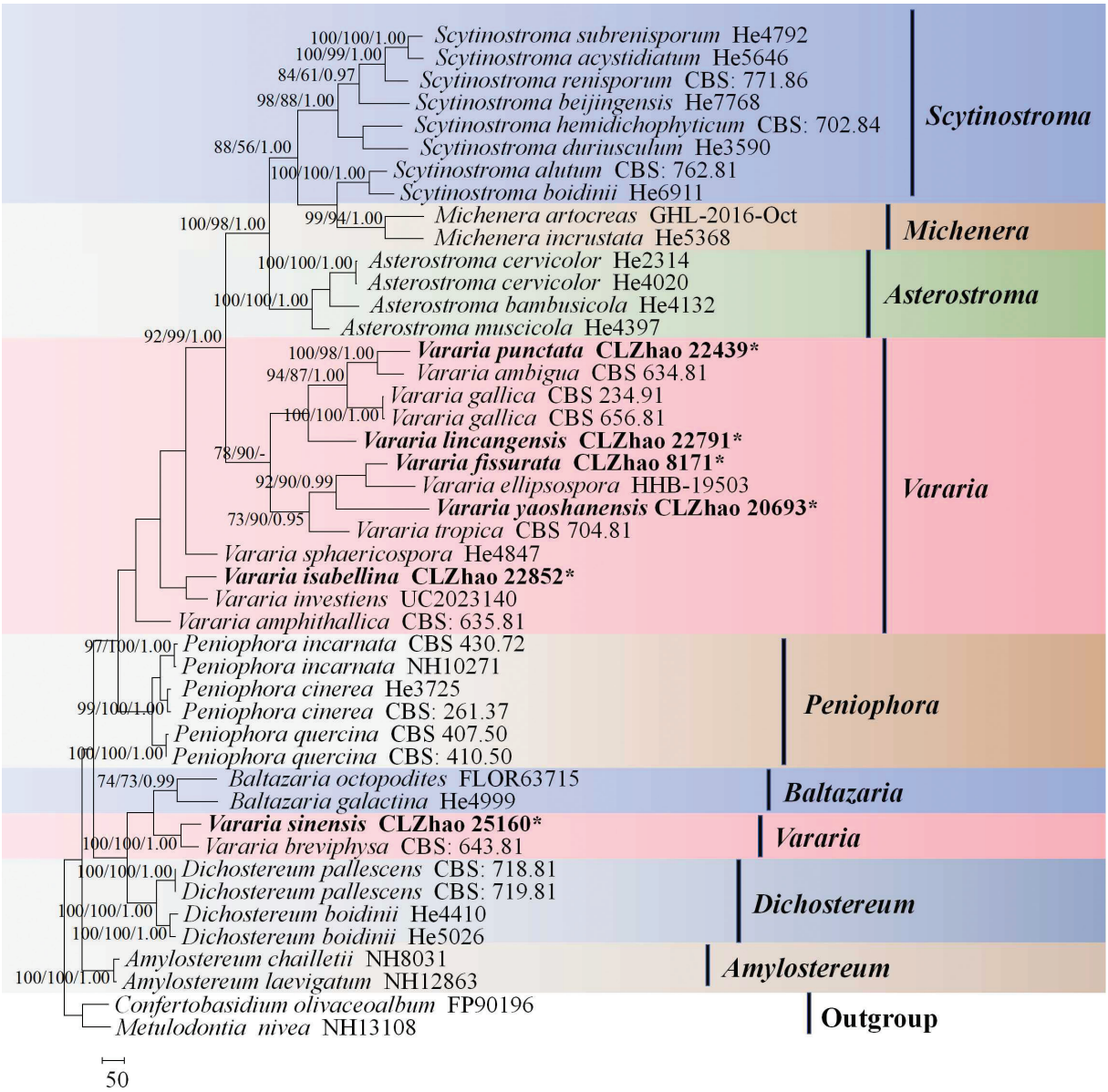

Figure 1. Maximum parsimony strict consensus tree illustrating the phylogeny of *Vararia* and related genera in the family Peniophoraceae based on ITS+LSU sequences. Branches are labelled with maximum likelihood bootstrap values > 70%, parsimony bootstrap values > 50% and Bayesian posterior probabilities > 0.95, respectively.

a previous study (Zhao and Wu 2017). All characters were equally weighted and gaps were treated as missing data. Trees were inferred using the heuristic search option with TBR branch swapping and 1,000 random sequence additions. Max-trees were set to 5,000, branches of zero length were collapsed and all parsimonious trees were saved. Clade robustness was assessed using bootstrap (BT) analysis with 1,000 pseudo replicates (Felsenstein 1985). Descriptive tree statistics – tree length (TL), composite consistency index (CI), composite retention index (RI), composite rescaled consistency index (RC) and composite homoplasy index (HI) – were calculated for each maximum parsimonious tree generated. The combined dataset was also analysed using Maximum Likelihood (ML) in RAxML-HPC2 through the CIPRES Science Gateway (Miller et al. 2012). Branch support (BS) for the ML analysis was determined by 1000 bootstrap pseudo replicates.

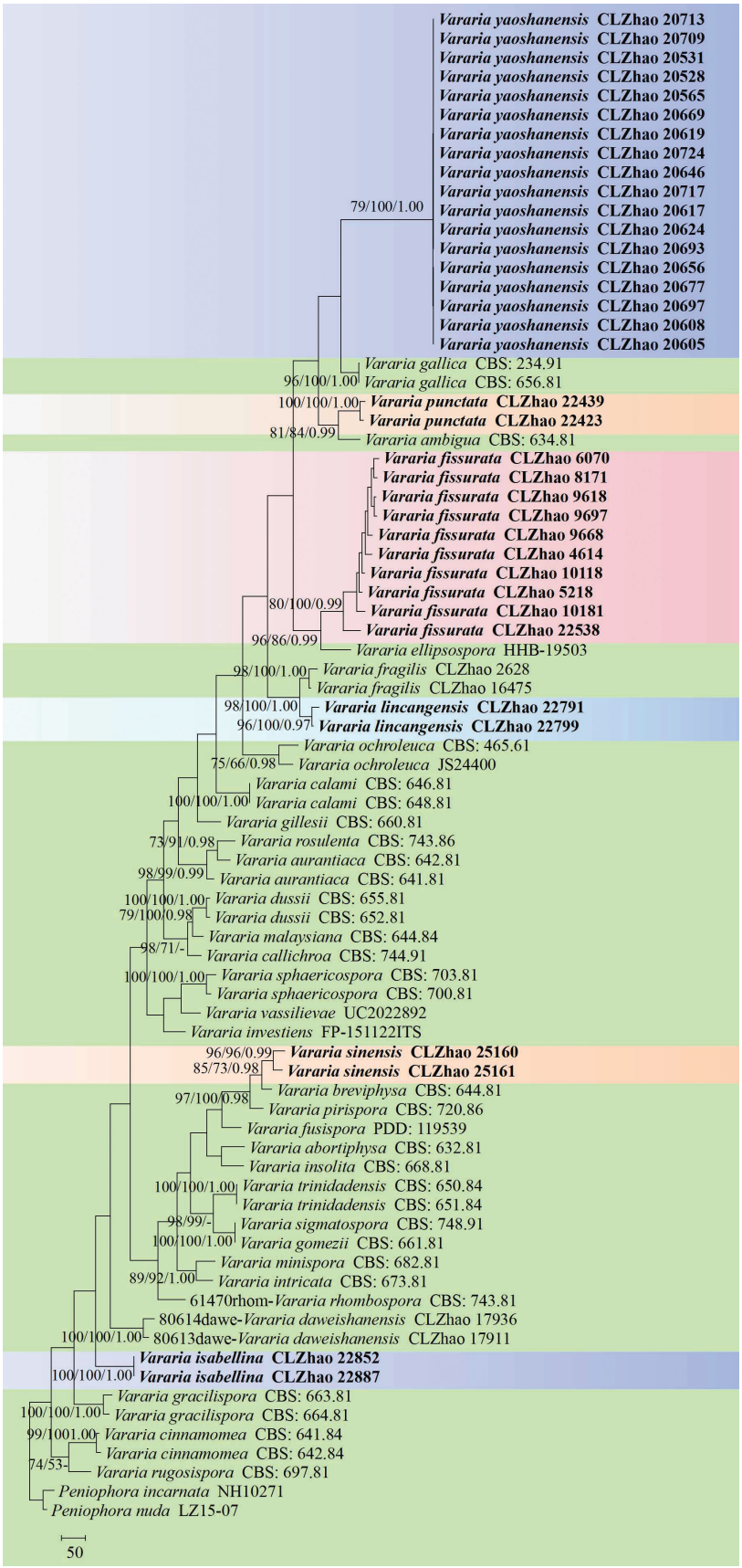

Figure 2. Maximum parsimony strict consensus tree illustrating the phylogeny of the two new species and related species in *Vararia*, based on ITS sequences. Branches are labelled with maximum likelihood bootstrap values > 70%, parsimony bootstrap values > 50% and Bayesian posterior probabilities > 0.95, respectively.

MrModeltest 2.3 (Nylander 2004) was used to determine the best-fit evolution model for each dataset for the purposes of Bayesian inference (BI) which was performed using MrBayes 3.2.7a with a GTR+I+G model of DNA substitution and a gamma distribution rate variation across sites (Ronquist et al. 2012). A total of four Markov chains were run for two runs from random starting trees for 1.2 million generations for ITS+LSU (Fig. 1); and 4 million generations for ITS (Fig. 2) with trees and parameters sampled every 1,000 generations. The first quarter of all the generations were discarded as burn-ins. A majority rule consensus tree was computed from the remaining trees. Branches were considered as significantly supported if they received a maximum likelihood bootstrap support value (BS) of > 70%, a maximum parsimony bootstrap support value (BT) of > 70% or a Bayesian posterior probability (BPP) of > 0.95.

Results

Molecular phylogeny

The ITS+LSU dataset (Fig. 1) comprised sequences from 45 fungal specimens representing 38 taxa. The dataset had an aligned length of 2,304 characters, of which 1,181 characters were constant, 346 were variable and parsimony-uninformative and 777 (50%) were parsimony-informative. Maximum parsimony analysis yielded 3 equally parsimonious trees (TL = 5,051, CI = 0.3985, HI = 0.6015, RI = 0.5522 and RC = 0.2201). The best model of nucleotide evolution for the ITS+LSU dataset estimated and applied in the Bayesian analysis was found to be GTR+I+G. Bayesian analysis and ML analysis resulted in a similar topology as in the MP analysis. The Bayesian analysis had an average standard deviation of split frequencies = 0.004451 (BI) and the effective sample size (ESS) across the two runs is double the average ESS (avg. ESS) = 324. The phylogram based on the ITS+LSU rDNA gene regions (Fig. 1) included eight genera within Peniophoraceae (Russulales), which were *Asterostroma*, *Amylostereum*, *Baltazaria*, *Dichostereum*, *Michenera*, *Peniophora*, *Scytinostroma* and *Vararia*, in which six new species were grouped into the genera *Vararia*.

The ITS dataset (Fig. 2) comprised sequences from 79 fungal specimens representing 38 taxa. The dataset had an aligned length of 849 characters, of which 199 characters were constant, 65 were variable and parsimony-uninformative and 585 (50%) were parsimony-informative. Maximum parsimony analysis yielded 1 equally parsimonious tree (TL = 4,058, CI = 0.3233, HI = 0.6767, RI = 0.7299 and RC = 0.2360). The best model of nucleotide evolution for the ITS dataset estimated and applied in the Bayesian analysis was found to be GTR+I+G. Bayesian analysis and ML analysis resulted in a similar topology as in the MP analysis. The Bayesian analysis had an average standard deviation of split frequencies = 0.001947 (BI) and the effective sample size (ESS) across the two runs is double the average ESS (avg. ESS) = 888. The phylogenetic tree (Fig. 2), inferred from the ITS sequences, highlighted that *V. fissurata* was the sister to *V. ellipsospora* G. Cunn. with strong supports. The new species *V. lincangensis* was clustered with *V. fragilis* L. Zou & C.L. Zhao. Furthermore, *V. punctata* was retrieved as a sister to *V. ambigua* Boidin, Lanq. & Gilles. Moreover, *V. isabellina* formed a monophyletic lineage, and it was then grouped closely with *V. daweishanensis* L. Zou & C.L. Zhao, and *V. gracilispora* Boidin &

Lanq. The species *V. sinensis* was grouped with five taxa as *Vararia breviphysa* Boidin & Lanq., *V. pirispora* Boidin, Gilles & Lanq., *V. fusispora* G. Cunn., *V. abortiphysa* Boidin & Lanq., and *V. insolita* Boidin & Lanq. In addition, *V. yaoshanensis* was sister to *V. gallica* (Bourdot & Galzin) Boidin with strong supports.

Taxonomy

Vararia fissurata **Y.L. Deng & C.L. Zhao, sp. nov.**
MycoBank No: MB851793
Figs 3, 4

Holotype. China. Yunnan Province, Yuxi, Xinping County, the Ancient Tea Horse Road, 23°57'10"N, 101°30'41"E, altitude 2600 m a.s.l., on the trunk of angiosperm, leg. C.L. Zhao, 21 August 2018, CLZhao 8171 (SWFC).

Etymology. *Fissurata* (Lat.): referring to the cracking hymenial surface.

Description. Basidiomata annual, resupinate, adnate, pruinose, brittle, without odor or taste when fresh, up to 12 cm long, 2.5 cm wide, and 100 μm thick. Hymenial surface smooth, white to olivaceous buff when fresh, and olivaceous buff upon drying, sparsely and deeply cracked with age. Sterile margin distinct, white, and up to 2 mm wide.

Hyphal system dimitic, generative hyphae with clamp connections, colorless, thin-walled, moderately branched, interwoven, 2–3 μm in diameter; IKI–, CB–, tissues unchanged in KOH. Dichohyphae predominate, yellowish, capillary, frequently branched, 1.5 μm in diameter, thick-walled, dichotomously to irregularly branched with main branches and acute tips, weakly to moderately dextrinoid in Melzer's reagent, CB–, tissues unchanged in KOH; subhymenial hyphae densely covered by a lot of bulk crystals.

Gloeocystidia empty or filled with refractive flocculent matter, two types: (1) Gloeocystidia subglobose, colorless, thin-walled, smooth, 11–23 × 6–12 μm; (2) Gloeocystidia subulate, usually containing refractive materials; slightly constricted at the neck, colorless, thin-walled, smooth, 25.5–43 × 7–11 μm. Basidia cylindrical, with four sterigmata and a basal clamp connection, 20–27 × 4–8 μm; basidioles dominant, in shape similar to basidia but slightly smaller.

Basidiospores ellipsoid to broadly ellipsoid, colorless, thin-walled, smooth, IKI–, CB–, 5–10 × 3–7 μm, L = 7.37 μm, W = 5.22 μm, Q = 1.38–1.44 (n = 150/5).

Additional specimens examined (paratypes). China. Yunnan Province, Yuxi, Xinping County, the Ancient Tea Horse Road, 23°57'10"N, 101°30'41"E, altitude 2600 m a.s.l., on fallen angiosperm branch, leg. C.L. Zhao, 13 January 2018, CLZhao 5218 (SWFC); Puer, Zhenyuan County, Heping Town, Damoshan, 23°56'21"N, 101°25'32"E, altitude 2240 m a.s.l., on fallen angiosperm branch, leg. C.L. Zhao, 16 January 2018, CLZhao 6070 (SWFC); Dali, Weishan Country, Qinghua Town, Green Peacock Nature Reserve, 25°23'35"N, 100°31'39"E, altitude 1500 m a.s.l., on the fallen branch of angiosperm, leg. C.L. Zhao, 18 July 2022, CLZhao 22538 (SWFC); Puer, Jingdong County, Wuliangshan National Nature Reserve, 24°34'45"N, 100°830'03"E, altitude 2000 m a.s.l., on fallen angiosperm branch, leg. C.L. Zhao, 6 October 2017, CLZhao 4614 (SWFC); 6 January 2019, CLZhao 9618, CLZhao 9668 and CLZhao 9697 (SWFC); Dali, Nanjian County, Lingbaoshan National Forest Park, 24°78'26"N, 100°51'30"E, altitude 2500 m a.s.l., on fallen angiosperm branch, leg. C.L. Zhao, 9 January 2019, CLZhao 10118, and CLZhao 10181 (SWFC).

Figure 3. Basidiomata of *Vararia fissurata* (holotype). Scale bars: 1 cm (**A**); 1 mm (**B**).

***Vararia isabellina* Y.L. Deng & C.L. Zhao, sp. nov.**
MycoBank No: MB851798
Figs 5, 6

Holotype. China. Yunnan Province, Lincang, Fengqing County, 24°67'18"N, 100°19'67"E, altitude 1660 m a.s.l., on the fallen angiosperm branch, leg. C.L. Zhao, 20 July 2022, CLZhao 22852 (SWFC).

Etymology. *Isabellina* (Lat.): referring to the isabelline to yellowish-brown basidiomata.

Description. Basidiomata annual, membranous, soft, and adnate, without odor or taste when fresh, up to 90 mm long, 10 mm wide, and 50–90 µm thick. Hymenial surface smooth, cream to isabelline when fresh, isabelline to slightly brown when dry. Sterile margin thinning out, cream to isabelline, and up to 1 mm wide.

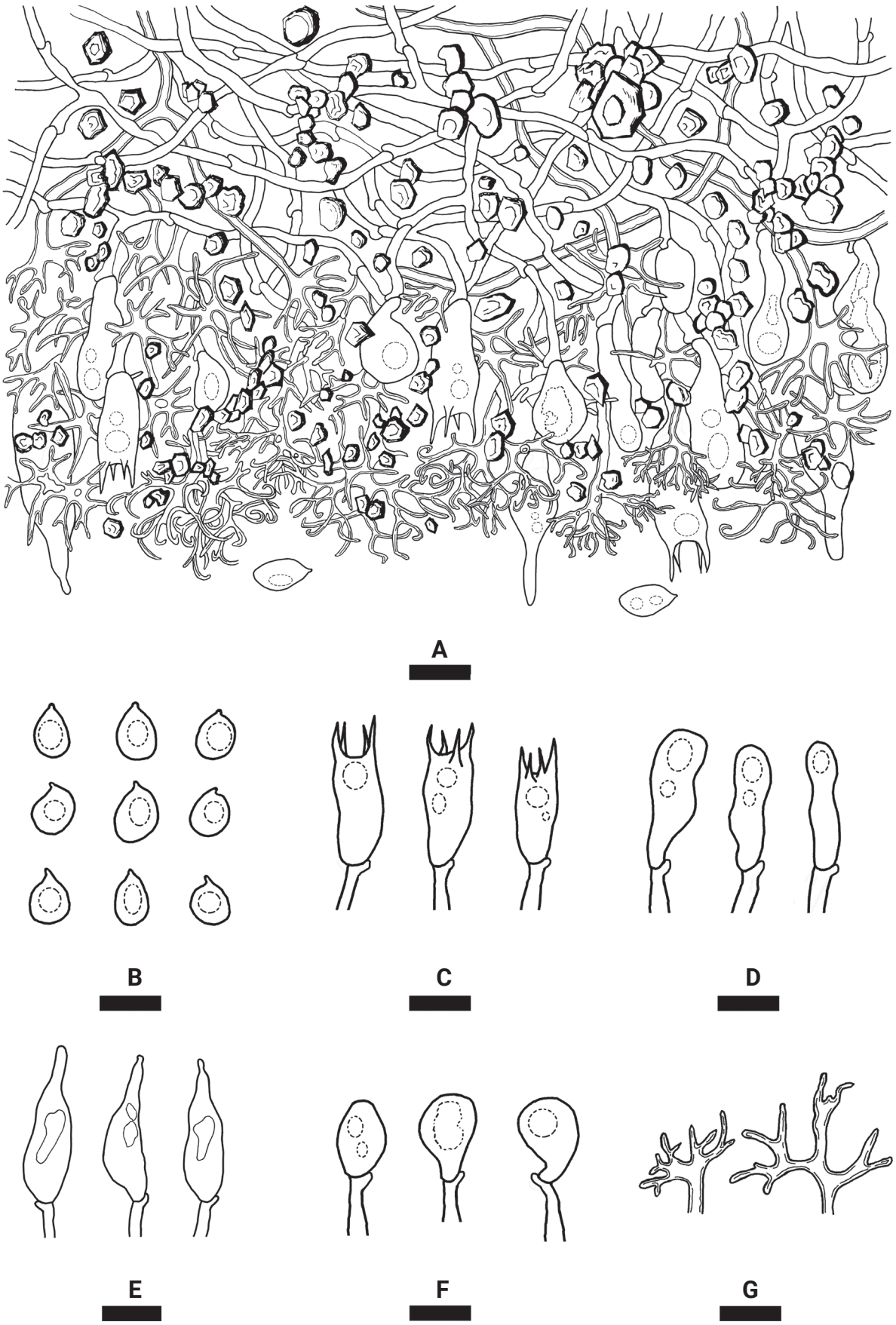

Figure 4. Microscopic structures of *Vararia fissurata* (holotype) **A** a section of hymenium **B** basidiospores **C** basidia **D** basidioles **E** gloeocystidia subulate **F** gloeocystidia subglobose **G** dichohyphae. Scale bars: 10 μm (**A–G**).

Hyphal system dimitic, generative hyphae bearing simple-septa, colorless, thin to slightly thick-walled, frequently branched, 2.5–4 µm in diameter, IKI–, CB–, tissues unchanged in KOH. Dichohyphae predominant, yellowish, distinctly thick-walled, dichotomously to irregularly branched with main branches up to 4 µm in diameter and with acute tips, moderately dextrinoid in Melzer's reagent, CB–, tissues unchanged in KOH; dichohyphae in hymenium similar to those in subiculum but more branched, with more narrow and shorter branches, with slightly curved tips and stronger.

Gloeocystidia spindle to subcylindrical, smooth, colorless, thin-walled, usually containing refractive materials, 38–47 × 8–13 µm. Basidia subcylindrical, slightly constricted at the neck, with four sterigmata and a basal simple septum connection, 33–39 × 7–9 µm; basidioles dominant, in shape similar to basidia, but slightly smaller.

Basidiospores sub-fusiform to navicular, colorless, smooth, with numerous oil-drops, thin-walled, IKI–, CB–, 9–13 × 5–8 µm, L = 11.66 µm, W = 6.69 µm, Q = 1.68–1.78 (n = 60/2).

Figure 5. Basidiomata of *Vararia isabellina* (holotype). Scale bars: 1 cm (**A**); 1 mm (**B**).

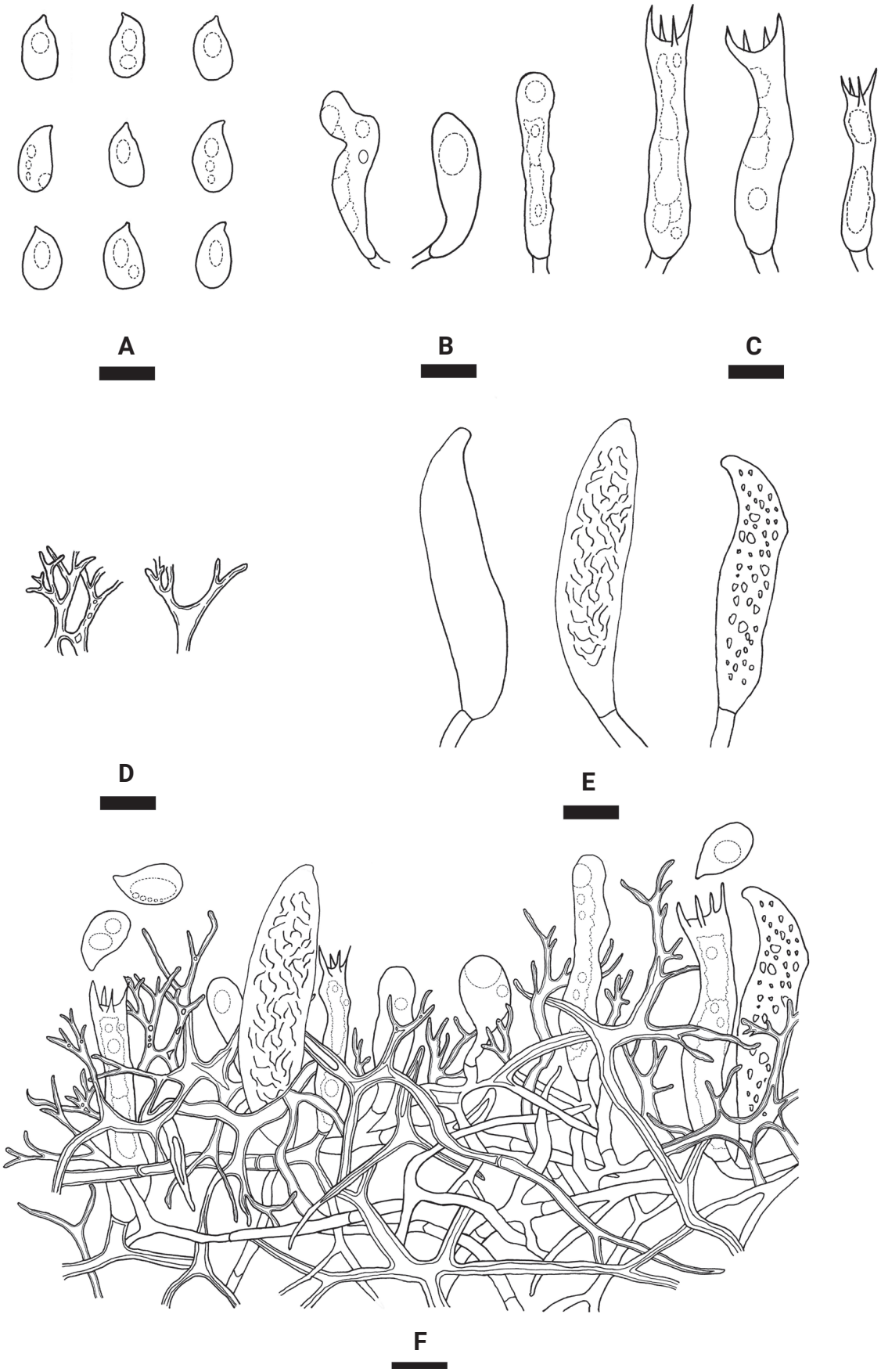

Figure 6. Microscopic structures of *Vararia isabellina* (holotype) **A** basidiospores **B** basidioles **C** basidia **D** dichohyphae **E** gloeocystidia **F** a section of hymenium. Scale bars: 10 μm (**A–F**).

Additional specimen examined (paratype). China. Yunnan Province, Lincang, Fengqing County, 24°67'18"N, 100°19'67"E, altitude 1660 m a.s.l., on the fallen angiosperm branch, leg. C.L. Zhao, 20 July 2022, CLZhao 22887 (SWFC).

***Vararia lincangensis* Y.L. Deng & C.L. Zhao, sp. nov.**
MycoBank No: MB851794
Figs 7, 8

Holotype. China. Yunnan Province, Lincang, Fengqing County, Yaojie Township, Xingyuan Village, 24°61'44"N, 100°17'21"E, altitude 1660 m a.s.l., on the fallen angiosperm branch, leg. C.L. Zhao, 20 July 2022, CLZhao 22791 (SWFC).

Etymology. *Lincangensis* (Lat.): referring to the locality (Lincang) of the type specimen.

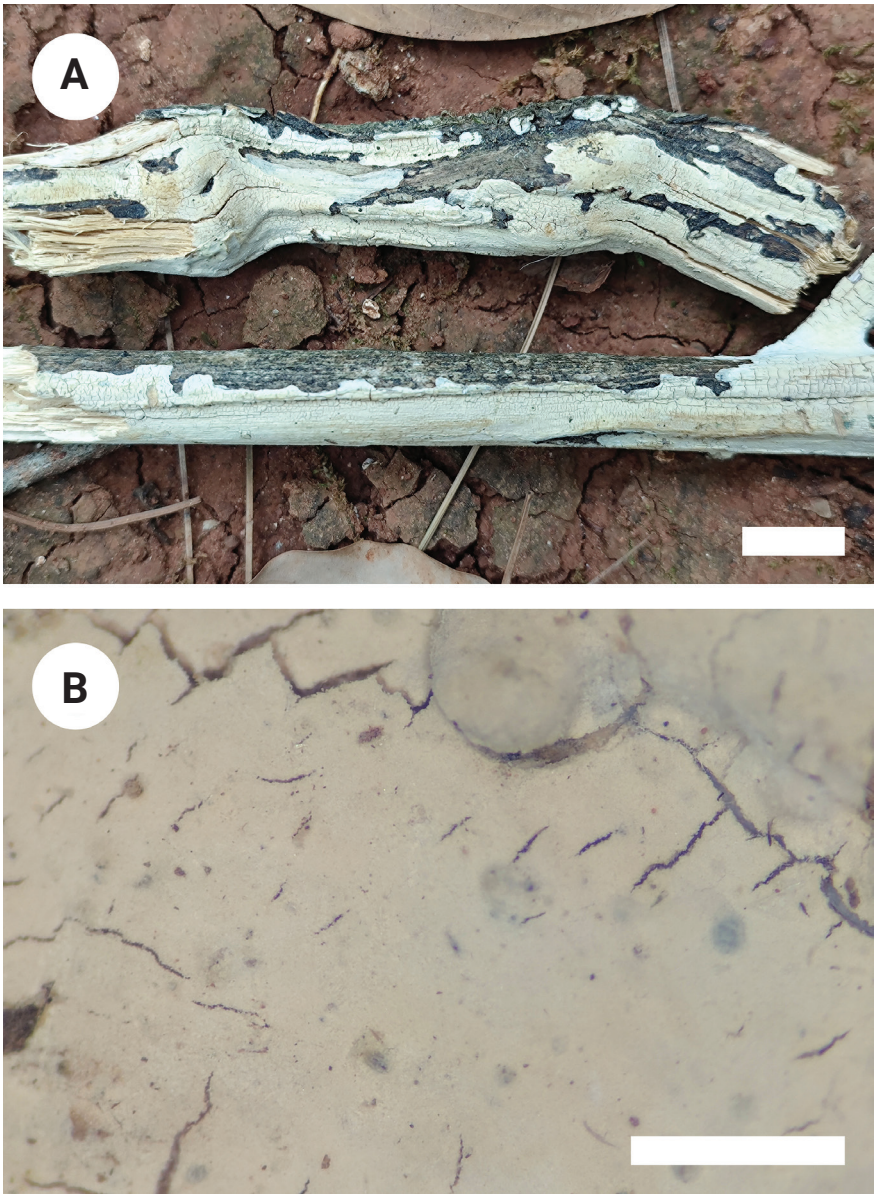

Figure 7. Basidiomata of *Vararia lincangensis* (holotype). Scale bars: 1 cm (**A**); 1 mm **(B)**.

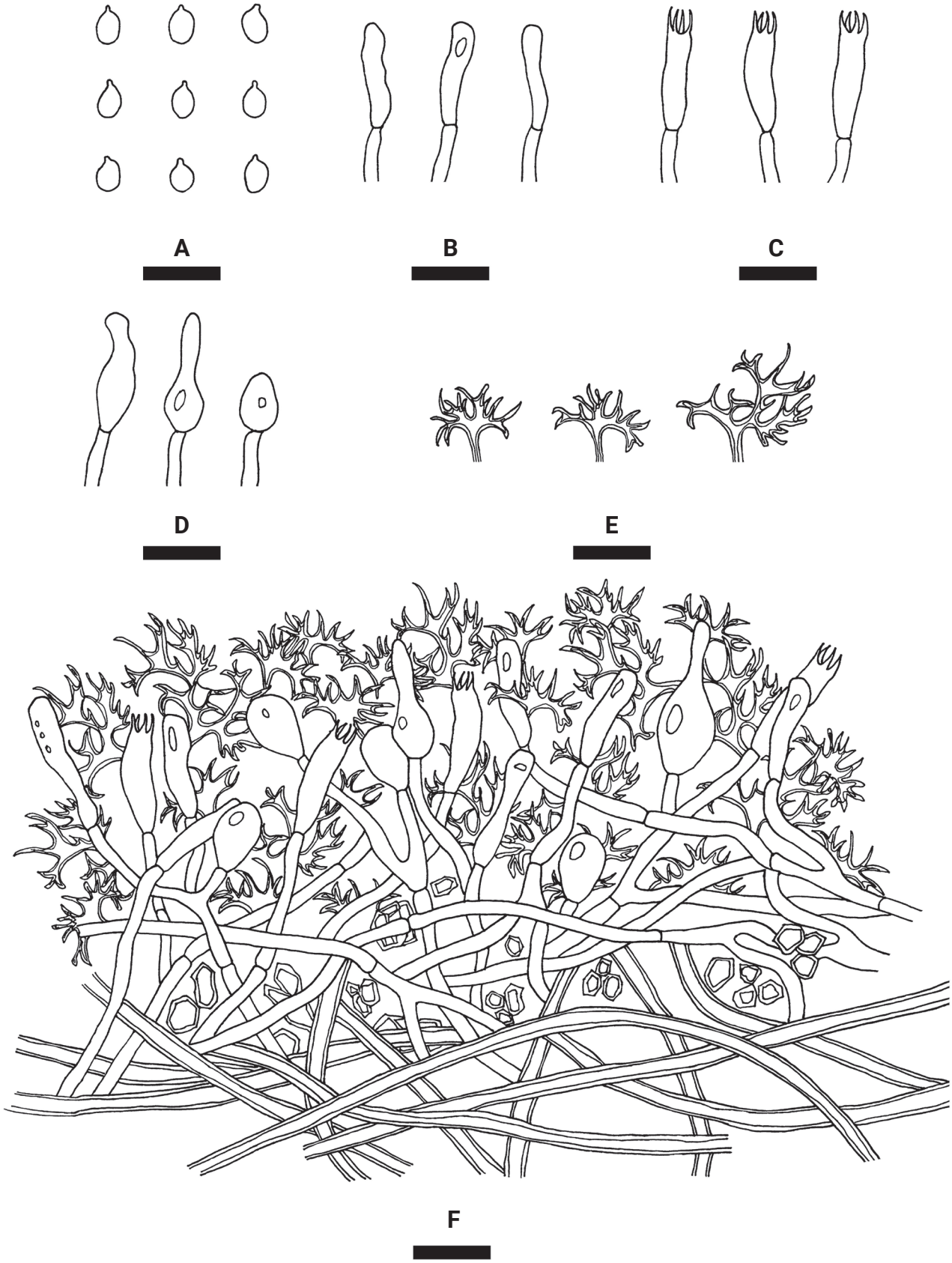

Figure 8. Microscopic structures of *Vararia lincangensis* (holotype) **A** basidiospores **B** basidioles **C** basidia **D** gloeocystidia **E** dichohyphae **F** a section of hymenium. Scale bars: 10 μm (**A–F**).

Description. Basidiomata annual, resupinate, membranous, soft and adnate, without odor or taste when fresh, up to 90 mm long, 20 mm wide, and 70–150 µm thick. Hymenial surface smooth, white to cream when fresh, cream upon drying, cracking with age. Sterile margin distinct, narrow, whitish, attached, and up to 1 mm wide.

Hyphal system dimitic, generative hyphae bearing simple-septa, rarely branched, colorless, thin-walled, 2–3 µm in diameter, IKI–, CB–, tissues unchanged in KOH; subhymenial hyphae densely covered by some crystals. Dichohyphae predominate, white to cream, capillary, thick-walled, frequently branched, dichotomously to irregularly branched with main branches and acute tips, 1–1.5 µm diameter, weakly to moderately dextrinoid in Melzer's reagent, CB–, tissues unchanged in KOH, subiculum composed of colorless. Skeletal hyphae colorless, thick-walled, 2–3 µm in diameter, IKI–, CB–, tissues unchanged in KOH.

Gloeocystidia subglobose, and clavate to fusiform, usually containing refractive materials, colorless, smooth, thin-walled, 6.5–16 × 3–5 µm. Basidia clavate, with four sterigmata and a basal simple septum, thin-walled, smooth, 11–17.5 × 2–4 µm; basidioles in shape similar to basidia, but slightly smaller.

Basidiospores ellipsoid, colorless, thin-walled, smooth, occasionally acyanophilous, CB–, (3–)3.5–5.5(–6) × (2–)2.5–4 µm, L = 4.18 µm, W = 3.11 µm, Q = 1.33–1.36 (n = 60/2).

Additional specimen examined (paratype). China. Yunnan Province, Lincang, Fengqing County, Yaojie Township, Xingyuan Village, 24°61'44"N, 100°17'21"E, altitude 1660 m a.s.l., on the fallen angiosperm branch, leg. C.L. Zhao, 20 July 2022, CLZhao 22799 (SWFC).

***Vararia punctata* Y.L. Deng & C.L. Zhao, sp. nov.**
MycoBank No: MB851795
Figs 9, 10

Holotype. China. Yunnan Province, Dali, Weishan Country, Qinghua Town, Green Peacock Nature Reserve, 25°23'35"N, 100°31'39"E, altitude 1500 m a.s.l., on the fallen branch of angiosperm, leg. C.L. Zhao, 18 July 2022, CLZhao 22439 (SWFC).

Etymology. *Punctata* (Lat.): referring to the species having cushion-shaped basidioma.

Description. Basidiomata annual, membranous, soft, adnate, without odor or taste when fresh, up to 50 mm long, 15 mm wide, and 90–150 µm thick. Hymenial surface smooth, and white to cream when fresh, cream when dry. Sterile margin thin, distinct, narrow, whitish, attached, and up to 1 mm.

Hyphal system dimitic, generative hyphae bearing simple-septa, colorless, thin to slightly thick-walled, rarely branched, interwoven, 2–3 µm in diameter, IKI–, CB–, tissues unchanged in KOH. Dichohyphae predominate, white to cream, capillary, frequently branched, thick-walled, 1 µm in diameter, dichotomously to irregularly branched with main branches and acute tips, weakly to moderately dextrinoid in Melzer's reagent, CB–, tissues unchanged in KOH. Skeletal hyphae colorless, thick-walled, 2–3 µm in diame-

Figure 9. Basidiomata of *Vararia punctata* (holotype). Scale bars: 1 cm (**A**); 1 mm (**B**).

ter, IKI–, CB–, tissues unchanged in KOH; subhymenial hyphae densely covered by bulk crystals.

Gloeocystidia clavate to cylindrical, usually containing oil droplets, colorless, smooth, thick-walled, and 12–21 × 5–9 µm. Basidia subcylindrical, with four sterigmata and a basal simple septum, 11–25 × 4–7 µm; basidioles in shape similar to basidia, but slightly smaller.

Basidiospores ellipsoid, colorless, thin-walled, smooth, with oil drops, amyloid, CB–, 6–10 × 4–6(–6.5) µm, L = 7.81 µm, W = 5.1 µm, Q = 1.51–1.56 (n = 120/4).

Additional specimen examined (paratype). China. Yunnan Province, Dali, Weishan Country, Qinghua Town, Green Peacock Nature Reserve, 25°23'35"N, 100°31'39"E, altitude 1500 m a.s.l., on the fallen branch of angiosperm, leg. C.L. Zhao, 18 July 2022, CLZhao 22423 (SWFC).

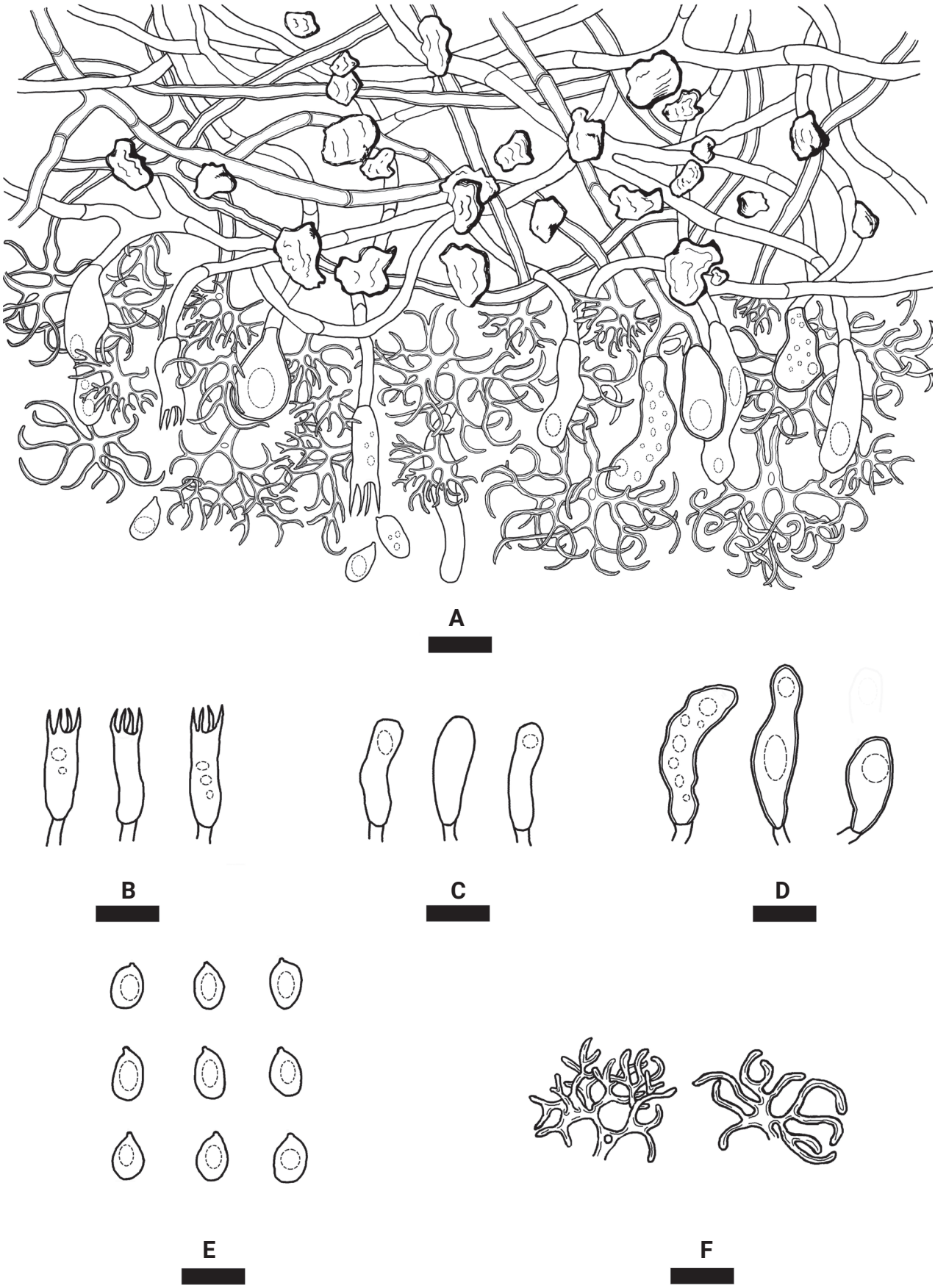

Figure 10. Microscopic structures of *Vararia punctata* (holotype) **A** a section of hymenium **B** basidia **C** basidioles **D** gloeocystidia **E** basidiospores **F** dichohyphae. Scale bars: 10 μm (**A–F**).

***Vararia sinensis* Y.L. Deng & C.L. Zhao, sp. nov.**
MycoBank No: MB851796
Figs 11, 12

Holotype. China. Yunnan Province, Lincang, Yun County, Dumu Village, 24°39'79"N, 100°18'17"E, altitude 1960 m a.s.l., on the fallen angiosperm branch, leg. C.L. Zhao, 20 October 2022, CLZhao 25160 (SWFC).

Etymology. *Sinensis* (Lat.): referring to the locality (China) of the type specimen.

Description. Basidiomata annual, membranous, and adnate, up to 70 mm long, 35 mm wide, and 80–160 μm thick. Hymenial surface smooth, white to slightly pink when fresh, pink upon drying. Sterile margin thinning out, narrow, whitish, attached, and up to 1 mm.

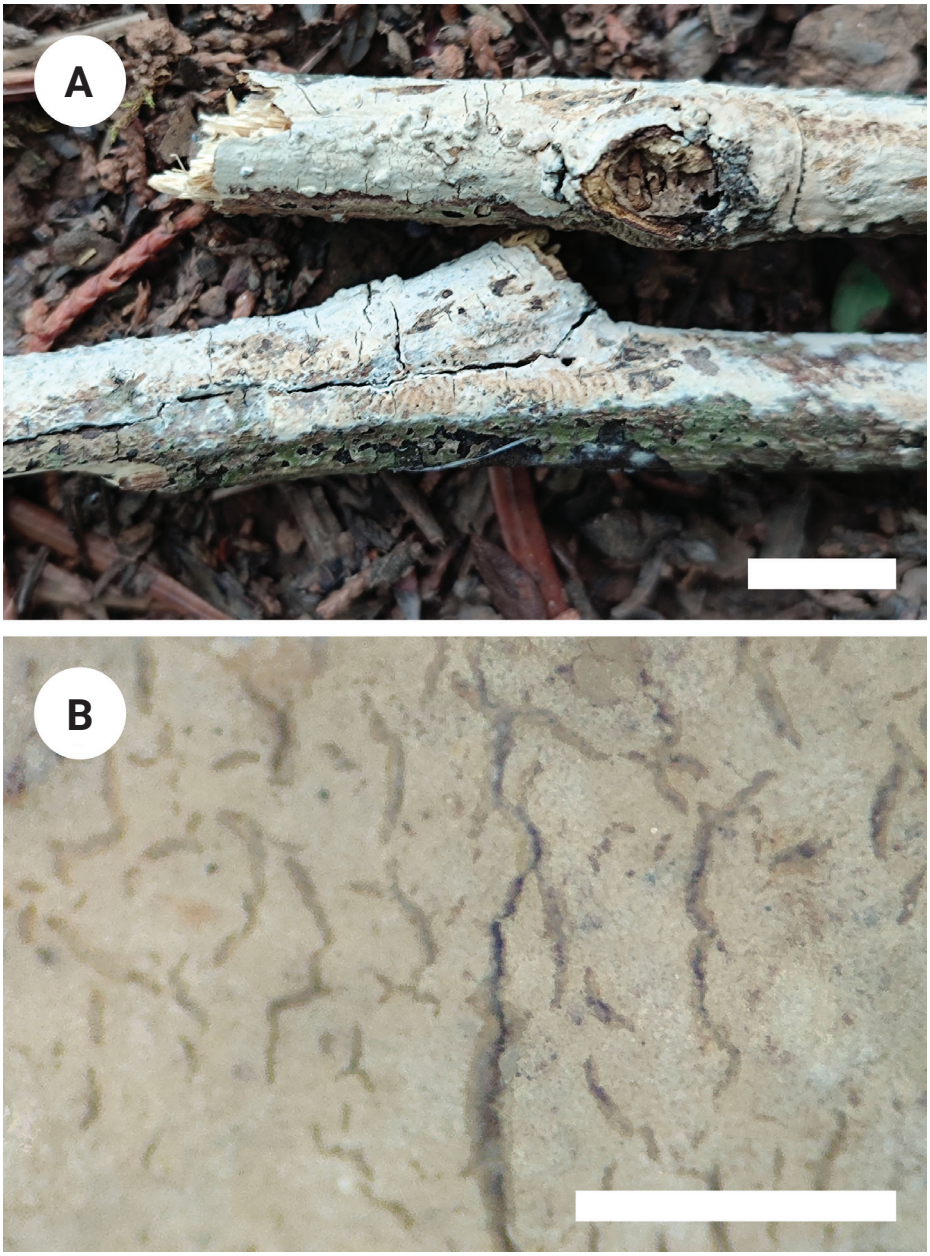

Figure 11. Basidiomata of *Vararia sinensis* (holotype). Scale bars: 1 cm (**A**); 1 mm (**B**).

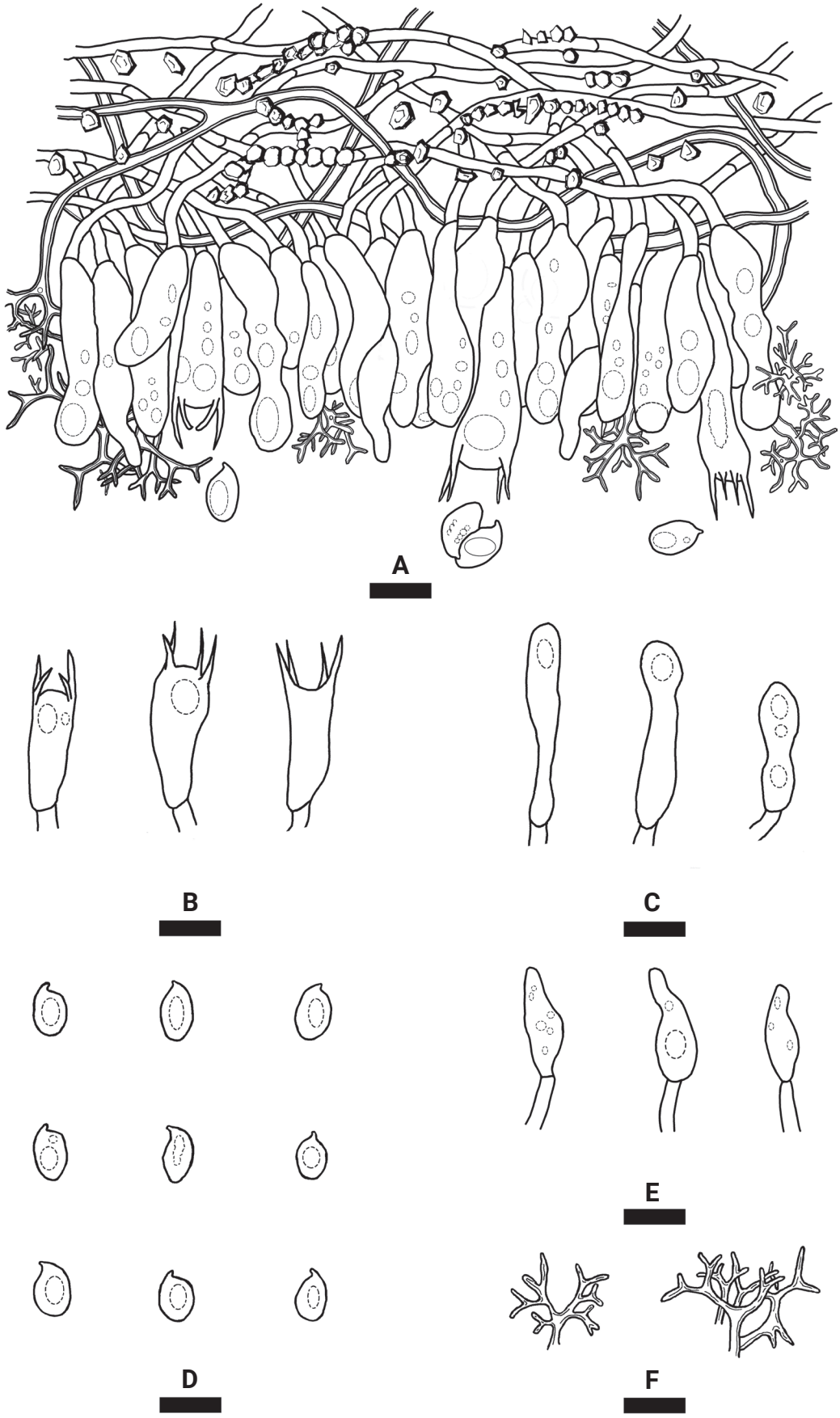

Figure 12. Microscopic structures of *Vararia sinensis* (holotype) **A** basidiospores **B** basidioles **C** basidia **D** dichohyphae **E** gloeocystidia subulate **F** a section of hymenium. Scale bars: 10 μm (**A–F**).

Hyphal system dimitic, generative hyphae bearing simple-septa, colorless, thin-walled, branched, 2.5–3 µm diameter, IKI–, CB–, tissues unchanged in KOH. Dichohyphae predominant, yellowish, thick-walled, dichotomously to irregularly branched with main branches up to 1.4 µm in diameter and with acute tips, moderately dextrinoid in Melzer's reagent, CB–, tissues unchanged in KOH, dichohyphae in hymenium similar to those in subiculum but more branched, with more narrow and shorter branches, with slightly curved tips and stronger, subhymenial hyphae densely covered by crystals. Skeletal hyphae rarely branched, interwoven, colorless, thick-walled, 2–3 µm in diameter, IKI–, CB–, tissues unchanged in KOH.

Gloeocystidia subulate, smooth, colorless, thin-walled, filled with refractive oil-like matter, 17–35 × 6–7 µm. Basidia clavate, with four sterigmata and a basal simple septum connection, 25–35 × 6–7 µm; basidioles dominant, in shape similar to basidia, but slightly smaller.

Basidiospores sub-fusiform to navicular, with a beaklike extension, colorless, smooth, with numerous oil-drops, thin-walled, IKI–, CB–, 6–11 × 4–6 µm, L = 8.21 µm, W = 4.88 µm, Q = 1.66–1.71 (n = 60/2).

Additional specimen examined (paratype). China. Yunnan Province, Lincang, Yun County, Dumu Village. GPS coordinates: 24°39'79"N, 100°18'17"E, altitude 1960 m a.s.l., on the fallen angiosperm branch, leg. C.L. Zhao, 20 October 2022, CLZhao 25161 (SWFC).

***Vararia yaoshanensis* Y.L. Deng & C.L. Zhao, sp. nov.**
MycoBank No: MB851797
Figs 13, 14

Holotype. China. Yunnan Province, Zhaotong, Qiaojia County, Yao Shan National Nature Reserve, 26°89'62"N, 102°95'04"E, altitude 2500 m a.s.l., on fallen branch of angiosperm, 21 August 2020, CLZhao 20693 (SWFC).

Etymology. *Yaoshanensis* (Lat.): referring to the provenance (Yaoshan) of the type specimen.

Description. Basidiomata annual, membranous, adnate, without odor or taste when fresh, up to 8 cm long, 4 cm wide, 80–120 µm thick. Hymenial surface smooth, cream to cinnamon-buff when fresh, pinkish buff to cinnamon-buff upon drying, cracking with age. Sterile margin thin, pinkish buff, up to 1 mm.

Hyphal system dimitic, generative hyphae bearing simple-septa, rarely branched, slightly thick-walled, 2–4 µm in diameter, IKI–, CB–, tissues unchanged in KOH. Dichohyphae, predominant, capillary, frequently branched, distinctly thick-walled, 1.6 µm diameter, dichotomously to irregularly branched with main branches and acute tips, weakly to moderately dextrinoid in Melzer's reagent, CB–, tissues unchanged in KOH.

Gloeocystidia with two types, (1) Gloeocystidia fusiform, colorless, thick-walled, smooth, tapered or gradually elongated apex, 28.5–50 × 6–12.5 µm; (2) Gloeocystidia subglobose, usually containing refractive materials, colorless, thick-walled, smooth, 11–27 × 7–11 µm. Basidia are subclavate to subcylindrical, thin-walled, with four sterigmatas and a basal simple septum, 23–46 × 5–8 µm; basidioles dominant, in shape similar to basidia, but slightly smaller.

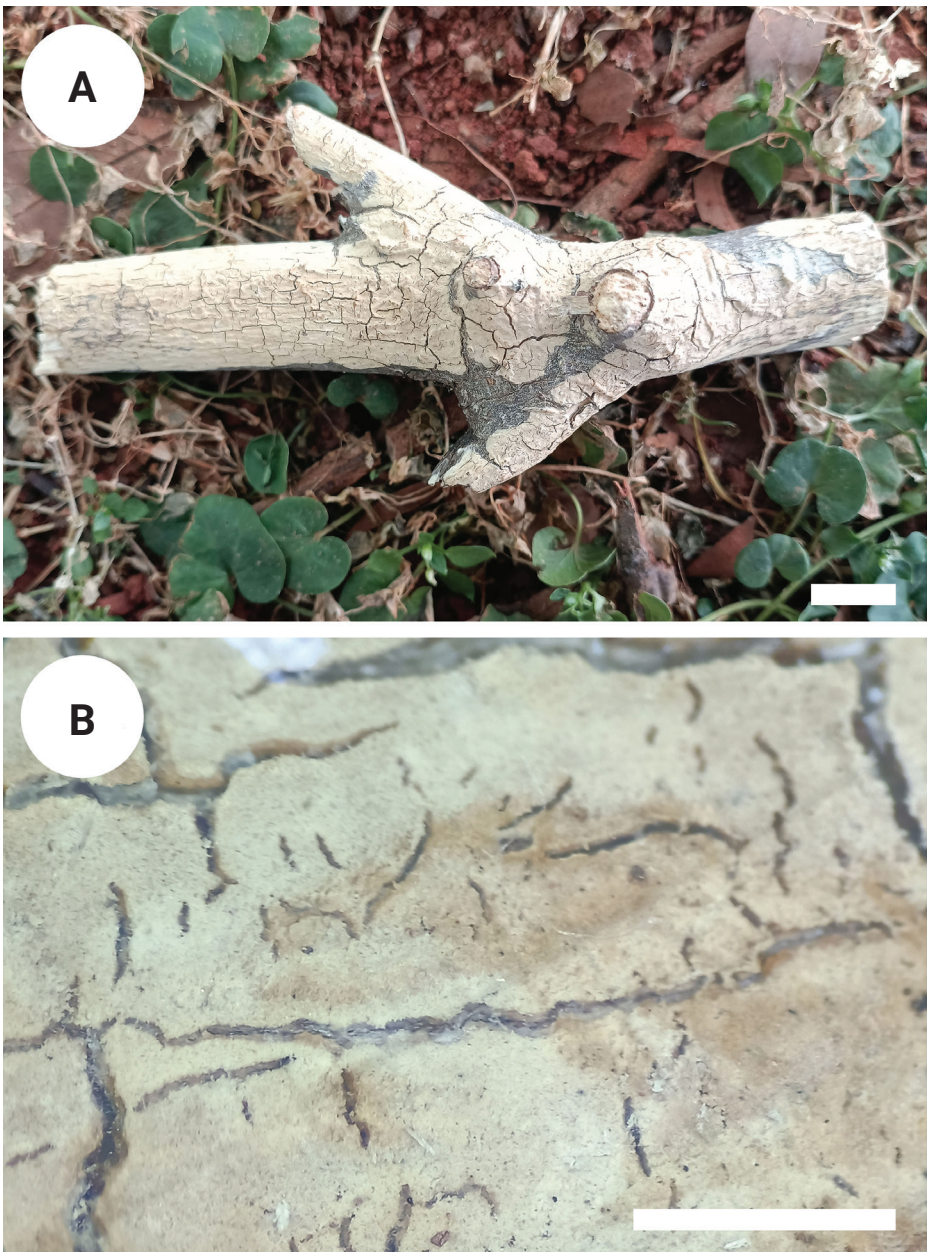

Figure 13. Basidiomata of *Vararia yaoshanensis* (holotype). Scale bars: 1 cm (**A**); 1 mm (**B**).

Basidiospores ellipsoid, colorless, slightly thick-walled, smooth, amyloid, CB–, (7.5–)7.6–10.8(–10.9) × (5.3–)5.7–7.8(–7.9) µm, L = 9.52 µm, W = 6.61 µm, Q = 1.4–1.5 (n = 210/7).

Additional specimens examined (paratypes). China. Yunnan Province, Zhaotong, Qiaojia County, Yao Shan National Nature Reserve, 26°89'62"N, 102°95'04"E, altitude 2500 m a.s.l., on fallen branch of angiosperm, 21 August 2020, CLZhao 20669, CLZhao 20677, CLZhao 20697, CLZhao 20709, CLZhao 20713, CLZhao 20717 and CLZhao 20724 (SWFC), 22 August 2020, CLZhao 20528, CLZhao 20531, CLZhao 20565, CLZhao 20605, CLZhao 20608, CLZhao 20617, CLZhao 20619, CLZhao 20624, CLZhao 20646 and CLZhao 20656 (SWFC).

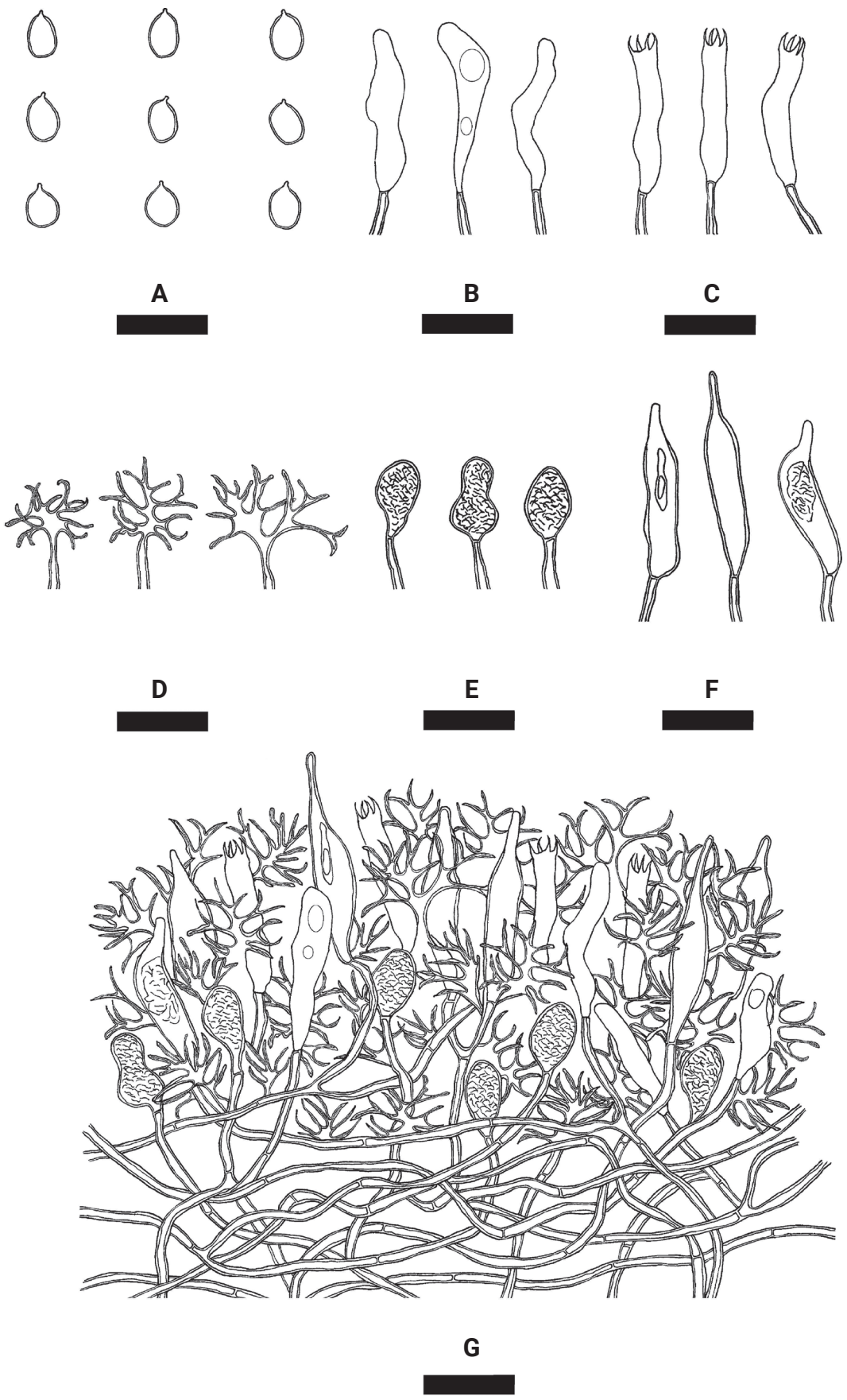

Figure 14. Microscopic structures of *Vararia yaoshanensis* (holotype) **A** basidiospores **B** basidia **C** basidioles **D** dichohyphae **E** gloeocystidia subglobose **F** gloeocystidia clavate to fusiform **G** a section of hymenium. Scale bars: 10 μm (**A–G**).

Discussion

Many recently described wood-inhabiting fungal taxa have been reported worldwide, including in the genera *Vararia* (Larsson 2007; Bernicchia and Gorjón 2010; Duhem and Buyck 2012; Sanyal et al. 2012; Nakasone 2015; Liu and He 2016; Leal-Dutra et al. 2018; Liu 2019; Dai et al. 2021; Zou et al. 2022; Deng and Zhao 2023; Li et al. 2023). Prior to this study, the following eleven *Vararia* species were reported from China, *V. amphithallica* Boidin, Lanq. & Gilles, *V. bispora* S.L. Liu & S.H. He, *V. breviphysa*, *V. cinnamomea* Boidin, Lanq. & Gilles, *V. daweishanensis*, *V. fragilis*, *V. investiens*, *V. montana* S.L. Liu & S.H. He, *V. racemosa* (Burt.) D.P. Rogers & H.S. Jacks., *V. sphaericospora* Gilb. and *V. yunnanensis* Y.L. Deng & C.L. Zhao (Dai 2011; Liu 2019; Dai et al. 2021; Zou et al. 2022; Deng and Zhao 2023). The present study (Figs 1, 2) reports six new species in *Vararia*, based on a combination of morphological features and molecular evidences.

Phylogenetically, based on the multiple loci in *Scytinostroma* s.s., nine genera, *Asterostroma*, *Baltazaria*, *Dichostereum*, *Gloiothele*, *Lachnocladium*, *Michenera*, *Peniophora*, *Vesiculomyces* and *Vararia* were divided in the family Peniophoraceae (Larsson and Larsson 2003, 2004; Larsson 2007; Leal-Dutra et al. 2018; Liu and He 2018; Zou et al. 2022; Li et al. 2023). In the present study, based on the ITS+LSU data (Fig. 1), *Vararia* was grouped with *Asterostroma*, *Baltazaria*, *Dichostereum*, and *Peniophora*, in which six new species were grouped into the genus *Vararia.* From the phylogram inferred from the ITS+LSU data (Fig. 1), the four new species *V. fissurata*, *V. punctata*, *V. isabellina* and *V. sinensis* were retrieved as a sister to *V. ellipsospora*, *V. ambigua*, *V. investiens* and *V. breviphysa*, respectively. Furthermore, the two new species *Vararia lincangensis* and *V. yaoshanensis* formed a monophyletic lineage respectively, and then *V. yaoshanensis* was clustered with *V. ellipsospora* and *V. tropica*. The species *V. lincangensis* was grouped closely with *V. ambigua*, *V. gallica* and *V. punctata*. However, morphologically, *V. investiens* can be delimited from *V. isabellina* by having the resupinate basidiomata with the yellowish cream to ochraceous hymenial surface, thin-walled, clamped generative hyphae, longer fusiform gloeocystidia (40–80 × 4–8 µm), longer basidia (30–50 × 4–5 µm), and smaller fusoid basidiospores measuring as 8–12 × 3–3.5 µm (Boidin and Lanquetin 1975). The taxon *V. ellipsospora* is different from *V. yaoshanensis* by having the smaller cylindrical basidia (24–30 × 5–6 µm), longer gloeocystidia (40–56 × 8–10 µm), and narrower basidiospores (8–12 × 5.5–6.5 µm; Cunningham 1955), and *V. tropica* is distinguished from *V. yaoshanensis* by its smaller subcylindrical gloeocystides (20–42 × 6.5–10 µm), and larger basidia (35–50 × 7–8.5 µm; Welden 1965). In addition, *V. ambigua* differs from *V. lincangensis* by having both larger gloeocystidia (15–32 × 3.5–7 µm), and basidiospores measuring as 6–7.3 × 3.4–5 µm (Boidin et al. 1980); *V. gallica* is different from *V. lincangensis* by its larger fusiform gloeocystidia (15–36 × 3.5–6.5 µm) and basidiospores (9–12 × 3.5–5 µm; Boidin and Lanquetin 1975; Grosse-Brauckmann and Kummer 2004).

Based on ITS topology (Fig. 2), the present study highlighted that *V. fissurata* was found to be the sister to *V. ellipsospora* with strong supports, and morphologically *V. ellipsospora* is different from *V. fissurata* by the fimbriate basidiomata, thick-walled generative hyphae, larger flexuous-cylindrical gloeocystid-

ia (40–56 × 8–10 μm), longer basidia (24–30 × 5–6 μm), and longer oblong ellipsoid basidiospores (8–12 × 5.5–6.5 μm; Cunningham 1955). In addition, *V. lincangensis* was clustered with *V. fragilis*, but morphologically *V. fragilis* is distinguished from *V. lincangensis* by the brittle basidiomata, with a buff to ochraceous hymenial surface and elliptical to ovoid gloeocystidia, both larger subulate gloeocystidia (16.5–27 × 4–7 μm) and subcylindrical basidia (13–23.5 × 3–4.5 μm; Zou et al. 2022). Furthermore, *V. punctata* was retrieved as a sister to *V. ambigua*, but morphologically *V. ambigua* differs from *V. punctata* by its cream to buff hymenophore, and larger fusiform gloeocystidia measuring as 15–32 × 3.5–7 μm (Boidin et al. 1980). Further, *V. isabellina* formed a monophyletic lineage and then was grouped closely with *V. daweishanensis* and *V. gracilispora* Boidin & Lanq. However, morphologically *V. daweishanensis* is distinguishable from *V. isabellina* by its pale yellowish hymenial surface, clamped generative hyphae, and smaller gloeocystidia (9–23 × 7–10.5 μm), longer basidia measuring as 26–46 × 5–8 μm, narrower allantoid basidiospores (9–13 × 3.5–5 μm; Zou et al. 2022). Moreover, *V. sinensis* was grouped with five taxa: *V. breviphysa*, *V. pirispora*, *V. fusispora*, *V. abortiphysa*, and *V. insolita*, however, morphologically, *V. breviphysa* is distinguishable from *V. sinensis* by having light yellow to light brown basidiomata, larger subcylindrical gloeocystides (50–65 × 6–8.5 μm), larger basidia (30–38 × 5.5–7 μm), and longer fusiform basidiospores (16–20 × 4–5 μm, Boidin and Lanquetin 1975; Liu et al. 2019); the species *V. pirispora* is distinct from *V. sinensis* by its larger subcylindrical gloeocystides (40–65 × 6–8 μm), longer basidia measuring as 36–52 × 6–7 μm, larger pyriform basidiospores (10–16.5 × 5–7 μm; Boidin et al. 1987); *V. fusispora* can be delimited from *V. sinensis* by having larger cylindrical gloeocystidia (40–60 × 5–6 μm) and oval to fusiform gloeocystidia (24–60 × 6–12 μm), subclavate basidia (35–56 × 6–9 μm), and larger fusiform basidiospores measuring as 14–17 × 4–6 μm (Cunningham 1955); *V. abortiphysa* is distinct from *V. sinensis* by its plagio and subcylindrical gloeocystides measuring as 25–45 × 4.5–9 μm, and longer cylindrical basidiospores (14–17 × 2.2–2.8 μm; Boidin and Lanquetin 1975); *V. insolita* is distinguishable from *V. sinensis* by having larger gloeocystidia measuring as 60–80 × 5–8 μm, longer subcylindrical basidia (30–78 × 5.5–6.5 μm), and longer subfusiform basidiospores (12–16 × 4.2–5.75 μm; Boidin and Lanquetin 1975). Then *V. yaoshanensis* was found to be the sister to *V. gallica* (Bourdot & Galzin) Boidin with strong supports. However, morphologically, *V. gallica* can be delimited from *V. yaoshanensis* by its thin-walled generative hyphae, smaller thin-walled fusiform gloeocystidia (15–36 × 3.5–6.5 μm), and thin-walled, narrower basidiospores measuring as 9–12 × 3.5–5 μm (Boidin and Lanquetin 1975; Grosse-Brauckmann and Kummer 2004).

Based on our phylogenetic and morphological research results, 17 species have been reported from China, including newly described in the present study and other recently published papers in this country (Dai 2011; Liu and He 2016; Liu 2019; Dai et al. 2021; Zou et al. 2022; Deng and Zhao 2023). It seems that the species diversity of *Vararia* is rich in China. Although *Vararia* taxa are well studied in the present paper, the species diversity, taxonomy and phylogeny of *Vararia* and related genera are still unresolved. A comprehensive study on this issue is urgently needed.

A key to 17 species of *Vararia* s.l. in China

1 Generative hyphae with clamp connections **2**
– Generative hyphae bearing simple-septa **3**
2 Basidia with 2 sterigmatas **4**
– Basidia with 4 sterigmatas **5**
3 Present thick-walled skeletal hyphae **6**
– Absent thick-walled skeletal hyphae **7**
4 Subcylindrical to fusiform basidiospores measuring as (10.5–)12–17(–20) × 4.5–5.5(–6.5) µm, slightly thick-walled, subglobose gloeocystidia (15–30(–35) × 6–8(–10) µm), and subcylindrical or gradually narrower gloeocystidia (25–40(–65) × 4.5–6(–18) µm) ..... ***V. amphithallica***
– Fusiform to cylindrical basidiospores measuring as (16–)18–22(–14) × 6–7.2(–8) µm, thick-walled, ventricose, gloeocystidia with an apical papilla (20–40 × 9–12 µm) ..... ***V. bispora***
5 Thin to thick-walled generative hyphae, subcylindrical basidia (26–46 × 5–8 µm), allantoid basidiospores measuring as (8.5–) 9–13 (–14) × 3.5–5 µm, and ellipsoid to ovoid to subcylindrical gloeocystidia (9–23 × 7–10.5 µm) ..... ***V. daweishanensis***
– Thin-walled generative hyphae **8**
6 Thin to slightly thick-walled generative hyphae, thick-walled, clavate to cylindrical gloeocystidia (12–21 × 5–9 µm), subcylindrical basidia (11–25 × 4–7 µm), and ellipsoid basidiospores (6–10 × 4–6(–6.5) µm) ..... ***V. punctata***
– Thin-walled generative hyphae, clavate basidia **9**
7 Slightly thick-walled generative hyphae **10**
– Thin-walled generative hyphae **11**
8 Gloeocystidia two kinds ..... ***V. fissurata***
– Gloeocystidia one kinds **12**
9 Ellipsoid basidiospores measuring as (3–)3.5–5.5(–6) × (2–)2.5–4 µm, subglobose, clavate to fusiform gloeocystidia (6.5–16 × 3–5 µm) ..... ***V. lincangensis***
– Subfusiform to navicular basidiospores (6–11 × 4–6 µm), subulate gloeocystidia (17–35 × 6–7 µm) ..... ***V. sinensis***
10 Slightly thick-walled, ellipsoid basidiospores measuring as (7.5–)7.6–10.8(–10.9) × (5.3–)5.7–7.8(–7.9) µm, thick-walled, fusiform gloeocystidia (28.5–50 × 6–12.5 µm), globose gloeocystidia (11–27 × 7–11 µm), subclavate to subcylindrical basidia (23–46 × 5–8 µm) ..... ***V. yaoshanensis***
– Thin-walled basidiospores, subcylindrical basidia **13**
11 Slightly thick-walled, ellipsoid basidiospores measuring as (5.1–)5.9–11.5(–11.8) × (4.3–)4.7–8.6(–9) µm, cylindrical basidia (17.5–32 × 5–9.5 µm), thin- to slightly thick-walled, subcylindrical gloeocystidia (16.5–58.5 × 4–10 µm), fusiform gloeocystidia (18.5–43.5 × 7–9 µm), tapering gloeocystidia (27.5–42 × 5.5–9 µm) ..... ***V. yunnanensis***
– Thin-walled basidiospores **14**
12 Basidiospores < 5 µm in diameter ..... ***V. investiens***
– Basidiospores > 5 µm in diameter **15**

13 Broad ellipsoid to ellipsoid basidiospores measuring as 3.5–5.5(–6) × 2.5–3.5 µm, elliptical to ovoid gloeocystidia (5.8–16 × 3.5–7 µm), subulate gloeocystidia (16.5–27 × 4–7 µm) ..... ***V. fragilis***

– Sub-fusiform to navicular basidiospores with numerous oil-drops measuring as 9–13 × 5–8 µm, spindle to subcylindrical gloeocystidia (38–47 × 8–13 µm) ..... ***V. isabellina***

14 Rose to orange subfusiform basidiospores measuring as (14–)16–19(–21.5) × 4.2–6 µm, cylindrical basidia (30–53 × 6.5–7.5 µm), thick-walled, subcylindrical Gloeocystides (50–65 × 6–7(–8.5) µm)..... ***V. breviphysa***

– Colorless basidiospores **16**

15 Broadly ellipsoid basidiospores measuring as (11–)12–16(–17) × (7.5–)9.5–13(–14) µm, clavate basidia (70–110 × 10–16 µm), clavate gloeocystidia (50–100 × 4–9 µm) ..... ***V. montana***

– Spherical basidiospores measuring as 8–10 × 7.5–8.5 µm, cylindrical to clavate basidia (40–45 × 6–7.5 µm), subcylindrical to fusiform gloeocystides (48–80(–105) × 7–11(–14) µm)..... ***V. sphaericospora***

16 Subcylindrical to fusiform gloeocystides (26–40 × 4.5–9 µm), cylindrical basidiospores (6–8 × 2–3 µm), cylindrical basidia (30–40 × 4–5 µm) .... ***V. racemosa***

– Absent gloeocystides, oblong to subellipsoid basidiospores measuring as 9–13 × 5–7.2 µm, and subcylindrical basidia (45–65 × 8–10 µm)..... ..... ***V. cinnamomea***

Additional information

Conflict of interest

The authors have declared that no competing interests exist.

Ethical statement

No ethical statement was reported.

Funding

The research was supported by the National Natural Science Foundation of China (Project Nos. 32170004, U2102220), and the High-level Talents Program of Yunnan Province (YNQR-QNRC-2018-111), and Forestry Innovation Programs of Southwest Forestry University (Grant No: LXXK-2023Z07).

Author contributions

Conceptualization: CZ. Data curation: YD, CZ. Formal analysis: CZ, YD, SJ. Funding acquisition: CZ. Investigation: YD, CZ, SJ. Methodology: SJ, YD, CZ. Project administration: CZ. Resources: CZ, YD. Software: YD, CZ. Supervision: YD, SJ, CZ. Validation: CZ. Visualization: CZ. Writing – original draft: YD, CZ, SJ. Writing – review and editing: YD, CZ.

Author ORCIDs

Yinglian Deng https://orcid.org/0000-0002-8220-508X
Sana Jabeen https://orcid.org/0000-0001-8839-7716
Changlin Zhao https://orcid.org/0000-0002-8668-1075

Data availability

All of the data that support the findings of this study are available in the main text.

References

Bernicchia A, Gorjón SP (2010) Fungi Europaei 12: *Corticiaceae* s.l. Edizioni Candusso, Alassio, Italy.

Boidin J (1967) Basidiomycètes Lachnocladiaceae résupinés de la Republique Centrafricaine. Cahiers de La Maboké 5: 23–35.

Boidin J (1980) Application du concept biologique del'espèce aux Basidiomycètes. Le genre *Vararia* section *Vararia* au Gabon. Cryptogamie. Mycologie 1: 265–384.

Boidin J, Gilles G (1999) Contribution à la connaissance du genre *Vararia* (Basidiomycotina). Bulletin de la Societe Mycologique de France 115: 115–139.

Boidin J, Lanquetin P (1975) *Vararia* subgenus *Vararia* (Basidiomycetes, Lachnocladiaceae): Étude spèciale des espèces d'Afrique intertropicale. Bulletin de la Société Mycologique de France 91: 457–513.

Boidin J, Lanquetin P (1987) Le genre *Scytinostroma* Donk (Basidiomycetes, Lachnocladiaceae). Bibliotheca Mycologica 114: 1–130.

Boidin J, Lanquetin P, Gilles G (1980) Application du concept biologique del'espèce aux Basidiomycètes. Le genre *Vararia* section *Vararia* au Gabon. Cryptogamie. Mycologie 1(4): 265–384.

Boidin J, Gilles G, Lanquetin P (1987) Basidiomycètes Aphyllophorales de l'Île de la Réunion. IX – Les genres *Dichostereum* Pilat et *Vararia* Karsten. Bulletin de la Société Mycologique de France 103(2): 119–135.

Boidin J, Mugnier J, Canales R (1998) Taxonomie moleculaire des Aphyllophorales. Mycotaxon 66: 445–491.

Cui BK, Li HJ, Ji X, Zhou JL, Song J, Si J, Yang ZL, Dai YC (2019) Species diversity, taxonomy and phylogeny of Polyporaceae (Basidiomycota) in China. Fungal Diversity 97(1): 137–392. https://doi.org/10.1007/s13225-019-00427-4

Cunningham GH (1955) Thelephoraceae of New Zealand. Part IV. The genus *Vararia*. Transactions and Proceedings of the Royal Society of New Zealand 82: 973–985.

Dai YC (2011) A revised checklist of corticioid and hydnoid fungi in China for 2010. Mycoscience 52(1): 69–79. https://doi.org/10.1007/S10267-010-0068-1

Dai YC, Yang ZL, Cui BK, Wu G, Yuan HS, Zhou LW, He SH, Ge ZW, Wu F, Wei YL, Yuan Y, Si J (2021) Diversity and systematics of the important macrofungi in Chinese forests. Mycosystema 40: 770–805. https://doi.org/10.13346/j.mycosystema.210036

Deng YL, Zhao CL (2023) The molecular phylogeny and morphology revealed a new wood-rotting fungus *Vararia yunnanensis* (Peniophoraceae, Russulales) in Yunnan Province, China. Phytotaxa 583: 039–049. https://doi.org/10.11646/phytotaxa.583.1.4

Duhem B, Buyck B (2012) On two new tropical *Vararia* (Russulales, Basidiomycota) with extremely small, racemose dichohyphidia. Cryptogamie. Mycologie 33(4): 427–437. https://doi.org/10.7872/crym.v33.iss4.2012.427

Felsenstein J (1985) Confidence intervals on phylogenetics: An approach using bootstrap. Evolution; International Journal of Organic Evolution 39(4): 783–791. https://doi.org/10.2307/2408678

Gilbertson RL (1965) Some species of *Vararia* from temperate North America. Papers of the Michigan Academy of Science, Arts and Letters 50: 161–184.

Grosse-Brauckman H, Kummer V (2004) Fünf bemerkenswerte funde corticioider Pilze aus Deutschland. Feddes Repertorium 115(1): 90–101. https://doi.org/10.1002/fedr.200311029

Guan QX, Huang J, Huang J, Zhao CL (2023) Five new species of Schizoporaceae (Basidiomycota, Hymenochaetales) from East Asia. MycoKeys 96: 25–56. https://doi.org/10.3897/mycokeys.96.99327

Hallenberg N (1985) The Lachnocladiaceae and Coniophoraceae of North Europe. Fungiflora.

Hyde KD (2022) The numbers of fungi. Fungal Diversity 114(1): 1. https://doi.org/10.1007/s13225-022-00507-y

Jiang N, Voglmayr H, Bian DR, Piao CG, Wnag SK, Li Y (2021) Morphology and phylogeny of *Gnomoniopsis* (Gnomoniaceae, Diaporthales) from fagaceae leaves in China. Journal of Fungi 7(10): 792. https://doi.org/10.3390/jof7100792

Karasinski D (2010) Polish resupinate Russulales: The genus *Vararia*. Acta Mycologica 45(1): 45–56. https://doi.org/10.5586/am.2010.007

Karnste PA (1898) Kritisk of versigt af Finlands Basidsvampar. Biology 3: 1–36.

Katoh K, Rozewicki J, Yamada KD (2019) MAFFT online service: Multiple sequence alignment, interactive sequence choice and visualization. Briefings in Bioinformatics 20(4): 1160–1166. https://doi.org/10.1093/bib/bbx108

Larsson KH (2007) Re-thinking the classification of corticioid fungi. Mycological Research 111(9): 1040–1063. https://doi.org/10.1016/j.mycres.2007.08.001

Larsson A (2014) AliView: A fast and lightweight alignment viewer and editor for large data sets. Bioinformatics 30(22): 3276–3278. https://doi.org/10.1093/bioinformatics/btu531

Larsson E, Larsson KH (2003) Phylogenetic relationships of russuloid basidiomycetes with emphasis on aphyllophoralean taxa. Mycologia 95(6): 1037–1065. https://doi.org/10.1080/15572536.2004.11833020

Larsson KH, Larsson E, Kõljalg U (2004) High phylogenetic diversity among corticioid homobasidiomycetes. Mycological Research 108: 983–1002. https://doi.org/10.1017/S0953756204000851

Leal-Dutra CA, Neves MA, Griffith GW, Reck MA, Clasen LA, Dentinger BTM (2018) Reclassification of *Parapterulicium* Corner (Pterulaceae, Agaricales), contributions to Lachnocladiaceae and Peniophoraceae (Russulales) and introduction of *Baltazaria* gen. nov. MycoKeys 37: 39–56. https://doi.org/10.3897/mycokeys.37.26303

Li Y, Xu WQ, Liu SL, Yang N, He SH (2023) Species diversity and taxonomy of *Scytinostroma* sensu stricto (Russulales, Basidiomycota) with descriptions of four new species from China. MycoKeys 98: 133–152. https://doi.org/10.3897/mycokeys.98.105632

Liu SL (2019) Taxonomy and phylogeny of *Vararia* and related genera in China. Ph.D. Thesis, Beijing Forestry University, Beijing,China.

Liu SL, He SH (2016) The genus *Vararia* (Russulales, Basidiomycota) in China. Two new species and two new Chinese records. Nordic Journal of Botany 1756–1051. https://doi.org/10.1111/njb.01170

Liu SL, He SH (2018) Taxonomy and phylogeny of *Dichostereum* (Russulales), with descriptions of three new species from southern China. MycoKeys 40: 111–126. https://doi.org/10.3897/mycokeys.40.28700

Liu SL, Tian Y, Nie T, Thawthong A, Hyde KD, Xu LL, He SH (2017) Updates on East Asian *Asterostroma* (Russulales, Basidiomycota): New species and new records from Thailand and China. Mycological Progress 16(6): 667–676. https://doi.org/10.1007/s11557-017-1301-5

Liu SL, Nakasone KK, He SH (2019) *Michenera incrustata* sp. nov. (Peniophoraceae, Russulales) from southern China. Nova Hedwigia 108(1-2): 197–206. https://doi.org/10.1127/nova_hedwigia/2018/0500

Miller SL, Larsson E, Larsson KH, Verbeken A, Nuytinck J (2006) Perspectives in the new Russulales. Mycologia 98(6): 960–970. https://doi.org/10.1080/15572536.2006.11832625

Miller MA, Pfeiffer W, Schwartz T (2012) The CIPRES Science Gateway: enabling high-impact science for phylogenetics researchers with limited resources. Association for Computing Machinery 39: 1–8. https://doi.org/10.1145/2335755.2335836

Nakasone KK (2015) Taxonomic studies in *Chrysoderma*, *Corneromyces*, *Dendrophysellum*, *Hyphoradulum*, and *Mycobonia*. Mycotaxon 130: 369–397. https://doi.org/10.5248/130.369

Nylander JAA (2004) MrModeltest v.2. Program Distributed by the Author; Evolutionary Biology Centre, Uppsala University: Uppsala, Sweden.

Petersen JH (1996) The danish mycological society's colour-chart. Foreningen til Svampekundskabens Fremme, Greve.

Pouzar Z (1982) Taxonomic studies in resupinate fungi I. Czech Mycology 36: 141–145.

Rehner SA, Samuels GJ (1994) Taxonomy and phylogeny of *Gliocladium* analysed from nuclear large subunit ribosomal DNA sequences. Mycological Research 98(6): 625–634. https://doi.org/10.1016/S0953-7562(09)80409-7

Riebesehl J, Langer E (2017) *Hyphodontia* s.l. (Hymenochaetales, Basidiomycota): 35 new combinations and new keys to currently all 120 species. Mycological Progress 16(6): 637–666. https://doi.org/10.1007/s11557-017-1299-8

Riebesehl J, Yurchenko E, Nakasone KK, Langer E (2019) Phylogenetic and morphological studies in *Xylodon* (Hymenochaetales, Basidiomycota) with the addition of four new species. MycoKeys 47: 97–137. https://doi.org/10.3897/mycokeys.47.31130

Ronquist F, Teslenko M, van der Mark P, Ayres DL, Darling A, Hohna S, Larget B, Liu L, Suchard MA, Huelsenbeck JP (2012) MrBayes 3.2: Efficient Bayesian phylogenetic inference and model choice across a large model space. Systematic Biology 61(3): 539–542. https://doi.org/10.1093/sysbio/sys029

Rosenthal LM, Larsson KH, Branco S, Chung JA, Glassman SI, Liao HL, Peay KG, Smith DP, Talbot JM, Taylor JW, Vellinga EC, Vilgalys R, Bruns TD (2017) Survey of corticioid fungi in North American pinaceous forests reveals hyperdiversity, underpopulated sequence databases, and species that are potentially ectomycorrhizal. Mycologia 109(1): 115–127. https://doi.org/10.1080/00275514.2017.1281677

Sanyal SK, Dhingra GS, Singh AP (2012) *Vararia longicystidiata* sp. nov. (Agaricomycetes) from India. Mycotaxon 120(1): 357–360. https://doi.org/10.5248/120.357

Stalpers JA (1996) The aphyllophoraceous fungi II. Keys to the species of the Hericiales. Studies in Mycology 40: 1–183.

Vilgalys R, Hester M (1990) Rapid genetic identification and mapping of enzymatically amplified ribosomal DNA from several *Cryptococcus* species. Journal of Bacteriology 172(8): 4238–4246. https://doi.org/10.1128/jb.172.8.4238-4246.1990

Vu D, Groenewald M, Vries M, Gehrmann T, Stielow B, Eberhardt U (2019) Large-scale generation and analysis of filamentous fungal DNA barcodes boosts coverage for kingdom fungi and reveals thresholds for fungal species and higher taxon delimitation. Studies in Mycology 92(1): 135–154. https://doi.org/10.1016/j.simyco.2018.05.001

Welden AL (1965) West Indian species of *Vararia* with notes on extralimital species. Mycologia 57(4): 502–520. https://doi.org/10.1080/00275514.1965.12018236

White TJ, Bruns T, Lee S, Taylor J (1990) Amplification and direct sequencing of fungal ribosomal RNA genes for phylogenetics. In: Innis MA, Gelfand DH, Sninsky JJ, White TJ (Eds) PCR protocols: A Guide to Methods And Applications. Academic Press, San Diego, 315–322. https://doi.org/10.1016/B978-0-12-372180-8.50042-1

Wu F, Zhou LW, Vlasák J, Dai YC (2022) Global diversity and systematics of Hymenochaetaceae with poroid hymenophore. Fungal Diversity 113(1): 1–192. https://doi.org/10.1007/s13225-021-00496-4

Yurchenko E, Wu SH (2016) A key to the species of *Hyphodontia* sensu lato. MycoKeys 12: 1–27. https://doi.org/10.3897/mycokeys.12.7568

Yurchenko E, Riebesehl J, Langer E (2017) Clarification of *Lyomyces sambuci* complex with the descriptions of four new species. Mycological Progress 16(9): 865–876. https://doi.org/10.1007/s11557-017-1321-1

Yurchenko E, Riebesehl J, Langer E (2020) *Fasciodontia* gen. nov. (Hymenochaetales, Basidiomycota) and the taxonomic status of *Deviodontia*. Mycological Progress 19(2): 171–184. https://doi.org/10.1007/s11557-019-01554-7

Zhao CL, Wu ZQ (2017) *Ceriporiopsis kunmingensis* sp. nov. (Polyporales, Basidiomycota) evidenced by morphological characters and phylogenetic analysis. Mycological Progress 16(1): 93–100. https://doi.org/10.1007/s11557-016-1259-8

Zhao YN, He SH, Nakasone KK, Wasantha KL, Chen CC, Liu SL, Ma HX, Huang MR (2021) Global phylogeny and taxonomy of the wood-decaying fungal genus *Phlebiopsis* (Polyporales, Basidiomycota). Frontiers in Microbiology 12: 622460. https://doi.org/10.3389/fmicb.2021.622460

Zhao CL, Qu MH, Huang RX, Karunarathna SC (2023) Multi-gene phylogeny and taxonomy of the wood-rotting fungal genus *Phlebia* sensu lato (Polyporales, Basidiomycota). Journal of Fungi 9(3): 1–41. https://doi.org/10.3390/jof9030320

Zou L, Zhang XL, Deng YL, Zhao CL (2022) Four new wood-inhabiting fungal species of Peniophoraceae (Russulales, Basidiomycota) from the Yunnan-Guizhou Plateau, China. Journal of Fungi 8(11): 1227. https://doi.org/10.3390/jof8111227

MycoKeys 103: 129–165 (2024)
DOI: 10.3897/mycokeys.103.107935

Research Article

Rostrupomyces, a new genus to accommodate *Xerocomus sisongkhramensis*, and a new *Hemileccinum* species (Xerocomoideae, Boletaceae) from Thailand

Santhiti Vadthanarat[1,2], Bhavesh Raghoonundon[1], Saisamorn Lumyong[3,4,5], Olivier Raspé[1,6,7]

1 *School of Science, Mae Fah Luang University, Chiang Rai, 57100, Thailand*
2 *Department of Biological Science, Faculty of Science, Ubon Ratchathani University, Ubon Ratchathani, 34190, Thailand*
3 *Department of Biology, Faculty of Science, Chiang Mai University, Chiang Mai, 50200, Thailand*
4 *Research Center of Microbial Diversity and Sustainable Utilization, Faculty of Science, Chiang Mai University, Chiang Mai, 50200, Thailand*
5 *Academy of Science, The Royal Society of Thailand, Bangkok, Thailand*
6 *Meise Botanic Garden, Nieuwelaan 38, 1860 Meise, Belgium*
7 *Service Général de l'Enseignement Supérieur et de la Recherche Scientifique, Fédération Wallonie-Bruxelles, Brussels, Belgium*

Corresponding author: Olivier Raspé (olivier.ras@mfu.ac.th)

Abstract

A new genus, *Rostrupomyces* is established to accommodate *Xerocomus sisongkhramensis* based on multiple protein-coding genes (*atp*6, *cox*3, *tef*1, and *rpb*2) analyses of a wide taxon sampling of Boletaceae. In our phylogeny, the new genus was sister to *Rubinosporus* in subfamily Xerocomoideae, phylogenetically distant from *Xerocomus*, which was highly supported as sister to *Phylloporus* in the same subfamily Xerocomoideae. *Rostrupomyces* is different from other genera in Boletaceae by the following combination of characters: rugulose to subrugulose pileus surface, white pores when young becoming pale yellow in age, subscabrous stipe surface scattered with granulose squamules, white basal mycelium, unchanging color in any parts, yellowish brown spore print, and broadly ellipsoid to ellipsoid, smooth basidiospores. In addition, *Hemileccinum inferius*, also from subfamily Xerocomoideae, is newly described. Detailed descriptions and illustrations of the new genus and new species are presented.

Key words: *atp*6, Boletales, *cox*3, fungal diversity, multigene phylogeny, one new species, taxonomy, Tropical Asia

This article is part of:
Diversity, taxonomy, and systematics of macrofungi from tropical Asia
Edited by Olivier Raspé, Rui-Lin Zhao, Jennifer Luangsa-ard

Academic editor: Rui-Lin Zhao
Received: 13 June 2023
Accepted: 6 March 2024
Published: 28 March 2024

Citation: Vadthanarat S, Raghoonundon B, Lumyong S, Raspé O (2024) *Rostrupomyces*, a new genus to accommodate *Xerocomus sisongkhramensis*, and a new *Hemileccinum* species (Xerocomoideae, Boletaceae) from Thailand. MycoKeys 103: 129–165. https://doi.org/10.3897/mycokeys.103.107935

Introduction

Xerocomoideae Singer, which is one of the six subfamilies in Boletaceae Chevall, was established in 1945 with *Xerocomus* Quél. as the typus. At present, the subfamily consists of 12 genera, namely *Alessioporus* Gelardi, Vizzini & Simonini, *Amylotrama* Bloomfield, Davoodian, Trappe & T. Lebel, *Aureoboletus* Pouzar, *Boletellus* Murrill, *Heimioporus* E. Horak, *Hemileccinum* Šutara, *Hourangia* Xue T. Zhu & Zhu L. Yang, *Phylloporus* Quél., *Pulchroboletus* Gelardi, Vizzini & Simonini, *Rubinosporus* Vadthanarat, Raspé & Lumyong, *Veloboletus* Fechner &

Halling, and *Xerocomus* (Šutara 2008; Gelardi et al. 2014; Wu et al. 2014; Zhu et al. 2015; Wu et al. 2016; Crous et al. 2020; Lebel et al. 2022; Vadthanarat et al. 2022). The typical characters of species in this subfamily are boletoid or phylloporoid, rarely sequestrate basidiomata; dry or viscid pileus with smooth or subtomentose to tomentose pellis; absence or rarely presence of a veil; off-white, yellowish white, yellowish to yellow context; at least some basidiome parts often bluing, sometimes reddening or unchanging; smooth or ornamented stipe surface; hymenophore yellowish to yellow to bright yellow or cream to dull yellow to yellow to gray in sequestrate forms; basidiospores with bacillate, reticulate, tiny warts, pinholes, longitudinally striate, pitted ornamentations, or occasionally smooth; spore deposit with more or less olive-brown tint, rarely dark ruby (e. g. Gelardi et al. 2014; Wu et al. 2014; Zhu et al. 2015; Wu et al. 2016; Crous et al. 2020; Lebel et al. 2022; Vadthanarat et al. 2022).

Hemileccinum, one of the genera belonging to the Xerocomoideae, was established in 2008 to accommodate two *Boletus* species, namely *B. depilatus* Redeuilh and *B. impolitus* Fr. In 2012, a new genus named *Corneroboletus* N.K. Zeng & Zhu L. Yang was established to accommodate *Boletus indecorus* Massee (Zeng et al. 2012). However, *Corneroboletus* was later synonymized with *Hemileccinum* (Wu et al. 2016). *Hemileccinum* currently comprises 13 species worldwide, namely *H. albidum* Mei Xiang Li, Zhu L. Yang & G. Wu, *H. brevisporum* Mei Xiang Li, Zhu L. Yang & G. Wu, *H. brunneotomentosum* (B. Ortiz) Nitson & J.L. Frank, *H. depilatum* (Redeuilh) Šutara, *H. ferrugineipes* Mei Xiang Li, Zhu L. Yang & G. Wu, *H. floridanum* J.A. Bolin, A.E. Bessette, A.R. Bessette, L.V. Kudzma, A. Farid & J.L. Frank, *H. hortonii* (A.H. Sm. & Thiers) M. Kuo & B. Ortiz, *H. impolitum* (Fr.) Šutara (typus), *H. indecorum* (Massee) G. Wu & Zhu L. Yang, *H. parvum* Mei Xiang Li, Zhu L. Yang & G. Wu, *H. rubropunctum* (Peck) Halling & B. Ortiz, *H. rugosum* G. Wu & Zhu L. Yang, *H. subglabripes* (Peck) Halling (Index Fungorum, accessed on 23 March 2023). *Hemileccinum* species share the following combination of characters: boletoid basidiomata, glabrous to subtomentose, smooth to rugose pileus surface, which turns violet with NH_3 vapours; tubes depressed around the stipe apex, pores at first light yellow to deep yellow becoming olive-yellow in age, concolorous with tubes, unchanging; olive spore deposit; central stipe, whose surface is always ornamented with scales concolorous with stipe, unchanging; pale yellow to light yellow context, unchanging; pileipellis a trichodermium with broad hyphae or an epithelium, sometime with filamentous terminal elements; pleurocystidia present, fusoid to lageniform; spores boletoid, subfusoid or ellipsoid in face view, smooth under light microscope, irregularly tiny warted and pinholed or rarely smooth under SEM; clamp connections absent (Šutara 2008; Halling et al. 2015; Wu et al. 2016; Index Fungorum 443:1, 2020; Kuo and Ortiz-Santana 2020; Farid et al. 2021; Li et al. 2021).

The first study of poroid mushrooms from Thailand was published in 1902, with descriptions of five new species, namely *Boletus lacunosus* Rostr. [current name: *Austroboletus rostrupii* (Syd. & P. Syd.) E. Horak], *Boletus costatus* Rostr., *Suillus changensis* Rostr. [current name: *Boletus changensis* (Rostr.) Sacc. & D. Sacc.], *Suillus hygrophanus* Rostr. [current name: *Boletus hygrophanus* (Rostr.) Sacc. & D. Sacc.], and *Suillus velatus* Rostr. [current name: *Veloporphyrellus velatus* (Rostr.) Y.C. Li & Zhu L. Yang] (Rostrup 1902; Saccardo and Saccardo 1905;

Horak 1980; Li et al. 2014). At that time, they were classified to belong to the Polyporaceae; however, later they were all moved to family Boletaceae. No new taxa in Boletaceae were described from Thailand during the following one hundred years. It is only in 2006 that again a new species, *Rhodactina incarnata* Zhu L. Yang, Trappe & Lumyong, was described from Chiang Mai Province, northern Thailand (Yang et al. 2006). In 2009, *Spongiforma thailandica* Desjardin, Manfr. Binder, Roekring & Flegel was described as a new genus and species from Nakorn Nayok Province, central Thailand (Desjardin et al. 2009). After that, molecular phylogenetic analyses have been widely used in Boletaceae taxonomy. Two more new Boletaceae genera including *Cacaoporus* Raspé & Vadthanarat and *Rubinosporus* Vadthanarat, Raspé & Lumyong were described from Chiang Mai Province, northern Thailand (Vadthanarat et al. 2019b, 2022). During that period, twenty-seven new species were also described from the country, among which nine belong in subfamily Xerocomoideae, namely *Heimioporus subcostatus* Vadthanarat, Raspé & Lumyong, *Phylloporus castanopsidis* M.A. Neves & Halling, *P. dimorphus* M.A. Neves & Halling, *P. infuscatus* M.A. Neves & Halling, *Phylloporus pusillus* Raspé, K.D. Hyde & Chuankid, *P. rubiginosus* M.A. Neves & Halling, *P. subrubeolus* Chuankid, K.D. Hyde & Raspé, *Rubinosporus auriporus* Vadthanarat, Raspé & Lumyong, *Xerocomus sisongkhramensis* Khamsuntorn, Pinruan & Luangsa-ard (Neves et al. 2012; Halling et al. 2014; Raspé et al. 2016; Vadthanarat et al. 2018; Chuankid et al. 2019; Vadthanarat et al. 2019a, 2019b, 2020; Chuankid et al. 2021; Raghoonundon et al. 2021; Vadthanarat et al. 2021; Tan et al. 2022; Vadthanarat et al. 2022).

In this study, several collections of boletes belonging to the subfamily Xerocomoideae were obtained from northern and northeastern Thailand. They were carefully studied based on morphology as well as family-wide and subfamily-wide phylogenetic analyses. Some of them were identified as a new *Hemileccinum* species. Some collections were identified as *X. sisongkhramensis* based on morphological characters and the megablast result of the ITS region. However, following multiple gene phylogenetic analyses based on four protein-coding gene (*atp*6, *cox*3, *tef*1, and *rpb*2), *X. sisongkhramensis* appeared phylogenetically distant from other *Xerocomus* species and distinct from existing genera in Boletaceae. Moreover, the detailed morphology did not fit any known Xerocomoideae genus. Therefore, *Rostrupomyces* is introduced to accommodate *X. sisongkhramensis*. Finally, a new *Hemileccinum* species is introduced with full descriptions and illustrations.

Materials and methods

Specimens collecting

Fresh basidiomata of boletes in subfamily *Xerocomoideae* were collected in Chiang Mai and Chiang Rai provinces in northern Thailand, and Ubon Ratchathani and Sisaket provinces in northeastern Thailand between 2015 and 2021. They were photographed in the field and then wrapped in aluminum foil for later description in the laboratory on the same day. The specimens were then dried in an electric drier at 45–50 °C. Examined specimens were deposited at MFU, BKF or CMUB herbaria.

Morphological study

Macroscopic descriptions were made based on the detailed field notes and photos of fresh basidiomata. Color codes were given based on Kornerup and Wanscher (1978). Macrochemical reactions (color reactions) were observed using aqueous solutions of 10% potassium hydroxide (KOH), and 28–30% NH_4OH. Microscopic structures were observed from dried specimens rehydrated in 5% KOH or 1% ammoniacal Congo red. For the measurements of microscopic features, a minimum of 50 basidiospores or 20 for other structures, were randomly chosen and measured under a Nikon Eclipse Ni compound microscope using NIS-Elements D version 5.10 software. The notation '[x/y/z]' represents the number of basidiospores 'x' measured from the number of basidiomata 'y' of the number of collections 'z'. The measurements of microscopic structures are presented in the following format (a–) b–c–d (–e), in which 'c' represents the average, 'b' is the 5th percentile, 'd' is the 95th percentile, and 'a' and 'e' the extreme values, shown in parentheses. *Q* is the length/width ratio. Sections of the pileipellis were cut radially, perpendicularly to the surface halfway between the centre and margin of pileus. Sections of stipitipellis were taken halfway along the stipe length (Li et al. 2011; Hosen et al. 2013; Li et al. 2014; Zhu et al. 2015). All line drawings of microscopic features were drawn by free hand using an Olympus compound microscope model CX41 with Olympus Camera Lucida model U–DA. For scanning electron microscopy, small fragments of dried hymenophore were mounted directly onto a SEM stub with double-sided carbon tape. The samples were coated with gold, examined and photographed using a TESCAN MIRA's 4th generation SEM.

DNA extraction, PCR amplification and DNA sequencing

Genomic DNA was extracted from tissue of dried specimen or fresh tissue preserved in CTAB, using a CTAB isolation procedure adapted from Doyle and Doyle (1990). Portions of the genes *atp*6, *cox*3, *rpb*2, and *tef*1 were amplified by polymerase chain reaction (PCR). The primer pairs ATP6-1M40F/ATP6-2M (Raspé et al. 2016), COX3M1-F/ COX3M1-R (Vadthanarat et al. 2019b), bRPB2-6F/bRPB2-7.1R (Matheny 2005), and EF1-983F/EF1-2218R (Rehner and Buckley 2005) were used to amplify *atp*6, *cox*3, *rpb*2, and *tef*1, respectively. PCR products were purified by adding 1 U of exonuclease I and 0.5 U FastAP alkaline phosphatase (Thermo Scientific, St. Leon-Rot, Germany) and incubated at 37 °C for 1 h, followed by inactivation at 80 °C for 15 min. Standard Sanger sequencing was performed in both directions by Macrogen with PCR primers, except for *atp*6, for which universal primers M13F-pUC(-40) and M13F(-20) were used. For *tef*1, additional sequencing was performed with two internal primers, EF1-1577F and EF1-1567R (Rehner and Buckley 2005).

Alignment and phylogeny inference

The two reads of newly generated sequences were assembled in GENEIOUS Pro v. 6.0.6 (Biomatters) and blasted against GenBank database to check that they were not from unrelated contamination. For the Boletaceae-wide tree, the introns in *rpb*2 and *tef*1 were removed based on the amino acid sequence of

previously published sequences. The sequence datasets including the newly generated sequences and selected sequences representative of the whole family downloaded from GenBank, were separately aligned for each gene using MAFFT on the server accessed at http://mafft.cbrc.jp/alignment/server/ (Katoh and Standley 2013). Before combining the four gene partitions (*atp*6, *cox*3, *rpb*2 exons + *tef*1 exons), topological incongruence between the datasets was assessed using maximum likelihood (ML) on each of mitochondrial genes (*atp*6 + *cox*3) dataset and nuclear genes (*rpb*2 exons + *tef*1 exons) dataset. Paired trees were examined for conflicts involving only nodes with ML bootstrap (BS) ≥ 70%. After that, the Maximum likelihood phylogenetic inference was performed using RAxML (Stamatakis 2006) on the CIPRES web portal (RAxML-HPC2 on XSEDE; Miller et al. 2009). The phylogenetic tree was inferred by a single partitioned analysis with four character sets (one for each gene), using the GTRCAT model with 25 categories. The outgroup consisted of two *Buchwaldoboletus* and seven *Chalciporus* species from subfamily Chalciporoideae, based on previously published phylogenies. Statistical support of clades was obtained with 1,000 rapid bootstrap replicates. For Bayesian Inference (BI), the best-fit model of substitution among those implementable in MrBayes was estimated separately for each region using jModel-test (Darriba et al. 2012) on the CIPRES portal, based on the Bayesian Information Criterion (BIC). The selected models were HKY+I+G for *atp*6, GTR+I+G for *cox*3, K80+I+G for *rpb*2 exons, and SYM+I+G for *tef*1 exons. Partitioned Bayesian analysis was performed on the CIPRES web portal (MrBayes on XSEDE; Ronquist et al. 2012). Two runs of five chains were run for 15,000,000 generations and sampled every 1,000 generations. At the end of the run, the average deviation of split frequencies was 0.008563. The PSRF values were equal or greater than 1, and ESS values were greater than 200 for all parameters. A total of 11,252 trees were used to construct a 50% majority rule consensus tree and calculate the Bayesian posterior probabilities (BPPs).

A second, Xerocomoideae-wide tree, was also inferred from sequences of selected taxa in Xerocomoideae. Sequences were also separately aligned for each of the genes using the MAFFT online software, with introns included. Then, the topological incongruence between the datasets was also assessed using ML on each gene of five character sets, *atp*6, *cox*3, *rpb*2 exons, *tef*1 exons, and the three introns of *tef*1 + an intron of *rpb*2. Since there was no supported conflict, the ML phylogenetic tree was inferred by a single partitioned analysis with the five character sets (*atp*6, *cox*3, *rpb*2 exons, *tef*1 exons, and *rpb*2 intron + *tef*1 introns), using the same software and model that was used for family Boletaceae-wide phylogeny. Based on the latter, three *Hourangia*, three *Phylloporus*, and three *Xerocomus* species in the same subfamily Xerocomoideae were used as the outgroup. For BI, partitioned Bayesian analysis was performed with MrBayes 3.2.6 software for Windows. The selected models were GTR+I+G for *atp*6 and *cox*3, K80+I+G for *rpb*2 exons, and SYM+I+G for *tef*1 exons, HKY+I+G intron of *rpb*2 + introns of *tef*1. Two runs of five chains were sampled every 200 generations and stopped after 700,000 generations. At the end of the run, the average deviation of split frequencies was 0.007178. The PSRF values were equal or greater than 1, and ESS values were greater than 200 for all parameters. A total of 2,495 trees were used to construct a 50% majority rule consensus tree and calculate the BPPs.

Results

Phylogenetic analyses

A total of 39 sequences were newly generated in this study and deposited in GenBank. The ML phylograms from the mitochondrial and nuclear datasets were similar in topology without any supported conflict. The Boletaceae-wide, two-genome alignment contained 743 sequences comprising four genes (146 for *atp*6, 110 for *cox*3, 231 for *rpb*2, 256 for *tef*1) from 262 voucher specimens (Table 1) corresponding to 254 species, and was 2946 characters long (DOI: 10.6084/m9.figshare.23301077). ML and BI trees of the concatenated four-character set showed similar topologies without any supported conflicts (Bootstrap Support values, BS ≥ 70% and posterior probabilities, PP ≥ 0.90; Fig. 1). In the four-gene ML phylogram, the six subfamily clades were retrieved, namely the Austroboletoideae G. Wu & Zhu L. Yang, Boletoideae Singer, Chalciporoideae G. Wu & Zhu L. Yang, Leccinoideae G. Wu & Zhu L. Yang, Xerocomoideae, and Zangioideae G. Wu, Yan C. Li & Zhu L. Yang. The *Pulveroboletus* group introduced by Wu et al. (2014, 2016) was not monophyletic; however, the monophyly of each genus in this group was highly supported. All the *Xerocomus* (*Rostrupomyces*) *sisongkhramensis* collections included formed a highly supported (BS = 100%, PP = 1) monophyletic group, sister to *Rubinosporus* (BS = 99%, PP = 1) clustered in subfamily Xerocomoideae with high support (BS = 99%, PP = 1). The other selected *Xerocomus* species, including the type species *X. subtomentosus* (voucher VDKO 0987), formed another, distinct monophyletic group (BS = 89%, PP = 1), sister to *Phylloporus* (BS = 79%, PP = 1). The two genera also clustered in a supported clade together with *Hourangia* (BS = 100%, PP = 1). Regarding *Hemileccinum*, all selected species formed a highly supported clade (BS = 100%, PP = 1) consisting of fourteen species-level clades, including twelve known species, one new species from Thailand (this study), and one undescribed species from China. The new species *Hemileccinum inferius* clustered in a supported clade (BS = 76%, PP = 0.98) together with the American *H. hortonii*, the Chinese *H. rugosum*, and an undescribed *Hemileccinum* species from China (voucher HKAS53421).

Table 1. List of collections used for DNA analyses, with origin, GenBank accession numbers, and reference(s).

Species	Voucher	Origin	*atp*6	*cox*3	*rpb*2	*tef*1	Reference(s)
Afroboletus aff. *multijugus*	JD671	Burundi	MH614651	MH614794	MH614747	MH614700	Vadthanarat et al. (2019b)
Afroboletus costatisporus	ADK4644	Togo	KT823958	MH614795*	KT823991	KT824024	Raspé et al. (2016); Vadthanarat et al. (2019b)*
Afroboletus luteolus	ADK4844	Togo	MH614652	MH614796	MH614748	MH614701	Vadthanarat et al. (2019b)
Amoenoboletus granulopunctatus	HKAS 86007	China	–	–	MW560079	MZ741478	Wu et al. (2021)
Amoenoboletus granulopunctatus	HKAS 80250	China	–	–	MW560080	MW566746	Wu et al. (2021)
Amylotrama banrockensis	AD-C58672	Australia	–	–	–	MN413637	Lebel et al. (2022)
Amylotrama clelandii	MEL2432546	Australia	–	–	–	MN413630	Lebel et al. (2022)
Anthracoporus cystidiatus	HKAS55375	China	–	–	MT110410	KT990816*	Li and Yang (2021); Wu et al. (2016)*
Anthracoporus holophaeus	HKAS59407	China	–	–	KT990506	KT990888	Wu et al. (2016)
Anthracoporus nigropurpureus	HKAS52685	China	–	–	KT990459	KT990821	Wu et al. (2016)

Species	Voucher	Origin	*atp6*	*cox3*	*rpb2*	*tef1*	Reference(s)
Aureoboletus auriflammeus	CFMR:BOS-699	USA	–	–	MK766269	MK721060	Kuo and Ortiz-Santana (2020)
Aureoboletus catenarius	HKAS54467	China	–	–	KT990349	KT990711	Wu et al. (2016)
Aureoboletus duplicatoporus	HKAS50498	China	–	–	KF112754	KF112230	Wu et al. (2014)
Aureoboletus formosus	GDGM44441	China	–	–	KT291751	KT291744	Zhang et al. (2015)
Aureoboletus gentilis	ADK4865	Belgium	KT823961	MH614797*	KT823994	KT824027	Raspé et al. (2016); Vadthanarat et al. (2019b)*
Aureoboletus glutinosus	GDGM44477	China	–	–	MH700229	MH700205	Zhang et al. (2019)
Aureoboletus innixus	CFMR:BOS-544	USA	–	–	MK766270	MK721061	Kuo and Ortiz-Santana (2020)
Aureoboletus moravicus	VDKO1120	Belgium	MG212528	MH614798*	MG212615	MG212573	Vadthanarat et al. (2018); Vadthanarat et al. (2019b)*
Aureoboletus nephrosporus	HKAS74929	China	–	–	KT990358	KT990721	Wu et al. (2016)
Aureoboletus pseudoauriporus	JAB 80	USA	–	–	MW737471	MW737490	Farid et al. (2021)
Aureoboletus raphanaceus	GDGM 53127	China	–	–	MN549706	MN549676	Zhang et al. (2019)
Aureoboletus singeri	CFMR:BOS-468	Belize	–	–	MK766274	MK721065	Kuo and Ortiz-Santana (2020)
Aureoboletus tenuis	GDGM42601	China	–	–	KT291754	KT291745	Zhang et al. (2015)
Aureoboletus thibetanus	AFTOL-ID-450	China	DQ534600*	–	DQ366279	DQ029199	Binder and Hibbett (2006)*; Unpublished
Aureoboletus tomentosus	HKAS90216	China	–	–	KT990355	KT990717	Wu et al. (2016)
Aureoboletus viscidipes	HKAS77103	China	–	–	KT990360	KT990723	Wu et al. (2016)
Aureoboletus viscosus	OR0361	Thailand	MH614655	MH614801	MH614751	MH614704	Vadthanarat et al. (2019b)
Australopilus palumanus	REH-9433	Australia	–	–	MK766276	MK721067	Kuo and Ortiz-Santana (2020)
Austroboletus cf. *dictyotus*	OR0045	Thailand	KT823966	MH614802*	KT823999	KT824032	Raspé et al. (2016); Vadthanarat et al. (2019b)*
Austroboletus cf. *subvirens*	OR0573	Thailand	MH614656	MH614803	MH614752	MH614705	Vadthanarat et al. (2019b)
Austroboletus olivaceoglutinosus	HKAS57756	China	–	–	KF112764	KF112212	Wu et al. (2014)
Baorangia major	OR0209	Thailand	MG897421	MK372295*	MG897441	MG897431	Phookamsak et al. (2019); Vadthanarat et al. (2019b)*
Baorangia pseudocalopus	HKAS63607	China	–	–	KF112677	KF112167	Wu et al. (2014)
Baorangia rufomaculata	BOTH4144	USA	MG897415	MH614805*	MG897435	MG897425	Phookamsak et al. 2019; Vadthanarat et al. (2019b)*
Binderoboletus segoi	TWH8035	Guyana	**OP358290**	**OP358307**	–	–	**This study**
Boletellus aff. *ananas*	NY815459	Costa Rica	–	–	KF112760	KF112308	Wu et al. (2014)
Boletellus aff. *emodensis*	OR0061	Thailand	KT823970	MH614806*	KT824003	KT824036	Raspé et al. (2016); Vadthanarat et al. (2019b)*
Boletellus ananas	K(M)123769	Belize	MH614658	MH614807	MH614754	MH614707	Vadthanarat et al. (2019b)
Boletellus areolatus	TNS-F-61444 or BLT-7	Japan	–	AB989025	AB999754	–	Sata and Hattori (2015)
Boletellus aurocontextus	TNS-F-61501 or BLT-65	Japan	–	AB989037	AB999770	–	Sata and Hattori (2015)
Boletellus emodensis	TNS-F-61564 or BLT-128	Japan	–	AB989053	AB999782	–	Sata and Hattori (2015)
Boletus aereus	VDKO1055	Belgium	MG212530	MH614809*	MG212617	MG212575	Vadthanarat et al. (2018); Vadthanarat et al. (2019b)*
Boletus albobrunnescens	OR0131	Thailand	KT823973	MH614810*	KT824006	KT824039	Raspé et al. (2016); Vadthanarat et al. (2019b)*
Boletus botryoides	HKAS53403	China	–	–	KT990375	KT990738	Wu et al. (2016)
Boletus edulis	VDKO0869	Belgium	MG212531	MH614811*	MG212618	MG212576	Vadthanarat et al. (2018); Vadthanarat et al. (2019b)*
Boletus rubriceps	MICH:KUO-08150719	USA	–	–	MK766284	MK721076	Kuo and Ortiz-Santana (2020)
Borofutus dhakanus	OR0345	Thailand	MH614660	MH614814	MH614755	MH614709	Vadthanarat et al. (2019b)
Buchwaldoboletus lignicola	HKAS76674	China	–	–	KF112819	KF112277	Wu et al. (2014)
Buchwaldoboletus lignicola	VDKO1140	Belgium	MH614661	MH614815	MH614756	MH614710	Vadthanarat et al. (2019b)

Species	Voucher	Origin	*atp6*	*cox3*	*rpb2*	*tef1*	Reference(s)
Butyriboletus appendiculatus	VDKO0193b	Belgium	MG212537	MH614816*	MG212624	MG212582	Vadthanarat et al. (2018); Vadthanarat et al. (2019b)*
Butyriboletus cf. *roseoflavus*	OR0230	China	KT823974	MH614819*	KT824007	KT824040	Raspé et al. (2016); Vadthanarat et al. (2019b)*
Butyriboletus pseudoregius	VDKO0925	Belgium	MG212538	MH614817*	MG212625	MG212583	Vadthanarat et al. (2018); Vadthanarat et al. (2019b)*
Butyriboletus roseopurpureus	BOTH4497	USA	MG897418	MH614818*	MG897438	MG897428	Phookamsak et al. (2019); Vadthanarat et al. (2019b)*
Butyriboletus subsplendidus	HKAS50444	China	–	–	KT990379	KT990742	Wu et al. (2016)
Butyriboletus yicibus	HKAS55413	China	–	–	KF112674	KF112157	Wu et al. (2014)
Cacaoporus pallidicarneus	SV0221	Thailand	MK372262	MK372299	MK372286	MK372273	Vadthanarat et al. (2019b)
Cacaoporus tenebrosus	SV0223	Thailand	MK372266	MK372303	MK372290	MK372277	Vadthanarat et al. (2019b)
Caloboletus calopus	ADK4087	Belgium	MG212539	MH614820	KP055030	KJ184566	Vadthanarat et al. (2018); Zhao et al. (2014a); Zhao et al. (2014b); Vadthanarat et al. (2019b)
Caloboletus firmus	BOS-372	Belize	–	–	MK766288	MK721080	Kuo and Ortiz-Santana (2020)
Caloboletus inedulis	BOTH3963	USA	MG897414	MH614821*	MG897434	MG897424	Phookamsak et al. (2019); Vadthanarat et al. (2019b)*
Caloboletus radicans	VDKO1187	Belgium	MG212540	MH614822*	MG212626	MG212584	Vadthanarat et al. (2018); Vadthanarat et al. (2019b)*
Caloboletus yunnanensis	HKAS69214	China	–	–	KT990396	KJ184568	Zhao et al. (2014a); Wu et al. (2016)
Chalciporus aff. *piperatus*	OR0586	Thailand	KT823976	MH614824*	KT824009	KT824042	Raspé et al. (2016); Vadthanarat et al. (2019b)*
Chalciporus aff. *rubinus*	OR0139	China	MH614663	–	MH614758	MH614712	Vadthanarat et al. (2019b)
Chalciporus africanus	JD517	Cameroon	KT823963	MH614825*	KT823996	KT824029	Raspé et al. (2016); Vadthanarat et al. (2019b)*
Chalciporus piperatus	VDKO1063	Belgium	MH614664	MH614826	MH614759	MH614713	Vadthanarat et al. (2019b)
Chalciporus rubinus	AF2835	Belgium	KT823962	–	KT823995	KT824028	Raspé et al. (2016)
Chalciporus sp.	OR0363	Thailand	MH645586	MH645607	MH645602	MH645594	Vadthanarat et al. (2019b)
Chalciporus sp.	OR0373	Thailand	MH645587	MH645608	MH645603	MH645595	Vadthanarat et al. (2019b)
Chamonixia brevicolumna	DBG_F28707	USA	–	–	MK766291	MK721083	Kuo and Ortiz-Santana (2020)
Chamonixia caespitosa	OSC117571	USA	–	–	MK766293	MK721085	Kuo and Ortiz-Santana (2020)
Chiua virens	OR0266	China	MG212541	MH614828*	MG212627	MG212585	Vadthanarat et al. (2018); Vadthanarat et al. (2019b)*
Chiua viridula	HKAS74928	China	–	–	KF112794	KF112273	Wu et al. (2014)
Crocinoboletus cf. *laetissimus*	OR0576	Thailand	KT823975	MH614833*	KT824008	KT824041	Raspé et al. (2016); Vadthanarat et al. (2019b)*
Crocinoboletus rufoaureus	HKAS53424	China	–	–	KF112710	KF112206	Wu et al. (2014)
Cupreoboletus poikilochromus	GS10070	Italy	–	–	KT157068	KT157072	Gelardi et al. (2015)
Cyanoboletus brunneoruber	OR0233	China	MG212542	MH614834*	MG212628	MG212586	Vadthanarat et al. (2018); Vadthanarat et al. (2019b)*
Cyanoboletus pulverulentus	RW109	Belgium	KT823980	MH614835*	KT824013	KT824046	Raspé et al. (2016); Vadthanarat et al. (2019b)*
Cyanoboletus sinopulverulentus	HKAS59609	China	–	–	KF112700	KF112193	Wu et al. (2014)
Erythrophylloporus aurantiacus	REH7271	Costa Rica	MH614666	MH614829	MH614761	MH614715	Vadthanarat et al. (2019a)
Erythrophylloporus fagicola	Garay215	Mexico	MH614667	MH614830	MH614762	MH614716	Vadthanarat et al. (2019a)
Erythrophylloporus paucicarpus	OR1151	Thailand	MH614670	MH614831	MH614765	MH614719	Vadthanarat et al. (2019a)
Erythrophylloporus suthepensis	SV0236	Thailand	MH614672	MH614832	MH614767	MH614721	Vadthanarat et al. (2019a)
Fistulinella prunicolor	REH9880	Australia	MH614676	MH614840	MH614771	MH614725	Vadthanarat et al. (2019b)
Harrya chromapes	HKAS50527	China	–	–	KF112792	KF112270	Wu et al. (2014)
Harrya moniliformis	HKAS49627	China	–	–	KT990500	KT990881	Wu et al. (2016)
Heimioporus conicus	HKAS53451	China	–	–	KF112805	KF112226	Wu et al. (2016)

Species	Voucher	Origin	*atp6*	*cox3*	*rpb2*	*tef1*	Reference(s)
Heimioporus australis	REH9288	Australia	–	–	–	KP327703	Halling et al. (2015)
Heimioporus cooloolae	REH9817	Australia	–	–	–	KP327710	Halling et al. (2015)
Heimioporus fruticicola	REH8962	Australia	–	–	–	KP327696	Halling et al. (2015)
Heimioporus gaojiaocong	HKAS80582	China	–	–	KT990409	KT990770	Wu et al. (2016)
Heimioporus ivoryi	REH8620	Costa Rica	–	–	–	KP327683	Halling et al. (2015)
Heimioporus japonicus	OR0114	Thailand	KT823971	–	KT824004	KT824037	Raspé et al. (2016)
Heimioporus japonicus	SV0016	Thailand	MT136776	–	MT136766	MT136771	Vadthanarat et al. (2020)
Heimioporus mandarinus	OR0218	Thailand	MG212546	–	MG212632	MG212590	Vadthanarat et al. (2018)
Heimioporus subcostatus	SV0235	Thailand	MT136780	–	MT136770	MT136775	Vadthanarat et al. (2020)
Hemileccinum albidum	KUN-HKAS81120	China	–	–	MZ936320	MZ936352	Li et. al. (2021)
Hemileccinum inferius	BR0260	Thailand	**OP358291**	–	**OP358312**	**OP358319**	**This study**
Hemileccinum inferius	SV0282	Thailand	**OP358292**	–	–	–	**This study**
Hemileccinum brevisporum	KUN-HKAS89150	China	–	–	MZ936328	MZ936362	Li et. al. (2021)
Hemileccinum brevisporum	HKAS59445	China	–	–	KT990414	KT990775	Wu et al. (2016)
Hemileccinum depilatum	AF2845	Belgium	MG212547	MH614843*	MG212633	MG212591	Vadthanarat et al. (2018); Vadthanarat et al. (2019b)*
Hemileccinum ferrugineipes	KUN-HKAS115554	China	–	–	MZ936330	MZ973011	Li et. al. (2021)
Hemileccinum floridanum	AB16	USA	–	–	–	MW737481	Farid et al. (2021)
Hemileccinum hortonii	MICH:KUO-07050706	USA	–	–	MK766377	MK721175	Kuo and Ortiz-Santana (2020)
Hemileccinum impolitum	ADK4078	Belgium	MG212548	MH614844*	MG212634	MG212592	Vadthanarat et al. (2018); Vadthanarat et al. (2019b)*
Hemileccinum indecorum	OR0863	Thailand	MH614677	MH614845	MH614772	MH614726	Vadthanarat et al. (2019b)
Hemileccinum parvum	KUN-HKAS115553	China	–	–	MZ936333	MZ973010	Li et. al. (2021)
Hemileccinum rubropunctum	REH-8501	USA	–	–	MK766327	MK721122	Kuo and Ortiz-Santana (2020)
Hemileccinum rugosum	HKAS84355	China	–	–	KT990413	KT990774	Wu et al. (2016)
Hemileccinum sp.	HKAS53421	China	–	–	KF112751	KF112235	Wu et al. (2014)
Hemileccinum subglabripes	MICH:KUO-07230802	USA	–	–	MK766300	MK721092	Kuo and Ortiz-Santana (2020)
Hortiboletus amygdalinus	HKAS54166	China	–	–	KT990416	KT990777	Wu et al. (2016)
Hortiboletus campestris	MICH:KUO-08240502	USA	–	–	MK766302	MK721094	Kuo and Ortiz-Santana (2020)
Hortiboletus rubellus	VDKO0403	Belgium	MH614679	MH614847	MH614774	–	Vadthanarat et al. (2019b)
Hortiboletus subpaludosus	HKAS59608	China	–	–	KF112696	KF112185	Wu et al. (2014)
Hourangia cf. *pumila*	OR0762	Thailand	MH614680	MH614848	MH614775	MH614728	Vadthanarat et al. (2019b)
Hourangia cheoi	HKAS52269	China	–	–	KF112773	KF112286	Zhu et al. (2015)
Hourangia microcarpa	HKAS53378	China	–	–	KF112775	KF112300	Wu et al. (2014)
Hourangia nigropunctata	HKAS 57427	China	–	–	KP136978	KP136927	Zhu et al. (2015)
Hymenoboletus luteopurpureus	HKAS46334	China	–	–	KF112795	KF112271	Wu et al. (2014)
Imleria badia	VDKO0709	Belgium	KT823983	MH614849*	KT824016	KT824049	Raspé et al. (2016); Vadthanarat et al. (2019b)*
Imleria obscurebrunnea	OR0263	China	MH614681	MH614850	MH614776	MH614729	Vadthanarat et al. (2019b)
Imleria pallidus	BOTH4356	USA	MH614659	MH614812	–	MH614708	Vadthanarat et al. (2019b)
Indoporus squamulosus	HKAS107153	China	–	–	MT110409	MT110335	Li and Yang (2021)
Ionosporus longipes	LEE1180	Malaysia	MT085461	–	MH712031*	MT085471	Chuankid et al. (2021); Khmelnitsky et al. (2019)
Kaziboletus rufescens	HKAS74706	Bangladesh	–	–	JQ928600	JQ928578	Hosen et al. (2021)

Species	Voucher	Origin	*atp6*	*cox3*	*rpb2*	*tef1*	Reference(s)
Lanmaoa angustispora	HKAS74752	China	–	–	KM605177	KM605154	Wu et al. (2015)
Lanmaoa asiatica	OR0228	China	MH614682	MH614851	MH614777	MH614730	Vadthanarat et al. (2019b)
Lanmaoa carminipes	BOTH4591	USA	MG897419	MH614852*	MG897439	MG897429	Phookamsak et al. (2019); Vadthanarat et al. (2019b)*
Lanmaoa pallidorosea	BOTH4432	USA	MG897417	MH614853*	MG897437	MG897427	Phookamsak et al. (2019); Vadthanarat et al. (2019b)*
Lanmaoa sublurida	Farid 1023	USA	–	–	MW737460	MW737485	Farid et al. (2021)
Leccinellum aff. *crocipodium*	HKAS76658	China	–	–	KF112728	KF112252	Wu et al. (2014)
Leccinellum aff. *griseum*	KPM-NC-0017832	Japan	KC552164	–	–	JN378450*	Unpublished; Orihara et al. (2012)*
Leccinellum cremeum	HKAS90639	China	–	–	KT990420	KT990781	Wu et al. (2016)
Leccinum scabrum	VDKO0938	Belgium	MG212549	MH614858*	MG212635	MG212593	Vadthanarat et al. (2018); Vadthanarat et al. (2019b)*
Leccinum schistophilum	VDKO1128	Belgium	KT823989	MH614859*	KT824022	KT824055	Raspé et al. (2016); Vadthanarat et al. (2019b)*
Leccinum variicolor	VDKO0844	Belgium	MG212550	MH614860*	MG212636	MG212594	Vadthanarat et al. (2018); Vadthanarat et al. (2019b)*
Leccinum versipelle	KPM-NC-0017833	Scotland	KC552172	–	–	JN378454	Orihara et al. (2016); Orihara et al. (2012)
Leccinum vulpinum	KPM-NC-0017834	Scotland	KC552171	–	–	JN378456	Orihara et al. (2016); Orihara et al. (2012)
Mucilopilus castaneiceps	HKAS75045	China	–	–	KF112735	KF112211	Wu et al. (2014)
Mucilopilus paracastaneiceps	HKAS50338	China	–	–	KT990391	KT990755	Wu et al. (2016)
Mucilopilus ruber	HKAS84555	China	–	–	MT110436	MT110364	Li and Yang (2021)
Mycoamaranthus cambodgensis	SV0197	Thailand	MZ355900	MZ355909	–	–	Vadthanarat et al. (2022)
Neoboletus brunneissimus	OR0249	China	MG212551	MH614861*	MG212637	MG212595	Vadthanarat et al. (2018); Vadthanarat et al. (2019b)*
Neoboletus ferrugineus	HKAS77718	China	–	–	KT990431	KT990789	Wu et al. (2016)
Neoboletus flavidus	HKAS59443	China	–	–	KU974144	KU974136	Wu et al. (2016)
Neoboletus hainanensis	HKAS59469	China	–	–	KF112669	KF112175	Wu et al. (2014)
Neoboletus junquilleus	AF2922	France	MG212552	MH614862*	MG212638	MG212596	Vadthanarat et al. (2018); Vadthanarat et al. (2019b)*
Neoboletus magnificus	HKAS74939	China	–	–	KF112653	KF112148	Wu et al. (2014)
Neoboletus obscureumbrinus	OR0553	Thailand	MK372271	–	MK372294	MK372282	Vadthanarat et al. (2019b)
Neoboletus tomentulosus	HKAS53369	China	–	–	KF112659	KF112154	Wu et al. (2014)
Neoboletus erythropus	VDKO0690	Belgium	KT823982	MH614864*	KT824015	KT824048	Raspé et al. (2016); Vadthanarat et al. (2019b)*
Octaviania asterosperma	AQUI3899	Italy	KC552159	–	–	KC552093	Orihara et al. (2016)
Octaviania cyanescens	PNW-FUNGI-5603	USA	KC552160	–	–	JN378438	Orihara et al. (2016); Orihara et al. (2012)
Octaviania tasmanica	MEL2128484	Australia	KC552157	–	–	JN378437	Orihara et al. (2016); Orihara et al. (2012)
Octaviania zelleri	MES270	USA	KC552161	–	–	JN378440	Orihara et al. (2016); Orihara et al. (2012)
Parvixerocomus pseudoaokii	OR0155	China	MG212553	MH614865	MG212597	MG212597	Vadthanarat et al. (2019b)
Paxilloboletus latisporus	ADK5072	Congo	–	–	MZ707870	MZ707866	Badou et al. (2022)
Paxilloboletus africanus	SAB0716	Guinea	–	–	MZ707869	MZ707865	Badou et al. (2022)
Phylloporus bellus	OR0473	China	MH580778	MH614866*	MH580818	MH580798	Chuankid et al. (2019); Vadthanarat et al. (2019b)*
Phylloporus brunneiceps	OR0050	Thailand	KT823968	MH614867*	KT824001	KT824034	Raspé et al. (2016); Vadthanarat et al. (2019b)*
Phylloporus castanopsidis	OR0052	Thailand	KT823969	MH614868*	KT824002	KT824035	Raspé et al. (2016); Vadthanarat et al. (2019b)*
Phylloporus maculatus	OR0285	China	MH580780	–	MH580820	MH580800	Chuankid et al. (2019)

Species	Voucher	Origin	*atp6*	*cox3*	*rpb2*	*tef1*	Reference(s)
Phylloporus pachycystidiatus	HKAS53422	China	–	–	KF112777	KF112288	Wu et al. (2014)
Phylloporus pelletieri	WU18746	Austria	MH580781	MH614869*	MH580821	MH580801	Chuankid et al. (2019); Vadthanarat et al. (2019b)*
Phylloporus pusillus	OR1158	Thailand	MH580783	MH614870*	MH580823	MH580803	Chuankid et al. (2019); Vadthanarat et al. (2019b)*
Phylloporus rhodoxanthus	WU17978	Austria	MH580785	MH614871*	MH580824	MH580805	Chuankid et al. (2019); Vadthanarat et al. (2019b)*
Phylloporus rubeolus	OR0251	China	MH580786	MH614872*	MH580825	MH580806	Chuankid et al. (2019); Vadthanarat et al. (2019b)*
Phylloporus rubiginosus	OR0169	China	MH580788	MH614873*	MH580827	MH580808	Chuankid et al. (2019); Vadthanarat et al. (2019b)*
Phylloporus rubrosquamosus	HKAS52552	China	–	–	KF112780	KF112289	Wu et al. (2014)
Phylloporus scabripes	CFMR:BOS-621	Belize	–	–	MK766359	MK721156	Kuo and Ortiz-Santana (2020)
Phylloporus subbacillisporus	OR0436	China	MH580792	MH614875*	MH580831	MH580812	Chuankid et al. (2019); Vadthanarat et al. (2019b)*
Phylloporus subrubeolus	BC022	Thailand	MH580793	MH614876*	MH580832	MH580813	Chuankid et al. (2019); Vadthanarat et al. (2019b)*
Phylloporus yunnanensis	OR0448	China	MG212554	MH614877*	MG212640	MG212598	Vadthanarat et al. (2018); Vadthanarat et al. (2019b)*
Porphyrellus castaneus	OR0241	China	MG212555	MH614878*	MG212641	MG212599	Vadthanarat et al. (2018); Vadthanarat et al. (2019b)*
Porphyrellus porphyrosporus	MB97 023	Germany	DQ534609	–	GU187800	GU187734	Binder and Hibbett (2006); Binder et al. (2010)
Pseudoaustroboletus valens	HKAS82644	China	–	–	MT110431	MT110359	Li and Yang (2021)
Pulchroboletus sclerotiorum	FLAS F 60333	USA	–	–	MF614169	MF614167	Crous et al. (2019)
Pulchroboletus sclerotiorum	FLAS F 60334	USA	–	–	MF614164	MF614165	Crous et al. (2019)
Pulveroboletus aff. *ravenelii*	ADK4360	Togo	KT823957	MH614882*	KT823990	KT824023	Raspé et al. (2016); Vadthanarat et al. (2019b)*
Pulveroboletus aff. *ravenelii*	ADK4650	Togo	KT823959	MH614883*	KT823992	KT824025	Raspé et al. (2016); Vadthanarat et al. (2019b)*
Pulveroboletus brunneopunctatus	HKAS55369	China	–	–	KT990455	KT990814	Wu et al. (2016)
Pulveroboletus fragrans	OR0673	Thailand	KT823977	MH614884*	KT824010	KT824043	Raspé et al. (2016); Vadthanarat et al. (2019b)*
Pulveroboletus ravenelii	REH2565	USA	KU665635	MH614885*	KU665637	KU665636	Raspé et al. (2016); Vadthanarat et al. (2019b)*
Retiboletus aff. *nigerrimus*	OR0049	Thailand	KT823967	MH614886*	KT824000	KT824033	Raspé et al. (2016); Vadthanarat et al. (2019b)*
Retiboletus brevibasidiatus	OR0570	Thailand	MT085469	–	MT085479	MT085476	Chuankid et al. (2021)
Retiboletus brunneolus	HKAS52680	China	–	–	KF112690	KF112179	Wu et al. (2014)
Retiboletus fuscus	OR0231	China	MG212556	MH614887*	MG212642	MG212600	Vadthanarat et al. (2018); Vadthanarat et al. (2019b)*
Retiboletus griseus	MB03 079	USA	KT823964	MH614888*	KT823997	KT824030	Raspé et al. (2016); Vadthanarat et al. (2019b)*
Retiboletus kauffmanii	OR0278	China	MG212557	MH614889*	MG212643	MG212601	Vadthanarat et al. (2018); Vadthanarat et al. (2019b)*
Retiboletus nigerrimus	HKAS53418	China	–	–	KT990462	KT990824	Wu et al. (2016)
Rhodactina himalayensis	CMU25117	Thailand	MG212558	–	–	MG212602, MG212603	Vadthanarat et al. (2018)
Rhodactina rostratispora	SV0170	Thailand	MG212560	–	MG212645	MG212605	Vadthanarat et al. (2018)
Rossbeevera cryptocyanea	KPM-NC17843	Japan	KT581441	–	–	KC552072	Orihara et al. (2016)
Rossbeevera eucyanea	TNS-F-36986	Japan	KC552115	–	–	KC552068	Orihara et al. (2016)
Rossbeevera griseovelutina	TNS-F-36989	Japan	KC552124	–	–	KC552076	Orihara et al. (2016)
Rossbeevera pachydermis	KPM-NC23336	New Zealand	KJ001064	–	–	KP222912	Orihara et al. (2016)
Rossbeevera vittatispora	TO-AUS-72	Australia	KC552108	–	–	KC552065	Orihara et al. (2016)

Species	Voucher	Origin	*atp6*	*cox3*	*rpb2*	*tef1*	Reference(s)
Rostrupomyces sisongkhramensis	BR0311	Thailand	**OP358293**	–	**OP358313**	**OP358320**	**This study**
Rostrupomyces sisongkhramensis	BR0313	Thailand	**OP358294**	–	**OP358314**	**OP358321**	**This study**
Rostrupomyces sisongkhramensis	BR0368	Thailand	**OP358295**	–	–	–	**This study**
Rostrupomyces sisongkhramensis	BR0371	Thailand	**OP358296**	–	–	**OP358322**	**This study**
Rostrupomyces sisongkhramensis	OR0915	Thailand	**OP358297**	–	–	–	**This study**
Rostrupomyces sisongkhramensis	OR0918	Thailand	**OP358298**	–	–	–	**This study**
Rostrupomyces sisongkhramensis	OR0919	Thailand	**OP358299**	**OP358308**	**OP358315**	**OP358323**	**This study**
Rostrupomyces sisongkhramensis	OR1004	Thailand	**OP358300**	–	–	–	**This study**
Rostrupomyces sisongkhramensis	OR1059	Thailand	**OP358301**	–	–	–	**This study**
Rostrupomyces sisongkhramensis	OR1392	Thailand	**OP358302**	–	–	–	**This study**
Rostrupomyces sisongkhramensis	OR1399	Thailand	**OP358303**	–	–	–	**This study**
Rostrupomyces sisongkhramensis	SV0155	Thailand	**OP358304**	**OP358309**	**OP358316**	**OP358324**	**This study**
Rostrupomyces sisongkhramensis	SV0219	Thailand	**OP358305**	**OP358310**	**OP358317**	**OP358325**	**This study**
Rostrupomyces sisongkhramensis	SV0225	Thailand	**OP358306**	**OP358311**	**OP358318**	**OP358326**	**This study**
Royoungia rubina	HKAS53379	China	–	–	KF112796	KF112274	Wu et al. (2014)
Rubinosporus auriporus	SV0101	Thailand	MZ355897	MZ355906	MZ355904	MZ355902	Vadthanarat et al. (2022)
Rubinosporus auriporus	SV0090	Thailand	MZ355896	MZ355905	MZ355903	MZ355901	Vadthanarat et al. (2022)
Rubroboletus legaliae	VDKO0936	Belgium	KT823985	MH614890*	KT824018	KT824051	Raspé et al. (2016); Vadthanarat et al. (2019b)*
Rubroboletus rhodosanguineus	BOTH4263	USA	MG897416	MH614891*	MG897436	MG897426	Phookamsak et al. (2019); Vadthanarat et al. (2019b)*
Rubroboletus rhodoxanthus	HKAS84879	China	–	–	KT990468	KT990831	Wu et al. (2016)
Rubroboletus satanas	VDKO0968	Belgium	KT823986	MH614892*	KT824019	KT824052	Raspé et al. (2016); Vadthanarat et al. (2019b)*
Rugiboletus andinus	REH-7705	Costa Rica	–	–	MK766316	MK721111	Kuo and Ortiz-Santana (2020)
Rugiboletus brunneiporus	HKAS83209	China	–	–	KM605168	KM605144	Wu et al. (2015)
Rugiboletus extremiorientalis	OR0406	Thailand	MG212562	MH614893*	MG212647	MG212607	Vadthanarat et al. (2018); Vadthanarat et al. (2019b)*
Singerocomus inundabilis	TWH9199	Guyana	MH645588	MH645609	LC043089*	MH645596	Henkel et al. (2016)*; Vadthanarat et al. (2019b)
Singerocomus rubriflavus	TWH9585	Guyana	MH645589	MH645610	–	MH645597	Vadthanarat et al. (2019b)
Spongiforma thailandica	DED7873	Thailand	MG212563	MH614894**	MG212648	KF030436*	Nuhn et al. (2013)*; Vadthanarat et al. (2018); Vadthanarat et al. (2019b)**
Spongispora temasekensis	SING 0206334	Singapore	–	–	MG674378	MG674377	Wu et al. (2018)
Spongispora temasekensis	ACMF5	Singapore	MZ803018	–	MZ824748	MZ803023	Raghoonundon et al. (2021)
Strobilomyces atrosquamosus	HKAS55368	China	–	–	KT990476	KT990839	Wu et al. (2016)
Strobilomyces echinocephalus	OR0243	China	MG212564	–	MG212649	MG212608	Vadthanarat et al. (2018)
Strobilomyces floccopus	RW103	Belgium	KT823978	MH614895*	KT824011	KT824044	Raspé et al. (2016); Vadthanarat et al. (2019b)*
Strobilomyces mirandus	OR0115	Thailand	KT823972	MH614896*	KT824005	KT824038	Raspé et al. (2016); Vadthanarat et al. (2019b)*
Strobilomyces verruculosus	HKAS55389	China	–	–	KF112813	KF112259	Wu et al. (2014)
Suillellus luridus	VDKO0241b	Belgium	KT823981	MH614901*	KT824014	KT824047	Raspé et al. (2016); Vadthanarat et al. (2019b)*
Suillellus queletii	VDKO1185	Belgium	MH645590	MH645611	MH645604	MH645598	Vadthanarat et al. (2019b)

Species	Voucher	Origin	*atp6*	*cox3*	*rpb2*	*tef1*	Reference(s)
Suillellus subamygdalinus	HKAS57262	China	–	–	KF112660	KF112174	Wu et al. (2014)
Sutorius australiensis	REH9441	Australia	MG212567	MK386576**	MG212652	JQ327032*	Halling et al. (2012)*; Vadthanarat et al. (2018); Vadthanarat et al. (2019b)**
Sutorius eximius	REH9400	USA	MG212568	MH614902**	MG212653	JQ327029*	Halling et al. (2012)*; Vadthanarat et al. (2018); Vadthanarat et al. (2019b)**
Sutorius pachypus	OR0411	Thailand	MN067465	–	MN067500	MN067484	Vadthanarat et al. (2021)
Sutorius pseudotylopilus	OR0378B	Thailand	MH614692	MH614903	MH614787	MH614740	Vadthanarat et al. (2019b)
Sutorius rubinus	OR0379	Thailand	MH614693	MH614904	MH614788	MH614741	Vadthanarat et al. (2019b)
Sutorius ubonensis	SV0032	Thailand	MN067472	–	MN067507	MN067491	Vadthanarat et al. (2021)
Tengioboletus glutinosus	HKAS53425	China	–	–	KF112800	KF112204	Wu et al. (2014)
Tengioboletus reticulatus	HKAS53426	China	–	–	KF112828	KF112313	Wu et al. (2014)
Turmalinea persicina	KPM-NC18001	Japan	KC552130	–	–	KC552082	Orihara et al. (2016)
Turmalinea yuwanensis	KPM-NC18011	Japan	KC552138	–	–	KC552089	Orihara et al. (2016)
Tylocinum griseolum	HKAS50281	China	–	–	KF112730	KF112284	Wu et al. (2014)
Tylopilus atripurpureus	HKAS50208	China	–	–	KF112799	KF112283	Wu et al. (2014)
Tylopilus felleus	VDKO0992	Belgium	KT823987	MH614906*	KT824020	KT824053	Raspé et al. (2016); Vadthanarat et al. (2019b)*
Tylopilus ferrugineus	BOTH3639	USA	MH614694	MH614907	MH614789	MH614742	Vadthanarat et al. (2019b)
Tylopilus otsuensis	HKAS53401	China	–	–	KF112797	KF112224	Wu et al. (2014)
Tylopilus vinaceipallidus	OR0137	China	MG212571	MH614912*	MG212656	MG212613	Vadthanarat et al. (2018); Vadthanarat et al. (2019b)*
Tylopilus violaceobrunneus	HKAS89443	China	–	–	KT990504	KT990886	Wu et al. (2016)
Veloboletus limbatus	REH9228	Australia	MT747398	–	MT747397	MN413636	Crous et al. (2019)
Veloporphyrellus conicus	REH8510	Belize	MH614698	MH614913	MH614792	MH614745	Vadthanarat et al. (2019b)
Veloporphyrellus gracilioides	HKAS53590	China	–	–	KF112734	KF112210	Wu et al. (2014)
Veloporphyrellus pseudovelatus	HKAS59444	China	JX984519	–	–	JX984553	Li et al. (2014)
Veloporphyrellus velatus	HKAS63668	China	JX984523	–	–	JX984554	Li et al. (2014)
Xanthoconium affine	NY00815399	USA	–	–	KT990486	KT990850	Wu et al. (2016)
Xanthoconium purpureum	MICH:KUO-07061405	USA	–	–	MK766372	MK721170	Kuo and Ortiz-Santana (2020)
Xanthoconium sinense	HKAS77651	China	–	–	KT990488	KT990853	Wu et al. (2016)
Xerocomellus chrysenteron	VDKO0821	Belgium	KT823984	MH614914*	KT824017	KT824050	Raspé et al. (2016); Vadthanarat et al. (2019b)*
Xerocomellus cisalpinus	ADK4864	Belgium	KT823960	MH614915*	KT823993	KT824026	Raspé et al. (2016); Vadthanarat et al. (2019b)*
Xerocomellus communis	HKAS50467	China	–	–	KT990494	KT990858	Wu et al. (2016)
Xerocomellus riparielus	VDKO0404	Belgium	MH614699	MH614916	MH614793	MH614746	Vadthanarat et al. (2019b)
Xerocomus ferrugineus	CFMR:BOS-545	USA	–	–	MK766375	MK721173	Kuo and Ortiz-Santana (2020)
Xerocomus fulvipes	HKAS76666	China	–	–	KF112789	KF112292	Wu et al. (2014)
Xerocomus magniporus	HKAS58000	China	–	–	KF112781	KF112293	Wu et al. (2014)
Xerocomus rugosellus	HKAS58865	China	–	–	KF112784	KF112294	Wu et al. (2014)
Xerocomus spadiceus var. *gracilis*	MICH:KUO-07080702	USA	–	–	MK766378	MK721176	Kuo and Ortiz-Santana (2020)
Xerocomus subtomentosus	VDKO0987	Belgium	MG212572	MH614919*	MG212657	MG212614	Vadthanarat et al. (2018); Vadthanarat et al. (2019b)*
Xerocomus tenax	MICH:KUO-08241404	USA	–	–	MK766379	MK721177	Kuo and Ortiz-Santana (2020)
Zangia citrina	HKAS52684	China	HQ326850	–	–	HQ326872	Li et al. (2011)
Zangia olivaceobrunnea	HKAS52272	China	HQ326857	–	–	HQ326876	Li et al. (2011)
Zangia roseola	HKAS51137	China	HQ326858	–	–	HQ326877	Li et al. (2011)

For the subfamily Xerocomoideae-wide phylogeny, no supported topological incongruence between the character sets was detected. Then, the Xerocomoideae-wide phylogeny was inferred based on the alignment containing 155 sequences of four genes (22 for *atp*6, 20 for *cox*3, 53 for *rpb*2, 60 for *tef*1) from 60 voucher specimens corresponding to 55 taxa, and was 3,161 characters long (DOI: 10.6084/m9.figshare.23301077). The ML and BI tree topologies

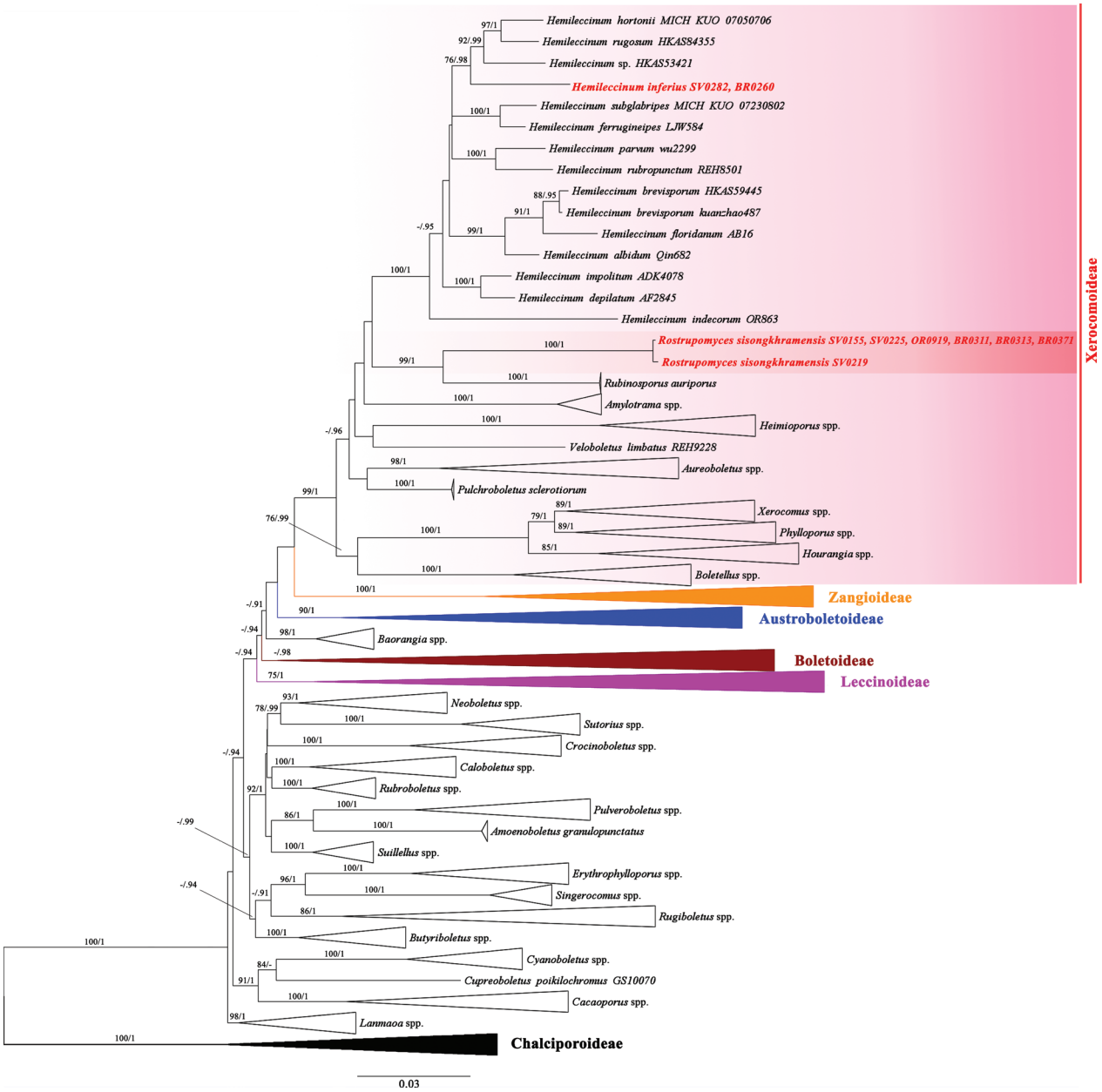

Figure 1. Boletaceae-wide Maximum Likelihood phylogenetic tree inferred from the four-gene dataset (*atp*6, *cox*3, *rpb*2, and *tef*1) (introns excluded), showing the position of the new genus *Rostrupomyces* in Xerocomoideae. Bootstrap support values (BS ≥ 70%) and the corresponding Bayesian posterior probabilities (PP ≥ 0.90) are shown above the supported branches. The two *Buchwaldoboletus* and seven *Chalciporus* species (subfamily Chalciporoideae) were used as outgroup. All taxa belonging to subfamilies Austroboletoideae, Boletoideae, Chalciporoideae, Leccinoideae, and Zangioideae were collapsed into subfamily clades. All generic clades in subfamily Xerocomoideae (excluding *Hemileccinum* and *Rostrupomyces*) and *Pulveroboletus* group with high supports, were also collapsed.

of the concatenated five-character-set alignment were similar without any supported conflict (Fig. 2). The Xerocomoideae-wide ML tree also showed a similar topology to the Boletaceae-wide tree. However, in this subfamily Xerocomoideae-wide tree, the support of the clade consisting of the new species *Hemileccinum inferius*, *H. hortonii*, *H. rugosum*, and an undescribed *Hemileccinum* species, was lower (BS = 53%, PP = 0.71) than in the Boletaceae-wide ML tree.

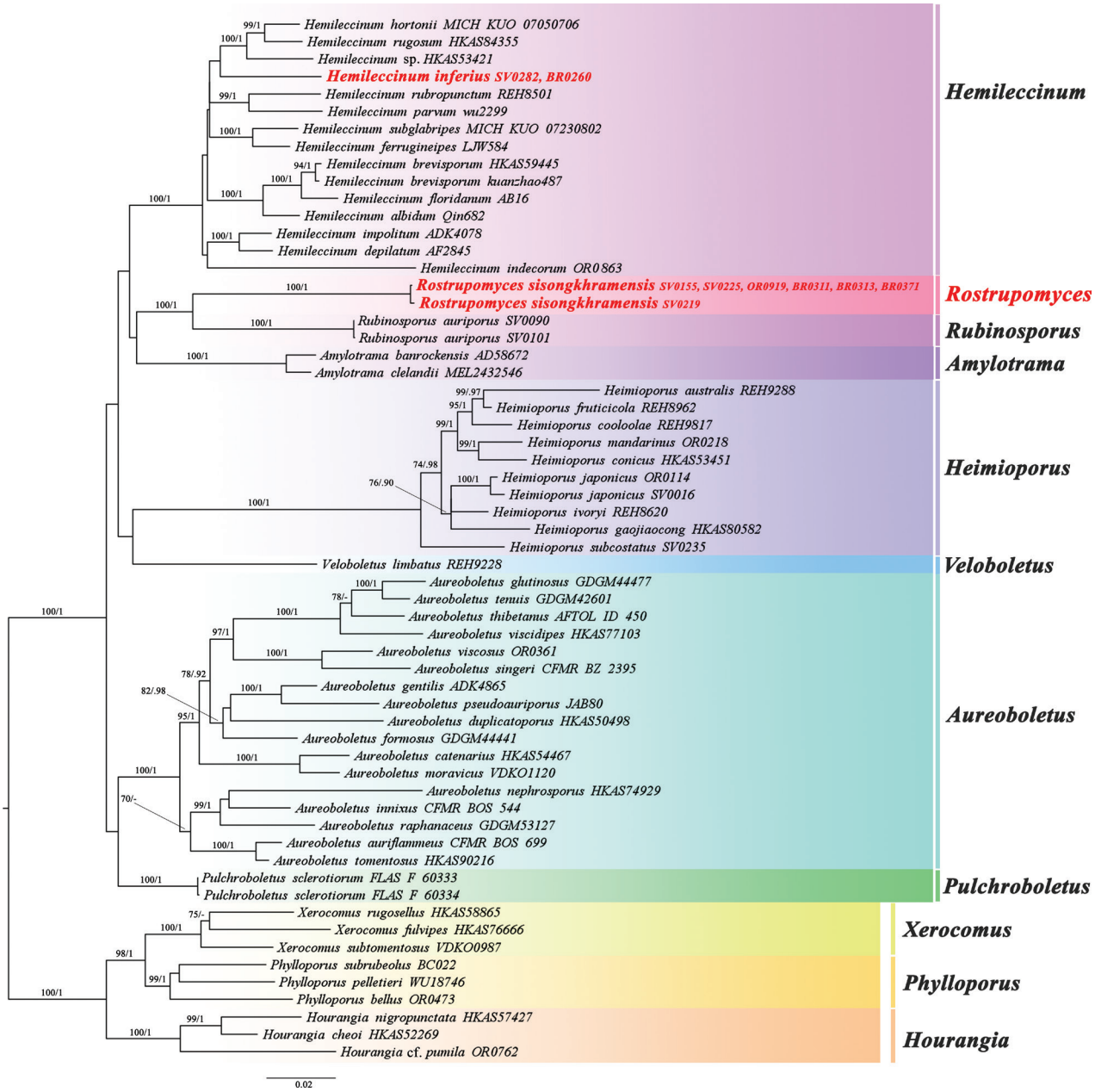

Figure 2. Xerocomoideae-wide phylogenetic tree inferred from the four-gene dataset (*atp*6, *cox*3, *rpb*2, and *tef*1) (introns included), including new genus *Rostrupomyces* and selected Xerocomoideae using Maximum Likelihood and Bayesian Inference methods (ML tree is presented). The three *Hourangia*, three *Phylloporus*, and three *Xerocomus* species in Xerocomoideae were used as outgroup. Bootstrap support values (BS ≥ 70%) and posterior probabilities (PP ≥ 0.90) are shown above the supported branches.

Taxonomy

***Rostrupomyces* Vadthanarat & Raspé, gen. nov.**
MycoBank No: 849050

Etymology. Named in honor of Frederik Georg Emil Rostrup (1831–1907), Danish botanist, mycologist, and plant pathologist, celebrating the 120 years of his describing the first new species of Boletaceae from Thailand in 1902.

Diagnosis. Differs from other genera in Boletaceae by the following combination of characters: rugulose to subrugulose pileus surface, white pore when young becoming grayish yellow in age, subscabrous stipe surface with scattered granulose squamules, white basal mycelium, unchanging color in any parts, yellowish brown spore print, and broadly ellipsoid to ellipsoid, smooth basidiospores.

Description. ***Basidiomata*** stipitate-pileate. ***Pileus*** convex then plano-convex to plane; ***surface*** at first rugulose then subrugulose in age, finely tomentose to tomentose, dark brown to reddish brown, becoming light brown to brown to grayish orange, unchanging when bruised; ***context*** off-white then yellowish to dull pale orange in age, unchanging when cut. ***Stipe*** central, terete, cylindrical; ***surface*** subscabrous, yellowish white to pale yellow to orange white, with scattered brown to dark brown to reddish brown granulose squamules, unchanging when bruised; ***basal mycelium*** white; ***context*** solid, white becoming off-white to yellowish white in age, unchanging when cut. ***Hymenophore*** tubulate, slightly depressed to depressed around the stipe. ***Tubes*** pale yellow then grayish yellow, separable from the pileus context, unchanging when cut. ***Pores*** roundish then subangular to angular with age; when young white then yellowish white becoming grayish yellow, unchanging when touched. ***Spore print*** yellowish brown. ***Basidiospores*** ellipsoid to broadly ellipsoid, thin-walled, smooth under light microscope and SEM. ***Basidia*** 4-spored, clavate without basal clamp connection. ***Cheilo- and pleurocystidia*** narrowly fusiform to fusiform or narrowly utriform, thin-walled. ***Pileipellis*** an intricate trichoderm, made of moderately interwoven to loosely interwoven, thin-walled hyphae. ***Stipitipellis*** arranged parallel to the surface of the stipe, composed of moderately interwoven, thin-walled hyphae, with scattered groups of rising cells to clusters of narrowly clavate to clavate cells. ***Clamp connections*** not seen in any tissue.

Typus generis. *Rostrupomyces sisongkhramensis* (Khamsuntorn, Pinruan & Luangsa-ard) Vadthanarat, Raghoonundon & Raspé.

Distribution. Currently known only from northern and northeastern Thailand.

Notes. *Rostrupomyces* can be morphologically separated from *Xerocomus* by the different shape and surface of basidiospores, which are ellipsoid to broadly ellipsoid with smooth under light microscope and SEM in the new genus, whereas *Xerocomus* produce more or less oblong to fusiform basidiospores, usually with bacillate surface under SEM (Wu et. al. 2016). *Rostrupomyces* also produces yellowish brown spore print, whereas *Xerocomus* produces olive-brown spore print. Moreover, color change upon bruising does not occur in any part of *Rostrupomyces* basidiomes, whereas context and hymenophore of *Xerocomus* always turn more or less bluish to blue when bruised or cut (Wu et. al. 2016). The most resembling genus, *Hemileccinum*, shares some similar characters including rugulose to subrugulose pileus surface, yellow hymeno-

phore which is depressed around the stipe apex, subscabrous stipe surface (less so in *Hemileccinum*), white basal mycelium, mostly unchanging color in any parts. However, *Rostrupomyces* can be morphologically distinguished from *Hemileccinum* by the differences in spore print color, and in the shape and surface of basidiospores. *Rostrupomyces* produces yellowish brown spore print, broadly ellipsoid to ellipsoid basidiospores with smooth surface under light microscope and SEM. *Hemileccinum* produces olive-brown spore prints, boletoid basidiospores that are smooth under light microscope, but ornamented with irregular warts and pinholes under SEM. Also, the pore surface of *Rostrupomyces* is white in young basidiomata and becomes pale yellow when mature whereas in *Hemileccinum*, the pore surface is yellow in all stages (Šutara 2008; Wu et al. 2016; Farid et al. 2021; Li et al. 2021).

***Rostrupomyces sisongkhramensis* (Khamsuntorn, Pinruan & Luangsa-ard) Vadthanarat, Raghoonundon & Raspé, comb. nov.**
Figs 3, 4, 5A–B
MycoBank No: 851393

Xerocomus sisongkhramensis Khamsuntorn, Pinruan & Luangsa-ard. Basionym.

Diagnosis. *Rostrupomyces sisongkhramensis* is characterised by having dark to reddish brown, becoming brown to grayish orange pileus, with rugulose to subrugulose, finely tomentose to tomentose surface; yellowish to orange white, subscabrous, longitudinally fissurate stipe surface, with moderately scattered brown to dark brown to reddish brown granulose squamules; yellow hymenophore; unchanging color in any parts; yellowish brown spore print; and broadly ellipsoid to ellipsoid smooth basidiospores.

Description. ***Basidiomata*** medium-sized. ***Pileus*** 37–94(118) mm in diameter, convex at first then plano-convex to plane, sometimes with sub-depressed at the centre; ***margin*** inflexed at first then deflexed in age, exact or slightly exceeding (up to 1 mm); ***surface*** at first rugulose especially near the margin then subrugulose in age, dull, dry to moist, finely tomentose to tomentose covered with greenish yellow (3A3–4, 3B4) matted hyphae at places (especially when young), at first dark brown to reddish brown (6–8F4–8), becoming light brown to brown to grayish orange (6D/E5–6, 5B4–5) on light yellow to brownish orange (4A3–5, 5C4) background in age, gradually paler to the margin, unchanging when bruised; ***context*** (3)5–10(14) mm thick half-way to the margin, at first firm then soft in age, color distribution even, at first off-white, slightly brownish (7D/E4–5) near the pileipellis, then yellowish to orange white (4–5A2) or occasionally yellowish (3A3–4) above the hymenium especially in age, unchanging when cut. ***Stipe*** (33)41–97(108) × 6(7)–19(20) mm, central, terete, usually cylindrical for the most part but often with wider base, rarely club-shaped; ***surface*** subscabrous longitudinally fissurate, slightly shiny, yellowish white to pale yellow to orange white (3A3 to 4A2 to 5A2), occasionally pale yellow (3A3–4) near the cap, with moderately scattered brown to dark brown to reddish brown (7D/E/F4–7) granulose squamules, unchanging when bruised; ***basal mycelium*** little developed, white (1A1); ***context*** solid, firm, at first white (1A1) becoming off-white to yellowish white (4A2) occasionally pale yellow (3A3–4) especially

in the above part near the stipe surface in age, yellowish to orange gray (4–5B2–3) virgate at places, unchanging when cut. ***Hymenophore*** tubulate, slightly depressed to depressed around the stipe, with slightly decurrent tooth, sometimes almost free, mostly segmentiform to subventricose. ***Tubes*** (3)4–13 mm long half-way to the margin, at first pale yellow (4A3) then grayish yellow (4B3)

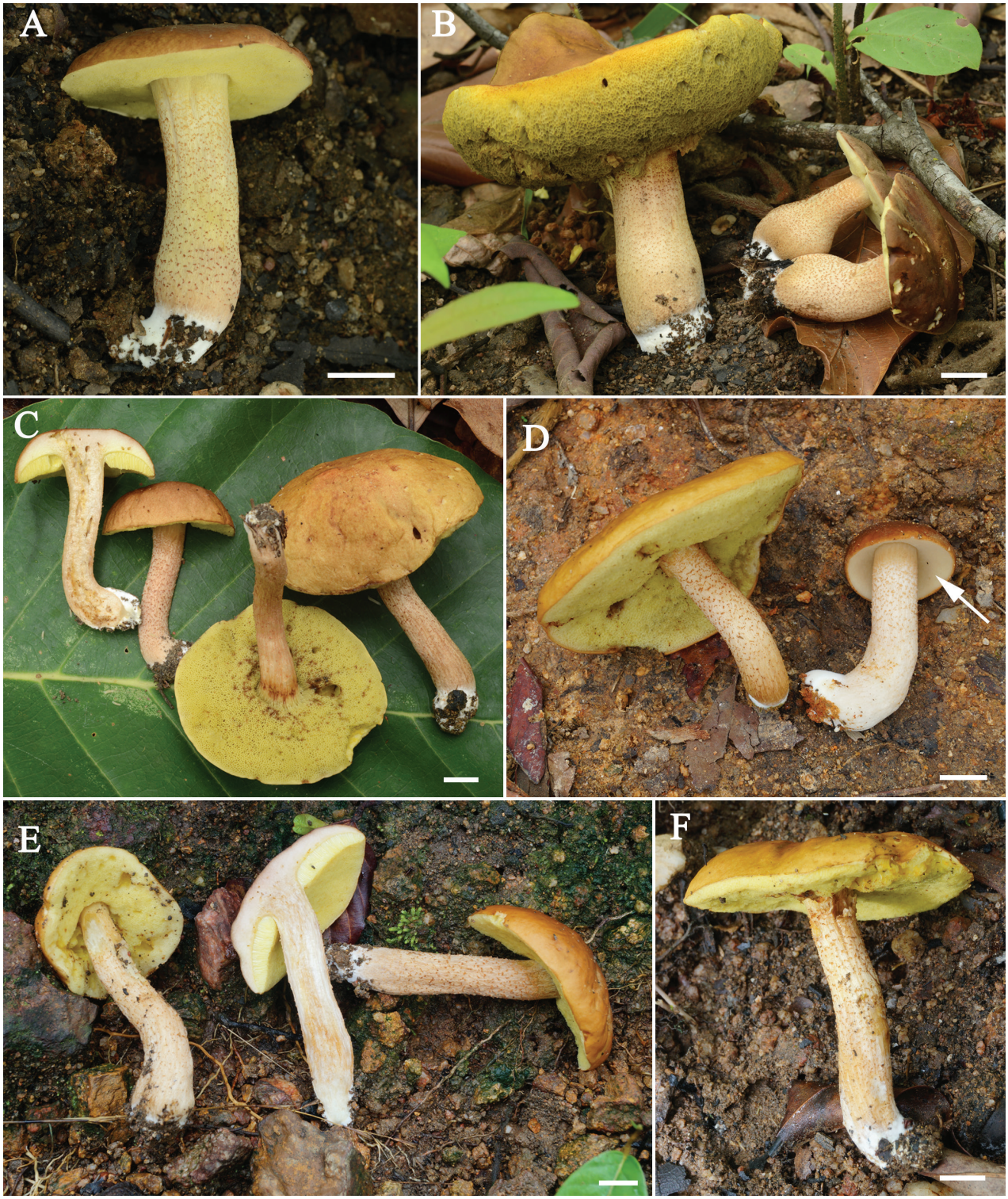

Figure 3. Fresh basidiomata of *Rostrupomyces sisongkhramensis* **A** OR0915 **B** OR0919 **C** OR1004 **D** SV0155, white pores surface in young basidioma (white arrow) **E** SV0219 **F** SV0225. Scale bars: 1 cm (**A–F**).

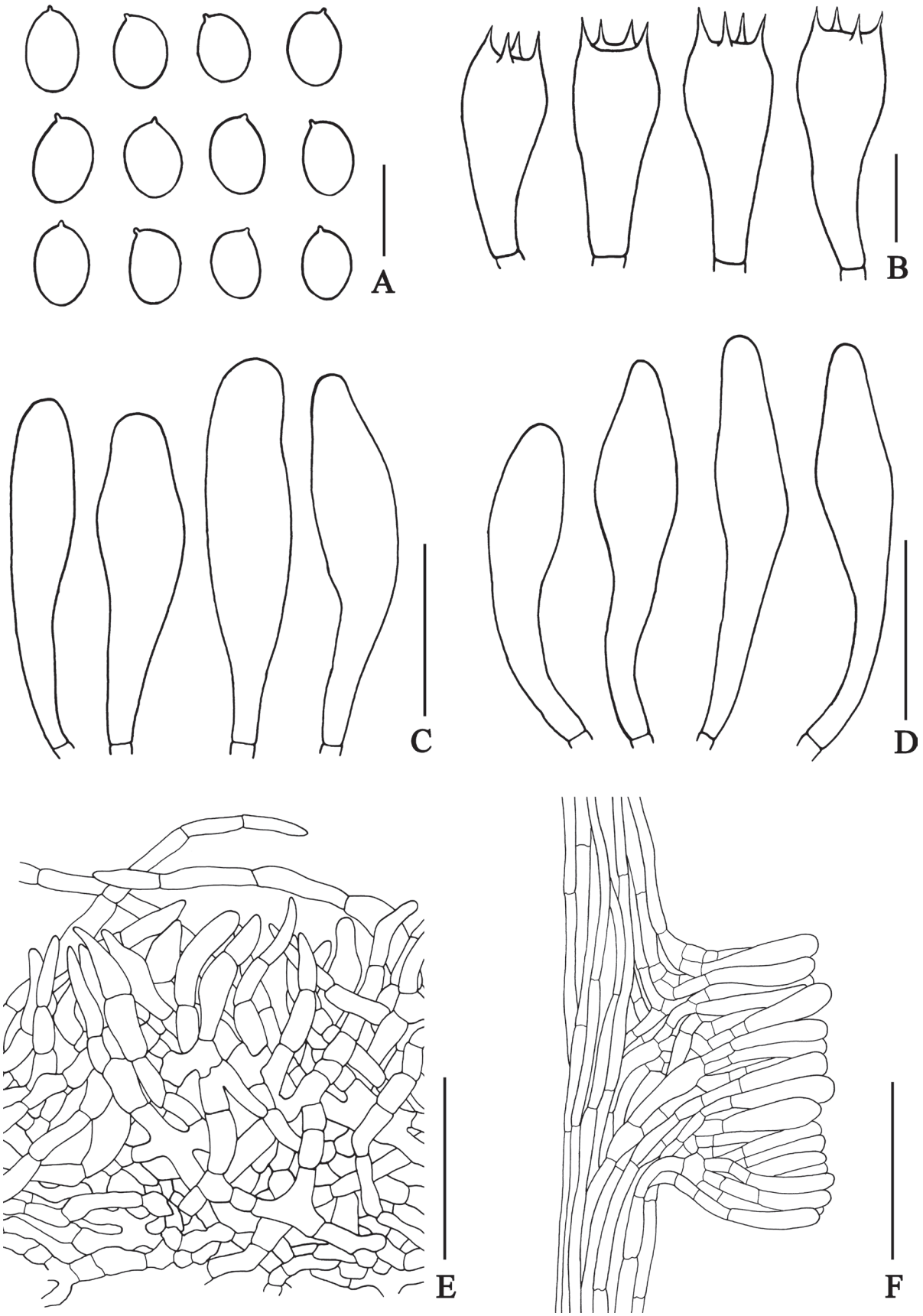

Figure 4. Microscopic features of *Rostrupomyces sisongkhramensis* **A** basidiospores **B** basidia **C** cheilocystidia **D** pleurocystidia **E** pileipellis **F** stipitipellis showing a cluster of narrowly clavate to clavate cells which slightly scattered on the stipe surface. Scale bars: 10 µm (**A–D**); 25 µm (**D–E**); 50 µm (**E–F**). All line drawings were made from SV0155.

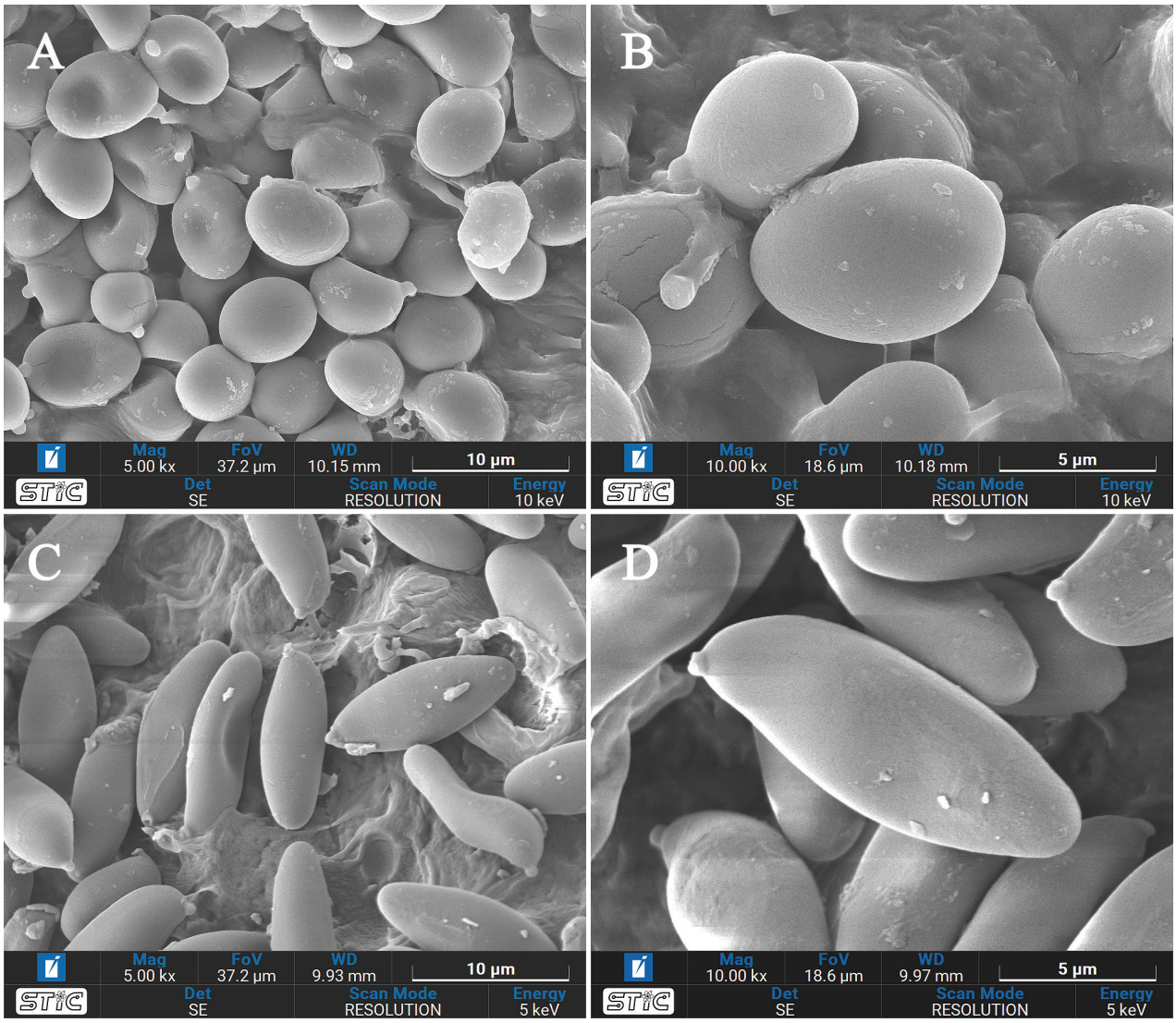

Figure 5. Scanning electron micrographs of basidiospores **A–B** *Rostrupomyces sisongkhramensis* (SV0155) **C–D** *Hemileccinum inferius* (SV0282).

when mature, separable from the pileus context, unchanging when cut. ***Pores*** 0.2–0.8(1.3) mm wide half-way to the margin, irregularly arranged, roundish then subangular to angular in age; topography subregular, composite pores frequent; color distribution even, when young white (1A1) then yellowish white (4A2) becoming grayish yellow (4B3–5) infrequently with reddish brown spots (7–8E/F8) at places in age, unchanging when touched. ***Odour*** mild fungoid. ***Taste*** mild. ***Spore print*** yellowish brown (5F5) in mass.

***Macrochemical reactions*:** KOH, brownish orange on pileus, yellowish to pale dull orange on pileus context and stipe surface, none or yellowish on stipe context, yellowish brown to brownish orange on hymenium; NH_4OH, yellowish to brownish orange (occasionally with purple aura) on pileus, yellowish to pale orange on stipe surface, yellowish to brownish on hymenium, none or yellowish on pileus context and stipe context.

Spores [591/10/10] (6.3–)6.9–7.9–9.1(–9.8) × (4.5–)4.8–5.5–6.2(–6.5) µm *Q* = (1.2–)1.29–1.44–1.63(–1.79). From the type (6.5–)6.9–7.7–8.8(–9.5) × (4.7–)5–5.5–6.2(–6.5) µm, *Q* = (1.2–)1.25–1.41–1.54(–1.63), *N* = 106, broad-

ly ellipsoid to ellipsoid, thin-walled, smooth under light microscope and SEM, yellowish hyaline in water or KOH, inamyloid. ***Basidia*** 4-spored, (22–)22–26–31(–31) × (9–)9–11–13(–13) µm, clavate without basal clamp connection, hyaline to yellowish hyaline in KOH; sterigmata up to 4 µm long. ***Cheilocystidia*** (30–)30–43–58(–59) × (9–)9–11–15(–15) µm, frequent, narrowly fusiform to fusiform with obtuse apex or narrowly utriform, thin-walled, hyaline in KOH. ***Pleurocystidia*** (33–)33–43–63(–63) × (8–)8–11–13(–13) µm, infrequent, narrowly fusiform to fusiform with obtuse apex, thin-walled, hyaline in KOH. ***Hymenophoral trama*** subregular to slightly divergent, 38–82 µm wide, with subregular mediostratum 8–24 µm wide, composed of cylindrical, 4–12 µm wide hyphae, hyaline in KOH. ***Pileipellis*** an intricate trichoderm, 70–130 mm thick, made of moderately interwoven (when young) to loosely interwoven in age, thin-walled, smooth, hyaline hyphae 4–18 mm wide, branching and anastomosing at places; terminal cells 12–65 × 4–18 mm, narrowly fusiform to fusiform to broadly fusiform with slightly acuminate or obtuse apex, hyaline to yellowish pale brown in KOH. ***Pileus context*** made of strongly interwoven, thin-walled hyphae, up to 12 µm wide, hyaline in KOH. ***Stipitipellis*** arranged parallel to the surface of the stipe, composed of moderately interwoven, cylindrical, thin-walled, 3–10 µm wide hyphae, anastomosing and branching at places, sparsely scattered with groups of rising cells to clusters (up to 87 µm high) of narrowly clavate to clavate cells (21–36 × 4–9 µm), hyaline to yellowish hyaline in KOH. ***Caulocystidia*** not seen. ***Stipe context*** parallelly arranged, composed of moderately interwoven, cylindrical, thin-walled, 3–18 µm wide hyphae, hyaline to yellowish hyaline in KOH. ***Clamp connections*** not seen in any tissue.

Habitat and distribution. Solitary or in small groups (up to 4 basidiomata), or fasciculate by 2 to 3 basidiomata, on sandy loam to sandy clay loam soil in open dry dipterocarp forest and dipterocarp forest dominated by Dipterocarpaceae trees namely *Anthoshorea roxburghii*, *Dipterocarpus obtusifolius*, *D. tuberculatus*, *D. intricatus*, *Pentacme siamensis*, and *Shorea obtusa* with or without scattered Fagaceae trees. Currently known from the type locality (Nakhon Phanom province), Sisaket and Ubon Ratchathani provinces in northeastern Thailand, and also in Chiang Mai and Chiang Rai provinces in northern Thailand.

Specimens examined. Thailand, Chiang Mai Province, Muang District, Doi Suthep-Pui National Park, 18°47'39.4"N, 98°55'21.5"E, elev. 915 m, 20 July 2015, *Olivier Raspé*, OR1004 (CMUB, BKF, BR); ibid., 18°48'04.2"N, 98°55'44.3"E, elev. 775 m, 21 July 2015, *Santhiti Vadthanarat*, SV0155 (CMUB, BKF); Mae On District, 18°51'57.4"N, 99°17'22.9"E, elev. 660 m, 1 June 2015, *Olivier Raspé*, OR0915 (CMUB, BR); ibid., 18°51'57.0"N, 99°17'23.0"E, elev. 660 m, 1 June 2015, *Olivier Raspé*, OR0918 (CMUB, BR); ibid., 18°51'57.0"N, 99°17'23.0"E, elev. 660 m, 1 June 2015, *Olivier Raspé*, OR0919 (CMUB, BR); ibid., 18°52'13.0"N, 99°18'25.0"E, elev. 760 m, 15 August 2015, *Santhiti Vadthanarat*, SV0219 (CMUB, BR); ibid., 18°51'57.4"N, 99°17'22.0"E, elev. 700 m, 16 August 2015, *Santhiti Vadthanarat*, SV0225 (CMUB, BR); ibid., 18°51'57.7"N, 99°17'26.5"E, elev. 685 m, 1 June 2017, *Santhiti Vadthanarat*, SV0397 (CMUB, BR); ibid., 18°52'15.6"N, 99°18'11.5"E, elev. 800 m, 11 July 2017, *Olivier Raspé*, OR1392 (CMUB, BR); ibid., 18°52'15.6"N, 99°18'11.5"E, elev. 800 m, 11 July 2017, *Olivier Raspé*, OR1399 (CMUB, BR); ibid., 18°52'16.7"N, 99°18'13.0"E, elev. 800 m, 9 June 2021, *Santhiti Vadthanarat*, SV0512 (CMUB, BR); ibid. 18°52'7.9"N, 99°17'42.0"E, elev. 780 m, 10 June 2021, *Santhiti Vadthanarat*, SV0517 (CMUB, BR); ibid. 18°52'16.4"N,

99°17'40.5"E, elev. 820 m, 10 June 2021, *Santhiti Vadthanarat*, SV0518 (CMUB, BR); ibid. 18°52'12.0"N, 99°17'31.2"E, elev. 700 m, 10 June 2021, *Bhavesh Raghoonundon*, BR0311; ibid. 18°52'26.8"N, 99°18'15.5"E, elev. 845 m, 10 June 2021, *Bhavesh Raghoonundon*, BR0313; Chiang Rai Province, Phan District, 19°48'50.0"N, 99°51'57.0"E, elev. 730 m, 22 June 2021, *Bhavesh Raghoonundon*, BR0368; ibid. 19°48'50.0"N, 99°51'57.0"E, elev. 730 m, 22 June 2021, *Bhavesh Raghoonundon*, BR0371; Sisaket Province, Kanthararom District, Kok Yang Yai roadside market, 17 September 2016, *Santhiti Vadthanarat*, SV0345 (CMUB); Ubon Ratchathani Province, Trakan Phuet Phon District, Huay Fai, 15°32'44.3"N, 105°10'17.4"E, elev. 165 m, 28 July 2015, *Olivier Raspé*, OR1059 (CMUB, BR).

ITS sequence accession number (SV0155): PP354891.

Notes. The BLAST result based on ITS sequence obtained from one of the examined specimens (voucher SV0155, GenBank accession number PP354891) was 100% identical to the holotype of *X. sisongkhramensis* (voucher BBH 48255, accession number OP462477) which was reported by Tan et al. 2022. This suggested that our collections belonged to *X. sisongkhramensis*. Morphological characters of our collections mostly fit the original description of the species. However, some variations were observed between ours and the original description as follows: Tan et al. (2022) mentioned the absence of cheilocystidia in *X. sisongkhramensis* while we could observe them in our collections; they were narrowly fusiform to fusiform with obtuse apex or narrowly utriform, thin-walled. The protologue mentioned broadly clavate to subclavate (40–60 × 8–15 µm) caulocystidia. However, in our observation only groups of rising terminal cells of shape and size similar to the caulocystidia in Tan et al. (2022), were observed. What Tan et al. (2022) considered as caulocystidia were what we described as undifferentiated terminal cells of the stipitipellis. In the species protologue, the pileipellis and stipitipellis were described as composed of thick-walled hyphae (no measurement mentioned). However, only thin-walled hyphae were observed in our collections.

Rostrupomyces sisongkhramensis is morphologically similar to *Hemileccinum duriusculum* Mei-Xiang Li, Zhu L. Yang & G. Wu, which was recently described from China. The two species share some morphological characters including basidiome size and color, scattering of granular squamules on the stipe surface, pale yellow to grayish yellow hymenophore that is depressed around the stipe apex, and unchanging color in any parts. However, *H. duriusculum* differs by its strikingly venose pileus surface, finer granular squamules on the stipe surface, and subfusiform basidiospores ornamented with irregular warts under SEM (Liu et al. 2024). *Rostrupomyces sisongkhramensis* is also somewhat similar to a European *Leccinum* species originally described from Italy, *Leccinum albostipitatum* den Bakker & Noordel., which has a similar shade of pileus color (light orange), whitish stipe covered with whitish squamules when young to reddish brown in age. However, *L. albostipitatum* can be differentiated by having an inflexed margin which exceeds the hymenophore by up to 4 mm, yellowish white to very pale brown hymenophore that becomes brownish when bruised, a clear blue discoloration of the stipe base when touched, context staining vinaceous then grayish to blackish when cut, smooth fusiform basidiospores, distribution in Europe, and association with *Populus* L. trees (den Bakker and Noordeloos 2005).

Phylogenetically, *R. sisongkhramensis* is closely related to *Rubinosporus auriporus* Vadthanarat, Raspé & Lumyong, the only known species in the genus, which was described from the same region as *Rostrupomyces* (northern Thailand). However, it can be differentiated from *R. sisongkhramensis* by having grayish red to pastel red to reddish brown pileus; even stipe surface with scattered bright yellow to yellowish white to orange to light brown minute squamules; shorter tubes especially when young; golden yellow hymenophore; and the striking dark ruby spore print (Vadthanarat et al. 2022).

Hemileccinum inferius **Vadthanarat, Raghoonundon & Raspé, sp. nov.**
MycoBank No: 849063
Figs 6, 7

Etymology. "inferius" refers to the only lower part of the stipe ornamented with reticulum

Holotype. Thailand, Chiang Mai Province, Muang District, Doi Suthep-Pui National Park, 18°47'52.8"N, 98°54'21.2"E, elev. 1,170 m, 1 July 2016, *Santhiti Vadthanarat*, SV0282 (holotype: CMUB, isotype: BKF, MFUB). ITS sequence accession number PP354892.

Diagnosis. *Hemileccinum inferius* can be differentiated from resembling *Hemileccinum* species by a grayish red to reddish brown to dark brown, plane to sub-depressed, subrugulose to pitted pileus; and yellow to yellowish white, cylindrical with subbulbous stipe, with surface even on the upper half and subscabrous to delicately reticulate on the lower half, as well as smooth basidiospores even when observed under SEM.

Description. ***Basidiomata*** medium-sized. ***Pileus*** 66–68 mm in diameter, plane to sub-depressed at the centre; ***margin*** deflexed in age, elastic, slightly exceeding (up to 1 mm); ***surface*** subrugulose to pitted especially near the margin, dull, moist to slippery when wet, tomentose, grayish red (8B/C3–4) to reddish brown (8D/E4–6) to dark brown to reddish brown (7–8F4–6), unchanging when bruised; ***context*** 8–10 mm thick haft-way to the margin, firm to soft, pale yellow (1A3), slightly brown (7E5) near the pileus surface, light yellow (1A4) above

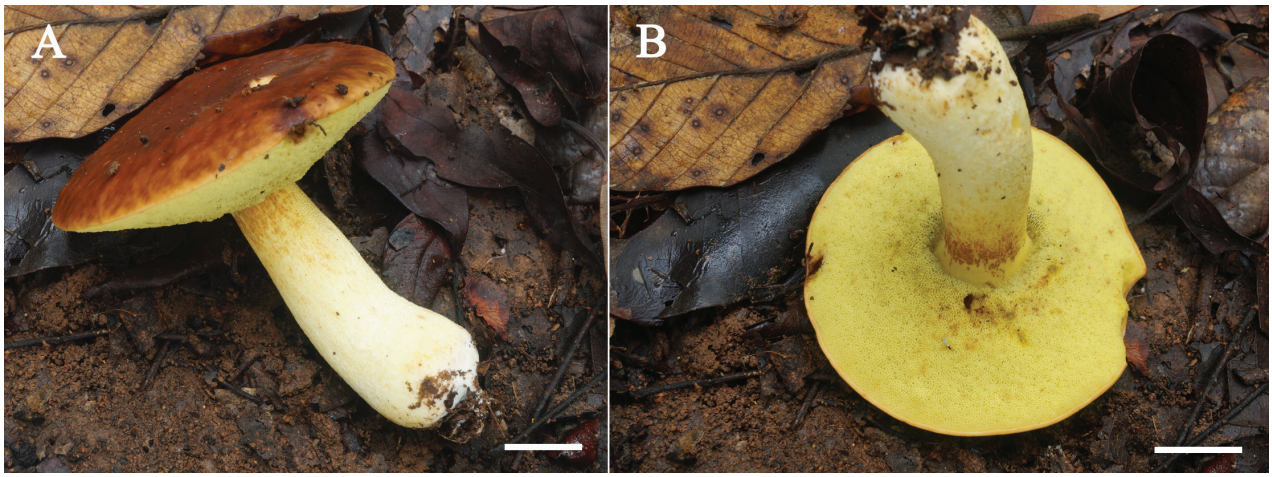

Figure 6. Fresh basidioma of *Hemileccinum inferius* **A, B** SV0282 (holotype). Scale bars: 1 cm (**A, B**).

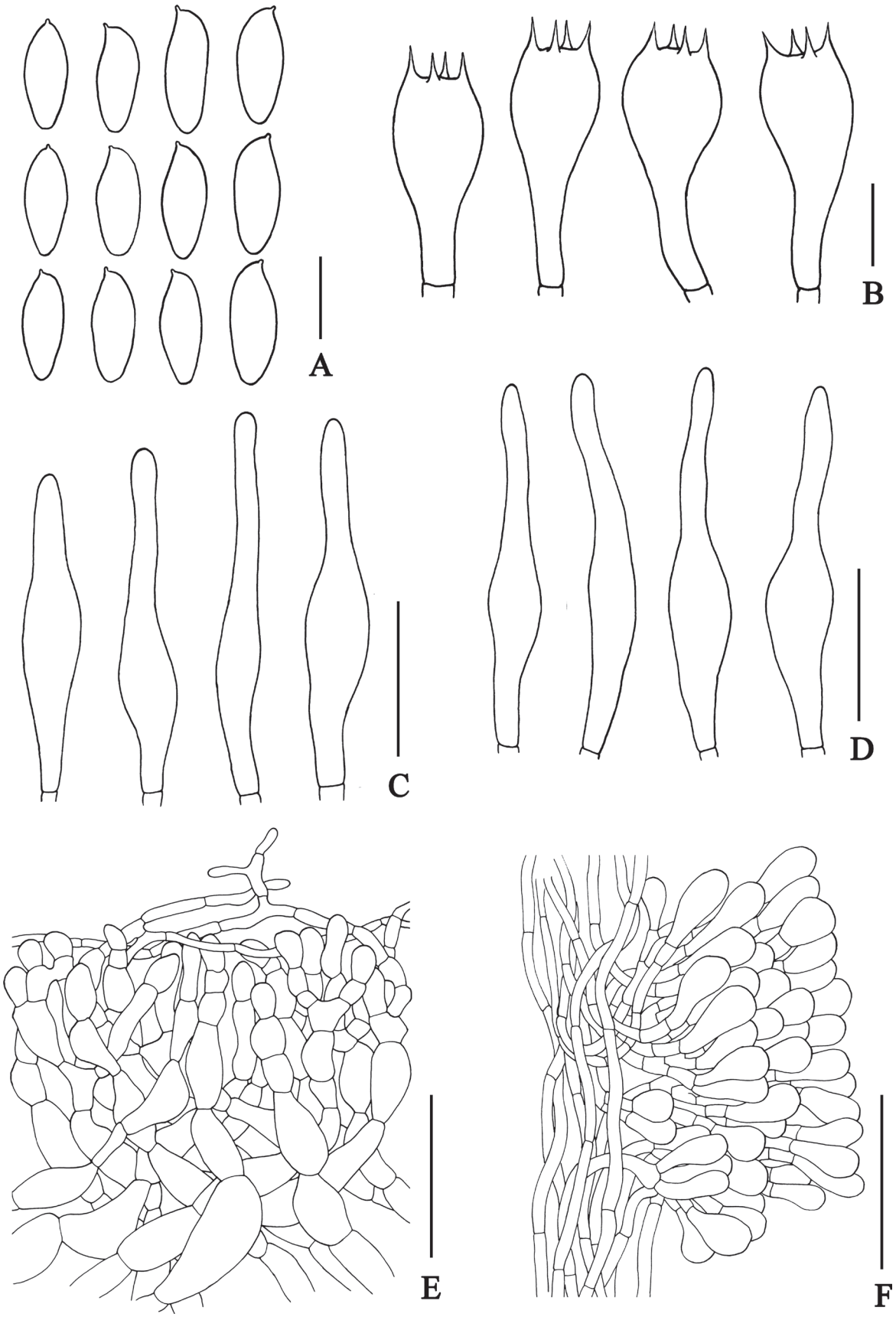

Figure 7. Microscopic features of *Hemileccinum inferius* **A** basidiospores **B** basidia **C** cheilocystidia **D** pleurocystidia **E** pileipellis **F** stipitipellis showing a cluster of clavate to boardy clavate like cells which moderately scattered on the stipitipellis. Scale bars: 10 µm (**A–D**); 25 µm (**D–E**); 50 µm (**E–F**). All drawings were made from holotype type (SV0282).

the hymenium in age, unchanging when cut. ***Stipe*** 65–76 × 14–18 mm, central, terete, cylindrical with subbulbous base; ***surface*** even on the upper half then subscabrous to delicately reticulate on the lower half, dull, dry to moist, light yellow (2A4–6) to yellowish white to pale yellow (2A2–3) at the base, occasionally with reddish brown to dark brown spots (8D5–8, 8F7) at places, minutely covered with pale yellow to light brown to dark brown (2A3–4 to 7D/E4, 7F8) squamules on the upper half, slightly fibrillose following a reticulate pattern at the middle of the stipe getting less so to the base, unchanging when bruised; ***basal mycelium*** white (1A1); ***context*** solid, firm, pale yellow (2A3–5) especially in the above half near the stipe surface becoming yellowish white (2A2) to off-white at the base, unchanging when cut. ***Hymenophore*** tubulate, slightly depressed around the stipe, with slightly decurrent tooth, subventricose. ***Tubes*** 7–8 mm long half-way to the margin, yellow to grayish yellow (2A7 to 2B7) near the pileus context then olive (2E5) near the pores, separable from the pileus context, unchanging when bruised. ***Pores*** 0.3–0.8(1.2) mm wide at mid-radius, subangular to angular, even, grayish yellow (2B5), unchanging when touched, irregularly arranged; topography subregular. ***Odour*** mild fungoid. ***Taste*** mild. ***Spore print*** olive brown (4E7).

***Macrochemical reactions*:** KOH, brownish orange on pileus and hymenophore, pale orange on pileus context and stipe surface, and stipe context; NH_4OH, brownish orange with purple aura on pileus, yellowish to brownish orange with purple aura on stipe surface, yellowish to greenish or slightly blue on pileus context and stipe context.

Spores [118/2/2] (10.5–)11.4–12.9–14.6(–15.3) × (3.8–)4.2–4.8–5.6(–6.1) µm *Q* = (2.06–)2.4–2.68–3.05(–3.32). From the type (10.8–)11.5–12.7–14.2(–14.5) × (4.1–)4.3–4.8–5.5(–6.1) µm, *Q* = (2.06–)2.33–2.66–3.06(–3.1), *N* = 68, narrowly ellipsoid to subcylindrical with a slight suprahilar depression, thin-walled, smooth under light microscope and SEM (Fig. 5C–D), yellowish to brownish hyaline in water, yellowish hyaline in KOH, inamyloid. ***Basidia*** 4-spored, (23–)24–27–31(–32) × (11–)11–12–14(–14) µm, clavate without basal clamp connection, hyaline to yellowish hyaline in KOH; sterigmata up to 4 µm long. ***Cheilocystidia*** (30–)34–54–72(–72) × (7–)8–10–14(–14) µm, narrowly fusiform with elongated obtuse apex, frequent, thin-walled, hyaline to yellowish hyaline in KOH. ***Pleurocystidia*** (34–)34–51–69(–70) × (10–)10–11–13(–13) µm, frequent near the pores, narrowly fusiform with elongated obtuse apex, thin-walled, hyaline to yellowish hyaline in KOH. ***Hymenophoral trama*** slightly divergent, 62–150 µm wide composed of cylindrical, 4–12 µm wide hyphae, with subregular mediostratum 30–100 µm wide, hyaline in KOH. ***Pileipellis*** a hyphoepithelium, 80–112 µm thick, the pileipellis composed of ellipsoid to broadly ellipsoid or cylindrical, thin-walled, more or less vertically arranged, occasionally branching or anastomosing, with metablematic, elongated-cylindrical hyphae (2–4 µm wide hyphae), branching or anastomosing at places, hyaline to yellowish hyaline in KOH; terminal cells of 2 types: 1) ellipsoid to broadly ellipsoid, 8–15 × 12–20 µm; and 2) clavate to broadly clavate with obtuse apex, 10–20 × 4–7 µm. ***Pileus context*** made of moderately interwoven, ellipsoid to broadly ellipsoid, thin-walled hyphae, 10–23 µm wide, hyaline in KOH. ***Stipitipellis*** arranged parallel to the surface of the stipe (40–50 µm thick), composed of moderately interwoven, cylindrical, thin-walled, 2.5–4 µm wide hyphae, anastomosing at places, moderately scattered with groups of rising cells to clus-

ters (50–60 µm high) of thin-walled clavate to broadly clavate cells (20–30 × 10–15 µm), hyaline to yellowish hyaline in KOH. ***Caulocystidia*** not seen. ***Stipe context*** composed of parallel, 8–22 µm wide hyphae, hyaline in KOH. ***Clamp connections*** not seen in any tissue.

Habitat and distribution. Solitary, on loamy soil in hill evergreen forest dominated by Fagaceae scattered with a few *Dipterocarpus obtusifolius*, at 985–1,170 m elevation. Currently known from Chiang Mai Province, northern Thailand.

Additional specimens examined. Thailand, Chiang Mai Province, Mae Taeng District, 19°06'59"N, 98°44'23"E, elev. 985 m, 6 June 2021, *Bhavesh Raghoonundon*, BR0260 (MFLU).

Notes. *Hemileccinum inferius* is described based on collections from Thailand. The comparison of the new species with the seven known Asian species follows. *Hemileccinum albidum* differs from *H. inferius* by gray-brown to chrome yellow to ochraceous or golden brown pileus; longer and slender stipe (up to 160 mm); shorter basidiospores (10–12.5 × 4.0–5.5 µm); occurrence at higher elevations (1,968–2,490 m; Li et al. 2021). *Hemileccinum brevisporum* is similar in pileus color but has shorter basidiospores (9–11 × 4–5 µm); and it occurs under Fagaceae and Pinaceae, at higher elevations (1,700–2,120 m); Li et al. 2021). *Hemileccinum duriusculum* is macromorphologically quite similar, but differs by a strongly venose pileus surface, even when young, the absence of reticulum on the lower half of the stipe, as well as shorter cheilo- and pleurocystidia (Liu et al. 2024). *Hemileccinum ferrugineipes* has similar pileus surface and color but can be differentiated by the apparent pale red-brown color on the lower part of the stipe; and shorter basidiospores (11.0–12.5 × 4–5 µm; Li et al. 2021). *Hemileccinum indecorum* is clearly different in having dark red to reddish brown basidiomata with mucilaginous surface densely covered with whitish to dirty white, small conical to subconical to irregularly shaped squamules; incurved margin; and yellowish hymenophore that slowly turns brownish to reddish brown when bruised (Horak 2011; Zeng et al. 2012). *Hemileccinum parvum* has smaller basidiomata (pileus 3.3–3.6 cm diam, stipe 60–97 × 4–9 mm); paler pileus (brownish to yellowish); pale yellow context that slowly turns pale blue when cut (Li et al. 2021). *Hemileccinum rugosum* has paler pileus (light orange to reddish orange); very distinctly rugose to wrinkled pileus surface; and shorter basidiospores (9–13 × 4–5 µm; Wu et al. 2016).

Hemileccinum inferius is also similar to an American species, *H. floridanum*, which has reddish brown to chestnut brown wrinkled and uneven pileus, whitish to pale yellow stipe, white basal mycelium, yellow hymenophore, and smooth basidiospore under both light microscope and SEM. However, the latter species is different by white context that slowly turns yellow often from the margin toward the center, longer basidiospores (10–17 × 4.5–6 µm), likely forms association with oak in northern America (Farid et al. 2021).

Phylogenetically, *H. inferius* was most closely related to *H. hortonii*, *H. rugosum*, and an undescribed specimen (voucher HKAS 53421) from China. *Hemileccinum hortonii*, an American species, can easily be distinguished by its conspicuously pitted pileus, smooth to lightly pruinose stipe that sometimes has delicate reticulation on the upper half, pores that occasionally turn blue on when touched, and slightly longer and narrower basidiospores (12–15 × 3.5–4.5; Kuo and Ortiz-Santana 2020; Farid et al. 2021). For morphological comparison with *H. rugosum* see the above paragraph.

Discussion

In this study, the morphological and phylogenetic evidence highly supported establishing *Rostrupomyces* as a new genus of Boletaceae to accommodate *Xerocomus sisongkhramensis*. The most important morphological characters used to differentiate the new genus from other Boletaceae genera are: subscabrous stipe surface with scattered granulose squamules; hymenophore that is white in young basidiomes and becomes yellow in age; yellowish brown spore print; and broadly ellipsoid to ellipsoid basidiospores with smooth surface.

The character of subscabrous to scabrous stipe surface dotted with scattered granulose squamules is also present in other Boletaceae genera such as *Hemileccinum* (see in notes under *Rostrupomyces*), *Leccinum* Gray, *Leccinellum* Bresinsky & Manfr. Binde, *Rugiboletus* G. Wu & Zhu L. Yang, and *Sutorius* Halling, Nuhn & N.A. Fechner. *Leccinum* can be separated from *Rostrupomyces* by having a white to pallid to light brown hymenophore while *Leccinellum* has yellow hymenophore similar to *Rostrupomyces*. However, both genera are different from *Rostrupomyces* by a more or less pronounced color change of hymenophore, stipe surface, and/or context, which can stain red, brown, yellow, or occasionally blue when bruised. *Leccinellum* and *Leccinum* produce boletoid basidiospores which are also different from *Rostrupomyces*. Moreover, they are phylogenetically distant and placed in another subfamily, the Leccinoideae (den Bakker and Noordeloos 2005; Wu et al. 2016; Xue et al. 2019; Meng et al. 2021). *Rugiboletus* differs from *Rostrupomyces* by its strongly wrinkled pileus (especially when young), yellow or brown or reddish brown hymenophore that is unchanging or turns bluish when bruised, subfusiform basidiospores, and phylogenetically distant and placed in *Pulveroboletus* group (Wu et al. 2015; Kuo and Ortiz-Santana 2020). *Sutorius* Halling, Nuhn & N.A. Fechner, is different in having chocolate to reddish brown or purplish brown basidiomata, grayish or reddish brown or brownish orange hymenophore, context always with scattered reddish or violet or dark brown encrustations that are visible with the naked eye, reddish brown spore deposit, and narrowly ellipsoid to subcylindrical basidiospores (Halling et al. 2012; Vadthanarat et al. 2021). Like *Rugiboletus*, *Sutorius* is phylogenetically distant from *Rostrupomyces*, belonging to the *Pulveroboletus* group (Vadthanarat et al. 2021).

Xerocomoideae genera other than *Rostrupomyces* also produce smooth basidiospores, including *Amylotrama*, *Aureoboletus*, *Alessioporus*, *Pulchroboletus*, *Rubinosporus*, and *Veloboletus*. Moreover, while most *Xerocomus* and *Phylloporus* species produce basidiospores with bacillate surface, a few species produce smooth basidiospores (Neves and Halling 2010; Wu et. al. 2016; Chuankid et al. 2019). However, only *Amylotrama* and *Rubinosporus* present the same shape of basidiospore as *Rostrupomyces*, whereas the others produce more or less oblong to ellipsoid to fusiform basidiospores (Gelardi et al. 2014; Wu et al. 2016; Farid et al. 2017; Frank et al. 2017; Zhang et al. 2019; Crous et al. 2020; Lebel et al. 2022; Vadthanarat et al. 2022). *Amylotrama* comprises two species from Australia, which are completely different from *Rostrupomyces* by their sequestrate basidiomata (Lebel et al. 2022). *Rubinosporus*, differs by having a strikingly thin hymenophore, especially when young; golden yellow hymenophore; and dark ruby spore print (Vadthanarat et al. 2022). *Aureoboletus* differs by the pileus usually having a viscid surface especially when moist; and golden

yellow hymenophore (Wu et al. 201; Zhang et al. 2019). *Alessioporus* is different by its reticulated stipe occasionally with a granular ring-like zone in the middle or lower half of the stipe, golden yellow hymenophore; blue staining of the stipe surface, hymenophore, and context; and distribution in Mediterranean Italy and subtropical USA (Gelardi et al. 2014; Frank et al. 2017). *Pulchroboletus* differs by the stipe surface with scattered red to reddish brown, occasionally with reticulum or longitudinal striations, and with a pseudo-annulus; golden yellow hymenophore; intense blue staining of the hymenophore and context; and occurrence only in Mediterranean Europe and tropical to subtropical America (Gelardi et al. 2014; Farid et al. 2017). The only *Veloboletus* species, is different by its basidiomata with a distinctive universal veil; blue staining of the pileus, stipe, hymenophore, and context, and distribution in Australia (Crous et al. 2020).

Tan et al. (2022) phylogeny was based on ITS and LSU sequences of only *Xerocomus* spp., and *Phylloporus* as outgroup, which resulted in the clustering of *X. sisongkhramensis* in *Xerocomus*. However, our phylogeny based on multiple protein-coding genes (*atp*6, *cox*3, *tef*1, and *rpb*2) and on a much wider taxon sampling of Boletaceae resolved *X. sisongkhramensis* in subfamily Xerocomoideae indeed, but distant from other *Xerocomus* species. Keeping *X. sisongkhramensis* would have rendered the genus polyphyletic. The erection of the new genus *Rostrupomyces*, which can also be morphologically separated from *Xerocomus*, was therefore necessary.

In the phylogeny, *Rostrupomyces* appeared sister to another monotypic genus, *Rubinosporus* (morphological comparison see in notes under *Rostrupomyces sisongkhramensis*). The two genera can be differentiated mainly by the spore print color, and color of hymenophore, two characters that do not vary between species in the same genus in Boletaceae. The characters have been primarily used to differentiate many genera in Boletaceae e.g., *Sutorius*, *Cacaoporus*, *Hourangia*, *Baorangia* (Halling et al. 2012; Wu et al. 2015; Zhu et al. 2015; Vadthanarat et al. 2019b). Additional morphological characters, including pileus color and stipe surface, could be useful to separate them. However, both genera so far comprise only a single species and the pileus color and stipe surface are found to be variable between species within the same genus. For example, in *Boletus* L. and *Tylopilus* P. Karst. the pileus color is variable from white, yellow, brown, orange, green, gray, and purple, and the stipe surface from even to reticulate to strongly reticulate (e.g., Cui et al. 2015; Wu et al. 2016; Li and Yang 2021). Hence, if more species in either of those two genera are described, the comparison between the two genera might need updating.

Rostrupomyces has been found so far on sandy loam to sandy clay loam soils at elevations lower than 1,000 m (165 to 915 m), in open dry dipterocarp and dipterocarp forest mainly dominated by ectomycorrhizal trees in family Dipterocarpaceae genera *Anthoshorea* (*A. roxburghii*), *Dipterocarpus* (*D. obtusifolius*, *D. tuberculatus*, *D. intricatus*), *Pentacme* (*P. siamensis*), and *Shorea* (*S. obtusa*), with scattered Fagaceae trees. In Thailand the Dipterocarpaceae tree species are mainly distributed in lowland (<800 m) to mid-elevation forests (800–1,200 m) whereas Fagaceae trees are mostly distribute in mid-elevation to highland forests (>1,200 m) (Gardner et al. 2007). During our surveys on the diversity of Boletaceae in Thailand, no *Rostrupomyces* collection was found in the forests above 1,000 m, where no *Anthoshorea*, *Dipterocarpus*, *Pentacme*, or

Shorea trees were observed or mentioned as occurring. This suggests that the distribution of *Rostrupomyces* depends on the distribution of the mentioned tree genera, and they are inferred as the associated tree hosts of *Rostrupomyces*. However, a more detailed study is needed to confirm the specificity of its relationship with ectomycorrhizal hosts.

In this study, some specimens of *Rostrupomyces sisongkhramensis* were collected from community forests and the species was found to be consumed by local people, in Ubon Ratchathani and Sisaket provinces in lower northeastern Thailand. It is found on sale on roadsides and local markets, along with other Boletaceae in genera such as *Baorangia*, *Boletus*, *Boletellus*, *Heimioporus*, *Retiboletus*, *Sutorius*, and *Tylopilus*. The species is called "Hed Phueng Waan" in which the words "Hed Phueng" refer to bolete and "Waan" means sweet. It can also be called "Hed Phueng Kaw" in which the words "Kaw" means rice. The same local names are also applied to the other bolete species that are mostly white and have sweet taste after cooking such as *Boletus* spp. In this region a local name can be used for different mushroom species which present similarly striking morphological characters. Conversely, one mushroom species may have more than one local name. *Rostrupomyces sisongkhramensis* is also found in the northern parts of Thailand in Chiang Rai and Chiang Mai provinces. However, during our survey in the region, the species has never been found being collected or on sale for consumption by the locals. The protologue of this species (collections from upper northeastern Thailand) did not mention the edibility (Tan et al. 2022).

To date, 15 *Hemileccinum* species have been described worldwide, among which eight are originally from Asia (China: *H. albidum*, *H. brevisporum*, *H. duriusculum*, *H. ferrugineipes*, *H. parvum*, *H. rugosum*; Singapore: *H. indecorum*; and Thailand: *H. inferius*), two species from France in Europe (*H. depilatum* and *H. impolitum*), four species from North America (*H. floridanum*, *H. hortonii*, *H. rubropunctum*, and *H. subglabripes*), and a single species, *H. brunneotomentosum*, from Belize in Central America (Šutara 2008; Halling et al. 2015; Wu et al. 2016; Kuo and Ortiz-Santana 2020; Nitson and Frank 2020; Farid et al. 2021; Li et al. 2021; Liu et al. 2024). Three *Hemileccinum* species have been previously reported to occur in Thailand, namely *H. depilatum* (reported as *Boletus depilatus* Redeuilh), *H. impolitum* (reported as *B. impolitus* Fr.), and *H. indecorum* (Chandrasrikul et al. 2011; Vadthanarat et al. 2019b). The first two species were originally described from France and were then reported from Thailand based on morphological identification only. As we know that the distribution of Boletaceae species depends on the distribution of their hosts, the ecology and host specificity are important characters in distinguishing species in Boletaceae (den Bakker et al. 2004; Dentinger et al. 2010; Cui et al. 2015; Loizides et al. 2019; Gelardi 2020). It is therefore doubtful that European species are also present in Southeast Asia where the forests are dominated by different tree species or families. Unfortunately, no specimens associated with the reports of occurrence in Thailand are available for molecular analysis to compare with European specimens. Moreover, molecular analysis of several *Hemileccinum* specimens obtained in our study showed none of them belong to those European species. It is therefore reasonable to assume that the identifications of the Thai collections as *H. depilatum* and *H. impolitum* were not correct. The

other recorded species, *H. indecorum* was originally described from Singapore in Southeast Asia (Horak 2011). Specimens collected from Thailand were identified based on both molecular and morphological evidences (Vadthanarat et al. 2019b). However, the full morphological description of this Thai collection has not yet been published. In the future, more detail on the species and more records of *Hemileccinum* will be reported.

Basidiospores with tiny warts and pinholes (when observed under SEM) are typical of *Hemileccinum*. However, a few *Hemileccinum* species produce basidiospores with smooth surface, including the new species (Kuo and Ortiz-Santana et al. 2020; Farid et al. 2021). This kind of exception is also found in other Xerocomoideae genera i.e., in *Phylloporus* and *Xerocomus*, In the latter two genera, most of the species produce basidiospores with bacillate surfaces, but a few produce smooth basidiospores (Neves and Halling 2010; Wu et. al. 2016; Chuankid et al. 2019).

A total of 39 new taxa (4 new genera and 35 new species), including those introduced in this paper, have been originally described from Thailand (Rostrup 1902; Yang et al. 2006; Desjardin et al. 2009; Choeyklin et al. 2012; Neves et al. 2012; Halling et al. 2014; Raspé et al. 2016; Vadthanarat et al. 2018; Chuankid et al. 2019; Phookamsak et al. 2019; Vadthanarat et al. 2019a, 2019b, 2020; Chuankid et al. 2021; Raghoonundon et al. 2021; Vadthanarat et al. 2021; Tan et al. 2022; Vadthanarat et al. 2022; This study). Our study on the diversity of Boletaceae in Thailand is still ongoing and is needed to uncover more new taxa and new distribution records for Thailand.

Acknowledgements

Authors are grateful for the permit number 0907.4/4769 granted by the Department of National Parks, Wildlife and Plant Conservation, Ministry of Natural Resources and Environment for collecting in Doi Suthep-Pui National Park.

Additional information

Conflict of interest

The authors have declared that no competing interests exist.

Ethical statement

No ethical statement was reported.

Funding

This research work was supported by a Postdoctoral Fellowship from Mae Fah Luang University to Santhiti Vadthanarat, and partially funded by the Mae Fah Luang University research grant 641A01003.

Author contributions

Conceptualization: SV, OR. Data curation: BR, SV. Formal analysis: SV. Funding acquisition: OR. Investigation: SV. Methodology: SV. Project administration: OR. Resources: BR, OR, SV. Software: SV. Supervision: OR. Validation: SL, OR. Visualization: SV. Writing – original draft: SV. Writing – review and editing: BR, OR, SL.

Author ORCIDs

Santhiti Vadthanarat https://orcid.org/0000-0002-9035-0375
Bhavesh Raghoonundon https://orcid.org/0000-0001-6671-2404
Olivier Raspé https://orcid.org/0000-0002-8426-2133

Data availability

All of the data that support the findings of this study are available in the main text.

References

Badou SA, Furneaux B, De Kesel A, Khan FK, Houdanon RD, Ryberg M, Yorou NS (2022) *Paxilloboletus* gen. nov., a new lamellate bolete genus from tropical Africa. Mycological Progress 21(1): 243–256. https://doi.org/10.1007/s11557-021-01756-y

Binder M, Hibbett DS (2006) Molecular systematics and biological diversification of Boletales. Mycologia 98(6): 971–981. https://doi.org/10.1080/15572536.2006.11832626

Binder M, Larsson KH, Matheny PB, Hibbett DS (2010) Amylocorticiales ord. nov. and Jaapiales ord. nov.: Early diverging clades of agaricomycetidae dominated by corticioid forms. Mycologia 102(4): 865–880. https://doi.org/10.3852/09-288

Chandrasrikul A, Suwanarit P, Sangwanit U, Lumyong S, Payapanon A, Sanoamuang N, Pukahuta C, Petcharat V, Sardsud U, Duengkae K, Klinhom U, Thongkantha S, Thongklam S (2011) Checklist of Mushrooms (Basidiomycetes) in Thailand. Office of Natural Resources and Environmental Policy and Planning, Bangkok, Thailand, 448 pp.

Choeyklin R, Boonpratuang T, Sommai S, Somrithipol S (2012) *Octaviania violascens*: A new sequestrate bolete from Thailand. Mycotaxon 120(1): 149–155. https://doi.org/10.5248/120.149

Chuankid B, Vadthanarat S, Hyde KD, Thongklang N, Zhao R, Lumyong S, Raspé O (2019) Three new *Phylloporus* species from tropical China and Thailand. Mycological Progress 18(5): 603–614. https://doi.org/10.1007/s11557-019-01474-6

Chuankid B, Vadthanarat S, Thongbai B, Stadler M, Lumyong S, Hyde KD, Raspé O (2021) *Retiboletus* (Boletaceae) in northern Thailand: One novel species and two first records. Mycoscience 62(5): 62. https://doi.org/10.47371/mycosci.2021.05.003

Crous PW, Wingfield MJ, Lombard L, Roets F, Swart WJ, Alvarado P, Carnegie AJ, Moreno G, Luangsa-Ard J, Thangavel R, Alexandrova AV, Baseia IG, Bellanger J-M, Bessette AE, Bessette AR, Delapeña-Lastra S, García D, Gené J, Pham THG, Heykoop M, Malysheva E, Malysheva V, Martín MP, Morozova OV, Noisripoom W, Overton BE, Rea AE, Sewall BJ, Smith ME, Smyth CW, Tasanathai K, Visagie CM, Adamík S, Alves A, Andrade JP, Aninat MJ, Araújo RVB, Bordallo JJ, Boufleur T, Baroncelli R, Barreto RW, Bolin J, Cabero J, Cabo M, Cafà G, Caffot MLH, Cai L, Carlavilla JR, Chávez R, Decastro RRL, Delgat L, Deschuyteneer D, Dios MM, Domínguez LS, Evans HC, Eyssartier G, Ferreira BW, Figueiredo CN, Liu F, Fournier J, Galli-Terasawa LV, Gil-Durán C, Glienke C, Gonçalves MFM, Gryta H, Guarro J, Himaman W, Hywel-Jones N, Iturrieta-González I, Ivanushkina NE, Jargeat P, Khalid AN, Khan J, Kiran M, Kiss L, Kochkina GA, Kolaík M, Kubátová A, Lodge DJ, Loizides M, Luque D, Manjón JL, Marbach PAS, Massolajr NS, Mata M, Miller AN, Mongkolsamrit S, Moreau P-A, Morte A, Mujic A, Navarro-Ródenas A, Németh MZ, Nóbrega TF, Nováková A, Olariaga I, Ozerskaya SM, Palma MA, Petters-Vandresen DAL, Piontelli E, Popov ES, Rodríguez A, Requejo Ó, Rodrigues ACM, Rong IH, Roux J, Seifert KA, Silva BDB, Sklená F, Smith JA, Sousa JO, Souza HG, Desouza JT, Vec K, Tanchaud P, Tanney JB, Terasawa F, Thanakitpi-

pattana D, Torres-Garcia D, Vaca I, Vaghefi N, Vaniperen AL, Vasilenko OV, Verbeken A, Yilmaz N, Zamora JC, Zapata M, Jurjević Ž, Groenewald JZ (2019) Fungal Planet description sheets: 951–1041. Persoonia 43(1): 223–425. https://doi.org/10.3767/persoonia.2019.43.06

Crous PW, Cowan DA, Maggs-Kölling G, Yilmaz N, Larsson E, Angelini C, Brandrud TE, Dearnaley JDW, Dima B, Dovana F, Fechner N, García D, Gené J, Halling RE, Houbraken J, Leonard P, Luangsa-ard JJ, Noisripoom W, Rea-Ireland AE, Ševčíková H, Smyth CW, Vizzini A, Adam JD, Adams GC, Alexandrova AV, Alizadeh A, Álvarez Duarte E, Andjic V, Antonín V, Arenas F, Assabgui R, Ballarà J, Banwell A, Berraf-Tebbal A, Bhatt VK, Bonito G, Botha W, Burgess TI, Caboň M, Calvert J, Carvalhais LC, Courtecuisse R, Cullington P, Davoodian N, Decock CA, Dimitrov R, Di Piazza S, Drenth A, Dumez S, Eichmeier A, Etayo J, Fernández I, Fiard J-P, Fournier J, Fuentes-Aponte S, Ghanbary MAT, Ghorbani G, Giraldo A, Glushakova AM, Gouliamova DE, Guarro J, Halleen F, Hampe F, Hernández-Restrepo M, Iturrieta-González I, Jeppson M, Kachalkin AV, Karimi O, Khalid AN, Khonsanit A, Kim JI, Kim K, Kiran M, Krisai-Greilhuber I, Kučera V, Kušan I, Langenhoven SD, Lebel T, Lebeuf R, Liimatainen K, Linde C, Lindner DL, Lombard L, Mahamedi AE, Matočec N, Maxwell A, May TW, McTaggart AR, Meijer M, Mešić A, Mileto AJ, Miller AN, Molia A, Mongkolsamrit S, Muñoz Cortés C, Muñoz-Mohedano J, Morte A, Morozova OV, Mostert L, Mostowfizadeh-Ghalamfarsa R, Nagy LG, Navarro-Ródenas A, Örstadius L, Overton BE, Papp V, Para R, Peintner U, Pham THG, Pordel A, Pošta A, Rodríguez A, Romberg M, Sandoval-Denis M, Seifert KA, Semwal KC, Sewall BJ, Shivas RG, Slovák M, Smith K, Spetik M, Spies CFJ, Syme K, Tasanathai K, Thorn RG, Tkalčec Z, Tomashevskaya MA, Torres-Garcia D, Ullah Z, Visagie CM, Voitk A, Winton LM, Groenewald JZ (2020) Fungal Planet description sheets: 1112–1181. Persoonia 45(1): 251–409. https://doi.org/10.3767/persoonia.2020.45.10

Cui YY, Feng B, Wu G, Xu J, Yang ZL (2015) Porcini mushrooms (*Boletus* sect. *Boletus*) from China. Fungal Diversity 81(1): 189–212. https://doi.org/10.1007/s13225-015-0336-7

Darriba D, Taboada GL, Doallo R, Posada D (2012) jModelTest 2: More models, new heuristics and parallel computing. Nature Methods 9(8): 772. https://doi.org/10.1038/nmeth.2109

den Bakker HC, Noordeloos ME (2005) A revision of European species of *Leccinum* Gray and notes on extralimital species. Persoonia 18: 511–587.

den Bakker HC, Zuccarello GC, Kuyper THW, Noordeloos ME (2004) Evolution and host specificity in the ectomycorrhizal genus *Leccinum*. The New Phytologist 163(1): 201–215. https://doi.org/10.1111/j.1469-8137.2004.01090.x

Dentinger BTM, Ammirati JF, Both EE, Desjardin DE, Halling RE, Henkel TW, Moreau PA, Nagasawa E, Soytong K, Taylor AF, Watlingm R, Moncalvo JM, McLaughlin DJ (2010) Molecular phylogenetics of porcini mushrooms (*Boletus* section *Boletus*). Molecular Phylogenetics and Evolution 57(3): 1276–1292. https://doi.org/10.1016/j.ympev.2010.10.004

Desjardin DE, Binder M, Roekring S, Flegel T (2009) *Spongiforma*, a new genus of gastroid boletes from Thailand. Fungal Diversity 37: 1–8.

Doyle JJ, Doyle JL (1990) Isolation of plant DNA from fresh tissue. Focus (San Francisco, Calif.) 12: 13–15.

Farid A, Franck AR, Garey JR (2017) *Boletus rubricitrinus* belongs in *Pulchroboletus* (Boletaceae). Czech Mycology 69(2): 143–162. https://doi.org/10.33585/cmy.69204

Farid A, Bessette AE, Bessette AR, Bolin JA, Kudzma LV, Franck AR, Garey JR (2021) Investigations in the boletes (Boletaceae) of southeastern USA: Four novel species and

three novel combinations. Mycosphere 12(1): 1038–1076. https://doi.org/10.5943/mycosphere/12/1/12

Frank JL, Bessette AR, Bessette AE (2017) *Alessioporus rubriflavus* (Boletaceae), a new species from the eastern United States. North American Fungi 12(2): 1–8.

Gardner S, Sidisunthorn P, Anusarnsunthorn V (2007) A field guide to forest trees of Northern Thailand, Bangkok, Thailand.

Gelardi M (2020) Diversity, Biogeographic Distribution, Ecology, and Ectomycorrhizal Relationships of the Edible Porcini Mushrooms (*Boletus* s. str., Boletaceae) Worldwide: State of the Art and an Annotated Checklist. In: Pérez-Moreno J, Guerin-Laguette A, Flores Arzú R, Yu FQ (Eds) Mushrooms, Humans and Nature in a Changing World. Springer, Cham, 223–271. https://doi.org/10.1007/978-3-030-37378-8_8

Gelardi M, Simonini G, Ercole E, Vizzini A (2014) *Alessioporus* and *Pulchroboletus* gen. nov. (Boletaceae, Boletineae), two novel genera to accommodate *Xerocomus ichnusanus* and *X. roseoalbidus* from European Mediterranean basin: Molecular and morphological evidence. Mycologia 106(6): 1168–1187. https://doi.org/10.3852/14-042

Gelardi M, Simonini G, Ercole E, Davoli P, Vizzini A (2015) *Cupreoboletus* (Boletaceae, Boletineae), a new monotypic genus segregated from *Boletus* sect. *Luridi* to reassign the Mediterranean species *B. poikilochromus.* Mycologia 107(6): 1254–1269. https://doi.org/10.3852/15-070

Halling RE, Nuhn M, Fechner NA, Osmandson TW, Soytong K, Arora D, Hibbett DS, Binder M (2012) *Sutorius*: A new genus for *Boletus eximius.* Mycologia 104(4): 951–961. https://doi.org/10.3852/11-376

Halling RE, Desjardin DE, Fechner N, Arora D, Soytong K, Dentinger BTM (2014) New porcini (*Boletus* sect. *Boletus*) from Australia and Thailand. Mycologia 106(4): 830–834. https://doi.org/10.3852/13-340

Halling RE, Fechner N, Nuhn M, Osmundson T, Soytong K, Arora D, Binder M, Hibbett D (2015) Evolutionary relationships of *Heimioporus* and *Boletellus* (Boletales), with an emphasis on Australian taxa including new species and new combinations in *Aureoboletus*, *Hemileccinum* and *Xerocomus.* Australian Systematic Botany 28(1): 1–22. https://doi.org/10.1071/SB14049

Henkel TW, Obase K, Husbands D, Uehling JK, Bonito G, Aime MC, Smith ME (2016) New Boletaceae taxa from Guyana: *Binderoboletus segoi* gen. and sp. nov., *Guyanaporus albipodus* gen. and sp. nov., *Singerocomus rubriflavus* gen. and sp. nov., and a new combination for *Xerocomus inundabilis.* Mycologia 108(1): 157–173. https://doi.org/10.3852/15-075

Horak E (1980) Supplementary remark to *Austroboletus* (Corner) Wolfe (Boletaceae). Sydowia 33: 71–87.

Horak E (2011) Revision of Malaysian species of Boletales s.l. (Basidiomycota) described by Corner EJH (1972, 1974). Forest Research Institute and Ministry of Natural Resources and Environment, Malaysia, 283 pp.

Hosen MI, Feng B, Wu G, Zhu XT, Li YC, Yang ZL (2013) *Borofutus*, a new genus of Boletaceae from tropical Asia: phylogeny, morphology and taxonomy. Fungal Diversity 58: 215–226. https://doi.org/10.1007/s13225-012-0211-8

Hosen MI, Yang ZL (2021) *Kaziboletus*, a new boletoid genus of Boletaceae associated with *Shorea robusta* in Bangladesh. Mycological Progress 20(9): 1145–1156. https://doi.org/10.1007/s11557-021-01723-7

Katoh K, Standley DM (2013) MAFFT Multiple sequence alignment software version 7: Improvements in performance and usability. Molecular Biology and Evolution 30(4): 772–780. https://doi.org/10.1093/molbev/mst010

Khmelnitsky O, Davoodian N, Singh P, Raspé O, Lee SML, Fechner N, Bonito G, Lebel T, Halling RE (2019) *Ionosporus*: A new genus for *Boletus longipes* (Boletaceae), with a new species, *I. australis*, from Australia. Mycological Progress 18(3): 439–451. https://doi.org/10.1007/s11557-018-01463-1

Kornerup A, Wanscher JH (1978) Methuen Handbook of Colour. 3rd edn. Eyre Methuen Ltd, London, 252 pp.

Kuo M, Ortiz-Santana B (2020) Revision of leccinoid fungi, with emphasis on North American taxa, based on molecular and morphological data. Mycologia 112(1): 197–211. https://doi.org/10.1080/00275514.2019.1685351

Lebel T, Davoodian N, Bloomfield MC, Syme K, May TW, Hosaka K, Castellano MA (2022) A mixed bag of sequestrate fungi from five different families: Boletaceae, Russulaceae, Psathyrellaceae, Strophariaceae, and Hysterangiaceae. Swainsona 36: 33–65.

Li YC, Yang ZL (2021) The Boletes of China: *Tylopilus* s.l. Springer, Singapore, 418 pp. https://doi.org/10.1007/978-981-16-2986-0_1

Li YC, Feng B, Yang ZL (2011) *Zangia*, a new genus of Boletaceae supported by molecular and morphological evidence. Fungal Diversity 49(1): 125–143. https://doi.org/10.1007/s13225-011-0096-y

Li YC, Ortiz-Santana B, Zeng NK, Feng B, Yang ZL (2014) Molecular phylogeny and taxonomy of the genus *Veloporphyrellus*. Mycologia 106(2): 291–306. https://doi.org/10.3852/106.2.291

Li MX, Wu G, Yang ZL (2021) Four new species of *Hemileccinum* (Xerocomoideae, Boletaceae) from Southwestern China. Journal of Fungi 7(10): 823. https://doi.org/10.3390/jof7100823

Liu SL, Wang XW, Li GJ, Deng CY, Rossi W, Leonardi M, Liimatainen K, Kekki T, Niskanen T, Smith ME, Ammirati J, Bojantchev D, Abdel-Wahab MA, Zhang M, Tian E, Lu Y-Z, Zhang J-Y, Ma J, Dutta AK, Acharya K, Du T-Y, Xu J, Kim JS, Lim YW, Gerlach A, Zeng N-K, Han Y-X, Razaghi P, Raza M, Cai L, Calabon MS, Jones EBG, Saha R, Kumar TKA, Krishnapriya K, Thomas A, Kaliyaperumal M, Kezo K, Gunaseelan S, Singh SK, Singh PN, Lagashetti AC, Pawar KS, Jiang S, Zhang C, Zhang H, Qing Y, Bau T, Peng X-C, Wen T-C, Ramirez NA, Niveiro N, Li M-X, Yang ZL, Wu G, Tarafder E, Tennakoon DS, Kuo C-H, da Silva TM, Souza-Motta CM, Bezerra JDP, He G, Ji X-H, Suwannarach N, Kumla J, Lumyong S, Wannathes N, Rana S, Hyde KD, Zhou L-W (2024) Fungal diversity notes 1717–1817: Taxonomic and phylogenetic contributions on genera and species of fungal taxa. Fungal Diversity 124(1): 1–216. https://doi.org/10.1007/s13225-023-00529-0

Loizides M, Bellanger JM, Assyov B, Moreau PA, Richard F (2019) Present status and future of boletoid fungi (Boletaceae) on the island of Cyprus: Cryptic and threatened diversity unravelled by ten-year study. Fungal Ecology 10: 65–81. https://doi.org/10.1016/j.funeco.2019.03.008

Matheny PB (2005) Improving phylogenetic inference of mushrooms with RPB1 and RPB2 nucleotide sequences (*Inocybe*; Agaricales). Molecular Phylogenetics and Evolution 35(1): 1–20. https://doi.org/10.1016/j.ympev.2004.11.014

Meng X, Wang GS, Wu G, Wang PM, Yang ZL, Li YC (2021) The genus *Leccinum* Boletaceae, Boletales) from China based on morphological and molecular data. Journal of Fungi (Basel, Switzerland) 7(9): 732. https://doi.org/10.3390/jof7090732

Miller MA, Holder MT, Vos R, Midford PE, Liebowitz T, Chan L, Hoover P, Warnow T (2009) The CIPRES portals. CIPRES. http://www.phylo.org/portal2/home

Neves MA, Halling RE (2010) Study on species of *Phylloporus* I: Neotropics and North America. Mycologia 102(4): 923–943. https://doi.org/10.3852/09-215

Neves MA, Binder M, Halling R, Hibbett D, Soytong K (2012) The phylogeny of selected *Phylloporus* species inferred from NUC-LSU and ITS sequences, and descriptions of new species from the Old World. Fungal Diversity 55(1): 109–123. https://doi.org/10.1007/s13225-012-0154-0

Nitson DD, Frank JL (2020) Nomenclatural novelties. Index Fungorum: Published Numbers 443: 1.

Nuhn ME, Binder M, Taylor AFS, Halling RE, Hibbett DS (2013) Phylogenetic overview of the Boletineae. Fungal Biology 117(7–8): 479–511. https://doi.org/10.1016/j.funbio.2013.04.008

Orihara T, Smith ME, Shimomura N, Iwase K, Maekawa N (2012) Diversity and systematics of the sequestrate genus *Octaviania* in Japan: Two new subgenera and eleven new species. Persoonia 28(1): 85–112. https://doi.org/10.3767/003158512X650121

Orihara T, Lebel T, Ge Z-W, Smith ME, Maekawa N (2016) Evolutionary history of the sequestrate genus *Rossbeevera* (Boletaceae) reveals a new genus *Turmalinea* and highlights the utility of ITS minisatellite-like insertions for molecular identification. Persoonia 37(1): 173–198. https://doi.org/10.3767/003158516X691212

Phookamsak R, Hyde KD, Wanasinghe DN, Jeewon R, Bhat DJ, Maharachchikumbura SSN, Raspé O, Karunarathna SC, Wanasinghe DN, Hongsanan S, Doilom M, Tennakoon DS, Machado AR, Firmino AL, Ghosh A, Karunarathna A, Mešić A, Dutta AK, Thongbai B, Devadatha B, Norphanphoun C, Senwanna C, Wei D, Pem D, Ackah FK, Wang G-N, Jiang H-B, Madrid H, Lee HB, Goonasekara ID, Manawasinghe IS, Kušan I, Cano J, Gené J, Li J, Das K, Acharya K, Raj KNA, Latha KPD, Chethana KWT, He M-Q, Dueñas M, Jadan M, Martín MP, Samarakoon MC, Dayarathne MC, Raza M, Park MS, Telleria MT, Chaiwan N, Matočec N, de Silva NI, Pereira OL, Singh PN, Manimohan P, Uniyal P, Shang Q-J, Bhatt RP, Perera RH, Alvarenga RLM, Nogal-Prata S, Singh SK, Vadthanarat S, Oh S-Y, Huang S-K, Rana S, Konta S, Paloi S, Jayasiri SC, Jeon SJ, Mehmood T, Gibertoni TB, Nguyen TTT, Singh U, Thiyagaraja V, Sarma VV, Dong W, Yu X-D, Lu Y-Z, Lim YW, Chen Y, Tkalčec Z, Zhang Z-F, Luo Z-L, Daranagama DA, Thambugala KM, Tibpromma S, Camporesi E, Bulgakov TS, Dissanayake AJ, Senanayake IC, Dai DQ, Tang L-Z, Khan S, Zhang H, Promputtha I, Cai L, Chomnunti P, Zhao R-L, Lumyong S, Boonmee S, Wen T-C, Mortimer PE, Xu J (2019) Fungal diversity notes 933–1040: Taxonomic and phylogenetic contributions on genera and species of fungal taxa. Fungal Diversity 95(1): 1–273. https://doi.org/10.1007/s13225-019-00421-w

Raghoonundon B, Davoodian N, Phonemany M, Raspé O (2021) *Tylocinum* is no longer monotypic: *Tylocinum brevisporum* sp. nov. (Boletales, Boletaceae) from northern Thailand. Biodiversity Data Journal 9: e75907. https://doi.org/10.3897/BDJ.9.e75907

Raspé O, Vadthanarat S, De Kesel A, Degreef J, Hyde KD, Lumyong S (2016) *Pulveroboletus fragrans*, a new Boletaceae species from Northern Thailand, with a remarkable aromatic odor. Mycological Progress 15(4): 38. https://doi.org/10.1007/s11557-016-1179-7

Rehner SA, Buckley E (2005) A *Beauveria* phylogeny inferred from nuclear ITS and EF1-α sequences: Evidence for cryptic diversification and links to *Cordyceps* teleomorphs. Mycologia 97(1): 84–98. https://doi.org/10.3852/mycologia.97.1.84

Ronquist F, Teslenko M, van der Mark P, Ayres D, Darling A, Höhna S, Larget B, Liu L, Suchard MA, Huelsenbeck JP (2012) MrBayes 3.2: Efficient Bayesian phylogenetic inference and model choice across a large model space. Systematic Biology 61(3): 539–542. https://doi.org/10.1093/sysbio/sys029

Rostrup E (1902) Fungi. In: Schmidt J (Ed.) Flora of Koh Chang, Contributions to the knowledge of the vegetation in the gulf of Siam, Part 6, Botanisk Tidsskrift 24: 355–367.

Saccardo PA, Saccardo D (1905) Sylloge fungorum omnium hucusque cognitorum Vol. 17.

Sato H, Hattori T (2015) New species of *Boletellus* section *Boletellus* (Boletaceae, Boletales) from Japan, *B. aurocontextus* sp. nov. and *B. areolatus* sp. nov. PLoS ONE 10(6): e0128184. https://doi.org/10.1371/journal.pone.0128184

Stamatakis A (2006) RAxML-vi-hpc: Maximum likelihood-based phylogenetic analyses with thousands of taxa and mixed models. Bioinformatics 22(21): 2688–2690. https://doi.org/10.1093/bioinformatics/btl446

Šutara J (2008) *Xerocomus* s. l. in the light of the present state of knowledge. Czech Mycology 60(1): 29–62. https://doi.org/10.33585/cmy.60104

Tan YP, Bishop-Hurley SL, Shivas RG, Cowan DA, Maggs-Kölling G, Maharachchikumbura SSN, et al. (2022) Fungal planet description sheets: 1436–1477. Persoonia 49: 261–350. https://doi.org/10.3767/persoonia.2022.49.08

Vadthanarat S, Raspé O, Lumyong S (2018) Phylogenetic affinities of the sequestrate genus *Rhodactina* (Boletaceae), with a new species, *R. rostratispora* from Thailand. MycoKeys 29: 63–80. https://doi.org/10.3897/mycokeys.29.22572

Vadthanarat S, Amalfi M, Halling RE, Bandala V, Lumyong S, Raspé O (2019a) Two new *Erythrophylloporus* species (Boletaceae) from Thailand, with two new combinations of American species. MycoKeys 55: 29–57. https://doi.org/10.3897/mycokeys.55.34570

Vadthanarat S, Lumyong S, Raspé O (2019b) *Cacaoporus*, a new Boletaceae genus, with two new species from Thailand. MycoKeys 54: 1–29. https://doi.org/10.3897/mycokeys.54.35018

Vadthanarat S, Lumyong S, Raspé O (2020) *Heimioporus subcostatus*, a new Boletaceae species from northern and northeastern Thailand. Phytotaxa 475(1):018–028.

Vadthanarat S, Halling RE, Amalfi M, Lumyong S, Raspé O (2021) An unexpectedly high number of new *Sutorius* (Boletaceae) species from northern and northeastern Thailand. Frontiers in Microbiology 12: 1–27. https://doi.org/10.3389/fmicb.2021.643505

Vadthanarat S, Raspé O, Lumyong S (2022) *Rubinosporus auriporus* gen. et sp. nov. (Boletaceae: Xerocomoideae) from tropical forests of Thailand, producing unusual dark ruby spore deposits. Journal of Fungi 8(3): 278. https://doi.org/10.3390/jof8030278

Wu G, Feng B, Xu J, Zhu XT, Li YC, Zeng NK, Hosen MI, Yang ZL (2014) Molecular phylogenetic analyses redefine seven major clades and reveal 22 new generic clades in the fungal family Boletaceae. Fungal Diversity 69(1): 93–115. https://doi.org/10.1007/s13225-014-0283-8

Wu G, Zhao K, Li YC, Zeng NK, Feng B, Halling RE, Yang ZL (2015) Four new genera of the fungal family Boletaceae. Fungal Diversity 81(1): 1–24. https://doi.org/10.1007/s13225-015-0322-0

Wu G, Li YC, Zhu XT, Zhao K, Han LH, Cui YY, Li F, Xu JP, Yang ZL (2016) One hundred noteworthy boletes from China. Fungal Diversity 81(1): 25–188. https://doi.org/10.1007/s13225-016-0375-8

Wu G, Lee SML, Horak E, Yang ZL (2018) *Spongispora temasekensis*, a new boletoid genus and species from Singapore. Mycologia 110(5): 919–929. https://doi.org/10.1080/00275514.2018.1496387

Wu G, Li MX, Horak E, Yang ZL (2021) Phylogenetic analysis reveals the new genus *Amoenoboletus* from Asia and New Zealand. Mycologia 114(1): 144–156. https://doi.org/10.1080/00275514.2021.1971450

Xue R, Wu LL, Jiang S, Hao YJ, Chai H, Liang ZQ, Zeng NK, Su MS (2019) Two new species of the genus *Leccinellum* (Boletaceae, Boletales) from the south of China. Phytotaxa 411(2): 093–104. https://doi.org/10.11646/phytotaxa.411.2.1

Yang ZL, Trappe JM, Binder M, Sanmee R, Lumyong P, Lumyong S (2006) The sequestrate genus *Rhodactina* (Basidiomycota, Boletales) in northern Thailand. Mycotaxon 96: 133–140.

Zeng NK, Cai Q, Yang ZL (2012) *Corneroboletus*, a new genus to accommodate the southeastern Asian *Boletus indecorus*. Mycologia 104(6): 1420–1432. https://doi.org/10.3852/11-326

Zhang M, Li TH, Wang C-Q, Song B, Xu J (2015) *Aureoboletus formosus*, a new bolete species from Hunan Province of China. Mycological Progress 14(12): 118. https://doi.org/10.1007/s11557-015-1142-z

Zhang M, Li TH, Wang C-Q, Zeng N-K, Deng W-Q (2019) Phylogenetic overview of *Aureoboletus* (Boletaceae, Boletales), with descriptions of six new species from China. MycoKeys 61: 111–145. https://doi.org/10.3897/mycokeys.61.47520

Zhao K, Wu G, Feng B, Yang ZL (2014a) Molecular phylogeny of *Caloboletus* (Boletaceae) and a new species in East Asia. Mycological Progress 13(4): 1127–1136. https://doi.org/10.1007/s11557-014-1001-3

Zhao K, Wu G, Yang ZL (2014b) A new genus, *Rubroboletus*, to accommodate *Boletus sinicus* and its allies. Phytotaxa 188(2): 61–77. https://doi.org/10.11646/phytotaxa.188.2.1

Zhu XT, Wu G, Zhao K, Halling RE, Yang ZL (2015) *Hourangia*, a new genus of Boletaceae to accommodate *Xerocomus cheoi* and its allied species. Mycological Progress 14(6): 37. https://doi.org/10.1007/s11557-015-1060-0

MycoKeys 103: 167–213 (2024)
DOI: 10.3897/mycokeys.103.115799

Research Article

Systematic revision of species of *Atractilina* and *Spiropes* hyperparasitic on Meliolales (Ascomycota) in the tropics

Miguel A. Bermúdez-Cova[1,2], Tina A. Hofmann[3], Nourou S. Yorou[4], Meike Piepenbring[1]

1 *Mycology Research Group, Faculty of Biological Sciences, Goethe University Frankfurt Am Main, Frankfurt Am Main, Germany*
2 *Departamento de Biología de Organismos, División de Ciencias Biológicas, Universidad Simón Bolívar, Caracas, Venezuela*
3 *Centro de Investigaciones Micológicas (CIMi), Herbario UCH, Universidad Autónoma de Chiriquí, David, Panama*
4 *Research Unit Tropical Mycology and Plants-Soil Fungi Interactions (MyTIPS), Faculty of Agronomy, University of Parakou, BP 123, Parakou, Benin*
Corresponding author: Miguel A. Bermúdez-Cova (miguelangelbermudez11@hotmail.com)

Abstract

Atractilina Dearn. & Barthol. and *Spiropes* Cif. are genera of asexual fungi that comprise species mainly hyperparasitic on black mildews (Meliolales, Ascomycota). Although a common group of anamorphic fungi, they have been described up to now only by morphology and their systematic position is unknown. The present study provides a morphological treatise of all known species of *Atractilina* and *Spiropes* hyperparasitic on Meliolales, including insights into their systematic position, based on DNA sequences generated here for the first time. The study was conducted, based on 33 herbarium specimens and 23 specimens recently collected in Benin and Panama. The obtained DNA sequence data (28S rDNA and ITS rDNA) of *A. parasitica* and of two species of *Spiropes* show systematic placements in the Dothideomycetes and Leotiomycetes, respectively. The sequence data of the two *Spiropes* spp. do not group together. Moreover, the anamorph-teleomorph connection between *Atractilina parasitica* and *Malacaria meliolicola*, a pseudothecioid fungus, is confirmed. Three species in the genus *Spiropes* are proposed as new to science, namely *S. angylocalycis*, *S. carpolobiae* and *S. croissantiformis*. Four species are reported for Benin for the first time, three species for Panama and one species for mainland America. *Atractilina* and *Spiropes* are currently two genera with highly heterogeneous species and they might have to be split in the future, once the taxonomic concepts are validated by morphology and molecular sequence data.

Key words: Anamorph-teleomorph connection, Benin, Dothideomycetes, Hyperparasitism, Leotiomycetes, Panama

Academic editor: Gerhard Rambold
Received: 27 November 2023
Accepted: 8 March 2024
Published: 11 April 2024

Citation: Bermúdez-Cova MA, Hofmann TA, Yorou NS, Piepenbring M (2024) Systematic revision of species of *Atractilina* and *Spiropes* hyperparasitic on Meliolales (Ascomycota) in the tropics. MycoKeys 103: 167–213. https://doi.org/10.3897/mycokeys.103.115799

Introduction

Meliolales (Sordariomycetes, Ascomycota) form a large order of biotrophic, obligate plant parasitic fungi in the Tropics and subtropics (Piepenbring et al. 2011; Hongsanan et al. 2015; Zeng et al. 2017). The order comprises two families, Armatellaceae and Meliolaceae, with *Armatella* Theiss. & Syd. and *Meliola* Fr. being the most species-rich genera of each family, respectively (Hosagoudar 2003; Jayawardena et al. 2020). They are commonly known as “black mildews”,

because they produce black colonies that are composed of dark, thick-walled, branched, superficial hyphae (Rodríguez Justavino et al. 2015).

Approximately 200 species of hyperparasitic fungi, i.e. fungi parasitic on other parasites, have been reported to grow on colonies of Meliolales (Bermúdez-Cova et al. 2022, 2023a). These hyperparasites mainly belong to the Dothideomycetes and the Sordariomycetes, although the systematic positions of a large number of these fungi still remain unknown (Bermúdez-Cova et al. 2022; Bermúdez-Cova et al. 2023a). Hyperparasitic fungi frequently overgrow entire colonies of black mildews, so the meliolalean host may be detected only by careful search with a light microscope (Stevens 1918; Ciferri 1955; Bermúdez-Cova et al. 2023a).

Amongst the hyperparasitic fungi, species of the anamorphic genera *Atractilina* Dearn. & Barthol. and *Spiropes* Cif. are common hyperparasites of black mildews in the tropics. In the past, they were regarded as conidial stages of Meliolales (Ciferri 1955; Bermúdez-Cova et al. 2023b) and nowadays as incertae sedis in the Ascomycota (Bermúdez-Cova et al. 2022). The genus *Atractilina* includes six species of mostly hyperparasitic hyphomycetes with true synnemata, denticulate conidiogenous loci and pale pluriseptate conidia (Deighton and Pirozynski 1972; Mel'nik and Braun 2013). On the other hand, the genus *Spiropes* comprises 34 species of dematiaceous, mostly hyperparasitic hyphomycetes with mononematous, fasciculate or synnematous conidiophores (Ellis 1968, 1971, 1976; Seifert and Hughes 2000; Bánki et al. 2023). Species of *Spiropes* are characterised by the presence of conidiogenous cells with conspicuous, flat and numerous scars, as well as pigmented conidia with 1–9 septa or pseudosepta (Ellis 1968).

Arthrobotryum Ces., *Cercospora* Fresen. ex Fuckel, *Helminthosporium* Link, *Pleurophragmium* Costantin and *Podosporium* Schwein. are only a few of the many genera to which species of *Atractilina* and *Spiropes* have been assigned in the past, although they were not congeneric with the type specimens of those genera (Ellis 1968; Deighton and Pirozynski 1972; Alcorn 1988). This resulted in taxonomic uncertainty with species being transferred from one genus to another. This problem was initially addressed by Ellis (1968) and Deighton and Pirozynski (1972), as they did an extensive morphological revision of taxa now assigned to *Atractilina* or *Spiropes*. For example, all the synnematous fungi, hyperparasitic on Meliolales formerly assigned to the genus *Arthrobotryum*, were transferred to the genus *Spiropes* by Ellis (1968), with the exception of *A. parasiticum* (Winter) Hansf., which was transferred to the genus *Atractilina* by Deighton and Pirozynski (1972).

There is currently one valid species of *Atractilina*, namely *A. parasitica* (G. Winter) Deighton & Piroz. and 19 species of the genus *Spiropes* known to be hyperparasitic on colonies of Meliolales (Ellis 1968; Deighton and Pirozynski 1972; Mel'nik and Braun 2013; Bermúdez-Cova et al. 2022). However, species delimitation within these two genera has up to now been done by morphology only, as species were described in the past before the molecular era and because of the challenges of isolating DNA from mixed infections (Bermúdez-Cova et al. 2022, 2023a, 2023b). As a result, the systematic position of both genera within the Ascomycota remained unknown. The present study revises the morphology of the species of *Atractilina* and *Spiropes* and provides the first insights into their systematic position according to molecular sequence data, with emphasis on the species hyperparasitic on Meliolales.

Materials and methods

Sample collection and morphological characterisation

Samples of leaves infected with black mildews were opportunistically collected in western Panama from January-March 2020 and in Benin in February as well as September-October 2022. For the present study, colonies of Meliolales hyperparasitised by *Atractilina parasitica* and species of *Spiropes* were considered. Infected leaves were dried in a plant press and deposited in the Herbarium at the Universidad Autónoma de Chiriquí (UCH, specimens from Panama) or in the Mycological Herbarium of the University of Parakou (UNIPAR) in Benin. Duplicates of large-sized samples were deposited in the Botanische Staatssammlung München (M). In some cases, fungal tissue was collected prior to drying of the specimens and preserved in CTAB buffer for subsequent DNA extraction.

Dried specimens were observed by stereomicroscopy and by light microscopy (LM). Measurements of at least 20 conidia and other structures have been made for each specimen at magnifications of 600× and 1000×. Measurements are presented as mean value ± standard deviation with extreme values in parentheses. Line drawings were made freehand on scaled paper. Scars on conidiophores are drawn in surface view although further cells of the conidiophore are drawn in optical sections. Images and drawings were edited with Photoshop (Adobe, San Jose, California). Specimens were also analysed morphologically by scanning electron microscopy (SEM). Materials used for SEM were prepared according to Hofmann et al. (2010).

Host plant identification

Host plants were identified by morphological characteristics and, in some cases, by molecular sequence data. Morphological identifications were made by comparison with herbarium specimens, literature (e.g. Akoègninou et al. (2006); Condit et al. (2011)) and with the help of local botanists. Molecular sequence data for species identifications were obtained by polymerase chain reaction (PCR) for the amplification of the partial region of chloroplast rbcL with the primer pairs rbcLa-F (Levin et al. 2003) and rbcLa-R (Kress et al. 2009). DNA was extracted from approx. 0.05 g of leaf tissue dried with silica gel using the innuPREP Plant DNA Kit (Analytik Jena, Germany) and following the manufacturer's instructions. Protocols for PCR were carried out as described by Fazekas et al. (2012).

DNA extraction, PCR amplification and sequencing of fungal DNA

DNA was isolated from the synnemata and hyphae of specimens using the E.Z.N.A Forensic DNA Extraction Kit, following the manufacturer's instructions. To extract total genomic DNA, a small amount of clean synnemata or single conidiophores were transferred into a sterile Eppendorf tube with approx. 200 µl of distilled water using sterilised tweezers and trying to avoid picking cells of any other organism associated with the leaves and the colonies of black mildews. For example, for the synnemata of *Atractilina parasitica* and *Spiropes melanoplaca*, only the upper parts were used for DNA extraction, in order to avoid the basal parts that are in direct contact with cells of other organisms.

The samples were frozen for 24 h at -20 °C, and later homogenised for 10–12 min. using a Retsch Mixer Mill MM301 with TL buffer and 2.5 mm Zirconia beads. Isolated DNA was re-suspended in elution buffer and stored at -20 °C.

Two partial nuclear gene regions (ribosomal loci) were amplified and sequenced: For the large subunit nuclear ribosomal DNA (nrLSU, 28S rDNA), the primers LR0R (Wagner and Ryvarden 2002) and LR5 (Vilgalys and Hester 1990) were used. For the internal transcribed spacer region of ribosomal DNA (ITS), the primers ITS5 and ITS4 (White et al. 1990) were used. The PCR mixtures consisted of 1 µl genomic DNA, 15× $MgCl_2$ reaction buffer (Bioline, Luckenwalde, Germany), 25 mM $MgCl_2$, 25 µM of each dNTP, 10 µM of each primer and 5 U Taq DNA polymerase (VWR) in a total volume of 30 µl. Cycling parameters of the PCR were as follows: initial denaturation at 94 °C for 3 min, followed by 35 cycles of amplification [denaturation at 94 °C for 30 s, primer annealing at 52 °C for 30 s and primer extension at 72 °C for 45 s] and a final extension at 72 °C for 5 min, followed by storage at 8 °C. PCR-products were checked on 1.5% agarose electrophoresis gels containing HDGreenPlus DNA stain. Amplified PCR products were purified with the Cycle Pure Kit (VWR-Omega, USA). Sequencing was performed at Seqlab GmbH, Germany.

Phylogenetic analyses

Consensus sequences of trace files were generated with Geneious 10.2.2 (https://www.geneious.com, Kearse et al. 2012) and searched against GenBank (https://www.ncbi.nlm.nih.gov/, Benson et al. 2014) with MegaBLAST. Ambiguous and miscalled bases were corrected, when possible, after examination of the corresponding chromatogram files. Sequences with a high similarity were aligned with MAFFT v. 7 using the L-INS-i algorithm (Nakamura et al. 2018). The alignments were manually checked by using MEGA v. 7 (Kumar et al. 2016). Gblocks v. 0.91b (Talavera and Castresana 2007) was used to remove poorly-aligned positions and divergent regions from the DNA alignment. Phylogenetic analyses of this study were conducted by applying Maximum Likelihood (ML) in RAxML-HPC2 v.8.2.12 (Stamatakis 2014) on XSEDE (Miller et al. 2010) and Bayesian phylogenetic inference with the programme MrBayes 3.2.6. (Ronquist et al. 2012) on XSEDE (Miller et al. 2010), available on the CIPRES Science Gateway web portal (http://www.phylo.org/sub_sections/portal/). The alignment and tree are included in Suppl. material 1.

We also used T-BAS 2.1 (Carbone et al. 2019) and the "Place Unknowns" tool to place newly-generated ITS sequences on to the Pezizomycotina tree version 2. Two FASTA files of the newly-generated ITS sequences of *Spiropes* were uploaded to the T-BAS interface. We selected the "de novo" option for the RAxML placement, with 500 bootstrap replicates.

Results

Taxonomy

Based on morphological evidence, the hyperparasitic fungi collected in Panama and Benin are assigned to the genera *Atractilina* or *Spiropes*. Amongst these, three species are proposed as new to science, all in the genus *Spiropes*.

Four species represent new reports for Benin and three for Panama. We also present a revision from herbarium material of 17 of the 19 known species of the genus *Spiropes* and one species of *Atractilina* hyperparasitic on Meliolales. All species synonyms, unless specified, are taken from Deighton and Pirozynski (1972) for *Atractilina parasitica* and from Ellis (1968) for species of *Spiropes*.

Atractilina **Dearn. & Barthol., Mycologia 16: 175, 1924.**

Atractilina parasitica **(G. Winter) Deighton & Piroz., Mycol. Pap. 128: 34, 1972**
Fig. 1

≡ *Arthrosporium parasiticum* G. Winter, Hedwigia 25: 103, 1886.
≡ *Arthrobotryum parasiticum* (G. Winter) Hansf., Proc. Linn. Soc. Lond. 155: 64, 1943.
= *Isariopsis penicillata* Ellis & Everh., Bull. Torrey bot. Club 22: 438, 1895.
≡ *Phaeoisariopsis penicillata* (Ellis & Everh.) S.C. Jong & E.F. Morris, Mycopath. Mycol. appl. 34: 271, 1968.
= *Arthrobotryum tecomae* Henn., Hedwigia 43: 397, 1904.
= *Arthrobotryum caudatum* Syd. & P. Sydow, Etudes sur la Flore du Bas et Moyen Congo 3(1): 22, 1909.
= *Arthrobotryum dieffenbachiae* F. Stevens, Bot. Gaz. 65: 237, 1918.
= *Atractilina callicarpae* Dearn. & Barthol., Mycologia 16: 175, 1924.
= *Podosporium pallidum* Pat., Scient. Surv. P. Rico 8(1) Bot.: 103, 1926.
= *Eriomycopsis bosquieae* Hansf., Bothalia 4(2): 466, 1942.
= *Arthrobotryum deightonii* Hansf., Mycol. Pap. 15: 218, 1946.
= *Malacaria meliolicola* Syd., Annls. Mycol. 28(1/2): 69, 1930. New synonym proposed in this study.
= *Paranectria flagellata* Hansf., Proc. Linn. Soc. London 153(1): 28, 1941. New synonym proposed in this study.
≡ *Malacaria flagellata* (Hansf.) Hansf., Mycol. Pap. 15: 128, 1946. New synonym proposed in this study.

Description. ***Colonies*** effuse, rust brown or pale brown, with hyphae that form large, erect, dark synnemata clearly visible under the stereomicroscope, but sometimes only loose unstalked tufts around the tips of the setae of the meliolalean host. ***Hyphae*** superficial, branched, septate, thin-walled, 1–2.5 µm wide, smooth. ***Conidiophores*** may form straw-coloured or pale olivaceous synnemata up to 1.5 mm long, 40 µm wide at the basal stalk-like part. Sometimes the synnemata grow around and up the setae of the meliolalean host. Individual conidiophores straight or sometimes flexuous, cylindrical, 2.5–5 µm thick towards the apex, pale olivaceous brown, with denticles. ***Conidia*** solitary, straight or slightly curved, fusiform, truncate at the base, tapering towards the apex and often terminating in a little bulbous swelling, 1 to mostly 3 septate, thin-walled, variable in size, (17–)30–37(–80) × (3.5–)7–8.5 µm, at first more or less colourless, at maturity becoming pale straw coloured, minutely rough-walled. As seen by SEM, the ornamentation of the surface of the conidia is distinctly reticulated, with thin networks and no ridges.

Specimens examined. On *Meliola* sp. on living leaves of *Opilia celtidifolia* (Opiliaceae), Benin, Campus University of Abomey-Calavi, botanical garden, 6°25'7"N,

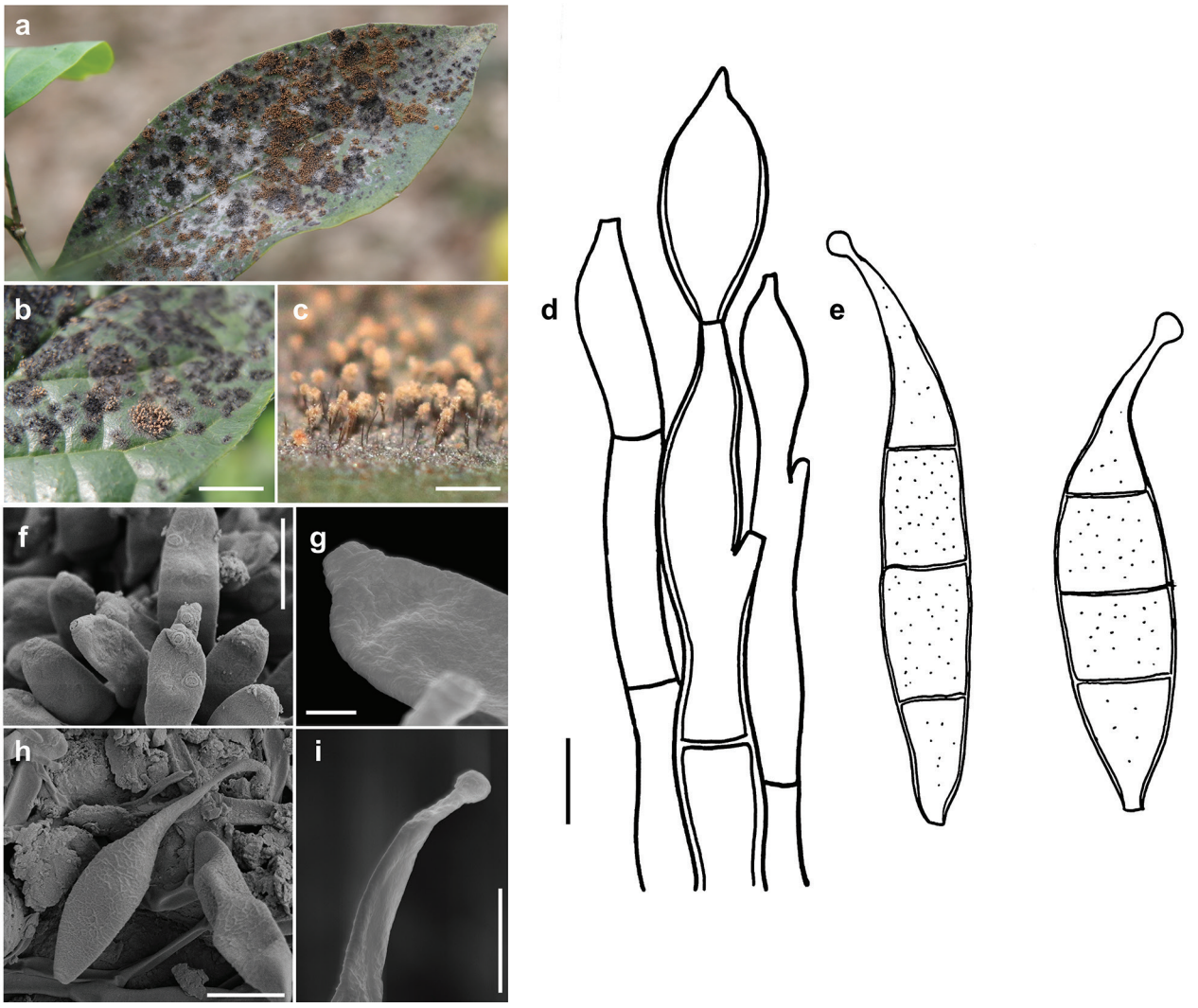

Figure 1. *Atractilina parasitica* (MB127, MB136) **a** synnemata (gold spots) on colonies of *Meliola* sp. (black spots) on a leaf of *Opilia celtidifolia* **b** synnemata of (gold spots) on colonies of *Meliola clerodendricola* (black spots) on a leaf of *Clerodendrum capitatum* **c** synnemata **d** conidiophores drawn in optical section. The thickness of the wall is indicated only in the drawing in the middle **e** conidia shown in optical section **f–i** as seen by SEM **f** conidiophores with denticles **g** a denticle at the tip of a conidiophore **h** conidium **i** bulbous swelling at the tip of a conidium. Scale bars: 1.5 mm (**b**); 1 mm (**c**); 5 µm (**d,e,i**); 8 µm (**f**); 1 µm (**g**); 6 µm (**h**).

2°20'34"E, 24 m a.s.l., 9 February 2022, M. A. Bermúdez-Cova, A. Tabé, D. Dongnima, O.P. Agbani, M. Piepenbring, N.S. Yorou, MB127 (UNIPAR, M); on *Meliola clerodendricola* on living leaves of *Clerodendrum capitatum* (Lamiaceae), Benin, Abomey-Calavi, Zopah, 6°30'8"N, 2°20'24"E, 37 m a.s.l., 12 February 2022, M. A. Bermúdez-Cova, A. Tabé, D. Dongnima, O.P. Agbani, M. Piepenbring, N.S. Yorou, MB133; on *Meliola clerodendricola* on living leaves of *Clerodendrum capitatum*, Benin, Allada, Sékou, 6°38'56"N, 2°11'38"E, 48 m a.s.l., 12 February 2022, M. A. Bermúdez-Cova, A. Tabé, D. Dongnima, O.P. Agbani, M. Piepenbring, N.S. Yorou, MB136 (UNIPAR, M, GenBank accession number: OR804686); on *Meliola* sp. on living leaves of *Pterocarpus santalinoides* (Fabaceae), Benin, Lokoli, border of forest, 7°3'41"N, 2°15'26"E, 22 m a.s.l., 20 February 2022, M. A. Bermúdez-Cova, A. Tabé, D. Dongnima, L. Konetche, M. Piepenbring, R. Hounkarin, MB160 (M);

on *Meliola* sp. on living leaves of *Coffea arabica* (Rubiaceae), Benin, Attogon, Niaouli, CRA-Sud center, 6°44'24"N, 2°8'25"E, 122 m a.s.l., 28 February 2022, M. A. Bermúdez-Cova, A. Tabé, I. Agonglo, M. Piepenbring, N.S. Yorou, O.P. Agbani, MB178 (UNIPAR, M, GenBank accession numbers: OR804685 and OR804687); on *Meliola* sp. on living leaves of *Coffea arabica*, Benin, Atlantique, Attogon, Niaouli Forest, 6°44'23"N, 2°8'26"E, 119 m a.s.l., 19 September 2022, A. Krauß, A. Tabé, O. Koukol, N.S. Yorou, AK06H (UNIPAR, M, GenBank accession number: OR804684); on *Meliola* sp. on living leaves of *Clerodendrum capitatum*, Benin, Atlantique, Attogon, Pahou Forest, 6°22'56"N, 2°9'35"E, 13 m a.s.l., 6 October 2022, A. Krauß, A. Tabé, O. Koukol, N.S. Yorou, AK61.

Additional specimens examined. On *Meliola lasiotricha* on leaves of unknown plant host, Puerto Rico, 1926, M.B. Ellis (IMI 130722, type specimen of *Podosporium pallidum*); On *Meliola clerodendri* on leaves of *Clerodendrum cyrtophyllum*, Taiwan, 1938, W. Yamamoto (IMI 31921b, type specimen of *Atractilina parasitica*).

Illustrations. This species was illustrated by Deighton and Pirozynski (1972).

Known hosts and distribution. On colonies of *Amazonia* spp., *Asteridiella* spp., *Irenopsis* spp. and *Meliola* spp. on living leaves of various plants in Congo, Ghana, Guinea, India, Mauritius, Nigeria, Perú, Philippines, Puerto Rico, Sierra Leone, St. Thomé, Taiwan, Tanzania, Uganda, U.S.A. and Venezuela. Only one single collection on *Balladyna* sp. (Balladynaceae, Dothideomycetes) as a fungal host (Deighton and Pirozynski 1972). *Atractilina parasitica* is reported here for the first time for Benin.

Notes. Only two species of the genus *Atractilina* with hyperparasitic lifestyle are known, namely *A. asterinae* and *A. parasitica* (Deighton and Pirozynski 1972). *Atractilina asterinae* differs from *A. parasitica* by the presence of 3–10 septate, thick-walled conidia.

The specimens of *A. parasitica* collected on leaves of *Coffea arabica* (MB 178, AK4H, AK06H) were found growing together with pseudothecia of *Malacaria meliolicola* Syd. (Tubeufiales, Dothideomycetes). According to Hansford (1941, as *Paranectria flagellata*; 1946), *M. flagellata* is most probably the perfect state of *A. parasitica*. The specimens collected by Hansford were also growing on coffee leaves. The latter and the fact that the DNA sequences we obtained from *A. parasitica* (GenBank accession numbers: OR804684, OR804686, OR804685 and OR804687) and *M. meliolicola* (GenBank accession numbers: OR805247 and OR805248) clustered together in one single strongly-supported clade (Fig. 22), confirm the anamorph-teleomorph connection between both species. For an updated species description of *M. meliolicola*, see Bermúdez-Cova et al. (2023b).

Spiropes Cif., Sydowia 9(1–6): 302, 1955

Spiropes angylocalycis Berm.-Cova & M. Piepenbr., sp. nov.

MycoBank No: 850990
Fig. 2

Holotype. On *Meliola* sp. on living leaves of *Angylocalyx oligophyllus* (Fabaceae), Benin, Atlantique, Attogon, Niaouli Forest, 6°44'42"N, 2°7'50"E, 69 m a.s.l.,

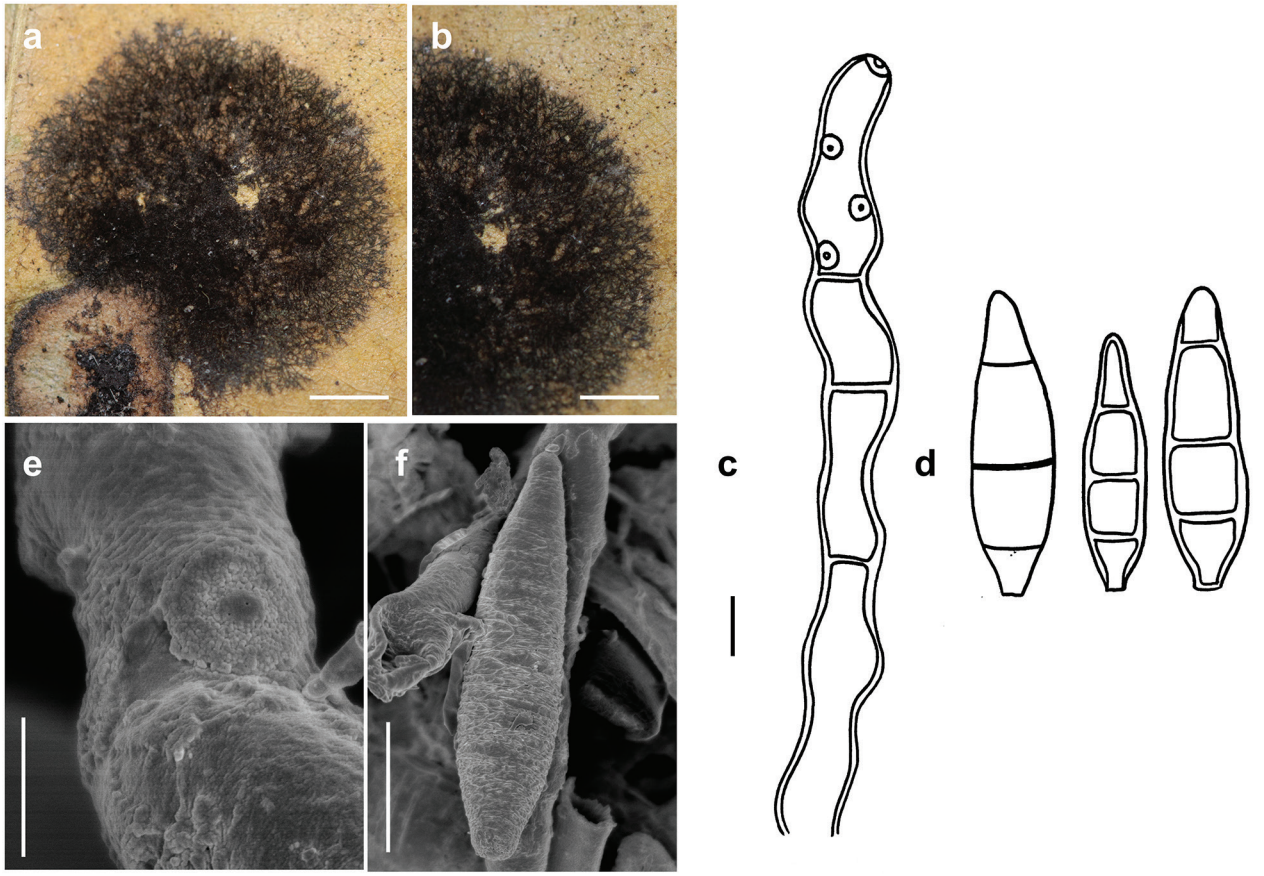

Figure 2. *Spiropes armatellae* (MB 167) **a, b** conidiophores growing intermingled with hyphae of *Meliola* sp. on leaves of *Angylocalyx oligophyllus* **c** conidiophore with scars **d** conidia shown in optical section. The thickness of the wall is shown in the two drawings on the right-hand side **e, f** as seen by SEM **e** part of a conidiophore with scar **f** conidium. Scale bars: 0.3 mm (**a**); 0.2 mm (**b**); 5 µm (**c, d**); 2 µm (**e**); 7 µm (**f**).

28 February 2022, M.A. Bermúdez, A. Tabé, D. Dongnima, I. Agonglo, O.P. Agbani, M. Piepenbring, N.S. Yorou, MB167 (M).

Etymology. Named after the genus of the host plant.

Description. ***Colonies*** effuse, dark brown to black, velvety to hairy. ***Hyphae*** superficial, branched, anastomosing, septate, 0.5–2 µm wide, straw-coloured, smooth. ***Conidiophores*** arising singly, erect or ascending, straight to flexuous, mostly flexuous at the tips, septate, up to 350 µm long, 4–6 µm thick, pale olivaceous-brown to brown, with rough surface, with scattered scars mostly in upper parts of the conidiophores. ***Conidia*** solitary, straight or slightly curved, fusiform to obclavate, 3–septate, (15–)17–25(–30) × 5–6.5 µm, 2–3 µm wide at the base, brown, the cells at each end pale brown, septa darker in colour, verrucose. As seen by SEM, the ornamentation of the spores is distinctly reticulated, with thin to thick networks and no ridges.

Known distribution. On colonies of *Meliola* sp. on living leaves of *Angylocalyx oligophyllus* in Benin.

Notes. *Spiropes angylocalycis* is similar to *S. clavatus* by the presence of 3–septate mostly fusiform conidia, with a similar size range (Ellis 1968). However, the conidiophores of *S. clavatus* are synnematous, while they are mononematous in *S. angylocalycis*.

***Spiropes armatellae* M.B. Ellis, Mycol. Pap. 125: 15, 1971**
Fig. 3

Type. On *Armatella cinnamomicola* on leaves of *Cinnamomum* sp. (Lauraceae), Sri Lanka, Ceylon, 1971, M.B. Ellis (IMI134405b. The type specimen was not available for loan).

Description. ***Colonies*** effuse, dark brown to black, hairy. ***Hyphae*** superficial, branched, septate, 1–3 µm wide, straw-coloured, smooth. ***Conidiophores*** arising singly, erect or ascending, straight to flexuous, mostly flexuous at their tips, septate, up to 300 µm long, 5–8 µm thick, brown to dark brown, paler towards the apex, with rough surface, with scattered scars in upper parts of the conidiophores. ***Conidia*** solitary, straight or slightly curved, obclavate to obpyriform, mostly 1–septate, (20–)30–42(–50) × (6–)7–8(–10) µm, 2–3.5 µm wide at the base, brown, paler towards the ends, verrucose when seen by LM and SEM.

Specimen examined. On *Armatella litseae* on leaves of *Daphnidium pulcherrimum* (Lauraceae), India, west Bengal, 1967, M.K. Maity (IMI 136371); on *Armatella cinnamomicola* on leaves of *Cinnamomum* sp., Myanmar, Thaton, 1971, M.M. Thaung, (IMI 161265).

Known hosts and distribution. On colonies of *Armatella* spp. on various plants in India, Myanmar and Sri Lanka (Ellis 1971).

Illustrations. This species was illustrated by Ellis (1971).

Notes. Two known species of *Spiropes* are hyperparasitic on species of the genus *Armatella* (Meliolales, Armatellaceae), namely *S. armatellae* and *S. armatellicola* (Ellis 1971, Hosagoudar et al. 2002). According to Hosagoudar et

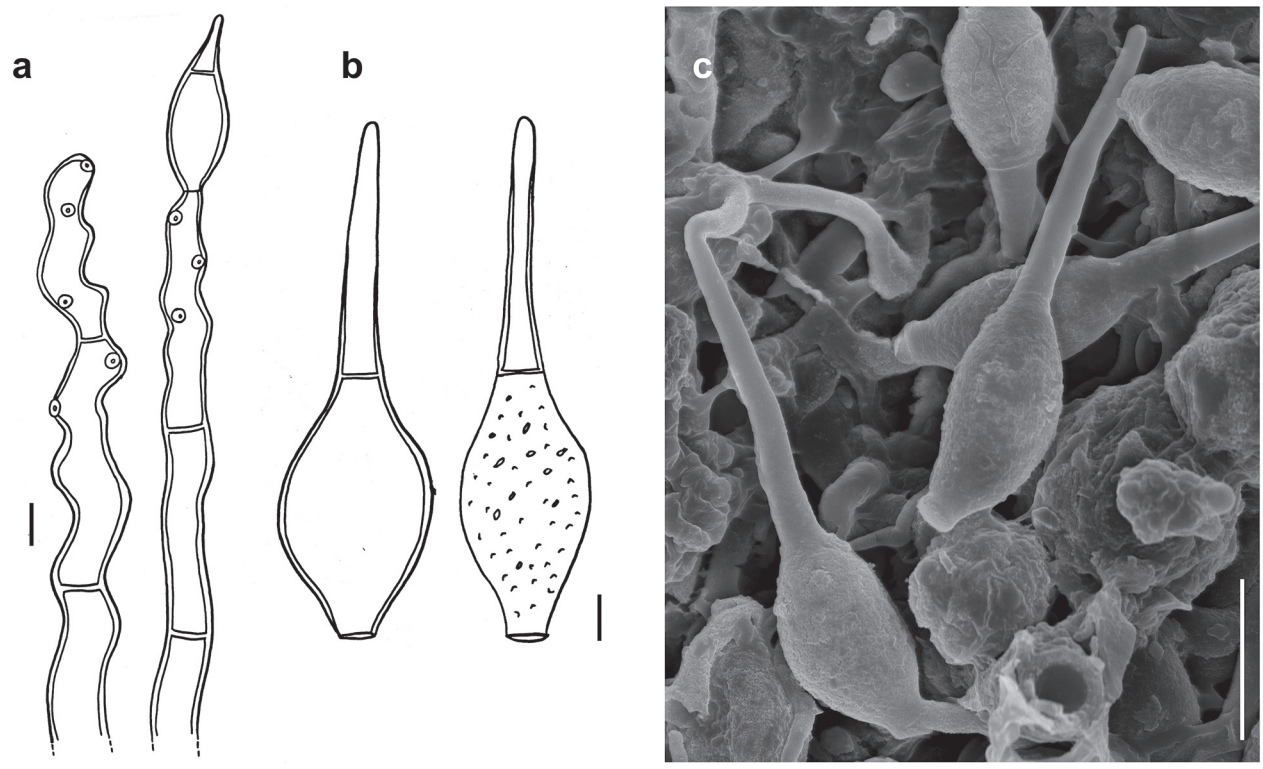

Figure 3. *Spiropes armatellae* (IMI 161265) **a** conidiophores with young conidium **b, c** conidia **b** shown in optical section. The thickness of the wall is indicated only in the drawing on the left-hand side **c** as seen by SEM. Scale bars: 5 µm (**a**); 2.5 µm (**b**); 10 µm (**c**).

al. (2002), both species are similar, but differ by the ornamentation of the conidia. The conidia of *S. armatellicola* are smooth, while those of *S. armatellae* are distinctly reticulated. However, it is sometimes difficult to observe the surface of the conidia by LM. Therefore, we recommend to analyse the ornamentation of the spores of *S. armatellicola* by SEM. The scars of *S. armatellae* could not be observed by SEM and it is necessary to collect fresh specimens of this fungus for further morphological analysis.

Spiropes armatellicola **M.B. Ellis, Mycol. Pap. 125: 15, 1971**

Type. On *Armatella* sp. on leaves of *Actinodaphne* sp. (Lauraceae), Banasuran Hills, Wyanad, Kerala, India, 16 April 1999, C.K. Biju (HCIO 43621. The type specimen was not available for loan by HCIO).

Species description. This species was described by Hosagoudar et al. (2002).

Known hosts and distribution. On colonies of *Armatella* sp. on living leaves of *Actinodaphne* sp. in India (Hosagoudar et al. 2002).

Illustrations. This species was illustrated by Hosagoudar et al. (2002).

Notes. This species is only known from the type specimen.

Spiropes capensis **(Thüm.) M.B. Ellis, Mycol. Pap. 114: 5, 1968**
Fig. 4

≡ *Cercospora capensis* (Thüm.) Sacc., Syll. fung. 4: 469, 1886.
≡ *Helminthosporium capense* (Thüm.) [as '*Helmisporium*'], Flora, Regensburg 59: 570, 1876.
≡ *Pleurophragmium capense* (Thüm.) S. Hughes, Can. J. Bot. 36: 796, 1958.
= *Helminthosporium carpocrinum* Cif. [as '*Helmisporium*'], Annls. Mycol. 36(2/3): 236, 1938.
= *Helminthosporium coffeae* Massee [as '*Helmisporium*'], Bull. Misc. Inf., Kew: 167, 1901.
≡ *Sporhelminthium coffeae* (Massee) Speg., Physis, Rev. Soc. Arg. Cienc. Nat. 4(no. 17): 292, 1918.
= *Helminthosporium fici* H.S. Yates [as '*ficuum*'], Philipp. J. Sci. (Bot.) 13: 382, 1918.
= *Helminthosporium ficinum* Sacc. [as '*Helmisporium*'], Atti Accad. Sci. Ven.-Trent.-Istr., Sér. 3, 10: 90, 1919.
= *Helminthosporium fumagineum* Sacc. [as '*Helmisporium*'], Atti Accad. Sci. Ven.-Trent.-Istr., Sér. 3, 10: 90, 1919.
= *Helminthosporium filicicola* Henn., Hedwigia 44: 71, 1905.
= *Helminthosporium glabroides* F. Stevens [as '*Helmisporium*'], Bot. Gaz. 65(3): 240, 1918.
= *Helminthosporium melioloides* Sacc. [as '*Helmisporium*'], Atti Accad. Sci. Ven.-Trent.-Istr., Sér. 3, 10: 89, 1919.
= *Helminthosporium orbiculare* Lév., Annls. Sci. Nat., Bot., Sér. 3, 5: 299, 1846.
= *Helminthosporium philippinum* Sacc. [as '*Helmisporium*'], Atti Accad. Sci. Ven.-Trent.-Istr., Sér. 3, 10: 89, 1919.

= *Helminthosporium subsimile* Sacc., Boll. Orto bot., Napoli 6: 23, 1921.
= *Helminthosporium tapurae* Allesch., Hedwigia 36(4): 245, 1897.
= *Napicladium portoricense* Speg., Boln Acad. nac. Cienc. Córdoba 26(2–4): 363, 1921.
≡ *Helminthosporium portoricense* (Speg.) Cif., Sydowia 9(1–6): 298, 1955.
= *Nascimentoa pseudoendogena* Cif. & Bat., Publicações Inst. Micol. Recife 44:4, 1956.

Description. ***Colonies*** effuse, dark brown to black, hairy (Ellis 1968). ***Hyphae*** superficial, branched, septate, 2–4 µm wide, pale olive to olivaceous-brown, smooth. ***Conidiophores*** arising singly or in groups, sometimes in large groups of 50–100 conidiophores, terminally or laterally from the hyphae, erect or ascending, straight or flexuous, septate, up to 600 µm long, 5–9 µm thick along most of their length, brown to dark brown, paler closer to the apex, with terminal and lateral scars. ***Conidia*** solitary, straight or curved, fusiform to obclavate, truncate at the base, 3–6 (usually 4 or 5) pseudosepta, (33–)50–60(–78) × (5.5–)6–11(–16) µm, 1–4 µm wide at the base, light brown to brown, smooth.

Specimen examined. On *Meliola* sp. on living leaves of *Coffea arabica*, Benin, Atlantique, Attogon, Niaouli Forest, 6°44'23"N, 2°8'26"E, 119 m a.s.l., 19 September 2022, A. Krauß, A. Tabé, O. Koukol, N.S. Yorou, AK06H.

Additional specimens examined. – On leaves of *Ficus ulmifolia* (Moraceae), Philippines, Los Baños, 1915, C.F. Baker, 451 (IMI 130940, type of *Helminthosporium fumagineum*); on *Meliola compositarum* on leaves of *Eupatorium portoricense*

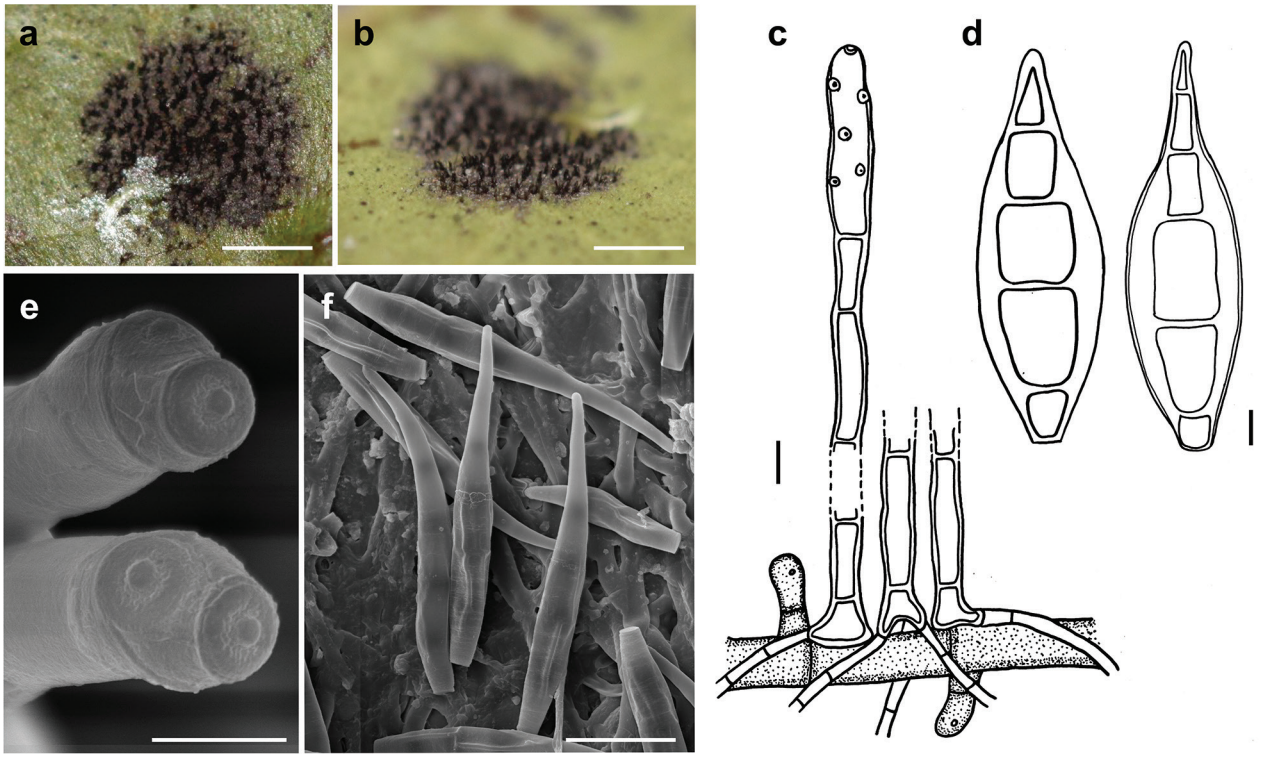

Figure 4. *Spiropes capensis* (AK06H) **a, b** groups of conidiophores growing on hyphae of *Meliola* sp **c** conidiophores growing on hyphae of *Meliola* sp. shown in optical section **d** conidia shown in optical section. The thickness of the outer wall layer is indicated only in the drawing on the right-hand side **e, f** as seen by SEM **e** conidiophores with scars **f** conidia. Scale bars: 1 mm (**a, b**); 8.5 µm (**c**); 5 µm (**d**); 5 µm (**e**); 20 µm (**f**).

(Asteraceae), Puerto Rico, Bega Vaja, 1921, no. 1753 (IMI 100331a, type of *Napicladium portoricense*).

Known hosts and distribution. On colonies of *Appendiculella* spp., *Asteridiella* spp., *Irenopsis* spp. and *Meliola* spp. on living leaves of various plants in Amboina, Bolivia, Brazil, Cameroon, Congo, Dominican Republic, Ghana, India, Jamaica, Malaya, Peru, Philippines, Puerto Rico, Sabah, Sierra Leone, South Africa, Tanzania, Trinidad, Uganda and Venezuela (Ellis 1968); on *Meliola* sp. on living leaves of *Coffea arabica* in Benin (this study). *Spiropes capensis* is reported here for the first time for Benin.

Illustrations. This species was illustrated by Ellis (1968).

Notes. According to the nomenclatural and taxonomic database Index Fungorum (http://www.IndexFungorum.org), the current name of the *Spiropes capensis* is *Pleurophragmium capense* (Thüm.) S. Hughes. The genus *Pleurophragmium* (*incertae sedis*, Ascomycota) was established by Costantin (1888) and it comprises species with brown to dark brown conidiophores and sympodially proliferating, denticulate conidiogenous cells producing holoblastic, simple, mostly 3–septate, brown to dark brown conidia (Abarca et al. 2007). According to Ellis (1968), the flat double scar is a good taxonomic character to distinguish species of *Spiropes* from *Pleurophragmium*, since, in the latter, the conidia are borne at the tips of tapered denticles. The morphological analysis of our samples and the type specimens (AK06H, IMI 100331a and IMI 130940) revealed the presence of flat double scars (Fig. 4e) and no denticles. We think that the examined species differs morphologically from species in the genus *Pleurophragmium* and, therefore, it should be retained in the genus *Spiropes*.

Spiropes caribensis **Hol.-Jech., Česká Mykol. 38(2): 113, 1984**
Fig. 5

Description. ***Colonies*** effuse, dark brown to black, velvety to hairy. ***Hyphae*** superficial, branched, septate, 1.5–3.5 µm wide, pale olivaceous-brown, smooth. ***Conidiophores*** arising singly, erect or ascending, straight or flexuous, septate, up to 240 µm long, 4–8 µm thick, pale brown to brown, smooth, with few scars. ***Conidia*** solitary, straight or slightly curved, obclavate, central cells barrel-shaped, 3-septate, (30–)36–48(–41.5) × (7.5–)9.5–11.5 µm, 4.5–6 µm wide at the truncate base, the central cells pale brown, the cells at the ends paler and almost hyaline, smooth.

Specimen examined. On *Meliola* sp. on leaves of an unknown palm-tree, Cuba, Isla de La Juventud (= Isla de Pinos), Los Indios, south-west of La Cañada, 1981, V. Holubová-Jechová (PRM 831531, holotype).

Known hosts and distribution. On *Meliola* sp. on living leaves of an unidentified palm tree in Cuba (Holubová-Jechová and Sierra 1984).

Illustrations. This species was illustrated by Holubová-Jechová and Sierra (1984).

Notes. *Spiropes caribensis* is similar to *S. helleri*, but differs from the latter by paler conidia, with wider truncate base (*S. helleri* has conidia with a truncate base 3–4 µm wide) and shorter conidiophores (up to 600 µm long in *S. helleri*; Holubová-Jechová and Sierra (1984)). As seen by SEM, conidia of *S. caribensis* are smooth (Fig. 5b), while conidia of *S. helleri* are distinctly

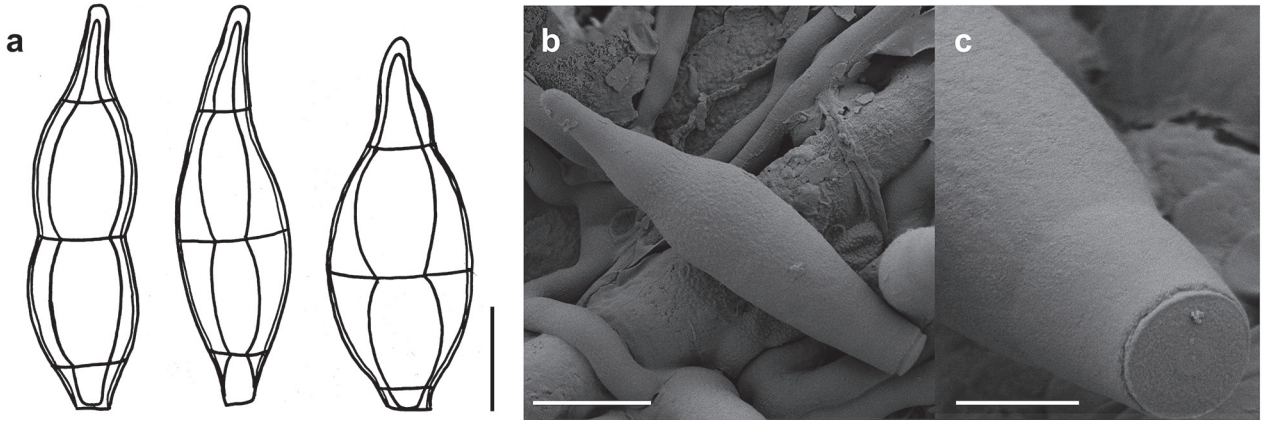

Figure 5. *Spiropes caribensis* (PRM 8311531) **a** conidia shown in optical section **b, c** as seen by SEM **b** conidium **c** basis of a conidium with a flat scar. Scale bars: 10 µm (**a**); 9 µm (**b**); 4 µm (**c**).

reticulated (Fig. 13e). The scars could not be observed by SEM and it is, therefore, necessary to collect fresh specimens of this fungus for further morphological analyses. *S. caribensis* is only known from the type specimen.

Spiropes carpolobiae **Berm.-Cova & M. Piepenbr., sp. nov.**
MycoBank No: 850987
Fig. 6

Holotype. On *Meliola* cf. *carpolobiae* on living leaves of *Carpolobia lutea* (Polygalaceae), Benin, Atlantique, Attogon, Niaouli Forest, 6°44'41"N, 2°7'52"E, 68 m a.s.l., 28 February 2022, M.A. Bermúdez, A. Tabé, D. Dongnima, I. Agonglo, O.P. Agbani, M. Piepenbring, N.S. Yorou, MB166 (M).

Etymology. Named after the genus of the host plant.

Description. ***Colonies*** effuse, dark brown to black, velvety to hairy. ***Hyphae*** superficial, branched, anastomosing, septate, 1–2 µm wide, straw-coloured, smooth. ***Conidiophores*** arising singly, erect or ascending, straight to flexuous, septate, up to 250 µm long, 2–5 µm thick, sometimes thicker at the apex, brown, not smooth, with scattered scars mostly in the upper parts of the conidiophores. ***Conidia*** solitary, straight or slightly curved, ovate to slightly fusiform, 3–septate, (12.5–)13–16(–19) × 5–7 µm, 2–2.5 µm wide at the base, brown, the cells at each end pale brown, septa darker, surface verrucose. As seen by SEM, the ornamentation of the conidia is distinctly reticulated, with thin to thick networks that can form ridges.

Known distribution. On colonies of *Meliola* cf. *carpolobiae* on living leaves of *Carpolobia lutea* in Benin.

Notes. *S. carpolobiae* is the only known species of *Spiropes* with ovate to slightly fusiform conidia.

Spiropes clavatus **(Ellis & Martin) M.B. Ellis, Mycol. Pap. 114: 25, 1968**
Fig. 7

≡ *Isariopsis clavata* Ellis & Martin, Am. Nat. 18: 188, 1884.

≡ *Arthrobotryum clavatum* (Ellis & Martin) Höhn, Sber. Akad. Wiss. Wien, Math.-naturw. Kl., Abt. 1, 125: 120, 1916.

≡ *Bitunicostilbe clavata* (Ellis & Martin) M. Morelet, Bull. Soc. Sci. nat. Arch. Toulon et du Var 7: 195, 1971.

= *Podosporium chlorophaeum* Speg., An. Mus. nac. Hist. nat. B. Aires 20: 450, 1910.

= *Arthrobotryum noz-moscatae* Bat. & J. Silva, Anais IV Congr. Soc. bot. Brasil: 144, 1953.

Description. ***Colonies*** effuse, brown to dark brown or black. ***Hyphae*** superficial, branched, anastomosing, septate, 1–3 µm wide, pale olivaceous-brown. ***Conidiophores*** tightly packed to form dark brown to blackish synnemata up to 700 µm long, 20–40 µm thick, often splaying out to a width of up to 110 µm at the apex. Individual hyphae straight or flexous, cylindrical, 1–3 µm thick near the base, 4–7 µm thick near the apex, dark brown, paler towards the apex, verrucose, with numerous conidial scars. ***Conidia*** solitary, fusiform to obclavate, mostly 3–, rarely 1–, 2– or 4–septate, (13–)18–25(–33) × (4–)5–7(–8) µm, tapering to about 1–1.5 µm at the apex and at the base, pale brown to brown,

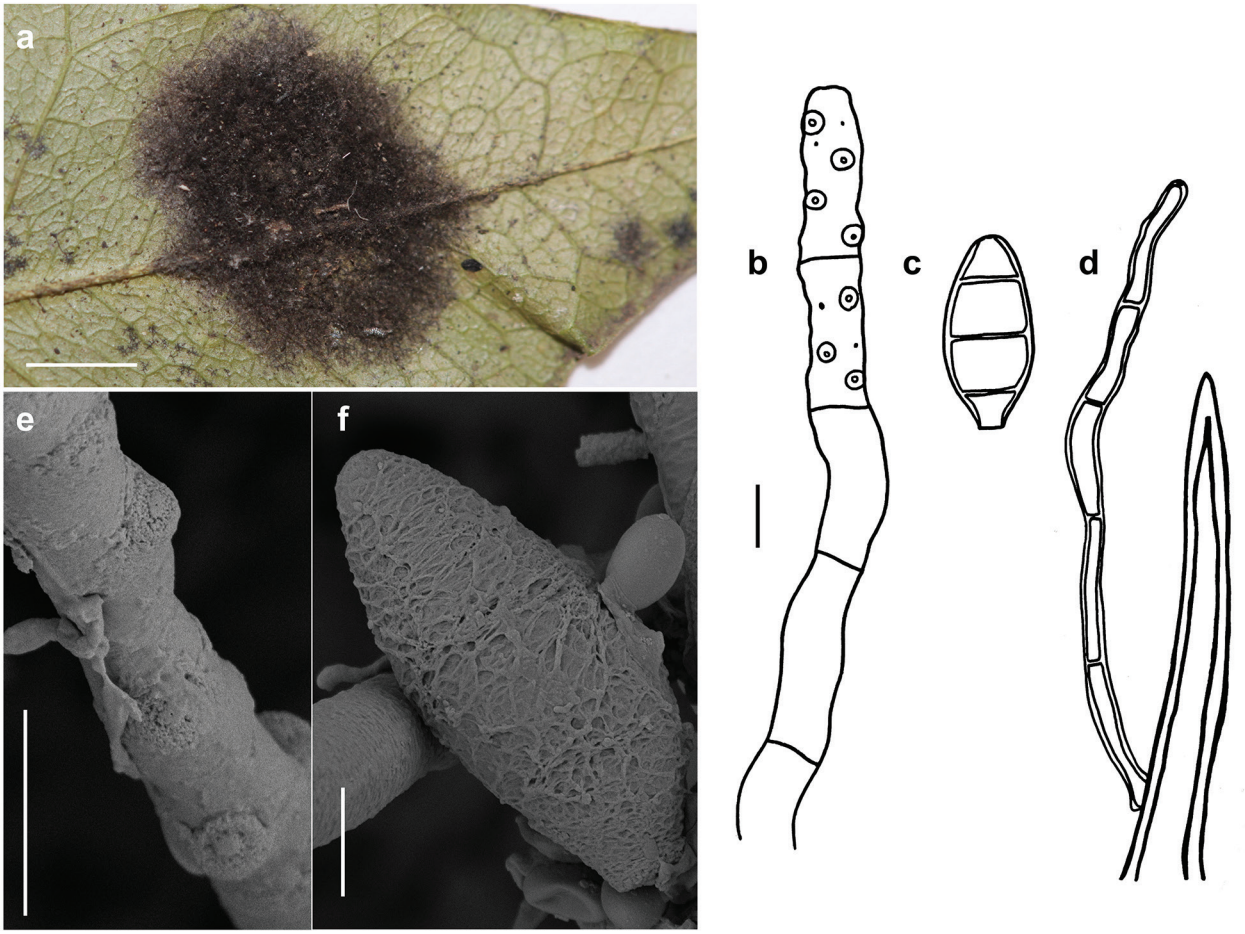

Figure 6. *Spiropes carpolobiae* (MB 166) **a** conidiophores growing intermingled with hyphae of *Meliola* sp. on a leaf of *Carpolobia lutea* **b** conidiophore with scars **c** Conidia shown in optical section. The thickness of the wall is shown in the left-hand drawing **d, e** as seen by SEM **d** conidiophore with scar **e** conidium. Scale bars: 0.3 mm (**a**); 5 µm (**b, c**); 5 µm (**d**); 3 µm (**e**).

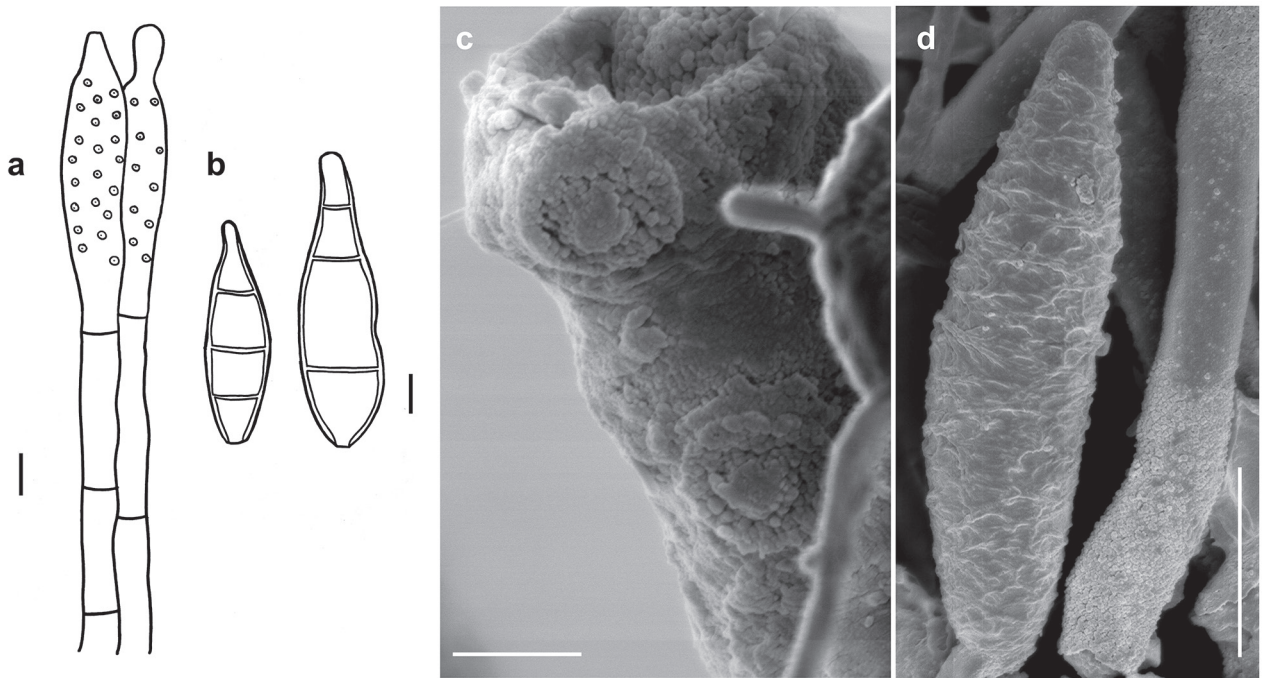

Figure 7. *Spiropes clavatus* (IMI 102772) **a** conidiophores with scars **b** conidia shown in optical section **c, d** as seen by SEM **c** conidiophore with scars **d** conidium. Scale bars: 5 µm (**a**); 2.5 µm (**b**); 1 µm (**c**); 5 µm (**d**).

the cells at each end paler, wrinkled. As seen by SEM, the ornamentation of the spores is distinctly reticulated, with thin to thick networks and no ridges.

Specimens examined. On *Meliola panici* on leaves of *Panicum glutinosa*, Puerto Rico, El Alto de la Bandera, 1913, F.L. Stevens & W.E. Hess, n°4368 (IMI 130764); on *Meliola* sp. on leaves of *Raphia monbuttorum*, Uganda, 1915, R. Dümmer, (IMI 102772); on *Meliola thouiniae* on leaves of an unknown plant, Brasil, São Paulo, 1940, A.R. Campos (IMI 130975, type of *Arthrobotryum noz-moscatae*).

Illustrations. This species was illustrated by Ellis (1968).

Known hosts and distribution. On colonies of Meliolales on living leaves of various plants in Argentina, Brazil, Ghana, Malaysia, Puerto Rico, Sierra Leone, Trinidad and Uganda (Ellis 1968).

Notes. In the nomenclatural and taxonomic database Index Fungorum (http://www.IndexFungorum.org), the current name of the *Spiropes clavatus* is *Bitunicostilbe clavata* (Ellis & Martin) M. Morelet. The genus *Bitunicostilbe* (*incertae sedis*, Ascomycota) was proposed by Morelet (1971) to accommodate two species, namely *B. clavata* and *B. linderae*, that were previously cited in other genera. Although the publication by Morelet was not available for this study, the morphological analysis of the herbarium specimens (IMI 130764, 130975) revealed that the features of these specimens are consistent with the description of *Spiropes clavatus* by Ellis (1968). The species has typical characteristics of the genus *Spiropes*, such as flat double scars (Fig. 7c) and, therefore, it should be classified in this genus. De Beer et al. (2013) analysed the type and additional specimens of *B. linderae* (as *Graphium linderae*) and concluded that this species should be also classified in the genus *Spiropes*.

***Spiropes croissantiformis* Berm.-Cova & M. Piepenbr., sp. nov.**
MycoBank No: 850984
Fig. 8

Holotype. On *Meliola* cf. *xylopiae* on living leaves of *Xylopia frutescens*, Panama, Chiriquí Province, Cochea, Cochea River Trail, 8°32'37"N, 82°23'03"W, 181 m a.s.l., 26 February 2020, M.A. Bermúdez, A. Sanjur, A. Villarreal, MB110 (UCH).

Etymology. Named after the shape of the conidia.

Description. ***Colonies*** effuse, dark brown to black, with tightly packed hyphae that form erect, dark synnemata clearly visible under the stereomicroscope. ***Hyphae*** superficial, branched, septate, 1–2 µm wide, straw-coloured, smooth. ***Conidiophores*** tightly packed to form dark brown to blackish synnemata up to 400 µm high, spreading out at the apex, up to 80 µm diam. Individual hyphae mostly straight, cylindrical, 3–5 µm thick, with numerous small scars, brown, paler towards the apex, rough. ***Conidia*** straight or curved, mostly crescent-shaped, sometimes fusiform, mostly 3(–5)–septate, (14–)20–24(–33) × (3.5–)5–6.5 µm, with two golden brown middle cells and paler cells at each. As

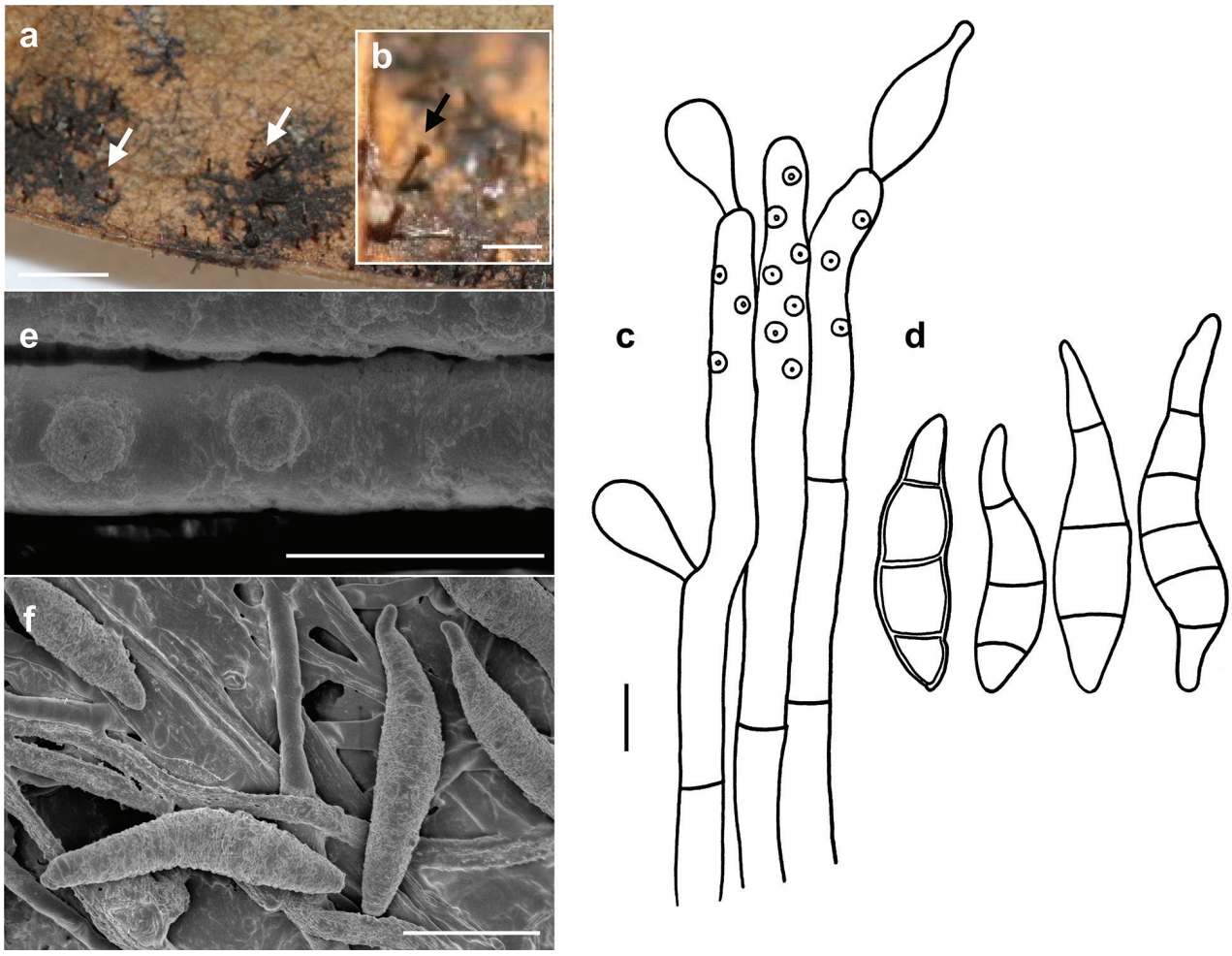

Figure 8. *Spiropes croissantiformis* (MB 110) **a** synnemata (indicated by white arrows) growing on colonies of *Meliola* cf. *xylopiae* **b** synnema (indicated by a black arrow) **c** conidiophores with scars and young conidia, shown in optical section **d** conidia shown in optical section. The thickness of the wall is only shown for the first spore from the left **e, f** as seen by SEM **e** part of a conidiophore with scars **f** conidia. Scale bars: 160 µm (**a**); 400 µm (**b**); 5 µm (**c, d**); 5 µm (**e**); 10 µm (**f**).

seen by SEM, the ornamentation of the spores is distinctly reticulated, with thin to thick networks and no ridges.

Known distribution. On colonies of *Meliola* cf. *xylopiae* on living leaves of *Xylopia frutescens* (Annonaceae) in Panama.

Notes. *Spiropes xylopiae* is a synnematous hyperparasitic species of *Spiropes* with the shortest synnemata (up to 400 µm), when compared to other synnematous species, such as *S. melanoplaca* with synnemata that can reach up to 1.5 mm and *S. penicillium* with synnemata up to 700 µm high. In addition to this, the new species has crescent-shaped conidia, a feature that is not present in any other known species of the genus.

Spiropes deightonii **M.B. Ellis, Mycol. Pap. 114: 18, 1968**
Fig. 9

Description. ***Colonies*** effuse, olive to olivaceous-brown, velvety or hairy. ***Hyphae*** superficial, branched, septate, 0.5–2 µm wide, pale olive to olivaceous-brown, smooth. ***Conidiophores*** arising singly or in groups terminally or laterally from the hyphae, erect or ascending, straight or flexous, septate, up to 400 µm long, 2–4 µm thick along most of their length, swollen towards the apex, 5–8 µm thick, brown, reticulate as seen by SEM, with scattered cylindrical scars. ***Conidia*** solitary, straight or slightly curved, obovate to clavate, truncate at their base, 3–septate, (10–)12–14(–15) × (5–)6–8 µm, 1.5–2 µm wide at the base, the cells

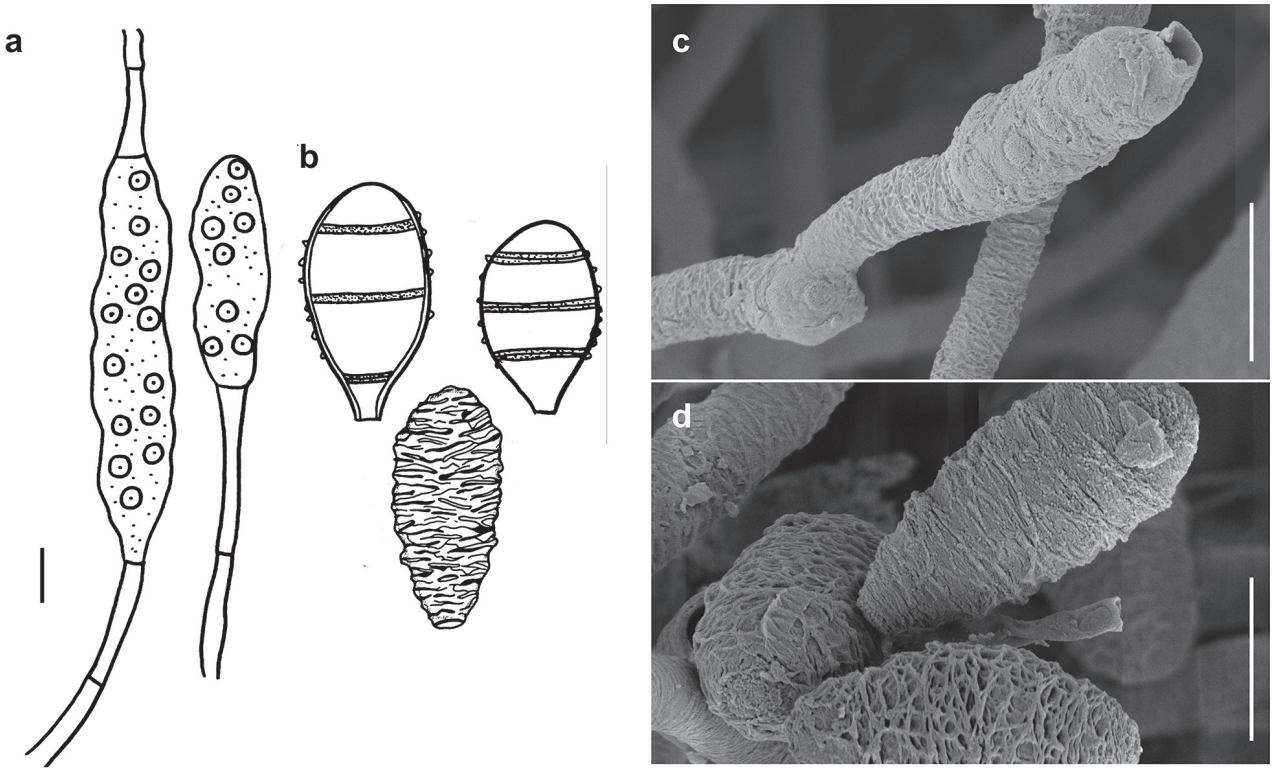

Figure 9. *Spiropes deightonii* (IMI48956a) **a** conidiophores **b** conidia, as seen by LM (two upper spores; the thickness of the wall is indicated only in the drawing on the left-hand side) and by SEM (bottom spore) **c, d** as seen by SEM **c** conidiophore **d** conidia. Scale bars: 5 µm (**a, b**); 8 µm (**c**); 5 µm (**d**).

at each end of a conidium subhyaline or pale brown, intermediate cells brown, ornamented. As seen by SEM, the ornamentation of the spores is distinctly reticulated, with thin to thick networks that can form ridges.

Specimen examined. On *Meliola borneensis* on *Uvaria chamae*, Sierra Leone, 1951, F.C. Deighton, (IMI 48956a, type of *S. deightonii*).

Illustrations. This species was illustrated by Ellis (1968).

Known hosts and distribution. On colonies of *Meliola borneensis* on living leaves of *Uvaria chamae* (Annonaceae) in Sierra Leone (Ellis 1968).

Notes. *Spiropes deightonii* and *Spiropes intricatus* are the only known species of the genus that present conidiophores that swell in the areas where conidia are formed (Figs 9, 14; Ellis (1968)). *Spiropes intricatus* differs from *S. deightonii* by the presence of larger conidia (16–23 µm long) that are more oblong-ellipsoid (Ellis 1968), rather than obovate or clavate. *S. deightonii* is only known from the type specimen.

***Spiropes dorycarpus* (Mont.) M.B. Ellis, Mycol. Pap. 114: 27, 1968**
Fig. 10

≡ *Helminthosporium dorycarpum* Mont., Annls Sci. nat., 2 Sér., 17: 120, 1842.
≡ *Pleurophragmium dorycarpum* (Mont.) Hughes, Can. J. Bot. 36: 797, 1958.
= *Helminthosporium orbiculare* Lév., Annls Sci. nat., 3 Sér., 5: 299, 1846.
= *Napicladium myrtacearum* Speg., An. Soc. cient. Argent. 26: 71, 1888.
≡ *Sporhelminthium myrtacearum* (Speg.) Speg., Physis 4(17): 292, 1918.
= *Helminthosporium conspicuum* McAlpine, Proc. Linn. Soc. N.S.W. 22: 40, 1897.
= *Podosporium densum* Pat., J. Bot. Paris 11: 373, 1897.
= *Helminthosporium asterinoides* Sacc. & P. Syd., apud Saccardo, Rc. Congr. Bot. Palermo, May 1902: 58, 1902.
≡ *Sporhelminthium asterinoides* (Sacc. & Syd.) Speg., Physis 4(17): 292, 1918.
= *Helminthosporium melastomacearum* F. Stevens, Bot. Gaz. 65: 242, 1918.
= *Helminthosporium panici* F. Stevens, Bot. Gaz. 65: 242, 1918.
= *Helminthosporium parathesicola* [as '*parathesicolum*'] F. Stevens, Bot. Gaz. 65: 242, 1918.

Description. ***Colonies*** effuse, brown to dark brown, hairy. ***Hyphae*** superficial, branched, septate, 1–3 µm wide, straw-coloured, pale brown, smooth. ***Conidiophores*** arising singly or in groups, terminally or laterally from the hyphae, erect or ascending, straight or flexous, septate, up to 700 µm long, 3–7 µm thick, straw-coloured, pale brown to brown, with scattered cylindrical scars towards the apex. ***Conidia*** solitary, straight or slightly curved, variable in shape, but mostly obclavate to fusiform, truncate at the base, mostly 3–septate, but sometimes with 4 to 5 septa, (16–)20–35(–40) × (4.5–)5–7 µm, straw-coloured to pale brown, middle cells slightly darker, wrinkled or verrucose. As seen by SEM, the ornamentation of the spores is distinctly reticulated, with thin to thick networks and no ridges.

Specimen examined. On *Meliola* sp. on living leaves of *Coffea arabica*, Benin, Atlantique, Attogon, Niaouli Forest, 6°44'23"N, 2°8'26"E, 119 m a.s.l., 19 September 2022, A. Krauß, A. Tabé, O. Koukol, N.S. Yorou, AK06H.

Additional specimens examined. On *Eugenia pungens*, Brasil, Guarapí, 1883, B. Balansa, 3939, (IMI 100322, type of *Napicladium myrtacearum*); on *Meliola* sp.

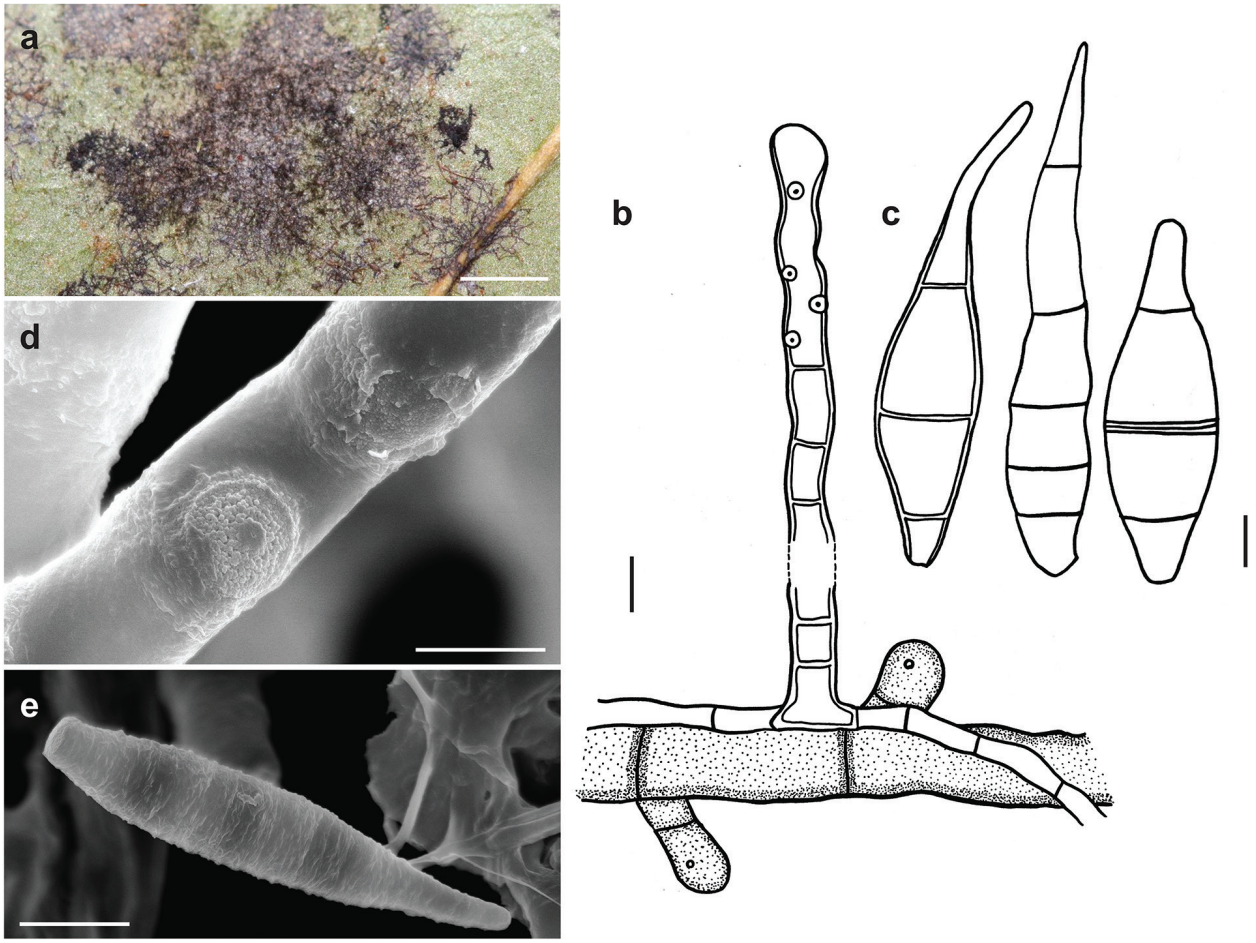

Figure 10. *Spiropes dorycarpus* (AK06H) **a** superficial hyphae growing on a colony of *Meliola* sp. on a leaf of *Coffea arabica* **b, c** in optical section **b** conidiophore growing on a hypha of *Meliola* sp. **c** conidia. The thickness of the wall is indicated only in the drawing on the left-hand side **d, e** As seen by SEM **d** conidiophore with a scar **e** conidium. Scale bars: 1 mm (**a**); 5 µm (**b**); 3.5 µm (**c**); 3 µm (**d**); 7 µm (**e**).

on leaves of an unknown plant, Cuba, R. de la Sagra (IMI 10002, type of *Helminthosporium dorycarpum*).

Illustrations. This species was illustrated by Ellis (1968).

Known hosts and distribution. On colonies of *Appendiculella* spp., *Asteridiella* spp., *Clypeolella* spp., *Irenopsis* spp., *Meliola* spp. and *Schiffnerula* spp., on living leaves of various plants in Australia, Brazil, Chile, Congo, Cuba, Dominican Republic, Ghana, Guyana, India, Malaysia, Nigeria, Puerto Rico, Sierra Leone, South Africa, Taiwan, Tanzania and Uganda (Ellis 1968). *Spiropes dorycarpus* is reported here for the first time for Benin.

Notes. *Spiropes dorycarpus* is similar to *S. effusus* and *S. helleri* by the presence of non-synnematous conidiophores and conidia mostly with three true septa. However, conidia of *S. effusus* are narrower (3–5 µm) than those of *S. helleri* (7–13 µm).

***Spiropes effusus* (Pat.) M.B. Ellis, Mycol. Pap. 114: 10, 1968**
Fig. 11

≡ *Podosporium effusum* Pat., Scient. Surv. P. Rico 8(1): 103, 1926.

= *Helminthosporium dorycarpum* var. *amazoniae* Hughes [as '*Helmisporium*'], Mycol. Pap. 50: 24, 1953.

≡ *Pleurophragmium dorycarpum* var. *amazoniae* (S. Hughes) S. Hughes, Can. J. Bot. 36: 797, 1958.

Description. ***Colonies*** effuse, olive to brown, hairy. ***Hyphae*** superficial, branched, septate, 1–2 µm wide, yellowish, olive or pale brown, smooth. ***Conidiophores*** arising singly or in groups, as terminal and lateral branches on the hyphae, erect, straight or flexous, septate, up to 300 µm long, 3–4 µm thick, slightly reticulated when seen by SEM, with few or many small conidial scars towards the apex. ***Conidia*** solitary, narrowly obclavate to fusiform, truncate at the base, mostly 3(–5)–septate, (15–)20–36 × (3–)3.8–4.5(–5) µm, pale brown, the central cells slightly darker, verruculose. As seen by SEM, the ornamentation of the spores is distinctly reticulated, with thin networks and no ridges.

Specimen examined. On meliolalean fungus on leaves of *Piper* sp., Puerto Rico, Río Piedras, 1926, Heller, 142 (IMI 130721, type of *Podosporium effusum*); on *Amazonia psychotriae* on leaves of *Psychotria warneckei*, Ghana, Togoland, 1938, F.C. Deighton M1617B (IMI 9996a).

Illustrations. This species was illustrated by Ellis (1968).

Known hosts and distribution. On colonies of Meliolales, especially *Amazonia* spp., on living leaves of various plants in Ghana, Puerto Rico, Sierra Leone and Venezuela. One record on *Asterina* sp. (Asterinales, Ascomycota) in Uganda (Ellis 1968).

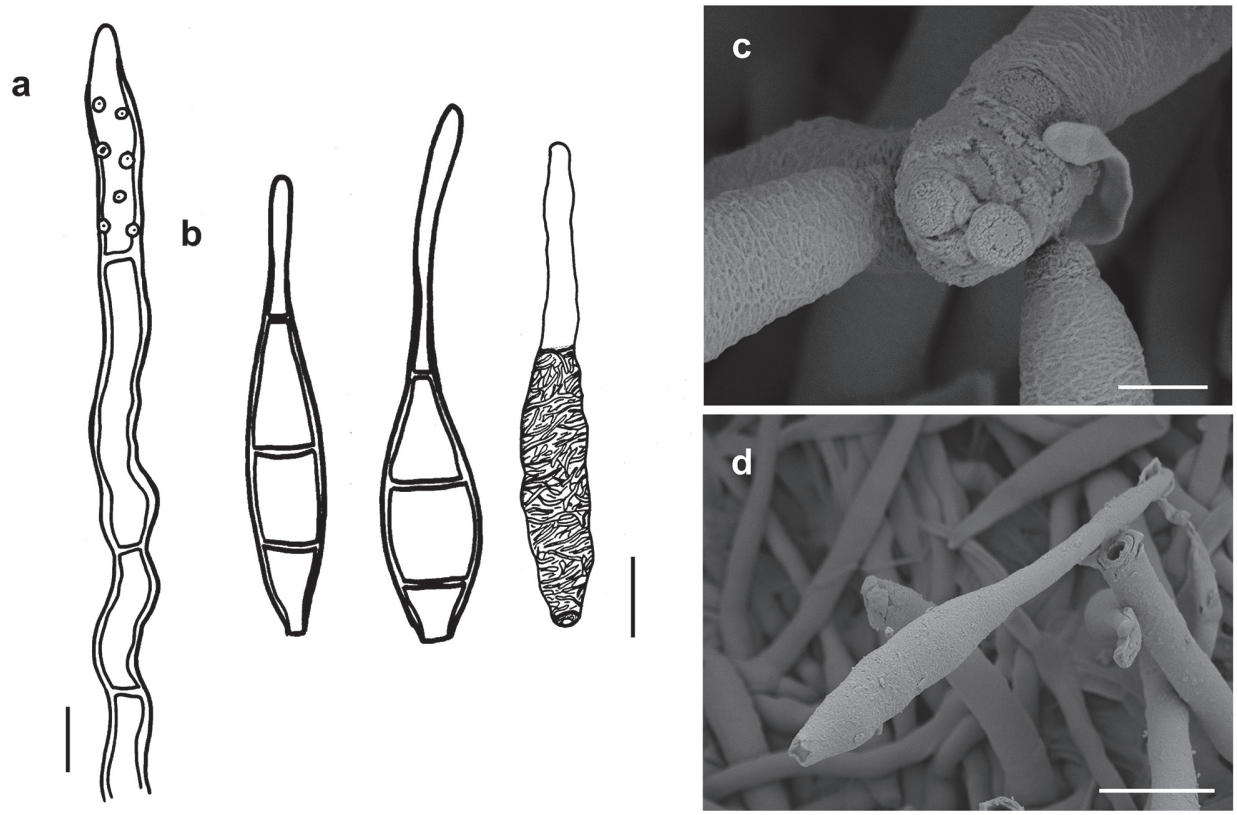

Figure 11. *Spiropes effusus* (IMI 130721) **a** conidiophore shown in optical section **b** conidia. The first two drawings show spores in optical section. The right-hand drawing shows a conidium as seen by SEM **c, d** as seen by SEM **c** conidiophore with scars and conidia **d** conidium. Scale bars: 5 µm (**a**); 8 µm (**b**); 2 µm (**c**); 8 µm (**d**).

Notes. *Spiropes effusus* has conidia similar in size to those of *S. dorycarpus*. However, conidia of *S. dorycarpus* are wider (5–7 µm) than in *S. effusus*.

***Spiropes fumosus* (Ellis & Martin) M.B. Ellis, Mycol. Pap. 114: 20, 1968.**

≡ *Helminthosporium fumosum* Ellis & Martin, Am. Nat. 18: 70, 1884.
≡ *Brachysporium fumosum* (Ellis & Martin) Sacc., Syll. Fung. 4: 428, 1886.

Type. On *Meliola* sp. on leaves of *Persea palustris* (Lauraceae), Florida, U.S.A, 1883, G. Martin (NY 830274. The type specimen was not available for loan by NY).

Species description. This species was described by Ellis (1968).

Known hosts and distribution. On colonies of *Meliola* sp. on living leaves of *Persea palustris* in the U.S.A. (Ellis 1968).

Specimen examined. On Meliolales on living leaves of *Persea palustris*, U.S.A, Florida, Cove Springs, 1890, G. Martin, (IMI 16307).

Illustrations. This species was illustrated by Ellis (1968).

Notes. The specimen IMI 16307 was analysed, but no fungal cells were seen.

***Spiropes guareicola* (F. Stevens) Cif., Sydowia 9(1–6): 302, 1955**
Fig. 12

≡ *Helminthosporium guareicola* F. Stevens [as '*Helmisporium guareicolum*'], Bot. Gaz. 65(3): 241, 1918.
≡ *Pleurophragmium guareicola* (F. Stevens) S. Hughes, Can. J. Bot. 36: 797, 1958.
= *Cladosporium elegans* var. *singaporense* Sacc., Bull. Orto Bot. Regia Univ. Napoli 6: 60, 1921.
= *Helminthosporium flagellatum* H.S. Yates [as '*Helmisporium*'], Philipp. J. Sci. (Bot.) 13: 383, 1918.
= *Helminthosporium spirotrichum* Sacc. [as '*Helmisporium*'], Boll. Orto bot. 6: 61, 1921.

Description. ***Colonies*** effuse, dark brown to black, hairy. ***Hyphae*** superficial, branched, septate, 2–4 µm wide, pale olivaceous-brown, smooth. ***Conidiophores*** arising singly or in groups, as lateral branches on the hyphae, erect, sterile lower part straight or flexuous, upper fertile part in zigzag shape, septate, up to 400 µm long, 6–9 µm thick, brown to dark brown, paler towards the apex, more or less smooth, with numerous well-defined, dark conidial scars. ***Conidia*** solitary, broadly fusiform, truncate at the base, with 3 to 5 pseudosepta, (25–)35–52(–60) × (7–)8–10(–13) µm, 3.5–5 µm wide at the base, pale to dark brown or olivaceous-brown, smooth as seen by SEM.

Specimen examined. On leaves of *Cyrtophyllum fragrans* (Gentianaceae), Singapore, 1921, Baker (IMI 49160, type of *Helminthosporium spirotrichum*); on *Meliola* sp. on leaves of *Daniellia thurifera* (Fabaceae), Sierra Leone, 1936, F.C. Deightonii M1267 (IMI 10010).

Illustrations. This species was illustrated by Ellis (1968).

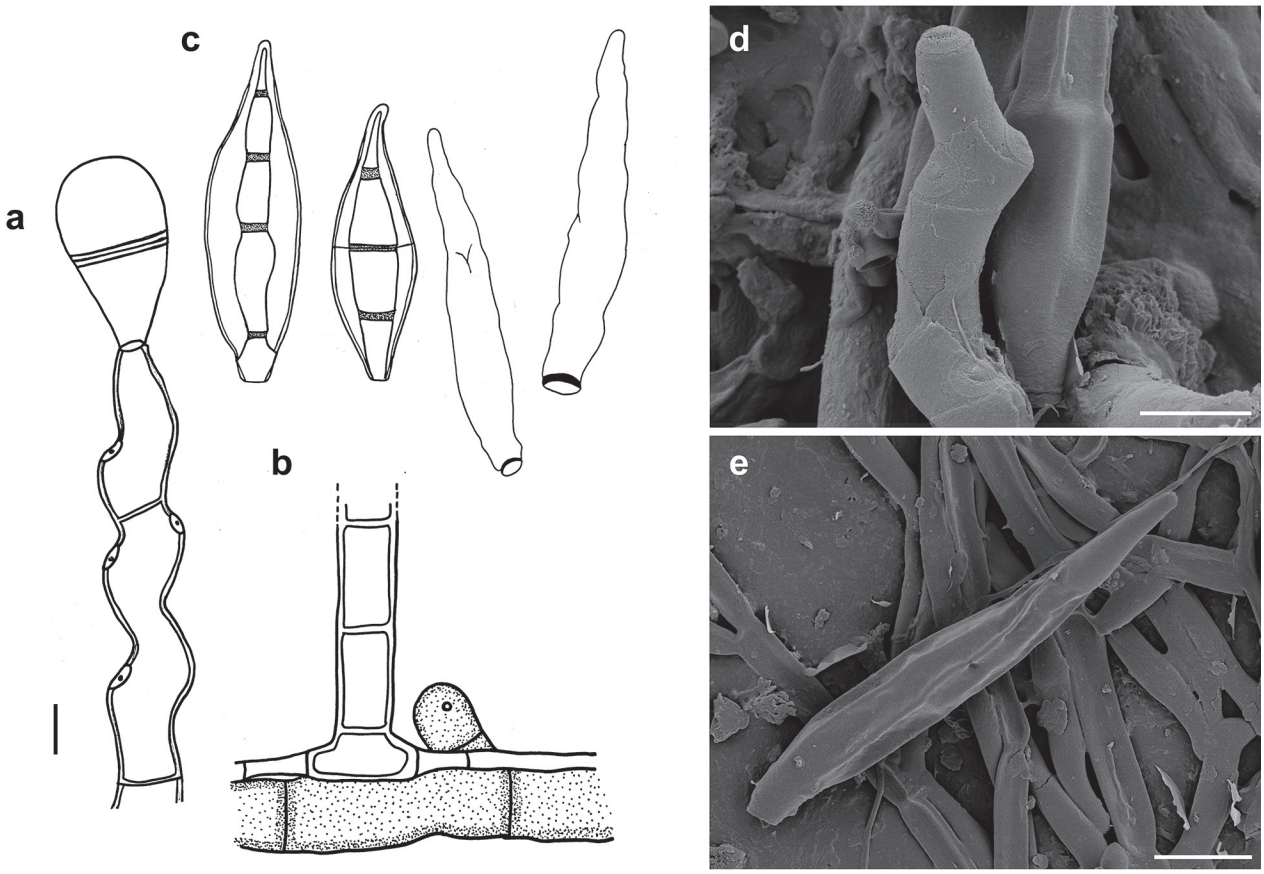

Figure 12. *Spiropes guareicola* (IMI 10010) **a** conidiophore with scars and a young conidium shown in optical section **b** base of a conidiophore growing on a hypha of *Meliola* sp. shown in optical section **c** conidia shown in optical section (two drawings on the left-hand side) and as seen by SEM (two drawings on the right-hand side) **d, e** as seen by SEM **d** zigzag-shaped conidiophore with scars **e** conidium. Scale bars: 5 µm (**a**–**c**); 8 µm (**d**); 10 µm (**e**).

Known hosts and distribution. On colonies of *Asteridiella* spp., *Irenopsis* spp. and *Meliola* spp. on living leaves of various plants in Bougainville Islands, Ghana, India, Indonesia, Malaysia, Philippines, Puerto Rico, Sabah, Sierra Leone, Solomon Islands and Uganda (Ellis 1968).

Notes. *Spiropes guareicola* is the type species of the genus *Spiropes* and it differs from other species of the genus by the presence of zigzag-shaped conidiophores in the fertile upper parts (Ellis 1968). *S. guareicola* presents smooth conidia, a feature that is only evident by SEM.

***Spiropes helleri* (F. Stevens) M.B. Ellis, Mycol. Pap. 114: 14, 1968**
Fig. 13

≡ *Helminthosporium helleri* F. Stevens [as '*Helmisporium*], Bot. Gaz. 65(3): 242, 1918.
= *Helminthosporium leucosykes* H.S. Yates [as '*Helmisporium leucosykeae*'], Philipp. J. Sci., C, Bot. 13(6): 382, 1918.
= *Helminthosporium maculosum* Sacc. [as '*Helmisporium*'], Atti Accad. Sci. Ven.-Trent.-Istr. 10: 91, 1919 [1917].
≡ *Pleurophragmium maculosum* (Sacc.) S. Hughes, Can. J. Bot. 36: 797, 1958.

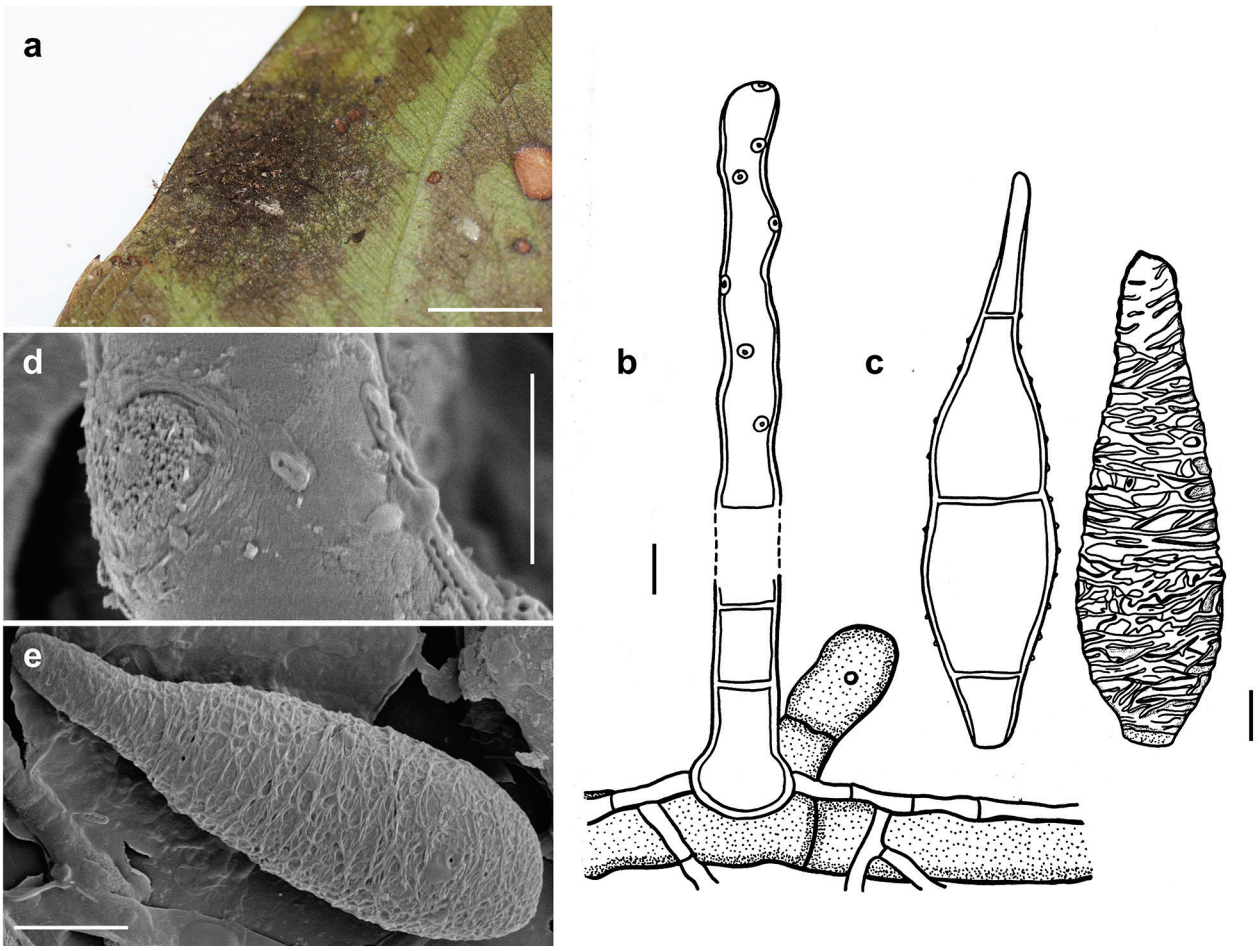

Figure 13. *Spiropes helleri* (IMI130940) **a** superficial hyphae growing on a colony of *Meliola* sp. on a leaf of *Cupania guatemalensis* **b** conidiophore growing on a hypha of *Meliola* sp. shown in optical section **c** conidia shown in optical section (drawing on the left-hand side) and as seen by SEM (drawing on the right-hand side) **d, e** as seen by SEM **d** part of a conidiophore with a scar **e** conidium. Scale bars: 1 mm (**a**); 5 µm (**b**); 6 µm (**c**); 4 µm (**b**); 5 µm (**c**).

Description. ***Colonies*** effused, dark brown to black, hairy. ***Hyphae*** superficial, branched, septate, 1–3 µm wide, straw-coloured or pale brown, smooth. ***Conidiophores*** arising singly as terminal or lateral branches on the hyphae, erect, straight or flexuous, septate, up to 600 µm long, 5–8 µm wide, brown to dark brown, paler towards the apex, smooth, with scattered conidial scars. ***Conidia*** solitary, obclavate, frequently rostrate, 3(–4)–septate, (26–)36–43(–50) × (6–)7–10(–13) µm, 3–4 µm wide at the truncate base, pale brown to brown, verruculose. As seen by SEM, the ornamentation of the spores is clearly reticulated, with thin networks and no ridges.

Specimens examined. On *Meliola* sp. on leaves of *Cupania guatemalensis* (Sapindaceae), Panama, Chiriquí Province, Botanical Garden of the Autonomous University of Chiriquí (UNACHI), 8°25'55"N, 82°27'03"W, 34 m a.s.l., 11 February 2020, M. A. Bermúdez-Cova, A. Sanjur MB92 (UCH15489, M); on *Meliola* sp. on living leaves of *Pterocarpus santalinoides* (Fabaceae), Benin, Atlantique, Attogon, Niaouli Forest, 6°44'40"N, 2°7'53"E, 72 m a.s.l., 20 September 2022, A. Krauß, A. Tabé, O. Koukol, N.S. Yorou, AK15 (M).

Additional specimens examined. On Meliolales on living leaves of an undetermined plant, Gold Coast Colony, Banau, 1949, S.J. Hughes 1141 (IMI44564);

on *Meliola* sp. on leaves of *Myrcia deflexa*, Puerto Rico, El Alto de la Bandera, F.L. Stevens 8268 (IMI9991, type of *Helminthosporium helleri*).

Illustrations. This species was illustrated by Ellis (1968).

Known hosts and distribution. On colonies of *Asteridiella* spp., *Irenopsis* spp. and *Meliola* spp. on living leaves of various plants in Ghana, Malaysia, New Caledonia, Philippines, Puerto Rico, Sabah, Sierra Leone and Uganda (Ellis 1968). *Spiropes helleri* is reported here for the first time for Benin and for mainland America (Panama).

Notes. *Spiropes helleri* is similar to *S. effusus*, *S. dorycarpus* and *S. leonensis* by the presence of obclavate to sometimes fusiform conidia, but differs from the first two by wider conidia (3.8–4.5 µm in *S. effusus* and 5–7 µm in *S. dorycarpus*) and from the last one by narrower ones (10–11µm).

***Spiropes intricatus* (Sacc.) M.B. Ellis, Mycol. Pap. 114: 9, 1968**
Fig. 14

≡ *Brachysporium intricatum* Sacc., Atti Accad. scient. Veneto-trent.-istriana, Ser. 3, 10: 88, 1919.
= *Spiropes pirozynskii* M.B. Ellis, Mycol. Pap. 114: 19, 1968. New synonym proposed in this study.

Description. ***Colonies*** effuse, straw-coloured, olive or olivaceous-brown, velvety or hairy. ***Hyphae*** superficial, branched, anastomosing, septate, 1–2 µm wide, pale olivaceous brown, smooth. ***Conidiophores*** arising singly or in groups, terminally or laterally from the hyphae, erect or ascending, straight or flexuous, septate, up to 900 µm long, 2–5 µm thick along most of their length, swollen to 4–9 µm towards the apex and in intercalary parts that produce conidia, pale olivaceous-brown to brown, reticulate as seen by SEM, with scattered cylindrical scars. ***Conidia*** solitary, straight or slightly curved, oblong-ellipsoid or obovate to clavate, truncate at the base, mostly 3–septate, (13–)16–23(–25) × (4.5–)6–8 µm, 1.5–3 µm wide at the base, the cells at each end of a conidium pale brown, intermediate cells brown, ornamented. As seen by SEM, the ornamentation of the spores is distinctly reticulated, with thin to thick networks that can form ridges.

Specimens examined. On *Irenopsis* sp. on *Lindackeria bukobensis* (Achariaceae), Tanzania, Kigoma, 1964, K.A. Pirozynski M418 b&c (IMI 106645b-c, type of *Spiropes pirozynskii*); on leaves of *Camellia drupifera* (Theaceae), Nepal, Kathmandu, Godawari, 1986, U. Budathoki KU294 (IMI323287).

Illustrations. This species was illustrated by Ellis (1968).

Known hosts and distribution. On colonies of Meliolales on living leaves of various plants in Ghana, Philippines and Tanzania (Ellis 1968).

Notes. *Spiropes intricatus* and *S. deightonii* are the only known species of the genus that present conidiophores that swell in the areas where conidia are formed (Figs 9, 14; Ellis (1968)). *Spiropes deightonii* differs from *S. intricatus* by the presence of smaller conidia (12–14 µm long) that are more obovate or clavate rather than oblong-ellipsoid. The type specimen of *S. pirozynskii* (IMI 106645b-c) is morphologically similar to *S. intricatus*. Both species present oblong-ellipsoid conidia with a similar size range (Fig. 15). Therefore, we propose *S. pirozynskii* as a synonym of *S. intricatus*.

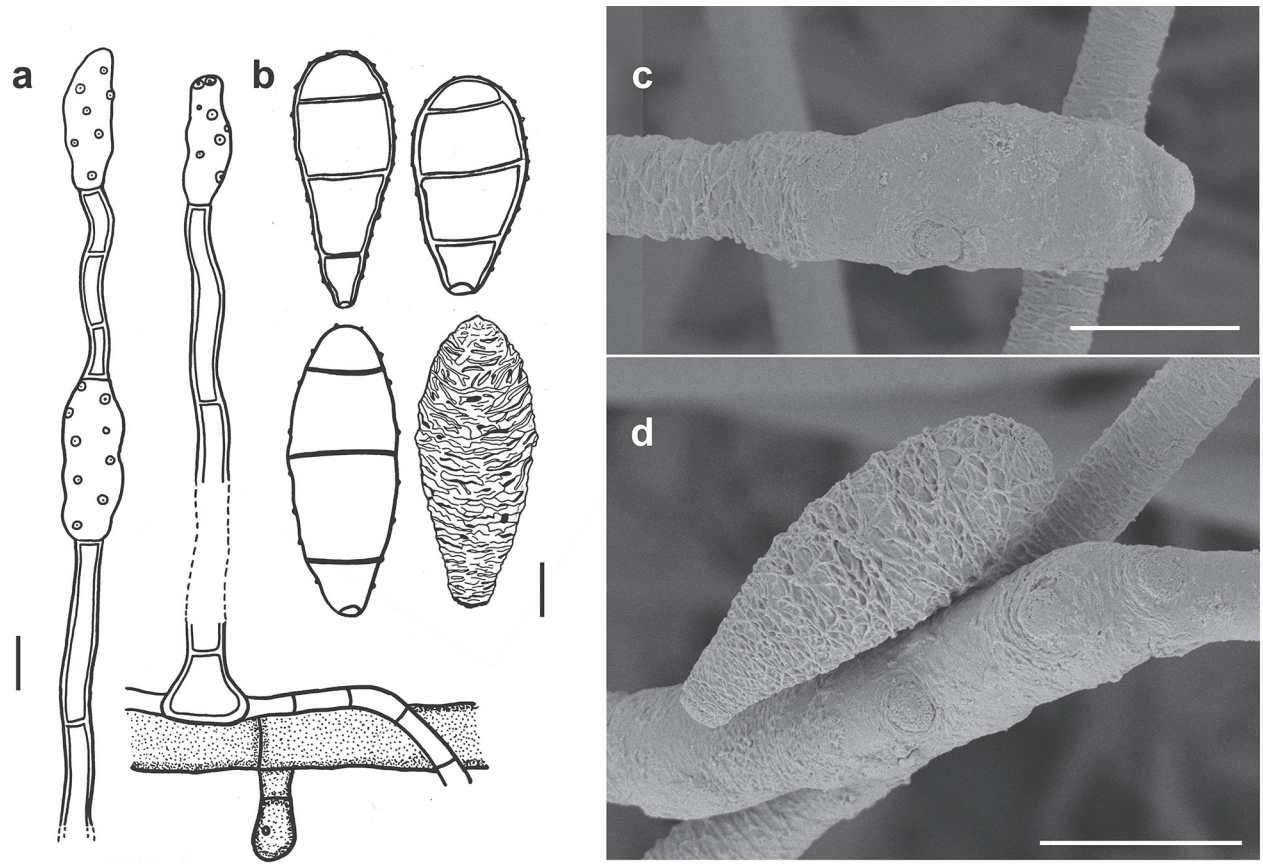

Figure 14. *Spiropes intricatus* (IMI 106645b-c) **a** conidiophores, growing on a hypha of *Irenopsis* sp., shown in optical section **b** conidia shown in optical section (the thickness of the wall is indicated only in the drawings on the upper row) and as seen by SEM (second row right) **c, d** as seen by SEM **c** conidiophore with scars **d** conidium. Scale bars: 5 µm (**a**); 3 µm (**b**); 7 µm (**c**); 8 µm (**c**).

Spiropes japonicus **(Henn.) M.B. Ellis, Mycol. Pap. 114: 22, 1968**
Fig. 16

≡ *Podosporium japonicum* Henn., Bot. Jb. 29: 152, 1900.
= *Helminthosporium insigne* Gaillard ex Sacc. [as '*Helmisporium*'], Atti Accad. Sci. Ven.-Trent.-Istr. 10: 89, 1917.

Description. ***Colonies*** effuse, amphigenous, sometimes dense, dark brown to black, with tightly packed hyphae that form large, erect, dark synnemata clearly visible under the stereomicroscope. ***Hyphae*** superficial, branched, septate, 1–4 µm wide, pale olivaceous-brown, smooth. ***Conidiophores*** tightly packed to form dark brown to blackish synnemata up to 1 mm high, spreading out at the apex and upper half of the synnemata; conidiophores individually flexuous or straight, thick-walled, septate, 6–8 µm thick, brown to dark brown at the base, paler towards the apex, smooth, with scattered cylindrical scars. ***Conidia*** solitary, fusiform to obclavate, with 4(–6) pseudosepta, (50–)67–80 × (7–)8–14 µm, 2–3 µm wide at the apex, 3–5 µm at the truncate base, pale brown to brown, striate.

Specimens examined. On *Meliola* sp. on living leaves of Asteraceae, Panama, Chiriquí Province, Boquerón District, Chuspa Hydroelectric, 8°32'20"N, 82°36'21"W, 281 m a.s.l., 6 March 2020, M. A. Bermúdez-Cova, A. Sanjur, S.

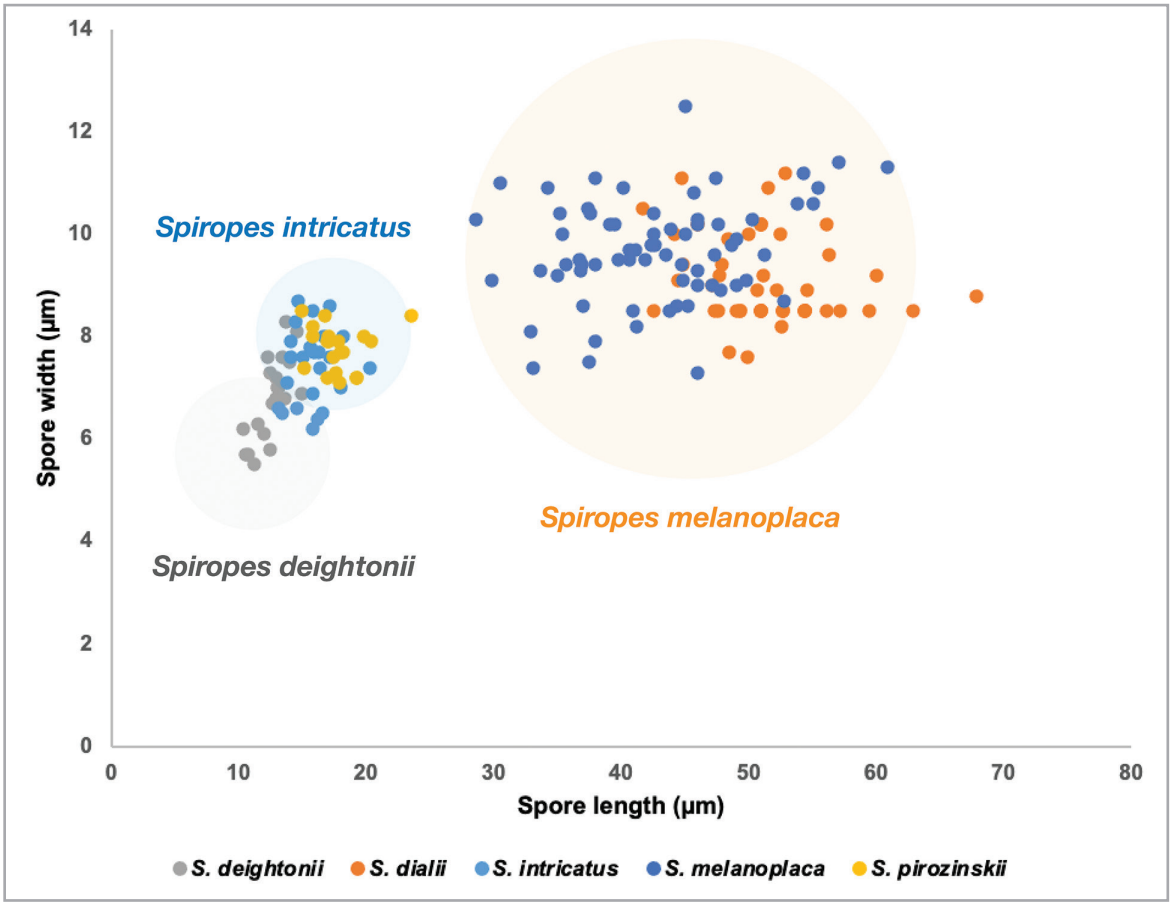

Figure 15. Scatter plot of spore size (width and length) of species of *Spiropes*.

Samaniego, MB120 (UCH15492); on *Meliola* sp. on living leaves of Fabaceae, Panama, Chiriquí Province, Bugaba District, area around Gariché River, 8°38'38.1"N, 82°41'19.6"W, 566 m a.s.l., 8 March 2020, M. A. Bermúdez-Cova, A. Sanjur, A. Villarreal, MB123 (UCH15493, M).

Additional specimens examined. On *Irenina entebbeensis* on *Alchornea hirtella* (Euphorbiaceae), Sierra Leone, 1939, Makump, M1774 (IMI 38813); on *Asteridiella aucubae* on *Aucuba japonica* (Garryaceae), Japan, Ise, 1899, P. Hennings (IMI 130973, type of *Podosporium japonicum*).

Illustrations. This species was illustrated by Ellis (1968).

Known hosts and distribution. On colonies of Meliolales on living leaves of various plants in the Cook Islands, Japan, Malaysia, Papua New Guinea and Sierra Leone (Ellis 1968). *Spiropes japonicus* is reported here for the first time for Panama.

Notes. *Spiropes japonicus* is the only known synnematous species of *Spiropes* that produces conidia with 4–6 pseudosepta, as well as synnemata that splay out at the apex and upper half (Ellis 1968).

***Spiropes leonensis* M.B. Ellis, Mycol. Pap. 114: 15, 1968**
Fig. 17

Description. ***Colonies*** effuse, grey to dark blackish-brown, hairy. ***Hyphae*** superficial, branched, septate, 2–6 µm wide, pale brown, smooth. ***Conidiophores***

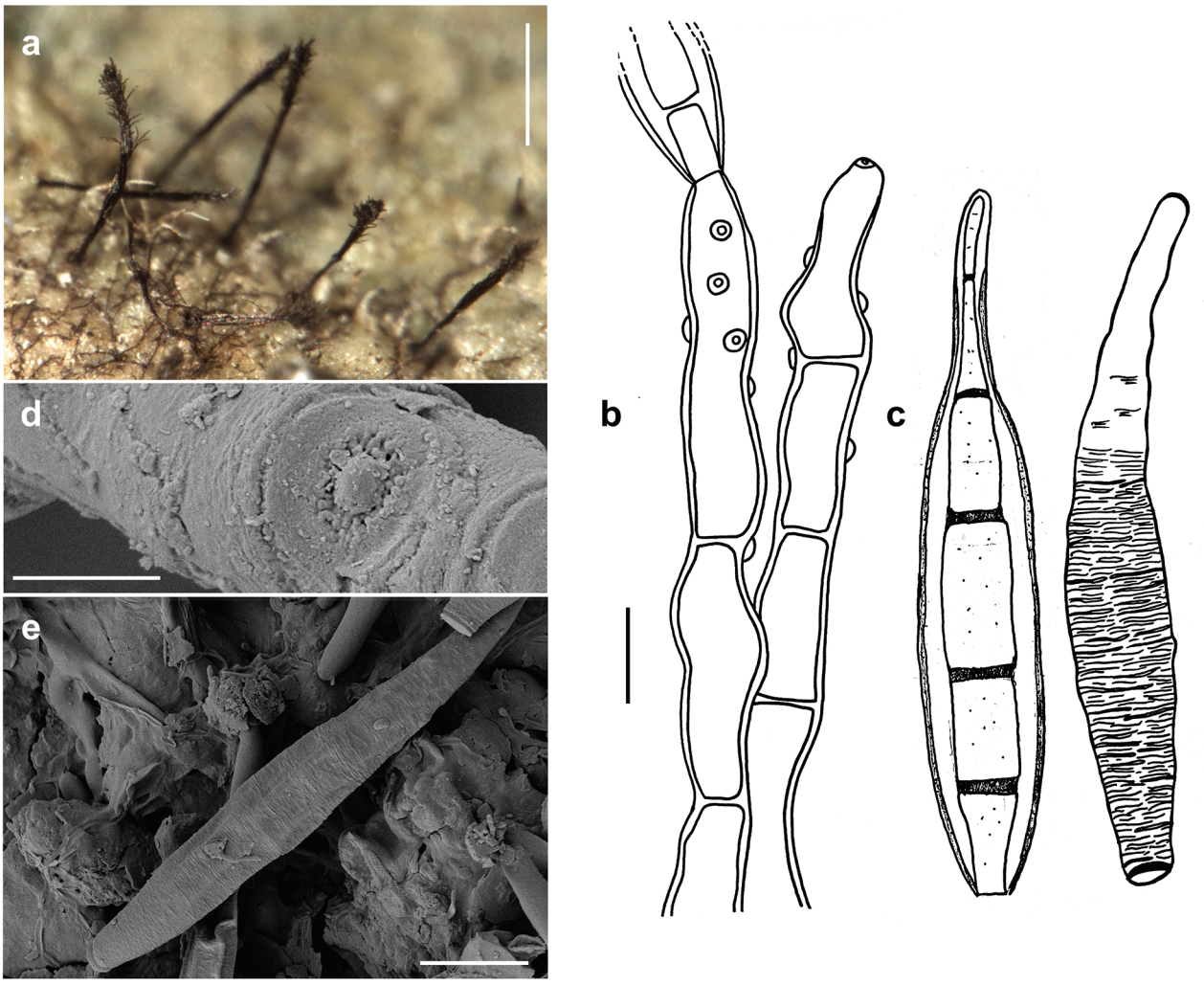

Figure 16. *Spiropes japonicus* (MB120, 123) **a** synnemata growing on a colony of *Meliola* sp. **b** conidiophores with scars and a young conidium, shown in optical section **c** a conidium shown in optical section (drawing on the left) and as seen by SEM (drawing on the right) **d, e** as seen by SEM **d** conidiophore with a scar **e** conidium. Scale bars: 1 mm (**a**); 10 µm (**b, c**); 3 µm (**d**); 9 µm (**d**).

arising singly, as terminal and lateral branches on the hyphae, erect, straight or flexuous, septate, up to 700 µm long, 8–12 µm thick, sometimes swollen to 16–17 µm at the base, dark brown to dark blackish-brown, paler towards the apex, smooth, with scattered conidial scars. ***Conidia*** solitary, obclavate, rostrate, 3(–4)–septate, (38–)40–54(–63) × (8–)10–11(–13) µm, 4–6 µm wide at the truncate base, pale brown to brown, verruculose. As seen by SEM, the ornamentation of the spores is distinctly reticulated, with thin networks and no ridges. It was not possible to see the scars by SEM.

Specimen examined. On *Meliola garciniae* on leaves of *Pentadesma butyracea* (Clusiaceae), Sierra Leone, Rokupr, 1951, F.C. Deighton M3920 (IMI 46589b, holotype); on *Meliola garciniae* on *Pentadesma butyracea*, Sierra Leone, near Rokupr, 1939, F.C. Deighton (IMI 9992a, type of *Spiropes leonensis*).

Illustrations. This species was illustrated by Ellis (1968).

Known hosts and distribution. On colonies of *Meliola garciniae* on living leaves of *Pentadesma butyracea* (Clusiaceae) in Sierra Leone (Ellis 1968).

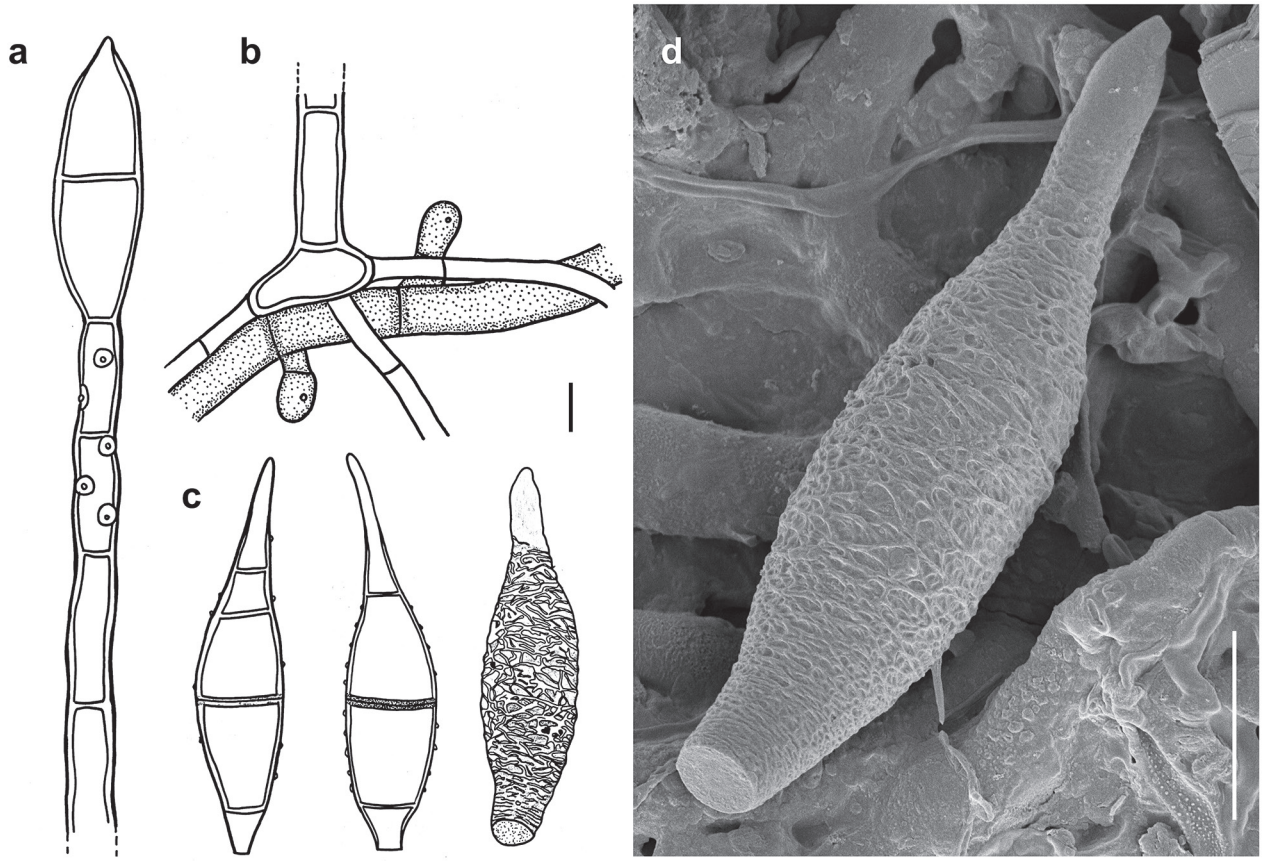

Figure 17. *Spiropes leonensis* (IMI 46589b) **a** conidiophore with scars and a young conidium, shown in optical section **b** part of a conidiophore growing on a hypha of *Meliola* sp., shown in optical section **c** conidia shown in optical section (first two drawings, from left to right) and as seen by SEM **d** conidium as seen by SEM. Scale bars: 8.5 µm (**a–c**); 7 µm (**d**).

Notes. *Spiropes leonensis* is similar to *S. helleri* by the presence of rostrate, obclavate, 3–septate conidia (Ellis 1968). However, conidia in *S. helleri* are smaller (36–43 µm).

***Spiropes melanoplaca* (Berk. & M.A. Curtis) M.B. Ellis, Mycol. Pap. 114: 28, 1968**
Fig. 18

= *Arthrobotryum melanoplaca* Berk. & M.A. Curtis, J. Linn. Soc. Bot. 10(46): 360, 1868.
≡ *Podosporium melanoplaca* (Berk. & M.A. Curtis) Cif., Sydowia 9(1–6): 310, 1955.
= *Podosporium dialii* Bat. [as '*dialiumii*'], Atas Inst. Micol. 1: 266, 1960. New synonym proposed in this study.
≡ *Spiropes dialii* (Bat.) M.B. Ellis, Mycol. Pap. 114: 27, 1968. New synonym proposed in this study.
= *Arthrobotryum scoparium* Henn., Hedwigia 43(6): 397, 1904. New synonym proposed in this study.

Description. ***Colonies*** effuse, dark brown to black, hairy, with tightly packed hyphae that form large, erect, dark synnemata clearly visible under the

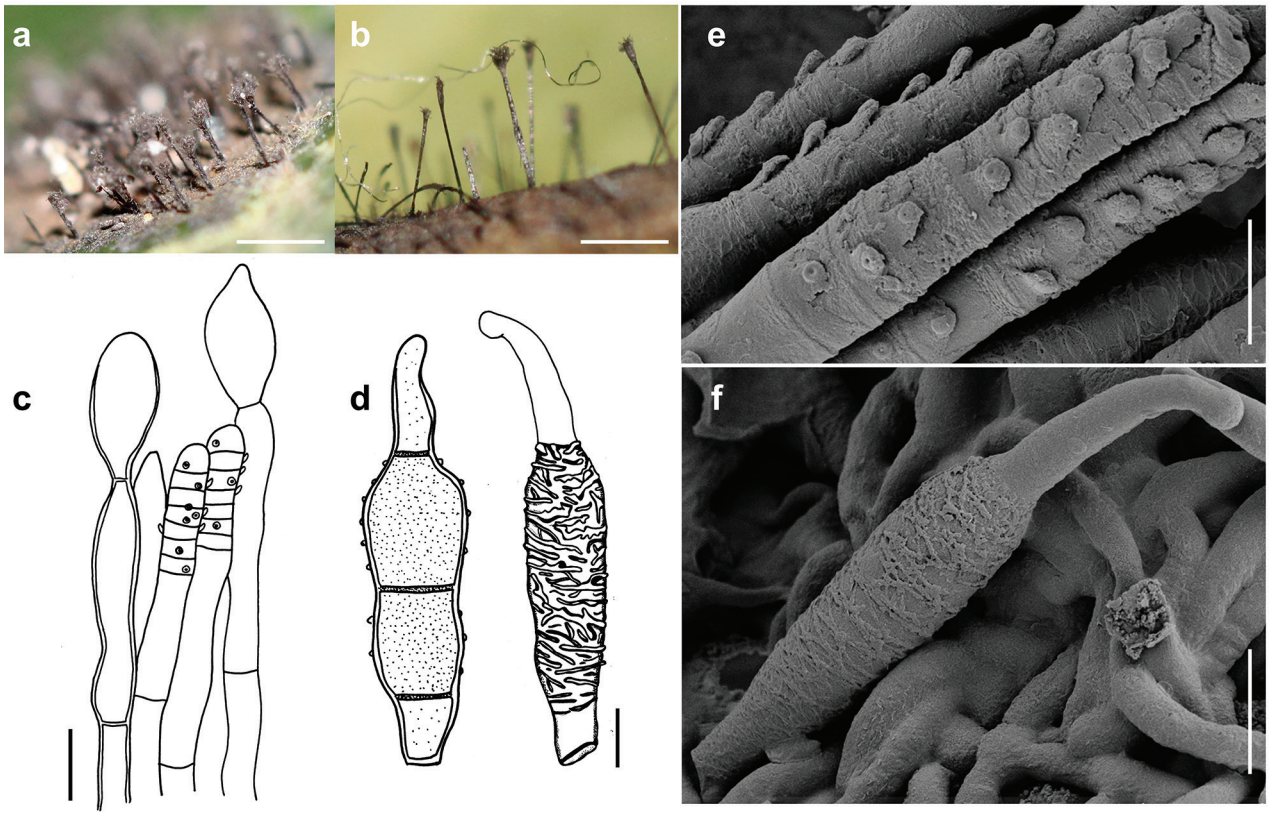

Figure 18. *Spiropes melanoplaca* (MB81, MB119, IMI189570a) **a, b** synnemata growing on hyphae of *Meliola mangiferae* on living leaves of *Mangifera indica* **c** conidiophores with scars and young conidia shown in optical section. The thickness of the wall is only shown in the first conidiophore, from left to right **d** conidia, shown in optical section (left-hand drawing) and as seen by SEM (right-hand drawing) **e, f** as seen by SEM **e** parts of conidiophores with scars **f** conidium. Scale bars: 1.5 mm (**a**); b); 0.9 mm (**c**); 8 µm (**d**); 7 µm (**e**); 8 µm (**f**).

stereomicroscope. ***Hyphae*** superficial, branched, septate, 1.5–6 µm wide, pale olivaceous, smooth. ***Conidiophores*** tightly packed to form dark brown to blackish synnemata up to 1.5 mm high, spreading out at the apex, 20–80 µm thick, splaying out at the apex. Individual hyphae straight or flexuous, cylindrical, 2–6 µm thick along most of their length, 5–8 µm thick near the apex, with numerous small scars that may overlap like scales. As evident by SEM, the scales are produced by the peeling of the outer wall layers where the scars are located. ***Conidia*** straight or curved, fusiform to obclavate, 3-septate, (30–)40–52(–68) × (7–)9–11(–14) µm, with the two middle cells usually golden brown or brown, warty and the cells at each end paler. As seen by SEM, the ornamentation of the spores is distinctly reticulated, with thin to thick networks and no ridges.

Specimens examined. On *Meliola mangiferae* on living leaves of *Mangifera indica* (Anacardiaceae), Panama, Chiriquí Province, Los Algarrobos, 8°31'05"N, 82°25'25"W, 168 m a.s.l., 20 January 2020, M. A. Bermúdez-Cova, MB81; same fungal and plant host, Panama, Chiriquí Province, Universidad Autónoma de Chiriquí (UNACHI), 8°25'57"N, 82°27'02"W, 37 m a.s.l., 23 January 2020, M. A. Bermúdez-Cova, MB85 (UCH15487); same fungal and plant host, Panama, Chiriquí Province, Los Algarrobos, Majagua River Trail, 8°28'56"N, 82°24'47"W, 101 m a.s.l., 23 January 2020, M. A. Bermúdez-Cova, MB89 (UCH15488, M); same fungal and plant host, Panama, Chiriquí Province, Meseta de Chorcha, 8°24'19"N, 82°13'26"W, 94 m a.s.l., 16 February 2020, M. A. Bermúdez-Cova, A. Sanjur, MB101 (UCH);

same fungal and plant host, Panama, Chiriquí Province, Boquerón District, Hidroeléctrica Chuspa, 8°33'37"N, 82°36'22"W, 331 m a.s.l., 6 March 2020, M. A. Bermúdez-Cova, A. Sanjur, S. Samaniego, MB119 (UCH15491); On *Meliola* sp. on living leaves of *Angylocalyx oligophyllus* (Fabaceae), Benin, Attogon, Niaouli, Niaouli Forest, 6°44'42"N, 2°7'50"E, 69 m a.s.l., 28 February 2022, M.A. Bermúdez-Cova, A. Tabé, I. Agonglo, O.P. Agbani, M. Piepenbring, N.S. Yorou, MB173 (M); on *Meliola mangiferae* on living leaves of *Mangifera indica*, Benin, Attogon, Niaouli, Niaouli Forest, 6°44'44"N, 2°7'49"E, 65 m a.s.l., 28 February 2022, M.A. Bermúdez-Cova, A. Tabé, I. Agonglo, O.P. Agbani, M. Piepenbring, N.S. Yorou, MB180 (M).

Additional specimens examined. On *Meliola mangiferae* on *Mangifera indica*, Brunei, 1974, W.T.H. Peregrine (IMI189570a); on *Meliola* sp. on *Psychotria* sp. (Rubiaceae), Cuba, 1879, C. Wright (IMI 105348 and IMI 105349, syntypes of *Arthrobotryum melanoplaca*).

Illustrations. This species was illustrated by Ellis (1968).

Known hosts and distribution. On colonies of Meliolales, especially *Meliola* spp., on living leaves of various plants in Brazil, Cuba, China, Dominican Republic, Ghana, Guadalcanal, India, Malaysia, Peru, Philippines, Sierra Leone, Tanzania, Trinidad and Uganda (Ellis 1968; Zhao et al. 1996; Dubey and Moonnambeth 2013). *Spiropes melanoplaca* is reported here for the first time for Benin and Panama.

Notes. According to Ellis (1968), the main difference between *Spiropes melanoplaca* and *S. dialii* is the range of spore width, with *S. melanoplaca* having wider spores (9–14 µm wide) than *S. dialii* (7–9 µm wide). However, after revision of several specimens and herbarium material from both species, we noticed that the aspect of the colonies, morphological features (both as seen in LM and by SEM) are similar between the species and both species present conidia with a similar size range (Fig. 15). Therefore, we propose *S. dialii* as a synonym of *S. melanoplaca*.

***Spiropes palmetto* (W.R. Gerard) M.B. Ellis, Mycol. Pap. 114: 16, 1968**
Fig. 19

≡ *Helminthosporium palmetto* W.R. Gerard, Grevillea 17(83): 68, 1889.
≡ *Pleurophragmium palmetto* (W.R. Gerard) S. Hughes, Can. J. Bot. 36: 778, 1958.

Description. ***Colonies*** effuse, dark brown to black, hairy. ***Hyphae*** superficial, branched, anastomosing, septate, 1–4 µm wide, pale olivaceous-brown, smooth. ***Conidiophores*** arising singly or in groups, as terminal and lateral branches on the hyphae, erect, straight or flexuous, septate, up to 400 µm long, 6–10 µm thick, dark brown, paler towards the apex, smooth, with scattered conidial scars. ***Conidia*** solitary, obclavate to fusiform, rostrate, with 2 septa delimiting a barrel-shaped central cell and often with an additional dark central pseudoseptum, (27–)30–46 × (7–)9–12(–15) µm, 3–5 µm wide at the truncate base, brown, middle cells pale brown, smooth as seen by LM and SEM.

Specimens examined. On *Meliola* sp. on leaves of *Elaeis guineensis* (Arecaceae), Ghana, Apremodo, 1949, S.J. Hughes 534 (IMI 38617); on *Meliola* sp. on leaves of *Sabal palmetto* (Arecaceae), U.S.A, Louisiana (IMI 10032, type of *Helminthosporium palmetto*).

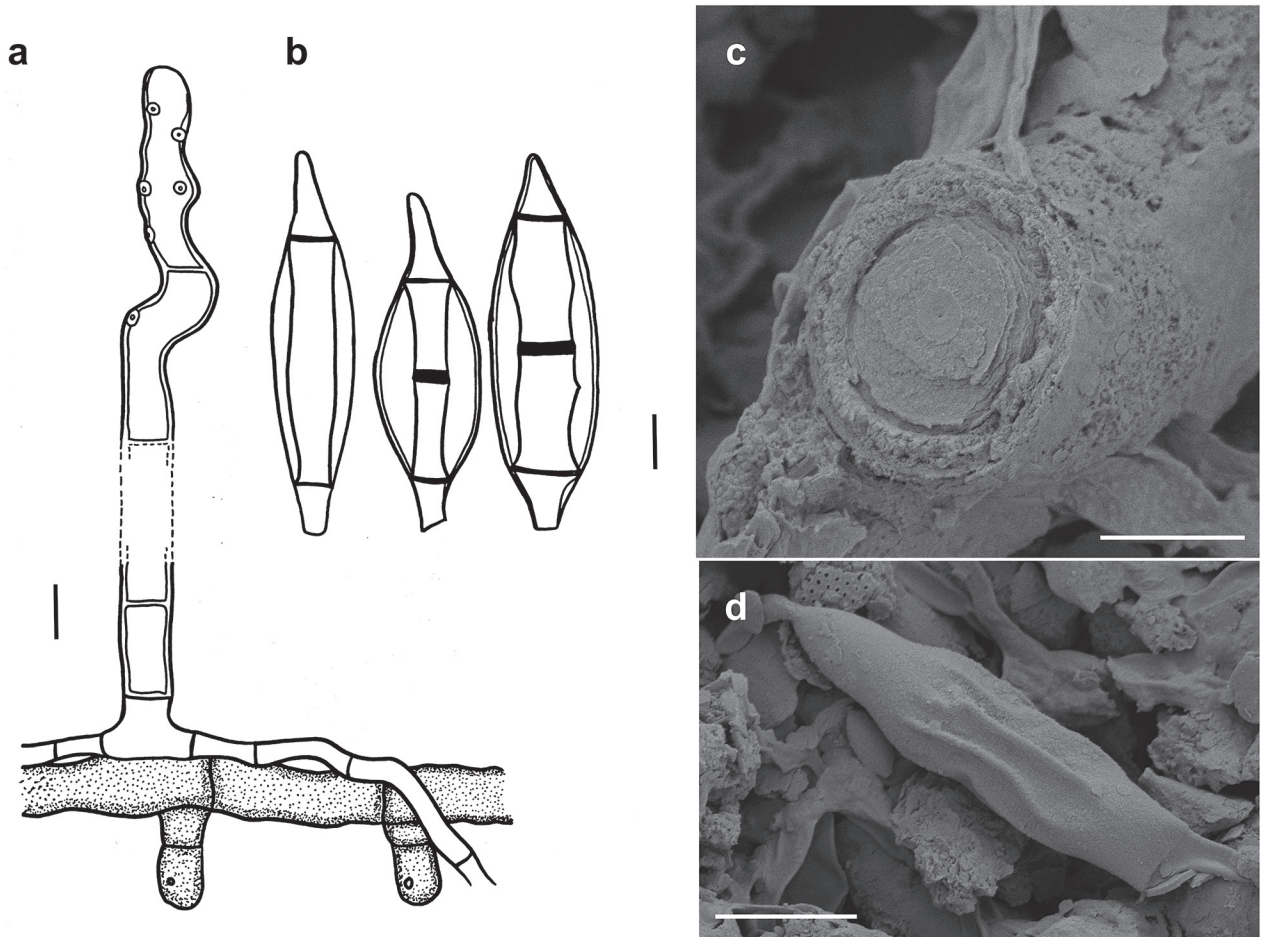

Figure 19. *Spiropes palmetto* (IMI 10032) **a** conidiophore growing on a hypha of *Meliola* sp., shown in optical section **b** conidia shown in optical section. The thickness of the walls is only shown in the two last drawings **c, d** as seen by SEM **c** part of a conidiophore with a scar **d** conidium. Scale bars: 7 µm (**a**); 5 µm (**b**); 6 µm (**c**); 7 µm (**d**).

Illustrations. This species was illustrated by Ellis (1968).

Known hosts and distribution. On colonies of *Irenopsis* spp. and *Meliola* spp. on living leaves of various plants in Ghana, Malaysia, New Zealand, Puerto Rico, Sierra Leone and the U.S.A. (Ellis 1968).

Notes. *Spiropes palmetto* can be easily recognised by the presence of conidia with two septa that delimit a barrel-shaped central cell and with a dark central pseudoseptum (Ellis 1968).

***Spiropes penicillium* (Speg.) M.B. Ellis, Mycol. Pap. 114: 23, 1968**
Fig. 20

≡ *Podosporium penicillium* Speg., Boln. Acad. nac. Cienc. Córdoba 11: 618, 1889.
≡ *Arthrobotryum penicillium* (Speg.) F. Stevens, Bot. Gaz. 65: 238, 1918.
= *Arthrobotryum strychni* Henn., Hedwigia 43: 397, 1904.
≡ *Podosporium strychni* (Henn.) Cif., Sydowia 9: 311, 1955.
= *Arthrobotryum glabroides* F. Stevens, Bot. Gaz. 65: 237, 1918.
≡ *Podosporium glabroides* (F. Stevens) Cif., Sydowia 9: 309, 1955.

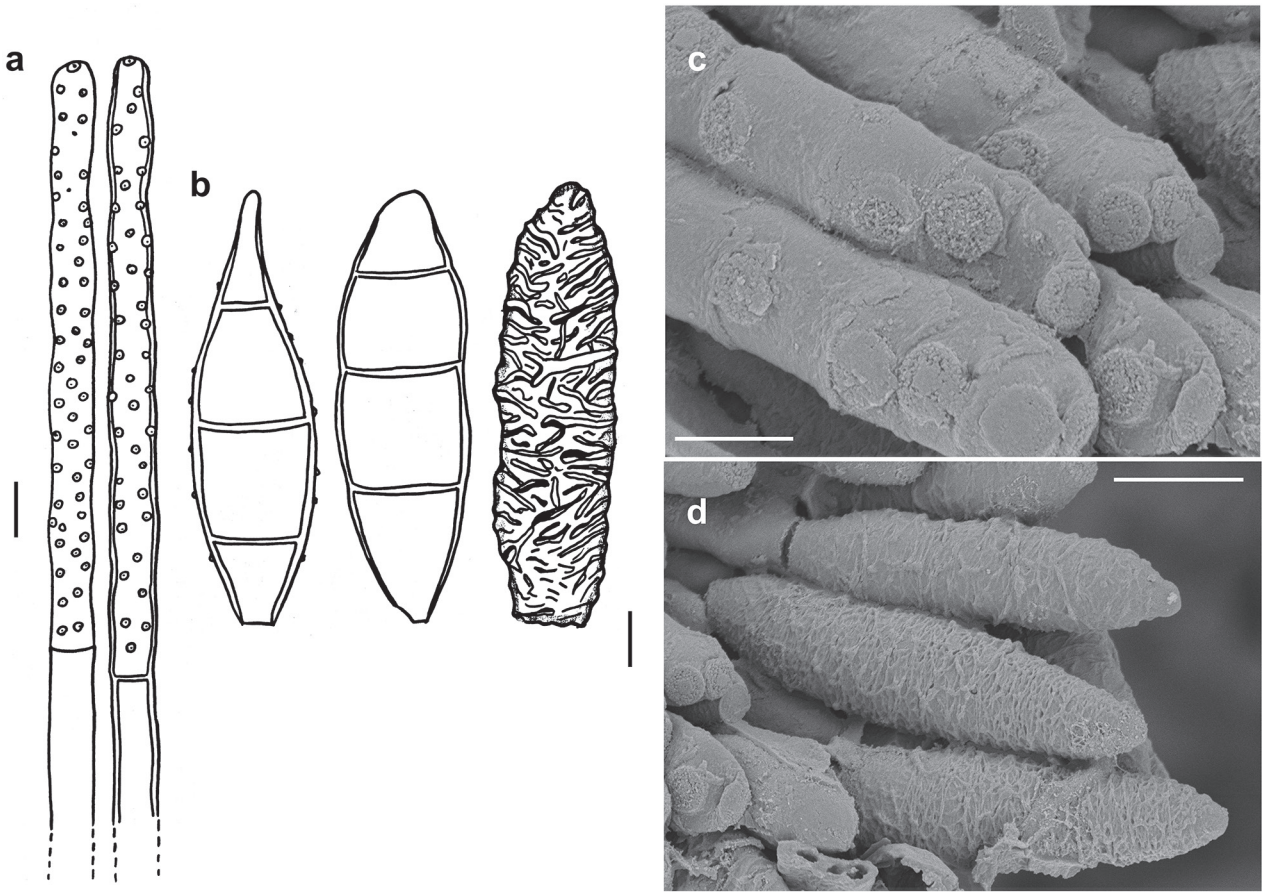

Figure 20. *Spiropes penicillium* (IMI 51664) **a** conidiophores with scars (the thickness of the wall is shown on the right-handed drawing) **b** conidia shown in optical section (first two left-hand drawings) and as seen by SEM **c, d** as seen by SEM **c** tips of conidiophores with scars **d** conidia. Scale bars: 5 µm (**a**); 2.5 µm (**b**); 3 µm (**c**); 5 µm (**d**).

Description. ***Colonies*** effuse, yellowish to dark olivaceous-brown, velvety, with tightly packed hyphae that form large, erect, dark synnemata clearly visible under the stereomicroscope. A bright yellow pigment diffuses out when colonies are mounted in lactic acid or lacto-phenol. ***Hyphae*** superficial, branched, septate, 1–2 µm wide, yellowish, pale olive, smooth. ***Conidiophores*** tightly packed to form dark brown to blackish synnemata up to 650 µm long, 10–40 µm thick, often splaying out to a width of 100 µm at the apex. Individual hyphae straight or flexuous, cylindrical, 1–2 µm thick near the base, 2–3.5 µm thick near the apex, pale olivaceous-brown, smooth, with numerous small conidial scars. ***Conidia*** solitary, fusiform or occasionally almost cylindrical, mostly 3(–5)–septate, 16–23(–37) × (3–)3.5–5(–7) µm, tapering to about 1 µm at the apex and base, middle cells pale brown, the cells at each end paler, surface wrinkled or verruculose. As seen by SEM, the ornamentation of the spores is distinctly reticulated, with thin to thick networks that can form ridges-like structures.

Specimen examined. On *Meliola calva* on leaves of Lauraceae, Brasil, S. Paulo, Apiahy, 1881, J. Puiggari 1483 (IMI 131184, type of *Podosporium penicillium*); on *Meliola* sp. on leaves of *Oxyanthus* sp. (Rybiaceae), Sierra Leone, 1951, D.S. Rennis (IMI 51664).

Illustrations. This species was illustrated by Ellis (1968).

Known hosts and distribution. On colonies of *Asteridiella* spp. and *Meliola* spp. on living leaves of various plants in Brazil, Congo, Costa Rica, Ghana, Ivory Coast, Nigeria, Sierra Leone and Uganda (Ellis 1968).

Notes. *Spiropes penicillium* is easily distinguishable from other known synnematous species of the genus *Spiropes* by the presence of fusiform to cylindrical conidia without rostra. In addition, a bright yellow pigment diffuses out of the cells when colonies are mounted in lactic acid or lacto-phenol (Ellis 1968).

Key to species of *Atractilina* and *Spiropes* hyperparasitic on Meliolales

1 Conidiophores synnematous **2**
– Conidiophores single or in groups **7**
2 Synnemata straw-coloured to pale olivaceous; conidiophores with denticulate conidiogenous loci; pale multiseptate conidia ..... ***A. parasitica***
– Synnemata dark brown to black; conidiophores with cicatrised conidiogenous loci; conidia pigmented and multiseptate **3**
3 Synnemata up to 400 µm long; conidia mostly crescent shape ..... ***S. croissantiformis***
– Synnemata longer, from 700 µm to 1.5 mm long; conidia fusiform to obclavate, occasionally cylindrical **4**
4 Conidia fusiform to almost cylindrical; a yellow pigment diffuses out when colonies are mounted in lactic acid or lacto-phenol ..... ***S. penicillium***
– Conidia fusiform to obclavate; no yellow pigment **5**
5 Conidia always 4–6 septate ..... ***S. japonicus***
– Conidia always 3–septate **6**
6 Conidia 17–25 × 5–6.5 µm ..... ***S. clavatus***
– Conidia 40–52 × 9–11 µm ..... ***S. melanoplaca***
7 Conidia with 3–6 pseudosepta **8**
– Conidia 1–3–septate **10**
8 Conidiophores in larger groups; conidia with 3–6 (usually 4 or 5) pseudosepta ..... ***S. capensis***
– Conidiophores single or in small groups; conidia with 3–5 pseudosepta **9**
9 Conidiophores with zigzag shape; conidia with 3–5 pseudosepta, fusiform to obclavate ..... ***S. guareicola***
– Conidiophores without zigzag shape; conidia with 3–4 pseudosepta, obovate ..... ***S. fumosus***
10 Conidia 1–septate **11**
– Conidia 3–septate **12**
11 Conidia obpyriform, verrucose ..... ***S. armatellae***
– Conidia obpyriform, smooth ..... ***S. armatellicola***
12 Conidia oblong-ellipsoid ..... ***S. intricatus***
– Conidia of various shapes, not oblong-ellipsoid **13**
13 Conidia obovate to clavate; conidiophores swollen towards the apex or in areas where conidia are produced ..... ***S. deightonii***
– Conidia ovate or fusiform to obclavate; conidiophores not swollen towards the apex or in areas where conidia are produced **14**

14 Conidia obclavate; central cells barrel-shaped.....**15**
– Conidia ovate or fusiform to obclavate; without central barrel-shaped cells.....**16**
15 Conidia with 3 true septa..... ***S. caribensis***
– Conidia with 2 septa and a dark central pseudoseptum.....***S. palmetto***
16 Conidia ovate.....***S. carpolobiae***
– Conidia fusiform to obclavate.....**17**
17 Conidia 3–4.5 µm wide.....***S. effusus***
– Conidia wider.....**18**
18 Conidia 17–25 µm long.....***S. angylocalycis***
– Conidia longer.....**19**
19 Conidia 20–35 µm long.....***S. dorycarpus***
– Conidia longer.....**20**
20 Conidia 36–48 µm long.....***S. helleri***
– Conidia 40–54 µm long.....***S. leonensis***

In Fig. 21, we propose a visual key to the known species of *Spiropes* hyperparasitic on Meliolales.

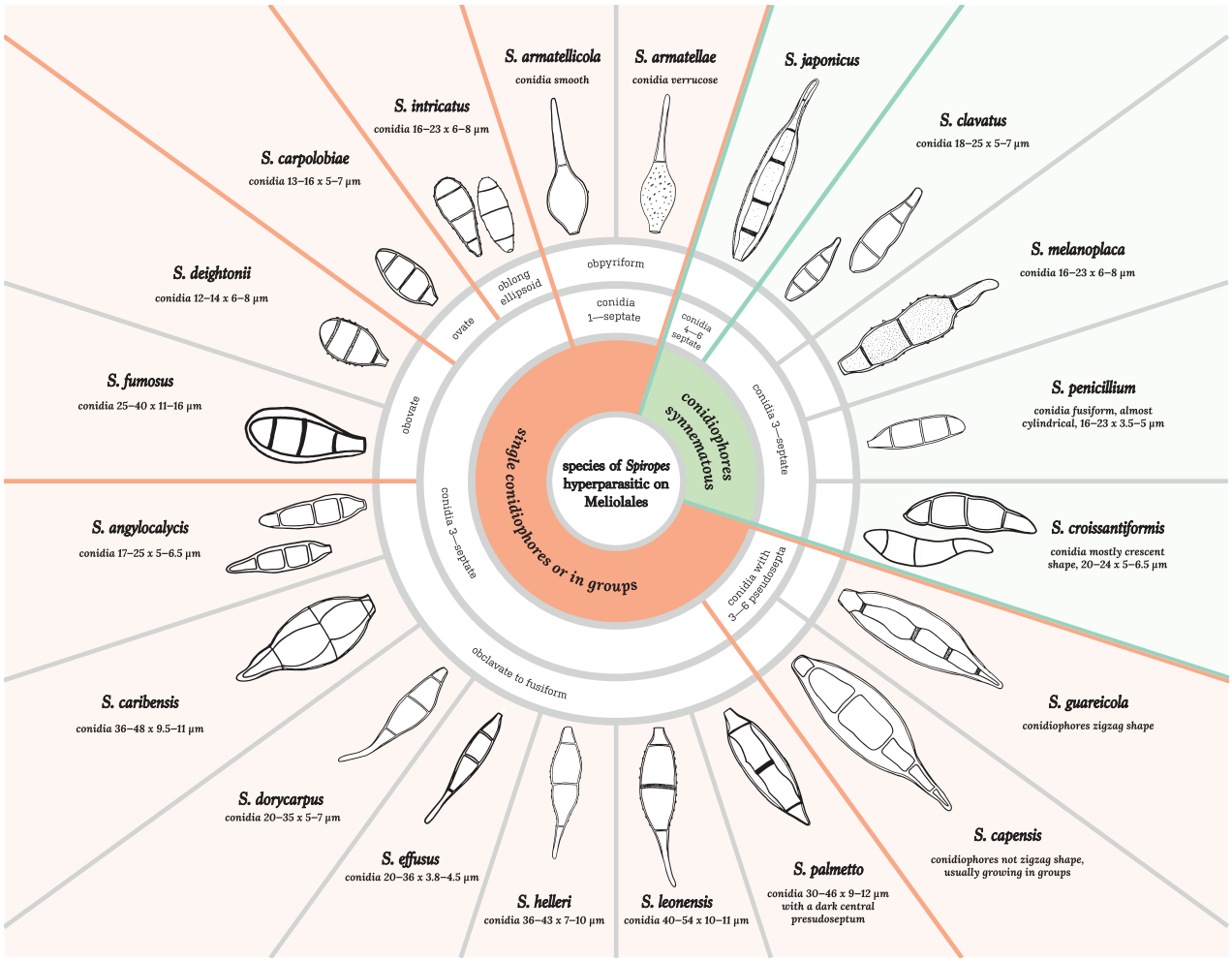

Figure 21. Visual key to known species of *Spiropes* hyperparasitic on Meliolales.

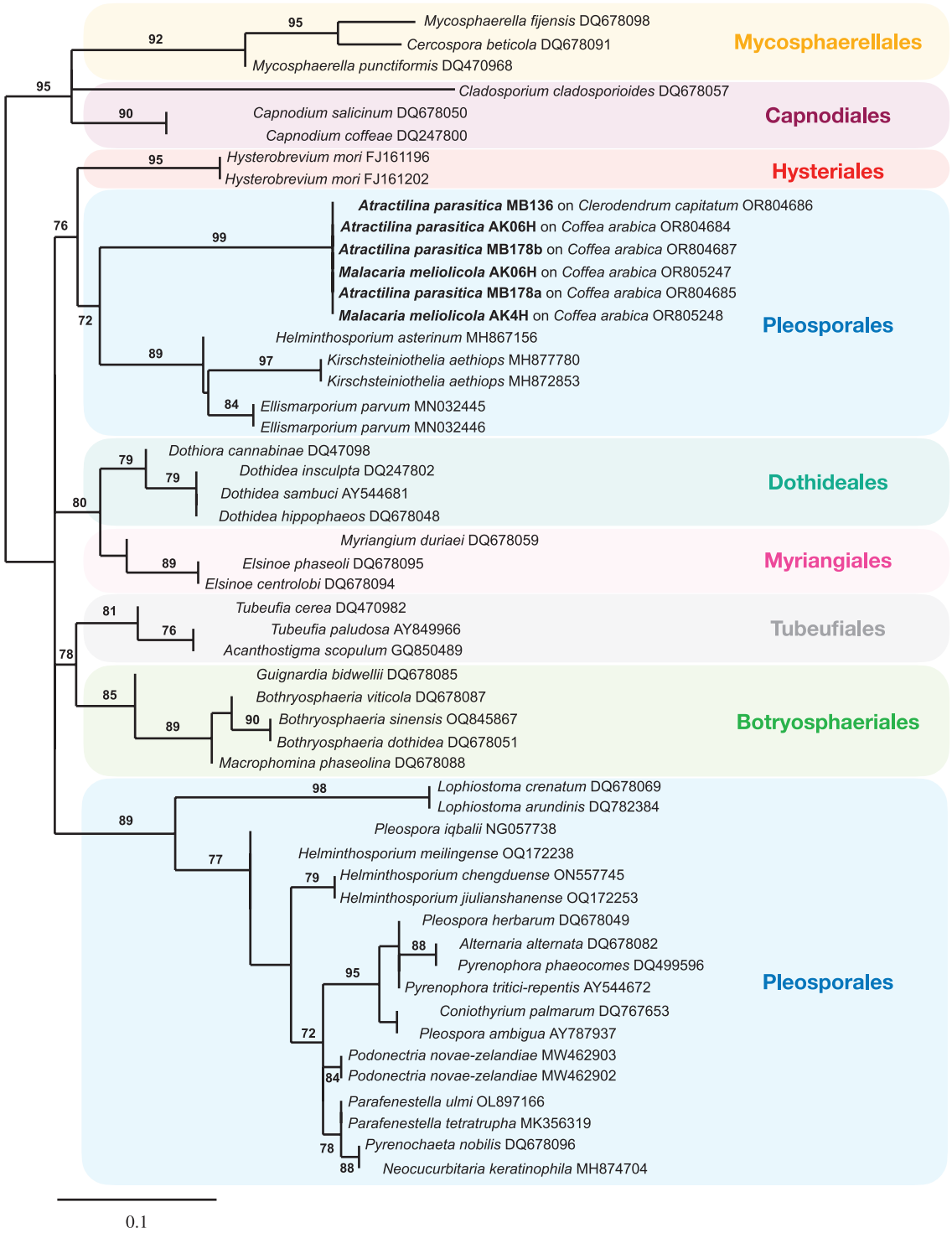

Figure 22. Phylogenetic tree inferred from a Maximum Likelihood analysis of nuc LSU rDNA sequences of members of the Dothideomycetes, including new sequences of *Atractilina parasitica* and *Malacaria meliolicola* (written with bold letters). The tree is rooted with sequences of species of the orders Capnodiales and Mycosphaerellales. Bootstrap values are indicated above the branches. Sequences downloaded from GenBank are given with accession numbers.

Molecular position of species of *Atractilina* and *Spiropes*

In order to know the systematic positions of species of *Atractilina* and *Spiropes* hyperparasitic on Meliolales, new sequences of recently-collected specimens were obtained.

The BLAST query revealed that the nrLSU sequences of *Atractilina parasitica* (specimens MB136 and MB178) show approximately 82% similarity with sequences of species of the Dothideomycetes, such as *Botryosphaeria* spp., *Helminthosporium asterinum* Cooke, *Hysterobrevium mori* (Schwein.) E. Boehm & C.L. Schoch and *Neoheleiosa lincangensis* Mortimer, amongst others. In the tree inferred from the analysis of LSU sequences of 45 specimens of several orders of Dothideomycetes (Fig. 22), the sequences of *A. parasitica* are located in a well-supported clade that comprises species of Pleosporales, such as *Ellismarsporium parvum* R.F. Castañeda & W.B. Kendr., *Kirschsteiniothelia aethiops* (Sacc.) D. Hawksw. and *Helminthosporium asterinum*. In addition, the sequences of *A. parasitica* cluster together in a strongly-supported clade with two DNA sequences we obtained from *Malacaria meliolicola* (specimens AK4H and AK06H), a hyperparasitic perithecioid fungus that usually grows amongst the synnemata of *A. parasitica* on coffee leaves (see Bermúdez-Cova et al. (2023b) for the updated species description of *M. meliolicola*).

As for species of *Spiropes*, the BLAST query revealed that the nrITS sequences of *Spiropes melanoplaca* (specimens MB81 and MB119) and *Spiropes japonicus* (specimen MB 120) are not closely related to each other (60% similarity) and show between 88 and 90% similarity with species of the Leotiomycetes, such as *Lophodermium actinothyrium* Fuckel and *Hypoderma* spp., amongst others. Placement on to the Pezizomycotina tree version 2 in T-BAS confirmed that the newly-generated ITS sequences for the two species of *Spiropes* are placed in the Leotiomycetes (Fig. 23).

Discussion

Atractilina and *Spiropes*, two genera with heterogeneous species

Morphology-based identification of a species can be very difficult, especially amongst asexual or non-sporulating fungi (Jeewon et al. 2002; Promputtha et al. 2005, 2007). However, it continues to be an essential tool, especially for understudied groups of fungi and when DNA sequences are not available or scarce (Raja et al. 2017). The morphological analyses and the literature review of specimens of *Atractilina* and *Spiropes* revealed that both genera include highly heterogeneous species that are not necessarily congeneric with the type species of each genus.

The type species of *Atractilina*, *Atractilina callicarpae* Dearn. & Barthol. (= *Atractilina parasitica* (G. Winter) Deighton & Piroz.), has consistently true synnematous conidiophores, denticulate conidiogenous loci, pale pluriseptate (phragmoseptate) conidia and a hyperparasitic lifestyle (Deighton and Pirozynski 1972; Mel'nik and Braun 2013). Based on these characteristics, only three species of the genus are congeneric with *A. parasitica*, namely *A. alinae* Melnik & U. Braun, *A. biseptata* R.F. Castañeda and *A. calycini* T.K. Jana, S.N. Ghosh & A.K. Das (Castañeda-Ruiz 1986; Jana et al. 2006; Mel'nik and Braun 2013). The remaining two species present non-synnematous conidiophores and are probably not congeneric. *Atractilina asterinae* (Hansf.) Deighton & Piroz. is a species hyperparasitic on Asterinales and presents single conidiophores and distoseptate conidia (Deighton and Pirozynski 1972). *Atractilina hymenaeae* Bat. & J.L. Bezerra (introduced as *Atractina hymenaeae* by the authors) is hyperparasitic

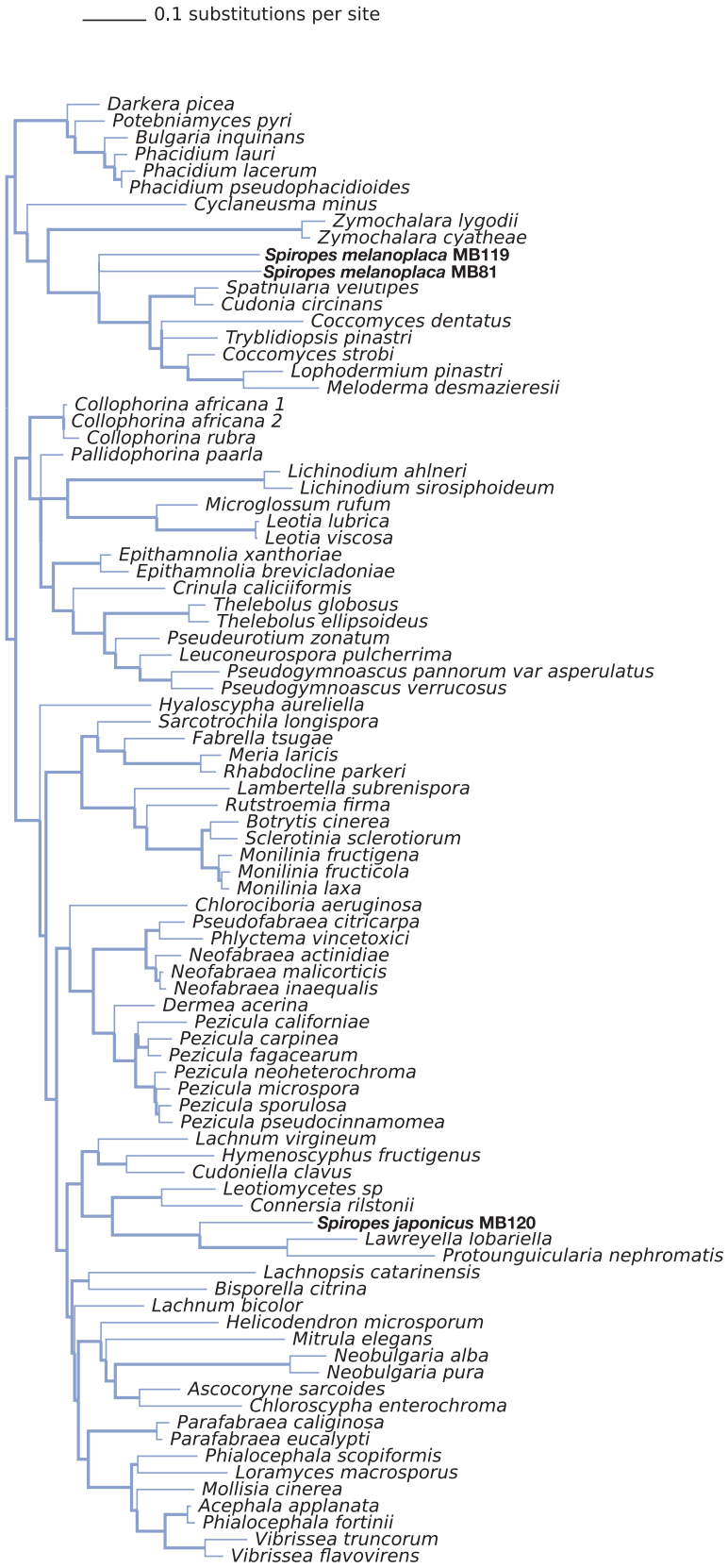

Figure 23. Placement of *Spiropes japonicus* and *S. melanoplaca* on to Pezizomycotina reference tree version 2 in T-Bas. Only the Leotiomycetes clade is shown. The tree is the result of RAxML analysis of nuc ITS rDNA with 500 bootstraps replicates. For each node, the Maximum Likelihood bootstrap (≥ 70%) is presented as thick branches. Names of *Spiropes* species with newly-generated sequence data are written in bold.

on Meliolales, but also with non-synnematous conidiophores and conidia with a variable number of septa (Batista and Bezerra 1961). Therefore, we believe that both species have been incorrectly assigned to the genus *Atractilina*.

The description of *A. parasitica* introduced by Deighton and Pirozynski (1972) is very broad. As a result, specimens with significant morphological variations are grouped into a single species concept. For example, Chen and Tzean (2007) described a parasitic fungus from Taiwan growing on decaying leaves of *Liquidambar* sp. (Altingiaceae), with conidia that resemble those of *A. parasitica*. However, conidiophores of this fungus are non-synnematous and very short (less than 15 µm long), a feature that has never been reported before for *A. parasitica*. It is necessary to re-evaluate this and other identifications, to narrow the species concept of *A. parasitica*, as well as to complement it with DNA sequence data.

The DNA molecular analyses of the nrLSU rDNA region of the specimens of *A. parasitica* from Benin revealed that this species belongs to the Dothideomycetes. The Dothideomycetes are the largest and most diverse class of fungi and comprise species that exhibit a broad range of lifestyles, including saprotrophs, plant pathogens, mycoparasites and hyperparasites, as well as lichenised and lichenicolous fungi (Pem et al. 2021). They typically produce flask-like structures called pseudothecia, though apothecial, hysterothecial and cleistothecioid ascomata also exist (Hessen and Jahns 1973; Valenzuela-Lopez et al. 2019). Bitunicate asci are one of the diagnostic characters for Dothideomycetes taxonomy (Von Arx and Müller 1975; Pem et al. 2021). Asexual stages are frequent amongst pathogenic genera in the families *Cladosporiaceae*, *Mycopsphaerellaceae*, *Pleosporaceae* and *Tubeufiaceae*, amongst others (Hyde et al. 2013; Wanasinghe et al. 2018; Hongsanan et al. 2020). Conidiophores in these anamorphic species are usually solitary or in groups forming synnemata (Thambugala et al. 2017). The sequences of *A. parasitica* showed 98% similarity with sequences of *Malacaria meliolicola* (Dothideomycetes, Ascomycota), a pseudothecioid hyperparasite that was found repeatedly amongst the synnemata of *A. parasitica* (Bermúdez-Cova et al. 2023b). The pseudothecia of *M. meliolicola* were also found to be growing without the presence of synnemata of *A. parasitica*. These colonies were used to extract the DNA of *M. meliolicola*. Therefore, the systematic position of *A. parasitica* in the Dothideomycetes and the anamorph-teleomorph connection between these two species are confirmed. This connection has been proposed in the past for these fungi on leaves of *Coffea arabica* (Hansford 1941, 1946; Bermúdez-Cova et al. 2023b). Here, a DNA sequence from a specimen of *A. parasitica* on *Meliola* sp. on leaves of *Clerodendrum capitatum* clustered with the aforementioned sequences in a highly-supported clade. The phylogenetic analysis of the nrLSU DNA locus showed that sequences of *A. parasitica* are located in a well-supported subclade together with other species of Pleosporales s.l., such as *Ellismarsporium parvum* (Zhang et al. 2020). Many species of the Dothideomycetes, especially the asexual genera, are known to be polyphyletic (Schoch et al. 2009). To confirm the systematic hypothesis and to determine the placement of *A. parasitica* at family level, the use of multi-loci phylogenies is necessary in the future.

As for the genus *Spiropes*, the generic diagnosis given by Ellis (1968, 1971) allows us to include in this genus all species with cicatrised conidiogenous cells and conspicuous, flat and numerous scars, as well as pigmented, mostly

obclavate phragmoconidia with 1–9 septa or pseudosepta. Seifert and Hughes (2000) proposed an amendment of this generic concept to also include species with dictyoconidia. As a result, *S. dictyosporus* is the only known species of the genus with muriform conidia. However, this morphological diagnosis allows for species with a wide range of types of conidiophores, conidiogenesis and conidia to be included in *Spiropes* (McTaggart et al. 2007). For example, the type species of the genus, *Spiropes guareicola* (F. Stevens) Cif., has distinctly sympodial-geniculate (zigzag-shaped) conidiophores, a character that is not present in any other known species of the genus (Ellis 1968). This species, in addition, presents distoseptate conidia, i.e. conidia with pseudosepta, a morphological feature that is present only in four species, namely *S. capensis*, *S. fumosus*, *S. guareicola* and *S. japonicus*. The remaining species of the genus present euseptate conidia (Ellis 1968, 1971). It is also possible to find a wide range of conidial shapes, such as obpyriform, obovate, ovate and oblong ellipsoid, to obclavate and fusiform (see the visual key to species of *Spiropes* in Fig. 21). Therefore, *Spiropes* is currently a genus with morphologically highly heterogeneous species and probably polyphyletic.

Identifying species of *Spiropes*, based on morphology alone, is not always easy. The most comprehensive key to species of the genus was proposed by Ellis (1968). However, this key is mainly based on the differences in the size range of the conidia of the species and, in some cases, these size differences are very subtle. Particular attention should be paid to herbarium specimens, as they may include immature or not well-preserved spores that can affect measurement results (Ordynets et al. 2021). We believe that other morphological characteristics that are not visible using standard light microscopy techniques should be considered when identifying species of *Spiropes* (e.g. Lutzoni et al. (2004)). Scanning electron Microscopy (SEM), for example, allowed us to observe for the first time the surface of the conidia of species of *Spiropes*. *Spiropes diallii* and *S. melanoplaca* were considered as different species by Ellis (1968). However, both species have overlapping spore-size ranges and the morphological analysis by SEM revealed that these species also have similar conidiogenesis and ornamentation patterns on conidia. This situation is similar for *S. intricatus* and *S. pirozynskii*. Therefore, we propose both groups of species as synonyms.

As for the molecular-based identification of species of *Spiropes*, there are currently no DNA sequences available in publicly-accessible databases. Species of the genus remain "incertae sedis" for many taxonomic ranks and it is difficult to assign new DNA sequences to species concepts (Bermúdez-Cova et al. 2022, 2023a). The DNA sequences generated for the first time in the context of this study suggest that species of *Spiropes* hyperparasitic on Meliolales may be polyphyletic in the Leotiomycetes. Fungi in the class Leotiomycetes are ecologically diverse and have been described as aquatic hyphomycetes, ectomycorrhizal parasites, endophytes, fungal parasites, mycorrhizal fungi, nematode-trapping fungi and plant-pathogens, amongst others (Wang et al. 2006a; Johnston et al. 2019). Many fungi have been suggested to belong to this class without any clear teleomorphic connection (Wang et al. 2006b). Up to date, no sexual stages have been linked to any species of *Spiropes* (Bermúdez-Cova et al. 2022). There is one genus with species morphologically similar to species of *Spiropes*, namely *Pseudospiropes* M.B. Ellis (Helotiales, Leotiomycetes; Ellis (1971)). Species of this genus differ from species of *Spiropes* by broadly enlarged, thickened, protuberant, strongly

melanised conidiogenous loci and distoseptate conidia only (Castañeda-Ruiz et al. 2001; McTaggart et al. 2007). Species of *Pseudospiropes* have *Strossmayeria* Schulzer (Helotiales, Leotiomycetes) teleomorphs (Iturriaga and Korf 1984, 1990; Castañeda-Ruiz et al. 2001). Thus, there is a possibility that species of the genus *Spiropes* also belong to the Leotiomycetes. It is necessary to continue generating new DNA sequences from the different species of the genus in order to confirm this hypothesis, especially from those species that form part of mixed infections.

It is difficult to obtain molecular sequence data from hyperparasites especially because of the fact that they develop intermingled with the primary parasite and many other organisms and, as a result, no specific set of molecular methods has been developed to study hyperparasites (Bermúdez-Cova et al. 2022; Bermúdez-Cova et al. 2023a). As a consequence, isolating and sequencing hyperparasitic fungi is a challenging task. There is also a lack of sequences of hyperparasitic fungi in public. Therefore, the sequences obtained can be related to existing species concepts only based on morphology databases (Bermúdez-Cova et al. 2023b). For hyperparasitic fungi on Meliolales, for example, it is advised to obtain the same or very similar DNA sequences repeatedly from a given morphospecies in order to be sure to have the correct DNA sequence of that morphospecies. Despite many attempts, it was not possible to obtain DNA sequences from some of the species included in this study. However, this research provides valuable information that lays the foundation for future research on hyperparasites in Meliolales, highlighting the importance of field work paired with molecular for the study of challenging fungal groups. Further methodologies, such as metabarcoding, could represent another way to try to isolate the DNA of these organisms.

The need for re-evaluation, resampling and epitypification

Applications of names based on morphological characteristics without DNA data is a challenge, resulting in the description of an excessive number of species or, in contrast, in the overlooking of cryptic species that can only be detected through molecular analyses (Hibbett et al. 2007; Crous et al. 2014; Jayasiri et al. 2015). The knowledge of morphological characteristics, however, is important to understand the evolution of fungal diversity (Raja et al. 2017). Instead of describing new species as part of *Atractilina* and *Spiropes*, a re-evaluation of the natural concepts of both genera is needed. Here we propose a list of actions that are necessary to carry out such a re-evaluation:

- Restudy the type species of each genus. When the type specimens of the type species are not in good condition or there is no more fungal material available for examination, it is necessary to recollect them. Epitypes and neotypes should be designated in these cases.
- After redefining the type species, all species belonging to the two genera need to be recollected, re-analysed morphologically and compared to the type species.
- The DNA of all existing species should be extracted, amplified and sequenced, in order to confirm or propose new concepts of genera and species. Multi-loci phylogenetic analyses are necessary to validate or propose new systematic hypotheses.

Atractilina and *Spiropes* are currently two repository genera of highly heterogeneous species and they may be split in the future, once species and genus concepts are validated respectively by morphology and molecular methods.

Acknowledgements

We are grateful to the University of Parakou and the University of Abomey-Calavi, Benin, for the support and facilities made available for this study. We acknowledge help by Dr. Pierre Agbani (Botanical Garden of the Université d'Abomey-Calavi) for his assistance with the identification of host plants and help by Daouda Dongnima during fieldwork. Special thanks to Affoussatou Tabé, Alicia Sanjur and Anna Krauss for their support and collecting efforts throughout the whole research process. We acknowledge the support and facilities made available by Orlando Cáceres and the Universidad Autónoma de Chiriquí (UNACHI) in Panama. The Environmental Ministry of Panama (MiAmbiente) is thanked for issuing the collection and export permits (SE/APHO-1-2019, SEX/H-5-2020, PA-01-ARG-049-2021). We are grateful to the Ministry of Environment of the Benin Republic for issuing the collecting permits and for the elaboration of the ABS Nagoya Protocol documents n° 636/DGEFC/ANC-APA/DCPRN/PF-APA.

Additional information

Conflict of interest

The authors have declared that no competing interests exist.

Ethical statement

No ethical statement was reported.

Funding

The first author acknowledges support from the German Academic Exchange Service (DAAD), within the framework of the scholarship programme for doctoral studies in Germany (Ref. no.: 91726217).

Author contributions

MB-C compiled and analyzed the data and wrote the first draft of the manuscript. MB-C, TH, NY and MP contributed to writing and editing the manuscript. All authors contributed to the article and approved the submitted version.

Author ORCIDs

Miguel A. Bermúdez-Cova https://orcid.org/0000-0002-7712-7347
Tina A. Hofmann https://orcid.org/0000-0003-1124-402X
Nourou S. Yorou https://orcid.org/0000-0001-6997-811X
Meike Piepenbring https://orcid.org/0000-0002-7043-5769

Data availability

All of the data that support the findings of this study are available in the main text or Supplementary Information.

References

Abarca GH, Ruiz RC, Arias RM, Saikawa M, Stadler M (2007) Anamorphic fungi from submerged plant material: *Acumispora verruculosa*, *Pleurophragmium aquaticum* and *P. miniumbonatum*. Mycotaxon 101: 89–97.

Akoègninou A, Van der Burg WJ, Van der Maesen LJG (2006) Flore Analytique du Bénin. Backhuys Publishers, Wageningen, 1034 pp.

Alcorn JL (1988) The taxonomy of "*Helminthosporium*" species. Annual Review of Phytopathology 26(1): 37–56. https://doi.org/10.1146/annurev.py.26.090188.000345

Bánki O, Roskov Y, Döring M, Ower G, Vandepitte L, Hobern D, Remsen D, Schalk P, DeWalt RE, Keping M, Miller J, Orrell T, Aalbu R, Abbott J, Adlard R, Adriaenssens EM, Aedo C, Aescht E, Akkari N, et al. (2023) Catalogue of Life Checklist [Version 2023-07-10]. Catalogue of Life. https://doi.org/10.48580/dfry

Batista AC, Bezerra JL (1961) Novos ou raros Deuteromycetes. Memórias da Sociedade Broteriana 14: 73–82.

Benson DA, Clark K, Karsch-Mizrachi I, Lipmanbn DJ, Ostell J, Sayers EW (2014) GenBank. Nucleic Acids Research 42(D1): D32–D37. https://doi.org/10.1093/nar/gkt1030

Bermúdez-Cova MA, Cruz-Laufer AJ, Piepenbring M (2022) Hyperparasitic fungi on black mildews (Meliolales, Ascomycota): Hidden fungal diversity in the tropics. Frontiers in Fungal Biology 3: 885279. https://doi.org/10.3389/ffunb.2022.885279

Bermúdez-Cova MA, Haelewaters D, de Bekker C, Piepenbring M, Schoutteten N, Quandt CA (2023a) Hyperparasitic fungi – definitions, diversity, ecology, and research. Authorea, June 27, 2023. https://doi.org/10.22541/au.168787020.07281183/v1

Bermúdez-Cova MA, Krauß A, Sanjur A, Tabé A, Hofmann TA, Yorou NS, Piepenbring M (2023b) Diversity of hyperparasitic fungi on Meliolales (Sordariomycetes, Ascomycota): New species, records, and molecular data from Benin and Panama. Mycological Progress 22(9): 65. https://doi.org/10.1007/s11557-023-01913-5

Carbone I, White JB, Miadlikowska J, Arnold AE, Miller MA, Magain N, U'Ren JM, Lutzoni F (2019) T-BAS version 2.1: Tree-Based Alignment Selector toolkit for evolutionary placement of DNA sequences and viewing alignments and specimen metadata on curated and custom trees. Microbiology Resource Announcements 8(29): e00328–e19.https://doi.org/10.1128/MRA.00328-19

Castañeda-Ruiz RF (1986) Fungi Cubenses, 20 pp.

Castañeda-Ruiz RF, Heredia G, Reyes M, Arias RM (2001) A revision of the genus *Pseudospiropes* and some new taxa. Cryptogamie. Mycologie 22(1): 3–18. https://doi.org/10.1016/S0181-1584(01)01057-0

Chen J-L, Tzean S-S (2007) Hyphomycetes from Taiwan. *Akanthomyces* and allied species. Fungal Science 22(3, 4): 63–77.

Ciferri R (1955) Observations on meliolicolous Hyphales from Santo Domingo. Sydowia 9(1–6): 296–335.

Condit R, Pérez R, Daguerre N (2011) Trees of Panama and Costa Rica. Princeton University Press, Princeton NJ, 481 pp. https://doi.org/10.1515/9781400836178

Costantin JN (1888) Les Mucédinées Simples. Histoire, Classification, Culture et Rôle des Champignons Inférieurs dans les Maladies des Végétaux et des Animaux. Klincksieck, Paris, i-viii, 210 pp.[, 190 figs]

Crous PW, Giraldo A, Hawksworth DL, Rober V, Kirk PM, Guarro J, Robbertse B, Schoch CL, Damm U, Trakunyingcharoen T, Groenewald JZ (2014) The Genera of Fungi: Fixing the application of type species of generic names. IMA Fungus 5(1): 141–160. https://doi.org/10.5598/imafungus.2014.05.01.14

De Beer ZW, Seifert KA, Wingfield MJ (2013) A nomenclator for ophiostomatoid genera and species in the Ophiostomatales and Microascales. Biodiversity Series 12: 245–322.

Deighton FC, Pirozynski KA (1972) Microfungi. V. More hyperparasitic hyphomycetes. Mycological Papers 128: 110.

Dubey R, Moonnambeth NA (2013) Hyperparasitism of *Isthmospora spinosa* Stevens and *Spiropes melanoplaca* (Berk. & Curtis) Ellis on *Meliola tylophorae – indicae* Hosag. parasitizing *Tylophora indica* (Burm. f.) Merill from India- A New Record. Journal on New Biological Reports 2(1): 64–66.

Ellis MB (1968) Dematiaceous Hyphomycetes. IX. *Spiropes* and *Pleurophragmium*. Mycological Papers 114: 1–44.

Ellis MB (1971) Dematiaceous Hyphomycetes. X. Mycological Papers 125: 1–30. https://doi.org/10.1079/9780851986180.0000

Ellis MB (1976) More Dematiaceous Hyphomycetes. Kew, Commonwealth Mycological Institute, 507 pp. https://doi.org/10.1079/9780851983653.0000

Fazekas AJ, Kuzmina ML, Newmaster SG, Hollingsworth PM (2012) DNA barcoding methods for land plants. In: Kress WJ, Erickson DL (Eds) DNA Barcodes. Methods in Molecular Biology. Humana, Totowa, 223–252. https://doi.org/10.1007/978-1-61779-591-6_11

Hansford CG (1941) Contribution towards the fungus flora of Uganda. III. Proceedings of the Linnean Society of London 153: 4–52. https://doi.org/10.1111/j.1095-8312.1941.tb01378.x

Hansford CG (1946) The foliicolous ascomycetes, their parasites and associated fungi. Mycological Papers 15.

Hessen A, Jahns HM (1973) '1974' lichens. Eine Einführung in die Flechtenkunde. Thiene, Stuttgart.

Hibbett DS, Binder M, Bischoff JF, Blackwell M, Cannon PF, Eriksson OE, Huhndorf S, James T, Kirk PM, Lücking R, Lumbsch HT, Lutzoni F, Mathenya PB, McLaughlin DJ, Powell MJ, Redhead S, Schoch CL, Spatafora JW, Stalpers JA, Vilgalys R, Aime MC, Aptroot A, Bauer R, Begerow D, Benny GL, Castlebury LA, Crous PW, Dair YC, Gams W, Geisers DM (2007) A higher-level phylogenetic classification of the fungi. Mycological Research 111(5): 509–547. https://doi.org/10.1016/j.mycres.2007.03.004

Hofmann TA, Kirschner R, Piepenbring M (2010) Phylogenetic relationships and new records of Asterinaceae (Dothideomycetes) from Panama. Fungal Diversity 43(1): 39–53. https://doi.org/10.1007/s13225-010-0042-4

Holubová-Jechová V, Sierra AM (1984) Studies on hyphomycetes from Cuba II. Hyphomycetes from the Isla de la Juventudeská. Česká Mykologie 38: 96–120.

Hongsanan S, Tian Q, Persoh D, Zeng X-Y, Hyde KD, Chomnunti P, Boonmee S, Bahkali AH, Wen T-C (2015) Meliolales. Fungal Diversity 74(1): 91–141. https://doi.org/10.1007/s13225-015-0344-7

Hongsanan S, Hyde KD, Phookamsak R, Wanasinghe DN, McKenzie EHC, Sarma VV, Boonmee S, Lücking R, Bhat DJ, Liu NG, Tennakoon DS, Pem D, Karunarathna A, Jiang SH, Jones EBG, Phillips AJL, Manawasinghe IS, Tibpromma S, Jayasiri SC, Sandamali DS, Jayawardena RS, Wijayawardene NN, Ekanayaka AH, Jeewon R, Lu YZ, Dissanayake AJ, Zeng XY, Luo ZL, Tian Q, Phukhamsakda C, Thambugala KM, Dai DQ, Chethana KWT, Samarakoon MC, Ertz D, Bao DF, Doilom M, Liu JK (2020) Refined families of Dothideomycetes: Dothideomycetidae and Pleosporomycetidae. Mycosphere : Journal of Fungal Biology 11(1): 1553–2107. https://doi.org/10.5943/mycosphere/11/1/13

Hosagoudar VB (2003) Armatellaceae, a new family segregated from the Meliolaceae. Sydowia 55: 162–167.

Hosagoudar VB, Biju CK, Abraham TK, Agarwal DK (2002) *Spiropes armatellicola* sp. nov. from Kerala, India. Journal of Economic and Taxonomic Botany 26(3): 603–604.

Hyde KD, Jones E, Liu JK, Ariyawansa H, Boehm E, Boonmee S, Braun U, Chomnunti P, Crous PW, Dai D-Q, Diederich P, Dissanayake A, Doilom M, Doveri F, Hongsanan S, Jayawardena R, Lawrey JD, Li Y-M, Liu Y-X, Lücking R, Monkai J, Muggia L, Nelsen MP, Pang K-L, Phookamsak R, Senanayake IC, Shearer CA, Suetrong S, Tanaka K, Thambugala KM, Wijayawardene NN, Wikee S, Wu H-X, Zhang Y, Aguirre-Hudson B, Alias SA, Aptroot A, Bahkali AH, Bezerra JL, Bhat DJ, Camporesi E, Chukeatirote E, Gueidan C, Hawksworth DL, Hirayama K, De Hoog S, Kang J-C, Knudsen K, Li W-J, Li X-H, Liu Z-Y, Mapook A, McKenzie EHC, Miller AN, Mortimer PE, Phillips AJL, Raja HA, Scheuer C, Schumm F, Taylor JE, Tian Q, Tibpromma S, Wanasinghe DN, Wang Y, Xu J-C, Yacharoen S, Yan J-Y, Zhang M (2013) Families of Dothideomycetes. Fungal Diversity 63(1): 1–313. https://doi.org/10.1007/s13225-013-0263-4

Iturriaga T, Korf RP (1984) Studies in the genus *Strossmayeria* (Helotiales). 1. generic delimitation. 2. Two lost species. 3. Three excluded taxa. Mycotaxon 20: 169–178.

Iturriaga T, Korf RP (1990) A monograph of the Discomycete genus *Strossmayeria* (Leotiaceae), with comments on its anamorph, *Pseudospiropes* (Dematiaceae). Mycotaxon 36: 383–454.

Jana TK, Das AK, Ghosh SN (2006) Studies on foliicolous fungi – I. Geobios (Jodhpur) 33(1): 9–16.

Jayasiri SC, Hyde KD, Ariyawansa HA, Bhat J, Buyck B, Cai L, Dai Y-C, Abd-Elsalam KA, Ertz D, Hidayat I, Jeewon R, Jones EBG, Bahkali AH, Karunarathna SC, Liu J-K, Luangsa-ard JJ, Lumbsch HT, Maharachchikumbura SSN, McKenzie EHC, Moncalvo J-M, Ghobad-Nejhad M, Nilsson H, Pang K-L, Pereira OL, Phillips AJL, Raspé O, Rollins AW, Romero AI, Etayo J, Selçuk F, Stephenson SL, Suetrong S, Taylor JE, Tsui CKM, Vizzini A, Abdel-Wahab MA, Wen T-C, Boonmee S, Dai DQ, Daranagama DA, Dissanayake AJ, Ekanayaka AH, Fryar SC, Hongsanan S, Jayawardena RS, Li W-J, Perera RH, Phookamsak R, de Silva NI, Thambugala KM, Tian Q, Wijayawardene NN, Zhao R-L, Zhao Q, Kang J-C, Promputtha I (2015) The Faces of Fungi database: Fungal names linked with morphology, phylogeny and human impacts. Fungal Diversity 74(1): 3–18. https://doi.org/10.1007/s13225-015-0351-8

Jayawardena RS, Hyde KD, Chen YJ, Papp V, Palla B, Papp D, et al. (2020) One stop shop IV: taxonomic update with molecular phylogeny for important phytopathogenic genera: 76–100 (2020). Fungal Diversity 103: 87–218. https://doi.org/10.1007/s13225-020-00460-8

Jeewon R, Liew ECY, Hyde KD (2002) Phylogenetic relationships of *Pestalotiopsis* and allied genera inferred from ribosomal DNA sequences and morphological characters. Molecular Phylogenetics and Evolution 25(3): 378–392. https://doi.org/10.1016/S1055-7903(02)00422-0

Johnston PR, Quijada L, Smith CA, Baral HO, Hosoya T, Baschien C, Pärtel K, Zhuang WY, Haelewaters D, Park D, Carl S, López-Giráldez F, Wang Z, Townsend JP (2019) A multigene phylogeny toward a new phylogenetic classification of Leotiomycetes. IMA Fungus 10(1): 1. https://doi.org/10.1186/s43008-019-0002-x

Kearse M, Moir R, Wilson A, Stones-Havas S, Cheung M, Sturrock S, Buxton S, Cooper A, Markowitz S, Duran C, Thierer T, Ashton B, Meintjes P, Drummond A (2012) Geneious basic: An integrated and extendable desktop software platform for the organization and analysis of sequence data. Bioinformatics (Oxford, England) 28(12): 1647–1649. https://doi.org/10.1093/bioinformatics/bts199

Kress WJ, Erickson DL, Jones FA, Swenson NG, Perez R, Sanjur O, Bermingham E (2009) Plant DNA barcodes and a community phylogeny of a tropical forest dynamics plot in

Panama. Proceedings of the National Academy of Sciences of the United States of America 106(44): 8621–18626. https://doi.org/10.1073/pnas.0909820106

Kumar S, Stecher G, Tamura K (2016) MEGA7: Molecular evolutionary genetics analysis version 7.0 for bigger datasets. Molecular Biology and Evolution 33(7): 1870–1874. https://doi.org/10.1093/molbev/msw054

Levin RA, Wagner WL, Hoch PC, Nepokroeff M, Pires JC, Zimmer EA, Sytsma KJ (2003) Family-level relationships of Onagraceae based on chloroplast rbcL and ndhF data. American Journal of Botany 90(1): 107–115. https://doi.org/10.3732/ajb.90.1.107

Lutzoni F, Kauff F, Cox CJ, McLaughlin D, Celio G, Dentinger B, Padamsee M, Hibbett D, James TY, Baloch E, Grube M, Reeb V, Hofstetter V, Schoch C, Arnold AE, Miadlikowska J, Spatafora J, Johnson D, Hambleton S, Crockett M, Shoemaker R, Sung GH, Lücking R, Lumbsch T, O'Donnell K, Binder M, Diederich P, Ertz D, Gueidan C, Hansen K, Harris RC, Hosaka K, Lim YW, Matheny B, Nishida H, Pfister D, Rogers J, Rossman A, Schmitt I, Sipman H, Stone J, Sugiyama J, Yahr R, Vilgalys R (2004) Assembling the fungal tree of life: Progress, classification, and evolution of subcellular traits. American Journal of Botany 91(10): 1446–1480. https://doi.org/10.3732/ajb.91.10.1446

McTaggart AR, Shivas RG, Braun U (2007) *Annellosympodia orbiculata* gen. et sp. nov. and *Scolecostigmina flagellariae* sp. nov. from Australia. Australasian Plant Pathology 36(6): 573–579. https://doi.org/10.1071/AP07061

Mel'nik VA, Braun U (2013) *Atractilina alinae* sp. nov. and *Neosporidesmium vietnamense* sp. nov. – two synnematous hyphomycetes from Vietnam. Mycobiota 3: 1–9. https://doi.org/10.12664/mycobiota.2013.03.01

Miller MA, Pfeiffer W, Schwartz T (2010) Creating the CIPRES science gateway for inference of large phylogenetic trees. 2010 Gateway Computing Environments Workshop (GCE). IEEE, New Orleans, 8. https://doi.org/10.1109/GCE.2010.5676129

Morelet M (1971) De aliquibus in mycologia novitatibus (5^{e} note). Bulletin de la Société de Sciences Naturelles et d 'Archéologie de Toulon et du Var 195: 7–8. https://doi.org/10.2113/gssgfbull.S7-XIII.1-2.195

Nakamura T, Yamada KD, Tomii K, Katoh K (2018) Parallelization of MAFFT for large-scale multiple sequence alignments. Bioinformatics (Oxford, England) 34(14): 2490–2492. https://doi.org/10.1093/bioinformatics/bty121

Ordynets A, Keßler S, Langer E (2021) Geometric morphometric analysis of spore shapes improves identification of fungi. PLOS ONE 16(8): e0250477. https://doi.org/10.1371/journal.pone.0250477

Pem D, Jeewon R, Chethana KWT, Hongsanan S, Doilom M, Suwannarach N, Hyde KD (2021) Species concepts of Dothideomycetes: Classification, phylogenetic inconsistencies and taxonomic standardization. Fungal Diversity 109(1): 283–319. https://doi.org/10.1007/s13225-021-00485-7

Piepenbring M, Hofmann TA, Kirschner R, Mangelsdorff R, Perdomo O, Rodríguez Justavino D, Trampe T (2011) Diversity patterns of Neotropical plant parasitic microfungi. Ecotropica (Bonn) 17: 27–40.

Promputtha I, Jeewon R, Lumyong S, McKenzie EHC, Hyde KD (2005) Ribosomal DNA fingerprinting in the identification of non-sporulating endophytes from *Magnolia liliifera* (Magnoliaceae). Fungal Diversity 20: 167–186.

Promputtha I, Lumyong S, Vijaykrishna D, McKenzie EHC, Hyde KD, Jeewon R (2007) A phylogenetic evaluation of whether endophytes become saprotrophs at host senescence. Microbial Ecology 53(4): 579–590. https://doi.org/10.1007/s00248-006-9117-x

Raja HA, Miller AN, Pearce CJ, Oberlies NH (2017) Fungal Identification Using Molecular Tools: A Primer for the Natural Products Research Community. Journal of Natural Products 24 80(3): 756–770. https://doi.org/10.1021/acs.jnatprod.6b01085

Rodríguez Justavino D, Kirschner R, Piepenbring M (2015) New species and new records of Meliolaceae from Panama. Fungal Diversity 70(1): 73–84. https://doi.org/10.1007/s13225-014-0292-7

Ronquist F, Teslenko M, van der Mark P, Ayres DL, Darling A, Höhna S, Larget B, Liu L, Suchard MA, Huelsenbeck JP (2012) MrBayes 3.2: Efficient bayesian phylogenetic inference and model choice across a large model space. Systematic Biology 61(3): 539–542. https://doi.org/10.1093/sysbio/sys029

Schoch CL, Crous PW, Groenewald JZ, Boehm EWA, Burgess TI, de Gruyter J, de Hoog GS, Dixon LJ, Grube M, Gueidan C, Harada Y, Hatakeyama S, Hirayama K, Hosoya T, Huhndorf SM, Hyde KD, Jones EBG, Kohlmeyer J, Kruys Å, Li YM, Lücking R, Lumbsch HT, Marvanová L, Mbatchou JS, McVay AH, Miller AN, Mugambi GK, Muggia L, Nelsen MP, Nelson P, Owensby CA, Phillips AJL, Phongpaichit S, Pointing SB, Pujade-Renaud V, Raja HA, Plata E Rivas, Robbertse B, Ruibal C, Sakayaroj J, Sano T, Selbmann L, Shearer CA, Shirouzu T, Slippers B, Suetrong S, Tanaka K, Volkmann-Kohlmeyer B, Wingfield MJ, Wood AR, Woudenberg JHC, Yonezawa H, Zhang Y, Spatafora JW (2009) A class-wide phylogenetic assessment of Dothideomycetes. Studies in Mycology 64: 1–15. https://doi.org/10.3114/sim.2009.64.01

Seifert KA, Hughes SJ (2000) *Spiropes dictyosporus*, a new synnematous fungus associated with sooty moulds. New Zealand Journal of Botany 38(3): 489–492. https://doi.org/10.1080/0028825X.2000.9512698

Stamatakis A (2014) RAxML version 8: A tool for phylogenetic analysis and post-analysis of large phylogenies. Bioinformatics (Oxford, England) 30(9): 1312–1313. https://doi.org/10.1093/bioinformatics/btu033

Stevens FL (1918) Some meliolicolous parasites and commensals from Porto Rico. Botanical Gazette (Chicago, Ill.) 65(3): 227–249. https://doi.org/10.1086/332230

Talavera G, Castresana J (2007) Improvement of phylogenies after removing divergent and ambiguously aligned blocks from protein sequence alignments. Systematic Biology 56(4): 564–577. https://doi.org/10.1080/10635150701472164

Thambugala KM, Wanasinghe DN, Phillips AJL, Camporesi E, Bulgakov TS, Phukhamsakda C, Ariyawansa HA, Goonasekara ID, Phookamsak R, Dissanayake A, Tennakoon DS, Tibpromma S, Chen YY, Liu ZY, Hyde KD (2017) Mycosphere notes 1–50: Grass (Poaceae) inhabiting Dothideomycetes. Mycosphere : Journal of Fungal Biology 8(4): 697–796. https://doi.org/10.5943/mycosphere/8/4/13

Valenzuela-Lopez N, Magaña-Dueñas V, Cano-Lira JF, Wiederhold N, Guarro J, Stchigel AM (2019) Two new species of *Gloniopsis* (Hysteriales, Ascomycota) from clinical specimens: Morphological and molecular characterization. Mycoses 62(12): 1164–1173. https://doi.org/10.1111/myc.13006

Vilgalys R, Hester M (1990) Rapid genetic identification and mapping of enzymatically amplified ribosomal DNA from several *Cryptococcus* species. Journal of Bacteriology 172(8): 4238–4246. https://doi.org/10.1128/jb.172.8.4238-4246.1990

Von Arx JA, Müller E (1975) A re-evaluation of the bitunicate ascomycetes with keys to families and genera. Studies in Mycology 9: 1–159.

Wagner T, Ryvarden L (2002) Phylogeny and taxonomy of the genus *Phylloporia* (Hymenochaetales). Mycological Progress 1(1): 105–116. https://doi.org/10.1007/s11557-006-0009-8

Wanasinghe DN, Phukhamsakda C, Hyde KD, Jeewon R, Lee HB, Jones EBG, Tibpromma S, Tennakoon DS, Dissanayake AJ, Jayasiri SC, Gafforov Y, Camporesi E, Bulgakov TS, Ekanayake AH, Perera RH, Samarakoon MC, Goonasekara ID, Mapook A, Li W-J, Senanayake IC, Li J, Norphanphoun C, Doilom M, Bahkali AH, Xu J, Mortimer PE, Tibell L, Tibell S, Karunarathna SC (2018) Fungal diversity notes 709–839: Taxonomic and phylogenetic contributions to fungal taxa with an emphasis on fungi on Rosaceae. Fungal Diversity 89(1): 1–236. https://doi.org/10.1007/s13225-018-0395-7

Wang Z, Johnston PR, Takamatsu S, Spatafora JW, Hibbett DS (2006a) Towards a phylogenetic classification of Leotiomycetes based on rDNA data. Mycologia 98(6): 1065–1075. https://doi.org/10.1080/15572536.2006.11832634

Wang Z, Binder M, Schoch CL, Johnston PR, Spatafora JW, Hibbett DS (2006b) Evolution of helotialean fungi (Leotiomycetes, Pezizomycotina): A nuclear rDNA phylogeny. Molecular Phylogenetics and Evolution 41(2): 295–312. https://doi.org/10.1016/j.ympev.2006.05.031

White TJ, Brun T, Lee S, Taylor J (1990) Amplification and direct sequencing of fungal ribosomal RNA genes for phylogenetics. In: Innis MA, Gelfand DH, Sninsky JJ, White TJ (Eds) PCR Protocols: a guide to methods and applications, Academic Press, San Diego. https://doi.org/10.1016/B978-0-12-372180-8.50042-1

Zeng XY, Zhao JJ, Hongsanan S, Chomnunti P, Boonmee S, Wen TC (2017) A checklist for identifying Meliolales species. Mycosphere: Journal of Fungal Biology 8(1): 218–359. https://doi.org/10.5943/mycosphere/8/1/16

Zhang K, Guo W, Sosa D, Magdama F, Serrano L, Malosso E, Li D-W, Castañeda-Ruiz RF (2020) Phylogeny and morphology of *Ellismarsporium parvum* and the new combination *E. varium*. Mycotaxon 135(2): 443–452. https://doi.org/10.5248/135.443

Zhao G, Wu Y, Li N (1996) Six fungi species of hyperparasite on Meliolaceae. Journal of Beijing Forestry University 18(1): 99–103.

Supplementary material 1

Alignments and tree generated during the analysis of the DNA sequences of *Atractilina parasitica*, *Malacaria meliolicola* and other members of the Dothideomycetes

Authors: Miguel A. Bermúdez-Cova, Tina A. Hofmann, Nourou S. Yorou, Meike Piepenbring

Data type: docx

Explanation note: Alignment is shown in NEXUS format. The tree is shown in Newick format.

Link: https://doi.org/10.3897/mycokeys.103.115799.suppl1